METABOLIC INTERACTIONS AND ACTIVITY PARTITIONING IN A METHANOGENIC, INTERDOMAIN BIOFILM

by

Laura Beth Camilleri

A dissertation submitted in partial fulfillment
of the requirements for the degree

of

Doctor of Philosophy

in

Microbiology and Immunology

MONTANA STATE UNIVERSITY
Bozeman, Montana

April 2019

©COPYRIGHT

by

Laura Beth Camilleri

2019

All Rights Reserved

DEDICATION

To my family and my friends,
To the strangers with a kind word or smile,
Thank You.

ACKNOWLEDGEMENTS

My parents have always had an appreciation for education and impressed this upon me from a very young age, but the joke is on them because now I am a professional student with a lifelong desire to keep learning all the secrets of the universe! I will forever be grateful to my Mom, Dad, Grandma, and Mormor for fostering my curiosity and giving me the courage to seek truth for myself. I also owe W.J., Torie, and Neerja my sincerest gratitude and love for being the supportive, wonderful, people they are!

I am also thankful for having Matthew Fields as my mentor and advisor through the years. I can’t imagine anybody else that would entertain my wild ideas let alone contribute to long, meaningful, and sometimes hypothetical, conversations every time a spontaneous thought crossed my mind. My time in the Center for Biofilm Engineering at Montana State University has been full of friendship, fun, inspiration, and comradery. It has been a welcoming environment full of encouraging and thoughtful people which is especially true of my committee members Christine Foreman, Robin Gerlach, and Mike Franklin.

I also owe my gratitude to Stephanie Cunningham who recognized my desire to study systems in their entirety and led me to becoming a fellow of the National Science Foundation – IGERT program. My education would not have been possible without it, or without the support of ENIGMA (Ecosystems and Networks Integrated with Genes and Molecular Assemblies), my friends and collaborators at Lawrence Berkeley National Laboratory, and the funding from the Department of Energy.

TABLE OF CONTENTS

1. INTRODUCTION 1

Interspecies Communication and Model Organisms 1
    Types of Symbiosis 4
    Sulfate-Reducing Bacteria 6
    Hydrogenotrophic Methanogenic Archaea 8
    Syntrophy between *Desulfovibrio* and *Methanococcus* 9
Biofilm Interactions 10
    Historical Significance 11
    Pure Culture Paradigm 15
Research Objectives 16
References 20

2. DIFFERENTIAL GENE EXPRESSION OF A BACTERIAL-ARCHAEAL INTERDOMAIN BIOFILM PRODUCING METHANE 30

Contributions of Authors 30
Manuscript Information 32
Abstract 33
Introduction 34
Materials and Methods 36
    Culture Conditions 36
    Sample Collection 36
    Total RNA Extraction 37
    Illumina Library Construction and Sequencing 37
    Transcriptome Assembly and Analyses 38
    RNA-Seq Expression Analysis 39
    Stoichiometric Modeling 40
Results 41
    Expression as a Result of Syntrophy 52
    Expression as a Result of Growth Mode 53
    Stoichiometric Modeling of Amino Acid Exchange 55
Discussion 59
References 65
Supplemental Material 70

TABLE OF CONTENTS – CONTINUED

3. ACTIVITY PARTITIONING IN AN ARCHAEAL-BACTERIAL BIOFILM 190

Contributions of Authors 190
Manuscript Information 191
Abstract 192
Introduction 193
Materials and Methods 195
- Culture Conditions 195
- Deuterium Oxide Addition 196
- Deuterium Proteomic Analysis 197
- Bioorthogonal Noncanonical Amino Acid Tagging and rRNA-targeted FISH 199

Results 201
- Biofilm Growth 201
- Deuterated Proteomics 202
- BONCAT – FISH of mono- and co- cultures 207

Discussion 220
References 227

4. METHANOCOCCUS MARIPALUDIS FACTOR CAUSES SLOWED GROWTH IN DESULFOVIBRIO VULGARIS HILDENBOROUGH....................232

Contributions of Authors 232
Manuscript Information 233
Abstract 234
Introduction 235
Materials and Methods 237
- Culture Conditions 237
- Gas Chromatography 238
- Sulfate Stress 238
- Cell Counts and Image Analysis of Co-culture Biofilm 239
- Spent Filtrate Preparation 240

Results 241
- Sulfate Stress of the Co-culture Biofilm Reactor 241
- Growth Effect of Filtered Media 245

Discussion 251
References 256
Supplemental Figures 259

TABLE OF CONTENTS – CONTINUED

5. GROWTH EFFECTS OF SULFOPYRUVATE AND SULFOACETATE ON THE SULFATE-REDUCING BACTERIUM, DESULFOVIBRIO VULGARIS HILDENBOROUGH, AND THE METHANOGENIC ARCHAEON METHANOCOCCUS MARIPALUDIS S2 260

Contributions of Authors 260
Manuscript Information 261
Abstract 262
Introduction 263
Materials and Methods 265
  Culture Conditions 265
  Sulfonate Compound Addition 265
Results and Discussion 266
  Desulfovibrio vulgaris Growth 266
  Methanococcus maripaludis Growth 270
Conclusion 276
References 277

6. EPILOGUE 280

References 290

REFERENCES CITED 294

APPENDICES 318

APPENDIX A: Methane production in *Pelosinus fermentans* JBW45 319
  Contributions of Authors 320
  Manuscript Information 321
  Abstract 322
  Introduction 323
  Materials and Methods 324
    Culture Conditions 324
    Cell Imaging 325
    Electron Microscopy 326
    Gas Chromatography 326
    Polymerase Chain Reaction 326
    Gas Chromatography – Mass Spectrometry 327

TABLE OF CONTENTS – CONTINUED

Results 328
Discussion 338
References 340
Supplemental Figures 344

APPENDIX B: Draft genome sequence of *Pelosinus fermentans* JBW45 isolated during *in situ* stimulation for Cr(VI) reduction 349
Contributions of Authors 350
Manuscript Information 351

APPENDIX C: Complete genome sequence of *Pelosinus fermentans* JBW45, a member of a remarkably competitive group of *Negativicutes* in the *Firmicutes* phylum 354
Contributions of Authors 355
Manuscript Information 356

APPENDIX D: Biofilm growth mode promotes maximum carrying capacity and community stability during product inhibition syntrophy 359
Contributions of Authors 360
Manuscript Information 361

APPENDIX E: 3D-Fluorescence *in situ* hybridization of intact, anaerobic biofilm 375
Contributions of Authors 376
Manuscript Information 377

LIST OF TABLES

Table Page

1. *Methanococcus maripaludis* S2 differentially expressed genes between co-culture biofilm and co-culture planktonic 50

2. Stoichiometric model predictions for *Desulfovibrio vulgaris* Hildenborough amino acids..56

3. Stoichiometric equations used for the *D. vulgaris* model 71

4. Stoichiometric equations used for the *M. maripaludis* model 87

5. Gene expression in *D. vulgaris* specific to the co-culture syntrophic growth with *M. maripaludis*. 155

6. Gene expression in *M. maripaludis* specific to the co-culture syntrophic growth with *D. vulgaris*..160

7. Co-culture biofilm specific gene expression in *D. vulgaris* 166

8. Co-culture biofilm specific gene expression in *M. maripaludis*......................179

9. *D. vulgaris* peptides deuterium labeled in co-culture biofilm and function in amino acid production, utilization, or transport 204

10. *M. maripaludis* peptides that were deuterium labeled in co-culture biofilm...205

11. *Pelosinus fermentans* JBW45 genes indicating heavy metal tolerance 337

LIST OF FIGURES

Figure Page

1. *Desulfovibrio vulgaris* Hildenborough and *Methanococcus maripaludis* S2 co-culture biofilm RNA-Seq analysis comparisons 39

2. *D. vulgaris* Hildenborough co-culture biofilm expression profile....................42

3. *M. maripaludis* co-culture biofilm expression profile 43

4. Statistically significant expression profile for *D. vulgaris* 44

5. Statistically significant expression profile for *M. maripaludis*..........................45

6. *D. vulgaris* expression for clusters of orthologous genes 47

7. *M. maripaludis* expression for clusters of orthologous genes 48

8. Transcriptomic differences in methanogenic-related electron and carbon processing genes for *M. maripaludis* in biofilm 51

9. *M. maripaludis* amino acid contribution to biomass modeling 57

10. *M. maripaludis* amino acid contribution to energy modeling..........................58

11. Enzymatic activity of co-culture alcohol and formate dehydrogenase 70

12. Deuterium oxide workflow for the co-culture biofilm system 197

13. Co-culture biofilm reactor profile with deuterium addition points................202

14. Late stage deuterium incorporation for key proteins 206

15. Apparent half-saturation time for deuterium incorporation in the early and late stage co-culture biofilm 207

16. Batch planktonic monocultures of *D. vulgaris* HPG-BONFISH labeled...209

17. Batch planktonic monocultures of *M. maripaludis* HPG-BONFISH labeled...210

LIST OF FIGURES CONTINUED

Figure Page

18. Batch planktonic co-cultures of *D. vulgaris* and *M. maripaludis* HPG-BONFISH labeled 211

19. *D. vulgaris* and *M. maripaludis* HPG-BONFISH labeled with 50 µM HPG in the co-culture biofilm reactor 212

20. Growth effect of 50 µM and 200 µM HPG on batch planktonic *M. maripaludis, D. vulgaris*, and the co-culture 213

21. Batch planktonic cultures of *M. maripaludis* and *D. vulgaris* grown with 50 µM HPG, filtered, and then re-inoculated with *D. vulgaris* to test for BONCAT labeling..215

22. Batch planktonic cultures of *M. maripaludis* and *D. vulgaris* grown with 50 µM HPG, filtered, and then re-inoculated with *M. maripaludis* to test for BONCAT labeling 216

23. BONFISH labeling for a short incubation using 50 µM HPG in a grown batch planktonic co-culture of *M. maripaludis* and *D. vulgaris* 217

24. EdU labeling of batch planktonic monocultures and co-cultures of *M. maripaludis* and *D. vulgaris* 219

25. Daily sampling for the co-culture biofilm reactors of *M. maripaludis* and *D. vulgaris* before and after sulfate stress 242

26. Co-culture population ratios before and after sulfate stress...........................243

27. FISH labeled co-culture biofilm from *M. maripaludis* and *D. vulgaris* before and after sulfate addition 245

28. Monoculture growth of *M. maripaludis* and *D. vulgaris* in 10 kDa co-culture reactor filtrate...246

29. *D. vulgaris, Desulfovibrio alaskensis* G20, and *Pseudomonas aeruginosa* growth in 10 kDa filtered spent media from *M. maripaludis* 249

LIST OF FIGURES CONTINUED

Figure Page

30. Effect of 10 kDa *M. maripaludis* filtrate on *D. vulgaris* and *D. alaskensis* G20 sulfate/lactate utilization 250

31. Effect of 10 kDa *M. maripaludis* filtrate on co-culture lactate utilization, H_2 and CH_4 production..251

32. Sulfide concentration in planktonic co-culture post sulfate addition............259

33. *D. vulgaris* growth on formate and pyruvate 267

34. *D. vulgaris* growth on lactate and sulfoacetate 268

35. *M. maripaludis* growth on H_2:CO_2 with and without acetate 271

36. *M. maripaludis* growth on formate and pyruvate 272

37. *M. maripaludis* growth with sulfopyruvate and sulfoacetate.........................273

38. Structural comparison of sulfopyruvate, sulfoacetate, Coenzyme M, and BES...275

39. Acridine orange stained *Pelosinus fermentans* JBW45.................................329

40. FE-SEM images of *P. fermentans* JBW45 330

41. Growth of *P. fermentans* JBW45 in glycerol...331

42. Growth of *P. fermentans* JBW45 in glucose, sucrose, fructose, and pyruvate...332

43. Growth of *P. fermentans* JBW45 in lactate with nitrate or sulfate, and formate with acetate 333

LIST OF FIGURES CONTINUED

Figure Page

44. PCR with McrA on *P. fermentans* JBW45 334

45. PCR with Arch30 on *P. fermentans* JBW45...334

46. FISH labeled *P. fermentans* JBW45 336

47. Headspace analysis showing CH_4 in *P. fermentans* JBW45..........................344

48. *P. fermentans* JBW45 GC-MS with $^{13}CO_2$ incubation 345

49. Growth of *P. fermentans* JBW45 with methionine and lactate 346

50. Growth of *P. fermentans* JBW45 on methylphosphonate 347

51. Growth of *P. fermentans* JBW45 in the presence of BES 348

ABSTRACT

Biofilms are an ancient survival strategy in which communities of organisms can grow as a cohesive unit, generally attached to a surface and/or at interfaces. Despite the paradigm that 99% of microorganisms grow as a biofilm in the environment, current research methods are largely limited to monoculture planktonic studies. Although more investigations are trying to improve culture complexity by evaluating interactions between two or more populations, experiments are still more readily performed with microorganisms in the planktonic growth mode. The research presented here aims to elucidate the complexity of interactions between two microorganisms from different domains of life that results in enhanced metabolism due to localization of cells in close proximity within an anaerobic biofilm. *Desulfovibrio vulgaris* Hildenborough (DvH) and *Methanococcus maripaludis* S2 (Mmp) form a syntrophic mutualism when grown in sulfate-limited media that requires electron flux from DvH to Mmp through what is commonly assumed to be interspecies hydrogen transfer, thereby establishing cross-feeding. The biofilm has been shown to promote a stable and more even carrying capacity for both populations that is likely linked to improved hydrogen transfer (and/or other potential carbon and electron co-metabolites) as compared to planktonic populations. Transcriptomic and proteomic analyses, utilizing RNA-seq and deuterated water respectively, were used to elucidate genes and proteins that contribute to the biofilm growth mode that results in a more efficient metabolism for the syntrophic co-culture (defined by biomass per substrate flux). The results demonstrate the expression of many genes with unknown functions, and others that contribute to cell-cell interactions as well as active proteins in electron processing (*e.g.*, lactate oxidation) in DvH and CO_2 reduction (*e.g.*, methanogenesis) in Mmp. A metabolic model of the coculture provided reinforcement for transcriptomic assumptions and aided in the identification of a sulfonate and other amino acids as important syntrophic metabolites. Assessment of biofilm co-culture activity utilizing a new method, Biorthogonal Noncanonical Amino Acid Tagging (BONCAT), showed Mmp was less active in the uptake of a methionine analog as compared to DvH. Alternate assessments confirmed that Mmp was in fact active (based upon methane generation) although translational activity was below the detection limit. Further investigation of the system under sulfate stress showed that the metabolic pairing is more stable than previously thought and could indicate survival strategies that drive the seemingly ‘mutualistic’ relationship as a forced cooperation. The sulfate stress response coincided with observed lags in DvH growth when grown in Mmp spent medium that was associated with a decoupling of lactate-oxidation and sulfate-reduction. Together the results demonstrate metabolic interactions and activity partitioning within a methanogenic archaeal-bacterial biofilm. The dogma of mutualism being synonymous with equal reciprocity is challenged as it pertains to this model biofilm system. Moreover, this unique bacterial-archaeal biofilm represents interdomain interactions that could represent systems that contributed shared metabolic processes that lead to the development of eukaryotic life.

CHAPTER ONE

INTRODUCTION

Interspecies Communication and Model Organisms

Microbial communities are heterogenous, diverse, and ubiquitous, and form complex networks of interactions between multiple species as well as the environment. Advancements in technology have illuminated the seemingly boundless expanse that microorganisms encompass and accompanied with it has been the shift away from the debate of what microorganisms exist in an environment, to an emphasis on the methodology to identify environmentally relevant populations and their respective biochemical capacity. Microbial communities have permeated every aspect of our daily lives in both a positive and negative fashion and have become essential to not only maintain, but advance modern life. Microorganisms are not just important to human health and disease, but they also help to provide us with technology for innumerable industrial applications from waste water treatment to the production of food and medication. To predict and alter microbial community physiology, the dynamic metabolic interactions between different populations must be better understood. The research outlined here utilizes model organisms to assess the dynamic interactions in an anaerobic biofilm assembly between the sulfate-reducing bacterium, *Desulfovibrio vulgaris* Hildenborough, and the archaeal methanogen, *Methanococcus maripaludis* S2.

Approximately 50 years ago, scientists discovered that bacteria could utilize cell-to-cell communication through the use of chemical signals (Nealson et al., 1970; Tomasz, 1965). The term quorum sensing was used to describe this signaling between bacteria of the same population since it was repeatedly discerned when a critical population density was reached, and further research has demonstrated that the signaling can impact different populations nearby (Fuqua et al., 1994). The observed outcome was due to an accumulation of chemical signal from an increasing population of cells which resulted in the coordinated expression of specific target genes within those bacterial members, thereby mimicking the behavior of a multicellular organism (Eberhard et al., 1981; Engebrecht et al., 1983; Matz, 2011). Unlike the planktonic growth mode, the diffusion limitations and close proximity of cells within a biofilm make chemical communication an idyllic route for interspecies interactions (Decho et al., 2010). For example, biofilm populations rely on chemical communication in order to overcome adverse environmental conditions thereby increasing the fitness of the assembled community (Keller & Surette, 2006).

While cell-to-cell communication has been rigorously studied, the ecological framework for the role of chemical signaling is still not well understood, as interactions are vast and complex (Keller & Surette, 2006). The types of chemical signaling molecules and pathways, along with the environmental and co-metabolic interactions that can be controlled, is an ever-expanding area of research as different microorganisms are cultivated under environmentally relevant conditions. Currently, quorum sensing is grouped into three different classes: N-acyl homoserine lactone based signaling by some Gram-negative bacteria, LuxS/autoinducer-2 signaling by some Gram-negative and Gram-positive bacteria, and oligopeptide signaling by some Gram-positive bacteria. The complexity of these communication molecules is exemplified by oligopeptide signaling. Oligopeptides can be highly specific to certain species while also exhibiting inhibitory or antimicrobial properties in other groups (Ji et al., 1997; Lyon et al., 2002; Mayville et al., 1999). Oligopeptide signals therefore not only coordinate cooperation but can also function in competition as well as having metabolic ramifications (*i.e*., utilization as carbon and/or energy source).

Interspecies communication infers that signals are released to elicit a directed response; however it can also be an unintentional cue that nearby community members can respond to as a result of cross-species signaling (Bassler, 1999). The need to better understand the ecological implications that signaling can have is particularly emphasized by recognizing that there are three general types of chemical interactions that can occur. Signaling is the primary interaction recognized which is an intentional, directed response that typically results in a behavior change. There can also be indirect effects, or cues, whereby bacteria passively recognize and modify gene expression due to chemical molecules that are produced by nearby community members of another species. Additionally, intentional chemical manipulation of one bacterium by another can occur, which typically functions to have a negative impact on the fitness of the recipient (Keller & Surette, 2006). Competition, defense mechanisms, and symbiosis can all be facilitated by chemical signaling (Matz, 2011).

Model organisms that have a well-studied genetic system, such as *Pseudomonas aeruginosa*, can have up to five percent of its total genes controlled by quorum sensing (Whiteley et al., 1999). The *P. aeruginosa* genes observed to be under signaling control include genes that are responsible for virulence, exoenzymes, and extracellular structures that are important for biofilm formation (Whiteley et al., 1999). There is also evidence of inter-domain communication such as the interference of the *P. aeruginosa* quorum sensing system that is modulated by compounds (*i.e.*, rosmarinic acid) secreted by plants (Corral-Lugo et al., 2016). Within the last 20 years, genomics, transcriptomics, proteomics, and metabolomics have become commonplace tools to elucidate the vast array of complex microbial interactions including novel signaling and communication pathways. Through these approaches, an understanding of the regulatory responses that microorganisms employ in their environment can be identified and biomined in an effort to control the effect microbial communities may have in a given setting. Therefore, in addition to the traditional modes of quorum sensing that can impact intra-population communication, direct metabolic interactions could be considered as a mechanism of inter-population communication that subsequently effects the optimization of resource sharing (*e.g.*, symbiosis).

Types of Symbiosis

Social behavior has been well documented throughout the biosphere, in and across all three domains of life, from microbes to ants to lions. The potential interactions in complex communities can be characterized as cooperative, altruistic, or hierarchal with the overarching goal to directly and/or indirectly improve reproductive success (Archetti et al., 2011; Hammerstein & Selten, 1994). With the advances in microbiological methodologies, ecological theories that were originally formed for the macroscopic world have become more applicable to microbial interactions. The discovery of quorum sensing, and the significant role communication has within microbial communities, has been the pinnacle that directed a new area of research deemed sociomicrobiology (Whiteley et al., 2017).

Many of the general characteristics observed in aggregations of animals can also be observed for microbial communities. The term social, or symbiosis, can erroneously lead people to envision an amicable, cooperative interaction that is generally assumed to be equally beneficial to the interacting populations. It is important to remember that social behavior on any scale is the product of competing interests for the organisms involved in terms of available resources, investment costs, and outcomes. Evolutionary theory emphasizes that social behavior is ultimately motivated by the desire to survive and reproduce (Hammerstein & Selten, 1994; Prosser et al., 2007).

Microbial relations form within complex ecological interactions and can be broadly defined as cooperative or competitive (Faust & Raes, 2012) The nature of the interaction is typically classified according to a “binary” model if each participant is benefitting, unchanged, negatively impacted, or a combination thereof (*e.g.*, +/-, -/+, +/+). Typical competitive or parasitic associations can be explained in a predator-prey dynamic with one benefitting at the expense of another to varying degrees of severity. When two organisms benefit from an interaction it is referred to as a mutualism. If the organisms are benefitting specifically due to the cross-feeding of metabolites, then it is considered to be a syntrophic mutualism.

Amensalism refers to conditions that harm one partner without affecting the other. An example of this would be the creation of a more acidic environment by *Lactobacillus* which would negatively impact organisms that are not acidophilic. Conversely, commensalism is when one partner benefits with neutral impact on the other partner. This type of interaction is common with biodegradation where a population of microorganisms is sustained off of the degradation products produced by another population.

These types of direct and indirect ecological interactions between microorganisms have been observed to produce pattern formations within multispecies biofilms. When the relationship is cooperative, the biofilm has an even intermixing of the populations throughout. If competitive interactions exist, the organisms spatially segregate within the biofilm as they compete for space and nutrients (Momeni et al., 2013). The research presented here studies ecological interactions in a controlled biofilm system that creates a syntrophic mutualism with even interspecies mixing between two model organisms, the sulfate-reducing bacterium, *Desulfovibrio vulgaris* Hildenborough, and an archaeal methanogen, *Methanococcus maripaludis* S2.

Sulfate-Reducing Bacteria

Anaerobic, sulfate-reducing bacteria (SRB) are the most common microbial induced corrosion (MIC)-associated organisms. Sulfate-reducing bacteria (SRB), such as *Desulfovibrio vulgaris* Hildenborough, and their biofilms on different surface types have been both of great interest and subject to scrutiny for the last several decades. SRB have been recognized as ideal organisms for bioremediation of sites that contain toxic hydrocarbons and soluble toxic heavy metals or radionuclides (Hamilton, 2003; Michel et al., 2001; Payne et al., 2002). They have gained attention due to their economic implications from oil field souring, steel and concrete corrosion, and metal pipe fouling. Hence, there is considerable interest in understanding and ultimately controlling the sulfidogenic activity of SRB, particularly at solid-liquid or liquid-liquid interfaces (*i.e.*, biofilms).

The SRB, *Desulfovibrio vulgaris* Hildenborough, has a fully sequenced genome and a genetic system that has transpired over the years as a result of the interest in understanding and controlling its physiology (Heidelberg et al., 2004). *D. vulgaris* Hildenborough, as a SRB, can generate energy by using an ancient metabolism that transfers electrons to sulfate which results in the production of sulfide, a reactive yet toxic product (Konhauser, 2006; Shen & Buick, 2004; Truper, 1984). *D. vulgaris* Hildenborough is valuable for bioremediation as it can also subsist by directing electrons to oxidized toxic metal ions such as uranium (VI) and chromium (VI), thereby converting these to less toxic, reduced, insoluble forms. Therefore, *D. vulgaris* is a model SRB for studying anaerobic metabolism, metal reduction, aerotolerance, and microbially-induced corrosion (Holman et al., 2009; Rabus et al., 2015), and numerous studies have characterized *Desulfovibrio* biofilms (Clark et al., 2006, 2012; Kurczy et al., 2015; Stylo et al., 2015). *Desulfovibrio* species represent an important guild in microbial communities that link the turnover of organic carbon with the cycling of sulfur and nitrogen compounds, and *Desulfovibrio* can also form syntrophic relationships with archaeal methanogens (Brileya et al., 2014b; Truper, 1984; Widdel, 1988).

Hydrogenotrophic Methanogenic Archaea

Hydrogen gas (H_2) is a crucial substrate for methanogens as well as a common source of energy for other organisms in both anaerobic and aerobic environments, including acetogens, sulfate- and sulfur- reducers, and hydrogen oxidizers (Ferrera et al., 2007; Petersen et al., 2011; Reysenbach et al., 2000). Hydrogenotrophic methanogens are obligate anaerobes that reduce carbon dioxide (CO_2) to methane (CH_4) by using hydrogen gas (H_2) as the electron donor. In addition to playing a role in the global carbon cycle, the methane that is generated from this ancient metabolism is a powerful greenhouse gas that has a global warming potential about 30 times higher than carbon dioxide (Thauer, 2012; Ueno et al., 2006; Yvon-Durocher et al., 2014). Understanding the ecological interactions of methanogens is important for elucidating early Earth processes and modern challenges such as determining the role methanogens play in the turnover of carbon in anaerobic environment, the formation of biogas, and human health (Conway de Macario & Macario, 2009; Jarrell et al., 2011).

Methanococcus maripaludis S2 is an anaerobic archaeon that can use H_2 or formate as an electron donor to reduce CO_2 to CH_4 and is considered a model mesophilic methanogen with its fully sequenced, and genetically tractable, genome. It was recently demonstrated that *Methanococcus maripaludis* could use hydrogen independent electromethanogenesis of carbon dioxide by cathodic electrons generated from a graphite electrode (Lohner et al., 2014). Additionally, it was observed that *Methanococcus maripaludis* can exhibit taxis toward hydrogen gas which may impart a competitive advantage in the environment and could help to maintain specific community interactions

(Brileya et al., 2013). Furthermore, *M. maripaludis* incorporates into *Desulfovibrio* biofilms under methanogenic and/or nitrogen-fixing conditions (Brileya et al., 2014b) (unpublished results).

Syntrophy between *Desulfovibrio* and *Methanococcus*

The syntrophy between sulfate-reducing bacteria and methanogenic archaea represent two different guilds that both contribute critical parts in various anaerobic environments. *Desulfovibrio* can use organic acids such as lactate, pyruvate, and formate as carbon and electron donors for sulfate reduction (Bryant et al., 1977; Hatchikian, 1975; Odom & Peck, 1981; Peck, 1960; Postgate, 1979). In the environment, *Desulfovibrio* will outcompete *Methanococcus* for free hydrogen (H_2) as sulfate reduction is more thermodynamically favorable compared to CO_2 reduction (Plugge et al., 2011). Conversely, when sulfate concentrations are low, some *Desulfovibrio* species can produce hydrogen (H_2) thereby facilitating a syntrophy with *Methanococcus* (and other methanogens) through interspecies hydrogen transfer (Bryant et al., 1977). This metabolic coupling is favorable when *Methanococcus* scavenges the hydrogen from *Desulfovibrio* because it keeps the partial pressure of hydrogen low and eliminates product inhibition feedback (Lupton et al., 1984). At the same time, this intricate interdomain interaction can be fleeting depending on the availability and flux of the substrates (Leloup et al., 2009; Plugge et al., 2011; Stams & Plugge, 2009).

In laboratory monocultures, *D. vulgaris* Hildenborough readily forms a biofilm that is flat and thin, but stable. While *M. maripaludis* has been observed to form a pellicle (Brileya et al., 2013), when grown in co-culture with *D. vulgaris* Hildenborough it doesn’t contribute to the initial biofilm formation, but is readily incorporated and evenly dispersed into an existing biofilm (Brileya et al., 2014b). The cooperative syntrophy in the co-culture also results in a thicker biofilm with topographical features such as ridges, spires, and valleys. It was recently shown that the biofilm promoted a stable, more even, carrying capacity with improved hydrogen transfer as compared to the planktonic bulk phase populations (Brileya et al., 2014b). Little work has been done to characterize the interactive populations in anaerobic biofilms and how structure impacts function within that community. The established model systems for *Desulfovibrio* and *Methanococcus* and the evidence for increased efficiency, as defined by biomass per substrate flux, within this biofilm mutualism via product inhibition syntrophy was the basis for further investigation presented here.

Biofilm Interactions

Microorganisms that grow as multicellular surface bound aggregates are termed a biofilm. Biofilms have been dated back to 3.4 billion years ago in deep-sea hydrothermal vents (Hall-Stoodley et al., 2004). In natural environments, over 99% of bacteria select to exist as high-density groups of surface attached communities (Costerton et al., 1987; Geesey et al., 1978). Biofilms provide many advantages as compared to the free-swimming planktonic state. Along with exhibiting a different phenotype, physiological activities of biofilms differ from the planktonic most likely driven by mass transport limitations dictated by flow regimes and biofilm composition. As an intricate three-dimensional structure, biofilms can concentrate nutrients, create microenvironments through gradients, communicate via signaling, and exhibit genetic heterogeneity. Furthermore, the cellular organization of biofilms effectually creates a protective outer layer that allows the inner community members to survive damaging UV, antibiotics, or other antimicrobials (Costerton & Wilson, 2004; Costerton, 1999). These factors make biofilms especially resilient to external stresses.

Biofilms are globally significant due to immense implications they have for the environment, medical field, and economy. Wastewater treatment facilities and bioremediation efforts commonly rely on the use of beneficial living biofilms. Unfortunately, the main driving force behind biofilm research has arisen from the negative aspects of biofilm formation. In the United States alone, it is estimated that $276 billion is spent on corrosion damage (Little & Lee, 2007). In other countries this cost accounts for 1-5% of the Gross National Product (Beech et al., 2005). Biofilms are believed to contribute over 50% of this total cost through microbial induced corrosion (MIC) (Flemming, 1996). Additionally, many chronic infections have been attributed to biofilms. Biofilm based infections are seldom resolved and can be detrimental even to those that have competent immune systems (Stewart & Costerton, 2001).

Historical Significance

Biofilms have been described from environments where there are liquid-solid, liquid-gas, or solid-solid interfaces that include terrestrial and deep sea hydrothermal features, riparian zones, ship hulls, metal pipes, saturated soils, and the human body (Hall-Stoodley et al., 2004). It is becoming increasingly clear that a mode of attached growth more closely resembles *in situ* conditions for many microorganisms in different environments and might likely be a universal feature that presents an important physiology to explore in addition to the typically conducted studies on planktonic cells (Dunne, 2002; Kolter, 2005; Shirtliff et al., 2002). As opposed to the individual free-swimming planktonic growth mode, cells growing as a biofilm are known to have different physiologies and properties such as increased resistance to external stresses such as antimicrobials, heavy metal exposure, desiccation, and substrate utilization (Clark et al., 2012; Kurczy et al., 2015; Stylo et al., 2015). This is in part due to the structure of the biofilm itself which can slow antibiotic penetration, alter the microenvironment in the inner layers, or provide a physical layer of protection by means of dead outer cells (Gross et al., 2007; Hall-Stoodley et al., 2004; Stewart & Costerton, 2001; Stewart & Franklin, 2008). Most microbial environments are physically dynamic habitats where fluxes in water, nutrients, temperature, pH, and osmolarity can create challenges for microorganisms to survive and thrive, and dehydration events can inhibit motility and limit nutrient availability that can result in decreased microbial activity (Or et al., 2007). Biofilm matrices can retain water, sorb nutrients, and protect against rapid changes in salinity, osmolarity, pH, nutrient availability, and redox, and these attributes significantly impact the cycling of C, N, S, and P in almost every environment on the planet.

Hardiness of biofilm cells can be attributed to the distinct physiological state of cells existing and growing in the biofilm growth mode and also to the secreted matrix components that interact with surfaces and the external environment. The biofilm EPS is an all-inclusive term for the extracellular macromolecules that enable cells to adhere to surfaces and each other. The understanding of the biofilm matrix has progressed to include, but are not limited to, polysaccharides, extracellular DNA, membrane vesicles, cell debris from lysed cells, enzymes, and structural proteins (Branda et al., 2005; Flemming & Wingender, 2010; Stewart & Franklin, 2008). While some of these components have been identified and a function established for a particular species, there are still many matrix components that have not been identified or described, including membrane vesicles and related structures, particularly for environmental microorganisms. Moreover, the biofilm matrix is increasingly being realized to contain a variety of intra- and inter- matrix interactions that contribute and may control biofilm behavior (D. E. Payne & Boles, 2016; Schooling & Beveridge, 2006).

In addition to aiding in surface attachment, the matrix can determine unique features of the biofilm such as structure and diffusion limitations (Braissant et al., 2007; Decho, 2000; Kreft et al., 2007; Lawrence et al., 2007; Loverdo et al., 2008; Nadell et al., 2008). Cells within the biofilm have the ability to move and it has been well documented that proximity of cells facilitates signaling (Stahl et al., 2011). Eukaryotic cells utilize filament tracks to shuttle large molecules around more rapidly than diffusion; therefore, it is possible that biofilms might function to exchange large signals similarly through the EPS (Loverdo et al., 2008). More recently, Hooper and Burstein posited that the minimization of extracellular space in prokaryotic (*i.e.*, *Bacteria* and Archaea) biofilms promoted cellular associations that impacted metabolism and may have contributed to the evolution of *Eukarya* (Hooper & Burstein, 2014). Thus, DvH and Mmp represent a good model system of an inter-domain biofilm to elucidate novel interactions.

The structure and function of multispecies biofilms can be more complex and difficult to cultivate than monocultures, but multispecies biofilms likely represent a natural state for *in situ* biofilms. Moreover, despite the ubiquity of biofilms and importance of anaerobes, little work has been done to understand how biofilm structure affects function in anaerobic microbial communities (Bernstein et al., 2012; Brenner & Arnold, 2011; Nielsen et al., 2000; Raskin et al., 1996). While interactions between SRB and methanogens have been studied, very little has been done to characterize the emergent properties of interactive populations in anerobic biofilms. *Desulfovibrio* and *Methanococcus* provide good model systems given the extent of importance, knowledge, and available resources (*e.g.*, genomes, mutants, Tn-Seq libraries).

Inhabitants of anaerobic ecosystems are assumed to function at the thermodynamic limit for energy generation and biomass production given system constraints (Bryant et al., 1977; Kato & Watanabe, 2010; McInerney et al., 2009; Thauer et al., 2008). When one metabolism is obligately coupled to another through interspecies H_2, formate, or electron transfer, organisms must persist by sharing the overall free energy of the reaction (Kato & Watanabe, 2010). Syntrophic physiology plays an important role in microbial communities dominated by fluctuations in nutrient availability and stress, where community interactions are thought to provide stability (Hansen et al., 2007).

In addition to the applied microbiology context, fundamentally, this unique bacterial-archaeal biofilm represents interdomain interactions that could have contributed to evolutionary processes that led to the development of eukaryotic life (Hooper &

Burstein, 2014; Wrede et al., 2012). The research presented here will provide insight into the internal and external biochemical environments that promoted differentiated, localized, and shared metabolism.

Pure Culture Paradigm

Natural biofilms represent multispecies communities of interacting microorganisms however; physiology and regulatory biofilm studies have been performed without excessive consideration of species-species interactions (Matz, 2011). Additionally, metabolic changes for adaptation to a syntrophic community may not be apparent when grown in pure culture. Transcriptomic studies of planktonic systems have repeatedly demonstrated that syntrophic growth resulted in the differential expression of hypothetical uncharacterized genes (Kato & Watanabe, 2010; Plugge et al., 2011; Walker et al., 2009).

Most studies utilize pure cultures for the ease of interpretation and analysis. Mixed cultures provide an added level of complexity, especially for transcriptomics (which measures mRNA transcript levels) and proteomics (which quantifies protein abundance), due to the significant computational efforts of individual organism assignment even with pre-established libraries to reference (Fondi & Liò, 2015; Gutleben et al., 2018; Zhang et al., 2010). Additionally, non-specific proteomics accomplished with deuterium oxide (D_2O) labeling can confound results when multiple populations are considered due to the intricacy of making peak assignments to individual proteins belonging to individual microorganisms. Pure culture studies are still invaluable in order to decipher microbial physiology and curate database annotations; however, they cannot fully unveil the complexities of microbial community interactions. Therefore, more studies are needed of mixed communities under anaerobic conditions in the biofilm growth mode to better elucidate a broader understanding of the emergent properties of complex bio-systems.

Research Objectives

While pure culture studies using simplified and controlled conditions are necessary to expand our basic understanding of microbial physiology, they are not necessarily relevant to understanding how individual microorganisms function in ecosystems, which are complex networks of interacting microorganisms. The work presented here focuses on the developed anaerobic co-culture biofilm system between the sulfate-reducing bacterium (SRB), *Desulfovibrio vulgaris* Hildenborough, and the archaeal hydrogenotrophic methanogen, *Methanococcus maripaludis* S2. Despite the efforts that have been put forth to study the interactions between SRB and methanogens, the emergent properties of interactive populations in anaerobic biofilms have not been well characterized. The environmentally relevant, genetically tractable, and well-studied *D. vulgaris* and *M. maripaludis* microorganisms provide a model system in which to assess ecological interactions. Further, *D. vulgaris* Hildenborough and *Methanococcus maripaludis* can metabolically pair themselves in what has been previously described as a product inhibition syntrophy (Dean, 1985). This occurs when *D. vulgaris* oxidizes lactate into acetate and H_2, which both can become inhibitory in excess concentrations. The methanogen, *M. maripaludis,* alleviates this burden on the SRB through the pursuit of its own energetic requirements which utilizes the H_2 and some acetate in order to run methanogenesis, which results in CH_4 production. The research goal here was to analyze the dynamic metabolic interactions of this syntrophic mutualism within the interdomain, anaerobic, biofilm in order to determine activity partitioning that may occur.

Previous work established that the syntrophic biofilm created between *D. vulgaris* and *M. maripaludis* enhanced the carrying capacity of the system as defined by mass flux of lactate or CH_4 (See Appendix D and E). Chapter 2 explores these findings and hypothesizes that the stability is due to unique carbon and electron cycling that is facilitated by the proximity of the populations within the biofilm. Furthermore, it was anticipated that there would be unique genetic expression in the biofilm growth mode in addition to expression differences unique to the co-culture environment. A full transcriptomic assessment utilizing RNA-seq on *D. vulgaris* and *M. maripaludis* grown as planktonic monocultures was used to compare expression profiles to that of the co-culture biofilm growth mode. Expression in the co-culture biofilm was also compared to the co-culture in the planktonic state. Additionally, the metabolic profile for each organism was used to create an elementary flux mode model that was used to make predictions about energetic requirements and how this could influence the interactions between the organisms.

The stability of the co-culture biofilm was further investigated in Chapter 3. It was hypothesized that in the presence of a more energetically desirable electron acceptor (*i.e.*, sulfate) that *D. vulgaris* would metabolically disassociate from *M. maripaludis*. Community interactions based upon interspecies hydrogen transfer were challenged in an established biofilm grown in a continuous culture reactor when it was exposed to a sulfate perturbation. Based on the results, further growth studies were conducted using filtered spent media from the organisms grown in planktonic monocultures. The filtrate was tested with various amendments and used as background medium for cross-inoculation growth studies. The results indicate that cell-free spent medium from *M. maripaludis* impacts *D. vulgaris* growth and sulfate-reduction.

Expression data alone are not always representative of actual function, as mRNA and protein expression can be uncorrelated (Binder & Liu, 1998; Bollmann et al., 2005; Morgenroth et al., 2000; Oda et al., 2000; Taniguchi et al., 2010). Therefore, Chapter 4 explores the translational activity for the co-culture biofilm. Deuterated water (^2H_2O) was added to the continuous co-culture biofilm reactor and used to assess activity for *D. vulgaris* and *M. maripaludis* at two developmental stages: the early, or developing, biofilm stage and the late, or steady state, biofilm stage. Newly synthesized proteins for the respective populations in the co-culture biofilm were determined from mass shifts occurring in liquid chromatography mass spectrometry (LC-MS) data. The protein activity results suggested from this analysis were further explored using a new method of Biorthogonal Noncanonical Amino Acid Tagging, or BONCAT (Hatzenpichler et al., 2014; Hatzenpichler & Orphan, 2015).

Chapter 5 explores the effect of sulfoacetate and sulfopyruvate on monoculture planktonic growth of the SRB and methanogen. Results from the previous studies outlined identified candidate metabolites, such as sulfonate compounds and amino acids that could be important for the syntrophic association between *D. vulgaris* and *M.*

maripaludis. Sulfonates are widespread and important contributors to the global sulfur cycle. Most of our knowledge on sulfonates has originated from the study of methanogenesis, specifically coenzyme M (2-mercaptoethanesulfonic acid). Reports have demonstrated the ability of microorganisms (e.g., *Cupriavidus necator* H16, *Rhodopseudomonas palustris*, *Desulfovibrio* IC1) to utilize sulfonates as terminal electron acceptors, sole carbon sources, or both (Denger et al., 2004; Lie et al., 1996; Weinitschke et al., 2007). The potential for sulfonate compounds to be used in this manner became of particular interest due to the implication that it could have for syntrophic interactions within this limited co-culture system and was therefore characterized.

Further emphasis on the importance of linking the distinction between genetic capacity and observed function was described for an environmental isolate in Appendix A. After a lactate amendment to stimulate sulfate-reducing bacteria in a chromium contaminated site was made, *Pelosinus fermentans* JBW45, was recovered. Initial analysis of functional annotations in the genome (See Appendix B and C) revealed unexpected capacities for heavy metal tolerance. Literature reviews revealed that other stimulated contaminated sites became enriched in *Pelosinus* spp. populations as well, which warranted further characterization. The subsequent physiological assessment is outlined along with the unexpected findings.

REFERENCES CITED

Archetti, M., Scheuring, I., Hoffman, M., Frederickson, M. E., Pierce, N. E., & Yu, D. W. (2011). Economic game theory for mutualism and cooperation. *Ecology Letters*, *14*(12), 1300–1312. http://doi.org/10.1111/j.1461-0248.2011.01697.x

Bassler, B. L. (1999). How bacteria talk to each other: regulation of gene expression by quorum sensing. *Current Opinion in Microbiology*, *2*(2), 582–587.

Beech, I. B., Sunner, J. A., & Hiraoka, K. (2005). Microbe-surface interactions in biofouling and biocorrosion processes. *International Microbiology*, *8*(3), 157–68. http://doi.org/16200494

Bernstein, H. C., Paulson, S. D., & Carlson, R. P. (2012). Synthetic Escherichia coli consortia engineered for syntrophy demonstrate enhanced biomass productivity. *Journal of Biotechnology*, *157*(1), 159–166. http://doi.org/10.1016/j.jbiotec.2011.10.001

Binder, B. J., & Liu, Y. C. (1998). Growth rate regulation of rRNA content of a marine Synechococcus (Cyanobacterium) strain. *Applied and Environmental Microbiology*, *64*(9), 3346–3351.

Bollmann, A., Schmidt, I., Saunders, A. M., & Nicolaisen, M. H. (2005). Influence of Starvation on Potential Ammonia-Oxidizing Activity and amoA mRNA Levels of Nitrosospira briensis. *Applied and Environmental Microbiology*, *71*(3), 1276–1282. http://doi.org/10.1128/AEM.71.3.1276

Braissant, O., Decho, A. W., Dupraz, C., Glunk, C., Przekop, K. M., & Visscher, P. T. (2007). Exopolymeric substances of sulfate-reducing bacteria: Interactions with calcium at alkaline pH and implication for formation of carbonate minerals. *Geobiology*, *5*(4), 401–411. http://doi.org/10.1111/j.1472-4669.2007.00117.x

Branda, S. S., Vik, S., Friedman, L., & Kolter, R. (2005). Biofilms: the matrix revisited. *Trends in Microbiology*, *13*(1), 20–6. http://doi.org/10.1016/j.tim.2004.11.006

Brenner, K., & Arnold, F. H. (2011). Self-Organization, Layered Structure, and Aggregation Enhance Persistence of a Synthetic Biofilm Consortium. *PLoS ONE*, *6*(2), e16791. http://doi.org/10.1371/journal.pone.0016791

Brileya, K. A., Camilleri, L. B., Zane, G. M., Wall, J. D., & Fields, M. W. (2014). Biofilm growth mode promotes maximum carrying capacity and community stability during product inhibition syntrophy. *Frontiers in Microbiology*, *5*(12), 693. http://doi.org/10.3389/fmicb.2014.00693

Brileya, K. A., Connolly, J. M., Downey, C., Gerlach, R., & Fields, M. W. (2013). Taxis toward hydrogen gas by Methanococcus maripaludis. *Scientific Reports*, *3*, 3140. http://doi.org/10.1038/srep03140

Bryant, M. P., Campbell, L. L., Reddy, C. A., & Crabill, M. R. (1977). Growth of Desulfovibrio in lactate or ethanol media low in sulfate in association with H2-utilizing methanogenic bacteria. *Applied and Environmental Microbiology*, *33*(5), 1162–9. Retrieved from http://www.ncbi.nlm.nih.gov/pubmed/879775

Clark, M. E., He, Q., He, Z., Huang, K. H., Alm, E. J., Wan, X.-F., … Fields, M. W. (2006). Temporal transcriptomic analysis as Desulfovibrio vulgaris Hildenborough transitions into stationary phase during electron donor depletion. *Applied and Environmental Microbiology*, *72*(8), 5578–88. http://doi.org/10.1128/AEM.00284-06

Clark, M. E., He, Z., Redding, A. M., Joachimiak, M. P., Keasling, J. D., Zhou, J. Z., … Fields, M. W. (2012). Transcriptomic and proteomic analyses of Desulfovibrio vulgaris biofilms: carbon and energy flow contribute to the distinct biofilm growth state. *BMC Genomics*, *13*(1), 138. http://doi.org/10.1186/1471-2164-13-138

Conway de Macario, E., & Macario, A. J. L. (2009). Methanogenic archaea in health and disease: A novel paradigm of microbial pathogenesis. *International Journal of Medical Microbiology*, *299*(2), 99–108. http://doi.org/10.1016/j.ijmm.2008.06.011

Corral-Lugo, A., Daddaoua, A., Ortega, A., Espinosa-Urgel, M., & Krell, T. (2016). So different and still so similar: The plant compound rosmarinic acid mimics bacterial homoserine lactone quorum sensing signals. *Communicative and Integrative Biology*, *9*(2), 1–4. http://doi.org/10.1080/19420889.2016.1156832

Costerton, J. W. (1999). Introduction to biofilm. *International Journal of Antimicrobial Agents*, *11*, 217–221.

Costerton, J. W., Cheng, K. J., Geesey, G. G., Ladd, T. I., Nickel, J. C., Dasgupta, M., & Marrie, T. J. (1987). Bacterial Biofilms in Nature and Disease. *Ann. Rev. Microbiol.*, *41*, 435–464. http://doi.org/10.1146/annurev.mi.41.100187.002251

Costerton, W. J., & Wilson, M. (2004). Introducing Biofilms. *Biofilms*, *1*(1), 1–4. http://doi.org/10.1017/S1479050504001164

Dean, A. M. (1985). The dynamics of microbial commensalisms and mutualisms. In D. H. Boucher (Ed.), *The Biology of Mutualism* (pp. 270–300). Oxford: Oxford University Press. Retrieved from https://books.google.com/books?hl=en&lr=&id=dWuQS_3F2P0C&oi=fnd&pg=PA270&ots=_vLqPPvfaW&sig=kQJWc5rcE0FIzy8fpfml3ZWn3-k#v=onepage&q&f=false

Decho, A. W. (2000). Exopolymer Microdomains as a Structuring Agent for Heterogeneity Within Microbial Biofilms. In R. E. Riding & S. M. Awramik (Eds.), *Microbial Sediments* (pp. 9–15). Berlin, Heidelberg: Springer-Verlag Berlin Heidelberg. http://doi.org/10.1007/978-3-662-04036-2_2

Decho, A. W., Norman, R. S., & Visscher, P. T. (2010). Quorum sensing in natural environments: emerging views from microbial mats. *Trends in Microbiology*, *18*(2), 73–80. http://doi.org/10.1016/j.tim.2009.12.008

Denger, K., Weinitschke, S., Hollemeyer, K., & Cook, A. M. (2004). Sulfoacetate generated by Rhodopseudomonas palustris from taurine. *Archives of Microbiology*, *182*(2–3), 254–8. http://doi.org/10.1007/s00203-004-0678-0

Dunne, W. M. J. (2002). aBacterial adhesion: seen any good biofilms lately? *Clinical Microbiology Reviews*, *15*(2), 155–166. http://doi.org/10.1128/CMR.15.2.155

Eberhard, A., Burlingame, A. L., Eberhard, C., Kenyon, G. L., Nealson, K. H., & Oppenheimer, N. J. (1981). Structural Identification of Autoinducer of Photobacterium fischeri Luciferase. *Biochemistry*, *20*(9), 2444–2449. http://doi.org/10.1021/bi00512a013

Engebrecht, J., Nealson, K., & Silverman, M. (1983). Bacterial Bioluminescence: Isolation and Genetic Analysis of Functions from Vibrio fischeri. *Cell*, *32*(3), 773–781. http://doi.org/10.1016/0092-8674(83)90063-6

Faust, K., & Raes, J. (2012). Microbial interactions: from networks to models. *Nature Reviews Microbiology*, *10*(8), 538–550. http://doi.org/10.1038/nrmicro2832

Ferrera, I., Longhorn, S., Banta, A. B., Liu, Y., Preston, D., & Reysenbach, A.-L. (2007). Diversity of 16S rRNA gene, ITS region and aclB gene of the Aquificales. *Extremophiles*, *11*(1), 57–64. http://doi.org/10.1007/s00792-006-0009-2

Flemming, H. C. (1996). Economical and Technical Overview. In E. Heitz, H. C. Flemming, & W. Sand (Eds.), *Microbially Influenced Corrosion of Materials* (pp. 6–14). New York: Springer-Verlag.

Flemming, H. C., & Wingender, J. (2010). The biofilm matrix. *Nature Reviews. Microbiology*, *8*(9), 623–33. http://doi.org/10.1038/nrmicro2415

Fondi, M., & Liò, P. (2015). Multi -omics and metabolic modelling pipelines: Challenges and tools for systems microbiology. *Microbiological Research*, *171*, 52–64. http://doi.org/10.1016/j.micres.2015.01.003

Fuqua, W. C., Winans, S. C., & Greenberg, E. P. (1994). Quorum Sensing in Bacteria: the LuxR-LuxI Family of Cell Density-Responsive Transcriptional Regulators. *Journal of Bacteriology*, *176*(2), 269–275. http://doi.org/10.1128/jb.176.2.269-

Geesey, G. G., Mutch, R., Costerton, J. W., & Green, R. B. (1978). Sessile Bacteria: An Important Component of the Microbial Population in Small Mountain Streams. *Limnology and Oceanography*, *23*(6), 1214–1223. Retrieved from https://www.jstor.org/stable/2835675

Gross, R., Hauer, B., Otto, K., & Schmid, A. (2007). Microbial biofilms: New catalysts for maximizing productivity of long-term biotransformations. *Biotechnology and Bioengineering*, *98*(6), 1123–1134. http://doi.org/10.1002/bit.21547

Gutleben, J., Chaib De Mares, M., van Elsas, J. D., Smidt, H., Overmann, J., & Sipkema, D. (2018). The multi-omics promise in context: from sequence to microbial isolate. *Critical Reviews in Microbiology*, *44*(2), 212–229. http://doi.org/10.1080/1040841X.2017.1332003

Hall-Stoodley, L., Costerton, J. W., & Stoodley, P. (2004). Bacterial biofilms: from the natural environment to infectious diseases. *Nature Reviews Microbiology*, *2*(2), 95–108. http://doi.org/10.1038/nrmicro821

Hamilton, W. A. (2003). Microbially Influenced Corrosion as a Model System for the Study of Metal Microbe Interactions: A Unifying Electron Transfer Hypothesis. *Biofouling*, *19*(1), 65–76. http://doi.org/10.1080/0892701021000041078

Hammerstein, P., & Selten, R. (1994). Game theory and evolutionary biology. In R. J. Aumann & S. Hart (Eds.), *Handbook of Game Theory with Economic Applications* (Vol. 2, pp. 929–993). Elsevier Science B.B. http://doi.org/10.1016/S1574-0005(05)80060-8

Hansen, S. K., Rainey, P. B., Haagensen, J. A. J., & Molin, S. (2007). Evolution of species interactions in a biofilm community. *Nature*, *445*(7127), 533–536. http://doi.org/10.1038/nature05514

Hatchikian, C. E. (1975). Purification and Properties of Thiosulfate Reductase from Desulfovibrio gigas. *Archives of Microbiology*, (105), 249–256. http://doi.org/10.1093/oxfordjournals.jbchem.a135144

Hatzenpichler, R., & Orphan, V. J. (2015). Detection of Protein-Synthesizing Microorganisms in the Environment via Bioorthogonal Noncanonical Amino Acid Tagging (BONCAT). In T. McGenity, K. Timmis, & B. Nogales (Eds.), *Hydrocarbon and Lipid Microbiology Protocols* (Springer P, pp. 145–157). Springer Berlin Heidelberg. http://doi.org/https://doi.org/10.1007/8623_2015_61

Hatzenpichler, R., Scheller, S., Tavormina, P. L., Babin, B. M., Tirrell, D. a., & Orphan, V. J. (2014). In situ visualization of newly synthesized proteins in environmental microbes using amino acid tagging and click chemistry. *Environmental Microbiology*, *16*(8), 2568–2590. http://doi.org/10.1111/1462-2920.12436

Heidelberg, J. F., Seshadri, R., Haveman, S. a, Hemme, C. L., Paulsen, I. T., Kolonay, J. F., … Fraser, C. M. (2004). The genome sequence of the anaerobic, sulfate-reducing bacterium Desulfovibrio vulgaris Hildenborough. *Nature Biotechnology*, *22*(5), 554–559. http://doi.org/10.1038/nbt959

Holman, H.-Y. N., Wozei, E., Lin, Z., Comolli, L. R., Ball, D. A., Borglin, S., … Downing, K. H. (2009). Real-time molecular monitoring of chemical environment in obligate anaerobes during oxygen adaptive response. *Proceedings of the National Academy of Sciences*, *106*(31), 12599–12604. http://doi.org/10.1073/pnas.0902070106

Hooper, S. L., & Burstein, H. J. (2014). Minimization of extracellular space as a driving force in prokaryote association and the origin of eukaryotes. *Biology Direct*, *9*(1), 24. http://doi.org/10.1186/1745-6150-9-24

Jarrell, K. F., Walters, A. D., Bochiwal, C., Borgia, J. M., Dickinson, T., & Chong, J. P. J. (2011). Major players on the microbial stage: why archaea are important. *Microbiology*, *157*(4), 919–936. http://doi.org/10.1099/mic.0.047837-0

Ji, G., Beavis, R., & Novick, R. P. (1997). Bacterial Interference Caused by Autoinducing Peptide Variants. *Science*, *276*(5321), 2027–2030. Retrieved from https://www.jstor.org/stable/2892976

Kato, S., & Watanabe, K. (2010). Ecological and Evolutionary Interactions in Syntrophic Methanogenic Consortia. *Microbes and Environments*, *25*(3), 145–151. http://doi.org/10.1264/jsme2.ME10122

Keller, L., & Surette, M. G. (2006). Communication in bacteria: An ecological and evolutionary perspective. *Nature Reviews Microbiology*, *4*(4), 249–258. http://doi.org/10.1038/nrmicro1383

Kolter, R. (2005). Surfacing views of biofilm biology. *Trends in Microbiology*, *13*(1), 1–2. http://doi.org/10.1016/j.tim.2004.11.003

Konhauser, K. O. (2006). *Introduction to Geomicrobiology* (illustrate, Vol. 10). Wiley.

Kreft, J.-U., Hartmann, A., Müller, J., Kuttler, C., Rothballer, M., & Hense, B. A. (2007). aDoes efficiency sensing unify diffusion and quorum sensing? *Nature Reviews Microbiology*, *5*(3), 230–239. http://doi.org/10.1038/nrmicro1600

Kurczy, M. E., Zhu, Z.-J., Ivanisevic, J., Schuyler, A. M., Lalwani, K., Santidrian, A. F., … Siuzdak, G. (2015). Comprehensive bioimaging with fluorinated nanoparticles using breathable liquids. *Nature Communications*, *6*(1), 5998. http://doi.org/10.1038/ncomms6998

Lawrence, J. R., Swerhone, G. D. W., Kuhlicke, U., & Neu, T. R. (2007). In situ evidence for microdomains in the polymer matrix of bacterial microcolonies. *Canadian Journal of Microbiology*, *53*(3), 450–458. http://doi.org/10.1139/W06-146

Leloup, J., Fossing, H., Kohls, K., Holmkvist, L., Borowski, C., & Jørgensen, B. B. (2009). Sulfate-reducing bacteria in marine sediment (Aarhus Bay, Denmark): abundance and diversity related to geochemical zonation. *Environmental Microbiology*, *11*(5), 1278–1291. http://doi.org/10.1111/j.1462-2920.2008.01855.x

Lie, T. J., Pitta, T., Leadbetter, E. R., Godchaux, W., & Leadbetter, J. R. (1996). Sulfonates: novel electron acceptors in anaerobic respiration. *Archives of Microbiology*, *166*(3), 204–10. http://doi.org/10.1007/s002030050376

Little, B. J., & Lee, J. S. (2007). Microbiologically Influenced Corrosion. In R. W. Revie (Ed.), *Wiley Series in Corrosion*. Hoboken, New Jersey: John Wiley & Sons, Inc. Retrieved from cfm.mines.edu/research.html

Lohner, S. T., Deutzmann, J. S., Logan, B. E., Leigh, J., & Spormann, A. M. (2014). Hydrogenase-independent uptake and metabolism of electrons by the archaeon Methanococcus maripaludis. *The ISME Journal*, *8*(8), 1673–1681. http://doi.org/10.1038/ismej.2014.82

Loverdo, C., Bénichou, O., Moreau, M., & Voituriez, R. (2008). Enhanced reaction kinetics in biological cells. *Nature Physics*, *4*(2), 134–137. http://doi.org/10.1038/nphys830

Lupton, F. S., Conrad, R., & Zeikus, J. G. (1984). Physiological Function of Hydrogen Metabolism During Growth of Sulfidogenic Bacteria on Organic Substrates. *Journal of Bacteriology*, *159*(3), 843–849.

Lyon, G. J., Wright, J. S., Muir, T. W., & Novick, R. P. (2002). Key Determinants of Receptor Activation in the agr Autoinducing Peptides of Staphylococcus aureus †. *Biochemistry*, *41*(31), 10095–10104. http://doi.org/10.1021/bi026049u

Matz, C. (2011). Competition, Communication, Cooperation: Molecular Crosstalk in Multi-species Biofilms. In H. C. Flemming, J. Wingender, & U. Szewzyk (Eds.), *Biofilm Highlights* (Springer S, Vol. 5, pp. 29–40). Springer Berlin Heidelberg. http://doi.org/10.1007/978-3-642-19940-0

Mayville, P., Ji, G., Beavis, R., Yang, H., Goger, M., Novick, R. P., & Muir, T. W. (1999). Structure-activity analysis of synthetic autoinducing thiolactone peptides from Staphylococcus aureus responsible for virulence. *Proceedings of the National Academy of Sciences of the United States of America*, *96*(4), 1218–23. Retrieved from http://www.pubmedcentral.nih.gov/articlerender.fcgi?artid=15443&tool=pmcentrez&rendertype=abstract

McInerney, M. J., Sieber, J. R., & Gunsalus, R. P. (2009). Syntrophy in anaerobic global carbon cycles. *Current Opinion in Biotechnology*, *20*(6), 623–632. http://doi.org/10.1016/j.copbio.2009.10.001

Michel, C., Brugna, M., Aubert, C., Bernadac, A., & Bruschi, M. (2001). Enzymatic reduction of chromate: comparative studies using sulfate-reducing bacteria. *Applied Microbiology and Biotechnology*, *55*(1), 95–100. http://doi.org/10.1007/s002530000467

Momeni, B., Brileya, K. A., Fields, M. W., & Shou, W. (2013). Strong inter-population cooperation leads to partner intermixing in microbial communities. *ELife*, *2*, e00230. http://doi.org/10.7554/eLife.00230

Morgenroth, E., Obermayer, A., Arnold, E., Brühl, A., Wagner, M., & Wilderer, P. A. (2000). Effect of long-term idle periods on the performance of sequencing batch reactors. *Water Science and Technology*, *41*(1), 105–113. http://doi.org/10.2166/wst.2000.0018

Nadell, C. D., Xavier, J. B., Levin, S. A., & Foster, K. R. (2008). The evolution of quorum sensing in bacterial biofilms. *PLoS Biology*, *6*(1), e14. http://doi.org/10.1371/journal.pbio.0060014

Nealson, K. H., Platt, T., & Hastings, J. W. (1970). Cellular control of the synthesis and activity of the bacterial luminescent system. *Journal of Bacteriology*, *104*(1), 313–322.

Nielsen, A. T., Tolker-Nielsen, T., Barken, K. B., & Molin, S. (2000). Role of commensal relationships on the spatial structure of a surface-attached microbial consortium. *Environmental Microbiology*, *2*(1), 59–68. http://doi.org/10.1046/j.1462-2920.2000.00084.x

Oda, Y., Slagman, S. J., Meijer, W. G., Forney, L. J., & Gottschal, J. C. (2000). Influence of growth rate and starvation on fluorescent in situ hybridization of Rhodopseudomonas palustris. *FEMS Microbiology Ecology*, *32*(3), 205–213. http://doi.org/10.1016/S0168-6496(00)00029-5

Odom, J. M., & Peck, H. D. (1981). Hydrogen cycling as a general mechanism for energy coupling in the sulfate-reducing bacteria, Desulfovibrio sp. *FEMS Microbiology Letters*, *12*, 47–50.

Or, D., Smets, B. F., Wraith, J. M., Dechesne, A., & Friedman, S. P. (2007). aPhysical constraints affecting bacterial habitats and activity in unsaturated porous media – a review. *Advances in Water Resources*, *30*(6–7), 1505–1527. http://doi.org/10.1016/j.advwatres.2006.05.025

Payne, D. E., & Boles, B. R. (2016). Emerging interactions between matrix components during biofilm development. *Current Genetics*, *62*(1), 137–141. http://doi.org/10.1007/s00294-015-0527-5

Payne, R. B., Gentry, D. M., Rapp-Giles, B. J., Casalot, L., & Wall, J. D. (2002). Uranium Reduction by Desulfovibrio desulfuricans Strain G20 and a Cytochrome c3 Mutant. *Applied and Environmental Microbiology*, *68*(6), 3129–3132. http://doi.org/10.1128/AEM.68.6.3129-3132.2002

Peck, H. D. (1960). Evidence for oxidative phosphorylation during the reduction of sulfate with hydrogen by Desulfovibrio desulfuricans. *The Journal of Biological Chemistry*, *235*(9), 2734–2738.

Petersen, J. M., Zielinski, F. U., Pape, T., Seifert, R., Moraru, C., Amann, R., … Dubilier, N. (2011). Hydrogen is an energy source for hydrothermal vent symbioses. *Nature*, *476*(7359), 176–180. http://doi.org/10.1038/nature10325

Plugge, C. M., Zhang, W., Scholten, J. C. M., & Stams, A. J. M. (2011). Metabolic Flexibility of Sulfate-Reducing Bacteria. *Frontiers in Microbiology*, *2*(5), 81. http://doi.org/10.3389/fmicb.2011.00081

Postgate, J. R. (1979). *The Sulphate-Reducing Bacteria*. Cambridge University Press.

Prosser, J. I., Bohannan, B. J. M., Curtis, T. P., Ellis, R. J., Firestone, M. K., Freckleton, R. P., … Young, J. P. W. (2007). The role of ecological theory in microbial ecology. *Nature Reviews Microbiology*, *5*(5), 384–392. http://doi.org/10.1038/nrmicro1643

Rabus, R., Venceslau, S. S., Wohlbrand, L., Voordouw, G., & Wall, J. D. (2015). A Post-Genomic View of the Ecophysiology, Catabolism and Biotechnological Relevance of Sulphate-Reducing Prokaryotes. In R. K. Poole (Ed.), *Advances in Microbial Physiology* (pp. 55–321). Elsevier. Retrieved from https://doi.org/10.1016/bs.ampbs.2015.05.002

Raskin, L., Rittmann, B. E., & Stahl, D. A. (1996). Competition and coexistence of sulfate-reducing and methanogenic populations in anaerobic biofilms. *Applied and Environmental Microbiology*, *62*(10), 3847–57. Retrieved from http://www.pubmedcentral.nih.gov/articlerender.fcgi?artid=1388966&tool=pmcentrez&rendertype=abstract

Reysenbach, A. L., Longnecker, K., & Kirshtein, J. (2000). Novel bacterial and archaeal lineages from an in situ growth chamber deployed at a Mid-Atlantic Ridge hydrothermal vent. *Applied and Environmental Microbiology*, *66*(9), 3798–806. http://doi.org/10.1128/AEM.66.9.3798-3806.2000.Updated

Schooling, S. R., & Beveridge, T. J. (2006). Membrane Vesicles: an Overlooked Component of the Matrices of Biofilms. *Journal of Bacteriology*, *188*(16), 5945–7

Shen, Y., & Buick, R. (2004). The antiquity of microbial sulfate reduction, *64*, 243–272. http://doi.org/10.1016/S0012-8252(03)00054-0

Shirtliff, M. E., Mader, J. T., & Camper, A. K. (2002). Molecular interactions in biofilms. *Chemistry and Biology*, *9*(8), 859–871.

Stahl, D. A., Hillesland, K. L., & Harcombe, W. (2011). Measuring the Costs of Microbial Mutualism. *Microbe Magazine*, *6*(10), 427–434. http://doi.org/10.1128/microbe.6.427.1

Stams, A. J. M., & Plugge, C. M. (2009). Electron transfer in syntrophic communities of anaerobic bacteria and archaea. *Nature Reviews Microbiology*, *7*(8), 568–577. http://doi.org/10.1038/nrmicro2166

Stewart, P. S., & Costerton, J. W. (2001). Antibiotic resistance of bacteria in biofilms. *Lancet*, *358*(9276), 135–8. Retrieved from http://www.ncbi.nlm.nih.gov/pubmed/11463434

Stewart, P. S., & Franklin, M. J. (2008). Physiological heterogeneity in biofilms. *Nature Reviews. Microbiology*, *6*(3), 199–210. http://doi.org/10.1038/nrmicro1838

Stylo, M., Neubert, N., Roebbert, Y., Weyer, S., & Bernier-Latmani, R. (2015). Mechanism of Uranium Reduction and Immobilization in Desulfovibrio vulgaris Biofilms. *Environmental Science & Technology*, *49*(17), 10553–10561. http://doi.org/10.1021/acs.est.5b01769

Taniguchi, Y., Choi, P. J., Li, G., Chen, H., Babu, M., Hearn, J., … Xie, X. S. (2010). Quantifying E. coli Proteome and Transcriptome with Single-Molecule Sensitivity in Single Cells. *Most*, *329*(5991), 533–538. http://doi.org/10.1126/science.1188308.

Thauer, R. K. (2012). aThe Wolfe cycle comes full circle. *Proceedings of the National Academy of Sciences*, *109*(38), 15084–15085. http://doi.org/10.1073/pnas.1213193109

Thauer, R. K., Kaster, A.-K., Seedorf, H., Buckel, W., & Hedderich, R. (2008). Methanogenic archaea: ecologically relevant differences in energy conservation. *Nature Reviews Microbiology*, *6*(8), 579–591. http://doi.org/10.1038/nrmicro1931

Tomasz, A. (1965). Control of the competent state in pneumococcus by a hormone-like cell product: An example for a new type of regulatory mechanism in bacteria. *Nature*, *208*(5006), 155–159. http://doi.org/10.1038/208155a0

Truper, H. (1984). Phototrophic bacteria and their sulfur metabolism. In A. Müller & B. Krebs (Eds.), *Sulfur: its significance for chemistry, for the geo-, bio- and cosmosphere, and technology* (Vol. 5, pp. 351–365). Amsterdam: Elsevier Science.

Ueno, Y., Yamada, K., Yoshida, N., Maruyama, S., & Isozaki, Y. (2006). Evidence from fluid inclusions for microbial methanogenesis in the early Archaean era. *Nature, 440*(7083), 516–519. http://doi.org/10.1038/nature04584

Walker, C. B., He, Z., Yang, Z. K., Ringbauer, J. a, He, Q., Zhou, J., … Stahl, D. A. (2009). The electron transfer system of syntrophically grown Desulfovibrio vulgaris. *Journal of Bacteriology, 191*(18), 5793–801. http://doi.org/10.1128/JB.00356-09

Weinitschke, S., Denger, K., Cook, A. M., & Smits, T. H. M. (2007). The DUF81 protein TauE in Cupriavidus necator H16, a sulfite exporter in the metabolism of C2 sulfonates. *Microbiology, 153*(9), 3055–3060. http://doi.org/10.1099/mic.0.2007/009845-0

Whiteley, M., Diggle, S. P., & Greenberg, E. P. (2017). Progress in and promise of bacterial quorum sensing research. *Nature*, *551*(7680), 313–320. http://doi.org/10.1038/nature24624

Whiteley, M., Lee, K. M., & Greenberg, E. P. (1999). Identification of genes controlled by quorum sensing in Pseudomonas aeruginosa. *Proceedings of the National Academy of Sciences*, *96*(24), 13904–13909. Retrieved from http://www.pnas.org/content/96/24/13904.full%5Cnpapers3://publication/uuid/831AA5C7-E5F1-44A1-914F-4B3548AC317E

Widdel, F. (1988). Microbiology and ecology of sulphate- and sulfur-reducing bacteria. In A. J. B. Zehnder (Ed.), *Biology of Anaerobic Microorganisms* (99th ed., pp. 469–585). New York: Wiley.

Wrede, C., Dreier, A., Kokoschka, S., & Hoppert, M. (2012). Archaea in Symbioses. *Archaea*, *2012*, 1–11. http://doi.org/10.1155/2012/596846

Yvon-Durocher, G., Allen, A. P., Bastviken, D., Conrad, R., Gudasz, C., St-Pierre, A., … del Giorgio, P. A. (2014). Methane fluxes show consistent temperature dependence across microbial to ecosystem scales. *Nature, 507*(7493), 488–491. http://doi.org/10.1038/nature13164

Zhang, W., Li, F., & Nie, L. (2010). Integrating multiple ‘ omics ’ analysis for microbial biology : application and methodologies. *Microbiology*, *156*, 287–301. http://doi.org/10.1099/mic.0.034793-0

CHAPTER TWO

DIFFERENTIAL GENE EXPRESSION OF A BACTERIAL-ARCHAEAL INTERDOMAIN BIOFILM PRODUCING METHANE

Contribution of Authors and Co-Authors

Manuscript in Chapter 2

Author: Laura B. Camilleri

Contributions: Developed experimental design, performed experiments, analyzed data, wrote and revised the manuscript.

Co-Author: Kristopher A. Hunt

Contributions: Performed stoichiometric modeling analysis.

Co-Author: Aurélien Mazurie

Contributions: Performed transcriptome assembly.

Co-Author: Jennifer Kuehl

Contributions: Constructed Illumina library and performed sequencing.

Co-Author: Alex Michaud

Contributions: Contributed data for stoichiometric model.

Co-Author: James Connolly

Contributions: Contributed data for stoichiometric model.

Co-Author: Egan Lohman

Contributions: Contributed data for stoichiometric model.

Co-Author: Zack Miller

Contributions: Contributed data for stoichiometric model.

Co-Author: Adam M. Deutschbauer

Contributions: P.I. for sequencing.

Co-Author: Matthew W. Fields

Contributions: Developed experimental design, analyzed data, wrote and revised the manuscript.

Manuscript Information

Laura B. Camilleri, Kristopher A. Hunt, Aurélien Mazurie, Jennifer Kuehl, Alex Michaud, James Connolly, Egan Lohman, Zack Miller, Adam M. Deutschbauer, and Matthew W. Fields

Biofilms

Status of Manuscript:
__x_ Prepared for submission to a peer-reviewed journal
____ Officially submitted to a peer-reviewed journal
____ Accepted by a peer-reviewed journal
____ Published in a peer-reviewed journal

ABSTRACT

Symbiosis is widespread throughout the biosphere with well-studied examples in and across all three domains of life. The syntrophy between sulfate-reducing bacteria (SRB) and methanogenic archaea is of interest because both guilds play crucial roles in many different anaerobic environments. *Methanococcus maripaludis* S2 and *Desulfovibrio vulgaris* Hildenborough can form a syntrophic mutualism when grown in the absence of sulfate. In order to better understand the interactions between *M. maripaludis* and *D. vulgaris*, RNA-Seq was used to create a transcriptomic profile of the co-culture biofilm as compared to the planktonic mono- and co- culture states to demonstrate unique expression and behavior in the biofilm state. Transcriptomic analysis indicated that the most differential expression for co-culture biofilm compared to planktonic monocultures occurred in *M. maripaludis*. The results demonstrated that key genes known to be involved in methanogenesis were down-expressed for *M. maripaludis* and electron transfer related genes were down-expressed for *D. vulgaris* Hildenborough. Many of the up-expressed genes for both populations included those encoding for hypothetical proteins, but also included genes known to encode for cell surface modifications, communication via small metabolites, N-cycling, and metal homeostasis. Insight into the interactions of this anaerobic syntrophy were also gained using stoichiometric modeling. Predictions about amino acid exchange in the two populations identified alanine, cysteine, glycine, and serine as integral to decreasing the hydrogen or carbon dioxide requirement in *M. maripaludis*. These results highlight unique gene expression and predicted metabolite sharing for the interdomain biofilm and indicate that the biofilm growth mode is both phenotypically and physiologically unique, most likely due to mass transport considerations and electrogenic flux balance that may be alleviated by amino acid sharing.

INTRODUCTION

Biofilms are an ancient adaptation as well as the predominant mode of growth for many microorganisms across a variety of natural environments (Flemming & Wuertz, 2019). Biofilms contribute to microbial tolerance of many physically dynamic habitats where fluxes in water, nutrients, temperature, pH, and osmolarity can create challenges for microorganisms to survive and thrive especially when limited nutrient availability can result in decreased microbial activity and/or niche space (Or et al., 2007). Therefore, biofilm physiology is important to explore in addition to the typical studies conducted on the more readily cultivated planktonic cells (Costerton, 2007; Dunne, 2002; Kolter, 2005; Wyndham & Costerton, 1981). Moreover, biofilms facilitate the development of complex interactions between community members and enhance metabolism by the localization of cells in close proximity such that cooperative interactions can be fostered, or competitive interactions minimized (Burmølle et al., 2014; Carlson et al., 2018) . Previous work has shown that the structure of a mixed biofilm community is dependent upon cooperative or competitive interactions and that the degree of intermixing of a two-member community is indicative of ecological interactions (*i.e*., cooperation/competition) (Momeni et al., 2013).

Desulfovibrio vulgaris Hildenborough (DvH) is a biofilm-forming, sulfate-reducing bacterium commonly grown with lactate and sulfate that results in oxidation to acetate and the reduction to sulfide (with transient H_2 production) (Clark et al., 2007; Odom & Peck, 1981; Pankhania et al., 1988; Peck, 1960; Voordouw, 2002).

Methanococcus maripaludis (Mmp) is a rapidly growing archaeal methanogen that uses H_2 as an electron donor to reduce carbon dioxide to methane by methanogenesis, which is possibly one of the oldest microbial metabolisms (Thauer, 2012; Ueno et al., 2006). The association of *Desulfovibrio vulgaris* Hildenborough with *Methanococcus maripaludis* under low sulfate conditions has been described as a product inhibition syntrophy due to the inhibitory effect excessive H_2 gas production has on *Desulfovibrio* during lactate oxidation in the absence of sulfate (Dean, 1985). The growth of these two species in the absence of sulfate results in a mutualistic, biofilm-forming, co-culture that self-assembles, but most of the work on the mutualism between *Desulfovibrio* and *Methanococcus* has been studied under planktonic conditions (Bryant et al., 1977; McInerney & Bryant, 1981; Plugge et al., 2010; Walker et al., 2009). Despite being model organisms that have been studied for over 50 years, relatively little is known about specific mechanisms of syntrophic interactions or how structure relates to function in terms of biofilm. With the recent demonstration of structural changes in the co-culture biofilm and the increased efficiency in terms of flux to biomass for a *Desulfovibrio*/*Methanococcus* biofilm compared to planktonic growth (Brileya et al., 2014), we hypothesized that the co-culture biofilm exhibited distinctly different metabolisms as compared to the planktonic physiology with altered carbon flux that could be identified through transcriptomic and metabolic model analyses to provide insight into potential investment strategies to gain benefit from metabolic interactions in a bacterial-archaeal biofilm.

MATERIALS AND METHODS

Culture Conditions

Desulfovibrio vulgaris Hildenborough and *Methanococcus maripaludis* S2 were anaerobically cultured in co-culture medium (CCM) with 80% N_2: 20% CO_2 sparged headspace at 30°C and shaking at 125 rpm (Walker et al., 2009). Batch, planktonic, monocultures of *D. vulgaris* Hildenborough were grown in serum bottles with the addition of 30 mM sulfate. Batch, planktonic, monocultures of *M. maripaludis* were grown in serum bottles and amended with 30 mM acetate instead of lactate, along with an over pressurization of 80% H_2: 20% CO_2 gas to 200 kPa. Co-culture biofilm was propagated on glass slides held in a modified, continuously stirred, 1 L CDC reactor as previously described (Brileya et al., 2014; Clark et al., 2006, 2012).

Sample Collection

Triplicates of each culture were harvested immediately upon reaching stationary phase, or steady state for biofilm samples based upon lactate consumption and methane production (~300 h; ~8.5 generations in planktonic phase). A 450 mL ice-water bath was made with 2 g of potassium chloride added. Sterile, coiled, stainless steel lines (4-5 mm) were submerged in the potassium chloride slurry and attached to a variable flow peristaltic pump (Fisher Scientific). A stand and clamp were used to hold the serum bottle containing the planktonic cultures upside down. A sterile filter and needle were attached to the nitrogen gas line then inserted into the bottle, while the sterile line connected to the pump was inserted. The pump was turned on slowly and allowed to flow into a sterile 50 mL conical on ice until the line was purged. The samples were immediately centrifuged at 10,000 x *g* for 10 minutes at 4°C. The supernatant was removed and the pellets were flash frozen using liquid nitrogen. For the co-culture biofilm, the replicate samples were scraped off the glass slides into sterile microcentrifuge tubes on ice under a stream of filter sterilized nitrogen gas before being centrifuged and frozen in liquid nitrogen. All samples were then stored at -80°C.

Total RNA Extraction

RNA was extracted from the triplicate samples using the RNeasy® Mini Kit (Qiagen, Valencia, CA, USA) as per manufacturer instructions with the optional DNase treatment performed. Biofilm was homogenized by passing it through a sterile, RNase free, 23-gauge needle. To increase RNA yield, 1X TE buffer was added to each RNA sample. RNA quantification was done using the Qubit™ Quant-iT™ RNA assay for the Qubit® fluorometer (Invitrogen, Carlsbad, CA, USA).

Illumina Library Construction and Sequencing

Total RNA samples (5 µg) were enriched for mRNA using the Ribo-Zero Metabacteria Kit (Epicentre, Madison, WI, USA), followed by a clean-up step using the RNA Clean & Concentrator (Zymo), the process was repeated for samples with more than 5% ribosomal RNA contamination. The mRNA enriched sample was fragmented to a 200-250 bp peak range using the Ambicon RNA Fragmentation kit (Ambicon, Austin, TX, USA). Complementary DNA synthesis was performed as described here (Gross et al., 2013). Briefly, cDNA was made by annealing random hexamers, then first strand synthesis was created using Superscript II (Invitrogen) and samples were purified using AMPure XP beads. For the second strand cDNA synthesis, a mixture of dNTPs, with dUTP instead of dTTP was used. A double AMpure XP SPRI bead purification was also utilized to select for a size range 250-500 bp. Indexed TruSeq libraries were made using manufacturer instructions (Illumina, San Diego, CA). Strands with dUTP incorporated were destroyed with AmpErase uracil N-glycosylase (Applied Biosystems, Foster City, CA). The sample was enriched for products with both adaptors with 10 cycles of PCR as is indicated in Illumina TruSeq DNA Sample Prep Kit. The library was sequenced on an Illumina HiSeq 2000.

Transcriptome Assembly and Analyses

Illumina Hi-Seq reads were checked for quality using the FastQC software [http://www.bioinformatics.babraham.ac.uk/projects/fastqc/], and checked for contaminants using the FastQ Screen (Wingett & Andrews, 2018) software together with a database of known Illumina adapters and vector sequences from NCBI UniVec. Following these quality checks, reads were trimmed with the Trimmomatic software (Bolger et al., 2014) to remove low-quality ends. Reads were then mapped against the *D. vulgaris* Hildenborough and *M. maripaludis* S2 genomes (NCBI references NC002937, NC005791 and NC005863) using Bowtie 2 (Langmead & Salzberg, 2012) and consistency across replicates assessed by PCA performed on counts of single and multiple hits. Counts of reads per CDS were calculated by HTSeq (Anders et al., 2015), and differential expression analysis based on these counts was performed by edgeR (Robinson et al., 2010).

RNA-Seq Expression Analysis

Expression was calculated for the following comparisons: *D. vulgaris* in the co-culture biofilm versus *D. vulgaris* batch planktonic monoculture, *M. maripaludis* in the co-culture biofilm versus *M. maripaludis* batch planktonic monoculture, and co-culture biofilm versus co-culture in batch planktonic (Figure 1). Genes with an adjusted p-value and FDR < 0.05, and fold change > 0.75 were identified as being differentially expressed.

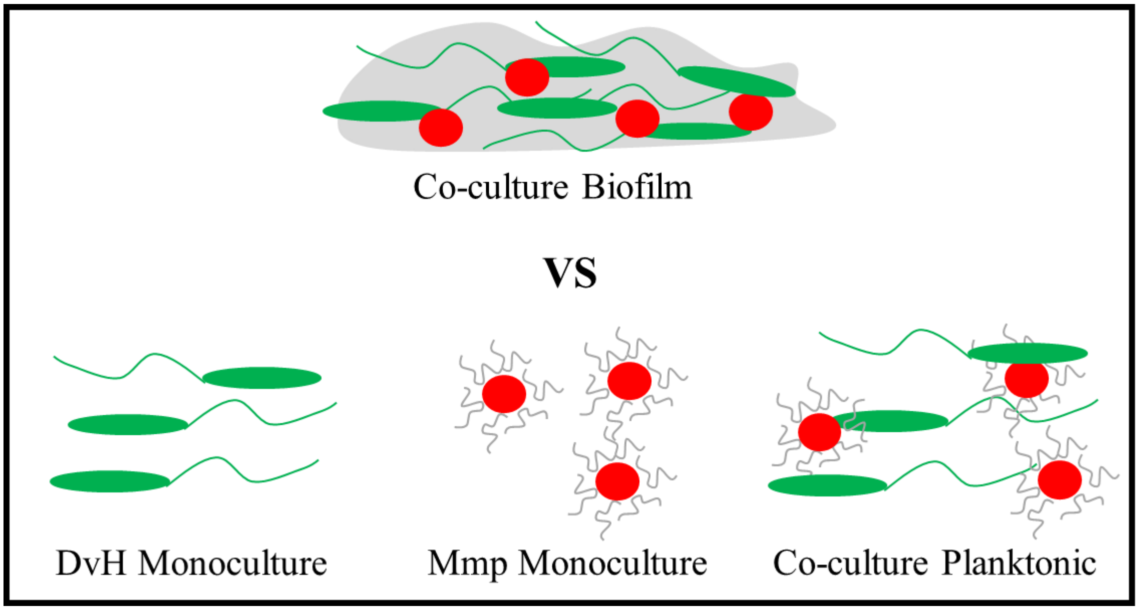

Figure 1. *D. vulgaris* Hildenborough (DvH, in green) and *M. maripaludis* (Mmp, in red) co-culture biofilm RNA-Seq transcript data was compared to planktonic cultures. RNA was harvested during the late exponential phase for the respective samples. The transcriptomic profile for *D. vulgaris* in the co-culture biofilm was compared against *D. vulgaris* expression in planktonic batch monoculture and planktonic batch co-culture. Similarly, *M. maripaludis* expression in the co-culture biofilm was compared to the expression in planktonic batch monoculture and planktonic batch co-culture.

Stoichiometric modeling

The online bioinformatics platform KBase (Arkin et al., 2018) was used to generate metabolic models for *Desulfovibrio vulgaris* Hildenborough and *Methanococcus maripaludis* S2 based on mapped genomic annotations from template models describing the metabolism of *Desulfovibrio alaskensis* G20 and *Methanospirillum hungatei* JF-1 (Table S1 and S2). Briefly, the template models were inputs to KBase using "FBA model from Excel," the proteomes of the template organism and intended organisms were compared using "Compare Two Proteomes," and the resulting output was used to develop the output models using "Propagate Model to New Genome." The resulting models were curated manually for elemental balance and metabolic functionality, including genes for the consumption and production of amino acids. Since neither organism is auxotrophic for amino acids in isolation, missing biosynthetic genes were added to complete synthesis pathways based on pathways described in the literature in phylogenetically similar organisms. Reaction rate distributions were obtained for single organism models using RegEFMTool version 3.3 (Gerstl et al., 2015; Gerstl et al., 2015) and analyzed for physiological context using in-house MATLAB scripts. Community analysis of DvH and Mmp used the overall reaction stoichiometries determined from individual models as inputs for linear optimization allowing for representative metabolic flexibility (*i.e.*, production or consumption of amino acids) with tractable ecological context (*i.e.*, individual organism minimizes carbon flux).

RESULTS

Transcriptomic comparisons were made from RNA-Seq data obtained from replicate *D. vulgaris* Hildenborough and *M. maripaludis* co-culture biofilm, monoculture planktonic, and co-culture planktonic growth conditions (Figure 1). The gene expression profiles revealed distinct physiological differences between the co-culture biofilm and planktonic growth modes for *D. vulgaris* (Figure 2) and *M. maripaludis* (Figure 3). *D. vulgaris* had approximately 220 genes that were significantly up-expressed compared to monoculture and were also at lower expression levels in the planktonic co-culture (Figure 2). Likewise, *D. vulgaris* had approximately 325 genes that were significantly down-expressed compared to monoculture that were also at higher expression levels in the planktonic co-culture (Figure 2). Between co-culture biofilm and planktonic, most genes displayed similar trends, although a small number were drastically lower (n=5) or higher (n=27) in co-culture. *M. maripaludis* displayed greater variability in expression levels for a greater number of genes, with most up-expressed genes (~300) and down-expressed genes (~250) showing a stronger respective change than the co-culture planktonic cells (Figure 3). Syntrophically-grown *Desulfovibrio* had 540 (43% of the 1257 genes with statistically significant expression changes) up-expressed genes and 717 (57% of the 1257 genes with statistically significant expression changes) down-expressed genes in the co-culture biofilm as compared with the planktonic monoculture (Figure 4A). Over half of the genes significantly up-expressed for co-culture biofilm and over a third of the genes significantly down-expressed for co-culture biofilm were annotated as hypothetical proteins (Figure 4A). Whereas the syntrophically-grown planktonic *Desulfovibrio* had 132 (43% of the 308 genes with statistically significant expression changes) up-expressed genes and 176 (57% of the 308 genes with statistically significant expression changes) down-expressed genes in the planktonic co-culture as compared with the planktonic monoculture and correspondingly a lower number of the significant changers were annotated as hypothetical proteins (Figure 4B).

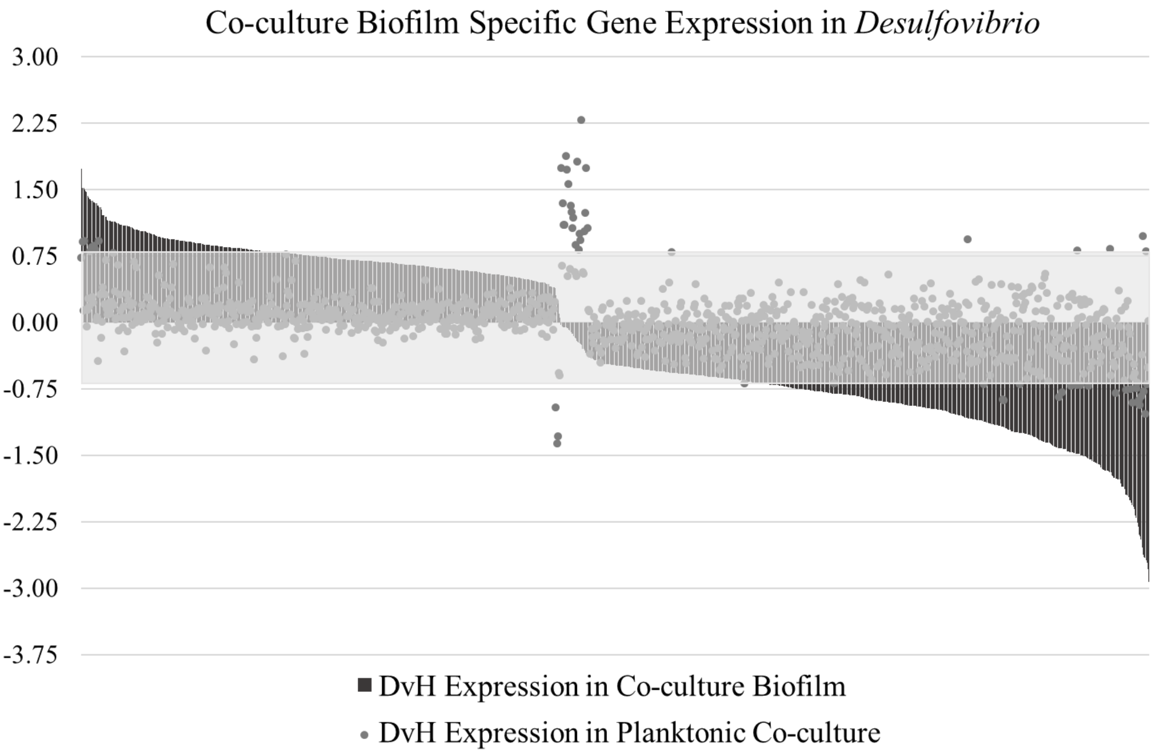

Figure 2. *D. vulgaris* Hildenborough (DvH) co-culture biofilm expression was plotted for all genes. The $\log_2$ fold-change profile for all *D. vulgaris* genes from greatest to least expressed in the co-culture biofilm (■) as compared to the planktonic monoculture, with the corresponding expression profile for the same genes in the planktonic co-culture (●). The grey box represents the cut-off threshold for significant expression levels (0.75<X<-0.75).

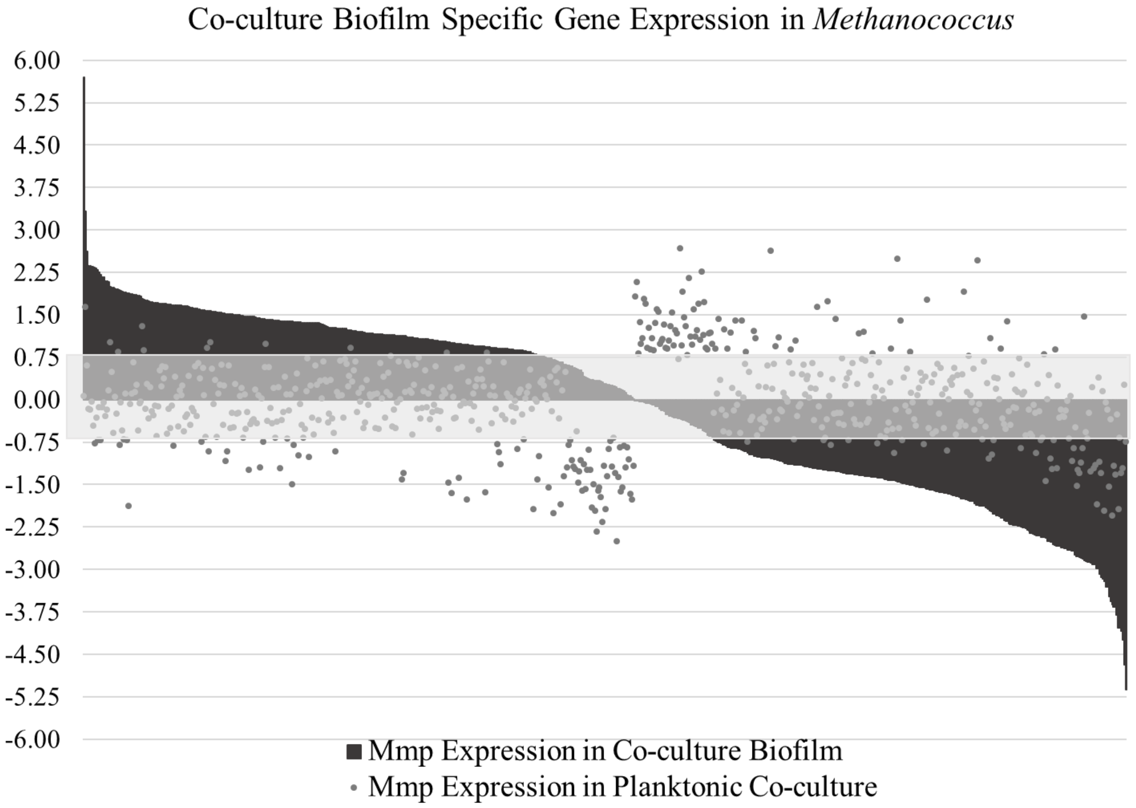

Figure 3. *M. maripaludis* (Mmp) co-culture biofilm expression was plotted for all genes. The $\log_2$ fold-change profile for all *M. maripaludis* genes from greatest to least expressed in the co-culture biofilm (■) as compared to the planktonic monoculture, with the corresponding expression profile for the same genes in the planktonic co-culture (●). The grey box represents the cut-off threshold for significant expression levels (0.75<X<-0.75).

(A) Statistically significant expression for *Desulfovibrio* in co-culture biofilm

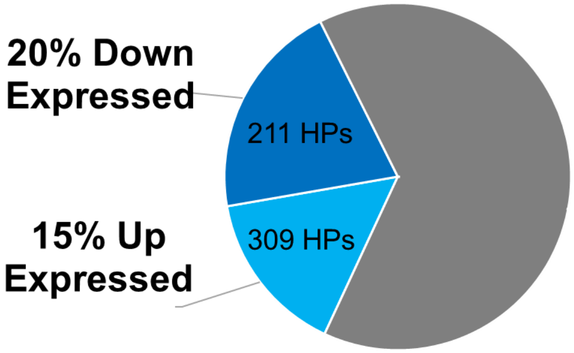

(B) Statistically significant expression for *Desulfovibrio* in planktonic co-culture

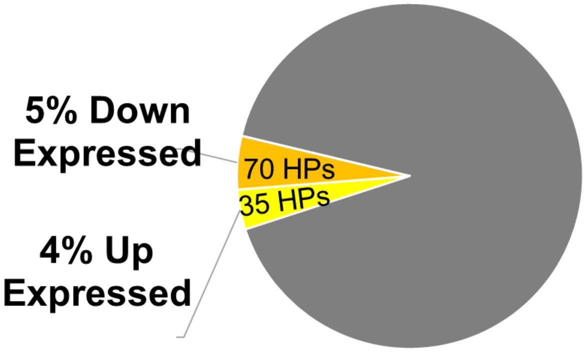

Figure 4. *D. vulgaris* Hildenborough co-culture statistically significant expressed genes were represented as a percentage of all genes in the genome. (A) The statistically significant gene fraction (using p-values and FDR <0.05) as compared to *D. vulgaris* planktonic monoculture for all annotated genes. The actual number of genes (down=211 and up=309) with altered expression annotated as hypothetical proteins (HP) for *D. vulgaris* in co-culture biofilm. (B) *D. vulgaris* in planktonic co-culture had 5% and 4% total genes display down-expression or up-expression, respectively. The actual number of genes (down=70 and up=35) with altered expression annotated as hypothetical proteins (HP) for *D. vulgaris* planktonic cells.

(A) Statistically significant expression for *Methanococcus* in co-culture biofilm

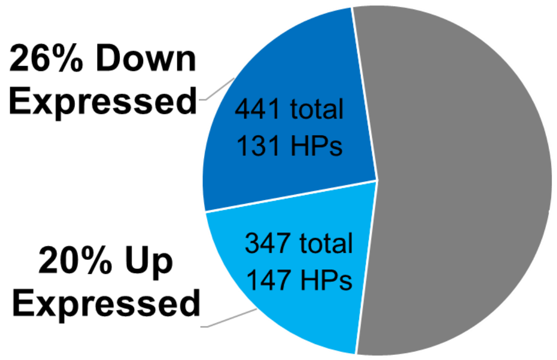

(B) Statistically significant expression for *Methanococcus* in planktonic co-culture

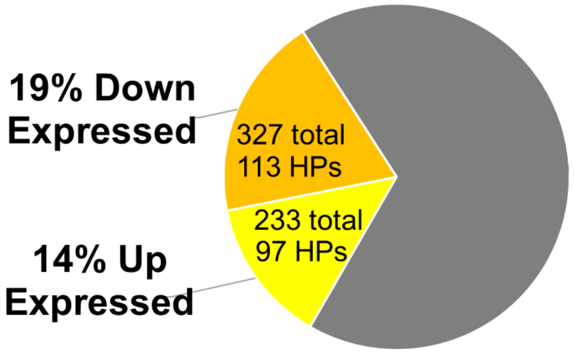

Figure 5. *M. maripaludis* co-culture statistically significant expressed genes were represented as a percentage of all genes in the genome. (A) The statistically significant gene fraction (using p-values and FDR <0.05) as compared to *M. maripaludis* planktonic monoculture for all annotated genes. The actual number of genes (down=131 and up=147) with altered expression annotated as hypothetical proteins (HP) for *M. maripaludis* in co-culture biofilm. (B) *M. maripaludis* in planktonic co-culture had 19% and 14% total genes display down-expression or up-expression, respectively of all annotated genes. The actual number of genes (down=113 and up=97) with altered expression annotated as hypothetical proteins (HP) for *M. maripaludis* planktonic cells.

Syntrophically-grown *Methanococcus* had 347 (44% of the 788 genes with statistically significant expression changes) up-expressed genes and 441 (56% of the 788 genes with statistically significant expression changes) down-expressed genes in the co-culture biofilm as compared with the planktonic monoculture (Figure 5A). Whereas the syntrophically-grown planktonic *Methanococcus* had 236 (42% of the 566 genes with statistically significant expression changes) statistically significant up-expressed genes and 330 (58% of the 566 genes with statistically significant expression changes) down-expressed genes in the planktonic co-culture as compared with the planktonic monoculture (Figure 5B). Between 25 to 50% of the genes with altered expression in *M. maripaludis* were annotated as hypothetical proteins (Figure 5).

Overall, there were more significant gene expression changes for both populations in the co-culture biofilm condition as compared to the planktonic monocultures (Figure 4 and 5). *Methanococcus* had 111 more genes both up and down-expressed in co-culture biofilm as compared to the planktonic co-culture, while *Desulfovibrio* showed 408 more genes up-expressed and 541 more genes down-expressed in co-culture biofilm as compared to planktonic co-culture. Interestingly, while *M. maripaludis* maintained similar relative abundances of up- and down-expressed genes between biofilm co-culture and planktonic conditions, *D. vulgaris* had a decline of significant changers for the planktonic co-culture condition.

D. vulgaris genes with significantly altered expression for co-culture biofilm were binned into COGs based upon cellular functions, and most of the COGs displayed a downward trend in gene expression (Figure 6). After hypothetical/general function, COG T (signal transduction), COG M (cell wall/membrane), COG L (replication/repair), COG E (amino acids), and COG C (energy production/conservation) were the next predominately changed categories (Figure 6). Interestingly, only three COGs had more up-expressed genes than down-expressed genes for *D. vulgaris* in the co-culture biofilm:

unknown function, general function, and defense. *M. maripaludis* genes with significantly altered expression for co-culture biofilm were binned into COGs based upon cellular functions, and the COGs displayed a mixed response (Figure 7). After general function and unknown function as the two largest up-expressed groups, COG V (defense), COG M (cell wall/membrane), COG J (translation/ribosome), COG H (coenzyme), COG E (amino acid), and COG C (energy production/conservation) were the most up-expressed (Figure 7). COGs that were mainly down-expressed for *M. maripaludis* in the co-culture biofilm included COG T (signal transduction), COG Q (secondary metabolites), COG L (replication/repair), COG K (transcription), COG I (lipids), and COG D (cell cycle).

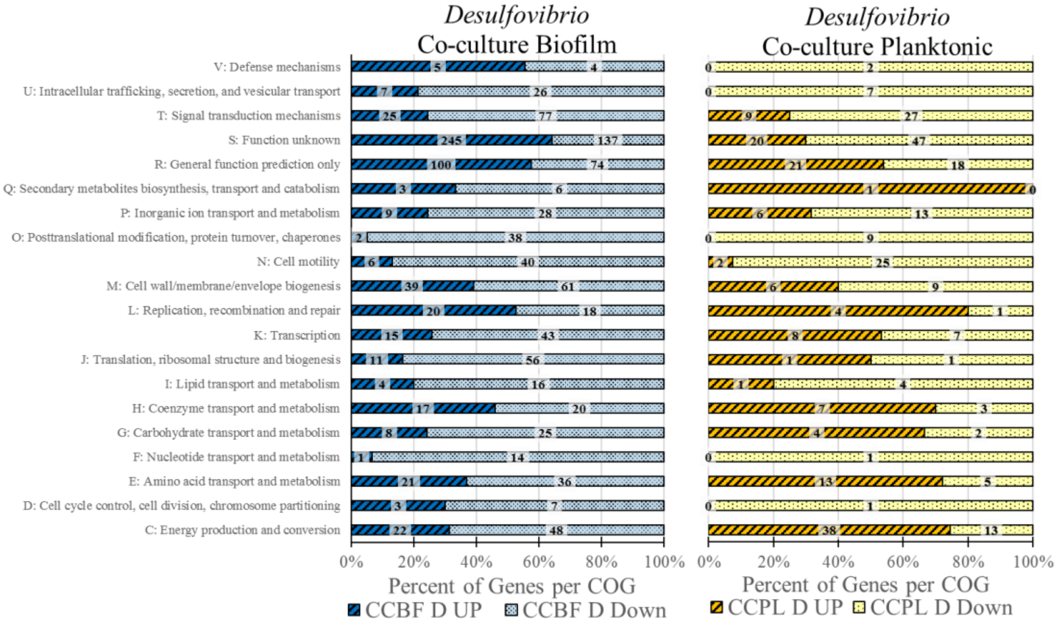

Figure 6. *D. vulgaris* Clusters of Orthologous Genes. The statistically significant genes with expression differences for *D. vulgaris* in the co-culture biofilm (CCBF D) or planktonic co-culture (CCPL D) as compared to the planktonic monoculture categorized into pre-defined COG categories. Each category is represented as a percentage of all the genes for each COG with the representative gene numbers listed in the boxes.

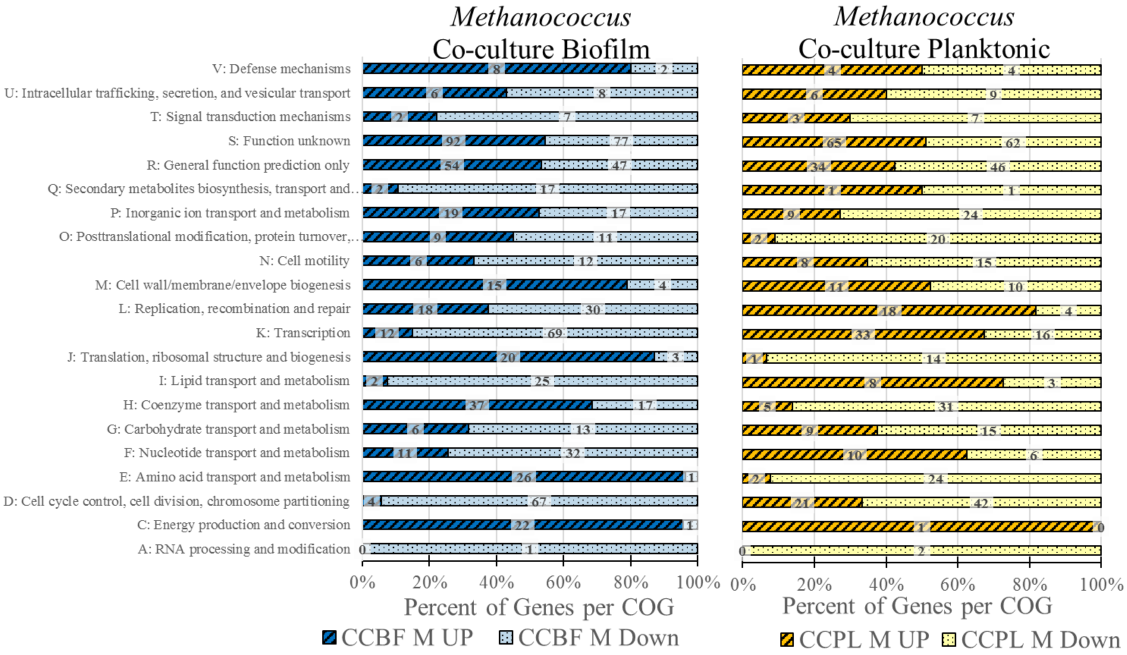

Figure 7. *M. maripaludis* Clusters of Orthologous Genes. The statistically significant genes with expression differences for *M. maripaludis* in the co-culture biofilm (CCBF M) or planktonic co-culture (CCPL M) as compared to the planktonic monoculture were categorized into pre-defined COG categories. Each category is represented as a percentage of all the genes for each COG with the representative gene numbers listed in the boxes.

D. vulgaris expression could be easily categorized into two groups, those that were unique to the co-culture biofilm and those that were specific to the co-culture (*i.e.* syntrophy) in general. Upon analysis, it was apparent that *Methanococcus* had a third group of genes that could only be classified as those genes that were statistically significant to the co-culture biofilm and planktonic co-culture (*i.e.*, co-culture), but also were differentially expressed. *M. maripaludis* had six statistically significant up-expressed genes in the co-culture biofilm that were also down-expressed in the planktonic co-culture (Table 1). For example, MMP0837 is annotated as a ribonuclease, and could play a role in control of cell activity through modulation of RNA molecules and/or ribosomes. Additionally, there were 19 statistically significant down-expressed genes in the co-culture biofilm that were significantly up-expressed in the planktonic co-culture (Table 1). Interestingly, five of these genes were annotated as ribosomal proteins and could be suggestive of a down-trend for overall translation. In the context of carbon processing, the co-culture biofilm (but not planktonic co-culture) down-expressed an annotated formate dehydrogenase subunit (MMP1297), a carbonic anhydrase (MMP1299), hypothetical protein (MMP1300), and formate transporter (MMP1301) (Figure 8). While the presumptive formate dehydrogenase for *M. maripaludis* was down-expressed, the formate dehydrogenase of *D. vulgaris* (DVU2811 and DVU2812) was significantly up-expressed. In addition, methyl viologen was used to measure formate dehydrogenase activity between co-culture planktonic and biofilm samples and the co-culture biofilm had 18-fold higher formate dehydrogenase activity (Figure S1).

Gene ID	CCBF Log$_2$FC	Gene ID	CCPl Log$_2$FC	Gene ID	CCBF vs CCPl Log$_2$FC	Description
MMP1179	1.3796	MMP1179	-1.4970	MMP1179	2.8771	methyltransferase
MMP0875	1.1266	MMP0875	-1.2987	MMP0875	2.4253	S layer protein
MMP0870	0.9010	MMP0870	-0.9315	MMP0870	1.8326	glycerate dehydrogenase
MMP0837	0.9007	MMP0837	-1.1361	MMP0837	2.0371	ribonuclease H
MMP1548	0.8736	MMP1548	-0.8664	MMP1548	1.7402	Fe-S type hydro-lyase tartrate/fumarate subunit beta
MMP1343	0.7864	MMP1343	-1.0023	MMP1343	1.7887	hypothetical protein [Superfamily, evalue = 9.77e-22]cl00446, Metallo-beta-lactamase superfamily
MMP1299	-2.8399	MMP1299	1.4750	MMP1299	-4.3150	carbonic anhydrase
MMP0252	-2.1474	MMP0252	1.3835	MMP0252	-3.5314	hypothetical protein
MMP1300	-1.8633	MMP1300	2.4679	MMP1300	-4.3312	hypothetical protein
MMP1301	-1.7551	MMP1301	1.9144	MMP1301	-3.6695	formate/nitrite transporter
MMP0457	-1.5796	MMP0457	1.7625	MMP0457	-3.3422	DEAD/DEAH box helicase domain-containing protein
MMP0948	-1.4648	MMP0948	1.4047	MMP0948	-2.8698	hypothetical protein
MMP1297	-1.4449	MMP1297	2.4984	MMP1297	-3.9433	formate dehydrogenase subunit beta
MMP0489	-1.3626	MMP0489	0.8174	MMP0489	-2.1805	hypothetical protein
MMP0443	-1.3438	MMP0443	1.1954	MMP0443	-2.5395	30S ribosomal protein S24e
MMP1147	-1.3326	MMP1147	1.1745	MMP1147	-2.5072	50S ribosomal protein L37e
MMP0577	-1.2607	MMP0577	1.4229	MMP0577	-2.6837	30S ribosomal protein S17e
MMP0578	-1.2482	MMP0578	1.7434	MMP0578	-2.9919	chorismate mutase
MMP1385	-1.2213	MMP1385	1.6418	MMP1385	-2.8631	coenzyme F420-reducing hydrogenase subunit beta
MMP0136	-1.1477	MMP0136	1.0504	MMP0136	-2.1983	3-isopropylmalate dehydratase small subunit
MMP1643	-1.0678	MMP1643	1.1082	MMP1643	-2.1761	hypothetical protein
MMP1658	-1.0594	MMP1658	0.9424	MMP1658	-2.0019	30S ribosomal protein S8e
MMP0062	-1.0026	MMP0062	1.2108	MMP0062	-2.2136	50S ribosomal protein L31e
MMP1505	-0.9191	MMP1505	0.8472	MMP1505	-1.7663	pyruvate oxidoreductase (synthase) subunit alpha
MMP1693	-0.9082	MMP1693	0.6299	MMP1693	-1.5382	F420 non-reducing hydrogenase subunit

Table 1. *M. maripaludis* had differential expression for a subset of genes. The statistically significant genes (using p-values and FDR <0.05) with differential expression (Log$_2$ Fold Change) between *M. maripaludis* (as compared to planktonic monoculture) in the co-culture biofilm (CCBF), co-culture planktonic (CCPl), and as the co-culture biofilm compared to the co-culture planktonic (CCBF vs CCPl).

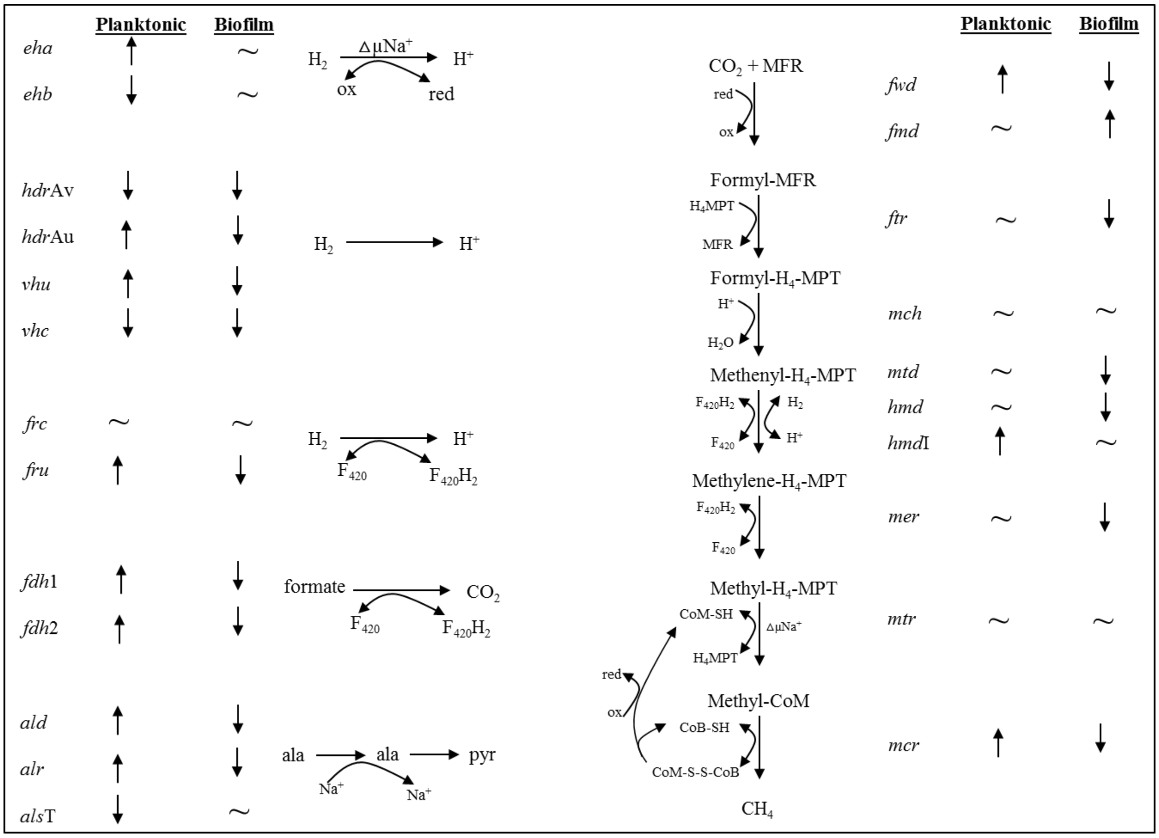
Planktonic
Biofilm
eha
ehb
ΔμNa+
H2
H+
ox
red
hdrAv
hdrAu
vhu
vhc
frc
fru
F420
F420H2
fdh1
fdh2
formate
CO2
ald
alr
alsT
ala
pyr
Na+
CO2 + MFR
Formyl-MFR
H4MPT
MFR
Formyl-H4-MPT
H2O
Methenyl-H4-MPT
Methylene-H4-MPT
Methyl-H4-MPT
CoM-SH
Methyl-CoM
CoB-SH
CoM-S-S-CoB
CH4
fwd
fmd
ftr
mch
mtd
hmd
hmdI
mer
mtr
mcr

Figure 8. Transcriptomic differences in methanogenic-related electron and carbon processing genes for *Methanococcus maripaludis* between planktonic co-culture and biofilm co-culture. $\Delta\mu Na^+$, Na^+ gradient; H_4MPT, tetrahydromethanopterin; MFR, methanofuran; CoM-SH, coenzyme M; CoB-SH, coenzyme B; CoM-S-S-CoB, heterodisulfide of CoM and CoB; F_{420}/$F_{420}H_2$, coenzyme F_{420}; ox/red (most likely ferredoxin); *eha*/*ehb*, hydrogenase A or B; *fdh*1/2, formate dehydrogenase; *ftr*, formyltransferase; *fmd*/*fwd*, formylmethanofuran dehydrogenase; *fru*/*frc*, F_{420}-reducing hydrogenase; *hdr*, heterodisulfide reductase; *hmd*, H_2-dependent methylene-H_4MPT dehydrogenase; *mch*, methenyl-H_4MPT cyclohydrolase; Mcr, methyl-CoM reductase; *mer*, methylene-H_4MPT reductase; *mtd*, F_{420}-dependent methylene-H_4MPT dehydrogenase; *mtr*, methyl-H_4MPT:CoM methyltransferase; *vhu*/*vhc*. Modified from Costa et al., 2013.

Expression as a Result of Syntrophy

Genes that showed similar expression trends and that were statistically significant to the co-culture biofilm and co-culture planktonic growth modes were identified as being important for syntrophic interactions. *Desulfovibrio* had 9 genes more than 2-fold up-expressed, and 30 genes more than 2-fold down-expressed that were co-culture specific (Table S3). The up-expressed genes greater than 2-fold were annotated as lactate permeases (DVU2451 and DVU3026), lipoproteins (DVU0147-8), a response regulator (DVU0145), and hypotheticals with predicted membrane associations (DVU0146, DVU0149-50, DVU1105). The genes with ≥ 2-fold down-expression in the co-culture biofilm were annotated as important for energy, cell motility, inorganic ion transport, and hypothetical proteins and included hypothetical proteins (DVU0304, DVU2681, DVU0303, DVU2108, DVU0772), flagellin (DVU2082, DVU1441), chemotaxis protein CheX (DVU0302), and ferrous iron transport proteins (DVU2571-2). These genes were similarly down-expressed in the planktonic co-culture however they were significantly more down-expressed in the co-culture biofilm growth mode in general.

Overall, a much wider range in expression changes were observed for *Methanococcus* in the co-culture biofilm despite having similar expression trends with the planktonic co-culture. The highest expressed genes related to syntrophic growth were for hypothetical proteins (MMP0501 a predicted homology to a hydrocarbon precursor of the pentalenolactone family of antibiotics, and MMP0998 a predicted virulence factor related to pectin that mediates adhesion to target cells), a surface protein with a collagen triple helix repeat (MMP1194), blue (type 1) copper domain protein (MMP0997 which is predicted to be similar to a cupredoxin for intermolecular electron transfer reactions), cobalt transport protein (MMP1483), glutamine amidotransferase (MMP1656), and aspartate racemase (MMP0739) among numerous other hypothetical proteins with no known function (Table S4). The most down-expressed genes for *Methanococcus* in co-culture were in hypothetical proteins (MMP0601, MMP1016, MMP0629, MMP1302, MMP0846, MMP0692, MMP1586, MMP0235, MMP1633), flagellin (MMP1666-7, MMP1670), nitrogenase (MMP0857), ammonia transporter (MMP0065), and genes central to the methanogenesis pathway such as coenzyme F420 non-reducing hydrogenase (MMP0822-4, MMP0817), methylenetetrahydromethanopterin reductase (MMP0058, MMP0127, MMP0372), and formylmethanofuran dehydrogenase (MMP1248-9); however, CH_4 production was steady under the tested growth conditions.

Expression as a Result of Growth Mode

Overall, *Desulfovibrio* did not exhibit changes in expression above log 2-fold change that could be identified as being co-culture biofilm specific (Table S5). The most up-expressed genes unique to the biofilm growth mode were annotated as lipoprotein (DVU1126, DVU2301), NiFe hydrogenase (DVU1922), tryptophanase (DVU2204), hypothetical alcohol dehydrogenase (DVU2603), metallo-beta-lactamase (DVU2804), predicted phage genes (DVU1107, DVU1140, DVU1139, DVU2716, DVU2723), and numerous hypothetical genes with no known function. The co-culture biofilm genes for *Desulfovibrio* that had the most down-expression were related to chemotaxis (DVU1904), RNA-binding (DVU1257, DVU2215), periplasmic [NiFeSe] hydrogenases

(DVU1918, DVU1917) which is preferentially used under lower hydrogen conditions, rubredoxin (DVU3093), rubrerythrin (DVU3094), acidic cytochrome c3 (DVU0263), type I secretion protein (DVU1013), lipoprotein A (DVU0407), universal stress protein (DVU0261), and hypothetical proteins.

Interestingly, in the co-culture biofilm condition, *Methanococcus* had 17 genes more than 2-fold up-expressed and 87 genes more than 2-fold down-expressed. Most of the annotations available for the most up-expressed genes were hypothetical with no known function (Table S6). The highest up-expressed genes for *Methanococcus* in the co-culture biofilm when compared to the planktonic co-culture were in hypothetical proteins (*e.g.*, MMP0750, MMP0775, MMP0467, MMP0466, MMP0745, MMP0211, MMP0782, MMP0518, MMP0530, MMP0462, MMP0673, MMP0747), cobalt ABC transporter inner membrane protein (MMP1483), thiamine-monophosphate kinase (MMP1124), molybdopterin biosynthesis protein (MMP0513), lysine/homoserine lactone exporter (MMP0849), and various other ATPase related genes (*e.g.*, MMP0408, MMP1649, MMP0520). The most down-expressed genes identified were annotated as a heterodisulfide reductase (MMP0825, MMP1053-4), 30S/50S ribosomal proteins (MMP1420, MMP1419, MMP1421), methyl-coenzyme M reductase I (MMP1556-9), tetrahydromethanopterin-S-methyltransferase (MMP1565-6, MMP1563), and alanine racemase/dehydrogenase (MMP1512/13).

Stoichiometric Modeling of Amino Acid Exchange

Model predictions revealed that when *D. vulgaris* is grown with lactate oxidation and sulfate reduction, the amino acids serine, alanine, cysteine, aspartate, valine, and glycine can be synthesized for the least mole of lactate oxidized per mole of amino acid produced (Table 2). While the more expensive amino acids per mole are tryptophan, tyrosine, phenylalanine, arginine, histidine, and isoleucine. Furthermore, the relative ranking of nutrient requirements was maintained for both electron donor and acceptor limited simulations. The relative nutrient requirements to produce these amino acids are also reflected in previous observations of amino acid excretion by *Desulfovibrio* (He et al., 2010), and extracellular detection coincides with predicted, relative less cost to synthesize (*i.e*., excrete the least expensive amino acids). Whereas, the amino acids that are predicted to be more expensive to synthesize are not detected at high levels extracellularly (He et al., 2010).

Simulations of amino acid utilization for *M. maripaludis* demonstrate that most amino acids are predicted to not contribute to the production of biomass beyond simple supplementation that could theoretically reduce the need to fix carbon. The baseline plot shows the condition in which amino acids were not fed and overlays all scenarios where the supplemental amino acids were fed. The close overlap of the physiological space for the H_2/biomass and CO_2/biomass (mmol/gCDW) for the baseline conditions indicate that *M. maripaludis* does not produce energy solely from these amino acids (Figure 9 and 10). In addition, the plots demonstrate that most of the amino acids do not contribute to the production of energy beyond supplementation. Whether the simulations are plotted as

CO_2 or H_2 consumed per unit biomass (Figure 9) or energy (Figure 10), the model predicts the amino acids alanine, cysteine, glycine and serine could result in less H_2 and/or CO_2 consumed per unit biomass or energy produced, and thus ultimately result in more biomass produced or lessen the direct need for both H_2 and/or CO_2 when the amino acids are available exogenously. The modes predict that alanine and cysteine would be converted to acetate, glycine would be oxidized via a THF-like (tetrahydrofolate) pathway, and serine could be indirectly converted to acetate through cysteine.

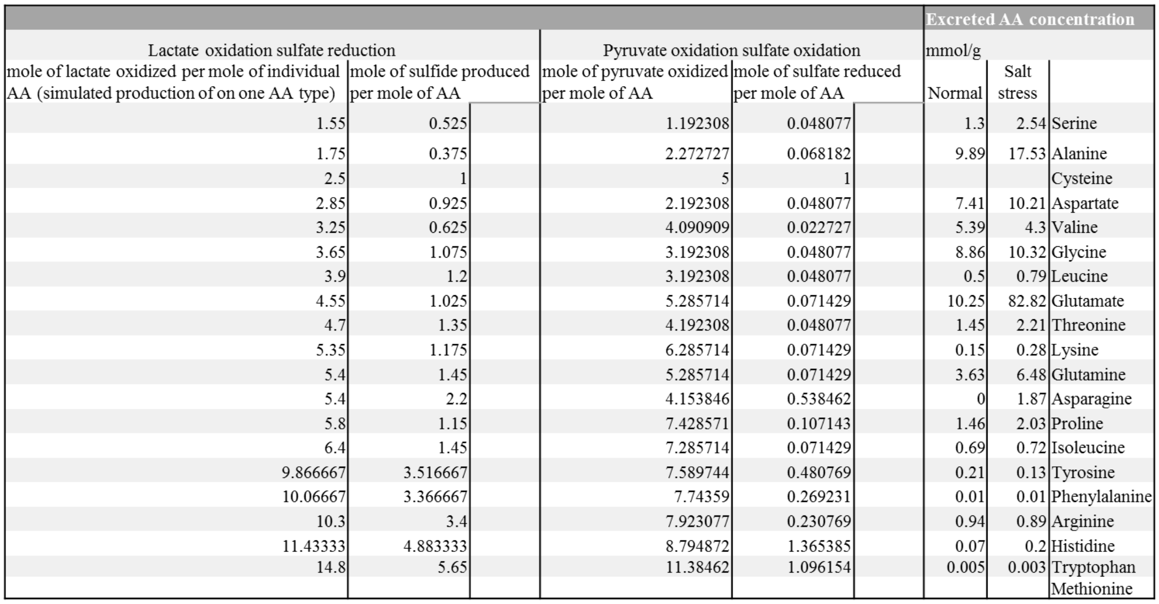

				Excreted AA concentration		
Lactate oxidation sulfate reduction		Pyruvate oxidation sulfate oxidation		mmol/g		
mole of lactate oxidized per mole of individual AA (simulated production of on one AA type)	mole of sulfide produced per mole of AA	mole of pyruvate oxidized per mole of AA	mole of sulfate reduced per mole of AA	Normal	Salt stress	
1.55	0.525	1.192308	0.048077	1.3	2.54	Serine
1.75	0.375	2.272727	0.068182	9.89	17.53	Alanine
2.5	1	5	1			Cysteine
2.85	0.925	2.192308	0.048077	7.41	10.21	Aspartate
3.25	0.625	4.090909	0.022727	5.39	4.3	Valine
3.65	1.075	3.192308	0.048077	8.86	10.32	Glycine
3.9	1.2	3.192308	0.048077	0.5	0.79	Leucine
4.55	1.025	5.285714	0.071429	10.25	82.82	Glutamate
4.7	1.35	4.192308	0.048077	1.45	2.21	Threonine
5.35	1.175	6.285714	0.071429	0.15	0.28	Lysine
5.4	1.45	5.285714	0.071429	3.63	6.48	Glutamine
5.4	2.2	4.153846	0.538462	0	1.87	Asparagine
5.8	1.15	7.428571	0.107143	1.46	2.03	Proline
6.4	1.45	7.285714	0.071429	0.69	0.72	Isoleucine
9.866667	3.516667	7.589744	0.480769	0.21	0.13	Tyrosine
10.06667	3.366667	7.74359	0.269231	0.01	0.01	Phenylalanine
10.3	3.4	7.923077	0.230769	0.94	0.89	Arginine
11.43333	4.883333	8.794872	1.365385	0.07	0.2	Histidine
14.8	5.65	11.38462	1.096154	0.005	0.003	Tryptophan
						Methionine

Table 2. Stoichiometric model predictions for *Desulfovibrio*. Mole of amino acids produced per mole of lactate oxidized from least (cheapest) to most (expensive).

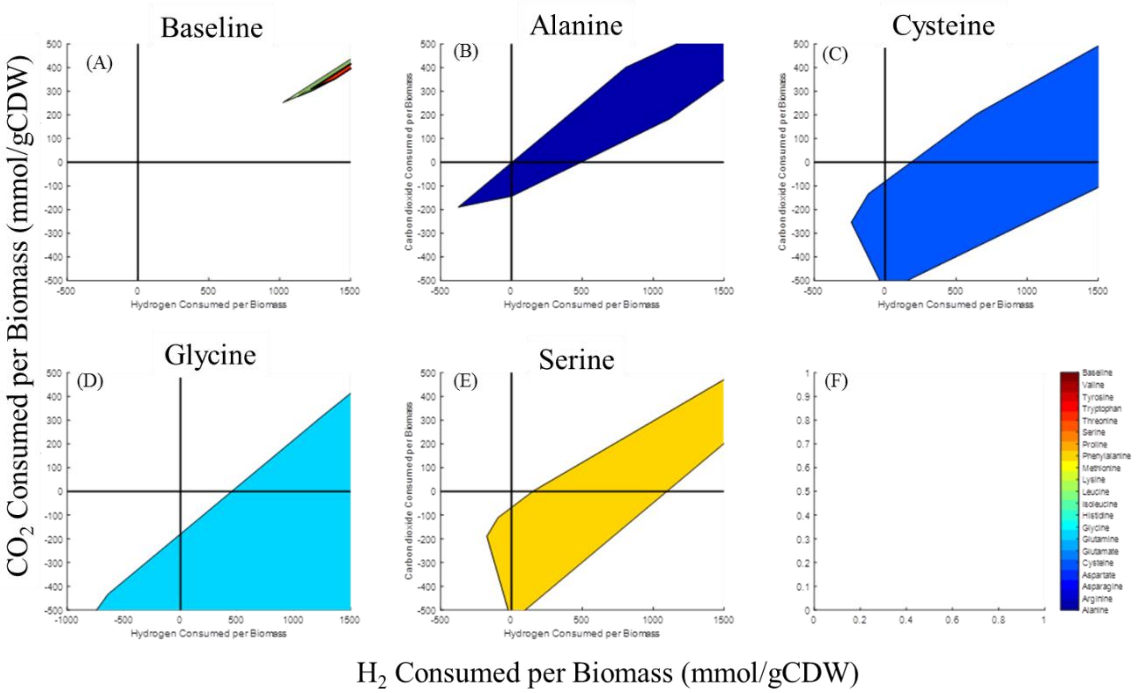

Figure 9. *M. maripaludis* modeling identified four amino acids that could be used for biomass. The plots demonstrate that most of the amino acids don't contribute to the production of biomass beyond supplementation, as evident by the close overlap of the physiological space on plot (A) where the baseline scenario depicts no amino acids fed and overlays all scenarios where the supplemental amino acids were fed. Scenarios for (B) Alanine, (C) Cysteine, (D) Glycine, (E) Serine, demonstrate hydrogen production and carbon dioxide consumption (upper left quadrant), biomass produced per carbon dioxide and hydrogen consumed for methanogenesis (upper right quadrant), hydrogen and carbon dioxide production (bottom left hand quadrant), and carbon dioxide production with hydrogen consumption.

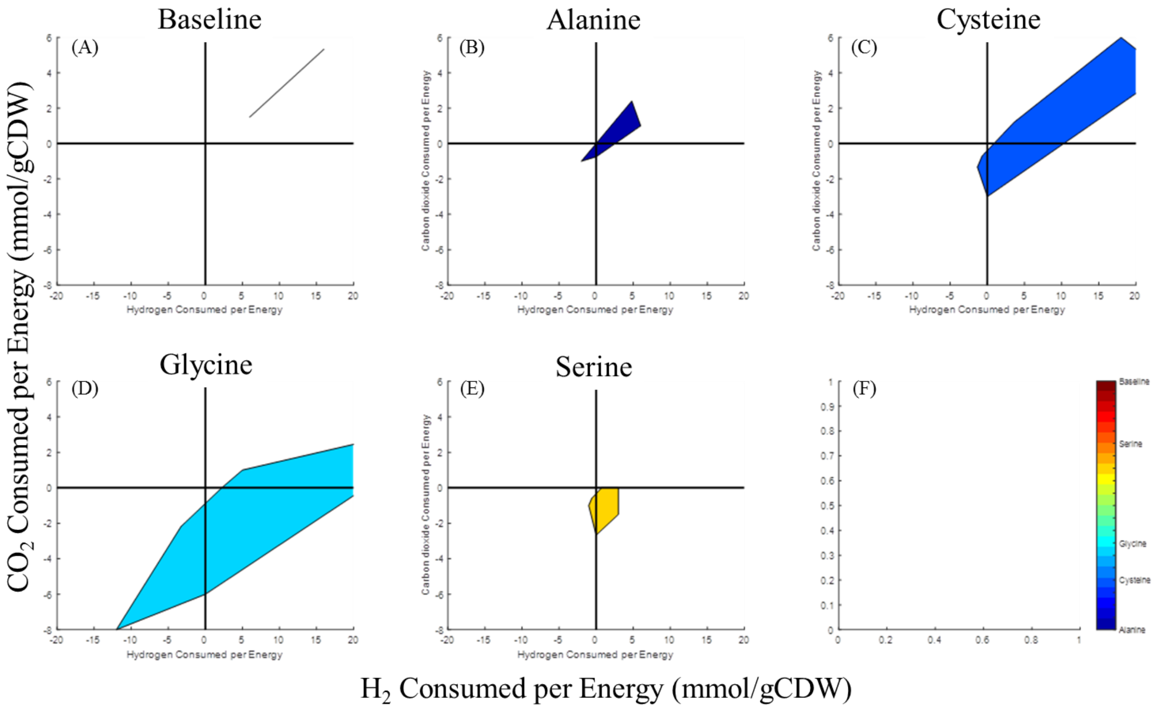

Figure 10. *M. maripaludis* modeling showed four amino acids could be used for energy production. The plots demonstrate carbon dioxide consumption and hydrogen consumption per energy, the (A) baseline shows the overlap of all the amino acids that cannot make energy. The amino acids (B) Alanine, (C) Cysteine, (D) Glycine, and (E) Serine can make energy for *M. maripaludis,* the closer to the origin, the more energy there is.

DISCUSSION

Previous work has demonstrated that the co-culture biofilm growth mode enhances the efficiency of the syntrophy between *Desulfovibrio vulgaris* Hildenborough and *Methanococcus maripaludis* S2 in terms of carbon flux (*e.g.* lactate or methane) to biomass (Brileya et al., 2014). Despite inherent variability and heterogeneity in biofilm structure, the co-culture biofilm appeared to promote cooperative resource sharing that resulted in maximized carrying-capacity for both species (Brileya et al., 2014). Our current hypothesis is that the SRB and methanogen biofilm could have multiple metabolic interactions in addition to (or rather than) the typically considered H_2 and/or predicted alanine (Walker et al., 2012). Particularly in light of the fact that previous work has not focused on the biofilm growth mode where cellular interactions and mass transport can be significantly different. While proximity of the two studied populations in biofilm is believed to facilitate metabolic exchanges, the full extent of possible metabolites and the underlying gene expressions that impact efficiency in the system in terms of carbon and electron flow is unknown. The role of metabolic dependencies such as amino acids as major drivers of community structure and function is being increasingly observed in different systems (Zelezniak et al., 2015), and model work with constructed consortia of varying genotypes has demonstrated that cross-feeding can be selected under a range of conditions (Pande et al., 2016). In addition, metabolite leakage is increasingly thought to be common (D’Souza et al., 2018), and therefore, metabolite exchange would most likely be even more pronounced for biofilm communities and possibly a selectable trait to encourage association.

The aim of this study was to identify genetic and metabolic components unique to a syntrophic co-culture biofilm that contained a metabolically-linked bacterium and archaeon, as previous transcriptomic work has only focused on the co-culture in the planktonic state (Walker et al., 2009, 2012). The results demonstrated a unique transcriptomic profile that was different from planktonic systems, and the methanogen showed much broader expression changes in the co-culture biofilm. In addition to the expected up-expression of membrane associated genes and a decrease in expression for cell motility, there was an increase in genes for both organisms that had homology to various antimicrobials which could indicate cell signaling pathways or possible antagonisms.

Previous work has identified genes important for syntrophy, yet the data presented here shows that a unique set of genes is important for biofilm syntrophy that maximizes lactate utilization and electron transfer. Many of the genes previously identified for the same co-culture grown in the planktonic state had different responses to the biofilm growth mode, although many of the differences between planktonic syntrophs and biofilm syntrophs were observed in the methanogen. One of the main differences for *D. vulgaris* was the increased expression for lactate permeases (DVU2451, DVU3026) compared to planktonic co-culture (Walker et al., 2009); suggesting that the biofilm might need to overcome mass transport limitations for lactate compared to planktonic cells.

Additionally, the co-culture biofilm had increased transcripts for electron processing genes that differed from described planktonic co-cultures. In the biofilm, the *vhu*, *vhc*, *fdh*1, *fdh*2, *hdr*Av, and *hdr*Au hydrogenases were down-expressed but the *vhu*, *fdh*1, *fdh*2, and *hdr*Au were up-expressed in the planktonic co-culture (Figure 8). Whereas *fru* was up-expressed in planktonic but down-expressed in biofilm. The *eha* and *ehb* expression was static in biofilm, but *eha* was increased and *ehb* decreased in planktonic (Figure 8). Although H_2 was never detected in the biofilm system as previously reported for the planktonic co-culture (Walker et al., 2009), expression of the NiFe hydrogenases (high-affinity H_2 oxidation) and the down-expression of the low affinity NiFeSe hydrogenases indicated that H_2 levels are not limiting (Krumholz et al., 2015). Another sign that H_2 availability is maximized within the co-culture biofilm is from the observed down-expression of the methanogenesis pathway for *M. maripaludis* which has been reported to increase mRNA abundance as a function of decreased H_2 availability (Hendrickson et al., 2007). Taken together, these results suggest that H_2 flux between the bacterium and archaeon have been optimized. Furthermore, the results are in line with previous reports of transcript discordance between expression and function and further work is needed to fully understand the role of mRNA and protein half-lives for different organisms in different physiological states.

The CO_2-reduction pathway also displayed differences for biofilm versus planktonic growth modes (Figure 8). The formyl-transfer related genes, *fwd* and *fmd*, were up-expressed or static, respectively in planktonic cells, but *fwd* was down-expressed and *fmd* was up-expressed in biofilm co-culture. The genes *ftr, mch, mtd,* and *mer* were static for planktonic co-culture but *ftr*, *mtd*, and *mer* expression were decreased in biofilm. The *por* was down-expressed in both planktonic and biofilm whereas *cdh* was static in biofilm but down-expressed in planktonic. The *hmd* and *hmd1* were static or down-expressed in biofilm but were static or up-expressed in planktonic. Lastly, *mcr*, the enzyme for the final methyl-reducing step, was up-expressed in planktonic but down-expressed in biofilm (Figure 8). Overall, the electron and carbon processing associated proteins for methanogenesis in *M. maripaludis* were mostly up-expressed in the planktonic condition and static to decreased for the biofilm. These results suggested the local environment of the syntrophic biofilm affords *M. maripaludis* the opportunity to modulate electron and carbon flow compared to conditions in the bulk aqueous phase. Further work is needed to elucidate the mechanisms of metabolic modulation in terms of the potential impacts of flux and/or additional e^-, carbon, and nitrogen inputs.

Although alanine was previously observed to be important for syntrophy in planktonic co-cultures, appreciable differences in growth rates or yields were not observed in the presence of alanine or with mutants (Walker et al., 2009). For the syntrophic biofilm, the alanine dehydrogenase and racemase were down-expressed compared to the planktonic state. Previous work has shown that *Methanococci* can assimilate alanine (Jones et al., 1987), and our metabolic models predicted that alanine could impact H_2/CO_2 consumption by *M. maripaludis*. In addition, the flux balance model predicted that alanine biosynthesis is relatively inexpensive for *D. vulgaris*. The down-expression for alanine related-genes in this case may be another instance of discordance between mRNA and protein. In addition, as put forth by Walker et al.

(2012), the cost of synthesis to one organism could be compensated for by an advantage provided by the partner. The co-culture biofilm also had increased expression in tryptophanase and tryptophan-specific transporters that could be involved in nitrogen cycling as well as biofilm formation (Hamilton et al., 2009). The decreased expression of the rare lipoprotein A genes and the outer membrane protein *omp*H in *D. vulgaris* suggests a response to an unknown antimicrobial possibly secreted by *M. maripaludis.* For example, MMP1103 annotated as a protein involved in trifolitoxin production and MMP0501 annotated as a terpenoid cyclase involved in antibiotic precursors were highly up-expressed. Further work is needed to ascertain to what degree the syntrophic biofilm may be experiencing a combination of syntrophic and antagonistic interactions.

The metabolic flux models for *M. maripaludis* predicted that most of the amino acids do not increase biomass production beyond supplementation which could reduce the need to fix carbon (acetyl-CoA) and indirectly provide negligible energy conservation. Alanine, cysteine, glycine, and serine were predicted to decrease the amount of H_2 or CO_2 consumed because these amino acids might be utilized as carbon backbone and/or electron source under different conditions. The alanine coincides with predictions for the planktonic co-culture (Walker et al., 2012), but cysteine, glycine, and serine have not been previously considered and no other amino acids have been shown to serve as energy, carbon, and/or nitrogen sources for *M. maripaludis*. Preliminary data suggests that cysteine could increase growth in *M. maripaludis*, and further work is needed to delineate growth impacts of different amino acids.

The co-culture biofilm represents a unique phenotypic and physiological state as evident by the majority of significant changes unique to the syntrophic biofilm compared to the same co-culture condition in the planktonic state. Given the unique differences to the biofilm state, the transcriptomic data suggested that the two populations modulated carbon and electron flow but also altered characteristics at the cell surface (membranes, defense). However, a majority of the significant changes were putative proteins with unknown function(s), and further work focused on the biofilm growth mode and the emergent properties of metabolic interactions are needed.

Acknowledgments. This material by ENIGMA- Ecosystems and Networks Integrated with Genes and Molecular Assemblies (http://enigma.lbl.gov), a Scientific Focus Area Program at Lawrence Berkeley National Laboratory is based upon work supported by the U.S. Department of Energy, Office of Science, Office of Biological & Environmental Research under contract number DE-AC02-05CH11231.

REFERENCES CITED

Anders, S., Pyl, P. T., & Huber, W. (2015). HTSeq--a Python framework to work with high-throughput sequencing data. *Bioinformatics*, *31*(2), 166–169. http://doi.org/10.1093/bioinformatics/btu638

Arkin, A. P., Cottingham, R. W., Henry, C. S., Harris, N. L., Stevens, R. L., Maslov, S., … Yu, D. (2018). KBase: The United States Department of Energy Systems Biology Knowledgebase. *Nature Biotechnology*, *36*(7), 566–569. http://doi.org/10.1038/nbt.4163

Bolger, A. M., Lohse, M., & Usadel, B. (2014). Trimmomatic: a flexible trimmer for Illumina sequence data. *Bioinformatics*, *30*(15), 2114–2120. http://doi.org/10.1093/bioinformatics/btu170

Brileya, K. A., Camilleri, L. B., Zane, G. M., Wall, J. D., & Fields, M. W. (2014). Biofilm growth mode promotes maximum carrying capacity and community stability during product inhibition syntrophy. *Frontiers in Microbiology*, *5*(12), 693. http://doi.org/10.3389/fmicb.2014.00693

Bryant, M. P., Campbell, L. L., Reddy, C. A., & Crabill, M. R. (1977). Growth of Desulfovibrio in lactate or ethanol media low in sulfate in association with H2-utilizing methanogenic bacteria. *Applied and Environmental Microbiology*, *33*(5), 1162–9. Retrieved from http://www.ncbi.nlm.nih.gov/pubmed/879775

Burmølle, M., Ren, D., Bjarnsholt, T., & Sørensen, S. J. (2014). Interactions in multispecies biofilms: do they actually matter? *Trends in Microbiology*, *22*(2), 84–91. http://doi.org/10.1016/j.tim.2013.12.004

Carlson, R. P., Beck, A. E., Phalak, P., Fields, M. W., Gedeon, T., Hanley, L., … Heys, J. J. (2018). Competitive resource allocation to metabolic pathways contributes to overflow metabolisms and emergent properties in cross-feeding microbial consortia. *Biochemical Society Transactions*, *46*(2), 269–284. http://doi.org/10.1042/BST20170242

Clark, M. E., Edelmann, R. E., Duley, M. L., Wall, J. D., & Fields, M. W. (2007). Biofilm formation in Desulfovibrio vulgaris Hildenborough is dependent upon protein filaments. *Environmental Microbiology*, *9*(11), 2844–54. http://doi.org/10.1111/j.1462-2920.2007.01398.x

Clark, M. E., He, Q., He, Z., Huang, K. H., Alm, E. J., Wan, X.-F., … Fields, M. W. (2006). Temporal transcriptomic analysis as Desulfovibrio vulgaris Hildenborough transitions into stationary phase during electron donor depletion. *Applied and Environmental Microbiology*, *72*(8), 5578–88. http://doi.org/10.1128/AEM.00284-06

Clark, M. E., He, Z., Redding, A. M., Joachimiak, M. P., Keasling, J. D., Zhou, J. Z., … Fields, M. W. (2012). Transcriptomic and proteomic analyses of Desulfovibrio vulgaris biofilms: carbon and energy flow contribute to the distinct biofilm growth state. *BMC Genomics*, *13*(1), 138. http://doi.org/10.1186/1471-2164-13-138

Costa, K. C., Yoon, S. H., Pan, M., Burn, J. A., Baliga, N. S., & Leigh, J. A. (2013). Effects of H2 and Formate on Growth Yield and Regulation of Methanogenesis in Methanococcus maripaludis. Journal of Bacteriology, 195(7), 1456–1462. http://doi.org/10.1128/JB.02141-12

Costerton, J. W. (2007). *The Biofilm Primer*. (J. W. Costerton, Ed.) (Vol. 1). Springer Berlin Heidelberg. http://doi.org/10.1007/b136878

D'Souza, G., Shitut, S., Preussger, D., Yousif, G., Waschina, S., & Kost, C. (2018). Ecology and evolution of metabolic cross-feeding interactions in bacteria. *Natural Product Reports*, *35*(5), 455–488. http://doi.org/10.1039/C8NP00009C

Dean, A. M. (1985). The dynamics of microbial commensalisms and mutualisms. In D. H. Boucher (Ed.), *The Biology of Mutualism* (pp. 270–300). Oxford: Oxford University Press. Retrieved from https://books.google.com/books?hl=en&lr=&id=dWuQS_3F2P0C&oi=fnd&pg=PA270&ots=_vLqPPvfaW&sig=kQJWc5rcE0FIzy8fpfml3ZWn3-k#v=onepage&q&f=false

Dunne, W. M. J. (2002). Bacterial adhesion: seen any good biofilms lately? *Clinical Microbiology Reviews*, *15*(2), 155–166. http://doi.org/10.1128/CMR.15.2.155

Flemming, H. C., & Wuertz, S. (2019). Bacteria and archaea on Earth and their abundance in biofilms. *Nature Reviews Microbiology*, *17*(4), 247–260. http://doi.org/10.1038/s41579-019-0158-9

Gerstl, M. P., Jungreuthmayer, C., & Zanghellini, J. (2015). tEFMA: computing thermodynamically feasible elementary flux modes in metabolic networks. *Bioinformatics*, *31*(13), 2232–2234. http://doi.org/10.1093/bioinformatics/btv111

Gerstl, M. P., Ruckerbauer, D. E., Mattanovich, D., Jungreuthmayer, C., & Zanghellini, J. (2015). Metabolomics integrated elementary flux mode analysis in large metabolic networks. *Scientific Reports*, *5*(1), 8930. http://doi.org/10.1038/srep08930

Gross, S. M., Martin, J. A., Simpson, J., Abraham-Juarez, M., Wang, Z., & Visel, A. (2013). De novo transcriptome assembly of drought tolerant CAM plants, Agave deserti and Agave tequilana. *BMC Genomics*, *14*(1), 563. http://doi.org/10.1186/1471-2164-14-563

Hamilton, S., Bongaerts, R. J., Mulholland, F., Cochrane, B., Porter, J., Lucchini, S., … Hinton, J. C. (2009). The transcriptional programme of Salmonella enterica serovar Typhimurium reveals a key role for tryptophan metabolism in biofilms. *BMC Genomics*, *10*(1), 599. http://doi.org/10.1186/1471-2164-10-599

He, Z., Zhou, A., Baidoo, E., He, Q., Joachimiak, M. P., Benke, P., … Zhou, J. (2010). Global Transcriptional, Physiological, and Metabolite Analyses of the Responses of Desulfovibrio vulgaris Hildenborough to Salt Adaptation. *Applied and Environmental Microbiology*, *76*(5), 1574–1586. http://doi.org/10.1128/AEM.02141-09

Hendrickson, E. L., Haydock, A. K., Moore, B. C., Whitman, W. B., & Leigh, J. A. (2007). Functionally distinct genes regulated by hydrogen limitation and growth rate in methanogenic Archaea. *Proceedings of the National Academy of Sciences of the United States of America.*, *104*(21), 8930–8934. http://doi.org/10.1073/pnas.0701157104

Jones, W. J., Nagle, D. P., & Whitman, W. B. (1987). Methanogens and the diversity of archaebacteria. *Microbiological Reviews*, *51*(1), 135–77. Retrieved from http://www.pubmedcentral.nih.gov/articlerender.fcgi?artid=373095&tool=pmcentrez&rendertype=abstract

Kolter, R. (2005). Surfacing views of biofilm biology. *Trends in Microbiology*, *13*(1), 1–2. http://doi.org/10.1016/j.tim.2004.11.003

Krumholz, L. R., Bradstock, P., Sheik, C. S., Diao, Y., Gazioglu, O., Gorby, Y., & McInerney, M. J. (2015). Syntrophic Growth of Desulfovibrio alaskensis Requires Genes for H 2 and Formate Metabolism as Well as Those for Flagellum and Biofilm Formation. *Applied and Environmental Microbiology*, *81*(7), 2339–2348. http://doi.org/10.1128/AEM.03358-14

Langmead, B., & Salzberg, S. L. (2012). Fast gapped-read alignment with Bowtie 2. *Nature Methods*, *9*(4), 357–359. http://doi.org/10.1038/nmeth.1923

McInerney, M. J., & Bryant, M. P. (1981). Anaerobic degradation of lactate by syntrophic associations of Methanosarcina barkeri and Desulfovibrio species and effect of H2 on acetate degradation. *Applied and Environmental Microbiology*, *41*(2), 346–354.

Momeni, B., Brileya, K. A., Fields, M. W., & Shou, W. (2013). Strong inter-population cooperation leads to partner intermixing in microbial communities. *ELife*, *2*, e00230. http://doi.org/10.7554/eLife.00230

Odom, J. M., & Peck, H. D. (1981). Hydrogen cycling as a general mechanism for energy coupling in the sulfate-reducing bacteria, Desulfovibrio sp. *FEMS Microbiology Letters*, *12*, 47–50.

Or, D., Smets, B. F., Wraith, J. M., Dechesne, A., & Friedman, S. P. (2007). Physical constraints affecting bacterial habitats and activity in unsaturated porous media – a review. *Advances in Water Resources*, *30*(6–7), 1505–1527. http://doi.org/10.1016/j.advwatres.2006.05.025

Pande, S., Kaftan, F., Lang, S., Svatoš, A., Germerodt, S., & Kost, C. (2016). Privatization of cooperative benefits stabilizes mutualistic cross-feeding interactions in spatially structured environments. *The ISME Journal*, *10*(6), 1413–1423. http://doi.org/10.1038/ismej.2015.212

Pankhania, I. P., Spormann, A. M., Hamilton, W. A., & Thauer, R. K. (1988). Lactate conversion to acetate, CO2 and H2 in cell suspensions of Desulfovibrio vulgaris (Marburg): indications for the involvement of an energy driven reaction. *Archives of Microbiology*, *150*(1), 26–31. http://doi.org/10.1007/BF00409713

Peck, H. D. (1960). Evidence for oxidative phosphorylation during the reduction of sulfate with hydrogen by Desulfovibrio desulfuricans. *The Journal of Biological Chemistry*, *235*(9), 2734–2738.

Plugge, C. M., Scholten, J. C. M., Culley, D. E., Nie, L., Brockman, F. J., & Zhang, W. (2010). Global transcriptomics analysis of the Desulfovibrio vulgaris change from syntrophic growth with Methanosarcina barkeri to sulfidogenic metabolism. *Microbiology*, *156*(Pt 9), 2746–56. http://doi.org/10.1099/mic.0.038539-0

Robinson, M. D., McCarthy, D. J., & Smyth, G. K. (2010). edgeR: a Bioconductor package for differential expression analysis of digital gene expression data. *Bioinformatics*, *26*(1), 139–140. http://doi.org/10.1093/bioinformatics/btp616

Thauer, R. K. (2012). The Wolfe cycle comes full circle. *Proceedings of the National Academy of Sciences*, *109*(38), 15084–15085. http://doi.org/10.1073/pnas.1213193109

Ueno, Y., Yamada, K., Yoshida, N., Maruyama, S., & Isozaki, Y. (2006). Evidence from fluid inclusions for microbial methanogenesis in the early Archaean era. *Nature*, *440*(7083), 516–519. http://doi.org/10.1038/nature04584

Voordouw, G. (2002). Carbon Monoxide Cycling by Desulfovibrio vulgaris Hildenborough, *184*(21), 5903–5911. http://doi.org/10.1128/JB.184.21.5903

Walker, C. B., He, Z., Yang, Z. K., Ringbauer, J. A, He, Q., Zhou, J., … Stahl, D. A. (2009). The electron transfer system of syntrophically grown Desulfovibrio vulgaris. *Journal of Bacteriology*, *191*(18), 5793–801. http://doi.org/10.1128/JB.00356-09

Walker, C. B., Redding-Johanson, A. M., Baidoo, E. E., Rajeev, L., He, Z., Hendrickson, E. L., … Stahl, D. A. (2012). Functional responses of methanogenic archaea to syntrophic growth. *The ISME Journal*, *6*(11), 2045–2055.

Wingett, S. W., & Andrews, S. (2018). FastQ Screen: A tool for multi-genome mapping and quality control. *F1000Research*, *7*(0), 1338. http://doi.org/10.12688/f1000research.15931.1

Wyndham, R. C., & Costerton, J. W. (1981). Heterotrophic potentials and hydrocarbon biodegradation potentials of sediment microorganisms within the athabasca oil sands deposit. *Applied and Environmental Microbiology*, *41*(3), 783–90. Retrieved from http://www.pubmedcentral.nih.gov/articlerender.fcgi?artid=243775&tool=pmcentrez&rendertype=abstract

Zelezniak, A., Andrejev, S., Ponomarova, O., & Mende, D. R. (2015). Metabolic dependencies drive species co-occurrence in diverse microbial communities. *Proceedings of the National Academy of Sciences*, *112*(20), 201522642. http://doi.org/10.1073/pnas.1522642113

SUPPLEMENTAL MATERIAL

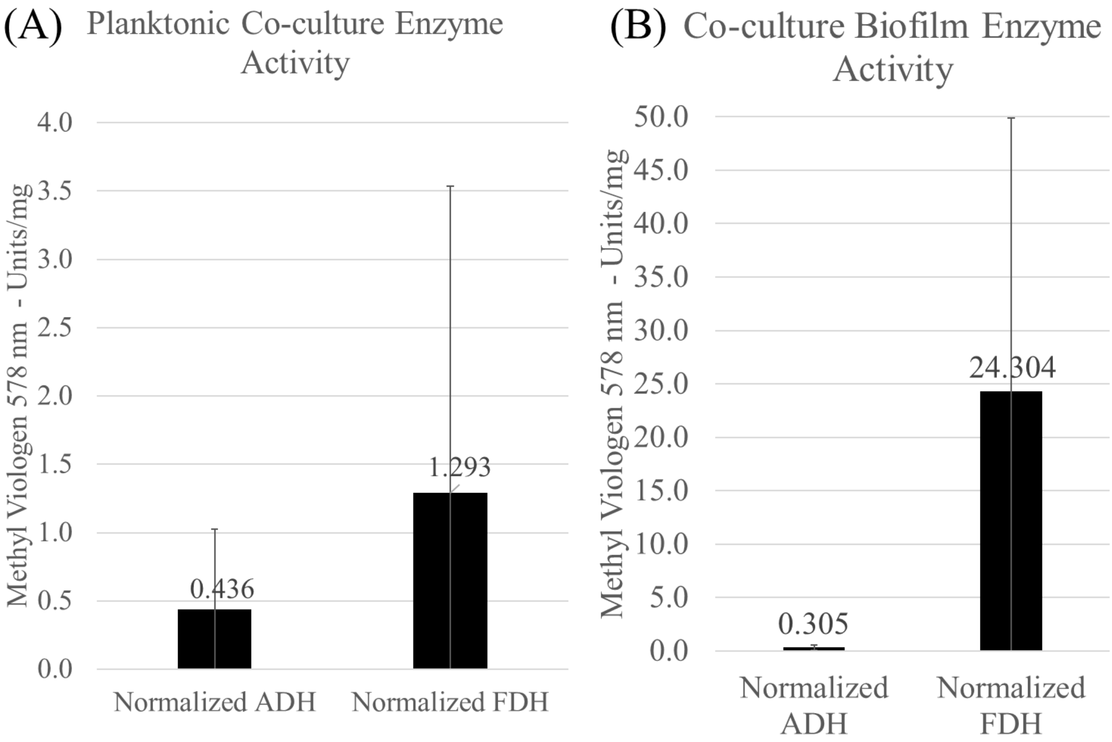

Figure S1. Enzymatic activity of co-culture was tested. Activity profiles for alcohol dehydrogenase (ADH) and formate dehydrogenase (FDH) were performed with methyl viologen (578 nm) and normalized to biomass levels for (A) Planktonic co-culture samples of *D. vulgaris* and *M. maripaludis*, and (B) Co-culture biofilm samples of *D. vulgaris* and *M. maripaludis*.

Table S1. Stoichiometric equations used for the *Desulfovibrio vulgaris* Hildenborough model.

		gpr	gene ID	KO	enzyme	definition
1	<->	kb|g.3562.peg.1908	DVU2147	K01752	4.3.1.17	(1) L-Threonine_c0[c0] <-> (1) NH3_c0[c0] + (1) 2-Oxobutyrate_c0[c0]
2	->	kb|g.3562.peg.2084	DVU0360	K01652	2.2.1.6	(1) Pyruvate_c0[c0] + (1) H+_c0[c0] + (1) 2-Oxobutyrate_c0[c0] <-> (1) CO2_c0[c0] + (1) 2-Aceto-2-hydroxybutanoate_c0[c0]
3	->	kb|g.3562.peg.2251	DVU0361	K01653	2.2.1.6	
4	->	kb|g.3562.peg.681	DVU1376	K01652	2.2.1.6	
5	->	kb|g.3562.peg.915	DVU1377	K01653	2.2.1.6	
6	<->	kb|g.3562.peg.365	DVU1378	K00053	1.1.1.86	(1) NADPH_c0[c0] + (1) H+_c0[c0] + (1) 2-Aceto-2-hydroxybutanoate_c0[c0] <-> (1) NADP_c0[c0] + (1) 2,3-Dihydroxy-3-methylvalerate_c0[c0]
7	->	kb|g.3562.peg.2111	DVU3373	K01687	4.2.1.9	(1) 2,3-Dihydroxy-3-methylvalerate_c0[c0] <-> (1) H2O_c0[c0] + (1) 3MOP_c0[c0]
8	<->	kb|g.3562.peg.2245	DVU3197	K00826	2.6.1.42	(1) 2-Oxoglutarate_c0[c0] + (1) L-Isoleucine_c0[c0] <-> (1) L-Glutamate_c0[c0] + (1) 3MOP_c0[c0]
9	->	kb|g.3562.peg.2084	DVU0360	K01652	2.2.1.6	(2) Pyruvate_c0[c0] + (1) H+_c0[c0] = (1) CO2_c0[c0] + (1) ALCTT_c0[c0]
10	->	kb|g.3562.peg.2251	DVU0361	K01653	2.2.1.6	
11	->	kb|g.3562.peg.681	DVU1376	K01652	2.2.1.6	
12	->	kb|g.3562.peg.915	DVU1377	K01653	2.2.1.6	
13	<->	kb|g.3562.peg.365	DVU1378	K00053	1.1.1.86	(1) NADPH_c0[c0] + (1) H+_c0[c0] + (1) ALCTT_c0[c0] <-> (1) NADP_c0[c0] + (1) 2,3-Dihydroxy-isovalerate_c0[c0]
14	->	kb|g.3562.peg.2111	DVU3373	K01687	4.2.1.9	(1) 2,3-Dihydroxy-isovalerate_c0[c0] <-> (1) H2O_c0[c0] + (1) 3-Methyl-2-oxobutanoate_c0[c0]
15	<->	kb|g.3562.peg.2245	DVU3197	K00826	2.6.1.42	(1) 2-Oxoglutarate_c0[c0] + (1) L-Valine_c0[c0] <-> (1) L-Glutamate_c0[c0] + (1) 3-Methyl-2-oxobutanoate_c0[c0]
16	->	kb|g.3562.peg.1204	DVU2981	K01649	2.3.3.13	(1) H2O_c0[c0] + (1) Acetyl-CoA_c0[c0] + (1) 3-Methyl-2-oxobutanoate_c0[c0] <-> (1) CoA_c0[c0] + (1) H+_c0[c0] + (1) 2-Isopropylmalate_c0[c0]
17	<->	kb|g.3562.peg.1682	DVU2982	K01703	4.2.1.33 +4.2.1.35	(1) 2-Isopropylmalate_c0[c0] <-> (1) H2O_c0[c0] + (1) 2-Isopropylmaleate_c0[c0]
18	<->	kb|g.3562.peg.1442	DVU2983	K01704	4.2.1.33 +4.2.1.35	
19	<->	kb|g.3562.peg.1682	DVU2982	K01703	4.2.1.33 +4.2.1.35	(1) 3-Isopropylmalate_c0[c0] <-> (1) H2O_c0[c0] + (1) 2-Isopropylmaleate_c0[c0]
20	->	kb|g.3562.peg.1442	DVU2983	K01704	4.2.1.33 +4.2.1.35	
21	->	kb|g.3562.peg.1699	DVU2985	K00052	1.1.1.85	(1) NAD_c0[c0] + (1) 3-Isopropylmalate_c0[c0] <-> (1) NADH_c0[c0] + (1) H+_c0[c0] + (1) 2-isopropyl-3-oxosuccinate_c0[c0]

		gpr	gene ID	KO	enzyme	definition
22	->	Spontaneous	Spontaneous	Spontaneous	Spontaneous	(1) H+_c0[c0] + (1) 2-isopropyl-3-oxosuccinate_c0[c0] <-> (1) CO2_c0[c0] + (1) 4MOP_c0[c0]
23	<->	kb|g.3562.peg.2245	DVU3197	K00826	2.6.1.42	(1) 2-Oxoglutarate_c0[c0] + (1) L-Leucine_c0[c0] <-> (1) L-Glutamate_c0[c0] + (1) 4MOP_c0[c0]
24	<->	kb|g.3562.peg.2501	DVU0462	K14170	5.4.99.5+4.2.1.51	(1) NAD_c0[c0] + (1) Prephenate_c0[c0] <-> (1) NADH_c0[c0] + (1) CO2_c0[c0] + (1) p-hydroxyphenylpyruvate_c0[c0]
25	<->	kb|g.3562.peg.3198	DVU0841	K11358	2.6.1.1	(1) 2-Oxoglutarate_c0[c0] + (1) L-Tyrosine_c0[c0] <-> (1) L-Glutamate_c0[c0] + (1) p-hydroxyphenylpyruvate_c0[c0]
26	<->	kb|g.3562.peg.2686	DVU3223	K00812	2.6.1.1	
27	<->	kb|g.3562.peg.2358	DVU0465	K01657	4.1.3.27	(1) L-Glutamine_c0[c0] + (1) Chorismate_c0[c0] <-> (1) Pyruvate_c0[c0] + (1) L-Glutamate_c0[c0] + (1) H+_c0[c0] + (1) Anthranilate_c0[c0]
28	<->	kb|g.3562.peg.2101	DVU0467	K00766	2.4.2.18	(1) PPi_c0[c0] + (1) N-5-phosphoribosyl-anthranilate_c0[c0] <-> (1) Anthranilate_c0[c0] + (1) PRPP_c0[c0]
29	<->	kb|g.3562.peg.2797	DVU0469	K01817	5.3.1.24	(1) N-5-phosphoribosyl-anthranilate_c0[c0] <-> (1) 1-(2-carboxyphenylamino)-1-deoxyribulose-5-phosphate_c0[c0]
30	<->	kb|g.3562.peg.2756	DVU0468	K01609	4.1.1.48	(1) H+_c0[c0] + (1) 1-(2-carboxyphenylamino)-1-deoxyribulose-5-phosphate_c0[c0] <-> (1) H2O_c0[c0] + (1) CO2_c0[c0] + (1) Indoleglycerol-phosphate_c0[c0]
31	<->	kb|g.3562.peg.2598	DVU0471	K01695	4.2.1.20	(1) L-Serine_c0[c0] + (1) Indoleglycerol-phosphate_c0[c0] <-> (1) H2O_c0[c0] + (1) L-Tryptophan_c0[c0] + (1) Glyceraldehyde3-phosphate_c0[c0]
32	<->	kb|g.3562.peg.2973	DVU0470	K01696	4.2.1.20	
33	<->	kb|g.3562.peg.2598	DVU0471	K01695	4.2.1.20	
34	<->	kb|g.3562.peg.3125	DVU0085	K01696	4.2.1.20	
35	<->	Unknown	#N/A	K00641	2.3.1.31	(1) Acetyl-CoA_c0[c0] + (1) L-Homoserine_c0[c0] <-> (1) CoA_c0[c0] + (1) O-Acetyl-L-homoserine_c0[c0]
36	<->	Unknown	#N/A	K01740	2.5.1.49	(1) H2S_c0[c0] + (1) O-Acetyl-L-homoserine_c0[c0] <-> (1) Acetate_c0[c0] + (1) Homocysteine_c0[c0] + (1) H+
37	->	kb|g.3562.peg.180	DVU1585	K00548	2.1.1.13	(1) Homocysteine_c0[c0] + (1) 5-Methyltetrahydrofolate_c0[c0] <-> (1) L-Methionine_c0[c0] + (1) THF_c0[c0]
38	<->	kb|g.3562.peg.3121	DVU0997	K00297	1.5.1.20	(1) NAD_c0[c0] + (1) 5-Methyltetrahydrofolate_c0[c0] <-> (1) NADH_c0[c0] + (1) H+_c0[c0] + (1) 5-10-Methylenetetrahydrofolate_c0[c0]
39	->	kb|g.3562.peg.3177	DVU0930	K00931	2.7.2.11	(1) ATP_c0[c0] + (1) L-Glutamate_c0[c0] + (1) H+ <-> (1) ADP_c0[c0] + (1) L-Glutamyl-5-phosphate_c0[c0]
40	<->	kb|g.3562.peg.916	DVU1953	K00147	1.2.1.41	(1) NADP_c0[c0] + (1) Phosphate_c0[c0] + (1) L-Glutamate5-semialdehyde_c0[c0] <-> (1) NADPH_c0[c0] + (1) L-Glutamyl-5-phosphate_c0[c0]
41	->	kb|g.3562.peg.2146	DVU3319	K00294	1.2.1.88	(1) L-Glutamate5-semialdehyde_c0[c0] + (1) NAD_c0[c0] + (1) H2O_c0[c0] = (1) L-

		gpr	gene ID	KO	enzyme	definition
						Glutamate_c0[c0] + (1) NADH_c0[c0] + (2) H+_c0[c0]
42	<->	Spontaneous	Spontaneous	Spontaneous	Spontaneous	(1) H2O_c0[c0] + (1) H+_c0[c0] + (1) 1-Pyrroline-5-carboxylate_c0[c0] <-> (1) L-Glutamate5-semialdehyde_c0[c0]
43	->	kb|g.3562.peg.1883	DVU2332	K00286	1.5.1.2	(1) NADPH_c0[c0] + (1) H+_c0[c0] + (1) 1-Pyrroline-5-carboxylate_c0[c0] <-> (1) NADP_c0[c0] + (1) L-Proline_c0[c0]
44	<->	kb|g.3562.peg.3198	DVU0841	K11358	2.6.1.1	(1) 2-Oxoglutarate_c0[c0] + (1) L-Aspartate_c0[c0] <-> (1) L-Glutamate_c0[c0] + (1) Oxaloacetate_c0[c0]
45	<->	kb|g.3562.peg.2686	DVU3223	K00812	2.6.1.1	
46	<->	kb|g.3562.peg.1183	DVU2476	K00266	1.4.1.13 +1.4.1.14	(1) H2O_c0[c0] + (1) NADP_c0[c0] + (1) L-Glutamate_c0[c0] <-> (1) NADPH_c0[c0] + (1) NH3_c0[c0] + (1) 2-Oxoglutarate_c0[c0] + (1) H+_c0[c0]
47	<->	kb|g.3562.peg.2718	DVU3392	K01915	6.3.1.2	(1) ATP_c0[c0] + (1) NH3_c0[c0] + (1) L-Glutamate_c0[c0] <-> (1) ADP_c0[c0] + (1) Phosphate_c0[c0] + (1) L-Glutamine_c0[c0] + (1) H+_c0[c0]
48	<->	kb|g.3562.peg.454	DVU1878	K01620	4.1.2.48	(1) L-Threonine_c0[c0] <-> (1) Glycine_c0[c0] + (1) Acetaldehyde_c0[c0]
49	<->	kb|g.3562.peg.1908	DVU2147	K01752	4.3.1.17	(1) L-Serine_c0[c0] <-> (1) NH3_c0[c0] + (1) Pyruvate_c0[c0]
50	<->	kb|g.3562.peg.12	DVU1913	K00928	2.7.2.4	(1) ATP_c0[c0] + (1) L-Aspartate_c0[c0] + (1) H+c0[c0] <-> (1) ADP_c0[c0] + (1) 4-Phospho-L-aspartate_c0[c0]
51	<->	kb|g.3562.peg.1576	DVU3048	K00133	1.2.1.11	(1) NADP_c0[c0] + (1) Phosphate_c0[c0] + (1) L-Aspartate4-semialdehyde_c0[c0] <-> (1) NADPH_c0[c0] + (1) 4-Phospho-L-aspartate_c0[c0]
52	<->	kb|g.3562.peg.3126	DVU0890	K00003	1.1.1.3	(1) NADP_c0[c0] + (1) L-Homoserine_c0[c0] <-> (1) NADPH_c0[c0] + (1) H+_c0[c0] + (1) L-Aspartate4-semialdehyde_c0[c0]
53	<->	kb|g.3562.peg.1681	DVU0292	no KO assigned	0	(1) ATP_c0[c0] + (1) L-Homoserine_c0[c0] <-> (1) ADP_c0[c0] + (1) O-Phospho-L-homoserine_c0[c0]
54	->	kb|g.3562.peg.2320	DVU3210	K01733	4.2.3.1	(1) H2O_c0[c0] + (1) O-Phospho-L-homoserine_c0[c0] <-> (1) Phosphate_c0[c0] + (1) L-Threonine_c0[c0] + (1) H+_c0[c0]
55	<->	kb|g.3562.peg.2156	DVU0662	K00640	2.3.1.30	(1) Acetyl-CoA_c0[c0] + (1) L-Serine_c0[c0] <-> (1) CoA_c0[c0] + (1) O-Acetyl-L-serine_c0[c0]
56	<->	kb|g.3562.peg.2524	DVU0663	K01738	2.5.1.47	(1) H2S_c0[c0] + (1) O-Acetyl-L-serine_c0[c0] <-> (1) Acetate_c0[c0] + (1) L-Cysteine_c0[c0] + (1) H+_c0[c0]
57	<->	kb|g.3562.peg.547	DVU1624	K01627	2.5.1.55	(1) H2O_c0[c0] + (1) Phosphoenolpyruvate_c0[c0] + (1) D-Erythrose4-phosphate_c0[c0] <-> (1) Phosphate_c0[c0] + (1) DAHP_c0[c0] + (1) H+_c0[c0]
58	<->	kb|g.3562.peg.2649	DVU0461	no KO assigned	0	(1) DAHP_c0[c0] <-> (1) Phosphate_c0[c0] + (1) 5-Dehydroquinate_c0[c0] + (1) H+_c0[c0]

		gpr	gene ID	KO	enzyme	definition
59	<->	kb|g.3562.peg.721	DVU1665	K03786	4.2.1.10	(1) 5-Dehydroquinate_c0[c0] <-> (1) H2O_c0[c0] + (1) 3-Dehydroshikimate_c0[c0]
60	<->	kb|g.3562.peg.463	DVU0115	K00014	1.1.1.25	(1) NADP_c0[c0] + (1) Shikimate_c0[c0] <-> (1) NADPH_c0[c0] + (1) H+_c0[c0] + (1) 3-Dehydroshikimate_c0[c0]
61	->	kb|g.3562.peg.1964	DVU2521	K00891	2.7.1.71	(1) ATP_c0[c0] + (1) Shikimate_c0[c0] <-> (1) ADP_c0[c0] + (1) 3-phosphoshikimate_c0[c0]
62	->	kb|g.3562.peg.3064	DVU0892	K00891	2.7.1.71	
63	<->	kb|g.3562.peg.2655	DVU0463	K00800	2.5.1.19	(1) Phosphoenolpyruvate_c0[c0] + (1) 3-phosphoshikimate_c0[c0] <-> (1) Phosphate_c0[c0] + (1) 5-O--1-Carboxyvinyl-3-phosphoshikimate_c0[c0] + (1) H+_c0[c0]
64	->	kb|g.3562.peg.3229	DVU0894	K01736	4.2.3.5	(1) 5-O--1-Carboxyvinyl-3-phosphoshikimate_c0[c0] <-> (1) Phosphate_c0[c0] + (1) Chorismate_c0[c0] + (1) H+_c0[c0]
65	<->	kb|g.3562.peg.547	DVU1624	K01627	2.5.1.55	(1) Chorismate_c0[c0] <-> (1) Prephenate_c0[c0]
66	<->	kb|g.3562.peg.2501	DVU0462	K14170	5.4.99.5 +4.2.1.51	(1) H+_c0[c0] + (1) Prephenate_c0[c0] <-> (1) H2O_c0[c0] + (1) CO2_c0[c0] + (1) Phenylpyruvate_c0[c0]
67	<->	kb|g.3562.peg.3198	DVU0841	K11358	2.6.1.1	(1) 2-Oxoglutarate_c0[c0] + (1) L-Phenylalanine_c0[c0] <-> (1) L-Glutamate_c0[c0] + (1) Phenylpyruvate_c0[c0]
68	<->	kb|g.3562.peg.2686	DVU3223	K00812	2.6.1.1	
69	->	kb|g.3562.peg.1091	DVU3014	K01953	6.3.5.4	(1) H2O_c0[c0] + (1) ATP_c0[c0] + (1) L-Aspartate_c0[c0] + (1) L-Glutamine_c0[c0] <-> (1) PPi_c0[c0] + (1) AMP_c0[c0] + (1) L-Glutamate_c0[c0] + (1) L-Asparagine_c0[c0]
70	<->	kb|g.3562.peg.905	DVU1868	K01714	4.3.3.7	(1) Pyruvate_c0[c0] + (1) L-Aspartate4-semialdehyde_c0[c0] <-> (2) H2O_c0[c0] + (1) H+_c0[c0] + (1) Dihydrodipicolinate_c0[c0]
71	->	kb|g.3562.peg.643	DVU1609	K00215	1.17.1.8	(1) NADPH_c0[c0] + (1) H+_c0[c0] + (1) Dihydrodipicolinate_c0[c0] <-> (1) NADP_c0[c0] + (1) tetrahydrodipicolinate_c0[c0]
72	<->	kb|g.3562.peg.401	DVU1655	K10206	2.6.1.83	(1) 2-Oxoglutarate_c0[c0] + (1) LL-2,6-Diaminopimelate_c0[c0] <-> (1) H2O_c0[c0] + (1) L-Glutamate_c0[c0] + (1) H+_c0[c0] + (1) tetrahydrodipicolinate_c0[c0]
73	<->	kb|g.3562.peg.47	DVU1867	K01778	5.1.1.7	(1) LL-2,6-Diaminopimelate_c0[c0] <-> (1) meso-2,6-Diaminopimelate_c0[c0]
74	->	kb|g.3562.peg.258	DVU1647	K01586	4.1.1.20	(1) H+_c0[c0] + (1) meso-2,6-Diaminopimelate_c0[c0] <-> (1) CO2_c0[c0] + (1) L-Lysine_c0[c0]
75	->	kb|g.3562.peg.1978	DVU2566	K01586	4.1.1.20	
76	->	kb|g.3562.peg.2545	DVU0823	K00620	2.3.1.35 +2.3.1.1	(1) Acetyl-CoA_c0[c0] + (1) L-Glutamate_c0[c0] <-> (1) CoA_c0[c0] + (1) H+_c0[c0] + (1) N-Acetyl-L-glutamate_c0[c0]
77	<->	kb|g.3562.peg.206	DVU1466	K00930	2.7.2.8	(1) ATP_c0[c0] + (1) N-Acetyl-L-glutamate_c0[c0] + (1) H+_c0[c0] <-> (1) ADP_c0[c0] + (1) n-acetylglutamyl-phosphate_c0[c0]

		gpr	gene ID	KO	enzyme	definition
78	<->	kb|g.3562.peg.2162	DVU0492	K00145	1.2.1.38	(1) NADP_c0[c0] + (1) Phosphate_c0[c0] + (1) 2-Acetamido-5-oxopentanoate_c0[c0] <-> (1) NADPH_c0[c0] + (1) n-acetylglutamyl-phosphate_c0[c0]
79	<->	kb|g.3562.peg.1885	DVU2347	K00821	2.6.1.11 +2.6.1.17	(1) 2-Oxoglutarate_c0[c0] + (1) N-Acetylornithine_c0[c0] <-> (1) L-Glutamate_c0[c0] + (1) 2-Acetamido-5-oxopentanoate_c0[c0]
80	->	kb|g.3562.peg.2545	DVU0823	K00620	2.3.1.35 +2.3.1.1	(1) L-Glutamate_c0[c0] + (1) N-Acetylornithine_c0[c0] <-> (1) N-Acetyl-L-glutamate_c0[c0] + (1) ornithine_c0[c0]
81	<->	kb|g.3562.peg.622	DVU0162	K01955	6.3.5.5	(1) H2O_c0[c0] + (2) ATP_c0[c0] + (1) L-Glutamine_c0[c0] + (1) H2CO3_c0[c0] <-> (2) ADP_c0[c0] + (1) Phosphate_c0[c0] + (1) L-Glutamate_c0[c0] + (1) H+_c0[c0] + (1) Carbamoylphosphate_c0[c0]
82	<->	kb|g.3562.peg.2343	DVU3113	K01956	6.3.5.5	
83	<->	kb|g.3562.peg.56	DVU1096	no KO assigned	0	(1) Carbamoylphosphate_c0[c0] + (1) Ornithine_c0[c0] <-> (1) Phosphate_c0[c0] + (2) H+_c0[c0] + (1) Citrulline_c0[c0]
84	<->	kb|g.3562.peg.195	DVU1095	K01940	6.3.4.5	(1) ATP_c0[c0] + (1) L-Aspartate_c0[c0] + (1) Citrulline_c0[c0] <-> (1) PPi_c0[c0] + (1) AMP_c0[c0] + (1) L-Argininosuccinate_c0[c0]
85	<->	kb|g.3562.peg.352	DVU1094	K01755	4.3.2.1	(1) L-Argininosuccinate_c0[c0] <-> (1) L-Arginine_c0[c0] + (1) Fumarate_c0[c0]
86	<->	kb|g.3562.peg.603	DVU0114	K00765	2.4.2.17	(1) PPi_c0[c0] + (1) Phosphoribosyl-ATP_c0[c0] <-> (1) ATP_c0[c0] + (1) PRPP_c0[c0]
87	->	kb|g.3562.peg.515	DVU0113	K01496	3.5.4.19	(1) H2O_c0[c0] + (1) Phosphoribosyl-ATP_c0[c0] <-> (1) PPi_c0[c0] + (1) Phosphoribosyl-AMP_c0[c0]
88	->	kb|g.3562.peg.515	DVU0113	K01496	3.5.4.19	(1) H2O_c0[c0] + (1) Phosphoribosyl-AMP_c0[c0] <-> (1) phosphoribosylformiminoaicar-phosphate_c0[c0]
89	->	kb|g.3562.peg.3234	DVU1038	K01814	5.3.1.16	(1) phosphoribosylformiminoaicar-phosphate_c0[c0] <-> (1) phosphoribulosylformimino-AICAR-phosphate_c0[c0]
90	->	kb|g.3562.peg.1962	DVU0285	K02501	2.4.2.-	(1) L-Glutamine_c0[c0] + (1) phosphoribulosylformimino-AICAR-phosphate_c0[c0] <-> (1) L-Glutamate_c0[c0] + (1) H+_c0[c0] + (1) D-erythro-imidazol-glycerol-phosphate_c0[c0] + (1) AICAR_c0[c0]
91	->	kb|g.3562.peg.1128	DVU0286	K02500	4.1.3.-	
92	->	kb|g.3562.peg.3159	DVU1040	K01693	4.2.1.19	(1) D-erythro-imidazol-glycerol-phosphate_c0[c0] <-> (1) H2O_c0[c0] + (1) imidazole-acetol-phosphate_c0[c0]
93	<->	kb|g.3562.peg.3026	DVU1029	K00817	2.6.1.9	(1) 2-Oxoglutarate_c0[c0] + (1) L-histidinol-phosphate_c0[c0] <-> (1) L-Glutamate_c0[c0] + (1) imidazole-acetol-phosphate_c0[c0]
94	->	kb|g.3562.peg.1308	DVU2490	K04486	3.1.3.15	(1) H2O_c0[c0] + (1) L-histidinol-phosphate_c0[c0] <-> (1) Phosphate_c0[c0] + (1) L-Histidinol_c0[c0] + (1) H+_c0[c0]

		gpr	gene ID	KO	enzyme	definition
95	->	kb|g.3562.peg.2553	DVU0796	K00013	1.1.1.23	(1) H2O_c0[c0] + (2) NAD_c0[c0] + (1) L-Histidinol_c0[c0] <-> (2) NADH_c0[c0] + (3) H+_c0[c0] + (1) L-Histidine_c0[c0]
96	<->	kb|g.3562.peg.2004	DVU0571	K00259	1.4.1.1	(1) H2O_c0[c0] + (1) NAD_c0[c0] + (1) Alanine_c0[c0] <-> (1) NADH_c0[c0] + (1) NH3_c0[c0] + (1) Pyruvate_c0[c0] + (1) H+_c0[c0]
97	<->	kb|g.3562.peg.1853	DVU2929	K03046	2.7.7.6	(1) H2O_c0[c0] + (1) N-Acetylornithine_c0[c0] <-> (1) Acetate_c0[c0] + (1) Ornithine_c0[c0]
98	->	Unknown	#N/A	#N/A	#N/A	11.5 Alanine_c0 + 1.5 L-cysteine_c0 + 5.7 L-aspartate_c0 + 5.9 L-glutamate_c0 + 3.6 L-phenylalanine_c0 + 8.6 Glycine_c0 + 2.4 L-histidine_c0 + 4.4 L-isoleucine_c0 + 3.1 L-lysine_c0 + 10.4 L-leucine_c0 + 2.8 L-methionine_c0 + 2.4 L-asparagine_c0 + 5.2 L-proline_c0 + 3 L-glutamine_c0 + 7.6 L-arginine_c0 + 5.2 L-serine_c0 + 5.5 L-threonine_c0 + 7.8 L-valine_c0 + 1.2 L-tryptophan_c0 + 2.3 L-tyrosine_c0 + 100 ATP_c0 + 198 GTP_c0 + 199 H2O_c0 = 198 phosphate_c0 + 100 PPi_c0 + 100 AMP_c0 + 198 GDP_c0 + 1 Protein_c0 + 193 H+_c0
99	->	Unknown	#N/A	#N/A	#N/A	0.1838 dATP_c0 + 0.1838 TTP_c0 + 0.3162 dGTP_c0 + 0.3162 dCTP_c0 = 1 DNA_c0 + 1 Ppi_c0
100	->	Unknown	#N/A	#N/A	#N/A	1.94 ATP_c0 + 2.5 UTP_c0 + 2.37 GTP_c0 + 3.19 CTP_c0 = 1 RNA_c0 + 10 PPi_c0
101	->	Unknown	#N/A	#N/A	#N/A	5 glucose-1-phosphate_c0 + 4 H2O_c0 = 1 Glycogen_c0 + 5 phosphate_c0 + 5 H+_c0
102	->	kb|g.3562.peg.445	DVU1636	K01507	3.6.1.1	(1) H2O_c0[c0] + (1) PPi_c0[c0] <-> (2) Phosphate_c0[c0] + (2) H+_c0[c0]
103	<->	kb|g.3562.peg.98	DVU1769	K00533	1.12.7.2	(1) H2_c0[c0] + (2) Ferricytochromec3_c0[c0] <-> (2) H+_e0[e0] + (2) Ferrocytochromec3_c0[c0]
104	<->	kb|g.3562.peg.96	DVU1770	K00534	1.12.7.3	
105	<->	kb|g.3562.peg.228	DVU1917			
106	<->	kb|g.3562.peg.611	DVU1921			
107	<->	kb|g.3562.peg.669	DVU1922			
108	->	kb|g.3562.peg.1806	DVU2399			(1) H2_c0[c0] + (1) NAD_c0[c0] <-> (1) NADH_c0[c0] + (1) H+_c0[c0]
109	->	kb|g.3562.peg.1568	DVU2400			
110	->	kb|g.3562.peg.1152	DVU2401			
111	->	kb|g.3562.peg.1160	DVU2402			
112	->	kb|g.3562.peg.1242	DVU2403			
113	->	kb|g.3562.peg.1420	DVU2404			
114	<->	kb|g.3562.peg.1957	DVU2286		1.6.99.5	(1) H2_c0[c0] + (2) H+_c0[c0] + (1) Menaquinone 8_c0[c0] <-> (2) H+_e0[e0] + (1) Menaquinol 8_c0[c0]
115	<->	kb|g.3562.peg.1514	DVU2287			
116	<->	kb|g.3562.peg.1644	DVU2288			
117	<->	kb|g.3562.peg.1241	DVU2289			
118	<->	kb|g.3562.peg.1102	DVU2290			
119	<->	kb|g.3562.peg.1528	DVU2291			
120	<->	kb|g.3562.peg.1415	DVU2292			

		gpr	gene ID	KO	enzyme	definition
121	<->	kb|g.3562.peg.1795	DVU2293			
122	<->	kb|g.3562.peg.2708	DVU0429		1.12.7.2	(1) H2_c0[c0] + (1) H+_e0[e0] + (2) Oxidizedferredoxin_c0[c0] <-> (3) H+_c0[c0] + (2) Reducedferredoxin_c0[c0]
123	<->	kb|g.3562.peg.2885	DVU0430			
124	<->	kb|g.3562.peg.2659	DVU0431			
125	<->	kb|g.3562.peg.2533	DVU0432			
126	<->	kb|g.3562.peg.2943	DVU0433			
127	<->	kb|g.3562.peg.2336	DVU0434			
128	<->	kb|g.3562.peg.2037	DVU0775	K02112	3.6.3.14	(1) H2O_c0[c0] + (1) ATP_c0[c0] + (2.4) H+_c0[c0] <-> (1) ADP_c0[c0] + (1) Phosphate_c0[c0] + (3.4) H+_e0[e0]
129	<->	kb|g.3562.peg.2498	DVU0777	K02111		
130	<->	kb|g.3562.peg.2377	DVU0776	K02115		
131	<->	kb|g.3562.peg.2627	DVU0778	K02113		
132	<->	kb|g.3562.peg.2805	DVU0774	K02114		
133	<->	kb|g.3562.peg.3214	DVU0917	K02110		
134	<->	kb|g.3562.peg.3178	DVU0918	K02108		
135	<->	kb|g.3562.peg.2504	DVU0779	K02109		
136	->	kb|g.3562.peg.2565	DVU0536	no KO assigned		(1) Reducedferredoxin_c0[c0] + (1) Ferricytochromec3_c0[c0] <-> (1) Oxidizedferredoxin_c0[c0] + (1) Ferrocytochromec3_c0[c0]
137	->	kb|g.3562.peg.2416	DVU0535			
138	->	kb|g.3562.peg.2314	DVU0534			
139	->	kb|g.3562.peg.2837	DVU0533			
140	->	kb|g.3562.peg.2911	DVU0532			
141	->	kb|g.3562.peg.2566	DVU0531			
142	->	DORF6830	DORF6830			(2) H+_c0[c0] + (1) Menaquinone 8_c0[c0] + (2) Ferrocytochromec3_c0[c0] <-> (2) Ferricytochromec3_c0[c0] + (1) Menaquinol 8_c0[c0]
143	->	kb|g.3562.peg.2241	DVU0694	no KO assigned		
144	->	kb|g.3562.peg.2827	DVU0693	K00184		
145	->	kb|g.3562.peg.2768	DVU0692	K00185		
146	<->	Unknown				1 formate_c0[c0] + 1 H_c0[c0] = 1 formate_e0[e0] + 1 H_e0[e0]
147	->	kb|g.3562.peg.1122	DVU2809	K00122	1.2.1.2	(1) Formate_c0[c0] + (2) Ferricytochromec3_c0[c0] <-> (1) CO2_c0[c0] + (2) Ferrocytochromec3_c0[c0] + (1) H+_c0[c0]
148	->	kb|g.3562.peg.1112	DVU2810	K02380		
149	->	kb|g.3562.peg.1409	DVU2811			
150	->	kb|g.3562.peg.1793	DVU2812			
151	->	kb|g.3562.peg.1722	DVU2481			
152	->	kb|g.3562.peg.1005	DVU2482			
153	->	kb|g.3562.peg.1232	DVU2483			
154	->	kb|g.3562.peg.1912	DVU2484			
155	->	kb|g.3562.peg.1897	DVU2485			

		gpr	gene ID	KO	enzyme	definition
156	->		DVU0586			
157	->	kb|g.3562.peg.2733	DVU0587			
158	->	kb|g.3562.peg.2613	DVU0588			
159	->	kb|g.3562.peg.736	DVU1290	K00374	1.7.5.1 +1.7.99.4	(1) Sulfite_c0[c0] + (6) Ferrocytochromec3_c0[c0] + (7) H+_c0[c0] <-> (3) H2O_c0[c0] + (1) H2S_c0[c0] + (6) Ferricytochromec3_c0[c0]
160	->	kb|g.3562.peg.381	DVU1289	no KO assigned		
161	->	kb|g.3562.peg.244	DVU1288	no KO assigned		
162	->	kb|g.3562.peg.461	DVU1287	K00184		
163	->	kb|g.3562.peg.85	DVU1286	K00185		
164	->	kb|g.3562.peg.2656	DVU0402	K11180		
165	->	kb|g.3562.peg.2747	DVU0403	K11181	1.8.99.5	
166	->	kb|g.3562.peg.2836	DVU0404			
167	->	kb|g.3562.peg.1750	DVU2776	K11179	2.8.1.-	
168	<->	kb|g.3562.peg.2004	DVU0571	K00259	1.4.1.1	(1) NAD_c0[c0] + (1) NADPH_c0[c0] <-> (1) NADH_c0[c0] + (1) NADP_c0[c0]
169	<->	kb|g.3562.peg.1529	DVU2791	K03615		(1) NADP_c0[c0] + (2) Reducedferredoxin_c0[c0] + (2) H_c0[c0] <-> (1) NADPH_c0[c0] + (1) H+_e0[e0] + (2) Oxidizedferredoxin_c0[c0]
170	<->	kb|g.3562.peg.1677	DVU2792			
171	<->	kb|g.3562.peg.1562	DVU2793	K03614		
172	<->	kb|g.3562.peg.1475	DVU2794	K03612		
173	<->	kb|g.3562.peg.1243	DVU2795	K03613		
174	<->	kb|g.3562.peg.1599	DVU2796	K03617		
175	<->	kb|g.3562.peg.1021	DVU2797	no KO assigned		
176	->	kb|g.3562.peg.757	DVU1295	K00958	2.7.7.4	(1) ATP_c0[c0] + (1) Sulfate_c0[c0] + (1) H+_c0[c0] <-> (1) PPi_c0[c0] + (1) APS_c0[c0]
177	->	kb|g.3562.peg.3158	DVU0847	K00394	1.8.99.2	(1) APS_c0[c0] + (1) Menaquinol 8_c0[c0] + (2) H+_c0[c0] <-> (1) AMP_c0[c0] + (1) Sulfite_c0[c0] + (1) Menaquinone 8_c0[c0] + (2) H+_e0[e0]
178	->	kb|g.3562.peg.3141	DVU0846	K00395		
179	->	kb|g.3562.peg.3086	DVU0848	K16885		
180	->	kb|g.3562.peg.3074	DVU0849	K16886		
181	->	kb|g.3562.peg.3189	DVU0850	K16887		
182	<->	kb|g.3562.peg.540	DVU1207	K00648	2.3.1.180	(1) Acetyl-CoA_c0[c0] + (1) ACP_c0[c0] <-> (1) CoA_c0[c0] + (1) Acetyl-ACP_c0[c0]
183	->	kb|g.3562.peg.1714	DVU2225	K01962	6.4.1.2	(1) ATP_c0[c0] + (1) Acetyl-CoA_c0[c0] + (1) H2CO3_c0[c0] <-> (1) ADP_c0[c0] + (1) Phosphate_c0[c0] + (1) H+_c0[c0] + (1) Malonyl-CoA_c0[c0]

		gpr	gene ID	KO	enzyme	definition
184	<->	kb|g.3562.peg.639	DVU1249	K00645	2.3.1.39	(1) H+_c0[c0] + (1) Malonyl-CoA_c0[c0] + (1) ACP_c0[c0] <-> (1) CoA_c0[c0] + (1) Malonyl-acyl-carrierprotein-_c0[c0]
185	->	kb|g.3562.peg.946	DVU1204	K09458	2.3.1.179	(2) NADPH_c0[c0] + (2) H+_c0[c0] + (1) Malonyl-acyl-carrierprotein-_c0[c0] + (1) Acetyl-ACP_c0[c0] <-> (1) H2O_c0[c0] + (2) NADP_c0[c0] + (1) CO2_c0[c0] + (1) Butyryl-ACP_c0[c0] + (1) ACP_c0[c0]
186	->	kb|g.3562.peg.112	DVU1206	K00059	1.1.1.100	
187	->	kb|g.3562.peg.1281	DVU2368	K02372	4.2.1.59	
188	->	kb|g.3562.peg.2345	DVU0794	K00208	1.3.1.9 +1.3.1.10	
189	->	kb|g.3562.peg.946	DVU1204	K09458	2.3.1.179	(2) NADPH_c0[c0] + (2) H+_c0[c0] + (1) Butyryl-ACP_c0[c0] + (1) Malonyl-acyl-carrierprotein-_c0[c0] <-> (1) H2O_c0[c0] + (2) NADP_c0[c0] + (1) CO2_c0[c0] + (1) Hexanoyl-ACP_c0[c0] + (1) ACP_c0[c0]
190	->	kb|g.3562.peg.112	DVU1206	K00059	1.1.1.100	
191	->	kb|g.3562.peg.1281	DVU2368	K02372	4.2.1.59	
192	->	kb|g.3562.peg.2345	DVU0794	K00208	1.3.1.9 +1.3.1.10	
193	->	kb|g.3562.peg.946	DVU1204	K09458	2.3.1.179	(2) NADPH_c0[c0] + (2) H+_c0[c0] + (1) Hexanoyl-ACP_c0[c0] + (1) Malonyl-acyl-carrierprotein-_c0[c0] <-> (1) H2O_c0[c0] + (2) NADP_c0[c0] + (1) CO2_c0[c0] + (1) Octanoyl-ACP_c0[c0] + (1) ACP_c0[c0]
194	->	kb|g.3562.peg.112	DVU1206	K00059	1.1.1.100	
195	->	kb|g.3562.peg.1281	DVU2368	K02372	4.2.1.59	
196	->	kb|g.3562.peg.2345	DVU0794	K00208	1.3.1.9 +1.3.1.10	
197	->	kb|g.3562.peg.946	DVU1204	K09458	2.3.1.179	(2) NADPH_c0[c0] + (2) H+_c0[c0] + (1) Octanoyl-ACP_c0[c0] + (1) Malonyl-acyl-carrierprotein-_c0[c0] <-> (1) H2O_c0[c0] + (2) NADP_c0[c0] + (1) CO2_c0[c0] + (1) Decanoyl-ACP_c0[c0] + (1) ACP_c0[c0]
198	->	kb|g.3562.peg.112	DVU1206	K00059	1.1.1.100	
199	->	kb|g.3562.peg.1281	DVU2368	K02372	4.2.1.59	
200	->	kb|g.3562.peg.2345	DVU0794	K00208	1.3.1.9 +1.3.1.10	
201	->	kb|g.3562.peg.946	DVU1204	K09458	2.3.1.179	(2) NADPH_c0[c0] + (2) H+_c0[c0] + (1) Decanoyl-ACP_c0[c0] + (1) Malonyl-acyl-carrierprotein-_c0[c0] <-> (1) H2O_c0[c0] + (2) NADP_c0[c0] + (1) CO2_c0[c0] + (1) Dodecanoyl-ACP_c0[c0] + (1) ACP_c0[c0]
202	->	kb|g.3562.peg.112	DVU1206	K00059	1.1.1.100	
203	->	kb|g.3562.peg.1281	DVU2368	K02372	4.2.1.59	

		gpr	gene ID	KO	enzyme	definition
204	->	kb|g.3562.peg.2345	DVU0794	K00208	1.3.1.9 +1.3.1.10	
205	->	kb|g.3562.peg.946	DVU1204	K09458	2.3.1.179	(2) NADPH_c0[c0] + (2) H+_c0[c0] + (1) Dodecanoyl-ACP_c0[c0] + (1) Malonyl-acyl-carrierprotein-_c0[c0] <-> (1) H2O_c0[c0] + (2) NADP_c0[c0] + (1) CO2_c0[c0] + (1) Myristoyl-ACP_c0[c0] + (1) ACP_c0[c0]
206	->	kb|g.3562.peg.112	DVU1206	K00059	1.1.1.100	
207	->	kb|g.3562.peg.1281	DVU2368	K02372	4.2.1.59	
208	->	kb|g.3562.peg.2345	DVU0794	K00208	1.3.1.9 +1.3.1.10	
209	->	kb|g.3562.peg.946	DVU1204	K09458	2.3.1.179	(2) NADPH_c0[c0] + (2) H+_c0[c0] + (1) Myristoyl-ACP_c0[c0] + (1) Malonyl-acyl-carrierprotein-_c0[c0] <-> (1) H2O_c0[c0] + (2) NADP_c0[c0] + (1) CO2_c0[c0] + (1) hexadecanoyl-acp_c0[c0] + (1) ACP_c0[c0]
210	->	kb|g.3562.peg.112	DVU1206	K00059	1.1.1.100	
211	->	kb|g.3562.peg.1281	DVU2368	K02372	4.2.1.59	
212	->	kb|g.3562.peg.2345	DVU0794	K00208	1.3.1.9 +1.3.1.10	
213	->	kb|g.3562.peg.946	DVU1204	K09458	2.3.1.179	(2) NADPH_c0[c0] + (2) H+_c0[c0] + (1) hexadecanoyl-acp_c0[c0] + (1) Malonyl-acyl-carrierprotein-_c0[c0] <-> (1) H2O_c0[c0] + (2) NADP_c0[c0] + (1) CO2_c0[c0] + (1) ACP_c0[c0] + (1) Octadecanoyl-ACP_c0[c0]
214	->	kb|g.3562.peg.112	DVU1206	K00059	1.1.1.100	
215	->	kb|g.3562.peg.1281	DVU2368	K02372	4.2.1.59	
216	->	kb|g.3562.peg.2345	DVU0794	K00208	1.3.1.9 +1.3.1.10	
217	<->	kb|g.3562.peg.288	DVU1428	K01835	5.4.2.2	(1) Glucose-1-phosphate_c0[c0] <-> (1) D-glucose-6-phosphate_c0[c0]
218	<->	kb|g.3562.peg.1171	DVU2143	K01624	4.1.2.13	(1) D-fructose-1,6-bisphosphate_c0[c0] <-> (1) Glycerone-phosphate_c0[c0] + (1) Glyceraldehyde3-phosphate_c0[c0]
219	->	kb|g.3562.peg.2712	DVU0748	K01895	6.2.1.1	(1) ATP_c0[c0] + (1) CoA_c0[c0] + (1) Acetate_c0[c0] + (1) H+_c0[c0] <-> (1) PPi_c0[c0] + (1) AMP_c0[c0] + (1) Acetyl-CoA_c0[c0]
220	->	kb|g.3562.peg.1700	DVU2969	K01895	6.2.1.1	
221	<->	kb|g.3562.peg.1895	DVU2885	K00001	1.1.1.1	(1) NAD_c0[c0] + (1) Ethanol_c0[c0] <-> (1) NADH_c0[c0] + (1) H+_c0[c0] + (1) Acetaldehyde_c0[c0]
222		kb|g.3562.peg.1654	DVU2405			
223	->	kb|g.3562.peg.848	DVU1179	K03738	1.2.7.5	(1) acetaldehyde_c0[c0] + (1) H2O_c0[c0] + (2) Oxidizedferredoxin_c0[c0] = (1) acetate_c0[c0] + (3) H_c0[c0] + (2) Reducedferredoxin_c0[c0]
224	<->	kb|g.3562.peg.2684	DVU3294	K04073	1.2.1.10	(1) acetaldehyde_c0[c0] + (1) CoA_c0[c0] + (1) NAD_c0[c0] = (1) acetyl-CoA_c0[c0] + (1) NADH_c0[c0] + (1) H_c0[c0]

		gpr	gene ID	KO	enzyme	definition
225		kb|g.3562.peg.1271	DVU2603			
226	<->	kb|g.3562.peg.188	DVU1677	K01803	5.3.1.1	(1) Glyceraldehyde3-phosphate_c0[c0] <-> (1) Glycerone-phosphate_c0[c0]
227	<->	kb|g.3562.peg.1387	DVU2784	no KO assigned	0	(1) Menaquinone 8_c0[c0] + (1) L-Lactate_c0[c0] <-> (1) Menaquinol 8_c0[c0] + (1) Pyruvate_c0[c0]
228		kb|g.3562.peg.1561	DVU3027			
229	<->	kb|g.3562.peg.2993	DVU3222	K01810	5.3.1.9	(1) D-glucose-6-phosphate_c0[c0] <-> (1) D-fructose-6-phosphate_c0[c0]
230	<->	kb|g.3562.peg.1110	DVU2144	K00134	1.2.1.12	(1) NAD_c0[c0] + (1) Phosphate_c0[c0] + (1) Glyceraldehyde3-phosphate_c0[c0] <-> (1) NADH_c0[c0] + (1) 1,3-Bisphospho-D-glycerate_c0[c0]
231	<->	kb|g.3562.peg.2261	DVU0565	K00134	1.2.1.12	
232	<->	kb|g.3562.peg.1981	DVU2529	K00927	2.7.2.3	(1) ATP_c0[c0] + (1) 3-Phosphoglycerate_c0[c0] + (1) H+_c0[c0] <-> (1) ADP_c0[c0] + (1) 1,3-Bisphospho-D-glycerate_c0[c0]
233	<->	kb|g.3562.peg.3153	DVU0889	K15635	5.4.2.12	(1) 2-Phospho-D-glycerate_c0[c0] <-> (1) 3-Phosphoglycerate_c0[c0]
234	<->	kb|g.3562.peg.2709	DVU0322	K01689	4.2.1.11	(1) 2-Phospho-D-glycerate_c0[c0] <-> (1) H2O_c0[c0] + (1) Phosphoenolpyruvate_c0[c0]
235	->	kb|g.3562.peg.1221	DVU2514	K00873	2.7.1.40	(1) ATP_c0[c0] + (1) Pyruvate_c0[c0] <-> (1) ADP_c0[c0] + (1) Phosphoenolpyruvate_c0[c0]
236	->	kb|g.3562.peg.404	DVU2061	K00850	2.7.1.11	(1) ATP_c0[c0] + (1) D-fructose-6-phosphate_c0[c0] <-> (1) ADP_c0[c0] + (1) D-fructose-1,6-bisphosphate_c0[c0]
237	->	kb|g.3562.peg.192	DVU1841	K03841	3.1.3.11	(1) H2O_c0[c0] + (1) D-fructose-1,6-bisphosphate_c0[c0] <-> (1) Phosphate_c0[c0] + (1) D-fructose-6-phosphate_c0[c0] + (1) H+_c0[c0]
238	->	kb|g.3562.peg.870	DVU1539	K02446	3.1.3.11	
239	<->	kb|g.3562.peg.2993	DVU3222	K01810	5.3.1.9	(1) D-glucose-6-phosphate_c0[c0] <-> (1) beta-D-Glucose-6-phosphate_c0[c0]
240	<->	kb|g.3562.peg.305	DVU1575	K00948	2.7.6.1	(1) ATP_c0[c0] + (1) ribose-5-phosphate_c0[c0] <-> (1) AMP_c0[c0] + (1) PRPP_c0[c0]
241	->	kb|g.3562.peg.1444	DVU2313	K01057	3.1.1.31	(1) H2O_c0[c0] + (1) 6-phospho-D-glucono-1-5-lactone_c0[c0] <-> (1) H+_c0[c0] + (1) 6-Phospho-D-gluconate_c0[c0]
242	<->	kb|g.3562.peg.2525	DVU0477	K00031	1.1.1.42	(1) NADP_c0[c0] + (1) 6-Phospho-D-gluconate_c0[c0] <-> (1) NADPH_c0[c0] + (1) CO2_c0[c0] + (1) D-Ribulose5-phosphate_c0[c0]
243	<->	kb|g.3562.peg.1217	DVU2531	K01783	5.1.3.1	(1) D-Ribulose5-phosphate_c0[c0] <-> (1) D-Xylulose5-phosphate_c0[c0]
244	<->	kb|g.3562.peg.1109	DVU2530	K00615	2.2.1.1	(1) D-fructose-6-phosphate_c0[c0] + (1) Glyceraldehyde3-phosphate_c0[c0] <-> (1) D-Xylulose5-phosphate_c0[c0] + (1) D-Erythrose4-phosphate_c0[c0]
245	<->	kb|g.3562.peg.67	DVU1658	K00616	2.2.1.2	(1) Glyceraldehyde3-phosphate_c0[c0] + (1) Sedoheptulose7-phosphate_c0[c0] <-> (1) D-fructose-6-phosphate_c0[c0] + (1) D-Erythrose4-phosphate_c0[c0]

		gpr	gene ID	KO	enzyme	definition
246	<->	kb|g.3562.peg.1109	DVU2530	K00615	2.2.1.1	(1) Glyceraldehyde3-phosphate_c0[c0] + (1) Sedoheptulose7-phosphate_c0[c0] <-> (1) ribose-5-phosphate_c0[c0] + (1) D-Xylulose5-phosphate_c0[c0]
247	<->	kb|g.3562.peg.68	DVU1580	K01808	5.3.1.6	(1) ribose-5-phosphate_c0[c0] <-> (1) D-Ribulose5-phosphate_c0[c0]
248	<->	kb|g.3562.peg.1227	DVU3079	no KO assigned	0	(1) (R) -S-Lactoylglutathione_c0[c0] <-> (1) GSH_c0[c0] + (1) 2-Oxopropanal_c0[c0]
249	<->	kb|g.3562.peg.1941	DVU2765	no KO assigned	0	(1) H2O_c0[c0] + (1) (R) -S-Lactoylglutathione_c0[c0] <-> (1) GSH_c0[c0] + (1) H+_c0[c0] + (1) D-Lactate_c0[c0]
250	<->	kb|g.3562.peg.1836	DVU0253	K18930	0	(1) NAD_c0[c0] + (1) D-Lactate_c0[c0] <-> (1) NADH_c0[c0] + (1) Pyruvate_c0[c0] + (1) H+_c0[c0]
251	->	kb|g.3562.peg.406	DVU1833	K01007	2.7.9.2	(1) H2O_c0[c0] + (1) ATP_c0[c0] + (1) Pyruvate_c0[c0] <-> (1) Phosphate_c0[c0] + (1) AMP_c0[c0] + (1) Phosphoenolpyruvate_c0[c0] + (1) H+_c0[c0]
252	<->	kb|g.3562.peg.1049	DVU2272	K00656	2.3.1.54	(1) Acetyl-CoA_c0[c0] + (1) Formate_c0[c0] <-> (1) CoA_c0[c0] + (1) Pyruvate_c0[c0]
253	<->	kb|g.3562.peg.1440	DVU2824	K00656	2.3.1.54	
254	<->	kb|g.3562.peg.1789	DVU3030	K00925	2.7.2.1	(1) ATP_c0[c0] + (1) Acetate_c0[c0] + (1) H+_c0[c0] <-> (1) ADP_c0[c0] + (1) Acetylphosphate_c0[c0]
255	<->	kb|g.3562.peg.1135	DVU3029	K13788	2.3.1.8	(1) Phosphate_c0[c0] + (1) Acetyl-CoA_c0[c0] + (1) H+_c0[c0] <-> (1) CoA_c0[c0] + (1) Acetylphosphate_c0[c0]
256	->	Unknown	#N/A	#N/A	#N/A	(1) L-Aspartate_c0[c0] + (1) PRPP_c0[c0] + (1) Carbamoylphosphate_c0[c0] + (1) menaquinone 8_c0[c0] <-> (1) H2O_c0[c0] + (1) Phosphate_c0[c0] + (1) CO2_c0[c0] + (1) PPi_c0[c0] + (1) UMP_c0[c0] + (1) Menaquinol 8_c0[c0]
257	<->	kb|g.3562.peg.3051	DVU0871	K09903	2.7.4.22	(1) ATP_c0[c0] + (1) UMP_c0[c0] <-> (1) ADP_c0[c0] + (1) UDP_c0[c0]
258	<->	kb|g.3562.peg.689	DVU1623	K01937	6.3.4.2	(1) H2O_c0[c0] + (1) ATP_c0[c0] + (1) L-Glutamine_c0[c0] + (1) UTP_c0[c0] <-> (1) ADP_c0[c0] + (1) Phosphate_c0[c0] + (1) L-Glutamate_c0[c0] + (1) CTP_c0[c0] + (2) H+_c0[c0]
259	->	kb|g.3562.peg.457	DVU1202	K01493	3.5.4.12	(1) H+_c0[c0] + (1) H2O_c0[c0] + (1) dCTP_c0[c0] <-> (1) NH3_c0[c0] + (1) dUTP_c0[c0]
260	->	kb|g.3562.peg.1647	DVU2140	K00943	2.7.4.9	(1) ATP_c0[c0] + (1) dTMP_c0[c0] <-> (1) ADP_c0[c0] + (1) dTDP_c0[c0]
261	<->	kb|g.3562.peg.1148	DVU2254	K03465	2.1.1.148	(1) 5-10-Methylenetetrahydrofolate_c0[c0] + (1) dUMP_c0[c0] <-> (1) dTMP_c0[c0] + (1) Dihydrofolate_c0[c0]
262	->	kb|g.3562.peg.2077	DVU0736	K11175	2.1.2.2	(2) H2O_c0[c0] + (4) ATP_c0[c0] + (1) CO2_c0[c0] + (1) Glycine_c0[c0] + (1) L-Aspartate_c0[c0] + (2) L-Glutamine_c0[c0] + (1) PRPP_c0[c0] + (1) 10-Formyltetrahydrofolate_c0[c0] <-> (4) ADP_c0[c0] + (4) Phosphate_c0[c0] + (1) PPi_c0[c0] + (2) L-Glutamate_c0[c0] + (7)

		gpr	gene ID	KO	enzyme	definition
						H+_c0[c0] + (1) Fumarate_c0[c0] + (1) AICAR_c0[c0] + (1) THF_c0[c0]
263	<->	kb|g.3562.peg.2828	DVU3206	K00602	2.1.2.3 +3.5.4.10	(1) 10-Formyltetrahydrofolate_c0[c0] + (1) AICAR_c0[c0] <-> (1) FAICAR_c0[c0] + (1) THF_c0[c0]
264	<->	kb|g.3562.peg.2561	DVU3235	no KO assigned	0	
265	<->	kb|g.3562.peg.2828	DVU3206	K00602	2.1.2.3 +3.5.4.10	(1) H2O_c0[c0] + (1) IMP_c0[c0] <-> (1) FAICAR_c0[c0]
266	<->	kb|g.3562.peg.2561	DVU3235	no KO assigned	0	
267	<->	kb|g.3562.peg.3162	DVU1044	K00088	1.1.1.205	(1) H2O_c0[c0] + (1) NAD_c0[c0] + (1) IMP_c0[c0] <-> (1) NADH_c0[c0] + (1) H+_c0[c0] + (1) XMP_c0[c0]
268	<->	kb|g.3562.peg.3150	DVU1043	K01951	6.3.5.2	(1) H2O_c0[c0] + (1) ATP_c0[c0] + (1) L-Glutamine_c0[c0] + (1) XMP_c0[c0] <-> (1) PPi_c0[c0] + (1) AMP_c0[c0] + (1) L-Glutamate_c0[c0] + (1) H+_c0[c0] + (1) GMP_c0[c0]
269	<->	kb|g.3562.peg.3100	DVU0900	K00942	2.7.4.8	(1) ATP_c0[c0] + (1) GMP_c0[c0] <-> (1) ADP_c0[c0] + (1) GDP_c0[c0]
270	<->	kb|g.3562.peg.1042	DVU2947	K00527	1.17.4.2	(1) ATP_c0[c0] + (1) trdrd_c0[c0] <-> (1) H2O_c0[c0] + (1) dATP_c0[c0] + (1) trdox_c0[c0]
271	<->	kb|g.3562.peg.1042	DVU2947	K00527	1.17.4.2	(1) GTP_c0[c0] + (1) trdrd_c0[c0] <-> (1) H2O_c0[c0] + (1) dGTP_c0[c0] + (1) trdox_c0[c0]
272	<->	kb|g.3562.peg.1042	DVU2947	K00527	1.17.4.2	(1) CTP_c0[c0] + (1) trdrd_c0[c0] <-> (1) H2O_c0[c0] + (1) dCTP_c0[c0] + (1) trdox_c0[c0]
273	<->	kb|g.3562.peg.1042	DVU2947	K00527	1.17.4.2	(1) UTP_c0[c0] + (1) trdrd_c0[c0] <-> (1) H2O_c0[c0] + (1) dUTP_c0[c0] + (1) trdox_c0[c0]
274	<->	kb|g.3562.peg.2330	DVU3204	K01939	6.3.4.4	(1) GTP_c0[c0] + (1) L-Aspartate_c0[c0] + (1) IMP_c0[c0] <-> (1) Phosphate_c0[c0] + (1) GDP_c0[c0] + (2) H+_c0[c0] + (1) Adenylosuccinate_c0[c0]
275	<->	kb|g.3562.peg.1494	DVU2942	K01756	4.3.2.2	(1) Adenylosuccinate_c0[c0] <-> (1) AMP_c0[c0] + (1) Fumarate_c0[c0]
276	<->	kb|g.3562.peg.683	DVU1932	K00939	2.7.4.3	(1) ATP_c0[c0] + (1) AMP_c0[c0] <-> (2) ADP_c0[c0]
277	<->	kb|g.3562.peg.1976	DVU2333	K00940	2.7.4.6	(1) ATP_c0[c0] + (1) dTDP_c0[c0] <-> (1) ADP_c0[c0] + (1) TTP_c0[c0]
278	<->	kb|g.3562.peg.1976	DVU2333	K00940	2.7.4.6	(1) ATP_c0[c0] + (1) GDP_c0[c0] <-> (1) ADP_c0[c0] + (1) GTP_c0[c0]
279	<->	kb|g.3562.peg.1976	DVU2333	K00940	2.7.4.6	(1) ATP_c0[c0] + (1) UDP_c0[c0] <-> (1) ADP_c0[c0] + (1) UTP_c0[c0]
280	->	kb|g.3562.peg.2896	DVU0377	K00384	1.8.1.9	(1) NADPH_c0[c0] + (1) H+_c0[c0] + (1) trdox_c0[c0] <-> (1) NADP_c0[c0] + (1) trdrd_c0[c0]
281	->	kb|g.3562.peg.2	DVU1457	K00384	1.8.1.9	

		gpr	gene ID	KO	enzyme	definition
282	<->	kb|g.3562.peg.1773	DVU2348	K01520	3.6.1.23	(1) H2O_c0[c0] + (1) dUTP_c0[c0] <-> (1) PPi_c0[c0] + (1) dUMP_c0[c0]
283	<->	kb|g.3562.peg.851	DVU1203	K00600	2.1.2.1	(1) L-Serine_c0[c0] + (1) THF_c0[c0] <-> (1) H2O_c0[c0] + (1) Glycine_c0[c0] + (1) 5-10-Methylenetetrahydrofolate_c0[c0]
284	<->	kb|g.3562.peg.1538	DVU2891	K07722	0	(1) NADPH_c0[c0] + (1) H+_c0[c0] + (1) Dihydrofolate_c0[c0] <-> (1) NADP_c0[c0] + (1) THF_c0[c0]
285	<->	kb|g.3562.peg.2077	DVU0736	K11175	2.1.2.2	(1) H2O_c0[c0] + (1) 10-Formyltetrahydrofolate_c0[c0] <-> (1) Formate_c0[c0] + (1) H+_c0[c0] + (1) THF_c0[c0]
286	->	kb|g.3562.peg.1713	DVU2226	no KO assigned	0	(1) ATP_c0[c0] + (1) Pyruvate_c0[c0] + (1) H2CO3_c0[c0] <-> (1) ADP_c0[c0] + (1) Phosphate_c0[c0] + (1) Oxaloacetate_c0[c0] + (1) H+_c0[c0]
287	->	kb|g.3562.peg.53	DVU1834	K01958	6.4.1.1	
288	<->	kb|g.3562.peg.2525	DVU0477	K00031	1.1.1.42	(1) NAD_c0[c0] + (1) Isocitrate_c0[c0] <-> (1) NADH_c0[c0] + (1) CO2_c0[c0] + (1) 2-Oxoglutarate_c0[c0]
289	<->	kb|g.3562.peg.2553	DVU0796	K00013	1.1.1.23	(1) NAD_c0[c0] + (1) L-Malate_c0[c0] <-> (1) NADH_c0[c0] + (1) Oxaloacetate_c0[c0] + (1) H+_c0[c0]
290	<->	kb|g.3562.peg.2161	DVU3262	K00244	1.3.5.4	(1) NAD_c0[c0] + (1) Succinate_c0[c0] <-> (1) NADH_c0[c0] + (1) H+_c0[c0] + (1) Fumarate_c0[c0]
291	<->	kb|g.3562.peg.44	DVU1569	K00174	1.2.7.3 +1.2.7.11	(1) CO2_c0[c0] + (1) Acetyl-CoA_c0[c0] + (1) H+_c0[c0] + (2) Reducedferredoxin_c0[c0] <-> (1) CoA_c0[c0] + (1) Pyruvate_c0[c0] + (2) Oxidizedferredoxin_c0[c0]
292	<->	kb|g.3562.peg.61	DVU1570			
293	<->	kb|g.3562.peg.1752	DVU3025	K03737	1.2.7.1 +1.2.7.-	
294	<->	kb|g.3562.peg.887	DVU1946	K00175	1.2.7.3 +1.2.7.11	
295	<->	kb|g.3562.peg.497	DVU1947	K00177	1.2.7.3	
296	<->	kb|g.3562.peg.891	DVU1945	K00174	1.2.7.3 +1.2.7.11	
297	<->	kb|g.3562.peg.423	DVU1064	K01681	4.2.1.3	(1) Citrate_c0[c0] <-> (1) Isocitrate_c0[c0]
298	<->	kb|g.3562.peg.61	DVU1570	K00175	1.2.7.3 +1.2.7.11	(1) CoA_c0[c0] + (1) 2-Oxoglutarate_c0[c0] + (2) Oxidizedferredoxin_c0[c0] <-> (1) CO2_c0[c0] + (1) H+_c0[c0] + (1) Succinyl-CoA_c0[c0] + (2) Reducedferredoxin_c0[c0]
299	<->	kb|g.3562.peg.1707	DVU2137	K01902	6.2.1.5	(1) ATP_c0[c0] + (1) CoA_c0[c0] + (1) Succinate_c0[c0] <-> (1) ADP_c0[c0] + (1) Phosphate_c0[c0] + (1) Succinyl-CoA_c0[c0]
300	->	kb|g.3562.peg.2161	DVU3262	K00244	1.3.5.4	(2) H_c0[c0] + (1) Fumarate_c0[c0] + (2) Reducedferredoxin_c0[c0] <-> (1) Succinate_c0[c0] + (2) Oxidizedferredoxin_c0[c0]
301	<->	kb|g.3562.peg.3163	DVU0080	K01679	4.2.1.2	(1) L-Malate_c0[c0] <-> (1) H2O_c0[c0] + (1) Fumarate_c0[c0]
302	->	kb|g.3562.peg.2243	DVU0446	K14393	0	(1) Ethanol_c0[c0] <-> (1) Ethanol_e0[e0]

		gpr	gene ID	KO	enzyme	definition
303	->	Unknown	#N/A	#N/A	#N/A	(1) H+_e0[e0] <-> (1) H+_c0[c0]
304	->	kb|g.3562.peg.842	DVU1231	K03320	0	(1) NH3_e0[e0] <-> (1) NH3_c0[c0]
305	<->	Unknown	#N/A	#N/A	#N/A	(1) Phosphate_c0[c0] <-> (1) Phosphate_e0[e0]
306	<->	Unknown	#N/A	#N/A	#N/A	(1) H+_c0[c0] + (1) H2CO3_c0[c0] <-> (1) H2O_c0[c0] + (1) CO2_c0[c0]
307	->	Unknown	#N/A	#N/A	#N/A	(1) H2O_c0[c0] + (1) ATP_c0[c0] <-> (1) ADP_c0[c0] + (1) Phosphate_c0[c0] + (1) H+_c0[c0]
308	->	kb|g.3562.peg.2549	DVU0747	K06857	3.6.3.55	(1) Sulfate_e0[e0] + (2) H+_e0[e0] <-> (1) Sulfate_c0[c0] + (2) H+_c0[c0]
309	->	kb|g.3562.peg.2243	DVU0446	K14393	0	(1) H+_e0[e0] + (1) L-Lactate_e0[e0] <-> (1) L-Lactate_c0[c0] + (1) H+_c0[c0]
310		kb|g.3562.peg.1712	DVU3026			
311			DVU2285			
312	->	Unknown	#N/A	#N/A	#N/A	(1) H2S_c0[c0] <-> (1) H2S_e0[e0]
313	<->	kb|g.3562.peg.2243	DVU0446	K14393	0	(1) Acetate_c0[c0] + (1) H+_c0[c0] <-> (1) Acetate_e0[e0] + (1) H+_e0[e0]
314	<->	Unknown	#N/A	#N/A	#N/A	(1) CO2_e0[e0] <-> (1) CO2_c0[c0]
315	<->	Unknown	#N/A	#N/A	#N/A	(1) H2_c0[c0] <-> (1) H2_e0[e0]
316	->		#N/A	#N/A	#N/A	0.055 Protein_c0 + 0.0648 DNA_c0 + 0.0501 RNA_c0 + 0.1329 Glycogen_c0 + 0.1634 Lipid_c0 + 139 ATP_c0 + 139 H2O_c0 = 1 Biomass_c0 + 139 ADP_c0 + 139 phosphate_c0 + 139 H+_c0
317	->					1 hexadecanoyl-acp_c0 + 1 octadecanoyl-acp_c0 + 1 glycerol-3-phosphate_c0 + 1 Lipid_c0 + 2 acp_c0
318	<->					1 sn-glycerol-3-phosphate_c0[c0] + 1 NAD+_c0[c0] = 1 Glycerone-phosphate_c0[c0] + 1 NADH_c0[c0] + 1 H+_c0[c0]
319	->					1 biomass_c0[c0] -> 1 biomass_e0[e0]
320	->				pyruvate transporter	(1) pyruvate_e0[e0] + (1) H+_e0[e0] = (1) pyruvate_c0[c0] + (1) H+_c0[c0]
321	<->					(1) H2O_e0 = (1) H2O_c0
322	<->				Alanine	(1) Alanine_c0 = (1) Alanine_e0
323	<->				L-Arginine	(1) L-Arginine_c0 = (1) L-Arginine_e0
324	<->				L-Asparagine	(1) L-Asparagine_c0 = (1) L-Asparagine_e0
325	<->				L-aspartate	(1) L-Aspartate_c0 = (1) L-Aspartate_e0
326	<->				L-cysteine	(1) L-Cysteine_c0 = (1) L-Cysteine_e0
327	<->				L-glutamate	(1) L-Glutamate_c0 = (1) L-Glutamate_e0

	gpr	gene ID	KO	enzyme	definition
328	<->			L-glutamine	(1) L-Glutamine_c0 = (1) L-Glutamine_e0
329	<->			Glycine	(1) Glycine_c0 = (1) Glycine_e0
330	<->			L-histidine	(1) L-Histidine_c0 = (1) L-Histidine_e0
331	<->			L-isoleucine	(1) L-Isoleucine_c0 = (1) L-Isoleucine_e0
332	<->			L-leucine	(1) L-Leucine_c0 = (1) L-Leucine_e0
333	<->			L-lysine	(1) L-Lysine_c0 = (1) L-Lysine_e0
334	<->			L-methionine	(1) L-Methionine_c0 = (1) L-Methionine_e0
335	<->			L-phenylalanine	(1) L-Phenylalanine_c0 = (1) L-Phenylalanine_e0
336	<->			L-proline	(1) L-Proline_c0 = (1) L-Proline_e0
337	<->			L-serine	(1) L-Serine_c0 = (1) L-Serine_e0
338	<->			L-threonine	(1) L-Threonine_c0 = (1) L-Threonine_e0
339	<->			L-tryptophan	(1) L-Tryptophan_c0 = (1) L-Tryptophan_e0
340	<->			L-tyrosine	(1) L-Tyrosine_c0 = (1) L-Tyrosine_e0
341	<->			L-valine	(1) L-Valine_c0 = (1) L-Valine_e0
342					(1) phosphoenolpyruvate + (1) sulfite => (1) (2R)-2-O-phospho-3-sulfolactate
343					(1) (2R)-2-O-phospho-3-sulfolactate + (1) H2O => (2R)-3-sulfolactate + (1) phosphate
344					(1) Sulfolactate_c0 => (1) pyurvate_c0 + (1) sulfite_c0

Table S2. Stoichiometric equations used for the *Methanococcus maripaludis* model.

		gpr	gene ID	KO	enzyme	definition
1	<->	kb|g.575.peg.690	MMP1212	K00626	2.3.1.9	(2) Acetyl-CoA_c0[c0] <-> (1) CoA_c0[c0] + (1) Acetoacetyl-CoA_c0[c0]
2	<->	kb|g.575.peg.380	MMP1211	K01641	2.3.3.10	(1) CoA_c0[c0] + (1) H+_c0[c0] + (1) HMG-CoA_c0[c0] <-> (1) H2O_c0[c0] + (1) Acetyl-CoA_c0[c0] + (1) Acetoacetyl-CoA_c0[c0]
3	<->	kb|g.575.peg.1425	MMP0087	K00021	1.1.1.34	(2) NAD_c0[c0] + (1) CoA_c0[c0] + (1) Mevalonic-acid_c0[c0] <-> (2) NADH_c0[c0] + (2) H+_c0[c0] + (1) HMG-CoA_c0[c0]
4	<->	kb|g.575.peg.824	MMP1387	K06990	4.1.1.99	(1) ATP_c0[c0] + (1) 5-phosphomevalonate_c0[c0] <-> (1) ADP_c0[c0] + (1) CO2_c0[c0] + (1) Isopentenyl-phosphate_c0[c0] + (1) Phosphate_c0[c0]
5	<->	kb|g.575.peg.1678	MMP0043	K01823	5.3.3.2	(1) Isopentenyldiphosphate_c0[c0] <-> (1) DMAPP_c0[c0]
6	<->	kb|g.575.peg.1086	MMP0045	K13787	2.5.1.1/2.5.1.10/2.5.1.29	(1) Isopentenyldiphosphate_c0[c0] + (1) DMAPP_c0[c0] <-> (1) PPi_c0[c0] + (1) Geranyldiphosphate_c0[c0]
7	<->	kb|g.575.peg.1086	MMP0045	K13787	2.5.1.10/2.5.1.1/2.5.1.29	(1) Isopentenyldiphosphate_c0[c0] + (1) Geranyldiphosphate_c0[c0] <-> (1) PPi_c0[c0] + (1) Farnesyldiphosphate_c0[c0]
8	->	kb|g.575.peg.1086	MMP0045	K13787	2.5.1.29/2.5.1.1/2.5.1.10	(1) Isopentenyldiphosphate_c0[c0] + (1) Farnesyldiphosphate_c0[c0] <-> (1) PPi_c0[c0] + (1) Geranylgeranyl-diphosphate_c0[c0]
9	<->	kb|g.575.peg.915	MMP0225	K00096	1.1.1.261	
10	->	kb|g.575.peg.487	MMP1677	K17105	2.5.1.42	1 Geranylgeranyl diphosphate_c0 + 1 sn-3-O-(Geranylgeranyl)glycerol 1-phosphate_c0 = 1 lipids_c0 + 1 Ppi_c0
11	->	kb|g.575.peg.702	MMP1146	K00764	2.4.2.14	(1) H2O_c0[c0] + (1) L-Glutamine_c0[c0] + (1) PRPP_c0[c0] <-> (1) PPi_c0[c0] + (1) L-Glutamate_c0[c0] + (1) 5-Phosphoribosylamine_c0[c0]
12	<->	kb|g.575.peg.1334	MMP0392	K01945	6.3.4.13	(1) ATP_c0[c0] + (1) Glycine_c0[c0] + (1) 5-Phosphoribosylamine_c0[c0] <-> (1) ADP_c0[c0] + (1) Phosphate_c0[c0] + (1) GAR_c0[c0] + (1) H+_c0[c0]
13	<->	kb|g.575.peg.21	MMP0179	K01952	6.3.5.3	(1) H2O_c0[c0] + (1) ATP_c0[c0] + (1) L-Glutamine_c0[c0] + (1) N-Formyl-GAR_c0[c0] <-> (1) ADP_c0[c0] + (1) Phosphate_c0[c0] + (1) L-

		gpr	gene ID	KO	enzyme		definition
							Glutamate_c0[c0] + (1) 5'-Phosphoribosylformylglycinamidine_c0[c0] + (1) H+_c0[c0]
14	<->	kb|g.575.peg.480	MMP0178	K01952	6.3.5.3		
15	->	kb|g.575.peg.180	MMP1254	K01933	6.3.3.1		(1) ATP_c0[c0] + (1) 5'-Phosphoribosylformylglycinamidine_c0[c0] <-> (1) ADP_c0[c0] + (1) Phosphate_c0[c0] + (1) AIR_c0[c0] + (1) H+_c0[c0]
16	<->	kb|g.575.peg.1712	MMP0809	K06898		0	(1) CO2_c0[c0] + (1) AIR_c0[c0] <-> (1) H+_e0[e0] + (1) 5'-Phosphoribosyl-4-carboxy-5-aminoimidazole_c0[c0]
17	<->	kb|g.575.peg.929	MMP0282	K01588	5.4.99.18		
18	<->	kb|g.575.peg.1450	MMP0876	K11780	2.5.1.77		(1) ATP_c0[c0] + (1) L-Aspartate_c0[c0] + (1) 5'-Phosphoribosyl-4-carboxy-5-aminoimidazole_c0[c0] <-> (1) ADP_c0[c0] + (1) Phosphate_c0[c0] + (1) H+_c0[c0] + (1) SAICAR_c0[c0]
19	<->	kb|g.575.peg.1293	MMP0971	K01756	4.3.2.2		(1) SAICAR_c0[c0] <-> (1) Fumarate_c0[c0] + (1) AICAR_c0[c0] + (1) H+_c0[c0]
20	<->	kb|g.575.peg.811	MMP0278	no KO assigned	1.1.1.205		
21	<->	kb|g.575.peg.59	MMP1282	no KO assigned	2.7.4.8		(1) ATP_c0[c0] + (1) GMP_c0[c0] <-> (1) ADP_c0[c0] + (1) GDP_c0[c0]
22	<->	kb|g.575.peg.225	MMP0227	K21636	1.1.98.6		(2) H+_c0[c0] + (1) ATP_c0[c0] + (1) Formate_c0[c0] <-> (1) H2O_c0[c0] + (1) dATP_c0[c0] + (1) CO2_c0[c0]
23	<->	kb|g.575.peg.225	MMP0227	K21636	1.1.98.6		(1) H+_c0[c0] + (1) GTP_c0[c0] + (1) Formate_c0[c0] <-> (1) H2O_c0[c0] + (1) dGTP_c0[c0] + (1) CO2_c0[c0]
24	<->	kb|g.575.peg.225	MMP0227	K21636	1.1.98.6		(1) H+_c0[c0] + (1) CTP_c0[c0] + (1) Formate_c0[c0] <-> (1) H2O_c0[c0] + (1) dCTP_c0[c0] + (1) CO2_c0[c0]
25	<->	kb|g.575.peg.225	MMP0227	K21636	1.1.98.6		(1) H+_c0[c0] + (1) UTP_c0[c0] + (1) Formate_c0[c0] <-> (1) H2O_c0[c0] + (1) dUTP_c0[c0] + (1) CO2_c0[c0]
26	<->	kb|g.575.peg.435	MMP1432	K01939	6.3.4.4		(1) GTP_c0[c0] + (1) L-Aspartate_c0[c0] + (1) IMP_c0[c0] <-> (1) Phosphate_c0[c0] + (1) GDP_c0[c0] + (2) H+_c0[c0] + (1) Adenylosuccinate_c0[c0]
27	<->	kb|g.575.peg.1293	MMP0971	K01756	4.3.2.2		(1) Adenylosuccinate_c0[c0] <-> (1) AMP_c0[c0] + (1) Fumarate_c0[c0]

		gpr	gene ID	KO	enzyme	definition
28	<->	kb|g.575.peg.59	MMP1282	no KO assigned	#N/A	
29	<->	kb|g.575.peg.587	MMP0283	K00940	2.7.4.6	(1) ATP_c0[c0] + (1) dTDP_c0[c0] <-> (1) ADP_c0[c0] + (1) TTP_c0[c0]
30	<->	kb|g.575.peg.587	MMP0283	K00940	2.7.4.6	(1) ATP_c0[c0] + (1) dUDP_c0[c0] <-> (1) ADP_c0[c0] + (1) dUTP_c0[c0]
31	<->	kb|g.575.peg.587	MMP0283	K00940	2.7.4.6	(1) ATP_c0[c0] + (1) GDP_c0[c0] <-> (1) ADP_c0[c0] + (1) GTP_c0[c0]
32	<->	kb|g.575.peg.587	MMP0283	K00940	2.7.4.6	(1) ATP_c0[c0] + (1) UDP_c0[c0] <-> (1) ADP_c0[c0] + (1) UTP_c0[c0]
33	<->	kb|g.575.peg.1061	MMP0959	K00384	1.8.1.9	(1) NADH_c0[c0] + (1) H+_c0[c0] + (1) trdox_c0[c0] <-> (1) NAD_c0[c0] + (1) trdrd_c0[c0]
34	->	kb|g.575.peg.656	MMP1589	K01956	6.3.5.5	(1) H2O_c0[c0] + (2) ATP_c0[c0] + (1) HCO3_c0[c0] + (1) L-Glutamine_c0[c0] <-> (2) ADP_c0[c0] + (1) Phosphate_c0[c0] + (1) L-Glutamate_c0[c0] + (1) Carbamoylphosphate_c0[c0] + (2) H+_c0[c0]
35	->	kb|g.575.peg.350	MMP1013	K01955	6.3.5.5	
36	<->	kb|g.575.peg.821	MMP1104	K00610	0	(1) L-Aspartate_c0[c0] + (1) Carbamoylphosphate_c0[c0] <-> (1) Phosphate_c0[c0] + (1) H+_c0[c0] + (1) N-Carbamoyl-L-aspartate_c0[c0]
37	<->	kb|g.575.peg.260	MMP1009	K01465	3.5.2.3	(1) H2O_c0[c0] + (1) S-Dihydroorotate_c0[c0] <-> (1) H+_c0[c0] + (1) N-Carbamoyl-L-aspartate_c0[c0]
38	<->	kb|g.575.peg.1474	MMP0439	K17828	1.3.1.14	(1) NAD_c0[c0] + (1) S-Dihydroorotate_c0[c0] <-> (1) NADH_c0[c0] + (1) H+_c0[c0] + (1) Orotate_c0[c0]
39	<->	kb|g.575.peg.1509	MMP0079	K00762	2.4.2.10	(1) PPi_c0[c0] + (1) Orotidylic-acid_c0[c0] <-> (1) PRPP_c0[c0] + (1) Orotate_c0[c0]
40	<->	kb|g.575.peg.596	MMP1492	K00762	2.4.2.10	
41	->	kb|g.575.peg.1241	MMP0602	K01591	4.1.1.23	(1) H+_c0[c0] + (1) Orotidylic-acid_c0[c0] <-> (1) CO2_c0[c0] + (1) UMP_c0[c0]
42	<->	kb|g.575.peg.1284	MMP0385	K09903	2.7.4.22	(1) ATP_c0[c0] + (1) UMP_c0[c0] <-> (1) ADP_c0[c0] + (1) UDP_c0[c0]
43	->	kb|g.575.peg.1719	MMP0893	K01937	6.3.4.2	(1) H2O_c0[c0] + (1) ATP_c0[c0] + (1) L-Glutamine_c0[c0] + (1) UTP_c0[c0] <-> (1) ADP_c0[c0] + (1) Phosphate_c0[c0] + (1) L-

		gpr	gene ID	KO	enzyme	definition
						Glutamate_c0[c0] + (1) CTP_c0[c0] + (2) H+_c0[c0]
44	<->	Unknown	Unknown	#N/A	1.5.1.50	(1) NAD_c0[c0] + (1) Tetrahydromethanopterin_c0[c0] <-> (1) NADH_c0[c0] + (1) H+_c0[c0] + (1) Dihydromethanopterin_c0[c0]
45	<->	kb|g.575.peg.228	MMP1605	K00873	2.7.1.40	
46	<->	kb|g.575.peg.370	MMP1094	K01007	2.7.9.2	
47	<->	kb|g.575.peg.1423	MMP0396	K01689	4.2.1.11	(1) 2-Phospho-D-glycerate_c0[c0] <-> (1) H2O_c0[c0] + (1) Phosphoenolpyruvate_c0[c0]
49	<->	kb|g.575.peg.387	MMP1439	K15635	5.4.2.12	(1) 2-Phospho-D-glycerate_c0[c0] <-> (1) 3-Phosphoglycerate_c0[c0]
50	<->	kb|g.575.peg.298	MMP1532	K00927	2.7.2.3	(1) ATP_c0[c0] + (1) 3-Phosphoglycerate_c0[c0] <-> (1) ADP_c0[c0] + (1) 1,3-Bisphospho-D-glycerate_c0[c0]
51	<->	kb|g.575.peg.517	MMP0325	K00150	1.2.1.59	(1) NAD_c0[c0] + (1) Phosphate_c0[c0] + (1) Glyceraldehyde3-phosphate_c0[c0] <-> (1) NADH_c0[c0] + (1) H+_c0[c0] + (1) 1,3-Bisphospho-D-glycerate_c0[c0]
52	<->	kb|g.575.peg.1288	MMP0687	K01803	5.3.1.1	(1) Glyceraldehyde3-phosphate_c0[c0] <-> (1) Glycerone-phosphate_c0[c0]
53	<->	kb|g.575.peg.646	MMP1077	K03431	5.4.2.10	(1) Glucose-1-phosphate_c0[c0] <-> (1) D-glucose-6-phosphate_c0[c0]
55	<->	kb|g.575.peg.572	MMP1189	K01807	5.3.1.6	(1) ribose-5-phosphate_c0[c0] <-> (1) D-Ribulose5-phosphate_c0[c0]
56	<->	kb|g.575.peg.1478	MMP0410	K00948	2.7.6.1	
57	->	kb|g.575.peg.373	MMP0148	K01895	6.2.1.1	(1) ATP_c0[c0] + (1) CoA_c0[c0] + (1) Acetate_c0[c0] <-> (1) PPi_c0[c0] + (1) AMP_c0[c0] + (1) Acetyl-CoA_c0[c0]
58	->	kb|g.575.peg.579	MMP1274	K01895	6.2.1.1	
59	->	kb|g.575.peg.454	MMP1505	K00169	1.2.7.1	
60	->	kb|g.575.peg.562	MMP1504	K00170	1.2.7.1	
61	->	kb|g.575.peg.673	MMP1507	K00172	1.2.7.1	
62	->	kb|g.575.peg.115	MMP1506	K00171	1.2.7.1	
63	->	kb|g.575.peg.454	MMP1505	K00169	1.2.7.1	

		gpr	gene ID	KO	enzyme	definition
64	->	kb|g.575.peg.562	MMP1504	K00170	1.2.7.1	
65	->	kb|g.575.peg.673	MMP1507	K00172	1.2.7.1	
66	<->	kb|g.575.peg.1400	MMP0341	K01959	6.4.1.1	
67	->	kb|g.575.peg.1305	MMP0340	K01960	6.4.1.1	
68	<->	kb|g.575.peg.1273	MMP0645	K00024	1.1.1.37	(1) NAD_c0[c0] + (1) L-Malate_c0[c0] <-> (1) NADH_c0[c0] + (1) Oxaloacetate_c0[c0] + (1) H+_c0[c0]
69	<->	kb|g.575.peg.713	MMP0130	K01677	4.2.1.2	(1) L-Malate_c0[c0] <-> (1) H2O_c0[c0] + (1) Fumarate_c0[c0]
70	->	kb|g.575.peg.426	MMP1548	K01678	4.2.1.2	
71	->	kb|g.575.peg.266	MMP1277	K18209	1.3.4.1	(2) H+_c0[c0] + (1) Fumarate_c0[c0] + (2) Reducedferredoxin_c0[c0] <-> (1) Succinate_c0[c0] + (2) Oxidizedferredoxin_c0[c0]
72	->	kb|g.575.peg.863	MMP1067	K18210	1.3.4.1	
73	<->	kb|g.575.peg.1554	MMP0955	K01902	6.2.1.5	(1) ATP_c0[c0] + (1) CoA_c0[c0] + (1) Succinate_c0[c0] <-> (1) ADP_c0[c0] + (1) Phosphate_c0[c0] + (1) Succinyl-CoA_c0[c0]
74	->	kb|g.575.peg.967	MMP1105	K01903	6.2.1.5	
75	<->	kb|g.575.peg.1700	MMP0003	K00174	1.2.7.3/1.2.7.11	(1) CO2_c0[c0] + (1) H+_c0[c0] + (1) Succinyl-CoA_c0[c0] + (2) Reducedferredoxin_c0[c0] <-> (1) CoA_c0[c0] + (1) 2-Oxoglutarate_c0[c0] + (2) Oxidizedferredoxin_c0[c0]
76	->	kb|g.575.peg.799	Unknown	#N/A		
77	->	kb|g.575.peg.975	MMP1315	K00177	1.2.7.3	
78	->	kb|g.575.peg.1700	MMP0003	K00174	1.2.7.3/1.2.7.11	
79	->	kb|g.575.peg.718	MMP0305	K00175	1.2.7.3/1.2.7.11	
80	->	kb|g.575.peg.975	MMP1315	K00177	1.2.7.3	
81	<->	kb|g.575.peg.881	MMP1457	K14101	1.12.7.2	(2) Oxidizedferredoxin_c0[c0] + (1) H2_c0[c0] + (2) Na+_e0[e0] <-> (2) H+_c0[c0] + (2) Reducedferredoxin_c0[c0] + (2) Na+_c0[c0]
82	<->	kb|g.575.peg.27	MMP1461	K14105	0	

		gpr	gene ID	KO	enzyme		definition
83	<->	kb|g.575.peg.295	MMP1462	K14106		0	
84	<->	kb|g.575.peg.680	MMP1248	K00200	1.2.99.5		(1) CO2_c0[c0] + (1) Methanofuran_c0[c0] + (2) Reducedferredoxin_c0[c0] <-> (1) H2O_c0[c0] + (1) Formylmethanofuran_c0[c0] + (2) Oxidizedferredoxin_c0[c0] + (1) H+_c0[c0]
85	->	kb|g.575.peg.680	MMP1248	K00200	1.2.99.5		
86	->	kb|g.575.peg.438	MMP1691	K00201	1.2.99.5		
87	->	kb|g.575.peg.481	MMP1249	K00202	1.2.99.5		
88	->	kb|g.575.peg.243	MMP1247	K00203	1.2.99.5		
89	<->	kb|g.575.peg.268	MMP1609	K00672	2.3.1.101		(3) H+_c0[c0] + (1) Formylmethanofuran_c0[c0] + (1) H4MPT_c0[c0] <-> (1) Methanofuran_c0[c0] + (1) 5-Formyl-H4MPT_c0[c0]
90	<->	kb|g.575.peg.509	MMP1191	K01499	3.5.4.27		(1) H2O_c0[c0] + (1) 5,10-Methenyltetrahydromethanopterin_c0[c0] <-> (1) H+_c0[c0] + (1) 5-Formyl-H4MPT_c0[c0]
91	<->	kb|g.575.peg.1316	MMP0372	K00319	1.5.98.1		(1) 5,10-Methenyltetrahydromethanopterin_c0[c0] + (1) coenzyme-ferredoxin-420-2(reduced)_c0[c0] <-> (1) H+_c0[c0] + (1) 5,10-Methylenetetrahydromethanopterin_c0[c0] + (1) coenzyme-ferredoxin-420-2(oxidized)_c0[c0]
92	<->	kb|g.575.peg.1082	MMP0058	K00320	1.5.98.2		(1) 5,10-Methylenetetrahydromethanopterin_c0[c0] + (1) coenzyme-ferredoxin-420-2(reduced)_c0[c0] <-> (1) 5-Methyl-H4MPT_c0[c0] + (1) coenzyme-ferredoxin-420-2(oxidized)_c0[c0]
93	<->	kb|g.575.peg.567	MMP1560	K00581	2.1.1.86		(1) CoM_c0[c0] + (1) 5-Methyl-H4MPT_c0[c0] + (2) Na+_c0[c0] <-> (1) H4MPT_c0[c0] + (2) Na+_e0[e0] + (1) Methyl-CoM_c0[c0]
94	<->	kb|g.575.peg.585	MMP1561	K00580	2.1.1.86		
95	<->	kb|g.575.peg.290	MMP1562	K00579	2.1.1.86		
96	<->	kb|g.575.peg.143	MMP1563	K00578	2.1.1.86		

		gpr	gene ID	KO	enzyme		definition
97	<->	kb|g.575.peg.11	MMP1564	K00577	2.1.1.86		
	<->	kb|g.575.peg.521	MMP1565	K00577	2.1.1.86		
	<->	kb|g.575.peg.655	MMP1566	K00583	2.1.1.86		
	<->	kb|g.575.peg.923	MMP1567	K00584	2.1.1.86		
98	<->	kb|g.575.peg.950	MMP1559	K00399	2.8.4.1		(1) Methyl-CoM_c0[c0] + (1) HTP_c0[c0] <-> (1) Methane_c0[c0] + (1) CoM-S-S-CoB_c0[c0] + (1) H+_c0[c0]
99	<->	kb|g.575.peg.442	MMP1555	K00401	2.8.4.1		
100	<->	kb|g.575.peg.119	MMP1558	K00402	2.8.4.1		
101	<->	kb|g.575.peg.1148	MMP0083	K00441	1.12.98.1		(1) H2_c0[c0] + (1) coenzyme-ferredoxin-420-2(oxidized)_c0[c0] <-> (1) coenzyme-ferredoxin-420-2(reduced)_c0[c0]
		kb|g.575.peg.1569	MMP0817	K00441	1.12.98.1		
		kb|g.575.peg.1511	MMP0818	K00443	1.12.98.1		
		kb|g.575.peg.1442	MMP0820	K00440	1.12.98.1		
		kb|g.575.peg.854	MMP1382	K00440	1.12.98.1		
		kb|g.575.peg.684	MMP1384	K00443	1.12.98.1		
		kb|g.575.peg.338	MMP1385	K00441	1.12.98.1		
		kb|g.575.peg.1343	MMP0819	K00442		0	
		kb|g.575.peg.546	MMP1337	K00442		0	
		kb|g.575.peg.696	MMP1383	K00442		0	
104	->	kb|g.575.peg.1104	MMP0825	K03388	1.8.98.1		(1) CoM-S-S-CoB_c0[c0] + (2) Oxidizedferredoxin_c0[c0] + (2) H2_c0[c0] <-> (1) H+_c0[c0] + (1) CoM_c0[c0] + (1) HTP_c0[c0] + (2) Reducedferredoxin_c0[c0]
105	->	kb|g.575.peg.120	MMP1053	K03389	1.8.98.1		
106	->	kb|g.575.peg.931	MMP1154	K03390	1.8.98.1		
107	->	kb|g.575.peg.1302	MMP0985	K00192	1.2.7.4		(1) CoA_c0[c0] + (1) CO2_c0[c0] + (2) H+_c0[c0] + (1) 5-Methyl-H4MPT_c0[c0] + (2) Reducedferredoxin_c0[c0] <-> (1) H2O_c0[c0] + (1) Acetyl-

		gpr	gene ID	KO	enzyme		definition
							CoA_c0[c0] + (1) H4MPT_c0[c0] + (2) Oxidizedferredoxin_c0[c0]
108	->	kb|g.575.peg.1353	MMP0983	K00193	2.3.1.-		
109	->	kb|g.575.peg.1628	MMP0984	K00195		0	
110	->	kb|g.575.peg.1190	MMP0981	K00194	2.1.1.245		
111	->	kb|g.575.peg.1081	MMP0980	K00197	2.1.1.245		
112	<->	kb|g.575.peg.328	MMP1044	K02117	3.6.3.14/3.6.3.15		
1307	<->	kb|g.575.peg.328	MMP1044	K02117	3.6.3.14/3.6.3.15		(1) H2O_c0[c0] + (1) ATP_c0[c0] + (3) H+_c0[c0] -> (1) ADP_c0[c0] + (1) Phosphate_c0[c0] + (4) H+_e0[e0]
113	<->	kb|g.575.peg.467	MMP1042	K02119		0	
114	<->	kb|g.575.peg.126	MMP1046	K02120		0	
115	<->	kb|g.575.peg.328	MMP1044	K02117	3.6.3.14/3.6.3.15		(1) H+_c0[c0] + (1) ADP_c0[c0] + (1) Phosphate_c0[c0] + (3) Na+_e0[e0] <-> (1) H2O_c0[c0] + (1) ATP_c0[c0] + (3) Na+_c0[c0]
116	<->	kb|g.575.peg.467	MMP1042	K02119		0	
117	<->	kb|g.575.peg.126	MMP1046	K02120		0	
118	<->	kb|g.575.peg.514	MMP0219	K15986	3.6.1.1		(1) H2O_c0[c0] + (1) PPi_c0[c0] <-> (2) Phosphate_c0[c0] + (1) H+_c0[c0]
119	->	kb|g.575.peg.334	MMP1234	K21029	2.7.7.80		
120	->	kb|g.575.peg.334	MMP1234	K21029	2.7.7.80		(1) ATP_c0[c0] + (1) C15810_c0[c0] <-> (1) PPi_c0[c0] + (1) C15813_c0[c0]
121	->	kb|g.575.peg.1429	MMP0571	K03639	4.1.99.22		
122	->	kb|g.575.peg.717	MMP1235	K03635	2.8.1.12		
123	->	kb|g.575.peg.1084	MMP0391	no KO assigned	2.6.1.44		(1) Glyoxalate_c0[c0] + (1) L-Alanine_c0[c0] <-> (1) Pyruvate_c0[c0] + (1) Glycine_c0[c0]
124	->	kb|g.575.peg.1084	MMP0391	no KO assigned	2.6.1.1		(1) 2-Oxoglutarate_c0[c0] + (1) Glycine_c0[c0] <-> (1) L-Glutamate_c0[c0] + (1) Glyoxalate_c0[c0]
125	<->	kb|g.575.peg.1632	MMP0553	K00611	2.1.3.3		(1) Ornithine_c0[c0] + (1) Carbamoylphosphate_c0[c0] <-> (1) Phosphate_c0[c0] + (1) H+_c0[c0] + (1) Citrulline_c0[c0]

		gpr	gene ID	KO	enzyme	definition
126	->	kb|g.575.peg.1265	MMP0073	K01940	6.3.4.5	(1) ATP_c0[c0] + (1) L-Aspartate_c0[c0] + (1) Citrulline_c0[c0] <-> (1) PPi_c0[c0] + (1) AMP_c0[c0] + (1) H+_c0[c0] + (1) L-Argininosuccinate_c0[c0]
127	<->	kb|g.575.peg.55	MMP0013	K01755	4.3.2.1	(1) L-Argininosuccinate_c0[c0] <-> (1) L-Arginine_c0[c0] + (1) Fumarate_c0[c0]
128	->	kb|g.575.peg.1662	MMP0918	K01953	6.3.5.4	(1) H2O_c0[c0] + (1) ATP_c0[c0] + (1) L-Aspartate_c0[c0] + (1) L-Glutamine_c0[c0] <-> (1) PPi_c0[c0] + (1) AMP_c0[c0] + (1) L-Glutamate_c0[c0] + (1) L-Asparagine_c0[c0] + (1) H+_c0[c0]
129	<->	kb|g.575.peg.93	MMP1072	K00812	2.6.1.1	(1) 2-Oxoglutarate_c0[c0] + (1) L-Aspartate_c0[c0] <-> (1) L-Glutamate_c0[c0] + (1) Oxaloacetate_c0[c0]
130	->	Unknown	Unknown	#N/A	#N/A	(1) Glycerone-phosphate_c0[c0] <-> (1) Phosphate_c0[c0] + (1) 2-Oxopropanal_c0[c0]
131	->	kb|g.575.peg.639	MMP1205	K00800	2.5.1.19	(1) Phosphoenolpyruvate_c0[c0] + (1) 3-phosphoshikimate_c0[c0] <-> (1) Phosphate_c0[c0] + (1) 5-O--1-Carboxyvinyl-3-phosphoshikimate_c0[c0]
132	->	kb|g.575.peg.593	MMP1333	K01736	4.2.3.5	(1) 5-O--1-Carboxyvinyl-3-phosphoshikimate_c0[c0] <-> (1) Phosphate_c0[c0] + (1) Chorismate_c0[c0]
54	<->	kb|g.575.peg.485	MMP0293	K16305	4.1.2.13/2.2.1.10	(1) D-fructose-1,6-bisphosphate_c0[c0] <-> (1) Glycerone-phosphate_c0[c0] + (1) Glyceraldehyde3-phosphate_c0[c0]
133	->	kb|g.575.peg.485	MMP0293	K16305	2.2.1.11/4.1.2.13	(1) D-fructose-1,6-bisphosphate_c0[c0] + (1) 2-Oxopropanal_c0[c0] <-> (1) Glyceraldehyde3-phosphate_c0[c0] + (1) 6-deoxy-5-ketofructose-1-phosphate_c0[c0]
134	->	kb|g.575.peg.1330	MMP0686	K16306	2.2.1.10/4.1.2.13	(2) H+_c0[c0] + (1) L-Aspartate4-semialdehyde_c0[c0] + (1) 6-deoxy-5-ketofructose-1-phosphate_c0[c0] <-> (1) Hydroxypyruvaldehyde phosphate_c0[c0] + (1) 2-Amino-3,7-dideoxy-D-threo-hept-6-ulosonic acid_c0[c0]
135	->	Unknown	Unknown	#N/A	1.2.1.3	(1) H2O_c0[c0] + (1) Hydroxypyruvaldehyde phosphate_c0[c0] + (1) NAD+_c0[c0] <-> (1) 3-Phosphonooxypyruvate_c0[c0] + (1) NADH_c0[c0] + (3) H+_c0[c0]

		gpr	gene ID	KO	enzyme	definition
136	<->	kb|g.575.peg.1383	MMP0006	K11646	1.4.1.24	
137	->	kb|g.575.peg.639	MMP1205	K00800	2.5.1.19	(1) Phosphoenolpyruvate_c0[c0] + (1) 3-phosphoshikimate_c0[c0] <-> (1) Phosphate_c0[c0] + (1) 5-O--1-Carboxyvinyl-3-phosphoshikimate_c0[c0]
138	<->	kb|g.575.peg.1465	MMP0936	K00014	1.1.1.25	(1) NAD_c0[c0] + (1) Shikimate_c0[c0] <-> (1) NADH_c0[c0] + (1) H+_c0[c0] + (1) 3-Dehydroshikimate_c0[c0]
139	<->	kb|g.575.peg.507	MMP1206	K01915	6.3.1.2	(1) ATP_c0[c0] + (1) NH3_c0[c0] + (1) L-Glutamate_c0[c0] <-> (1) ADP_c0[c0] + (1) Phosphate_c0[c0] + (1) L-Glutamine_c0[c0] + (1) H+_c0[c0]
140	<->	kb|g.575.peg.362	MMP1018	K09011	2.3.1.182	(1) H2O_c0[c0] + (1) Pyruvate_c0[c0] + (1) Acetyl-CoA_c0[c0] <-> (1) CoA_c0[c0] + (1) H+_c0[c0] + (1) D-Citramalate_c0[c0]
142	<->	kb|g.575.peg.406	MMP0136	K01704	4.2.1.33/4.2.1.35	(1) H2O_c0[c0] + (1) Citraconate_c0[c0] <-> (1) D-erythro-3-Methylmalate_c0[c0]
143	<->	kb|g.575.peg.1107	MMP0880	K10978	1.1.1.87/1.1.1.-	(1) NAD_c0[c0] + (1) Homoisocitrate_c0[c0] <-> (1) NADH_c0[c0] + (1) CO2_c0[c0] + (1) 2-Oxoadipate_c0[c0]
144	->	kb|g.575.peg.1371	MMP0651	K01653	2.2.1.6	(1) Pyruvate_c0[c0] + (1) H+_c0[c0] + (1) 2-Oxobutyrate_c0[c0] <-> (1) CO2_c0[c0] + (1) 2-Aceto-2-hydroxybutanoate_c0[c0]
145	->	kb|g.575.peg.998	MMP0654	K00053	1.1.1.86	(1) NADPH_c0[c0] + (1) H+_c0[c0] + (1) 2-Aceto-2-hydroxybutanoate_c0[c0] <-> (1) NADP_c0[c0] + (1) 2,3-Dihydroxy-3-methylvalerate_c0[c0]
146	->	kb|g.575.peg.591	MMP0318	K01687	4.2.1.9	(1) 2,3-Dihydroxy-3-methylvalerate_c0[c0] <-> (1) H2O_c0[c0] + (1) 3MOP_c0[c0]
147	<->	kb|g.575.peg.974	MMP0132	K00826	2.6.1.42	(1) 2-Oxoglutarate_c0[c0] + (1) L-Isoleucine_c0[c0] <-> (1) L-Glutamate_c0[c0] + (1) 3MOP_c0[c0]
141	<->	kb|g.575.peg.406	MMP0136	K01704	4.2.1.35/4.2.1.33	(1) D-Citramalate_c0[c0] <-> (1) H2O_c0[c0] + (1) Citraconate_c0[c0]
148	<->	kb|g.575.peg.23	MMP1149	K01703	4.2.1.33/4.2.1.35	(1) 2-Isopropylmalate_c0[c0] <-> (1) H2O_c0[c0] + (1) 2-Isopropylmaleate_c0[c0]
149	<->	kb|g.575.peg.23	MMP1149	K01703	4.2.1.33/4.2.1.35	(1) 3-Isopropylmalate_c0[c0] = (1) 2-Isopropylmaleate_c0[c0] + (1) H2O_c0

		gpr	gene ID	KO	enzyme	definition
150	<->	kb|g.575.peg.1107	MMP0880	K10978	1.1.1.87/1.1.1.-	(1) NAD_c0[c0] + (1) 3-Isopropylmalate_c0[c0] <-> (1) NADH_c0[c0] + (1) H+_c0[c0] + (1) 2-isopropyl-3-oxosuccinate_c0[c0]
151	<->	Unknown	MMP0539	K00052	1.1.1.85	(1) CO2_c0[c0] + (1) 4MOP_c0[c0] <-> (1) 2-isopropyl-3-oxosuccinate_c0[c0] + (1) H+_c0[c0]
152	<->	kb|g.575.peg.974	MMP0132	K00826	2.6.1.42	(1) 2-Oxoglutarate_c0[c0] + (1) L-Leucine_c0[c0] <-> (1) L-Glutamate_c0[c0] + (1) 4MOP_c0[c0]
153	<->	kb|g.575.peg.695	MMP1017	K00928	2.7.2.4	
154	<->	kb|g.575.peg.870	MMP1391	K00133	1.2.1.11	(1) NADP_c0[c0] + (1) Phosphate_c0[c0] + (1) L-Aspartate4-semialdehyde_c0[c0] <-> (1) NADPH_c0[c0] + (1) H+_c0[c0] + (1) 4-Phospho-L-aspartate_c0[c0]
155	<->	kb|g.575.peg.1531	MMP0576	K01714	4.3.3.7	(1) Pyruvate_c0[c0] + (1) L-Aspartate4-semialdehyde_c0[c0] <-> (2) H2O_c0[c0] + (1) H+_c0[c0] + (1) Dihydrodipicolinate_c0[c0]
156	<->	kb|g.575.peg.1716	MMP0923	K00215	1.17.1.8	(1) NAD_c0[c0] + (1) tetrahydrodipicolinate_c0[c0] <-> (1) NADH_c0[c0] + (1) H+_c0[c0] + (1) Dihydrodipicolinate_c0[c0]
157	<->	kb|g.575.peg.432	MMP1527	K10206	2.6.1.83	(1) 2-Oxoglutarate_c0[c0] + (1) LL-2,6-Diaminopimelate_c0[c0] <-> (1) H2O_c0[c0] + (1) L-Glutamate_c0[c0] + (1) tetrahydrodipicolinate_c0[c0] + (1) H+_c0[c0]
136	<->	kb|g.575.peg.432	MMP1527		2.6.1.1	(1) 2-Oxoglutarate_c0[c0] + (1) L-phenylalanine_c0[c0] <-> (1) L-Glutamate_c0[c0] + (1) Phenylpyruvate_c0[c0]
158	<->	kb|g.575.peg.1580	MMP0917	K01778	5.1.1.7	(1) LL-2,6-Diaminopimelate_c0[c0] <-> (1) meso-2,6-Diaminopimelate_c0[c0]
159	<->	kb|g.575.peg.689	MMP1200	K01586	4.1.1.20	(1) H+_c0[c0] + (1) meso-2,6-Diaminopimelate_c0[c0] <-> (1) CO2_c0[c0] + (1) L-Lysine_c0[c0]
160	<->	kb|g.575.peg.1520	MMP0401	K00549	2.1.1.14	(1) Homocysteine_c0[c0] + (1) 5-Methyltetrahydromethanopterin_c0[c0] <-> (1) L-Methionine_c0[c0] + (1) Tetrahydromethanopterin_c0[c0]
161	<->	Unknown	Unknown	#N/A	#N/A	(1) NAD_c0[c0] + (1) 5-Methyltetrahydromethanopterin_c0[c0] <-> (1) NADH_c0[c0] + (1) H+_c0[c0] + (1) 5-10-Methylenetetrahydromethanopterin_c0[c0]

		gpr	gene ID	KO	enzyme	definition
162	->	Unknown	Unknown	#N/A	1.5.7.1	(2) H+_c0[c0] + (1) 5-10-Methylenetetrahydromethanopterin_c0[c0] + (2) Reducedferredoxin_c0[c0] <-> (1) 5-Methyltetrahydromethanopterin_c0[c0] + (2) Oxidizedferredoxin_c0[c0]
163	<->	kb|g.575.peg.508	MMP1528	K04518	4.2.1.51	(1) H+_c0[c0] + (1) Prephenate_c0[c0] <-> (1) H2O_c0[c0] + (1) CO2_c0[c0] + (1) Phenylpyruvate_c0[c0]
164	<->	kb|g.575.peg.93	MMP1072	K00812	2.6.1.1	
439	<->	kb|g.575.peg.819	MMP1216	K00817	2.6.1.9	
165	->	kb|g.575.peg.1240	MMP0897	K00620	2.3.1.35/2.3.1.1	(1) L-Glutamate_c0[c0] + (1) N-Acetylornithine_c0[c0] <-> (1) Ornithine_c0[c0] + (1) N-Acetyl-L-glutamate_c0[c0]
166	->	kb|g.575.peg.1101	MMP0063	K00930	2.7.2.8	
167	<->	kb|g.575.peg.987	MMP0116	K00145	1.2.1.38	(1) NADP_c0[c0] + (1) Phosphate_c0[c0] + (1) 2-Acetamido-5-oxopentanoate_c0[c0] <-> (1) NADPH_c0[c0] + (1) H+_c0[c0] + (1) n-acetylglutamyl-phosphate_c0[c0]
168	<->	kb|g.575.peg.462	MMP1101	K00821	2.6.1.11/2.6.1.17	(1) 2-Oxoglutarate_c0[c0] + (1) N-Acetylornithine_c0[c0] <-> (1) L-Glutamate_c0[c0] + (1) 2-Acetamido-5-oxopentanoate_c0[c0]
169	<->	kb|g.575.peg.237	MMP1702	K00003	1.1.1.3	(1) NAD_c0[c0] + (1) L-Homoserine_c0[c0] <-> (1) NADH_c0[c0] + (1) H+_c0[c0] + (1) L-Aspartate4-semialdehyde_c0[c0]
170	<->	Unknown	Unknown	#N/A	2.7.1.39	
171	->	kb|g.575.peg.288	MMP0135	K01733	4.2.3.1	(1) H2O_c0[c0] + (1) O-Phospho-L-homoserine_c0[c0] <-> (1) Phosphate_c0[c0] + (1) L-Threonine_c0[c0]
172	->	kb|g.575.peg.60	MMP1006	K01657	4.1.3.27	(1) L-Glutamine_c0[c0] + (1) Chorismate_c0[c0] <-> (1) Pyruvate_c0[c0] + (1) L-Glutamate_c0[c0] + (1) Anthranilate_c0[c0] + (1) H+_c0[c0]
173	->	kb|g.575.peg.184	MMP1005	K01658	4.1.3.27	

		gpr	gene ID	KO	enzyme	definition
174	<->	kb|g.575.peg.916	MMP1007	K00766	2.4.2.18	(1) PPi_c0[c0] + (1) N-5-phosphoribosyl-anthranilate_c0[c0] <-> (1) Anthranilate_c0[c0] + (1) PRPP_c0[c0]
175	->	kb|g.575.peg.10	MMP1008	K01609	4.1.1.48	(1) H+_c0[c0] + (1) 1-(2-carboxyphenylamino)-1-deoxyribulose-5-phosphate_c0[c0] <-> (1) H2O_c0[c0] + (1) CO2_c0[c0] + (1) Indoleglycerol-phosphate_c0[c0]
176	->	kb|g.575.peg.551	MMP1002	K01695	4.2.1.20	(1) L-Serine_c0[c0] + (1) Indoleglycerol-phosphate_c0[c0] <-> (1) H2O_c0[c0] + (1) L-Tryptophan_c0[c0] + (1) Glyceraldehyde3-phosphate_c0[c0]
177	->	kb|g.575.peg.367	MMP1003	K01696	4.2.1.20	
178	<->	kb|g.575.peg.518	MMP1514	K04517	1.3.1.12	(1) NAD_c0[c0] + (1) Prephenate_c0[c0] <-> (1) NADH_c0[c0] + (1) CO2_c0[c0] + (1) p-hydroxyphenylpyruvate_c0[c0]
179	<->	kb|g.575.peg.93	MMP1072	K00812	2.6.1.1	(1) 2-Oxoglutarate_c0[c0] + (1) L-Tyrosine_c0[c0] <-> (1) L-Glutamate_c0[c0] + (1) p-hydroxyphenylpyruvate_c0[c0]
180	->	kb|g.575.peg.1371	MMP0651	K01653	2.2.1.6	(2) Pyruvate_c0[c0] + (1) H+_c0[c0] <-> (1) CO2_c0[c0] + (1) ALCTT_c0[c0]
181	->	kb|g.575.peg.1467	MMP0650	K01652	2.2.1.6	
182	<->	kb|g.575.peg.998	MMP0654	K00053	1.1.1.86	(1) NADPH_c0[c0] + (1) H+_c0[c0] + (1) ALCTT_c0[c0] <-> (1) NADP_c0[c0] + (1) 2,3-Dihydroxy-isovalerate_c0[c0]
183	->	kb|g.575.peg.591	MMP0318	K01687	4.2.1.9	(1) 2,3-Dihydroxy-isovalerate_c0[c0] <-> (1) H2O_c0[c0] + (1) 3-Methyl-2-oxobutanoate_c0[c0]
184	<->	kb|g.575.peg.974	MMP0132	K00826	2.6.1.42	(1) 2-Oxoglutarate_c0[c0] + (1) L-Valine_c0[c0] <-> (1) L-Glutamate_c0[c0] + (1) 3-Methyl-2-oxobutanoate_c0[c0]
185	<->	kb|g.575.peg.1660	MMP0947	K00765	2.4.2.17	(1) PPi_c0[c0] + (1) Phosphoribosyl-ATP_c0[c0] <-> (1) ATP_c0[c0] + (1) PRPP_c0[c0] + (1) H+_c0[c0]
186	->	kb|g.575.peg.205	MMP0280	K01496	3.5.4.19	(1) H2O_c0[c0] + (1) Phosphoribosyl-AMP_c0[c0] <-> (1) phosphoribosylformiminoaicar-phosphate_c0[c0]
187	->	kb|g.575.peg.124	MMP1690	K01814	5.3.1.16	(1) phosphoribosylformiminoaicar-phosphate_c0[c0] <-> (1) phosphoribulosylformimino-AICAR-phosphate_c0[c0]
188	->	kb|g.575.peg.1272	MMP0417	K01814	5.3.1.16	

		gpr	gene ID	KO	enzyme	definition
189	->	kb|g.575.peg.732	MMP1722	K02500	4.1.3.-	(1) L-Glutamine_c0[c0] + (1) phosphoribulosylformimino-AICAR-phosphate_c0[c0] <-> (1) L-Glutamate_c0[c0] + (1) H+_c0[c0] + (1) D-erythro-imidazol-glycerol-phosphate_c0[c0] + (1) AICAR_c0[c0]
190	->	kb|g.575.peg.1388	MMP0548	K01693	4.2.1.19	(1) D-erythro-imidazol-glycerol-phosphate_c0[c0] <-> (1) H2O_c0[c0] + (1) imidazole-acetol-phosphate_c0[c0]
191	<->	kb|g.575.peg.819	MMP1216	K00817	2.6.1.9	(1) 2-Oxoglutarate_c0[c0] + (1) L-histidinol-phosphate_c0[c0] <-> (1) L-Glutamate_c0[c0] + (1) imidazole-acetol-phosphate_c0[c0]
192	->	Unknown	Unknown	#N/A	3.1.3.15	(1) H2O_c0[c0] + (1) L-histidinol-phosphate_c0[c0] <-> (1) Phosphate_c0[c0] + (1) L-Histidinol_c0[c0]
193	->	kb|g.575.peg.1455	MMP0968	K00013	1.1.1.23	(1) H2O_c0[c0] + (2) NAD_c0[c0] + (1) L-Histidinol_c0[c0] <-> (2) NADH_c0[c0] + (3) H+_c0[c0] + (1) L-Histidine_c0[c0]
194	->	Unknown	Unknown	#N/A	#N/A	5.7 L-Alanyl-tRNA_c0 + 1.3 L-cysteinyl-tRNA(Cys)_c0 + 5.6 L-aspartyl-tRNA(Asp)_c0 + 8.1 L-glutamyl-tRNA-Glu_c0 + 4.3 L-phenylalanyl-tRNA(Phe)_c0 + 6.7 Glycyl-tRNA(Gly)_c0 + 1.5 L-histidyl-tRNA(His)_c0 + 9.4 L-isoleucyl-tRNA(Ile)_c0 + 8.9 L-lysyl-tRNA_c0 + 9.1 L-leucyl-tRNA_c0 + 2.6 L-methionyl-tRNA_c0 + 5.7 Asn-tRNA(Asn)_c0 + 3.4 L-prolyl-tRNA(Pro)_c0 + 1.9 Gln-tRNA(Gln)_c0 + 3.1 L-arginyl-tRNA_c0 + 6.3 L-seryl-tRNA(Ser)_c0 + 5 L-threonyl-tRNA(Thr)_c0 + 7 L-valyl-tRNA(Val)_c0 + 0.7 L-tryptophanyl-tRNA(Trp)_c0 + 3.9 L-tyrosyl-tRNA(Tyr)_c0 + 198 GTP_c0 + 199 H2O_c0 = 5.7 tRNA(Ala)_c0 + 1.3 tRNA(Cys)_c0 + 5.6 tRNA(Asp)_c0 + 8.1 tRNA(Glu)_c0 + 4.3 tRNA(Phe)_c0 + 6.7 tRNA(Gly)_c0 + 1.5 tRNA(His)_c0 + 9.4 tRNA(Ile)_c0 + 8.9 tRNA(Lys)_c0 + 9.1 tRNA(Leu)_c0 + 2.6 tRNA(Met)_c0 + 5.7 tRNA(Asn)_c0 + 3.4 tRNA(Pro)_c0 + 1.9 tRNA(Gln)_c0 + 3.1

		gpr	gene ID	KO	enzyme	definition
						tRNA(Arg)_c0 + 6.3 tRNA(Ser)_c0 + 5 tRNA(Thr)_c0 + 7 tRNA(Val)_c0 + 0.7 tRNA(Trp)_c0 + 3.9 tRNA(Tyr)_c0 + 198 phosphate_c0 + 198 GDP_c0 + 1 Protein_c0 + 298 H+_c0
195	->	Unknown	Unknown	#N/A	#N/A	0.3345 dATP_c0 + 0.3345 TTP_c0 + 0.1655 dGTP_c0 + 0.1655 dCTP_c0 = 1 DNA_c0 + 1 Ppi_c0
196	->	Unknown	Unknown	#N/A	#N/A	2.12 ATP_c0 + 2.46 UTP_c0 + 2.33 GTP_c0 + 3.09 CTP_c0 = 1 RNA_c0 + 10 PPi_c0
197	->	Unknown	Unknown	#N/A	2.4.1.1	5 glucose-1-phosphate_c0 + 1 H2O_c0 = 1 Glycogen_c0 + 5 phosphate_c0
200	<->	Unknown	Unknown	#N/A	#N/A	(1) Methane_e0[e0] <-> (1) Methane_c0[c0]
201	<->	Unknown	Unknown	#N/A	#N/A	(1) CO2_e0[e0] <-> (1) CO2_c0[c0]
202	<->	Unknown	Unknown	#N/A	#N/A	(1) H2O_e0[e0] <-> (1) H2O_c0[c0]
203	<->	Unknown	Unknown	#N/A	#N/A	(1) H2_c0[c0] <-> (1) H2_e0[e0]
204	->	Unknown	Unknown	#N/A	#N/A	(1) H+_e0[e0] <-> (1) H+_c0[c0]
205	<->	Unknown	Unknown	#N/A	#N/A	(1) Acetate_c0[c0] <-> (1) Acetate_e0[e0]
206	<->	Unknown	Unknown	#N/A	#N/A	(1) NH3_e0[e0] <-> (1) NH3_c0[c0]
207	<->	Unknown	Unknown	#N/A	#N/A	(1) H2S_c0[c0] <-> (1) H2S_e0[e0]
208	<->	Unknown	Unknown	#N/A	#N/A	(1) Phosphate_c0[c0] <-> (1) Phosphate_e0[e0]
209	<->	Unknown	Unknown	#N/A	#N/A	(1) NAD_c0[c0] + (1) NADPH_c0[c0] <-> (1) NADH_c0[c0] + (1) NADP_c0[c0]
210	->		Unknown	#N/A	#N/A	0.0533 Protein_c0 + 0.0649 DNA_c0 + 0.0502 RNA_c0 + 0.1329 Glycogen_c0 + 0.1538 Lipids_c0 + 139 ATP_c0 + 139 H2O_c0 = 1 Biomass_c0 + 139 ADP_c0 + 139 phosphate_c0 + 139 H+_c0
1308	->					(1) Biomass_c0[c0] = (1) Biomass_e0[e0]

	gpr	gene ID	KO	enzyme	definition
332	kb|g.575.peg.600	MMP0228	K00555	2.1.1.215+2.1.1.216	
333	kb|g.575.peg.749	MMP1375	K07442	2.1.1.219+2.1.1.220	
359	kb|g.575.peg.1009	MMP0649	K00612	2.1.3.-	
372	kb|g.575.peg.1394	MMP0892	K03817	2.3.1.-	
391	kb|g.575.peg.1559	MMP0516	K03813	2.4.2.-	
472	kb|g.575.peg.1537	MMP0009	K18882	2.7.7.-	
473	kb|g.575.peg.1183	MMP0071	K02683	2.7.7.-	
508	kb|g.575.peg.986	MMP0308	K04085	2.8.1.-	
509	kb|g.575.peg.12	MMP0309	K07235	2.8.1.-	
516	kb|g.575.peg.1172	MMP0900	K06917	2.9.1.-	
519	kb|g.575.peg.529	MMP1313	K04799	3.-.-.-	
520	kb|g.575.peg.1189	MMP0044	K12574	3.1.-.-	
521	kb|g.575.peg.1475	MMP0374	K07060	3.1.-.-	
528	kb|g.575.peg.1679	MMP0567	K07107	3.1.2.-	
529	kb|g.575.peg.1096	MMP0755	K07452	3.1.21.-	
530	kb|g.575.peg.506	MMP1570	K03424	3.1.21.-	
546	kb|g.575.peg.1038	MMP0559	K05520	3.2.-.-	
549	kb|g.575.peg.1620	MMP0387	K13280	3.4.-.-	
550	kb|g.575.peg.1699	MMP0659	K08303	3.4.-.-	
553	kb|g.575.peg.845	MMP1069	K04773	3.4.21.-	
554	kb|g.575.peg.586	MMP1186	K04076	3.4.21.-	
558	kb|g.575.peg.1393	MMP0399	K03799	3.4.24.-	
574	kb|g.575.peg.316	MMP1284	K03725	3.6.1.-	
581	kb|g.575.peg.1140	MMP0363	K03924	3.6.3.-	
583	kb|g.575.peg.328	MMP1044	K02117	3.6.3.14+3.6.3.15	
590	kb|g.575.peg.615	MMP0216	K01534	3.6.3.3+3.6.3.5	
598	kb|g.575.peg.968	MMP0030	K10726	3.6.4.-	
599	kb|g.575.peg.1234	MMP0890	K03726	3.6.4.-	

		gpr	gene ID	KO	enzyme	definition
600		kb|g.575.peg.978	MMP1024	K10726	3.6.4.-	
601		kb|g.575.peg.84	MMP1141	K03724	3.6.4.-	
638		kb|g.575.peg.88	MMP0254	K17758/K17759	4.2.1.136/5.1.99.6	
694		kb|g.575.peg.1197	MMP0094	K07583	5.4.99.-	
695		kb|g.575.peg.841	MMP1686	K11131	5.4.99.-	
726		kb|g.575.peg.1017	MMP0566	K00666	6.2.1.-	
739		kb|g.575.peg.280	MMP1600	K05844	6.3.2.-	
774		kb|g.575.peg.1199	MMP0612	K01975	6.5.1.-	
1262		#N/A	RNA_21	K14220	#N/A	
403	<->	kb|g.575.peg.850	MMP0327	K18931	2.4.2.57	(2) H+_c0[c0] + (1) AMP_c0[c0] + (1) Orthophosphate_c0[c0] <-> (1) Adenine_c0[c0] + (1) D-Ribose 1,5-bisphosphate_c0[c0]
298	->	kb|g.575.peg.863	MMP1067	K18210	1.3.4.1	(1) Fumarate_c0[c0] + (1) Coenzyme M_c0[c0] + (1) Coenzyme B_c0[c0] <-> (1) Succinate_c0[c0] + (1) Coenzyme M 7-mercaptoheptanoylthreonine-phosphate heterodisulfide_c0[c0] + (1) H+_c0[c0]
299	->	kb|g.575.peg.266	MMP1277	K18209	1.3.4.1	
573	<->	kb|g.575.peg.1421	MMP0034	K17488	3.5.4.39	(1) GTP_c0[c0] + (1) H2O_c0[c0] <-> (1) 7,8-Dihydroneopterin 2',3'-cyclic phosphate_c0[c0] + (1) Formate_c0[c0] + (1) Diphosphate_c0[c0] + (1) H+_c0[c0]
545	<->	kb|g.575.peg.409	MMP0230	K17487	3.1.4.56	(1) 7,8-Dihydroneopterin 2',3'-cyclic phosphate_c0[c0] + (1) H2O_c0[c0] <-> (1) Dihydroneopterin phosphate_c0[c0] + (1) H+_c0[c0]
402	<->	kb|g.575.peg.526	MMP0279	K06984	2.4.2.54	(1) H+_c0[c0] + (1) 5-Phospho-alpha-D-ribose 1-diphosphate_c0[c0] + (1) 4-Aminobenzoate_c0[c0] <-> (1) 4-(beta-D-Ribofuranosyl)aniline 5'-phosphate_c0[c0] + (1) CO2_c0[c0] + (1) Diphosphate_c0[c0]
660	<->	kb|g.575.peg.1531	MMP0576	K01714	4.3.3.7	(1) H+_c0[c0] + (1) L-Aspartate 4-semialdehyde_c0[c0] + (1) Pyruvate_c0[c0] <-> (1) (2S,4S)-4-Hydroxy-2,3,4,5-tetrahydrodipicolinate_c0[c0] + (1) H2O_c0[c0]

		gpr	gene ID	KO	enzyme	definition
464	<->	kb|g.575.peg.719	MMP1645	K06981	2.7.4.26	(1) ATP_c0[c0] + (1) Isopentenyl phosphate_c0[c0] <-> (1) ADP_c0[c0] + (1) Isopentenyl diphosphate_c0[c0]
661	<->	kb|g.575.peg.1692	MMP0077	K10026	4.3.99.3	(1) H+_c0[c0] + (1) 6-Carboxy-5,6,7,8-tetrahydropterin_c0[c0] <-> (1) 7-Carboxy-7-carbaguanine_c0[c0] + (1) Ammonia_c0[c0]
1302	<->	kb|g.575.peg.856	MMP1151	K16179	0	(1) Dimethylamine_c0[c0] + (1) Coenzyme M_c0[c0] <-> (1) 2-(Methylthio)ethanesulfonate_c0[c0] + (1) Methylamine_c0[c0]
751	<->	kb|g.575.peg.336	MMP0226	K06920	6.3.4.20	(1) 7-Carboxy-7-carbaguanine_c0[c0] + (1) Ammonia_c0[c0] + (1) ATP_c0[c0] <-> (1) 7-Cyano-7-carbaguanine_c0[c0] + (1) ADP_c0[c0] + (1) Orthophosphate_c0[c0] + (1) H2O_c0[c0] + (1) H+_c0[c0]
579	<->	kb|g.575.peg.169	MMP0339	K03574	3.6.1.55	(1) 8-Oxo-dGTP_c0[c0] + (1) H2O_c0[c0] <-> (1) 8-Oxo-dGMP_c0[c0] + (1) Diphosphate_c0[c0] + (3) H+_c0[c0]
362	<->	kb|g.575.peg.258	MMP0201	K03750	2.10.1.1	(1) Adenylated molybdopterin_c0[c0] + (1) Molybdate_c0[c0] <-> (1) Molybdoenzyme molybdenum cofactor_c0[c0] + (1) AMP_c0[c0] + (1) H2O_c0[c0] + (2) H+_c0[c0]
363	<->	kb|g.575.peg.1498	MMP0513	K03750	2.10.1.1	
364	-	kb|g.575.peg.1115	MMP0545	K07219/K03750	2.7.7.75	(1) ATP_c0[c0] + (1) Molybdopterin_c0[c0] + (5) H+_c0[c0] = (1) Diphosphate_c0[c0] + (1) Adenylated molybdopterin_c0[c0]
365	<->	kb|g.575.peg.512	MMP1619	K03750	2.10.1.1	
429	<->	kb|g.575.peg.90	MMP1345	K15888	2.5.1.89	(1) Geranylgeranyl diphosphate_c0[c0] + (7) Isopentenyl diphosphate_c0[c0] <-> (7) Diphosphate_c0[c0] + (1) tritrans,heptacis-Undecaprenyl diphosphate_c0[c0]
401	<->	kb|g.575.peg.779	MMP0213	K05966	2.4.2.52	(1) H+_c0[c0] + (1) ATP_c0[c0] + (1) Dephospho-CoA_c0[c0] <-> (1) 2'-(5-Triphosphoribosyl)-3'-dephospho-CoA_c0[c0] + (1) Adenine_c0[c0]
572	<->	kb|g.575.peg.942	MMP1491	K12960	3.5.4.31+3.5.4.28	(1) H+_c0[c0] + (1) 5'-Methylthioadenosine_c0[c0] + (1) H2O_c0[c0] <-> (1) 5'-S-Methyl-

		gpr	gene ID	KO	enzyme	definition
						5'-thioinosine_c0[c0] + (1) Ammonia_c0[c0]
742	<->	kb|g.575.peg.1512	MMP0702	K15740	6.3.2.33	(1) ATP_c0[c0] + (1) 5,6,7,8-Tetrahydromethanopterin_c0[c0] + (1) L-Glutamate_c0[c0] <-> (1) ADP_c0[c0] + (1) Orthophosphate_c0[c0] + (1) Tetrahydrosarcinapterin_c0[c0] + (1) H+_c0[c0]
741	<->	kb|g.575.peg.927	MMP0170	K14940	6.3.2.32	(1) ATP_c0[c0] + (1) Coenzyme F420_c0[c0] + (1) L-Glutamate_c0[c0] <-> (1) ADP_c0[c0] + (1) Coenzyme F420-3_c0[c0] + (1) Orthophosphate_c0[c0] + (1) H+_c0[c0]
740	<->	kb|g.575.peg.1328	MMP0937	K12234	6.3.2.31+6.3.2.34	(1) Coenzyme F420-0_c0[c0] + (1) GTP_c0[c0] + (1) L-Glutamate_c0[c0] <-> (1) Coenzyme F420-1_c0[c0] + (1) GDP_c0[c0] + (1) Orthophosphate_c0[c0] + (1) H+_c0[c0]
504	<->	kb|g.575.peg.1595	MMP0404	K11212	2.7.8.28	(1) 7,8-Didemethyl-8-hydroxy-5-deazariboflavin_c0[c0] + (1) (2S)-Lactyl-2-diphospho-5'-guanosine_c0[c0] <-> (1) Coenzyme F420-0_c0[c0] + (1) GMP_c0[c0] + (1) H+_c0[c0]
493	<->	kb|g.575.peg.440	MMP0117	K14941	2.7.7.68	(1) (2S)-2-Phospholactate_c0[c0] + (1) GTP_c0[c0] + (1) H+_c0[c0] <-> (1) (2S)-Lactyl-2-diphospho-5'-guanosine_c0[c0] + (1) Diphosphate_c0[c0]
425	<->	kb|g.575.peg.1626	MMP0056	K11781	2.5.1.77	(1) 3-(4-Hydroxyphenyl)pyruvate_c0[c0] + (1) 5-Amino-6-(1-D-ribitylamino)uracil_c0[c0] + (2) S-Adenosyl-L-methionine_c0[c0] + (1) H2O_c0[c0] <-> (1) 7,8-Didemethyl-8-hydroxy-5-deazariboflavin_c0[c0] + (2) L-Methionine_c0[c0] + (2) 5'-Deoxyadenosine_c0[c0] + (1) Oxalate_c0[c0] + (1) Ammonia_c0[c0] + (3) H+_c0[c0]
426	<->	kb|g.575.peg.1545	MMP0057	K11781	2.5.1.77	
427	<->	kb|g.575.peg.1450	MMP0876	K11780	2.5.1.77	
510	<->	kb|g.575.peg.717	MMP1235	K03635	2.8.1.12	(1) Precursor Z_c0[c0] + (2) Thiocarboxy-[sulfur-carrier protein]_c0[c0] + (1) H2O_c0[c0] <-> (1) Molybdopterin_c0[c0] + (2) Sulfur-carrier protein_c0[c0] + (1) H+_c0[c0]

		gpr	gene ID	KO	enzyme	definition
743	<->	kb|g.575.peg.631	MMP1306	K09722	6.3.2.36	(1) ATP_c0[c0] + (1) (R)-4-Phosphopantoate_c0[c0] + (1) beta-Alanine_c0[c0] <-> (1) AMP_c0[c0] + (1) Diphosphate_c0[c0] + (1) D-4'-Phosphopantothenate_c0[c0] + (1) H+_c0[c0]
445	<->	kb|g.575.peg.1485	MMP0398	K06982	2.7.1.169	(1) ATP_c0[c0] + (1) (R)-Pantoate_c0[c0] <-> (1) ADP_c0[c0] + (1) (R)-4-Phosphopantoate_c0[c0] + (1) H+_c0[c0]
220	<->	kb|g.575.peg.222	MMP1348	K14654	1.1.1.302	(1) 2,5-Diamino-6-(5-phospho-D-ribosylamino)pyrimidin-4(3H)-one_c0[c0] + (1) NADH_c0[c0] + (1) H+_c0[c0] <-> (1) 2,5-Diamino-6-(5-phospho-D-ribitylamino)pyrimidin-4(3H)-one_c0[c0] + (1) NAD+_c0[c0]
561	<->	kb|g.575.peg.963	MMP1705	K14653	3.5.1.102	(1) 2-Amino-5-formylamino-6-(5-phospho-D-ribosylamino)pyrimidin-4(3H)-one_c0[c0] + (1) H2O_c0[c0] <-> (1) 2,5-Diamino-6-(5-phospho-D-ribosylamino)pyrimidin-4(3H)-one_c0[c0] + (1) Formate_c0[c0] + (1) H+_c0[c0]
337	<->	kb|g.575.peg.1382	MMP0831	K14080	2.1.1.246	(1) Methanol_c0[c0] + (1) Coenzyme M_c0[c0] <-> (1) 2-(Methylthio)ethanesulfonate_c0[c0] + (1) H2O_c0[c0]
335	<->	kb|g.575.peg.1081	MMP0980	K00197	2.1.1.245	(1) Acetyl-CoA_c0[c0] + (1) 5,6,7,8-Tetrahydromethanopterin_c0[c0] <-> (1) 5-Methyl-5,6,7,8-tetrahydromethanopterin_c0[c0] + (1) CO_c0[c0] + (1) CoA_c0[c0]
336	<->	kb|g.575.peg.1190	MMP0981	K00194	2.1.1.245	
373	<->	kb|g.575.peg.1353	MMP0983	K00193	2.3.1.-	
492	<->	kb|g.575.peg.89	MMP1698	K19664	2.7.7.67	(2) H+_c0[c0] + (1) CTP_c0[c0] + (1) 2,3-Bis-O-(geranylgeranyl)glycerol 1-phosphate_c0[c0] <-> (1) Diphosphate_c0[c0] + (1) CDP-2,3-bis-O-(geranylgeranyl)-sn-glycerol_c0[c0]
424	<->	kb|g.575.peg.767	MMP1240	K06868	2.5.1.73	(1) O-Phosphoseryl-tRNA(Cys)_c0[c0] + (1) Hydrogen sulfide_c0[c0] <-> (1) L-Cysteinyl-tRNA(Cys)_c0[c0] + (1) Orthophosphate_c0[c0]
719	<->	kb|g.575.peg.1119	MMP0688	K07587	6.1.1.27	(1) O-Phospho-L-serine_c0[c0] + (1) tRNA(Cys)_c0[c0] + (1) ATP_c0[c0] <-> (1) O-

		gpr	gene ID	KO	enzyme	definition
						Phosphoseryl-tRNA(Cys)_c0[c0] + (1) Diphosphate_c0[c0] + (1) AMP_c0[c0]
443	<->	kb|g.575.peg.167	MMP0184	K07732	2.7.1.161	(1) CTP_c0[c0] + (1) Riboflavin_c0[c0] <-> (1) CDP_c0[c0] + (1) FMN_c0[c0]
302	<->	kb|g.575.peg.1383	MMP0006	K11646	1.4.1.24	(1) 2-Amino-3,7-dideoxy-D-threo-hept-6-ulosonic acid_c0[c0] + (1) H2O_c0[c0] + (1) NAD+_c0[c0] <-> (1) 3-Dehydroquinate_c0[c0] + (1) Ammonia_c0[c0] + (1) NADH_c0[c0] + (1) H+_c0[c0]
518	->	kb|g.575.peg.1021	MMP0595	K03341	2.9.1.2	(1) O-Phosphoseryl-tRNA(Sec)_c0[c0] + (1) Selenophosphoric acid_c0[c0] + (1) H2O_c0[c0] <-> (1) L-Selenocysteinyl-tRNA(Sec)_c0[c0] + (2) Orthophosphate_c0[c0]
444	<->	kb|g.575.peg.98	MMP1490	K10837	2.7.1.164	(1) L-Seryl-tRNA(Sec)_c0[c0] + (1) ATP_c0[c0] <-> (1) O-Phosphoseryl-tRNA(Sec)_c0[c0] + (1) ADP_c0[c0] + (1) H+_c0[c0]
517	<->	kb|g.575.peg.807	MMP0002	K01042	2.9.1.1	(1) L-Seryl-tRNA(Sec)_c0[c0] + (1) Selenophosphoric acid_c0[c0] <-> (1) L-Selenocysteinyl-tRNA(Sec)_c0[c0] + (1) Orthophosphate_c0[c0]
328	<->	kb|g.575.peg.94	MMP1203	K02188	2.1.1.195	(1) Cobalt-precorrin 5B_c0[c0] + (1) S-Adenosyl-L-methionine_c0[c0] <-> (1) Cobalt-precorrin 6_c0[c0] + (1) S-Adenosyl-L-homocysteine_c0[c0] + (1) H+_c0[c0]
606	<->	kb|g.575.peg.165	MMP1591	K02189	3.7.1.12	(1) Cobalt-precorrin 5A_c0[c0] + (1) H2O_c0[c0] <-> (1) Cobalt-precorrin 5B_c0[c0] + (1) Acetaldehyde_c0[c0] + (1) H+_c0[c0]
662	<->	kb|g.575.peg.429	MMP0273	K08097	4.4.1.19	(1) (2R)-O-Phospho-3-sulfolactate_c0[c0] <-> (1) Sulfite_c0[c0] + (1) Phosphoenolpyruvate_c0[c0] + (1) H+_c0[c0]
944	<->	kb|g.575.peg.760	MMP1354	K03151	2.8.1.11	(1) [Enzyme]-S-sulfanylcysteine_c0[c0] + (1) Adenylyl-[sulfur-carrier protein]_c0[c0] + (1) Reduced acceptor_c0[c0] <-> (1) AMP_c0[c0] + (1) Thiocarboxy-[sulfur-carrier protein]_c0[c0] + (1) [Enzyme]-cysteine_c0[c0] + (1) Acceptor_c0[c0]
499	<->	kb|g.575.peg.334	MMP1234	K21029	2.7.7.80	
658	<->	kb|g.575.peg.561	MMP0103	K06215	4.3.3.6	(1) D-Glyceraldehyde 3-phosphate_c0[c0] + (1) D-Ribulose 5-phosphate_c0[c0] + (1) L-

		gpr	gene ID	KO	enzyme	definition
659	<->	kb|g.575.peg.721	MMP1656	K08681	4.3.3.6	Glutamine_c0[c0] <-> (1) Pyridoxal phosphate_c0[c0] + (1) L-Glutamate_c0[c0] + (1) Orthophosphate_c0[c0] + (3) H2O_c0[c0] + (1) H+_c0[c0]
301	<->	kb|g.575.peg.1338	MMP0737	K06989	1.4.1.21	(1) L-Aspartate_c0[c0] + (1) NADP+_c0[c0] <-> (1) Iminoaspartate_c0[c0] + (1) NADPH_c0[c0] + (2) H+_c0[c0]
697	<->	kb|g.575.peg.929	MMP0282	K01588	5.4.99.18	(1) 5-Carboxyamino-1-(5-phospho-D-ribosyl)imidazole_c0[c0] <-> (1) 1-(5-Phospho-D-ribosyl)-5-amino-4-imidazolecarboxylate_c0[c0]
377	<->	kb|g.575.peg.362	MMP1018	K09011	2.3.1.182	
571	<->	kb|g.575.peg.588	MMP1426	K09887	3.5.4.30	(1) dCTP_c0[c0] + (2) H2O_c0[c0] <-> (1) dUMP_c0[c0] + (1) Diphosphate_c0[c0] + (1) Ammonia_c0[c0]
570	<->	kb|g.575.peg.1579	MMP0405	K08096	3.5.4.29	(1) GTP_c0[c0] + (3) H2O_c0[c0] <-> (1) 2-Amino-5-formylamino-6-(5-phospho-D-ribosylamino)pyrimidin-4(3H)-one_c0[c0] + (2) Orthophosphate_c0[c0] + (2) H+_c0[c0]
630	<->	kb|g.575.peg.57	MMP0183	K02858	4.1.99.12	(1) D-Ribulose 5-phosphate_c0[c0] <-> (1) L-3,4-Dihydroxybutan-2-one 4-phosphate_c0[c0] + (1) Formate_c0[c0]
230	<->	kb|g.575.peg.104	MMP1174	K03386	1.11.1.15	(1) ROOH_c0[c0] + (2) Thiol-containing reductant_c0[c0] <-> (1) Alcohol_c0[c0] + (1) H2O_c0[c0] + (1) Oxidized thiol-containing reductant_c0[c0]
305	<->	kb|g.575.peg.849	MMP1259	K17870	1.6.3.3	(1) NADH_c0[c0] + (1) H+_c0[c0] + (1) Oxygen_c0[c0] <-> (1) NAD+_c0[c0] + (1) Hydrogen peroxide_c0[c0]
277	<->	kb|g.575.peg.17	MMP0315	K00180	1.2.7.8	(1) Indolepyruvate_c0[c0] + (1) CoA_c0[c0] + (2) Oxidized ferredoxin_c0[c0] <-> (1) S-2-(Indol-3-yl)acetyl-CoA_c0[c0] + (1) CO2_c0[c0] + (2) Reduced ferredoxin_c0[c0] + (1) H+_c0[c0]
278	<->	kb|g.575.peg.414	MMP0316	K00179	1.2.7.8	
279	<->	kb|g.575.peg.1471	MMP0713	K00179	1.2.7.8	
280	<->	kb|g.575.peg.1118	MMP0714	K00180	1.2.7.8	

		gpr	gene ID	KO	enzyme		definition
274	<->	kb|g.575.peg.50	MMP1271	K00187	1.2.7.7		(1) 3-Methyl-2-oxobutanoic acid_c0[c0] + (1) CoA_c0[c0] + (2) Oxidized ferredoxin_c0[c0] <-> (1) 2-Methylpropanoyl-CoA_c0[c0] + (1) CO2_c0[c0] + (2) Reduced ferredoxin_c0[c0]
275	<->	kb|g.575.peg.558	MMP1272	K00186	1.2.7.7		
276	<->	kb|g.575.peg.729	MMP1273	K00188	1.2.7.7		
273	<->	kb|g.575.peg.1186	MMP0945	K11389	1.2.7.6		(1) D-Glyceraldehyde 3-phosphate_c0[c0] + (1) H2O_c0[c0] + (2) Oxidized ferredoxin_c0[c0] <-> (1) 3-Phospho-D-glycerate_c0[c0] + (3) H+_c0[c0] + (2) Reduced ferredoxin_c0[c0]
781	<->	kb|g.575.peg.952	MMP1502	K00196		0	(1) CO_c0[c0] + (1) H2O_c0[c0] + (2) Oxidized ferredoxin_c0[c0] <-> (1) CO2_c0[c0] + (2) Reduced ferredoxin_c0[c0] + (2) H+_c0[c0]
782	<->	kb|g.575.peg.693	MMP1503	K00196		0	
272	<->	kb|g.575.peg.1302	MMP0985	K00192	1.2.7.4		
780	<->	kb|g.575.peg.1628	MMP0984	K00195		0	
222	<->	kb|g.575.peg.708	MMP1133	K05884	1.1.1.337		
753	<->	kb|g.575.peg.56	MMP1373	K06863	6.3.4.23		(1) Formate_c0[c0] + (1) ATP_c0[c0] + (1) 1-(5'-Phosphoribosyl)-5-amino-4-imidazolecarboxamide_c0[c0] <-> (1) ADP_c0[c0] + (1) Orthophosphate_c0[c0] + (1) 1-(5'-Phosphoribosyl)-5-formamido-4-imidazolecarboxamide_c0[c0]
736	<->	kb|g.575.peg.1067	MMP0951	K02227	6.3.1.10		(1) Adenosyl cobyrinate hexaamide_c0[c0] + (1) D-1-Aminopropan-2-ol O-phosphate_c0[c0] + (1) ATP_c0[c0] <-> (1) Adenosyl cobinamide phosphate_c0[c0] + (1) ADP_c0[c0] + (1) Orthophosphate_c0[c0] + (1) H+_c0[c0]
502	<->	kb|g.575.peg.846	MMP1423	K01001	2.7.8.15		(1) UDP-N-acetyl-alpha-D-glucosamine_c0[c0] + (1) Dolichyl phosphate_c0[c0] <-> (1) UMP_c0[c0] + (1) N-Acetyl-D-glucosaminyldiphosphodolichol_c0[c0]

		gpr	gene ID	KO	enzyme	definition
340	<->	kb|g.575.peg.981	MMP1227	K03399	2.1.1.289	(1) Cobalt-dihydro-precorrin 6_c0[c0] + (2) S-Adenosyl-L-methionine_c0[c0] <-> (1) Cobalt-precorrin 8_c0[c0] + (2) S-Adenosyl-L-homocysteine_c0[c0] + (1) CO2_c0[c0] + (1) H+_c0[c0]
329	<->	kb|g.575.peg.340	MMP1221	K02191	2.1.1.196	
667	<->	kb|g.575.peg.417	MMP0164	K03795	4.99.1.3	(1) Sirohydrochlorin_c0[c0] + (1) Cobalt ion_c0[c0] <-> (1) Cobalt-sirohydrochlorin_c0[c0] + (2) H+_c0[c0]
441	<->	kb|g.575.peg.793	MMP1296	K00918	2.7.1.146+2.7.1.147	(1) ADP_c0[c0] + (1) D-Fructose 6-phosphate_c0[c0] <-> (1) AMP_c0[c0] + (1) D-Fructose 1,6-bisphosphate_c0[c0] + (1) H+_c0[c0]
543	<->	kb|g.575.peg.692	MMP0161	K05979	3.1.3.71	(1) (2R)-O-Phospho-3-sulfolactate_c0[c0] + (1) H2O_c0[c0] <-> (1) (2R)-3-Sulfolactate_c0[c0] + (1) Orthophosphate_c0[c0] + (1) H+_c0[c0]
617	<->	kb|g.575.peg.1408	MMP0411	K06034	4.1.1.79	(1) H+_c0[c0] + (1) 3-Sulfopyruvate_c0[c0] <-> (1) Sulfoacetaldehyde_c0[c0] + (1) CO2_c0[c0]
618	<->	kb|g.575.peg.314	MMP1689	K13039	4.1.1.79	
245	<->	kb|g.575.peg.663	MMP1157	K05919	1.15.1.2	(1) Reduced rubredoxin_c0[c0] + (1) O2.-_c0[c0] + (1) H+_c0[c0] <-> (1) Oxidized rubredoxin_c0[c0] + (1) Hydrogen peroxide_c0[c0]
217	<->	kb|g.575.peg.915	MMP0225	K00096	1.1.1.261	(1) sn-Glycerol 1-phosphate_c0[c0] + (1) NAD+_c0[c0] <-> (1) Glycerone phosphate_c0[c0] + (1) NADH_c0[c0] + (2) H+_c0[c0]
577	<->	kb|g.575.peg.922	MMP1144	K06153	3.6.1.27	(1) di-trans,poly-cis-Undecaprenyl diphosphate_c0[c0] + (1) H2O_c0[c0] <-> (1) di-trans,poly-cis-Undecaprenyl phosphate_c0[c0] + (1) Orthophosphate_c0[c0] + (1) H+_c0[c0]
713	<->	kb|g.575.peg.728	MMP1011	K01885	6.1.1.17	(1) tRNA(Glu)_c0[c0] + (1) L-Glutamate_c0[c0] + (1) ATP_c0[c0] <-> (1) L-Glutamyl-tRNA(Glu)_c0[c0] + (1) Diphosphate_c0[c0] + (1) AMP_c0[c0]
703	<->					(1) tRNA(Gln)_c0[c0] + (1) L-Glutamate_c0[c0] + (1) ATP_c0[c0] <-> (1) L-Glutamyl-tRNA(Gln)_c0[c0] + (1) Diphosphate_c0[c0] + (1) AMP_c0[c0]

		gpr	gene ID	KO	enzyme	definition
709	<->	kb|g.575.peg.627	MMP1616	K01876	6.1.1.12	(1) tRNA(Asn)_c0[c0] + (1) L-Aspartate_c0[c0] + (1) ATP_c0[c0] <-> (1) L-Aspartyl-tRNA(Asn)_c0[c0] + (1) Diphosphate_c0[c0] + (1) AMP_c0[c0]
704	<->					(1) tRNA(Asp)_c0[c0] + (1) L-Aspartate_c0[c0] + (1) ATP_c0[c0] <-> (1) L-Aspartyl-tRNA(Asp)_c0[c0] + (1) Diphosphate_c0[c0] + (1) AMP_c0[c0]
624	<->	kb|g.575.peg.888	MMP1270	K13831	4.1.2.43+5.3.1.27	(1) D-Ribulose 5-phosphate_c0[c0] + (1) Formaldehyde_c0[c0] <-> (1) D-arabino-Hex-3-ulose 6-phosphate_c0[c0]
420	<->	kb|g.575.peg.781	MMP0137	K00809	2.5.1.46	(1) [eIF5A-precursor]-lysine_c0[c0] + (1) Spermidine_c0[c0] <-> (1) [eIF5A-precursor]-deoxyhypusine_c0[c0] + (1) 1,3-Diaminopropane_c0[c0] + (1) H+_c0[c0]
779	<->	kb|g.575.peg.1420	MMP0493	K02230	6.6.1.2	(1) Hydrogenobyrinate a,c diamide_c0[c0] + (1) Cobalt ion_c0[c0] + (1) ATP_c0[c0] + (1) H2O_c0[c0] <-> (1) Cob(II)yrinate a,c diamide_c0[c0] + (1) Orthophosphate_c0[c0] + (1) ADP_c0[c0] + (3) H+_c0[c0]
757	<->	kb|g.575.peg.955	MMP1215	K02232	6.3.5.10	(1) Adenosyl cobyrinate a,c diamide_c0[c0] + (4) L-Glutamine_c0[c0] + (4) ATP_c0[c0] + (4) H2O_c0[c0] <-> (1) Adenosyl cobyrinate hexaamide_c0[c0] + (4) L-Glutamate_c0[c0] + (4) Orthophosphate_c0[c0] + (4) ADP_c0[c0] + (4) H+_c0[c0]
770	<->	kb|g.575.peg.913	MMP1477	K02224	6.3.5.9+6.3.5.11	(1) Hydrogenobyrinate_c0[c0] + (2) L-Glutamine_c0[c0] + (2) ATP_c0[c0] + (2) H2O_c0[c0] <-> (1) Hydrogenobyrinate a,c diamide_c0[c0] + (2) Orthophosphate_c0[c0] + (2) L-Glutamate_c0[c0] + (2) ADP_c0[c0] + (2) H+_c0[c0]
771	<->	kb|g.575.peg.860	MMP1478	K02224	6.3.5.9+6.3.5.11	
503	<->	kb|g.575.peg.1315	MMP0938	K02233	2.7.8.26	(1) H+_c0[c0] + (1) Cobamide coenzyme_c0[c0] + (1) GMP_c0[c0] <-> (1) Adenosine-GDP-cobinamide_c0[c0] + (1) alpha-Ribazole_c0[c0]
491	<->	kb|g.575.peg.1091	MMP0915	K19712	2.7.7.62	(1) Adenosyl cobinamide phosphate_c0[c0] + (1) GTP_c0[c0] + (1) H+_c0[c0] <-> (1) Adenosine-GDP-

		gpr	gene ID	KO	enzyme	definition
						cobinamide_c0[c0] + (1) Diphosphate_c0[c0]
249	<->	kb|g.575.peg.495	MMP0147	K02588	1.18.6.1	(16) ATP_c0[c0] + (1) Nitrogen_c0[c0] + (8) Reduced ferredoxin_c0[c0] + (16) H2O_c0[c0] <-> (16) Orthophosphate_c0[c0] + (16) ADP_c0[c0] + (8) Oxidized ferredoxin_c0[c0] + (2) Ammonia_c0[c0] + (1) Hydrogen_c0[c0] + (6) H+_c0[c0]
250	<->	kb|g.575.peg.1689	MMP0853	K02588	1.18.6.1	
251	<->	kb|g.575.peg.1035	MMP0856	K02586	1.18.6.1	
252	<->	kb|g.575.peg.1227	MMP0857	K02591	1.18.6.1	
322	<->	kb|g.575.peg.812	MMP1662	K05936	2.1.1.133+2.1.1.271	(1) S-Adenosyl-L-methionine_c0[c0] + (1) Precorrin 4_c0[c0] <-> (1) S-Adenosyl-L-homocysteine_c0[c0] + (1) Precorrin 5_c0[c0] + (1) H+_c0[c0]
321	<->	kb|g.575.peg.1384	MMP0953	K05934	2.1.1.131	(1) S-Adenosyl-L-methionine_c0[c0] + (1) Precorrin 3B_c0[c0] <-> (1) S-Adenosyl-L-homocysteine_c0[c0] + (1) Precorrin 4_c0[c0] + (2) H+_c0[c0]
702	<->	kb|g.575.peg.896	MMP0330	K06042	5.4.99.61+5.4.99.60	(1) H+_c0[c0] + (1) Precorrin 8X_c0[c0] <-> (1) Hydrogenobyrinate_c0[c0]
296	<->	kb|g.575.peg.1357	MMP0599	K05895	1.3.1.54+1.3.1.106	(1) Precorrin 6Y_c0[c0] + (1) NADP+_c0[c0] <-> (1) Precorrin 6X_c0[c0] + (1) NADPH_c0[c0] + (1) H+_c0[c0]
342	<->	kb|g.575.peg.168	MMP0011	K00558	2.1.1.37	(1) S-Adenosyl-L-methionine_c0[c0] + (1) DNA cytosine_c0[c0] <-> (1) S-Adenosyl-L-homocysteine_c0[c0] + (1) DNA 5-methylcytosine_c0[c0] + (1) H+_c0[c0]
317	<->	kb|g.575.peg.1610	MMP0544	K04069	1.97.1.4	(1) S-Adenosyl-L-methionine_c0[c0] + (1) Dihydroflavodoxin_c0[c0] + (1) Protein glycine_c0[c0] <-> (1) 5'-Deoxyadenosine_c0[c0] + (1) L-Methionine_c0[c0] + (1) Flavodoxin semiquinone_c0[c0] + (1) Protein glycin-2-yl radical_c0[c0] + (1) H+_c0[c0]
318	<->	kb|g.575.peg.1516	MMP0580	K04069	1.97.1.4	

		gpr	gene ID	KO	enzyme	definition
680	<->	kb|g.575.peg.1272	MMP0417	K01814	5.3.1.16	
681	<->	kb|g.575.peg.124	MMP1690	K01814	5.3.1.16	
744	<->	kb|g.575.peg.1454	MMP0540	K01923	6.3.2.6	
390	<->	kb|g.575.peg.519	MMP0256	K02501	2.4.2.-	
392	<->	kb|g.575.peg.296	MMP1082	K02501	2.4.2.-	
625	<->	kb|g.575.peg.448	MMP1083	K02500	4.1.3.-	
626	<->	kb|g.575.peg.732	MMP1722	K02500	4.1.3.-	
513	<->	kb|g.575.peg.442	MMP1555	K00401	2.8.4.1	
514	<->	kb|g.575.peg.119	MMP1558	K00402	2.8.4.1	
515	<->	kb|g.575.peg.950	MMP1559	K00399	2.8.4.1	
311	<->	kb|g.575.peg.1104	MMP0825	K03388	1.8.98.1	(1) H+_c0[c0] + (1) Coenzyme M 7-mercaptoheptanoylthreonine-phosphate heterodisulfide_c0[c0] + (1) Dihydromethanophenazine_c0[c0] <-> (1) Coenzyme B_c0[c0] + (1) Coenzyme M_c0[c0] + (1) Methanophenazine_c0[c0]
312	<->	kb|g.575.peg.120	MMP1053	K03389	1.8.98.1	
313	<->	kb|g.575.peg.566	MMP1054	K03390	1.8.98.1	
314	<->	kb|g.575.peg.931	MMP1154	K03390	1.8.98.1	
315	<->	kb|g.575.peg.883	MMP1155	K03389	1.8.98.1	
316	<->	kb|g.575.peg.223	MMP1697	K03388	1.8.98.1	
419	<->	kb|g.575.peg.487	MMP1677	K17105	2.5.1.42	

		gpr	gene ID	KO	enzyme	definition
357	<->	kb|g.575.peg.1590	MMP0588	K20215	2.1.1.98	(1) S-Adenosyl-L-methionine_c0[c0] + (1) Peptide 2-(3-carboxy-3-aminopropyl)-L-histidine_c0[c0] <-> (1) S-Adenosyl-L-homocysteine_c0[c0] + (1) Peptide 2-[3-carboxy-3-(methylammonio)propyl]-L-histidine_c0[c0] + (1) H+_c0[c0]
304	<->	kb|g.575.peg.1082	MMP0058	K00320	1.5.98.2	
760	<->	kb|g.575.peg.480	MMP0178	K01952	6.3.5.3	
761	<->	kb|g.575.peg.21	MMP0179	K01952	6.3.5.3	
428	<->	kb|g.575.peg.1238	MMP0050	K00794	2.5.1.78	(1) 5-Amino-6-(1-D-ribitylamino)uracil_c0[c0] + (1) L-3,4-Dihydroxybutan-2-one 4-phosphate_c0[c0] <-> (1) 6,7-Dimethyl-8-(D-ribityl)lumazine_c0[c0] + (2) H2O_c0[c0] + (1) Orthophosphate_c0[c0] + (1) H+_c0[c0]
303	<->	kb|g.575.peg.1316	MMP0372	K00319	1.5.98.1	(1) H+_c0[c0] + (1) 5,10-Methylenetetrahydromethanopterin_c0[c0] + (1) Coenzyme F420_c0[c0] <-> (1) 5,10-Methenyltetrahydromethanopterin_c0[c0] + (1) Reduced coenzyme F420_c0[c0]
238	<->	kb|g.575.peg.422	MMP0127	K13942	1.12.98.2	(1) 5,10-Methenyltetrahydromethanopterin_c0[c0] + (1) Hydrogen_c0[c0] <-> (1) 5,10-Methylenetetrahydromethanopterin_c0[c0] + (1) H+_c0[c0]
451	<->	kb|g.575.peg.898	MMP1138	K00878	2.7.1.50	(1) ATP_c0[c0] + (1) 5-(2-Hydroxyethyl)-4-methylthiazole_c0[c0] <-> (1) ADP_c0[c0] + (1) 4-Methyl-5-(2-phosphooxyethyl)thiazole_c0[c0] + (1) H+_c0[c0]
682	<->	kb|g.575.peg.957	MMP1618	K08963	5.3.1.23	(1) S-Methyl-5-thio-D-ribose 1-phosphate_c0[c0] <-> (1) S-Methyl-5-thio-D-ribulose 1-phosphate_c0[c0]
358	<->	kb|g.575.peg.555	MMP0123	K08289	2.1.2.2	(1) 10-Formyltetrahydromethanopterin_c0[c0] + (1) 5'-Phosphoribosylglycinamide_c0[c0] <-> (1) Tetrahydromethanopterin_c0[c0] + (1) 5'-Phosphoribosyl-N-formylglycinamide_c0[c0] + (1) H+_c0[c0]

		gpr	gene ID	KO	enzyme	definition
375	<->	kb|g.575.peg.378	MMP1184	K03789	2.3.1.128	(1) Acetyl-CoA_c0[c0] + (1) Ribosomal-protein L-alanine_c0[c0] <-> (1) CoA_c0[c0] + (1) Ribosomal-protein N-acetyl-L-alanine_c0[c0]
376	<->	kb|g.575.peg.285	MMP1351	K03789	2.3.1.128	
423	<->	kb|g.575.peg.147	MMP1242	K03517	2.5.1.72	(1) Quinolinate_c0[c0] + (2) H2O_c0[c0] + (1) Orthophosphate_c0[c0] <-> (1) Iminoaspartate_c0[c0] + (1) Glycerone phosphate_c0[c0]
651	<->	kb|g.575.peg.678	MMP1250	K01737	4.2.3.12+4.1.2.50	(1) 7,8-Dihydroneopterin 3'-triphosphate_c0[c0] <-> (1) 6-Pyruvoyltetrahydropterin_c0[c0] + (1) Triphosphate_c0[c0] + (1) H+_c0[c0]
778	<->	kb|g.575.peg.1597	MMP0648	K01974	6.5.1.4	(1) ATP_c0[c0] + (1) RNA 3'-terminal-phosphate_c0[c0] <-> (1) AMP_c0[c0] + (1) Diphosphate_c0[c0] + (1) RNA terminal-2',3'-cyclic-phosphate_c0[c0] + (1) H+_c0[c0]
675	<->	kb|g.575.peg.1332	MMP0572	K03775	5.2.1.8	(1) Peptidylproline (omega-180)_c0[c0] <-> (1) Peptidylproline (omega-0)_c0[c0]
676	<->	kb|g.575.peg.800	MMP1128	K03768	5.2.1.8	
677	<->	kb|g.575.peg.874	MMP1129	K03768	5.2.1.8	
678	<->	kb|g.575.peg.447	MMP1190	K01802	5.2.1.8	
745	<->	kb|g.575.peg.1663	MMP0882	K01933	6.3.3.1	
746	<->	kb|g.575.peg.180	MMP1254	K01933	6.3.3.1	
247	<->	kb|g.575.peg.1716	MMP0923	K00215	1.17.1.8	(1) H+_c0[c0] + (1) 2,3,4,5-Tetrahydrodipicolinate_c0[c0] + (1) NAD+_c0[c0] + (1) H2O_c0[c0] <-> (1) (2S,4S)-4-Hydroxy-2,3,4,5-tetrahydrodipicolinate_c0[c0] + (1) NADH_c0[c0]
347	<->	kb|g.575.peg.704	MMP0102	K00573	2.1.1.77	(1) S-Adenosyl-L-methionine_c0[c0] + (1) Protein L-isoaspartate_c0[c0] <-> (1) S-Adenosyl-L-homocysteine_c0[c0] + (1) Protein L-isoaspartate methyl ester_c0[c0]
418	<->	kb|g.575.peg.1213	MMP0007	K17104	2.5.1.41	(1) Geranylgeranyl diphosphate_c0[c0] + (1) sn-Glycerol 1-phosphate_c0[c0] <->

		gpr	gene ID	KO	enzyme	definition
						(1) Diphosphate_c0[c0] + (1) 3-(O-Geranylgeranyl)-sn-glycerol 1-phosphate_c0[c0]
748	<->	kb|g.575.peg.1334	MMP0392	K01945	6.3.4.13	
309	<->	kb|g.575.peg.1329	MMP0848	K07304	1.8.4.11	(1) Peptide-L-methionine_c0[c0] + (1) Thioredoxin disulfide_c0[c0] + (1) H2O_c0[c0] <-> (1) Peptide-L-methionine (S)-S-oxide_c0[c0] + (1) Thioredoxin_c0[c0]
261	<->	kb|g.575.peg.1049	MMP0088	K02492	1.2.1.70	(1) L-Glutamyl-tRNA(Glu)_c0[c0] + (1) NADPH_c0[c0] + (1) H+_c0[c0] <-> (1) (S)-4-Amino-5-oxopentanoate_c0[c0] + (1) tRNA(Glu)_c0[c0] + (1) NADP+_c0[c0]
568	<->	kb|g.575.peg.205	MMP0280	K01496	3.5.4.19	
578	<->	kb|g.575.peg.1110	MMP0051	K01523	3.6.1.31	(1) 1-(5-Phospho-D-ribosyl)-ATP_c0[c0] + (1) H2O_c0[c0] <-> (1) Phosphoribosyl-AMP_c0[c0] + (1) Diphosphate_c0[c0] + (2) H+_c0[c0]
686	<->	kb|g.575.peg.1387	MMP0912	K01821	5.3.2.6	(1) 2-Hydroxymuconate_c0[c0] <-> (1) gamma-Oxalocrotonate_c0[c0]
320	<->	kb|g.575.peg.437	MMP0319	K03394	2.1.1.130+2.1.1.151	(1) H+_c0[c0] + (1) S-Adenosyl-L-methionine_c0[c0] + (1) Precorrin 2_c0[c0] <-> (1) S-Adenosyl-L-homocysteine_c0[c0] + (1) Precorrin 3A_c0[c0]
765	<->	kb|g.575.peg.1681	MMP0575	K02435	6.3.5.6+6.3.5.7	(1) Glutaminyl-tRNA(Gln)_c0[c0] + (1) L-Glutamate_c0[c0] + (1) Orthophosphate_c0[c0] + (1) ADP_c0[c0] + (1) H+_c0[c0] <-> (1) L-Glutamyl-tRNA(Gln)_c0[c0] + (1) L-Glutamine_c0[c0] + (1) ATP_c0[c0] + (1) H2O_c0[c0]
766	<->	kb|g.575.peg.1253	MMP0946	K02434	6.3.5.6+6.3.5.7	(1) L-glutamine_c0 + (1) L-aspartyl-tRNA(Asn) = (1) L-glutamate_c0 + (1) L-asparaginyl-tRNA(Asn)_c0
767	<->	kb|g.575.peg.83	MMP1510	K02433	6.3.5.6+6.3.5.7	
768	<->	kb|g.575.peg.326	MMP1265	K03330	6.3.5.7	
769	<->	kb|g.575.peg.221	MMP1266	K09482	6.3.5.7	
1160	<->	kb|g.575.peg.523	MMP1535	K08971	0	

		gpr	gene ID	KO	enzyme	definition
725	<->	kb|g.575.peg.1126	MMP0584	K01873	6.1.1.9	(1) ATP_c0[c0] + (1) L-Valine_c0[c0] + (1) tRNA(Val)_c0[c0] <-> (1) AMP_c0[c0] + (1) Diphosphate_c0[c0] + (1) L-Valyl-tRNA(Val)_c0[c0]
715	<->	kb|g.575.peg.611	MMP1592	K01867	6.1.1.2	(1) ATP_c0[c0] + (1) L-Tryptophan_c0[c0] + (1) tRNA(Trp)_c0[c0] <-> (1) AMP_c0[c0] + (1) Diphosphate_c0[c0] + (1) L-Tryptophanyl-tRNA(Trp)_c0[c0]
720	<->	kb|g.575.peg.1068	MMP0414	K01868	6.1.1.3	(1) ATP_c0[c0] + (1) L-Threonine_c0[c0] + (1) tRNA(Thr)_c0[c0] <-> (1) AMP_c0[c0] + (1) Diphosphate_c0[c0] + (1) L-Threonyl-tRNA(Thr)_c0[c0]
708	<->	kb|g.575.peg.1246	MMP0879	K01875	6.1.1.11	(1) ATP_c0[c0] + (1) L-Serine_c0[c0] + (1) tRNA(Ser)_c0[c0] <-> (1) AMP_c0[c0] + (1) Diphosphate_c0[c0] + (1) L-Seryl-tRNA(Ser)_c0[c0]
711	<->	kb|g.575.peg.1103	MMP0696	K01881	6.1.1.15	(1) ATP_c0[c0] + (1) L-Proline_c0[c0] + (1) tRNA(Pro)_c0[c0] <-> (1) AMP_c0[c0] + (1) Diphosphate_c0[c0] + (1) L-Prolyl-tRNA(Pro)_c0[c0]
716	<->	kb|g.575.peg.451	MMP1255	K01890	6.1.1.20	(1) ATP_c0[c0] + (1) L-Phenylalanine_c0[c0] + (1) tRNA(Phe)_c0[c0] <-> (1) AMP_c0[c0] + (1) Diphosphate_c0[c0] + (1) L-Phenylalanyl-tRNA(Phe)_c0[c0]
717	<->	kb|g.575.peg.137	MMP1496	K01889	6.1.1.20	
707	<->	kb|g.575.peg.878	MMP0326	K01874	6.1.1.10	(1) ATP_c0[c0] + (1) L-Methionine_c0[c0] + (1) tRNA(Met)_c0[c0] <-> (1) AMP_c0[c0] + (1) Diphosphate_c0[c0] + (1) L-Methionyl-tRNA_c0[c0]
723	<->	kb|g.575.peg.38	MMP1318	K04566	6.1.1.6	(1) ATP_c0[c0] + (1) L-Lysine_c0[c0] + (1) tRNA(Lys)_c0[c0] <-> (1) AMP_c0[c0] + (1) Diphosphate_c0[c0] + (1) L-Lysyl-tRNA_c0[c0]
721	<->	kb|g.575.peg.1022	MMP0697	K01869	6.1.1.4	(1) ATP_c0[c0] + (1) L-Leucine_c0[c0] + (1) tRNA(Leu)_c0[c0] <-> (1) AMP_c0[c0] + (1) Diphosphate_c0[c0] + (1) L-Leucyl-tRNA_c0[c0]

		gpr	gene ID	KO	enzyme	definition
722	<->	kb|g.575.peg.386	MMP1474	K01870	6.1.1.5	(1) ATP_c0[c0] + (1) L-Isoleucine_c0[c0] + (1) tRNA(Ile)_c0[c0] <-> (1) AMP_c0[c0] + (1) Diphosphate_c0[c0] + (1) L-Isoleucyl-tRNA(Ile)_c0[c0]
718	<->	kb|g.575.peg.488	MMP1614	K01892	6.1.1.21	(1) ATP_c0[c0] + (1) L-Histidine_c0[c0] + (1) tRNA(His)_c0[c0] <-> (1) AMP_c0[c0] + (1) Diphosphate_c0[c0] + (1) L-Histidyl-tRNA(His)_c0[c0]
710	<->	kb|g.575.peg.182	MMP0212	K01880	6.1.1.14	(1) ATP_c0[c0] + (1) Glycine_c0[c0] + (1) tRNA(Gly)_c0[c0] <-> (1) AMP_c0[c0] + (1) Diphosphate_c0[c0] + (1) Glycyl-tRNA(Gly)_c0[c0]
712	<->	kb|g.575.peg.251	MMP1060	K01883	6.1.1.16	(1) ATP_c0[c0] + (1) L-Cysteine_c0[c0] + (1) tRNA(Cys)_c0[c0] <-> (1) AMP_c0[c0] + (1) Diphosphate_c0[c0] + (1) L-Cysteinyl-tRNA(Cys)_c0[c0]
714	<->	kb|g.575.peg.723	MMP1026	K01887	6.1.1.19	(1) ATP_c0[c0] + (1) L-Arginine_c0[c0] + (1) tRNA(Arg)_c0[c0] <-> (1) AMP_c0[c0] + (1) Diphosphate_c0[c0] + (1) L-Arginyl-tRNA(Arg)_c0[c0]
507	<->	kb|g.575.peg.637	MMP0904	K01008	2.7.9.3	(1) ATP_c0[c0] + (1) Hydrogen selenide_c0[c0] + (1) H2O_c0[c0] <-> (1) AMP_c0[c0] + (1) Selenophosphoric acid_c0[c0] + (1) Orthophosphate_c0[c0] + (2) H+_c0[c0]
683	<->	kb|g.575.peg.302	MMP1004	K01817	5.3.1.24	(1) N-(5-Phospho-D-ribosyl)anthranilate_c0[c0] <-> (1) 1-(2-Carboxyphenylamino)-1-deoxy-D-ribulose 5-phosphate_c0[c0]
614	<->	kb|g.575.peg.10	MMP1008	K01609	4.1.1.48	
623	<->	kb|g.575.peg.893	MMP0243	K09739	4.1.2.25	(1) 2-Amino-4-hydroxy-6-(D-erythro-1,2,3-trihydroxypropyl)-7,8-dihydropteridine_c0[c0] <-> (1) Glycolaldehyde_c0[c0] + (1) 2-Amino-4-hydroxy-6-hydroxymethyl-7,8-dihydropteridine_c0[c0]
471	<->	kb|g.575.peg.1411	MMP0579	K07142	2.7.6.3	(1) ATP_c0[c0] + (1) 2-Amino-4-hydroxy-6-hydroxymethyl-7,8-dihydropteridine_c0[c0] <-> (1) AMP_c0[c0] + (1) 2-Amino-7,8-dihydro-4-hydroxy-6-(diphosphooxymethyl)pteridine_c0[c0]

		gpr	gene ID	KO	enzyme	definition
631	<->	kb|g.575.peg.810	MMP0187	K03147	4.1.99.17	(1) Aminoimidazole ribotide_c0[c0] + (1) S-Adenosyl-L-methionine_c0[c0] <-> (1) 4-Amino-2-methyl-5-(phosphooxymethyl)pyrimidine_c0[c0] + (1) 5'-Deoxyadenosine_c0[c0] + (1) L-Methionine_c0[c0] + (1) Formate_c0[c0] + (1) CO_c0[c0] + (2) H+_c0[c0]
569	<->	kb|g.575.peg.509	MMP1191	K01499	3.5.4.27	
416	<->	kb|g.575.peg.639	MMP1205	K00800	2.5.1.19	
639	<->	kb|g.575.peg.1388	MMP0548	K01693	4.2.1.19	
636	<->	kb|g.575.peg.1256	MMP0381	K16793	4.2.1.114	(1) (R)-2-Hydroxybutane-1,2,4-tricarboxylate_c0[c0] <-> (1) (Z)-But-1-ene-1,2,4-tricarboxylate_c0[c0] + (1) H2O_c0[c0]
637	<->	kb|g.575.peg.204	MMP1480	K16792	4.2.1.114	
374	<->	kb|g.575.peg.268	MMP1609	K00672	2.3.1.101	
398	<->	kb|g.575.peg.1543	MMP0877	K00767	2.4.2.19	(1) Nicotinate D-ribonucleotide_c0[c0] + (1) Diphosphate_c0[c0] + (1) CO2_c0[c0] <-> (1) Quinolinate_c0[c0] + (1) 5-Phospho-alpha-D-ribose 1-diphosphate_c0[c0] + (2) H+_c0[c0]
221	<->	kb|g.575.peg.1286	MMP0706	K02472	1.1.1.336	(1) UDP-N-acetyl-D-mannosamine_c0[c0] + (2) NAD+_c0[c0] + (1) H2O_c0[c0] <-> (1) UDP-N-acetyl-D-mannosaminouronate_c0[c0] + (2) NADH_c0[c0] + (3) H+_c0[c0]
611	<->	kb|g.575.peg.29	MMP1606	K13038	4.1.1.36+6.3.2.5	(1) H+_c0[c0] + (1) (R)-4'-Phosphopantothenoyl-L-cysteine_c0[c0] <-> (1) Pantetheine 4'-phosphate_c0[c0] + (1) CO2_c0[c0]
437	<->	kb|g.575.peg.1280	MMP0865	K00833	2.6.1.62	(1) S-Adenosyl-L-methionine_c0[c0] + (1) 8-Amino-7-oxononanoate_c0[c0] <-> (1) S-Adenosyl-4-methylthio-2-oxobutanoate_c0[c0] + (1) 7,8-Diaminononanoate_c0[c0]
417	<->	kb|g.575.peg.773	MMP1139	K00788	2.5.1.3	(1) H+_c0[c0] + (1) 4-Amino-5-hydroxymethyl-2-methylpyrimidine

		gpr	gene ID	KO	enzyme	definition
450	<->	kb|g.575.peg.337	MMP1639	K21219	2.7.1.49+2.7.4.7+2.5.1.3	diphosphate_c0[c0] + (1) 4-Methyl-5-(2-phosphooxyethyl)thiazole_c0[c0] <-> (1) Diphosphate_c0[c0] + (1) Thiamin monophosphate_c0[c0]
381	<->	kb|g.575.peg.404	MMP1574	K00652	2.3.1.47	(1) 6-Carboxyhexanoyl-CoA_c0[c0] + (1) L-Alanine_c0[c0] <-> (1) 8-Amino-7-oxononanoate_c0[c0] + (1) CoA_c0[c0] + (1) CO2_c0[c0]
730	<->	kb|g.575.peg.924	MMP1575	K01906	6.2.1.14	(1) H+_c0[c0] + (1) ATP_c0[c0] + (1) Pimelate_c0[c0] + (1) CoA_c0[c0] <-> (1) AMP_c0[c0] + (1) Diphosphate_c0[c0] + (1) 6-Carboxyhexanoyl-CoA_c0[c0]
612	<->	kb|g.575.peg.1228	MMP0830	K01599	4.1.1.37	(4) H+_c0[c0] + (1) Uroporphyrinogen III_c0[c0] <-> (1) Coproporphyrinogen III_c0[c0] + (4) CO2_c0[c0]
613	<->	kb|g.575.peg.871	MMP1150	K01599	4.1.1.37	
319	<->	kb|g.575.peg.1277	MMP0966	K02303	2.1.1.107	(2) S-Adenosyl-L-methionine_c0[c0] + (1) Uroporphyrinogen III_c0[c0] <-> (2) S-Adenosyl-L-homocysteine_c0[c0] + (1) Precorrin 2_c0[c0] + (2) H+_c0[c0]
747	<->	kb|g.575.peg.47	MMP1573	K01935	6.3.3.3	(1) ATP_c0[c0] + (1) 7,8-Diaminononanoate_c0[c0] + (1) CO2_c0[c0] <-> (1) ADP_c0[c0] + (1) Orthophosphate_c0[c0] + (1) Dethiobiotin_c0[c0] + (3) H+_c0[c0]
648	<->	kb|g.575.peg.1650	MMP0394	K01719	4.2.1.75	(1) Hydroxymethylbilane_c0[c0] <-> (1) Uroporphyrinogen III_c0[c0] + (1) H2O_c0[c0]
634	<->	kb|g.575.peg.439	MMP1394	K03785	4.2.1.10	(1) 3-Dehydroquinate_c0[c0] <-> (1) 3-Dehydroshikimate_c0[c0] + (1) H2O_c0[c0]
379	<->	kb|g.575.peg.578	MMP1355	K00638	2.3.1.28	(1) Acetyl-CoA_c0[c0] + (1) Chloramphenicol_c0[c0] <-> (1) CoA_c0[c0] + (1) Chloramphenicol 3-acetate_c0[c0]
724	<->	kb|g.575.peg.1629	MMP0397	K01872	6.1.1.7	(1) ATP_c0[c0] + (1) L-Alanine_c0[c0] + (1) tRNA(Ala)_c0[c0] <-> (1) AMP_c0[c0] + (1) Diphosphate_c0[c0] + (1) L-Alanyl-tRNA_c0[c0]
477	<->	kb|g.575.peg.958	MMP1093	K02201	2.7.7.3	(1) ATP_c0[c0] + (1) Pantetheine 4'-phosphate_c0[c0] <-> (1) Diphosphate_c0[c0] + (1) Dephospho-CoA_c0[c0]

		gpr	gene ID	KO	enzyme	definition
231	<->	kb|g.575.peg.1148	MMP0083	K00441	1.12.98.1	(1) Coenzyme F420_c0[c0] + (1) Hydrogen_c0[c0] <-> (1) Reduced coenzyme F420_c0[c0]
232	<->	kb|g.575.peg.1569	MMP0817	K00441	1.12.98.1	
233	<->	kb|g.575.peg.1511	MMP0818	K00443	1.12.98.1	
234	<->	kb|g.575.peg.1442	MMP0820	K00440	1.12.98.1	
235	<->	kb|g.575.peg.854	MMP1382	K00440	1.12.98.1	
236	<->	kb|g.575.peg.684	MMP1384	K00443	1.12.98.1	
237	<->	kb|g.575.peg.338	MMP1385	K00441	1.12.98.1	
787	<->	kb|g.575.peg.1343	MMP0819	K00442	0	
788	<->	kb|g.575.peg.546	MMP1337	K00442	0	
789	<->	kb|g.575.peg.696	MMP1383	K00442	0	
281	<->	kb|g.575.peg.1389	MMP0070	K00202	1.2.99.5	
282	<->	kb|g.575.peg.179	MMP0200	K11261	1.2.99.5	
283	<->	kb|g.575.peg.1600	MMP0508	K11261	1.2.99.5	
284	<->	kb|g.575.peg.1331	MMP0509	K00200	1.2.99.5	
285	<->	kb|g.575.peg.1482	MMP0510	K00202	1.2.99.5	
286	<->	kb|g.575.peg.1571	MMP0511	K00201	1.2.99.5	
287	<->	kb|g.575.peg.1587	MMP0512	K00201	1.2.99.5	
288	<->	kb|g.575.peg.1184	MMP0965	K11261	1.2.99.5	
289	<->	kb|g.575.peg.243	MMP1247	K00203	1.2.99.5	

		gpr	gene ID	KO	enzyme	definition
290	<->	kb|g.575.peg.680	MMP1248	K00200	1.2.99.5	
291	<->	kb|g.575.peg.481	MMP1249	K00202	1.2.99.5	
292	<->	kb|g.575.peg.438	MMP1691	K00201	1.2.99.5	
783	<->	kb|g.575.peg.401	MMP1244	K00204	0	
784	<->	kb|g.575.peg.103	MMP1245	K00205	0	
1222	<->	kb|g.575.peg.133	MMP1246	K11260	0	
346	<->	kb|g.575.peg.1170	MMP0735	K06223	2.1.1.72	(1) S-Adenosyl-L-methionine_c0[c0] + (1) DNA adenine_c0[c0] <-> (1) S-Adenosyl-L-homocysteine_c0[c0] + (1) DNA 6-methylaminopurine_c0[c0] + (1) H+_c0[c0]
413	<->	kb|g.575.peg.745	MMP1552	K03186	2.5.1.129	(1) H+_c0[c0] + (1) 4-Coumarate_c0[c0] <-> (1) 4-Hydroxystyrene_c0[c0] + (1) CO2_c0[c0]
615	<->	kb|g.575.peg.1462	MMP0613	K01575	4.1.1.5	(1) H+_c0[c0] + (1) (S)-2-Acetolactate_c0[c0] <-> (1) (R)-Acetoin_c0[c0] + (1) CO2_c0[c0]
706	<->	kb|g.575.peg.739	MMP0263	K01866	6.1.1.1	(1) ATP_c0[c0] + (1) L-Tyrosine_c0[c0] + (1) tRNA(Tyr)_c0[c0] <-> (1) AMP_c0[c0] + (1) Diphosphate_c0[c0] + (1) L-Tyrosyl-tRNA(Tyr)_c0[c0]
297	<->	kb|g.575.peg.1720	MMP0089	K02304	1.3.1.76+4.99.1.4	(1) Siroheme_c0[c0] + (2) H+_c0[c0] <-> (1) Fe2+_c0[c0] + (1) Sirohydrochlorin_c0[c0]
685	<->	kb|g.575.peg.903	MMP1295	K01810	5.3.1.9	(1) H+_c0[c0] + (1) alpha-D-Glucose 6-phosphate_c0[c0] <-> (1) beta-D-Glucose 6-phosphate_c0[c0]
687	<->	kb|g.575.peg.903	MMP1295	K01810	5.3.1.9	(1) alpha-D-Glucose 6-phosphate_c0[c0] <-> (1) beta-D-fructose 6-phosphate_c0[c0]
562	<->	kb|g.575.peg.801	MMP1398	K01439	3.5.1.18	(1) N-Succinyl-LL-2,6-diaminoheptanedioate_c0[c0] + (1) H2O_c0[c0] <-> (1) Succinate_c0[c0] + (1) LL-2,6-Diaminoheptanedioate_c0[c0]
457	<->	kb|g.575.peg.108	MMP1431	K05715	2.7.2.-	(1) 2-Phospho-D-glycerate_c0[c0] + (1) ATP_c0[c0] <-> (1) 2,3-Bisphospho-D-glycerate_c0[c0] + (1) ADP_c0[c0]

		gpr	gene ID	KO	enzyme	definition
460	<->	kb|g.575.peg.1101	MMP0063	K00930	2.7.2.8	(1) ATP_c0[c0] + (1) N-Acetyl-L-glutamate_c0[c0] <-> (1) ADP_c0[c0] + (1) N-Acetyl-L-glutamate 5-phosphate_c0[c0]
523	->	kb|g.575.peg.1171	MMP0926	K03412	3.1.1.61	(1) Protein glutamate methyl ester_c0[c0] + (1) H2O_c0[c0] <-> (1) Protein glutamate_c0[c0] + (1) Methanol_c0[c0] + (1) H+_c0[c0]
348	<->	kb|g.575.peg.1373	MMP0930	K00575	2.1.1.80	(1) S-Adenosyl-L-methionine_c0[c0] + (1) Protein glutamate_c0[c0] <-> (1) S-Adenosyl-L-homocysteine_c0[c0] + (1) Protein glutamate methyl ester_c0[c0]
563	<->	kb|g.575.peg.1401	MMP0928	K03411	3.5.1.44	(1) Protein glutamine_c0[c0] + (1) H2O_c0[c0] <-> (1) Protein glutamate_c0[c0] + (1) Ammonia_c0[c0]
731	<->	kb|g.575.peg.201	MMP0160	K01912	6.2.1.30	(1) ATP_c0[c0] + (1) Phenylacetic acid_c0[c0] + (1) CoA_c0[c0] <-> (1) AMP_c0[c0] + (1) Diphosphate_c0[c0] + (1) Phenylacetyl-CoA_c0[c0]
732	<->	kb|g.575.peg.245	MMP0314	K01912	6.2.1.30	
733	<->	kb|g.575.peg.1146	MMP0715	K01912	6.2.1.30	
212	<->	kb|g.575.peg.1433	MMP0672	K00077	1.1.1.169	(1) (R)-Pantoate_c0[c0] + (1) NADP+_c0[c0] <-> (1) 2-Dehydropantoate_c0[c0] + (1) NADPH_c0[c0] + (1) H+_c0[c0]
216	<->	kb|g.575.peg.1465	MMP0936	K00014	1.1.1.25	(1) Shikimate_c0[c0] + (1) NADP+_c0[c0] <-> (1) 3-Dehydroshikimate_c0[c0] + (1) NADPH_c0[c0] + (1) H+_c0[c0]
452	<->	kb|g.575.peg.8	MMP0320	K00891	2.7.1.71	(1) ATP_c0[c0] + (1) Shikimate_c0[c0] <-> (1) ADP_c0[c0] + (1) Shikimate 3-phosphate_c0[c0] + (1) H+_c0[c0]
693	<->	kb|g.575.peg.18	MMP0224	K01845	5.4.3.8	(1) 5-Aminolevulinate_c0[c0] <-> (1) (S)-4-Amino-5-oxopentanoate_c0[c0]
622	<->	kb|g.575.peg.730	MMP1187	K01628	4.1.2.17	(1) L-Fuculose 1-phosphate_c0[c0] <-> (1) Glycerone phosphate_c0[c0] + (1) (S)-Lactaldehyde_c0[c0] + (1) H+_c0[c0]
447	<->	kb|g.575.peg.766	MMP1335	K00869	2.7.1.36	(1) ATP_c0[c0] + (1) (R)-Mevalonate_c0[c0] <-> (1) ADP_c0[c0] + (1) (R)-5-Phosphomevalonate_c0[c0] + (1) H+_c0[c0]
387	<->	kb|g.575.peg.725	MMP1220	K00688	2.4.1.1	(1) Starch_c0[c0] + (1) Orthophosphate_c0[c0] <-> (1) Amylose_c0[c0] + (1) D-Glucose 1-phosphate_c0[c0]

		gpr	gene ID	KO	enzyme	definition
343	<->	kb|g.575.peg.1060	MMP0986	K00560	2.1.1.45	(1) dUMP_c0[c0] + (1) 5,10-Methylenetetrahydromethanopterin_c0[c0] <-> (1) Dihydromethanopterin_c0[c0] + (1) dTMP_c0[c0]
344	<->	kb|g.575.peg.106	MMP1379	K00560	2.1.1.45	
576	<->	kb|g.575.peg.385	MMP1075	K01520	3.6.1.23	(1) dUTP_c0[c0] + (1) H2O_c0[c0] <-> (1) dUMP_c0[c0] + (1) Diphosphate_c0[c0] + (1) H+_c0[c0]
469	<->	kb|g.575.peg.632	MMP1034	K00943	2.7.4.9	(1) ATP_c0[c0] + (1) dTMP_c0[c0] <-> (1) ADP_c0[c0] + (1) dTDP_c0[c0]
688	<->	kb|g.575.peg.646	MMP1077	K03431	5.4.2.10	(1) alpha-D-Glucosamine 1-phosphate_c0[c0] <-> (1) D-Glucosamine 6-phosphate_c0[c0]
310	<->	kb|g.575.peg.1159	MMP0941	K00390	1.8.4.8+1.8.4.10	(1) Thioredoxin_c0[c0] + (1) 3'-Phosphoadenylyl sulfate_c0[c0] <-> (1) Thioredoxin disulfide_c0[c0] + (1) Sulfite_c0[c0] + (1) Adenosine 3',5'-bisphosphate_c0[c0]
564	<->	kb|g.575.peg.260	MMP1009	K01465	3.5.2.3	
384	<->	kb|g.575.peg.380	MMP1211	K01641	2.3.3.10	
756	<->	kb|g.575.peg.1265	MMP0073	K01940	6.3.4.5	
431	<->	kb|g.575.peg.1415	MMP0096	K05825	2.6.1.-	(1) L-2-Aminoadipate_c0[c0] + (1) 2-Oxoglutarate_c0[c0] <-> (1) 2-Oxoadipate_c0[c0] + (1) L-Glutamate_c0[c0]
228	<->	kb|g.575.peg.1107	MMP0880	K10978	1.1.1.87+1.1.1.-	
415	<->	kb|g.575.peg.24	MMP1584	K00797	2.5.1.16	(1) S-Adenosylmethioninamine_c0[c0] + (1) Putrescine_c0[c0] <-> (1) 5'-Methylthioadenosine_c0[c0] + (1) Spermidine_c0[c0] + (1) H+_c0[c0]
394	<->	kb|g.575.peg.596	MMP1492	K00762	2.4.2.10	
368	<->	kb|g.575.peg.564	MMP1308	K00616	2.2.1.2	(1) Sedoheptulose 7-phosphate_c0[c0] + (1) D-Glyceraldehyde 3-phosphate_c0[c0] <-> (1) D-Erythrose 4-phosphate_c0[c0] + (1) beta-D-Fructose 6-phosphate_c0[c0]

		gpr	gene ID	KO	enzyme	definition
691	<->	kb|g.575.peg.419	MMP1372	K01840	5.4.2.8	(1) D-Mannose 6-phosphate_c0[c0] <-> (1) D-Mannose 1-phosphate_c0[c0]
505	<->	kb|g.575.peg.148	MMP1171	K17103	2.7.8.8	(1) CDP-diacylglycerol_c0[c0] + (1) L-Serine_c0[c0] <-> (1) CMP_c0[c0] + (1) Phosphatidylserine_c0[c0] + (1) H+_c0[c0]
448	<->	kb|g.575.peg.620	MMP0295	K00872	2.7.1.39	(1) ATP_c0[c0] + (1) L-Homoserine_c0[c0] <-> (1) ADP_c0[c0] + (1) O-Phospho-L-homoserine_c0[c0] + (1) H+_c0[c0]
294	<->	kb|g.575.peg.518	MMP1514	K04517	1.3.1.12	
701	<->	kb|g.575.peg.999	MMP0578	K04093	5.4.99.5	(1) Chorismate_c0[c0] <-> (1) Prephenate_c0[c0]
653	<->	kb|g.575.peg.593	MMP1333	K01736	4.2.3.5	
671	<->	kb|g.575.peg.190	MMP1114	K01783	5.1.3.1	(1) H+_c0[c0] + (1) D-Ribulose 5-phosphate_c0[c0] <-> (1) D-Xylulose 5-phosphate_c0[c0]
689	<->	kb|g.575.peg.341	MMP0112	K15635	5.4.2.12	
229	<->	kb|g.575.peg.500	MMP1588	K00058	1.1.1.95	(1) 3-Phospho-D-glycerate_c0[c0] + (1) NAD+_c0[c0] <-> (1) 3-Phosphonooxypyruvate_c0[c0] + (1) NADH_c0[c0]
458	<->	kb|g.575.peg.298	MMP1532	K00927	2.7.2.3	
650	<->	kb|g.575.peg.288	MMP0135	K01733	4.2.3.1	
258	<->	kb|g.575.peg.765	MMP1487	K19266	1.2.1.22	(1) (S)-Lactaldehyde_c0[c0] + (1) NAD+_c0[c0] + (1) H2O_c0[c0] <-> (1) (S)-Lactate_c0[c0] + (1) NADH_c0[c0] + (2) H+_c0[c0]
399	<->	kb|g.575.peg.604	MMP0185	K00772	2.4.2.28	(1) H+_c0[c0] + (1) 5'-Methylthioadenosine_c0[c0] + (1) Orthophosphate_c0[c0] <-> (1) Adenine_c0[c0] + (1) S-Methyl-5-thio-D-ribose 1-phosphate_c0[c0]
361	<->	kb|g.575.peg.1632	MMP0553	K00611	2.1.3.3	
360	<->	kb|g.575.peg.531	MMP1659	K00609	2.1.3.2	
790	<->	kb|g.575.peg.821	MMP1104	K00610	0	

		gpr	gene ID	KO	enzyme	definition
758	<->	kb|g.575.peg.1584	MMP0894	K01951	6.3.5.2	(1) ATP_c0[c0] + (1) Xanthosine 5'-phosphate_c0[c0] + (1) Ammonia_c0[c0] <-> (1) AMP_c0[c0] + (1) Diphosphate_c0[c0] + (1) GMP_c0[c0] + (2) H+_c0[c0]
759	<->	kb|g.575.peg.430	MMP1445	K01951	6.3.5.2	
307	<->	kb|g.575.peg.935	MMP1332	K00382	1.8.1.4	(1) Glycine_c0[c0] + (1) Tetrahydromethanopterin_c0[c0] + (1) NAD+_c0[c0] <-> (1) 5,10-Methylenetetrahydromethanopterin_c0[c0] + (1) Ammonia_c0[c0] + (1) CO2_c0[c0] + (1) NADH_c0[c0]
385	<->	kb|g.575.peg.212	MMP1063	K01649	2.3.3.13	(1) H+_c0[c0] + (1) alpha-Isopropylmalate_c0[c0] + (1) CoA_c0[c0] <-> (1) Acetyl-CoA_c0[c0] + (1) 3-Methyl-2-oxobutanoic acid_c0[c0] + (1) H2O_c0[c0]
649	<->	kb|g.575.peg.591	MMP0318	K01687	4.2.1.9	
266	<->	kb|g.575.peg.975	MMP1315	K00177	1.2.7.3	
267	<->	kb|g.575.peg.236	MMP1687	K00176	1.2.7.3	
262	<->	kb|g.575.peg.562	MMP1504	K00170	1.2.7.1	(2) Reduced ferredoxin_c0[c0] + (1) Acetyl-CoA_c0[c0] + (1) CO2_c0[c0] + (1) H+_c0[c0] <-> (2) Oxidized ferredoxin_c0[c0] + (1) Pyruvate_c0[c0] + (1) CoA_c0[c0]
263	<->	kb|g.575.peg.454	MMP1505	K00169	1.2.7.1	
264	<->	kb|g.575.peg.115	MMP1506	K00171	1.2.7.1	
265	<->	kb|g.575.peg.673	MMP1507	K00172	1.2.7.1	
268	<->	kb|g.575.peg.1700	MMP0003	K00174	1.2.7.3+1.2.7.11	
269	<->	kb|g.575.peg.718	MMP0305	K00175	1.2.7.3+1.2.7.11	
270	<->	kb|g.575.peg.261	MMP0306	K00174	1.2.7.3+1.2.7.11	
271	<->	kb|g.575.peg.799	MMP1316	K00175	1.2.7.3+1.2.7.11	

		gpr	gene ID	KO	enzyme	definition
215	<->	kb|g.575.peg.1455	MMP0968	K00013	1.1.1.23	
565	<->	kb|g.575.peg.150	MMP1585	K01480	3.5.3.11	(1) Agmatine_c0[c0] + (1) H2O_c0[c0] <-> (1) Putrescine_c0[c0] + (1) Urea_c0[c0]
755	<->	kb|g.575.peg.435	MMP1432	K01939	6.3.4.4	
213	<->	kb|g.575.peg.166	MMP0133	K00088	1.1.1.205	(1) IMP_c0[c0] + (1) NAD+_c0[c0] + (1) H2O_c0[c0] <-> (1) Xanthosine 5'-phosphate_c0[c0] + (1) NADH_c0[c0] + (1) H+_c0[c0]
214	<->	kb|g.575.peg.64	MMP0287	K00088	1.1.1.205	
567	<->	kb|g.575.peg.436	MMP1310	K11176	3.5.4.10	(1) IMP_c0[c0] + (1) H2O_c0[c0] <-> (1) 1-(5'-Phosphoribosyl)-5-formamido-4-imidazolecarboxamide_c0[c0]
656	<->	kb|g.575.peg.55	MMP0013	K01755	4.3.2.1	
640	<->	kb|g.575.peg.713	MMP0130	K01677	4.2.1.2	
641	<->	kb|g.575.peg.426	MMP1548	K01678	4.2.1.2	
511	<->	kb|g.575.peg.949	MMP0126	K01012	2.8.1.6	(1) Dethiobiotin_c0[c0] + (1) Sulfur donor_c0[c0] + (2) S-Adenosyl-L-methionine_c0[c0] + (2) Reducedferredoxin_c0[c0] <-> (1) Biotin_c0[c0] + (2) L-Methionine_c0[c0] + (2) 5'-Deoxyadenosine_c0[c0] + (2) Reducedferredoxin_c0[c0]
512	<->	kb|g.575.peg.598	MMP1238	K01012	2.8.1.6	
749	<->	kb|g.575.peg.701	MMP0119	K03524	6.3.4.15	(1) H+_c0[c0] + (1) ATP_c0[c0] + (1) Biotin_c0[c0] <-> (1) Diphosphate_c0[c0] + (1) Biotinyl-5'-AMP_c0[c0]
395	<->	kb|g.575.peg.702	MMP1146	K00764	2.4.2.14	
366	<->	kb|g.575.peg.573	MMP1113	K00615	2.2.1.1	(2) H+_c0[c0] + (1) D-Fructose 6-phosphate_c0[c0] + (1) D-Glyceraldehyde 3-phosphate_c0[c0] <-> (1) D-Erythrose 4-phosphate_c0[c0] + (1) D-Xylulose 5-phosphate_c0[c0]
367	<->	kb|g.575.peg.294	MMP1115	K00615	2.2.1.1	(1) D-ribose 5-phosphate_c0[c0] + (1) D-xylulose 5-phosphate_c0[c0] <-> (1) D-sedoheptulose 7-

		gpr	gene ID	KO	enzyme	definition
						phosphate_c0[c0] + (1) D-glyceraldehyde 3-phosphate_c0[c0]
442	<->	kb|g.575.peg.1398	MMP0418	K00852	2.7.1.15	(1) ATP_c0[c0] + (1) D-Ribose_c0[c0] <-> (1) ADP_c0[c0] + (1) D-Ribose 5-phosphate_c0[c0] + (1) H+_c0[c0]
470	<->	kb|g.575.peg.1478	MMP0410	K00948	2.7.6.1	(1) ATP_c0[c0] + (1) D-Ribose 5-phosphate_c0[c0] <-> (1) AMP_c0[c0] + (1) 5-Phospho-alpha-D-ribose 1-diphosphate_c0[c0] + (1) H+_c0[c0]
226	<->	kb|g.575.peg.1160	MMP0539	K00052	1.1.1.85	(1) 2-Oxobutanoate_c0[c0] + (1) CO2_c0[c0] + (1) NADH_c0[c0] <-> (1) D-erythro-3-Methylmalate_c0[c0] + (1) NAD+_c0[c0]
627	<->	kb|g.575.peg.184	MMP1005	K01658	4.1.3.27	(1) Chorismate_c0[c0] + (1) Ammonia_c0[c0] <-> (1) Anthranilate_c0[c0] + (1) Pyruvate_c0[c0] + (1) H2O_c0[c0] + (1) H+_c0[c0]
628	<->	kb|g.575.peg.60	MMP1006	K01657	4.1.3.27	
566	<->	kb|g.575.peg.1658	MMP0869	K01485	3.5.4.1	(1) H+_c0[c0] + (1) Cytosine_c0[c0] + (1) H2O_c0[c0] <-> (1) Uracil_c0[c0] + (1) Ammonia_c0[c0]
406	<->	kb|g.575.peg.1348	MMP0680	K00761	2.4.2.9	(1) UMP_c0[c0] + (1) Diphosphate_c0[c0] <-> (1) Uracil_c0[c0] + (1) 5-Phospho-alpha-D-ribose 1-diphosphate_c0[c0]
609	<->	kb|g.575.peg.1241	MMP0602	K01591	4.1.1.23	
663	<->	kb|g.575.peg.156	MMP1468	K20021	4.4.1.28	(1) L-Cysteine_c0[c0] + (1) H2O_c0[c0] <-> (1) Hydrogen sulfide_c0[c0] + (1) Pyruvate_c0[c0] + (1) Ammonia_c0[c0] + (1) H+_c0[c0]
435	<->	kb|g.575.peg.22	MMP1680	K00820	2.6.1.16	(1) L-Glutamine_c0[c0] + (1) D-Fructose 6-phosphate_c0[c0] <-> (1) L-Glutamate_c0[c0] + (1) D-Glucosamine 6-phosphate_c0[c0]
621	<->	kb|g.575.peg.187	MMP0317	K01622	4.1.2.13+3.1.3.11	(1) D-Fructose 1,6-bisphosphate_c0[c0] + (1) H2O_c0[c0] <-> (1) D-Fructose 6-phosphate_c0[c0] + (1) Orthophosphate_c0[c0]
218	<->	kb|g.575.peg.1376	MMP0870	K00018	1.1.1.29	(1) Glycolate_c0[c0] + (1) NAD+_c0[c0] <-> (1) Glyoxylate_c0[c0] + (1) NADH_c0[c0] + (1) H+_c0[c0]
647	<->	kb|g.575.peg.508	MMP1528	K04518	4.2.1.51	(1) H+_c0[c0] + (1) L-Arogenate_c0[c0] <-> (1) L-

		gpr	gene ID	KO	enzyme	definition
642	<->	kb|g.575.peg.551	MMP1002	K01695	4.2.1.20	Phenylalanine_c0[c0] + (1) H2O_c0[c0] + (1) CO2_c0[c0] (1) L-Serine_c0[c0] + (1) Indole_c0[c0] <-> (1) L-Tryptophan_c0[c0] + (1) H2O_c0[c0]
643	<->	kb|g.575.peg.367	MMP1003	K01696	4.2.1.20	
211	<->	kb|g.575.peg.1457	MMP0802	K00001	1.1.1.1	(1) Primary alcohol_c0[c0] + (1) NAD+_c0[c0] <-> (1) Aldehyde_c0[c0] + (1) NADH_c0[c0] + (1) H+_c0[c0]
461	<->	kb|g.575.peg.560	MMP1124	K00946	2.7.4.16	(1) ATP_c0[c0] + (1) Thiamin monophosphate_c0[c0] <-> (1) ADP_c0[c0] + (1) Thiamin diphosphate_c0[c0]
541	<->	kb|g.575.peg.1211	MMP0541	K01079	3.1.3.3	(1) O-Phospho-L-serine_c0[c0] + (1) H2O_c0[c0] <-> (1) L-Serine_c0[c0] + (1) Orthophosphate_c0[c0] + (1) H+_c0[c0]
762	<->	kb|g.575.peg.1662	MMP0918	K01953	6.3.5.4	
750	->	kb|g.575.peg.1719	MMP0893	K01937	6.3.4.2	(1) ATP_c0[c0] + (1) UTP_c0[c0] + (1) Ammonia_c0[c0] <-> (1) ADP_c0[c0] + (1) Orthophosphate_c0[c0] + (1) CTP_c0[c0] + (2) H+_c0[c0]
607	<->	kb|g.575.peg.214	MMP1582	K02626	4.1.1.19	(1) H+_c0[c0] + (1) L-Arginine_c0[c0] <-> (1) Agmatine_c0[c0] + (1) CO2_c0[c0]
254	<->	kb|g.575.peg.674	MMP0138	K00123	1.2.1.2	(1) Formate_c0[c0] + (1) NAD+_c0[c0] <-> (1) CO2_c0[c0] + (1) NADH_c0[c0]
255	<->	kb|g.575.peg.32	MMP0139	K00125	1.2.1.2	
256	<->	kb|g.575.peg.185	MMP1297	K00125	1.2.1.2	
257	<->	kb|g.575.peg.215	MMP1298	K00123	1.2.1.2	
669	<->	kb|g.575.peg.1553	MMP0739	K01779	5.1.1.13	(1) L-Aspartate_c0[c0] <-> (1) D-Aspartate_c0[c0]
610	<->	kb|g.575.peg.830	MMP0131	K18933	4.1.1.25+4.1.1.11	(1) H+_c0[c0] + (1) L-Aspartate_c0[c0] <-> (1) beta-Alanine_c0[c0] + (1) CO2_c0[c0]
459	<->	kb|g.575.peg.695	MMP1017	K00928	2.7.2.4	(1) ATP_c0[c0] + (1) L-Aspartate_c0[c0] <-> (1) ADP_c0[c0] + (1) 4-Phospho-L-aspartate_c0[c0]

		gpr	gene ID	KO	enzyme	definition
692	<->	kb|g.575.peg.1311	MMP0861	K01843	5.4.3.2	(1) L-Lysine_c0[c0] <-> (1) (3S)-3,6-Diaminohexanoate_c0[c0]
608	<->	kb|g.575.peg.689	MMP1200	K01586	4.1.1.20	
580	->	kb|g.575.peg.420	MMP0214	K02428	3.6.1.66	(1) GTP_c0[c0] + (1) H2O_c0[c0] <-> (1) GMP_c0[c0] + (1) Diphosphate_c0[c0] + (1) H+_c0[c0]
672	<->	kb|g.575.peg.1709	MMP0357	K01791	5.1.3.14	(1) UDP-N-acetyl-alpha-D-glucosamine_c0[c0] <-> (1) UDP-N-acetyl-D-mannosamine_c0[c0] + (2) H+_c0[c0]
673	<->	kb|g.575.peg.1702	MMP0705	K01791	5.1.3.14	
476	<->	kb|g.575.peg.502	MMP1076	K04042	2.7.7.23+2.3.1.157	(1) H+_c0[c0] + (1) UTP_c0[c0] + (1) N-Acetyl-alpha-D-glucosamine 1-phosphate_c0[c0] <-> (1) Diphosphate_c0[c0] + (1) UDP-N-acetyl-alpha-D-glucosamine_c0[c0]
734	<->	kb|g.575.peg.1554	MMP0955	K01902	6.2.1.5	
735	<->	kb|g.575.peg.967	MMP1105	K01903	6.2.1.5	
668	<->	kb|g.575.peg.736	MMP1512	K01775	5.1.1.1	(1) L-Alanine_c0[c0] <-> (1) D-Alanine_c0[c0]
300	<->	kb|g.575.peg.494	MMP1513	K00259	1.4.1.1	(1) L-Alanine_c0[c0] + (1) NAD+_c0[c0] + (1) H2O_c0[c0] <-> (1) Pyruvate_c0[c0] + (1) Ammonia_c0[c0] + (1) NADH_c0[c0] + (1) H+_c0[c0]
772	<->	kb|g.575.peg.1305	MMP0340	K01960	6.4.1.1	(1) ATP_c0[c0] + (1) Pyruvate_c0[c0] + (1) HCO3-_c0[c0] <-> (1) ADP_c0[c0] + (1) Orthophosphate_c0[c0] + (1) Oxaloacetate_c0[c0] + (1) H+_c0[c0]
773	<->	kb|g.575.peg.1400	MMP0341	K01959	6.4.1.1	
224	<->	kb|g.575.peg.1273	MMP0645	K00024	1.1.1.37	(1) (2R)-3-Sulfolactate_c0[c0] + (1) NAD+_c0[c0] <-> (1) 3-Sulfopyruvate_c0[c0] + (1) NADH_c0[c0] + (1) H+_c0[c0]
605	->	kb|g.575.peg.852	MMP1551	K03106	3.6.5.4	(1) GTP_c0[c0] + (1) H2O_c0[c0] <-> (1) GDP_c0[c0] + (1) Orthophosphate_c0[c0] + (1) H+_c0[c0]
674	<->	kb|g.575.peg.802	MMP1090	K01784	5.1.3.2	(1) UDP-glucose_c0[c0] <-> (1) UDP-alpha-D-galactose_c0[c0]

		gpr	gene ID	KO	enzyme	definition
501	<->	kb|g.575.peg.945	MMP1091	K00963	2.7.7.9	(1) H+_c0[c0] + (1) UTP_c0[c0] + (1) D-Glucose 1-phosphate_c0[c0] <-> (1) Diphosphate_c0[c0] + (1) UDP-glucose_c0[c0]
386	<->	kb|g.575.peg.543	MMP0153	K10977	2.3.3.14+2.3.3.-	(1) Acetyl-CoA_c0[c0] + (1) H2O_c0[c0] + (1) 2-Oxoglutarate_c0[c0] <-> (1) (R)-2-Hydroxybutane-1,2,4-tricarboxylate_c0[c0] + (1) CoA_c0[c0] + (1) H+_c0[c0]
380	<->	kb|g.575.peg.1240	MMP0897	K00620	2.3.1.35+2.3.1.1	(1) Acetyl-CoA_c0[c0] + (1) L-Glutamate_c0[c0] <-> (1) CoA_c0[c0] + (1) N-Acetyl-L-glutamate_c0[c0] + (1) H+_c0[c0]
763	->	kb|g.575.peg.350	MMP1013	K01955	6.3.5.5	
764	<->	kb|g.575.peg.656	MMP1589	K01956	6.3.5.5	
737	<->	kb|g.575.peg.507	MMP1206	K01915	6.3.1.2	
727	->	kb|g.575.peg.373	MMP0148	K01895	6.2.1.1	
728	<->	kb|g.575.peg.579	MMP1274	K01895	6.2.1.1	
729	<->	kb|g.575.peg.477	MMP0253	K01905	6.2.1.13	(1) ATP_c0[c0] + (1) Acetate_c0[c0] + (1) CoA_c0[c0] <-> (1) ADP_c0[c0] + (1) Acetyl-CoA_c0[c0] + (1) Orthophosphate_c0[c0]
449	<->	kb|g.575.peg.228	MMP1605	K00873	2.7.1.40	(1) ATP_c0[c0] + (1) Pyruvate_c0[c0] <-> (1) ADP_c0[c0] + (1) Phosphoenolpyruvate_c0[c0] + (1) H+_c0[c0]
506	->	kb|g.575.peg.370	MMP1094	K01007	2.7.9.2	(1) ATP_c0[c0] + (1) Pyruvate_c0[c0] + (1) H2O_c0[c0] <-> (1) AMP_c0[c0] + (1) Phosphoenolpyruvate_c0[c0] + (1) Orthophosphate_c0[c0] + (2) H+_c0[c0]
548	<->	kb|g.575.peg.1362	MMP0920	K01251	3.3.1.1	(1) S-Adenosyl-L-homocysteine_c0[c0] + (1) H2O_c0[c0] <-> (1) Adenosine_c0[c0] + (1) L-Homocysteine_c0[c0]
404	<->	kb|g.575.peg.758	MMP0145	K00759	2.4.2.7	(1) AMP_c0[c0] + (1) Diphosphate_c0[c0] <-> (1) Adenine_c0[c0] + (1) 5-Phospho-alpha-D-ribose 1-diphosphate_c0[c0]
405	<->	kb|g.575.peg.1147	MMP0660	K00759	2.4.2.7	

		gpr	gene ID	KO	enzyme	definition
738	<->	kb|g.575.peg.699	MMP1349	K01916	6.3.1.5	(1) ATP_c0[c0] + (1) Deamino-NAD+_c0[c0] + (1) Ammonia_c0[c0] <-> (1) AMP_c0[c0] + (1) Diphosphate_c0[c0] + (1) NAD+_c0[c0] + (1) H+_c0[c0]
542	<->	kb|g.575.peg.85	MMP1051	K03787	3.1.3.5	(1) AMP_c0[c0] + (1) H2O_c0[c0] <-> (1) Adenosine_c0[c0] + (1) Orthophosphate_c0[c0]
616	<->	kb|g.575.peg.757	MMP1583	K01611	4.1.1.50	(1) S-Adenosyl-L-methionine_c0[c0] + (1) H+_c0[c0] <-> (1) S-Adenosylmethioninamine_c0[c0] + (1) CO2_c0[c0]
421	->	kb|g.575.peg.234	MMP1640	K00789	2.5.1.6	(1) ATP_c0[c0] + (1) L-Methionine_c0[c0] + (1) H2O_c0[c0] -> (1) Orthophosphate_c0[c0] + (1) Diphosphate_c0[c0] + (1) S-Adenosyl-L-methionine_c0[c0]
475	<->	kb|g.575.peg.1254	MMP0943	K14656	2.7.7.2	(1) ATP_c0[c0] + (1) FMN_c0[c0] <-> (1) Diphosphate_c0[c0] + (1) FAD_c0[c0]
463	<->	kb|g.575.peg.1337	MMP0626	K00945	2.7.4.25	(1) ATP_c0[c0] + (1) dCMP_c0[c0] <-> (1) ADP_c0[c0] + (1) dCDP_c0[c0]
462	<->	kb|g.575.peg.85	MMP1051		3.1.3.5	(1) dCMP_c0[c0] + (1) H2O_c0[c0] <-> (1) Deoxycytidine_c0[c0] + (1) Orthophosphate_c0[c0] + (1) H+_c0[c0]
306	<->	kb|g.575.peg.1477	MMP0720	K05601	1.7.99.1	(1) Ammonia_c0[c0] + (1) NAD+_c0[c0] + (1) H2O_c0[c0] <-> (1) Hydroxylamine_c0[c0] + (1) NADH_c0[c0] + (2) H+_c0[c0]
474	<->	kb|g.575.peg.46	MMP1578	K00952	2.7.7.1	(1) ATP_c0[c0] + (1) Nicotinamide D-ribonucleotide_c0[c0] <-> (1) Diphosphate_c0[c0] + (1) NAD+_c0[c0]
633	<->	kb|g.575.peg.654	MMP1299	K01673	4.2.1.1	(1) H+_c0[c0] + (1) Carbonic acid_c0[c0] <-> (1) CO2_c0[c0] + (1) H2O_c0[c0]
465	<->	kb|g.575.peg.482	MMP1031	K00939	2.7.4.3	(1) ATP_c0[c0] + (1) AMP_c0[c0] <-> (2) ADP_c0[c0]
466	<->	kb|g.575.peg.77	MMP1534	K18532	2.7.4.3	
446	<->	kb|g.575.peg.418	MMP1489	K00858	2.7.1.23	(1) ATP_c0[c0] + (1) NAD+_c0[c0] <-> (1) ADP_c0[c0] + (1) NADP+_c0[c0] + (1) H+_c0[c0]
664	<->	kb|g.575.peg.210	MMP1064	K05873	4.6.1.1	(1) ATP_c0[c0] <-> (1) 3',5'-Cyclic AMP_c0[c0] + (1) Diphosphate_c0[c0]
584	->	kb|g.575.peg.267	MMP0163	K01551	3.6.3.16	(1) ATP_c0[c0] + (1) H2O_c0[c0] <-> (1) ADP_c0[c0] + (1)

		gpr	gene ID	KO	enzyme	definition
						Orthophosphate_c0[c0] + (1) H+_c0[c0]
585	<->	kb|g.575.peg.731	MMP0229	K02028	3.6.3.21	
586	<->	kb|g.575.peg.895	MMP1098	K02036	3.6.3.27	
587	<->	kb|g.575.peg.100	MMP0207	K02017	3.6.3.29	
588	<->	kb|g.575.peg.1195	MMP0504	K02017	3.6.3.29	
589	<->	kb|g.575.peg.345	MMP1649	K02017	3.6.3.29	
591	<->	kb|g.575.peg.501	MMP0110	K02010	3.6.3.30	
592	<->	kb|g.575.peg.1005	MMP0868	K02000	3.6.3.32	
593	<->	kb|g.575.peg.499	MMP0198	K02013	3.6.3.34	
594	<->	kb|g.575.peg.247	MMP1183	K02013	3.6.3.34	
595	<->	kb|g.575.peg.122	MMP1165	K17686	3.6.3.54	
596	<->	kb|g.575.peg.344	MMP1641	K17686	3.6.3.54	
597	<->	kb|g.575.peg.1224	MMP0520	K01537	3.6.3.8	
602	<->	kb|g.575.peg.1268	MMP0460	K03655	3.6.4.12	
603	<->	kb|g.575.peg.907	MMP1219	K03722	3.6.4.12	
604	<->	kb|g.575.peg.1506	MMP0457	K05592	3.6.4.13	
422	<->	kb|g.575.peg.1201	MMP0872	K01749	2.5.1.61	(4) Porphobilinogen_c0[c0] + (1) H2O_c0[c0] <-> (1) Hydroxymethylbilane_c0[c0] + (4) Ammonia_c0[c0]
430	<->	kb|g.575.peg.948	MMP0180	K00793	2.5.1.9	(2) 6,7-Dimethyl-8-(D-ribityl)lumazine_c0[c0] <-> (1) Riboflavin_c0[c0] + (1) 5-Amino-6-(1-D-ribitylamino)uracil_c0[c0]
644	<->	kb|g.575.peg.200	MMP1258	K01698	4.2.1.24	(2) 5-Aminolevulinate_c0[c0] <-> (1) Porphobilinogen_c0[c0] + (2) H2O_c0[c0] + (1) H+_c0[c0]

		gpr	gene ID	KO	enzyme	definition
239	<->	kb|g.575.peg.1346	MMP0821	K14127	1.12.99.-	
240	<->	kb|g.575.peg.1321	MMP0822	K14128	1.12.99.-	
241	<->	kb|g.575.peg.1167	MMP0823	K14126	1.12.99.-	
242	<->	#N/A	MMP1694	K14126	1.12.99.-	
243	<->	kb|g.575.peg.899	MMP1695	K14128	1.12.99.-	
244	<->	kb|g.575.peg.570	MMP1696	K14127	1.12.99.-	
369	<->	kb|g.575.peg.307	MMP0142	K01652	2.2.1.6	
370	<->	kb|g.575.peg.1467	MMP0650	K01652	2.2.1.6	
371	<->	kb|g.575.peg.1371	MMP0651	K01653	2.2.1.6	
575	<->	kb|g.575.peg.514	MMP0219	K15986	3.6.1.1	
382	<->	kb|g.575.peg.96	MMP1577	K07739	2.3.1.48	(1) Acetyl-CoA_c0[c0] + (1) Histone-L-lysine_c0[c0] <-> (1) CoA_c0[c0] + (1) Histone N6-acetyl-L-lysine_c0[c0]
246		kb|g.575.peg.641	MMP1159	K02217	1.16.3.2	
324		kb|g.575.peg.1575	MMP0606	K02427	2.1.1.166	
325		kb|g.575.peg.755	MMP1037	K00783	2.1.1.177	
327		kb|g.575.peg.599	MMP1307	K06969	2.1.1.191	
330		kb|g.575.peg.199	MMP1425	K07254	2.1.1.206	
331		kb|g.575.peg.780	MMP0149	K07446	2.1.1.213	
338		kb|g.575.peg.1041	MMP0924	K16317	2.1.1.257	
400		kb|g.575.peg.1412	MMP0610	K18779	2.4.2.48	
407		kb|g.575.peg.97	MMP1424	K21306	2.4.99.21	
440		kb|g.575.peg.293	MMP1595	K07557	2.6.1.97	
455		kb|g.575.peg.1270	MMP0927	K03407	2.7.13.3	
456		kb|g.575.peg.69	MMP1120	K02484	2.7.13.3	

	gpr	gene ID	KO	enzyme	definition
524	kb|g.575.peg.1368	MMP0990	K09716	3.1.1.96	
525	kb|g.575.peg.227	MMP1012	K01142	3.1.11.2	
526	kb|g.575.peg.1447	MMP0731	K03602	3.1.11.6	
527	kb|g.575.peg.1622	MMP0732	K03601	3.1.11.6	
531	kb|g.575.peg.791	MMP1678	K01151	3.1.21.2	
532	kb|g.575.peg.834	MMP0336	K03552	3.1.22.4	
533	kb|g.575.peg.1356	MMP0906	K00784	3.1.26.11	
534	kb|g.575.peg.289	MMP1526	K03685	3.1.26.3	
535	kb|g.575.peg.1205	MMP0837	K03469	3.1.26.4	
536	kb|g.575.peg.186	MMP1374	K03470	3.1.26.4	
537	kb|g.575.peg.1494	MMP0430	K03539	3.1.26.5	
538	kb|g.575.peg.1294	MMP0878	K03537	3.1.26.5	
539	kb|g.575.peg.1439	MMP0921	K03540	3.1.26.5	
540	kb|g.575.peg.198	MMP1407	K03538	3.1.26.5	
544	kb|g.575.peg.257	MMP1201	K01174	3.1.31.1	
551	kb|g.575.peg.209	MMP1444	K01265	3.4.11.18	
552	kb|g.575.peg.213	MMP1204	K01271	3.4.13.9	
555	kb|g.575.peg.479	MMP1185	K08315	3.4.23.51	
556	kb|g.575.peg.208	MMP0232	K07991	3.4.23.52	
557	kb|g.575.peg.1483	MMP0555	K07991	3.4.23.52	
559	kb|g.575.peg.783	MMP0251	K03432	3.4.25.1	
560	kb|g.575.peg.1599	MMP0695	K03433	3.4.25.1	
654	kb|g.575.peg.574	MMP0304	K01741	4.2.99.18	
655	kb|g.575.peg.1364	MMP0537	K10773	4.2.99.18	
665	kb|g.575.peg.584	MMP1132	K01170	4.6.1.16	
698	kb|g.575.peg.595	MMP1010	K06180	5.4.99.23	
699	kb|g.575.peg.866	MMP0014	K06176	5.4.99.27	
700	kb|g.575.peg.1317	MMP0615	K06176	5.4.99.27	
703	kb|g.575.peg.1470	MMP0956	K03168	5.99.1.2	

	gpr	gene ID	KO	enzyme	definition
704	kb|g.575.peg.1683	MMP0989	K03167	5.99.1.3	
705	kb|g.575.peg.25	MMP1437	K03166	5.99.1.3	
785	kb|g.575.peg.1514	MMP0620	K00400	0	
786	kb|g.575.peg.325	MMP1630	K00400	0	
791	#N/A	RNA_39	K01977	0	
792	#N/A	RNA_41	K01977	0	
793	#N/A	RNA_44	K01977	0	
794	#N/A	RNA_45	K01978	0	
795	#N/A	RNA_38	K01980	0	
796	#N/A	RNA_40	K01980	0	
797	#N/A	RNA_42	K01980	0	
798	#N/A	RNA_49	K01983	0	
799	#N/A	RNA_46	K01985	0	
800	#N/A	RNA_47	K01985	0	
801	#N/A	RNA_48	K01985	0	
802	#N/A	RNA_37	K01985	0	
803	kb|g.575.peg.139	MMP0167	K01990	0	
804	kb|g.575.peg.130	MMP0165	K01992	0	
805	kb|g.575.peg.1193	MMP0867	K02001	0	
806	kb|g.575.peg.1269	MMP0866	K02002	0	
807	kb|g.575.peg.1419	MMP0523	K02003	0	
808	kb|g.575.peg.1099	MMP0635	K02003	0	
809	kb|g.575.peg.1565	MMP0521	K02004	0	
810	kb|g.575.peg.1446	MMP0634	K02004	0	
811	kb|g.575.peg.1505	MMP0871	K02004	0	
812	kb|g.575.peg.668	MMP1484	K02006	0	
813	kb|g.575.peg.1456	MMP0889	K02007	0	
814	kb|g.575.peg.76	MMP1481	K02007	0	
815	kb|g.575.peg.1694	MMP0886	K02008	0	

	gpr	gene ID	KO	enzyme	definition
816	kb|g.575.peg.263	MMP1483	K02008	0	
817	kb|g.575.peg.1533	MMP0888	K02009	0	
818	kb|g.575.peg.121	MMP1482	K02009	0	
819	kb|g.575.peg.608	MMP0109	K02011	0	
820	kb|g.575.peg.946	MMP0108	K02012	0	
821	kb|g.575.peg.642	MMP0197	K02015	0	
822	kb|g.575.peg.157	MMP1182	K02015	0	
823	kb|g.575.peg.894	MMP0196	K02016	0	
824	kb|g.575.peg.914	MMP1176	K02016	0	
825	kb|g.575.peg.577	MMP1177	K02016	0	
826	kb|g.575.peg.709	MMP1178	K02016	0	
827	kb|g.575.peg.951	MMP1181	K02016	0	
828	kb|g.575.peg.936	MMP0206	K02018	0	
829	kb|g.575.peg.1030	MMP0506	K02018	0	
830	kb|g.575.peg.1634	MMP0515	K02018	0	
831	kb|g.575.peg.542	MMP1650	K02018	0	
832	kb|g.575.peg.759	MMP0205	K02020	0	
833	kb|g.575.peg.1123	MMP0507	K02020	0	
834	kb|g.575.peg.1347	MMP0514	K02020	0	
835	kb|g.575.peg.1230	MMP0975	K02020	0	
836	kb|g.575.peg.622	MMP1651	K02020	0	
837	kb|g.575.peg.1707	MMP0551	K02029	0	
838	kb|g.575.peg.1646	MMP0455	K02030	0	
839	kb|g.575.peg.1381	MMP0550	K02030	0	
840	kb|g.575.peg.1349	MMP0770	K02030	0	
841	kb|g.575.peg.175	MMP1224	K02030	0	
842	kb|g.575.peg.398	MMP1632	K02030	0	
843	kb|g.575.peg.665	MMP1096	K02037	0	
844	kb|g.575.peg.270	MMP1097	K02038	0	

		gpr	gene ID	KO	enzyme	definition
845		kb|g.575.peg.545	MMP1099	K02039	0	
846		kb|g.575.peg.737	MMP1199	K02039	0	
847		kb|g.575.peg.1180	MMP0345	K02040	0	
848		kb|g.575.peg.48	MMP1095	K02040	0	
849		kb|g.575.peg.189	MMP1198	K02049	0	
850		kb|g.575.peg.472	MMP1197	K02050	0	
851		kb|g.575.peg.118	MMP1260	K02051	0	
852		kb|g.575.peg.412	MMP0171	K02069	0	
853		kb|g.575.peg.158	MMP1038	K02107	0	
854		kb|g.575.peg.476	MMP1045	K02118	0	
855		kb|g.575.peg.467	MMP1042	K02119	0	
856		kb|g.575.peg.126	MMP1046	K02120	0	
857		kb|g.575.peg.128	MMP1041	K02121	0	
858		kb|g.575.peg.330	MMP1043	K02122	0	
859		kb|g.575.peg.3	MMP1039	K02123	0	
860		kb|g.575.peg.784	MMP1040	K02124	0	
861		kb|g.575.peg.905	MMP1233	K02379	0	
862		kb|g.575.peg.1020	MMP0963	K02440	0	
863		kb|g.575.peg.544	MMP0331	K02503	0	
864	<->	kb|g.575.peg.1451	MMP0658	K02585	4.1.99.22	(1) GTP_c0[c0] + (1) S-Adenosyl-L-methionine_c0[c0] + (1) Reduced acceptor_c0[c0] + (1) H+_c0[c0] = (1) C21310_c0[c0] + (1) 5'-Deoxyadenosine_c0[c0] + (1) L-Methionine_c0[c0] + (1) Acceptor_c0[c0]
865		kb|g.575.peg.1534	MMP0858	K02587	0	
866		kb|g.575.peg.1056	MMP0854	K02589	0	
867		kb|g.575.peg.1122	MMP0855	K02590	0	
868		kb|g.575.peg.1072	MMP0859	K02592	0	
869		kb|g.575.peg.726	MMP1366	K02600	0	
870		kb|g.575.peg.724	MMP1434	K02601	0	

	gpr	gene ID	KO	enzyme	definition
871	kb|g.575.peg.1424	MMP0919	K02823	0	
872	kb|g.575.peg.170	MMP0260	K02863	0	
873	kb|g.575.peg.5	MMP0259	K02864	0	
874	kb|g.575.peg.557	MMP1289	K02866	0	
875	kb|g.575.peg.677	MMP1433	K02867	0	
876	kb|g.575.peg.256	MMP0258	K02869	0	
877	kb|g.575.peg.445	MMP1324	K02871	0	
878	kb|g.575.peg.504	MMP1409	K02874	0	
879	kb|g.575.peg.1259	MMP0625	K02875	0	
880	kb|g.575.peg.496	MMP1421	K02876	0	
881	kb|g.575.peg.446	MMP0298	K02877	0	
882	kb|g.575.peg.283	MMP1418	K02881	0	
883	kb|g.575.peg.583	MMP1323	K02883	0	
884	kb|g.575.peg.41	MMP1417	K02885	0	
885	kb|g.575.peg.764	MMP1546	K02886	0	
886	kb|g.575.peg.1714	MMP0093	K02889	0	
887	kb|g.575.peg.917	MMP1403	K02890	0	
888	kb|g.575.peg.141	MMP1545	K02892	0	
889	kb|g.575.peg.652	MMP1410	K02895	0	
890	kb|g.575.peg.1708	MMP0639	K02896	0	
891	kb|g.575.peg.670	MMP1405	K02904	0	
892	kb|g.575.peg.803	MMP1543	K02906	0	
893	kb|g.575.peg.873	MMP1420	K02907	0	
894	kb|g.575.peg.795	MMP1365	K02908	0	
895	kb|g.575.peg.1493	MMP0062	K02910	0	
896	kb|g.575.peg.369	MMP1416	K02912	0	
897	kb|g.575.peg.1434	MMP0627	K02915	0	
898	kb|g.575.peg.315	MMP0249	K02921	0	
899	kb|g.575.peg.396	MMP1147	K02922	0	

	gpr	gene ID	KO	enzyme	definition
900	kb|g.575.peg.823	MMP0159	K02924	0	
901	kb|g.575.peg.287	MMP0151	K02927	0	
902	kb|g.575.peg.308	MMP1709	K02929	0	
903	kb|g.575.peg.910	MMP1544	K02930	0	
904	kb|g.575.peg.862	MMP1412	K02931	0	
905	kb|g.575.peg.828	MMP1415	K02933	0	
906	kb|g.575.peg.1120	MMP0641	K02936	0	
907	kb|g.575.peg.1385	MMP0060	K02944	0	
908	kb|g.575.peg.301	MMP1371	K02946	0	
909	kb|g.575.peg.638	MMP1321	K02948	0	
910	kb|g.575.peg.660	MMP1367	K02950	0	
911	kb|g.575.peg.80	MMP1319	K02952	0	
912	kb|g.575.peg.885	MMP1413	K02954	0	
913	kb|g.575.peg.679	MMP1579	K02956	0	
914	kb|g.575.peg.427	MMP1408	K02961	0	
915	kb|g.575.peg.1088	MMP0577	K02962	0	
916	kb|g.575.peg.273	MMP1547	K02965	0	
917	kb|g.575.peg.219	MMP0156	K02966	0	
918	kb|g.575.peg.1295	MMP0667	K02967	0	
919	kb|g.575.peg.1379	MMP0443	K02974	0	
920	kb|g.575.peg.1023	MMP0444	K02977	0	
921	kb|g.575.peg.403	MMP1708	K02978	0	
922	kb|g.575.peg.1491	MMP0640	K02979	0	
923	kb|g.575.peg.535	MMP1404	K02982	0	
924	kb|g.575.peg.1688	MMP0669	K02984	0	
925	kb|g.575.peg.751	MMP1320	K02986	0	
926	kb|g.575.peg.306	MMP1411	K02987	0	
927	kb|g.575.peg.381	MMP1419	K02988	0	
928	kb|g.575.peg.911	MMP1207	K02991	0	

	gpr	gene ID	KO	enzyme	definition
929	kb|g.575.peg.775	MMP1368	K02992	0	
930	kb|g.575.peg.181	MMP1414	K02994	0	
931	kb|g.575.peg.649	MMP1658	K02995	0	
932	kb|g.575.peg.323	MMP1325	K02996	0	
933	kb|g.575.peg.683	MMP1429	K03057	0	
934	kb|g.575.peg.813	MMP1523	K03072	0	
935	kb|g.575.peg.67	MMP1524	K03074	0	
936	kb|g.575.peg.250	MMP1422	K03076	0	
937	kb|g.575.peg.568	MMP1107	K03105	0	
938	kb|g.575.peg.1552	MMP0683	K03110	0	
939	kb|g.575.peg.70	MMP1406	K03113	0	
940	kb|g.575.peg.415	MMP0257	K03120	0	
941	kb|g.575.peg.1687	MMP0041	K03124	0	
942	kb|g.575.peg.1596	MMP0036	K03136	0	
945	kb|g.575.peg.1216	MMP0655	K03154	0	
946	kb|g.575.peg.534	MMP1370	K03231	0	
947	kb|g.575.peg.153	MMP1401	K03232	0	
948	kb|g.575.peg.970	MMP1369	K03234	0	
949	kb|g.575.peg.1141	MMP0603	K03236	0	
950	kb|g.575.peg.548	MMP1707	K03237	0	
951	kb|g.575.peg.132	MMP0297	K03238	0	
952	kb|g.575.peg.754	MMP1208	K03242	0	
953	kb|g.575.peg.694	MMP0284	K03243	0	
954	kb|g.575.peg.1198	MMP0952	K03263	0	
955	kb|g.575.peg.1677	MMP0061	K03264	0	
956	kb|g.575.peg.921	MMP1131	K03265	0	
957	kb|g.575.peg.1278	MMP0711	K03284	0	
958	kb|g.575.peg.576	MMP1108	K03284	0	
959	kb|g.575.peg.1375	MMP0850	K03294	0	

	gpr	gene ID	KO	enzyme	definition
960	kb|g.575.peg.264	MMP1700	K03307	0	
961	kb|g.575.peg.1513	MMP0419	K03308	0	
962	kb|g.575.peg.814	MMP1511	K03310	0	
963	kb|g.575.peg.1603	MMP0065	K03320	0	
964	kb|g.575.peg.1452	MMP0529	K03321	0	
965	kb|g.575.peg.1577	MMP0663	K03321	0	
966	kb|g.575.peg.1069	MMP0666	K03324	0	
967	kb|g.575.peg.1077	MMP0413	K03406	0	
968	kb|g.575.peg.1339	MMP0487	K03406	0	
969	kb|g.575.peg.1176	MMP0929	K03406	0	
970	kb|g.575.peg.1087	MMP0925	K03408	0	
971	kb|g.575.peg.1282	MMP0931	K03410	0	
972	kb|g.575.peg.1137	MMP0932	K03410	0	
973	kb|g.575.peg.1063	MMP0933	K03413	0	
974	kb|g.575.peg.19	MMP1647	K03420	0	
975	kb|g.575.peg.346	MMP1557	K03421	0	
976	kb|g.575.peg.310	MMP1556	K03422	0	
977	kb|g.575.peg.1255	MMP0796	K03445	0	
978	kb|g.575.peg.1616	MMP0653	K03453	0	
979	kb|g.575.peg.1138	MMP0681	K03458	0	
980	kb|g.575.peg.131	MMP1430	K03498	0	
981	kb|g.575.peg.770	MMP1599	K03499	0	
982	kb|g.575.peg.906	MMP1397	K03529	0	
983	kb|g.575.peg.920	MMP1436	K03531	0	
984	kb|g.575.peg.146	MMP1500	K03531	0	
985	kb|g.575.peg.848	MMP1341	K03546	0	
986	kb|g.575.peg.74	MMP1488	K03568	0	
987	kb|g.575.peg.197	MMP1525	K03592	0	
988	kb|g.575.peg.1501	MMP0593	K03609	0	

	gpr	gene ID	KO	enzyme	definition
989	kb|g.575.peg.613	MMP1145	K03609	0	
990	kb|g.575.peg.901	MMP1613	K03622	0	
991	kb|g.575.peg.890	MMP0290	K03626	0	
992	kb|g.575.peg.900	MMP1646	K03627	0	
993	kb|g.575.peg.160	MMP1357	K03636	0	
994	kb|g.575.peg.540	MMP1485	K03638	0	
995	kb|g.575.peg.1557	MMP0958	K03671	0	
996	kb|g.575.peg.1336	MMP0729	K03701	0	
997	kb|g.575.peg.1572	MMP0727	K03702	0	
998	kb|g.575.peg.1502	MMP0728	K03703	0	
999	kb|g.575.peg.1047	MMP0631	K03709	0	
1000	kb|g.575.peg.933	MMP1137	K03718	0	
1001	kb|g.575.peg.861	MMP1441	K03753	0	
1002	kb|g.575.peg.232	MMP1336	K03833	0	
1003	kb|g.575.peg.983	MMP1442	K03892	0	
1004	kb|g.575.peg.321	MMP1163	K03926	0	
1005	kb|g.575.peg.522	MMP1376	K03973	0	
1006	kb|g.575.peg.324	MMP1222	K04483	0	
1007	kb|g.575.peg.1145	MMP0617	K04484	0	
1008	kb|g.575.peg.484	MMP0301	K04651	0	
1009	kb|g.575.peg.612	MMP1520	K04652	0	
1010	kb|g.575.peg.28	MMP1330	K04653	0	
1011	kb|g.575.peg.960	MMP0289	K04654	0	
1012	kb|g.575.peg.715	MMP0274	K04655	0	
1013	kb|g.575.peg.662	MMP0140	K04656	0	
1014	kb|g.575.peg.1154	MMP0064	K04751	0	
1015	kb|g.575.peg.1342	MMP0066	K04751	0	
1016	kb|g.575.peg.1468	MMP0067	K04751	0	
1017	kb|g.575.peg.1594	MMP0630	K04759	0	

	gpr	gene ID	KO	enzyme	definition
1018	kb|g.575.peg.1504	MMP0472	K04763	0	
1019	kb|g.575.peg.1263	MMP0743	K04763	0	
1020	kb|g.575.peg.1560	MMP0597	K04795	0	
1021	kb|g.575.peg.475	MMP1148	K04796	0	
1022	kb|g.575.peg.743	MMP1470	K04797	0	
1023	kb|g.575.peg.575	MMP0245	K04798	0	
1024	kb|g.575.peg.352	MMP0322	K04800	0	
1025	kb|g.575.peg.1125	MMP0427	K04801	0	
1026	kb|g.575.peg.707	MMP1711	K04802	0	
1027	kb|g.575.peg.45	MMP0266	K05595	0	
1028	kb|g.575.peg.203	MMP1516	K05896	0	
1029	kb|g.575.peg.1245	MMP0594	K06024	0	
1030	kb|g.575.peg.1608	MMP0382	K06174	0	
1031	kb|g.575.peg.1605	MMP0957	K06196	0	
1032	kb|g.575.peg.15	MMP1279	K06199	0	
1033	kb|g.575.peg.1251	MMP0400	K06862	0	
1034	kb|g.575.peg.768	MMP1239	K06864	0	
1035	kb|g.575.peg.835	MMP0281	K06865	0	
1036	kb|g.575.peg.1174	MMP0914	K06869	0	
1037	kb|g.575.peg.459	MMP1062	K06870	0	
1038	kb|g.575.peg.313	MMP1446	K06874	0	
1039	kb|g.575.peg.368	MMP0157	K06875	0	
1040	kb|g.575.peg.1601	MMP0494	K06877	0	
1041	kb|g.575.peg.478	MMP1642	K06883	0	
1042	kb|g.575.peg.423	MMP0174	K06885	0	
1043	kb|g.575.peg.460	MMP0191	K06889	0	
1044	kb|g.575.peg.1535	MMP0792	K06889	0	
1045	kb|g.575.peg.1712	MMP0809	K06898	0	
1046	kb|g.575.peg.1684	MMP0689	K06901	0	

	gpr	gene ID	KO	enzyme	definition
1047	kb|g.575.peg.1484	MMP0035	K06913	0	
1048	kb|g.575.peg.714	MMP1264	K06915	0	
1049	kb|g.575.peg.1004	MMP0676	K06923	0	
1050	kb|g.575.peg.366	MMP0012	K06929	0	
1051	kb|g.575.peg.868	MMP1536	K06931	0	
1052	kb|g.575.peg.1664	MMP0375	K06935	0	
1053	kb|g.575.peg.886	MMP1014	K06936	0	
1054	kb|g.575.peg.159	MMP0270	K06939	0	
1055	kb|g.575.peg.966	MMP1117	K06940	0	
1056	kb|g.575.peg.511	MMP1263	K06940	0	
1057	kb|g.575.peg.722	MMP1122	K06942	0	
1058	kb|g.575.peg.1152	MMP0901	K06943	0	
1059	kb|g.575.peg.822	MMP1443	K06944	0	
1060	kb|g.575.peg.37	MMP1715	K06945	0	
1061	kb|g.575.peg.1640	MMP0037	K06950	0	
1062	kb|g.575.peg.788	MMP1142	K06953	0	
1063	kb|g.575.peg.239	MMP1127	K06959	0	
1064	kb|g.575.peg.1314	MMP0605	K06961	0	
1065	kb|g.575.peg.1476	MMP0978	K06964	0	
1066	kb|g.575.peg.1306	MMP0085	K06965	0	
1067	kb|g.575.peg.155	MMP1285	K06986	0	
1068	kb|g.575.peg.934	MMP1550	K06988	0	
1069	kb|g.575.peg.824	MMP1387	K06990	0	
1070	kb|g.575.peg.804	MMP1022	K07003	0	
1071	kb|g.575.peg.1674	MMP0852	K07005	0	
1072	kb|g.575.peg.996	MMP0624	K07006	0	
1073	kb|g.575.peg.1210	MMP0939	K07025	0	
1074	kb|g.575.peg.1144	MMP0767	K07027	0	
1075	kb|g.575.peg.716	MMP1522	K07027	0	

	gpr	gene ID	KO	enzyme	definition
1076	kb|g.575.peg.129	MMP1169	K07033	0	
1077	kb|g.575.peg.1561	MMP0348	K07034	0	
1078	kb|g.575.peg.741	MMP0124	K07038	0	
1079	kb|g.575.peg.1538	MMP0694	K07041	0	
1080	kb|g.575.peg.1121	MMP0838	K07043	0	
1081	kb|g.575.peg.1203	MMP0556	K07049	0	
1082	kb|g.575.peg.1661	MMP0432	K07051	0	
1083	kb|g.575.peg.1693	MMP0485	K07052	0	
1084	kb|g.575.peg.614	MMP1213	K07068	0	
1085	kb|g.575.peg.762	MMP0208	K07079	0	
1086	kb|g.575.peg.1527	MMP0803	K07079	0	
1087	kb|g.575.peg.1540	MMP0808	K07079	0	
1088	kb|g.575.peg.154	MMP1092	K07088	0	
1089	kb|g.575.peg.408	MMP0202	K07089	0	
1090	kb|g.575.peg.997	MMP0801	K07089	0	
1091	kb|g.575.peg.1410	MMP0973	K07089	0	
1092	kb|g.575.peg.1547	MMP0942	K07090	0	
1093	kb|g.575.peg.177	MMP1634	K07092	0	
1094	kb|g.575.peg.1635	MMP0393	K07095	0	
1095	kb|g.575.peg.589	MMP1501	K07095	0	
1096	kb|g.575.peg.626	MMP1684	K07096	0	
1097	kb|g.575.peg.926	MMP1377	K07111	0	
1098	kb|g.575.peg.740	MMP1538	K07112	0	
1099	kb|g.575.peg.40	MMP1531	K07123	0	
1100	kb|g.575.peg.667	MMP1192	K07129	0	
1101	kb|g.575.peg.464	MMP1714	K07131	0	
1102	kb|g.575.peg.382	MMP1590	K07134	0	
1103	kb|g.575.peg.163	MMP1059	K07137	0	
1104	kb|g.575.peg.1615	MMP0800	K07138	0	

	gpr	gene ID	KO	enzyme	definition
1105	kb|g.575.peg.785	MMP1495	K07139	0	
1106	kb|g.575.peg.820	MMP0134	K07143	0	
1107	kb|g.575.peg.756	MMP1342	K07158	0	
1108	kb|g.575.peg.606	MMP1611	K07159	0	
1109	kb|g.575.peg.49	MMP0231	K07162	0	
1110	kb|g.575.peg.1487	MMP0657	K07166	0	
1111	kb|g.575.peg.805	MMP1612	K07176	0	
1112	kb|g.575.peg.474	MMP1173	K07238	0	
1113	kb|g.575.peg.102	MMP0190	K07301	0	
1114	kb|g.575.peg.229	MMP1068	K07301	0	
1115	kb|g.575.peg.1405	MMP0977	K07321	0	
1116	kb|g.575.peg.1264	MMP0982	K07321	0	
1117	kb|g.575.peg.355	MMP1666	K07325	0	
1118	kb|g.575.peg.191	MMP1667	K07325	0	
1119	kb|g.575.peg.394	MMP1668	K07325	0	
1120	kb|g.575.peg.536	MMP1670	K07327	0	
1121	kb|g.575.peg.489	MMP1671	K07328	0	
1122	kb|g.575.peg.1090	MMP0342	K07329	0	
1123	kb|g.575.peg.14	MMP1672	K07329	0	
1124	kb|g.575.peg.867	MMP1673	K07330	0	
1125	kb|g.575.peg.282	MMP1674	K07331	0	
1126	kb|g.575.peg.1602	MMP0040	K07332	0	
1127	kb|g.575.peg.113	MMP1675	K07332	0	
1128	kb|g.575.peg.1098	MMP0039	K07333	0	
1129	kb|g.575.peg.610	MMP1676	K07333	0	
1130	kb|g.575.peg.909	MMP1435	K07342	0	
1131	kb|g.575.peg.13	MMP0291	K07388	0	
1132	kb|g.575.peg.269	MMP0024	K07392	0	
1133	kb|g.575.peg.1114	MMP0586	K07457	0	

	gpr	gene ID	KO	enzyme	definition
1134	kb|g.575.peg.1322	MMP0547	K07463	0	
1135	kb|g.575.peg.912	MMP1314	K07463	0	
1136	kb|g.575.peg.253	MMP1682	K07463	0	
1137	kb|g.575.peg.372	MMP1032	K07466	0	
1138	kb|g.575.peg.580	MMP1542	K07477	0	
1139	kb|g.575.peg.1713	MMP0495	K07502	0	
1140	kb|g.575.peg.782	MMP0296	K07562	0	
1141	kb|g.575.peg.687	MMP0016	K07565	0	
1142	kb|g.575.peg.1031	MMP0042	K07569	0	
1143	kb|g.575.peg.1499	MMP0091	K07572	0	
1144	kb|g.575.peg.827	MMP0155	K07574	0	
1145	kb|g.575.peg.1503	MMP0055	K07575	0	
1146	kb|g.575.peg.1377	MMP0431	K07577	0	
1147	kb|g.575.peg.1445	MMP0685	K07579	0	
1148	kb|g.575.peg.35	MMP1400	K07580	0	
1149	kb|g.575.peg.358	MMP0300	K07581	0	
1150	kb|g.575.peg.20	MMP0158	K07585	0	
1151	kb|g.575.peg.292	MMP0020	K07722	0	
1152	kb|g.575.peg.1303	MMP0719	K07722	0	
1153	kb|g.575.peg.1109	MMP0678	K07728	0	
1154	kb|g.575.peg.1242	MMP0674	K07729	0	
1155	kb|g.575.peg.1136	MMP0993	K07729	0	
1156	kb|g.575.peg.930	MMP1052	K07730	0	
1157	kb|g.575.peg.16	MMP1210	K07731	0	
1158	kb|g.575.peg.1018	MMP0052	K07744	0	
1159	kb|g.575.peg.277	MMP1669	K07822	0	
1161	kb|g.575.peg.712	MMP1109	K08975	0	
1162	kb|g.575.peg.309	MMP1587	K08978	0	
1163	kb|g.575.peg.530	MMP0022	K09005	0	

	gpr	gene ID	KO	enzyme	definition
1164	kb|g.575.peg.940	MMP1472	K09006	0	
1165	kb|g.575.peg.220	MMP1168	K09013	0	
1166	kb|g.575.peg.242	MMP1253	K09116	0	
1167	kb|g.575.peg.388	MMP1607	K09120	0	
1168	kb|g.575.peg.582	MMP0269	K09121	0	
1169	kb|g.575.peg.1093	MMP0806	K09121	0	
1170	kb|g.575.peg.904	MMP1663	K09123	0	
1171	kb|g.575.peg.1078	MMP0810	K09125	0	
1172	kb|g.575.peg.1453	MMP0905	K09126	0	
1173	kb|g.575.peg.1058	MMP0902	K09128	0	
1174	kb|g.575.peg.700	MMP1055	K09131	0	
1175	kb|g.575.peg.1279	MMP0913	K09135	0	
1176	kb|g.575.peg.272	MMP1056	K09136	0	
1177	kb|g.575.peg.383	MMP1278	K09137	0	
1178	kb|g.575.peg.988	MMP0199	K09138	0	
1179	kb|g.575.peg.647	MMP1494	K09139	0	
1180	kb|g.575.peg.117	MMP0150	K09140	0	
1181	kb|g.575.peg.1236	MMP0546	K09141	0	
1182	kb|g.575.peg.1212	MMP0535	K09149	0	
1183	kb|g.575.peg.640	MMP1643	K09152	0	
1184	kb|g.575.peg.537	MMP1660	K09153	0	
1185	kb|g.575.peg.443	MMP0321	K09154	0	
1186	kb|g.575.peg.1656	MMP0934	K09156	0	
1187	kb|g.575.peg.275	MMP1427	K09157	0	
1188	kb|g.575.peg.1659	MMP0074	K09160	0	
1189	kb|g.575.peg.1163	MMP0570	K09705	0	
1190	kb|g.575.peg.1175	MMP0557	K09713	0	
1191	kb|g.575.peg.1444	MMP0086	K09714	0	
1192	kb|g.575.peg.463	MMP0286	K09715	0	

	gpr	gene ID	KO	enzyme	definition
1193	kb|g.575.peg.151	MMP1230	K09717	0	
1194	kb|g.575.peg.1631	MMP0991	K09718	0	
1195	kb|g.575.peg.1490	MMP0607	K09720	0	
1196	kb|g.575.peg.826	MMP1188	K09721	0	
1197	kb|g.575.peg.1257	MMP0950	K09724	0	
1198	kb|g.575.peg.1226	MMP0358	K09726	0	
1199	kb|g.575.peg.1625	MMP0643	K09726	0	
1200	kb|g.575.peg.815	MMP1473	K09727	0	
1201	kb|g.575.peg.300	MMP1508	K09728	0	
1202	kb|g.575.peg.829	MMP0162	K09729	0	
1203	kb|g.575.peg.831	MMP1679	K09730	0	
1204	kb|g.575.peg.617	MMP1509	K09731	0	
1205	kb|g.575.peg.1351	MMP0429	K09732	0	
1206	kb|g.575.peg.1564	MMP0442	K09735	0	
1207	kb|g.575.peg.720	MMP1071	K09736	0	
1208	kb|g.575.peg.858	MMP1048	K09737	0	
1209	kb|g.575.peg.348	MMP1393	K09738	0	
1210	kb|g.575.peg.81	MMP1236	K09740	0	
1211	kb|g.575.peg.688	MMP0246	K09741	0	
1212	kb|g.575.peg.538	MMP0262	K09742	0	
1213	kb|g.575.peg.116	MMP1718	K09745	0	
1214	kb|g.575.peg.390	MMP0120	K09746	0	
1215	kb|g.575.peg.1026	MMP0434	K09779	0	
1216	kb|g.575.peg.796	MMP1280	K09922	0	
1217	kb|g.575.peg.872	MMP0265	K09936	0	
1218	kb|g.575.peg.202	MMP0027	K10716	0	
1219	kb|g.575.peg.605	MMP1395	K10896	0	
1220	kb|g.575.peg.1717	MMP0789	K10974	0	
1221	kb|g.575.peg.676	MMP1706	K11130	0	

	gpr	gene ID	KO	enzyme	definition
1223	kb|g.575.peg.727	MMP0221	K11928	0	
1224	kb|g.575.peg.206	MMP0176	K13525	0	
1225	kb|g.575.peg.1466	MMP0684	K13993	0	
1226	kb|g.575.peg.490	MMP1448	K14092	0	
1227	kb|g.575.peg.876	MMP1449	K14093	0	
1228	kb|g.575.peg.364	MMP1450	K14094	0	
1229	kb|g.575.peg.259	MMP1451	K14095	0	
1230	kb|g.575.peg.195	MMP1452	K14096	0	
1231	kb|g.575.peg.78	MMP1453	K14097	0	
1232	kb|g.575.peg.932	MMP1454	K14098	0	
1233	kb|g.575.peg.554	MMP1455	K14099	0	
1234	kb|g.575.peg.144	MMP1456	K14100	0	
1235	kb|g.575.peg.881	MMP1457	K14101	0	
1236	kb|g.575.peg.86	MMP1458	K14102	0	
1237	kb|g.575.peg.235	MMP1459	K14103	0	
1238	kb|g.575.peg.405	MMP1460	K14104	0	
1239	kb|g.575.peg.27	MMP1461	K14105	0	
1240	kb|g.575.peg.295	MMP1462	K14106	0	
1241	kb|g.575.peg.416	MMP1463	K14107	0	
1242	kb|g.575.peg.2	MMP1469	K14110	0	
1243	kb|g.575.peg.252	MMP1049	K14111	0	
1244	kb|g.575.peg.194	MMP1073	K14112	0	
1245	kb|g.575.peg.354	MMP1074	K14113	0	
1246	kb|g.575.peg.928	MMP1629	K14114	0	
1247	kb|g.575.peg.61	MMP1628	K14115	0	
1248	kb|g.575.peg.650	MMP1627	K14116	0	
1249	kb|g.575.peg.977	MMP1626	K14118	0	
1250	kb|g.575.peg.374	MMP1625	K14119	0	
1251	kb|g.575.peg.553	MMP1624	K14120	0	

	gpr	gene ID	KO	enzyme	definition
1252	kb|g.575.peg.68	MMP1623	K14121	0	
1253	kb|g.575.peg.400	MMP1622	K14122	0	
1254	kb|g.575.peg.515	MMP1153	K14123	0	
1255	kb|g.575.peg.984	MMP1621	K14124	0	
1256	kb|g.575.peg.1669	MMP0940	K14125	0	
1257	#N/A	RNA_36	K14218	0	
1258	#N/A	RNA_31	K14218	0	
1259	#N/A	RNA_10	K14219	0	
1260	#N/A	RNA_14	K14219	0	
1261	#N/A	RNA_15	K14219	0	
1263	#N/A	RNA_6	K14221	0	
1264	#N/A	RNA_8	K14221	0	
1265	#N/A	RNA_28	K14222	0	
1266	#N/A	RNA_1	K14223	0	
1267	#N/A	RNA_11	K14224	0	
1268	#N/A	RNA_23	K14224	0	
1269	#N/A	RNA_30	K14225	0	
1270	#N/A	RNA_29	K14225	0	
1271	#N/A	RNA_25	K14226	0	
1272	#N/A	RNA_18	K14227	0	
1273	#N/A	RNA_9	K14228	0	
1274	#N/A	RNA_26	K14228	0	
1275	#N/A	RNA_24	K14228	0	
1276	#N/A	RNA_5	K14229	0	
1277	#N/A	RNA_7	K14229	0	
1278	#N/A	RNA_34	K14230	0	
1279	#N/A	RNA_33	K14230	0	
1280	#N/A	RNA_19	K14230	0	
1281	#N/A	RNA_22	K14230	0	

		gpr	gene ID	KO	enzyme	definition
1282		#N/A	RNA_20	K14231	0	
1283		#N/A	RNA_3	K14232	0	
1284		#N/A	RNA_17	K14232	0	
1285		#N/A	RNA_13	K14233	0	
1286		#N/A	RNA_32	K14233	0	
1287		#N/A	RNA_16	K14233	0	
1288		#N/A	RNA_35	K14234	0	
1289		#N/A	RNA_2	K14234	0	
1290		#N/A	RNA_43	K14235	0	
1291		#N/A	RNA_4	K14236	0	
1292		#N/A	RNA_12	K14237	0	
1293		#N/A	RNA_27	K14237	0	
1294		#N/A	RNA_50	K14238	0	
1295		kb|g.575.peg.1604	MMP0638	K14475	0	
1296		kb|g.575.peg.532	MMP0247	K14561	0	
1297		kb|g.575.peg.1113	MMP0596	K14564	0	
1298		kb|g.575.peg.569	MMP0250	K14574	0	
1299		kb|g.575.peg.363	MMP1652	K15495	0	
1300		kb|g.575.peg.838	MMP1519	K15496	0	
1301		kb|g.575.peg.763	MMP0264	K16052	0	
1303		kb|g.575.peg.286	MMP0106	K16923	0	
1304		kb|g.575.peg.1135	MMP0416	K16923	0	
1305		kb|g.575.peg.1188	MMP0756	K19147	0	
1306		kb|g.575.peg.681	MMP1136	K19824	0	0
1309	<->	kb|g.575.peg.498	MMP1066	K03637	4.6.1.17	(1) C21310[c0] = (1) Precursor Z_c0[c0] + (1) Diphosphate_c0[c0]
1310	<->				2.8.1.7	(1) L-Cysteine_c0[c0] + (1) Protein-L-cysteine_c0[c0] = (1) L-Alanine_c0[c0] + (1) C21440_c0[c0]
1311	<->	kb|g.575.peg.359	MMP1359			(1) asparatate semialdehyde_c0[c0] + (1) sulfide_c0[c0] + (2) reducedferredoxin + (3) H+ = (2)

		gpr	gene ID	KO	enzyme	definition
						reducedferredoxin + (1) H2O_c0[c0] + (1) homocysteine_c0[c0]
1312	<->					(1) ornithine_c0[c0] = (1) NH3_c0[c0] + (1) L-proline_c0[c0]
1313	->					(1) 5,10-methenyltetrahydromethanopterin[c0] + (1) H2O[c0] = (1) 10-formyl-tetrahydromethanopterin[c0] + (1) H+[c0]
1314	->					(1) ATP_c0[c0] + (1) H2O_c0[c0] <-> (1) ADP_c0[c0] + (1) Orthophosphate_c0[c0] + (1) H+_c0[c0] + (1) energy
1315	->					(1) energy_c0 = (1) energy_e0
1316						(1) L-Alanine_e0 = (1) L-Alanine_c0
1317						(1) L-Arginine_e0 = (1) L-Arginine_c0
1318						(1) L-Asparagine_e0 = (1) L-Asparagine_c0
1319						(1) L-Aspartate_e0 = (1) L-Aspartate_c0
1320						(1) L-Cysteine_e0 = (1) L-Cysteine_c0
1321						(1) L-Glutamate_e0 = (1) L-Glutamate_c0
1322						(1) L-Glutamine_e0 = (1) L-Glutamine_c0
1323						(1) Glycine_e0 = (1) Glycine_c0
1324						(1) L-Histidine_e0 = (1) L-Histidine_c0
1325						(1) L-Isoleucine_e0 = (1) L-Isoleucine_c0
1326						(1) L-Leucine_e0 = (1) L-Leucine_c0
1327						(1) L-Lysine_e0 = (1) L-Lysine_c0
1328						(1) L-Methionine_e0 = (1) L-Methionine_c0
1329						(1) L-Phenylalanine_e0 = (1) L-Phenylalanine_c0
1330						(1) L-Proline_e0 = (1) L-Proline_c0
1331						(1) L-Serine_e0 = (1) L-Serine_c0
1332						(1) L-Threonine_e0 = (1) L-Threonine_c0
1333						(1) L-Tryptophan_e0 = (1) L-Tryptophan_c0
1334						(1) L-Tyrosine_e0 = (1) L-Tyrosine_c0
1335						(1) L-Valine_e0 = (1) L-Valine_c0

Table S3. Syntrophic Expression. Gene expression in *D. vulgaris* specific to the co-culture syntrophic growth with *M. maripaludis*.

Desulfovibrio vulgaris **Hildenborough**

	GeneID	**CC Biofilm Log$_2$FC**	**GeneID**	**CC Planktonic Log$_2$FC**	**product**	**COG**
1	DVU0149	4.4110	DVU0149	5.0098	hypothetical protein	R
2	DVU0150	4.3809	DVU0150	4.9622	hypothetical protein	M
3	DVU0148	4.1365	DVU0148	5.1717	lipoprotein	M
4	DVU0147	2.4720	DVU0147	3.5133	lipoprotein	M
5	DVU0146	2.3824	DVU0146	2.9193	hypothetical protein	S
6	DVU0145	2.3808	DVU0145	3.4271	response regulator	T
7	DVU2451	2.0019	DVU2451	1.2640	L-lactate permease	C
8	DVU3026	1.9650	DVU3026	1.5117	L-lactate permease	C
9	DVU1105	1.9167	DVU1105	0.9775	hypothetical protein	RX
10	DVU1102	1.8698	DVU1102	0.8767	baseplate assembly protein	S
11	DVU1112	1.8118	DVU1112	0.8727	hypothetical protein	S
12	DVU1134	1.7784	DVU1134	0.8925	DNA-binding protein HU subunit beta	L
13	DVU1101	1.7552	DVU1101	1.0436	hypothetical protein	S
14	DVU1128	1.7531	DVU1128	0.7858	lysozyme	M
15	DVU0359	1.7268	DVU0359	2.2181	HesB-like domain-containing protein	S
16	DVU1113	1.7188	DVU1113	0.8852	hypothetical protein	S
17	DVU1117	1.6982	DVU1117	0.7005	hypothetical protein	RX
18	DVU1108	1.6574	DVU1108	0.7623	hypothetical protein	S
19	DVU1106	1.6089	DVU1106	0.8925	hypothetical protein	S
20	DVU2752	1.6086	DVU2752	2.2055	rhodanese-like domain-containing protein	P
21	DVU1129	1.6016	DVU1129	0.8345	hypothetical protein	S
22	DVU1123	1.5994	DVU1123	0.9345	hypothetical protein	S
23	DVU2667	1.5893	DVU2667	2.0258	phosphate ABC transporter substrate-binding protein	P
24	DVU1133	1.5770	DVU1133	0.8441	hypothetical protein	S
25	DVU1115	1.5569	DVU1115	0.8269	hypothetical protein	S
26	DVU1103	1.5187	DVU1103	0.8928	baseplate assembly protein	RX
27	DVU1118	1.5128	DVU1118	0.8297	hypothetical protein	RX
28	DVU2652	1.5049	DVU2652	2.0860	hypothetical protein	S
29	DVU0770	1.4982	DVU0770	0.7697	hypothetical protein	R
30	DVU1138	1.4880	DVU1138	0.7772	hypothetical protein	K
31	DVU1100	1.4880	DVU1100	0.8630	tail fiber protein	RX
32	DVU1104	1.4793	DVU1104	0.9514	baseplate assembly protein	RX
33	DVU1122	1.4388	DVU1122	0.8280	portal protein	R
34	DVU1142	1.4051	DVU1142	0.7557	transcriptional regulator	K
35	DVU3028	1.3892	DVU3028	1.5488	iron-sulfur cluster-binding protein	C
36	DVU1296	1.3818	DVU1296	1.7586	hypothetical protein	S
37	DVU1114	1.3790	DVU1114	0.9559	virion morphogenesis protein	R
38	DVU3027	1.2491	DVU3027	1.7150	glycolate oxidase subunit GlcD	C
39	DVU1099	1.2373	DVU1099	0.6433	tail fiber assembly protein	RX
40	DVU1119	1.2040	DVU1119	0.8981	virion morphogenesis protein	RX
41	DVU1636	1.1537	DVU1636	1.9582	manganese-dependent inorganic pyrophosphatase	C
42	DVU1111	1.1245	DVU1111	0.7711	hypothetical protein	RX
43	DVU1121	1.0740	DVU1121	0.8419	hypothetical protein	R
44	DVU0536	1.0135	DVU0536	2.2095	high-molecular-weight cytochrome C	C

45	DVU2359	1.0011	DVU2359	1.9224	sigma-54 dependent transcriptional regulator	KT
46	DVU3384	0.9923	DVU3384	1.4221	zinc resistance-associated protein	R
47	DVU0531	0.9056	DVU0531	2.1555	hmc operon protein 6	C
48	DVU1144	0.8638	DVU1144	0.7631	Cro/CI family transcriptional regulator	K
49	DVU0599	0.7732	DVU0599	1.4758	carbon starvation protein A	T
50	DVU0529	0.7323	DVU0529	1.5901	Rrf2 family transcriptional regulator	K
51	DVU0152	0.6593	DVU0152	0.6258	phosphoenolpyruvate synthase	G
52	DVU0598	0.6432	DVU0598	1.0638	carbon starvation protein A	T
53	DVU3133	0.5899	DVU3133	0.5376	glycerol uptake facilitator protein	G
54	DVU2565	0.5881	DVU2565	0.5403	dethiobiotin synthetase	H
55	DVU2800	0.5367	DVU2800	0.6742	heavy metal translocating P-type ATPase	P
56	DVU1534	-0.4235	DVU1534	-0.9363	hypothetical protein	M
57	DVU0421	-0.4308	DVU0421	-0.5270	agmatinase	E
58	DVU0513	-0.4344	DVU0513	-0.7245	flagellar basal body rod protein FlgG	N
59	DVU0572	-0.4729	DVU0572	-0.9282	hypothetical protein	U
60	DVU0516	-0.5087	DVU0516	-0.5440	flagellar basal body P-ring protein	N
61	DVU1535	-0.5216	DVU1535	-0.7146	hypothetical protein	M
62	DVU0576	-0.5441	DVU0576	-0.8920	methionine sulfoxide reductase B	O
63	DVU1596	-0.5676	DVU1596	-0.5831	protein-glutamate methylesterase CheB	NT
64	DVU2551	-0.5711	DVU2551	-0.4647	HD domain-containing protein	RT
65	DVU2556	-0.5854	DVU2556	-0.8328	hypothetical protein	S
66	DVU1443	-0.5973	DVU1443	-1.1704	flagellar hook protein FlgE	N
67	DVU0596	-0.6066	DVU0596	-0.4697	DNA-binding response regulator LytR	KT
68	DVU0588	-0.6105	DVU0588	-0.6920	formate dehydrogenase subunit beta	C
69	DVU1536	-0.6108	DVU1536	-0.7004	Slt family transglycosylase	M
70	DVU1339	-0.6200	DVU1339	-0.9239	lipoprotein	M
71	DVU2419	-0.6368	DVU2419	-0.7509	hypothetical protein	R
72	DVU0592	-0.6375	DVU0592	-1.0735	chemotaxis protein CheW	NT
73	DVU1341	-0.7280	DVU1341	-0.8964	cation ABC transporter permease	P
74	DVU2387	-0.7336	DVU2387	-1.0211	ABC transporter ATP-binding protein	R
75	DVU2384	-0.7643	DVU2384	-1.3116	ABC transporter periplasmic substrate-binding protein	E
76	DVU1548	-0.7667	DVU1548	-0.9796	OmpP1/FadL/TodX family outer membrane transporter	I
77	DVU2410	-0.7926	DVU2410	-0.7961	superoxide dismutase, Fe	P
78	DVU2473	-0.8155	DVU2473	-0.5901	hypothetical protein	S
79	DVU0307	-0.8157	DVU0307	-0.6763	flagella basal body rod domain-containing protein	N
80	DVU0602	-0.8262	DVU0602	-0.6990	hypothetical protein	S
81	DVU0512	-0.8291	DVU0512	-0.8193	flagellar basal-body rod protein	N
82	DVU2381	-0.8519	DVU2381	-1.2787	hypothetical protein	S
83	DVU2494	-0.8528	DVU2494	-0.9033	M48 family peptidase	O

84	DVUA0092	-0.8620	DVUA0092	-0.6651	hypothetical protein	S
85	DVU1338	-0.8658	DVU1338	-0.9121	hypothetical protein	S
86	DVU2448	-0.8679	DVU2448	-0.7442	pantoate--beta-alanine ligase	H
87	DVU2422	-0.8944	DVU2422	-0.8152	nitroreductase	C
88	DVU0591	-0.8972	DVU0591	-1.1482	methyl-accepting chemotaxis protein	NT
89	DVU2529	-0.9055	DVU2529	-0.6060	phosphoglycerate kinase	G
90	DVU0949	-0.9070	DVU0949	-1.1312	hypothetical protein	P
91	DVU0053	-0.9073	DVU0053	-0.7630	sulfate permease	P
92	DVU1342	-0.9092	DVU1342	-1.0550	cation ABC transporter ATP-binding protein	P
93	DVU2390	-0.9103	DVU2390	-1.0643	TonB domain-containing protein	M
94	DVU2964	-0.9118	DVU2964	-1.0278	hypothetical protein	T
95	DVU1442	-0.9213	DVU1442	-1.3342	flagellin FlaG	N
96	DVU2377	-0.9232	DVU2377	-1.5001	hypothetical protein	S
97	DVU2626	-0.9287	DVU2626	-1.0038	hypothetical protein	S
98	DVU1875	-0.9412	DVU1875	-0.6498	dafA protein	T
99	DVU0056	-0.9427	DVU0056	-0.5444	chemotaxis protein CheV	NT
100	DVU2627	-0.9585	DVU2627	-1.1422	hypothetical protein	R
101	DVU1594	-0.9660	DVU1594	-0.9249	chemotaxis protein CheA	NT
102	DVU2382	-0.9906	DVU2382	-1.3621	hypothetical protein	S
103	DVU2918	-0.9948	DVU2918	-1.0544	hypothetical protein	S
104	DVU0420	-1.0105	DVU0420	-1.3104	hypothetical protein	S
105	DVU1419	-1.0187	DVU1419	-0.7215	sigma-54 dependent transcriptional regulator/response regulator	T
106	DVU0174	-1.0248	DVU0174	-0.9992	hypothetical protein	S
107	DVU0587	-1.0304	DVU0587	-0.8258	formate dehydrogenase subunit alpha	C
108	DVU0111	-1.0374	DVU0111	-0.5122	response regulator	T
109	DVU2548	-1.0769	DVU2548	-0.6983	ACP phosphodiesterase	I
110	DVU2676	-1.0788	DVU2676	-1.4689	hypothetical protein	S
111	DVU2946	-1.0846	DVU2946	-0.6970	hypothetical protein	S
112	DVU2324	-1.0865	DVU2324	-1.1119	copper-translocating P-type ATPase	P
113	DVU2893	-1.1173	DVU2893	-0.8652	flagellar basal-body rod protein	N
114	DVU2958	-1.1310	DVU2958	-1.5625	hypothetical protein	R
115	DVU0518	-1.1320	DVU0518	-1.0193	hypothetical protein	N
116	DVU0664	-1.1553	DVU0664	-0.6018	cysteine desulfurase	E
117	DVU0863	-1.1658	DVU0863	-1.0580	flagellar hook-associated protein 2	N
118	DVU1457	-1.1719	DVU1457	-0.7464	thioredoxin reductase	O
119	DVU2966	-1.1883	DVU2966	-0.9633	response regulator	T
120	DVU2442	-1.2077	DVU2442	-1.7762	HSP20 family protein	O
121	DVU0825	-1.2103	DVU0825	-0.7448	preprotein translocase subunit SecA	U
122	DVU0240	-1.2388	DVU0240	-0.8041	hypothetical protein	U
123	DVUA0023	-1.2729	DVUA0023	-0.7651	ABC transporter permease	V
124	DVU1805	-1.2870	DVU1805	-0.9570	diguanylate cyclase	T
125	DVU0072	-1.3125	DVU0072	-0.5097	glucose-1-phosphate cytidylyltransferase	MJ
126	DVU0251	-1.3149	DVU0251	-1.2834	hypothetical protein	R
127	DVU0977	-1.3249	DVU0977	-1.3335	hypothetical protein	S
128	DVU1343	-1.3328	DVU1343	-1.3213	cation ABC transporter periplasmc-binding protein	P
129	DVU2385	-1.3384	DVU2385	-1.4291	ABC transporter permease	R

130	DVU1444	-1.3414	DVU1444	-1.3070	basal-body rod modification protein FlgD	N
131	DVU2235	-1.3438	DVU2235	-0.8073	hypothetical protein	S
132	DVU2388	-1.3510	DVU2388	-1.2760	tolQ protein	U
133	DVU0948	-1.3536	DVU0948	-0.7667	hypothetical protein	R
134	DVU2441	-1.3764	DVU2441	-1.7687	HSP20 family protein	O
135	DVU0153	-1.3806	DVU0153	-0.8998	hypothetical protein	S
136	DVU2963	-1.3807	DVU2963	-1.3890	response regulator	T
137	DVU0186	-1.3829	DVU0186	-1.5612	hypothetical protein	S
138	DVU0665	-1.4088	DVU0665	-0.5955	nitrogen fixation protein nifU	C
139	DVU1783	-1.4179	DVU1783	-0.6726	hypothetical protein	C
140	DVU1592	-1.4259	DVU1592	-0.9913	arginine N-succinyltransferase subunit beta	NT
141	DVU2919	-1.4861	DVU2919	-0.6809	hypothetical protein	S
142	DVU2389	-1.4900	DVU2389	-1.2438	biopolymer ExbD/TolR family transporter	U
143	DVU0423	-1.5119	DVU0423	-1.3190	universal stress protein	T
144	DVU2201	-1.5134	DVU2201	-1.0990	iron-containing alcohol dehydrogenase	C
145	DVU0486	-1.5226	DVU0486	-0.9872	hypothetical protein	S
146	DVU0595	-1.5321	DVU0595	-0.8394	hypothetical protein	S
147	DVU0006	-1.5332	DVU0006	-0.9874	universal stress protein	T
148	DVU3282	-1.5600	DVU3282	-0.8101	ADP-ribosylglycohydrolase	O
149	DVU1032	-1.5626	DVU1032	-1.2712	hypothetical protein	S
150	DVU2488	-1.5723	DVU2488	-0.7320	hypothetical protein	S
151	DVU2947	-1.5771	DVU2947	-0.9324	anaerobic ribonucleoside triphosphate reductase	F
152	DVU2421	-1.6069	DVU2421	-0.6881	4-oxalocrotonate tautomerase	R
153	DVU0729	-1.6082	DVU0729	-1.4177	hypothetical protein	S
154	DVU0523	-1.6188	DVU0523	-1.0369	negative regulator of flagellin synthesis FlgM	K
155	DVU1593	-1.6346	DVU1593	-1.0737	chemotaxis protein CheY	T
156	DVU2380	-1.6442	DVU2380	-1.6524	ABC transporter ATP-binding protein	V
157	DVU2383	-1.6661	DVU2383	-1.5338	TonB dependent receptor domain-containing protein	I
158	DVU0318	-1.6933	DVU0318	-1.4777	hypothetical protein	NU
159	DVU3095	-1.7048	DVU3095	-1.4168	Fur family transcriptional regulator	P
160	DVU0410	-1.7147	DVU0410	-1.5105	hypothetical protein	S
161	DVU0764	-1.7494	DVU0764	-1.1251	DNA-binding protein HU	L
162	DVU4007	-1.7558	DVU4007	-1.2683	hypothetical protein	S
163	DVU2935	-1.7694	DVU2935	-1.0921	phosphoglyceromutase	G
164	DVU0944	-1.7839	DVU0944	-1.0112	hypothetical protein	S
165	DVU0763	-1.8760	DVU0763	-1.8735	diguanylate cyclase	T
166	DVU0524	-1.8951	DVU0524	-1.0976	hypothetical protein	S
167	DVU0409	-1.8967	DVU0409	-1.1566	hypothetical protein	S
168	DVU2959	-1.9008	DVU2959	-2.0082	hypothetical protein	R
169	DVU2379	-1.9516	DVU2379	-2.0882	M16 family peptidase	R
170	DVU2297	-1.9845	DVU2297	-1.1734	glycine betaine/L-proline ABC transporter substrate-binding protein	E
171	DVU2378	-2.0110	DVU2378	-2.3647	AraC family transcriptional regulator	K
172	DVU1441	-2.0188	DVU1441	-1.7012	flagellin	N
173	DVU2318	-2.1064	DVU2318	-1.5300	rubrerythrin	C
174	DVU2936	-2.1273	DVU2936	-1.0503	hypothetical protein	S
175	DVU2082	-2.2863	DVU2082	-1.9776	flagellin	N

176	DVU0024	-2.3736	DVU0024	-1.8144	hypothetical protein	RK
177	DVU0650	-2.4233	DVU0650	-1.5698	chelatase	H
178	DVU2325	-2.6145	DVU2325	-1.8051	mercuric transport periplasmic protein	P
179	DVU0273	-2.8452	DVU0273	-1.3100	hypothetical protein	RI
180	DVU2573	-2.8714	DVU2573	-2.4047	hypothetical protein	S
181	DVU2103	-2.8805	DVU2103	-1.5106	iron-sulfur cluster-binding/ATPase	C
182	DVU2574	-2.9477	DVU2574	-2.3490	ferrous ion transport protein	P
183	DVU2917	-2.9845	DVU2917	-2.2848	UDP-3-O-[3-hydroxymyristoyl] N-acetylglucosaminedeacetylase	M
184	DVU2109	-3.3154	DVU2109	-1.1725	hypothetical protein	D
185	DVU0036	-3.3200	DVU0036	-3.1522	hypothetical protein	T
186	DVU2444	-3.3203	DVU2444	-2.4171	flagellin	N
187	DVU2104	-3.4710	DVU2104	-2.0116	iron-sulfur cluster-binding/ATPase	C
188	DVU0302	-3.5123	DVU0302	-1.8697	chemotaxis protein CheX	N
189	DVU0772	-3.5632	DVU0772	-2.7488	hypothetical protein	S
190	DVU2108	-3.8166	DVU2108	-1.4451	hypothetical protein	S
191	DVU2247	-3.8248	DVU2247	-3.0816	anti-oxidant AhpCTSA family protein	O
192	DVU2680	-3.8726	DVU2680	-2.2038	flavodoxin	C
193	DVU2107	-4.0614	DVU2107	-1.3692	hypothetical protein	H
194	DVU2105	-4.1577	DVU2105	-2.9324	hypothetical protein	S
195	DVU2572	-4.2056	DVU2572	-2.5714	ferrous iron transport protein A	P
196	DVU2571	-4.2597	DVU2571	-1.7381	ferrous iron transport protein B	P
197	DVU0303	-4.8910	DVU0303	-3.1524	hypothetical protein	R
198	DVU2681	-5.0602	DVU2681	-2.1677	hypothetical protein	S
199	DVU0304	-5.0610	DVU0304	-3.2320	hypothetical protein	S

DvH:	Unique to Co-culture	> 2 LogFC	< -2 LogFC
Up-Expressed	55	6	18
Down-Expressed	144		
TOTAL	199		

Table S4. Syntrophic Expression. Gene expression in *M. maripaludis* specific to the co-culture syntrophic growth with *D. vulgaris*.

Methanococcus maripaludis S2

	GeneID	**CC Biofilm Log$_2$FC**	**GeneID**	**CC Planktonic Log$_2$FC**	**Product**	**COG**
1	MMP0501	6.7381	MMP0501	2.6701	hypothetical protein	MV
2	MMP1194	4.8998	MMP1194	4.5599	triple helix repeat-containing collagen	M
3	MMP1193	4.7082	MMP1193	5.8001	hypothetical protein	L
4	MMP0479	4.0149	MMP0479	1.4317	hypothetical protein	S
5	MMP0997	3.0561	MMP0997	0.9387	blue (type1) copper domain-containing protein	C
6	MMP0502	2.3632	MMP0502	2.8728	hypothetical protein	S
7	MMP0210	2.2347	MMP0210	1.4804	hypothetical protein	GER
8	MMP1656	1.9867	MMP1656	0.8939	glutamine amidotransferase subunit PdxT	H
9	MMP1351	1.7152	MMP1351	1.4320	hypothetical protein	R
10	MMP0031	1.7012	MMP0031	1.5384	hypothetical protein	K
11	MMP0324	1.5147	MMP0324	1.3506	hypothetical protein	S
12	MMP1600	1.4938	MMP1600	0.9077	ribosomal protein S6 modification protein	HJ
13	MMP1519	1.4837	MMP1519	1.2713	anion transport system permease	O
14	MMP0079	1.4646	MMP0079	1.4448	orotate phosphoribosyltransferase-like protein	F
15	MMP1518	1.3675	MMP1518	1.1610	sulfate/molybdate ABC-transporter ATPase subunit	E
16	MMP0718	1.3507	MMP0718	1.2988	hypothetical protein	E
17	MMP0899	1.3483	MMP0899	1.8240	ATP/GTP-binding motif-containing protein	R
18	MMP0682	1.3310	MMP0682	2.0734	hypothetical protein	R
19	MMP0223	1.3302	MMP0223	1.4563	hypothetical protein	S
20	MMP0288	1.3104	MMP0288	2.6469	hypothetical protein	S
21	MMP1660	1.3066	MMP1660	2.1048	hypothetical protein	S
22	MMP0839	1.2903	MMP0839	1.4400	hypothetical protein	S
23	MMP0048	1.2874	MMP0048	1.1787	hypothetical protein	S
24	MMP1596	1.2409	MMP1596	1.6960	hypothetical protein	S
25	MMP1132	1.2014	MMP1132	1.1191	tRNA-splicing endonuclease subunit alpha	J
26	MMP0366	1.1583	MMP0366	1.4409	hypothetical protein	S
27	MMP0010	1.1497	MMP0010	0.8085	hypothetical protein	L
28	MMP0919	1.1496	MMP0919	0.6981	dihydroorotate dehydrogenase electron transfer subunit	HC
29	MMP0209	1.1453	MMP0209	0.9059	hypothetical protein	KX
30	MMP0795	1.1120	MMP0795	0.8477	hypothetical protein	S
31	MMP0702	1.1087	MMP0702	1.8900	hypothetical protein	HJ
32	MMP0285	1.0841	MMP0285	1.8904	TrkA-N domain-containing protein	R
33	MMP0099	1.0457	MMP0099	1.0303	major facilitator transporter	G
34	MMP1257	0.9918	MMP1257	0.7923	NERD domain-containing protein	RL
35	MMP0935	0.9868	MMP0935	1.4770	hypothetical protein	S
36	MMP0184	0.9863	MMP0184	0.9428	riboflavin kinase	H
37	MMP1281	0.9713	MMP1281	1.1355	GCN5-like N-acetyltransferase	R

38	MMP1491	0.9519	MMP1491	0.7537	amidohydrolase	FR
39	MMP0100	0.9370	MMP0100	1.3865	Na(+)/H(+) exchanger family protein	P
40	MMP1626	0.9226	MMP1626	1.3045	monovalent cation/H+ antiporter subunit B	P
41	MMP1082	0.9036	MMP1082	1.0101	imidazole glycerol phosphate synthase subunit HisH	E
42	MMP1084	0.8765	MMP1084	0.6867	hypothetical protein	E
43	MMP0938	0.8762	MMP0938	1.0805	cobalamin (5'-phosphate) synthase	H
44	MMP1065	0.8013	MMP1065	1.9232	BadM/Rrf2 family transcriptional regulator	K
45	MMP0934	0.7653	MMP0934	0.6987	hypothetical protein	S
46	MMP0688	0.6957	MMP0688	0.7394	O-phosphoseryl-tRNA synthetase	J
47	MMP0598	-0.6911	MMP0598	-1.3763	phosphoglycerate mutase-related	G
48	MMP0644	-0.7236	MMP0644	-1.1447	cation diffusion facilitator family transporter	P
49	MMP1138	-0.7252	MMP1138	-0.6894	hydroxyethylthiazole kinase	H
50	MMP0683	-0.7468	MMP0683	-0.8641	signal recognition particle-docking protein FtsY	U
51	MMP1052	-0.7753	MMP1052	-1.0922	hypothetical protein	K
52	MMP0969	-0.8005	MMP0969	-0.8376	hypothetical protein	S
53	MMP1295	-0.8246	MMP1295	-1.8281	glucose-6-phosphate isomerase	G
54	MMP1294	-0.8715	MMP1294	-1.6486	starch synthase	G
55	MMP0725	-0.9227	MMP0725	-0.8165	integral membrane protein	S
56	MMP0650	-0.9229	MMP0650	-0.9475	acetolactate synthase catalytic subunit	EH
57	MMP1250	-0.9388	MMP1250	-0.9629	6-pyruvoyl tetrahydropterin synthase	H
58	MMP1283	-0.9490	MMP1283	-0.9120	hypothetical protein	R
59	MMP0394	-0.9587	MMP0394	-2.0715	uroporphyrinogen III synthase	H
60	MMP0926	-0.9611	MMP0926	-0.7844	response regulator receiver modulated CheB methylesterase	NT
61	MMP1241	-0.9855	MMP1241	-0.9768	hypothetical protein	S
62	MMP1477	-0.9861	MMP1477	-0.9272	cobyrinic acid a,c-diamide synthase	H
63	MMP0959	-0.9866	MMP0959	-1.3553	FAD-dependent pyridine nucleotide-disulfide oxidoreductase	O
64	MMP0304	-0.9947	MMP0304	-1.4866	N-glycosylase/DNA lyase	S
65	MMP0972	-0.9994	MMP0972	-1.0043	hypothetical protein	S
66	MMP0687	-1.0141	MMP0687	-0.9625	triosephosphate isomerase	G
67	MMP0911	-1.0208	MMP0911	-0.8755	iron-sulfur flavoprotein	R
68	MMP0927	-1.0301	MMP0927	-0.8245	CheA signal transduction histidine kinase	NT
69	MMP1187	-1.0424	MMP1187	-1.8065	class II aldolase/adducin family protein	G
70	MMP1072	-1.0578	MMP1072	-1.6409	aminotransferase (subgroup I) aromatic aminotransferase	E
71	MMP0306	-1.0800	MMP0306	-2.2420	oxidoreductase member subunit alpha	C
72	MMP0482	-1.0931	MMP0482	-1.0407	hypothetical protein	S
73	MMP1459	-1.1037	MMP1459	-0.9503	hypothetical protein	S
74	MMP1183	-1.1189	MMP1183	-2.2852	iron ABC transporter ATPase subunit	PH
75	MMP0856	-1.1482	MMP0856	-1.2887	nitrogenase subunit alpha	C

76	MMP0569	-1.1552	MMP0569	-2.1716	hypothetical protein	M
77	MMP0958	-1.2038	MMP0958	-1.5603	hypothetical protein	OC
78	MMP0645	-1.2204	MMP0645	-1.4292	malate dehydrogenase	C
79	MMP1569	-1.2207	MMP1569	-0.9293	hypothetical protein	S
80	MMP0427	-1.2221	MMP0427	-0.7788	replication factor C small subunit	L
81	MMP0980	-1.2228	MMP0980	-1.4464	acetyl-CoA decarbonylase/synthase complex subunit gamma	C
82	MMP0853	-1.2418	MMP0853	-1.1061	nitrogenase reductase	P
83	MMP0914	-1.2471	MMP0914	-1.1658	hypothetical protein	R
84	MMP1139	-1.2491	MMP1139	-0.9593	thiamine-phosphate pyrophosphorylase	H
85	MMP0722	-1.2497	MMP0722	-1.6909	hypothetical protein	C
86	MMP1177	-1.2516	MMP1177	-2.2495	iron transport system substrate-binding protein,C-term half	P
87	MMP0528	-1.2580	MMP0528	-1.1524	hypothetical protein	R
88	MMP1653	-1.2697	MMP1653	-1.2743	hypothetical protein	S
89	MMP0676	-1.2749	MMP0676	-1.8273	intermediate filament protein	R
90	MMP0599	-1.2765	MMP0599	-1.7479	precorrin-6x reductase CbiJ/CobK	H
91	MMP1166	-1.2788	MMP1166	-1.5596	iron-sulfur flavoprotein	R
92	MMP0787	-1.3016	MMP0787	-2.4846	MarR family transcriptional regulator	K
93	MMP1019	-1.3164	MMP1019	-1.0930	PEGA domain-containing protein	S
94	MMP0102	-1.3218	MMP0102	-2.7446	protein-L-isoaspartate O-methyltransferase	O
95	MMP0187	-1.3246	MMP0187	-1.7769	thiamine biosynthesis protein ThiC	H
96	MMP0545	-1.3364	MMP0545	-1.6856	molybdopterin biosynthesis protein MoeA/LysR substrate binding-domain-containing protein	H
97	MMP0612	-1.3425	MMP0612	-2.0545	2'-5' RNA ligase	J
98	MMP1462	-1.3507	MMP1462	-1.1727	energy conserving hydrogenase A large subunit	C
99	MMP0885	-1.3544	MMP0885	-0.9198	ATP/GTP-binding motif-containing protein	NU
100	MMP0912	-1.3545	MMP0912	-1.3142	4-oxalocrotonate tautomerase	R
101	MMP1486	-1.3596	MMP1486	-1.2499	mechanosensitive ion channel MscS	M
102	MMP0698	-1.3785	MMP0698	-1.1240	hypothetical protein	S
103	MMP1364	-1.3821	MMP1364	-1.2782	DNA-directed RNA polymerase subunit A"	K
104	MMP1022	-1.4080	MMP1022	-1.1478	hypothetical protein	M
105	MMP0416	-1.4177	MMP0416	-2.6440	hypothetical protein	M
106	MMP0563	-1.4599	MMP0563	-1.5112	hypothetical protein	S
107	MMP1186	-1.5056	MMP1186	-1.1949	thiol (cysteine) protease	O
108	MMP1164	-1.5136	MMP1164	-1.8927	heavy metal transport/detoxification protein	P
109	MMP1445	-1.5247	MMP1445	-0.9465	GMP synthase subunit A	F
110	MMP0979	-1.5489	MMP0979	-1.7166	hypothetical protein	C
111	MMP0883	-1.5629	MMP0883	-1.2006	hypothetical protein	S
112	MMP1061	-1.5942	MMP1061	-1.1790	hypothetical protein	S
113	MMP0241	-1.5957	MMP0241	-1.2003	hypothetical protein	U
114	MMP0426	-1.5964	MMP0426	-1.6101	nitroreductase	C
115	MMP0293	-1.6078	MMP0293	-1.9983	aldolase	G

116	MMP0981	-1.6253	MMP0981	-1.1225	acetyl-CoA decarbonylase/synthase complex subunit delta	C
117	MMP0636	-1.6296	MMP0636	-1.0893	hypothetical protein	M
118	MMP0816	-1.6439	MMP0816	-1.2370	seryl-tRNA synthetase-like protein	S
119	MMP1647	-1.6472	MMP1647	-1.0658	proteasome-activating nucleotidase	O
120	MMP1165	-1.6646	MMP1165	-2.5969	heavy metal translocating P-type ATPase	P
121	MMP1465	-1.6694	MMP1465	-1.6088	hypothetical protein	C
122	MMP0175	-1.6733	MMP0175	-0.9930	hypothetical protein	S
123	MMP1236	-1.6997	MMP1236	-2.1896	hypothetical protein	S
124	MMP1029	-1.7063	MMP1029	-0.9846	hypothetical protein	S
125	MMP1467	-1.7067	MMP1467	-1.4851	hypothetical protein	K
126	MMP1063	-1.7121	MMP1063	-0.9604	2-isopropylmalate synthase	E
127	MMP0835	-1.7159	MMP0835	-2.4796	hypothetical protein	G
128	MMP0432	-1.7599	MMP0432	-1.4774	TatD-like deoxyribonuclease	R
129	MMP1460	-1.7752	MMP1460	-1.0221	hypothetical protein	S
130	MMP0622	-1.7922	MMP0622	-1.5922	ADP-ribosylation/crystallin J1	O
131	MMP0278	-1.8042	MMP0278	-1.5462	CBS domain-containing signal transduction protein	R
132	MMP0904	-1.8147	MMP0904	-1.0777	selenophosphate synthetase	E
133	MMP0122	-1.8191	MMP0122	-1.3199	hypothetical protein	J
134	MMP0280	-1.8327	MMP0280	-0.9928	phosphoribosyl-AMP cyclohydrolase	E
135	MMP1463	-1.8462	MMP1463	-1.1422	polyferredoxin	C
136	MMP1568	-1.8736	MMP1568	-1.2888	hypothetical protein	S
137	MMP1167	-1.8928	MMP1167	-2.4580	flavoprotein-like protein	C
138	MMP1665	-1.9151	MMP1665	-1.9144	HEAT domain-containing protein	RU
139	MMP1168	-1.9263	MMP1168	-1.2401	ABC transporter ATP-binding protein	O
140	MMP0465	-1.9328	MMP0465	-2.1117	hypothetical protein	K
141	MMP0858	-1.9511	MMP0858	-1.9261	nitrogenase MoFe cofactor biosynthesis protein NifE	C
142	MMP0623	-1.9676	MMP0623	-2.6145	hypothetical protein	S
143	MMP1668	-1.9811	MMP1668	-2.4036	flagellin	N
144	MMP1021	-1.9915	MMP1021	-1.3204	hypothetical protein	M
145	MMP0020	-2.0380	MMP0020	-1.0070	nickel responsive regulator	K
146	MMP1200	-2.0390	MMP1200	-2.6206	diaminopimelate decarboxylase	E
147	MMP1163	-2.0581	MMP1163	-1.0797	CutA1 divalent ion tolerance protein	P
148	MMP1669	-2.0808	MMP1669	-2.0051	flagella accessory C family protein	N
149	MMP0543	-2.1260	MMP0543	-1.6925	hypothetical protein	H
150	MMP0413	-2.1277	MMP0413	-1.7126	hypothetical protein	NT
151	MMP1553	-2.1456	MMP1553	-2.1234	nitroreductase	C
152	MMP0327	-2.1558	MMP0327	-2.5719	thymidine phosphorylase	F
153	MMP0294	-2.1684	MMP0294	-1.0304	Pyrrolo-quinoline quinone	S
154	MMP1461	-2.1768	MMP1461	-2.0152	energy conserving hydrogenase A small subunit	C
155	MMP0305	-2.1789	MMP0305	-2.3589	2-oxoacid ferredoxin oxidoreductase subunit beta	C
156	MMP1671	-2.1943	MMP1671	-1.5773	flagella protein	N
157	MMP0282	-2.2098	MMP0282	-1.8524	phosphoribosylaminoimidazole carboxylase catalytic subunit	F

158	MMP1251	-2.2185	MMP1251	-1.7919	CBS domain-containing signal transduction protein	R
159	MMP0638	-2.2190	MMP0638	-1.9865	hypothetical protein	R
160	MMP0292	-2.2257	MMP0292	-1.8059	hypothetical protein	S
161	MMP0490	-2.2365	MMP0490	-2.3500	hypothetical protein	S
162	MMP1071	-2.2370	MMP1071	-2.0576	hypothetical protein	S
163	MMP1150	-2.2383	MMP1150	-1.9446	uroporphyrinogen decarboxylase	H
164	MMP1282	-2.2603	MMP1282	-1.1761	hypothetical protein	H
165	MMP0065	-2.2626	MMP0065	-1.2469	ammonium transporter	P
166	MMP0929	-2.2653	MMP0929	-1.7688	methyl-accepting chemotaxis sensory transducer	NT
167	MMP0628	-2.3011	MMP0628	-3.3151	TOBE domain-containing protein	H
168	MMP0605	-2.3121	MMP0605	-0.9485	RNA-processing protein	R
169	MMP0257	-2.3155	MMP0257	-1.2201	transcription factor	K
170	MMP0215	-2.3188	MMP0215	-1.8019	hypothetical protein	K
171	MMP0684	-2.3269	MMP0684	-1.9453	heat shock protein Hsp20	O
172	MMP1034	-2.3899	MMP1034	-0.9251	thymidylate kinase	F
173	MMP0884	-2.4048	MMP0884	-1.3236	hypothetical protein	S
174	MMP1235	-2.4081	MMP1235	-1.9728	molybdopterin biosynthesis MoaE	H
175	MMP0312	-2.4188	MMP0312	-1.6286	hypothetical protein	S
176	MMP1464	-2.4311	MMP1464	-1.2525	hypothetical protein	C
177	MMP0406	-2.4373	MMP0406	-0.8480	TIM-barrel protein	J
178	MMP1550	-2.4454	MMP1550	-1.4440	NADP oxidoreductase, coenzyme F420-dependent	R
179	MMP0256	-2.4497	MMP0256	-1.8507	imidazole glycerol phosphate synthase subunit HisH	E
180	MMP0963	-2.4585	MMP0963	-1.7058	MIP family channel protein	G
181	MMP1670	-2.5017	MMP1670	-2.1210	flagella protein	N
182	MMP0204	-2.5080	MMP0204	-0.8876	hypothetical protein	C
183	MMP0857	-2.5364	MMP0857	-1.9403	nitrogenase	C
184	MMP1346	-2.6010	MMP1346	-3.2737	basic helix-loop-helix dimerization domain-containing protein	R
185	MMP0177	-2.6314	MMP0177	-2.3340	hypothetical protein	J
186	MMP0723	-2.6331	MMP0723	-2.2151	hypothetical protein	S
187	MMP1666	-2.6905	MMP1666	-2.9720	flagellin	N
188	MMP0313	-2.6981	MMP0313	-1.8875	hypothetical protein	S
189	MMP1134	-2.7663	MMP1134	-1.7534	type A flavoprotein	C
190	MMP1162	-2.7801	MMP1162	-2.0899	beta-lactamase domain-containing protein	C
191	MMP0325	-2.8353	MMP0325	-2.3341	glyceraldehyde-3-phosphate dehydrogenase	G
192	MMP1169	-2.8366	MMP1169	-1.7327	SufBD protein	O
193	MMP1135	-2.8398	MMP1135	-1.4632	flavodoxin:beta-lactamase-like	C
194	MMP0527	-2.8564	MMP0527	-0.8191	hypothetical protein	K
195	MMP1154	-2.8843	MMP1154	-1.3946	heterosulfide reductase subunit C1	C
196	MMP1157	-2.8875	MMP1157	-1.5475	desulfoferrodoxin, ferrous iron-binding site	C
197	MMP1252	-2.8915	MMP1252	-2.5881	CBS domain-containing protein	K
198	MMP1035	-2.9116	MMP1035	-1.5827	hypothetical protein	OU
199	MMP0234	-2.9175	MMP0234	-1.1332	hypothetical protein	S
200	MMP1159	-2.9197	MMP1159	-1.6503	Ferritin	P
201	MMP1442	-2.9676	MMP1442	-0.9571	transcription regulator ArsR	K

202	MMP0167	-2.9831	MMP0167	-1.2394	ABC transporter ATP-binding protein	V
203	MMP1634	-2.9835	MMP1634	-1.7612	DsrE family protein	R
204	MMP1667	-3.0348	MMP1667	-3.0387	flagellin	N
205	MMP1033	-3.0730	MMP1033	-1.5511	hypothetical protein	R
206	MMP0693	-3.1196	MMP0693	-3.2252	aminoacyl-tRNA synthetase, class II	j
207	MMP0002	-3.2193	MMP0002	-2.5535	L-seryl-tRNA selenium transferase	E
208	MMP1161	-3.2224	MMP1161	-1.7352	hypothetical protein	P
209	MMP0641	-3.3217	MMP0641	-1.7080	50S ribosomal protein L7Ae	J
210	MMP0245	-3.3666	MMP0245	-1.8590	prefoldin subunit beta	O
211	MMP1636	-3.3946	MMP1636	-1.7844	major facilitator transporter	P
212	MMP1036	-3.4637	MMP1036	-2.2982	hypothetical protein	O
213	MMP0600	-3.4926	MMP0600	-2.6107	hypothetical protein	R
214	MMP0373	-3.4998	MMP0373	-2.2113	hypothetical protein	S
215	MMP0624	-3.5841	MMP0624	-1.9765	hypothetical protein	R
216	MMP0176	-3.6110	MMP0176	-2.7656	cell division protein CDC48	O
217	MMP0431	-3.6535	MMP0431	-3.8664	rhodopsin-like GPCR superfamily protein	J
218	MMP0246	-3.7227	MMP0246	-1.6322	hypothetical protein	S
219	MMP0633	-3.7517	MMP0633	-2.1682	rubrerythrin	C
220	MMP1633	-3.8437	MMP1633	-2.7716	hypothetical protein	S
221	MMP0235	-3.8728	MMP0235	-1.6707	hypothetical protein	S
222	MMP1586	-3.9843	MMP1586	-1.9365	hypothetical protein	S
223	MMP0247	-4.0439	MMP0247	-1.9685	ribosomal biogenesis protein	JA
224	MMP0846	-4.4463	MMP0846	-1.2561	hypothetical protein	S
225	MMP0629	-5.1439	MMP0629	-2.5642	hypothetical protein	K
226	MMP1016	-5.4161	MMP1016	-4.3693	CBS domain-containing signal transduction protein	K
227	MMP0601	-5.7086	MMP0601	-3.1158	hypothetical protein	R

Mmp:	Unique to Co-culture	> 2 LogFC	< -2 LogFC
Up-Expressed	46	4	43
Down-Expressed	181		
TOTAL	227		

Table S5. Co-culture biofilm specific gene expression in *D. vulgaris*.

***Desulfovibrio vulgaris* Hildenborough**

	GeneID	**Co-culture Biofilm Log$_2$FC**	**Product**	**COG**
1	DVU1126	1.7382	lipoprotein	M
2	DVU1107	1.5222	tail tape measure protein	RX
3	DVU1155	1.5220	hypothetical protein	S
4	DVU1922	1.4958	periplasmic [NiFe] hydrogenase large subunit, isozyme 1	C
5	DVU3302	1.4834	hypothetical protein	S
6	DVU2274	1.4716	hypothetical protein	S
7	DVU2406	1.4230	hypothetical protein	S
8	DVU3299	1.4069	hypothetical protein	R
9	DVU1297	1.3926	hypothetical protein	S
10	DVU1140	1.3920	bacteriophage transposase A protein	RX
11	DVU1127	1.3761	hypothetical protein	S
12	DVU2015	1.3740	hypothetical protein	S
13	DVU3301	1.3572	hypothetical protein	S
14	DVU1131	1.3558	hypothetical protein	S
15	DVU1116	1.3464	hypothetical protein	RX
16	DVU0672	1.3433	hypothetical protein	S
17	DVU2115	1.3208	hypothetical protein	S
18	DVU2803	1.3166	hypothetical protein	M
19	DVU1120	1.3044	hypothetical protein	S
20	DVU3300	1.2990	hypothetical protein	S
21	DVU2452	1.2736	hypothetical protein	S
22	DVU2301	1.2099	lipoprotein	M
23	DVU2699	1.2096	transglycosylase	M
24	DVU3115	1.2088	hypothetical protein	S
25	DVU2000	1.1951	hypothetical protein	S
26	DVU1125	1.1934	hypothetical protein	S
27	DVU2622	1.1600	hypothetical protein	S
28	DVU2701	1.1510	hypothetical protein	S
29	DVU1715	1.1475	hypothetical protein	S
30	DVU0368	1.1431	hypothetical protein	S
31	DVU0613	1.1420	hypothetical protein	S
32	DVU2703	1.1394	hypothetical protein	S
33	DVU1130	1.1375	DNA-binding protein	R
34	DVU2875	1.1363	DNA-binding protein	R
35	DVU0623	1.1349	hypothetical protein	S
36	DVU0678	1.1260	hypothetical protein	S
37	DVU1507	1.1188	hypothetical protein	S
38	DVU0782	1.1175	hypothetical protein	S
39	DVU2204	1.1143	tryptophanase	E
40	DVU1393	1.1021	hypothetical protein	S
41	DVU2597	1.1010	hypothetical protein	S
42	DVU2915	1.0989	hypothetical protein	S
43	DVU2603	1.0967	hypothetical protein	C
44	DVU1970	1.0931	response regulator	T
45	DVU2804	1.0922	metallo-beta-lactamase	R
46	DVU2594	1.0922	hypothetical protein	S
47	DVU2540	1.0894	2-hydroxyglutaryl-CoA dehydratase subunit D	E
48	DVU2745	1.0822	hypothetical protein	S
49	DVU1966	1.0818	hypothetical protein	S
50	DVU1476	1.0815	hypothetical protein	S
51	DVU2207	1.0755	hypothetical protein	S

52	DVU1727	1.0710	hypothetical protein	S
53	DVU1474	1.0662	hypothetical protein	S
54	DVU2712	1.0584	hypothetical protein	M
55	DVU1141	1.0489	hypothetical protein	S
56	DVU2722	1.0481	hypothetical protein	R
57	DVU1139	1.0470	bacteriophage DNA transposition B protein	R
58	DVU1259	1.0460	hypothetical protein	S
59	DVU2599	1.0377	hypothetical protein	S
60	DVU1711	1.0362	hypothetical protein	S
61	DVU2604	1.0334	hypothetical protein	RX
62	DVU2595	1.0325	hypothetical protein	S
63	DVU0497	1.0322	hypothetical protein	RC
64	DVU1697	1.0322	hypothetical protein	S
65	DVU2716	1.0313	tail sheath protein	R
66	DVU2723	1.0309	tail protein	R
67	DVU1972	1.0212	hypothetical protein	S
68	DVU1736	1.0147	hypothetical protein	S
69	DVU1872	1.0118	hypothetical protein	S
70	DVU2596	1.0090	hypothetical protein	RX
71	DVU2700	1.0021	hypothetical protein	S
72	DVU1741	0.9989	hypothetical protein	S
73	DVU1716	0.9956	hypothetical protein	S
74	DVU1713	0.9929	hypothetical protein	S
75	DVU1717	0.9901	hypothetical protein	S
76	DVU1516	0.9841	hypothetical protein	S
77	DVU2203	0.9787	L-PSP family endoribonuclease	J
78	DVU2821	0.9721	hypothetical protein	S
79	DVU1699	0.9704	hypothetical protein	S
80	DVU2167	0.9628	hypothetical protein	J
81	DVU1749	0.9625	hypothetical protein	S
82	DVU1498	0.9611	hypothetical protein	RX
83	DVU0617	0.9547	hypothetical protein	S
84	DVU2213	0.9537	nuclease domain-containing protein	L
85	DVU0537	0.9510	hypothetical protein	S
86	DVU2173	0.9502	hypothetical protein	S
87	DVU2598	0.9495	hypothetical protein	RX
88	DVU1732	0.9453	hypothetical protein	S
89	DVU2089	0.9451	hypothetical protein	S
90	DVU1714	0.9418	hypothetical protein	S
91	DVU3160	0.9384	hypothetical protein	S
92	DVU2713	0.9379	hypothetical protein	S
93	DVU3120	0.9379	hypothetical protein	S
94	DVU1513	0.9378	hypothetical protein	L
95	DVU2539	0.9367	hypothetical protein	S
96	DVU2729	0.9353	tail protein	S
97	DVU2027	0.9311	hypothetical protein	S
98	DVU2704	0.9309	hypothetical protein	S
99	DVU2632	0.9299	hypothetical protein	S
100	DVU2563	0.9285	beta-ketoacyl synthase	IQ
101	DVU1151	0.9249	hypothetical protein	S
102	DVU1989	0.9229	hypothetical protein	S
103	DVU1227	0.9214	hypothetical protein	S
104	DVU1525	0.9203	hypothetical protein	RJ
105	DVU0781	0.9183	hypothetical protein	S
106	DVU1963	0.9176	hypothetical protein	S
107	DVU2710	0.9162	hypothetical protein	R
108	DVU2541	0.9159	CoA-substrate-specific enzyme activase	I
109	DVU2715	0.9147	hypothetical protein	RX

110	DVU1735	0.9130	hypothetical protein	S
111	DVU2605	0.9121	hypothetical protein	S
112	DVU0297	0.9084	hypothetical protein	S
113	DVU0184	0.9081	hypothetical protein	S
114	DVU2728	0.9048	tail protein	S
115	DVU1725	0.9020	hypothetical protein	S
116	DVU1994	0.8996	hypothetical protein	S
117	DVU2180	0.8978	hypothetical protein	S
118	DVU1162	0.8973	hypothetical protein	S
119	DVU1161	0.8966	hypothetical protein	L
120	DVU0618	0.8958	hypothetical protein	S
121	DVU1521	0.8956	hypothetical protein	S
122	DVU1723	0.8945	hypothetical protein	J
123	DVU0443	0.8926	exonulcease	L
124	DVU1965	0.8815	hypothetical protein	S
125	DVU2631	0.8812	hypothetical protein	L
126	DVU3285	0.8798	hypothetical protein	S
127	DVU3380	0.8790	hypothetical protein	S
128	DVU1229	0.8789	hypothetical protein	S
129	DVU1213	0.8764	rhomboid family protein	R
130	DVU0188	0.8759	hypothetical protein	S
131	DVU2153	0.8754	tail fiber protein	RX
132	DVU2666	0.8730	phosphate ABC transporter permease	P
133	DVU1527	0.8709	phage integrase site specific recombinase	L
134	DVU0444	0.8708	hypothetical protein	RT
135	DVU1744	0.8706	DNA-binding protein	K
136	DVU3131	0.8655	transcriptional regulator	K
137	DVU0673	0.8644	hypothetical protein	S
138	DVU0728	0.8629	hypothetical protein	S
139	DVU1694	0.8628	C4-type zinc finger DksA/TraR family protein	RTX
140	DVU1555	0.8622	hypothetical protein	C
141	DVU2152	0.8621	hypothetical protein	S
142	DVU1705	0.8603	type I restriction-modification enzyme, S subunit	V
143	DVU1554	0.8595	radical SAM domain-containing protein	R
144	DVU2711	0.8559	major head subunit	R
145	DVU2602	0.8540	hypothetical protein	RX
146	DVU0431	0.8527	ech hydrogenase subunit EchD	C
147	DVU3269	0.8526	sensory box histidine kinase/response regulator	T
148	DVU2116	0.8512	pilin	U
149	DVU1143	0.8505	hypothetical protein	S
150	DVU1721	0.8498	hypothetical protein	RX
151	DVU1700	0.8457	metallo-beta-lactamase	J
152	DVU2606	0.8454	hypothetical protein	S
153	DVU1719	0.8445	hypothetical protein	S
154	DVU1761	0.8433	hypothetical protein	S
155	DVU2186	0.8417	hypothetical protein	S
156	DVU0710	0.8417	competence protein comM	O
157	DVU2790	0.8400	hypothetical protein	S
158	DVUA0045	0.8397	aminotransferase	M
159	DVU1488	0.8385	minor tail protein	R
160	DVU1938	0.8385	hypothetical protein	S
161	DVU1712	0.8381	hypothetical protein	S
162	DVU0605	0.8376	hypothetical protein	S
163	DVU2192	0.8376	hypothetical protein	S
164	DVU2205	0.8372	tryptophan-specific transport protein	E
165	DVU0345	0.8335	hypothetical protein	S

166	DVU2647	0.8315	L-PSP family endoribonuclease	J
167	DVU2852	0.8303	tail protein	S
168	DVU1230	0.8299	hypothetical protein	S
169	DVU2187	0.8299	hypothetical protein	S
170	DVU2273	0.8277	hypothetical protein	S
171	DVU1166	0.8256	hypothetical protein	S
172	DVU0365	0.8210	hypothetical protein	S
173	DVU1742	0.8208	prevent-host-death family protein	D
174	DVU1522	0.8203	hypothetical protein	S
175	DVU3060	0.8193	hypothetical protein	S
176	DVU3124	0.8152	hypothetical protein	S
177	DVU2248	0.8143	hypothetical protein	S
178	DVU2638	0.8136	hypothetical protein	S
179	DVU2315	0.8118	hypothetical protein	S
180	DVU2693	0.8096	hypothetical protein	I
181	DVUA0089	0.8096	hypothetical protein	M
182	DVU2122	0.8086	type II/IV secretion system protein	U
183	DVU0651	0.8083	hypothetical protein	S
184	DVU2721	0.8078	TP901 family phage tail tape measure protein	RX
185	DVU2564	0.8069	8-amino-7-oxononanoate synthase	H
186	DVU1154	0.8055	hypothetical protein	S
187	DVU2026	0.8054	hypothetical protein	S
188	DVU3391	0.8048	hypothetical protein	S
189	DVU1216	0.8043	hypothetical protein	S
190	DVU0820	0.8036	hypothetical protein	S
191	DVU3303	0.8025	ATP-dependent protease La	T
192	DVU3321	0.8011	hypothetical protein	S
193	DVU2028	0.8000	hypothetical protein	R
194	DVU2189	0.7994	transcriptional regulator cII	K
195	DVU1485	0.7993	hypothetical protein	S
196	DVU3063	0.7973	integral membrane protein MviN	R
197	DVU1226	0.7970	hypothetical protein	S
198	DVU2087	0.7965	hypothetical protein	S
199	DVU1239	0.7960	hypothetical protein	S
200	DVU2044	0.7958	hypothetical protein	S
201	DVU1967	0.7957	Rrf2 family transcriptional regulator	K
202	DVU0217	0.7953	tail protein	S
203	DVU2184	0.7929	DNA-binding protein	RTX
204	DVU1773	0.7921	hypothetical protein	S
205	DVU2520	0.7917	hypothetical protein	S
206	DVU2559	0.7887	adenosylmethionine--8-amino-7-oxononanoate aminotransferase	H
207	DVU0369	0.7869	hypothetical protein	S
208	DVU2137	0.7846	succinyl-CoA synthase subunit beta	C
209	DVU2269	0.7829	hypothetical protein	S
210	DVU1098	0.7820	adenine specific DNA methyltransferase	L
211	DVU1194	0.7810	hypothetical protein	L
212	DVU1637	0.7806	hypothetical protein	S
213	DVU2665	0.7798	phosphate ABC transporter permease	P
214	DVU1858	0.7789	cold shock domain-containing protein	K
215	DVU2939	0.7780	hypothetical protein	R
216	DVU2038	0.7772	hypothetical protein	R
217	DVU2909	0.7768	MarR family transcriptional regulator	K
218	DVU2134	0.7765	hypothetical protein	S
219	DVUA0030	0.7748	hypothetical protein	M
220	DVU1669	0.7725	ribosomal large subunit pseudouridine synthase B	J
221	DVU0332	0.7693	hypothetical protein	S

222	DVU3325	0.7691	hypothetical protein	S
223	DVU2853	0.7668	phage baseplate assembly protein V	S
224	DVUA0032	0.7665	hypothetical protein	M
225	DVU2989	0.7663	psp operon transcriptional activator	T
226	DVUA0046	0.7637	glycosyl transferase, group 2 family protein	M
227	DVU2434	0.7614	hypothetical protein	S
228	DVU1757	0.7605	phage integrase site specific recombinase	L
229	DVU1031	0.7600	hypothetical protein	S
230	DVU2786	0.7595	hypothetical protein	S
231	DVU2874	0.7577	hypothetical protein	R
232	DVU2199	0.7576	hypothetical protein	S
233	DVU1494	0.7546	hypothetical protein	S
234	DVU2808	0.7528	TonB domain-containing protein	M
235	DVU2698	0.7517	lipoprotein	M
236	DVU3394	0.7504	hypothetical protein	S
237	DVU3311	0.7492	hypothetical protein	S
238	DVU3143	0.7492	iron-sulfur cluster-binding protein	C
239	DVU1710	0.7487	hypothetical protein	S
240	DVU0926	0.7460	hypothetical protein	S
241	DVU2159	0.7457	hypothetical protein	S
242	DVU3318	0.7441	hypothetical protein	S
243	DVU3346	0.7430	hypothetical protein	S
244	DVU0475	0.7428	membrane protein , truncation	M
245	DVU0667	0.7423	HD domain-containing protein	RT
246	DVU0038	0.7403	acyltransferase domain-containing protein	R
247	DVU0124	0.7401	hypothetical protein	S
248	DVU1391	0.7396	hypothetical protein	S
249	DVU0615	0.7388	hypothetical protein	S
250	DVU2158	0.7386	hypothetical protein	S
251	DVU0083	0.7377	hypothetical protein	S
252	DVU2037	0.7352	cobS protein	R
253	DVU1502	0.7344	HK97 family portal protein	S
254	DVU3338	0.7280	K+-transporting ATPase subunit B	P
255	DVU4017	0.7278	hypothetical protein	S
256	DVU1701	0.7256	hypothetical protein	S
257	DVU0049	0.7246	OmpA family protein	N
258	DVUA0144	0.7243	hypothetical protein	S
259	DVU1731	0.7217	hypothetical protein	S
260	DVU0105	-0.7206	glutamine ABC transporter ATP-binding protein	E
261	DVU0274	-0.7268	hypothetical protein	S
262	DVU2061	-0.7278	diphosphate--fructose-6-phosphate 1-phosphotransferase	G
263	DVU0606	-0.7286	ArsR family transcriptional regulator	H
264	DVU0060	-0.7320	RND family efflux transporter MFP subunit	M
265	DVU0612	-0.7320	STAS domain-containing protein	Q
266	DVUA0086	-0.7334	response regulator	KT
267	DVU2684	-0.7380	hypothetical protein	U
268	DVU0627	-0.7413	phosphotransbutyrylase	C
269	DVU3070	-0.7447	hypothetical protein	L
270	DVU2787	-0.7455	hypothetical protein	S
271	DVU0448	-0.7464	GDP-mannose 4,6-dehydratase	M
272	DVU3204	-0.7486	adenylosuccinate synthetase	F
273	DVU1086	-0.7486	hypothetical protein	S
274	DVU2983	-0.7492	3-isopropylmalate dehydratase small subunit	E

275	DVU3045	-0.7498	sensory box histidine kinase/response regulator	T
276	DVU2781	-0.7500	hypothetical protein	S
277	DVU0035	-0.7537	hypothetical protein	S
278	DVU1174	-0.7541	hypothetical protein	S
279	DVU3379	-0.7546	ribonucleotide-diphosphate reductase subunit alpha	F
280	DVU3272	-0.7552	hypothetical protein	NU
281	DVU2607	-0.7611	hypothetical protein	S
282	DVU2833	-0.7629	hypothetical protein	S
283	DVU0945	-0.7639	sensor histidine kinase	T
284	DVU0910	-0.7640	flagellar motor switch protein FliM	N
285	DVU2545	-0.7642	iron-containing alcohol dehydrogenase	C
286	DVU2075	-0.7648	ParA family protein	D
287	DVU3353	-0.7669	phosphopantothenoylcysteine decarboxylase/phosphopantothenate--cysteine ligase	H
288	DVU1333	-0.7706	hypothetical protein	S
289	DVU0979	-0.7707	dihydroxyacetone kinase subunit DhaK	G
290	DVUA0088	-0.7717	hypothetical protein	R
291	DVU2608	-0.7763	flagellar motor protein MotA	N
292	DVU2501	-0.7765	cell division protein FtsQ	M
293	DVU1648	-0.7776	lipoprotein	M
294	DVU0898	-0.7795	hypothetical protein	S
295	DVU0074	-0.7809	polysaccharide biosynthesis domain-containing protein	M
296	DVU2553	-0.7818	NifU family protein	O
297	DVU1924	-0.7820	hydrogenase assembly chaperone HypC/HupF	O
298	DVU2484	-0.7821	cytochrome c family protein	C
299	DVU1569	-0.7823	pyruvate ferredoxin oxidoreductase subunit alpha	C
300	DVU1914	-0.7848	alpha-isopropylmalate/homocitrate synthase transferase	E
301	DVU0859	-0.7873	hypothetical protein	RU
302	DVU2259	-0.7873	hypothetical protein	S
303	DVU1075	-0.7908	ribonuclease P protein component	K
304	DVU1658	-0.7917	translaldolase	G
305	DVU0278	-0.7940	glyoxalase	E
306	DVU3112	-0.7957	hypothetical protein	U
307	DVU1210	-0.7972	hypothetical protein	R
308	DVU0638	-0.7978	hypothetical protein	M
309	DVU2513	-0.8018	cell division protein MraZ	S
310	DVU3123	-0.8023	HD domain-containing protein	RT
311	DVU2965	-0.8026	hypothetical protein	S
312	DVU1589	-0.8040	hypothetical protein	S
313	DVU1207	-0.8048	3-oxoacyl-ACP synthase	I
314	DVU2510	-0.8062	penicillin-binding protein	M
315	DVU2224	-0.8062	hypothetical protein	S
316	DVU2417	-0.8075	SlyX protein	S
317	DVU1692	-0.8078	hypothetical protein	S
318	DVU0424	-0.8097	cardiolipin synthetase	I
319	DVU0293	-0.8105	dksA/traR C4-type zinc finger family protein	T
320	DVU0766	-0.8112	transporter	R
321	DVU0241	-0.8113	hypothetical protein	S
322	DVU0703	-0.8119	GTP-binding protein LepA	M
323	DVU1901	-0.8135	peptidyl-prolyl cis-trans isomerase domain-containing protein	O

324	DVU1912	-0.8154	hypothetical protein	R
325	DVU0902	-0.8167	hypothetical protein	R
326	DVU0812	-0.8196	heat shock protein GrpE	O
327	DVU1038	-0.8224	1-(5-phosphoribosyl)-5-[(5-phosphoribosylamino)methylideneamino] imidazole-4-carboxamide isomerase	E
328	DVU1601	-0.8227	ATP-dependent Clp protease adaptor protein ClpS	S
329	DVU1679	-0.8250	isopentenyl-diphosphate delta-isomerase	I
330	DVU0063	-0.8251	MarR family transcriptional regulator	K
331	DVU1197	-0.8257	N utilization substance protein B	K
332	DVU0510	-0.8274	transcription elongation factor NusA	K
333	DVU2144	-0.8277	glyceraldehyde 3-phosphate dehydrogenase	G
334	DVU0713	-0.8339	branched-chain amino acid ABC transporter permease	E
335	DVUA0108	-0.8369	hypothetical protein	S
336	DVU0939	-0.8373	hypothetical protein	S
337	DVU4006	-0.8378	hypothetical protein	S
338	DVU1843	-0.8379	hypothetical protein	T
339	DVU1865	-0.8404	hypothetical protein	S
340	DVU2827	-0.8455	sigma-54 dependent transcriptional regulator	KT
341	DVU2929	-0.8497	DNA-directed RNA polymerase subunit beta'	K
342	DVU1196	-0.8523	leucyl-tRNA synthetase	J
343	DVUA0111	-0.8589	type III secretion system protein IpaC family	U
344	DVU2245	-0.8590	mutT/nudix family protein	F
345	DVU1582	-0.8620	hypothetical protein	S
346	DVU1628	-0.8688	RNA polymerase sigma-54 factor	K
347	DVU2835	-0.8706	transcriptional regulator	K
348	DVU1923	-0.8716	hydrogenase expression/formation protein HupD	C
349	DVU0893	-0.8745	universal stress protein	T
350	DVU2961	-0.8749	hypothetical protein	H
351	DVU0899	-0.8768	hypothetical protein	S
352	DVU1618	-0.8803	iojap family protein	S
353	DVU1408	-0.8815	hypothetical protein	S
354	DVU1801	-0.8843	hypothetical protein	S
355	DVU1241	-0.8859	hypothetical protein	S
356	DVU1248	-0.8865	arginyl-tRNA synthetase	J
357	DVU0900	-0.8890	guanylate kinase	F
358	DVU0508	-0.8890	translation initiation factor IF-2	J
359	DVU0242	-0.8914	SecC motif-containing protein	S
360	DVU1199	-0.8920	3,4-dihydroxy-2-butanone 4-phosphate synthase	H
361	DVU3149	-0.8935	signal peptide peptidase SppA, 36K type	OU
362	DVU2836	-0.8943	hypothetical protein	KX
363	DVU1564	-0.8944	hypothetical protein	S
364	DVU2738	-0.8950	methyl-accepting chemotaxis protein	NT
365	DVU0837	-0.8986	16S rRNA processing protein RimM	J
366	DVU0556	-0.8989	ISDvu3, transposase OrfA	L
367	DVU1676	-0.9022	preprotein translocase subunit SecG	U
368	DVU3356	-0.9032	NAD-dependent epimerase/dehydratase	MG
369	DVU2532	-0.9032	MerR family transcriptional regulator	K
370	DVU2483	-0.9046	cytochrome c family protein	C
371	DVU0941	-0.9075	M16 family peptidase	R

372	DVU1048	-0.9086	cytochrome c-type biogenesis protein CcmB	O
373	DVU1409	-0.9094	hypothetical protein	R
374	DVU2938	-0.9098	hypothetical protein	S
375	DVU0276	-0.9106	hypothetical protein	S
376	DVU3242	-0.9111	DNA-directed RNA polymerase subunit omega	K
377	DVU0935	-0.9115	methyl-accepting chemotaxis protein	NT
378	DVU1033	-0.9150	competence/damage-inducible protein CinA protein, truncation	R
379	DVU3097	-0.9175	outer membrane efflux protein	MU
380	DVU0228	-0.9192	hypothetical protein	S
381	DVU1198	-0.9202	6,7-dimethyl-8-ribityllumazine synthase	H
382	DVU0936	-0.9245	hypothetical protein	R
383	DVUA0079	-0.9307	adenylylsulfate kinase	P
384	DVU2655	-0.9321	D-alanyl-D-alanine carboxypeptidase	M
385	DVU0715	-0.9337	branched-chain amino acid ABC transporter ATP-binding protein	E
386	DVU1043	-0.9368	GMP synthase	F
387	DVU0511	-0.9377	hypothetical protein	S
388	DVUA0073	-0.9399	asparagine synthase (glutamine-hydrolyzing)	E
389	DVU2937	-0.9406	TPR domain/response regulator receiver domain-containing protein	RT
390	DVU0412	-0.9427	potassium uptake protein TrkA	P
391	DVU0321	-0.9427	pantothenate kinase	K
392	DVU0181	-0.9443	molybdenum ABC transporter permease	P
393	DVU3190	-0.9445	hypothetical protein	U
394	DVU0341	-0.9453	3-deoxy-manno-octulosonate cytidylyltransferase	M
395	DVU0942	-0.9456	Fur family transcriptional regulator	P
396	DVU2078	-0.9475	protein-glutamate methylesterase CheB	NT
397	DVU2074	-0.9500	chemotaxis protein CheW	NT
398	DVU1570	-0.9516	pyruvate ferredoxin oxidoreductase subunit beta	C
399	DVU2309	-0.9520	methyl-accepting chemotaxis protein	NT
400	DVU0269	-0.9527	Rrf2 family transcriptional regulator	K
401	DVU2226	-0.9558	acetyl-CoA carboxylase, biotin carboxylase	I
402	DVU2416	-0.9582	hypothetical protein	S
403	DVU1204	-0.9592	3-oxoacyl-ACP synthase	IQ
404	DVU2500	-0.9639	cell division protein FtsA	D
405	DVU2590	-0.9677	sensory box protein	S
406	DVU0938	-0.9685	isoamylase N-terminal domain-containing protein	R
407	DVUA0080	-0.9687	glycosyl transferase, group 2 family protein	M
408	DVU2674	-0.9690	succinate dehydrogenase and fumarate reductase iron-sulfur protein	C
409	DVU1050	-0.9706	cytochrome c-type biogenesis protein CcmF	O
410	DVU0177	-0.9753	molybdenum ABC transporter periplasmic molybdenum-binding protein	P
411	DVU1336	-0.9753	ATP-dependent protease ATP-binding subunit ClpX	O
412	DVU0299	-0.9754	anaerobic ribonucleoside triphosphate reductase	F
413	DVU1334	-0.9765	trigger factor	O
414	DVU2076	-0.9770	chemotaxis protein methyltransferase	NT

415	DVU0701	-0.9776	malate synthase G	C
416	DVU3083	-0.9782	hypothetical protein	S
417	DVU2774	-0.9830	hypothetical protein	R
418	DVU2903	-0.9843	HD domain-containing protein	J
419	DVU0928	-0.9849	50S ribosomal protein L27	J
420	DVU0880	-0.9871	hypothetical protein	S
421	DVU3173	-0.9903	hypothetical protein	S
422	DVU1655	-0.9945	LL-diaminopimelate aminotransferase	E
423	DVU2371	-0.9952	N-acetylmuramoyl-L-alanine amidase	M
424	DVU2368	-0.9970	(3R)-hydroxymyristoyl-ACP dehydratase	I
425	DVU0915	-0.9977	hypothetical protein	S
426	DVU2323	-1.0041	hypothetical protein	S
427	DVU1278	-1.0090	cell division protein FtsH	O
428	DVUA0074	-1.0114	sulfotransferase family protein	R
429	DVU1044	-1.0244	inosine-5`-monophosphate dehydrogenase	F
430	DVU0704	-1.0255	signal peptidase I	U
431	DVU2968	-1.0303	sensor histidine kinase/response regulator	T
432	DVU2374	-1.0309	lipoprotein releasing system, ATP-binding protein	V
433	DVU0856	-1.0334	delta-aminolevulinic acid dehydratase	H
434	DVU1851	-1.0367	M24/M37 family peptidase	M
435	DVU0789	-1.0380	rod shape-determining protein MreB	D
436	DVU1087	-1.0400	hypothetical protein	S
437	DVU1049	-1.0401	ABC transporter ATP-binding protein	P
438	DVU1579	-1.0474	cysteinyl-tRNA synthetase	J
439	DVUA0072	-1.0477	glycosyl transferase, group 1 family protein	M
440	DVU0824	-1.0508	hypothetical protein	S
441	DVU1396	-1.0511	hypothetical protein	S
442	DVU2769	-1.0575	hypothetical protein	P
443	DVUA0116	-1.0596	hypothetical protein	R
444	DVU0004	-1.0718	DNA gyrase subunit A	L
445	DVU2669	-1.0763	hypothetical protein	D
446	DVU0958	-1.0805	50S ribosomal protein L9	J
447	DVU3352	-1.0815	lipoprotein	M
448	DVU0464	-1.0825	prephenate dehydrogenase	E
449	DVU2227	-1.0836	hypothetical protein	U
450	DVU2073	-1.0869	chemotaxis protein CheY	T
451	DVU1816	-1.0878	hypothetical protein	R
452	DVU3392	-1.0885	glutamine synthetase, type I	E
453	DVU1042	-1.0943	twin-arginine translocation protein TatB	U
454	DVU2671	-1.0959	phosphodiesterase	R
455	DVU2547	-1.0978	transcriptional regulator	T
456	DVU0064	-1.0978	hypothetical protein	S
457	DVU3228	-1.1011	chemotaxis protein CheY	T
458	DVU1005	-1.1032	hypothetical protein	S
459	DVU0854	-1.1041	NirD protein	K
460	DVU2077	-1.1058	hypothetical protein	C
461	DVU2973	-1.1064	integration host factor subunit beta	L
462	DVU2222	-1.1091	single-strand binding protein	L
463	DVU1597	-1.1131	sulfite reductase, assimilatory-type	C
464	DVU0811	-1.1198	molecular chaperone DnaK	O
465	DVU2367	-1.1211	UDP-N-acetylglucosamine acyltransferase	M
466	DVU1427	-1.1261	response regulator	T
467	DVU1845	-1.1273	hypothetical protein	S
468	DVU0916	-1.1278	redox-sensing transcriptional repressor Rex	R

469	DVU1612	-1.1381	ACT domain-containing protein	R
470	DVU1448	-1.1382	hypothetical protein	L
471	DVU2988	-1.1384	phage shock protein A	KT
472	DVU2216	-1.1459	translation initiation factor IF-1	J
473	DVU0884	-1.1462	hypothetical protein	C
474	DVU2481	-1.1490	formate dehydrogenase subunit beta	C
475	DVU0794	-1.1548	enoyl-ACP reductase	I
476	DVU1580	-1.1550	ribose 5-phosphate isomerase	G
477	DVU0566	-1.1574	GAF domain-containing protein	T
478	DVU1864	-1.1584	DNA-binding protein HU subunit beta	L
479	DVU1943	-1.1639	hypothetical protein	S
480	DVU0626	-1.1684	acetolactate synthase small subunit	E
481	DVU1039	-1.1694	lipoprotein	M
482	DVU1896	-1.1756	30S ribosomal protein S20	J
483	DVU1781	-1.1792	hypothetical protein	S
484	DVU2869	-1.1796	major head protein	RX
485	DVU0200	-1.1850	major head protein	RX
486	DVU0503	-1.1922	polynucleotide phosphorylase/polyadenylase	J
487	DVU2482	-1.1960	formate dehydrogenase subunit alpha	C
488	DVU2411	-1.2028	EF hand domain-containing protein	R
489	DVU0793	-1.2114	hypothetical protein	S
490	DVU3330	-1.2136	hypothetical protein	P
491	DVU0005	-1.2153	lipoprotein	M
492	DVU1985	-1.2272	hypothetical protein	R
493	DVU1206	-1.2306	3-oxoacyl-ACP reductase	IQR
494	DVU1833	-1.2329	phosphoenolpyruvate synthase	G
495	DVU1666	-1.2369	elongation factor P	J
496	DVU0133	-1.2411	hypothetical protein	S
497	DVU1317	-1.2413	30S ribosomal protein S8	J
498	DVU1307	-1.2418	30S ribosomal protein S19	J
499	DVU1820	-1.2445	preprotein translocase subunit YajC	U
500	DVU1298	-1.2453	30S ribosomal protein S12	J
501	DVU1629	-1.2491	ribosomal subunit interface protein	J
502	DVU1040	-1.2499	imidazoleglycerol-phosphate dehydratase	E
503	DVU1319	-1.2528	50S ribosomal protein L18	J
504	DVU0509	-1.2533	hypothetical protein	K
505	DVU1302	-1.2535	30S ribosomal protein S10	J
506	DVU1300	-1.2544	elongation factor G	J
507	DVU2912	-1.2568	50S ribosomal protein L31	J
508	DVU1030	-1.2627	universal stress protein	T
509	DVU1337	-1.2653	ATP-dependent protease La	O
510	DVU1397	-1.2679	bacterioferritin	P
511	DVU1315	-1.2694	50S ribosomal protein L5	J
512	DVU0987	-1.2721	heavy metal-binding domain-containing protein	RP
513	DVU1313	-1.2738	50S ribosomal protein L14	J
514	DVU2577	-1.2826	LuxR family transcriptional regulator	TK
515	DVU2349	-1.2937	carbohydrate phosphorylase	G
516	DVU3185	-1.2950	rubredoxin-oxygen oxidoreductase	C
517	DVU1657	-1.2954	hypothetical protein	J
518	DVU2426	-1.3062	hypothetical protein	S
519	DVU1243	-1.3122	hypothetical protein	Q
520	DVU1309	-1.3200	30S ribosomal protein S3	J
521	DVU3217	-1.3318	hypothetical protein	S
522	DVU0253	-1.3340	oxidoreductase	C
523	DVU2531	-1.3366	ribulose-phosphate 3-epimerase	G
524	DVU1314	-1.3419	50S ribosomal protein L24	J
525	DVU2370	-1.3486	outer membrane protein OmpH	M

526	DVU1324	-1.3492	methionine aminopeptidase	J
527	DVU1421	-1.3535	hypothetical protein	S
528	DVU1377	-1.3541	acetolactate synthase 3 regulatory subunit	E
529	DVU1971	-1.3581	hypothetical protein	R
530	DVU2967	-1.3614	sensor histidine kinase/response regulator	KT
531	DVU1873	-1.3621	peptidyl-prolyl cis-trans isomerase B	O
532	DVU2072	-1.3706	chemotaxis protein CheA	NT
533	DVU1917	-1.3800	periplasmic [NiFeSe] hydrogenase small subunit	C
534	DVU1012	-1.3866	hemolysin-type calcium-binding repeat-containingprotein	R
535	DVU0565	-1.3956	glyceraldehyde 3-phosphate dehydrogenase	G
536	DVU2519	-1.4021	30S ribosomal protein S9	J
537	DVU2198	-1.4066	hypothetical protein	C
538	DVU1990	-1.4107	hypothetical protein	S
539	DVU1303	-1.4145	50S ribosomal protein L3	J
540	DVU1568	-1.4172	ferritin	P
541	DVU3122	-1.4195	hypothetical protein	S
542	DVU2980	-1.4238	CDP-diacylglycerol--serine O-phosphatidyltransferase	I
543	DVU3212	-1.4239	pyridine nucleotide-disulfide oxidoreductase	R
544	DVU0995	-1.4244	ThiJ/PfpI family protein	R
545	DVU1420	-1.4282	Hpt domain-containing protein	T
546	DVU1381	-1.4297	hypothetical protein	S
547	DVU0607	-1.4298	S-adenosyl-L-homocysteine hydrolase	H
548	DVU0305	-1.4315	ferredoxin II	C
549	DVU1045	-1.4558	hypothetical protein	R
550	DVU1468	-1.4574	peptidase/PDZ domain-containing protein	O
551	DVU1310	-1.4600	50S ribosomal protein L16	J
552	DVU1316	-1.4620	30S ribosomal protein S14	J
553	DVU0283	-1.4642	AhpF family protein/thioredoxin reductase	O
554	DVU0857	-1.4658	radical SAM domain-containing protein	R
555	DVU1537	-1.4684	lipoprotein	M
556	DVU2130	-1.4722	hypothetical protein	S
557	DVU1691	-1.4786	hypothetical protein	S
558	DVU1572	-1.4807	CarD family transcriptional regulator	K
559	DVU2236	-1.4814	hypothetical protein	S
560	DVU1205	-1.4823	acyl carrier protein	IQ
561	DVU0505	-1.4852	tRNA pseudouridine synthase B	J
562	DVU1330	-1.4866	50S ribosomal protein L17	J
563	DVU2427	-1.4985	hypothetical protein	S
564	DVU3183	-1.5011	desulfoferrodoxin	C
565	DVU1299	-1.5062	30S ribosomal protein S7	J
566	DVU0322	-1.5083	phosphopyruvate hydratase	G
567	DVU1074	-1.5107	50S ribosomal protein L34	J
568	DVU1308	-1.5124	50S ribosomal protein L22	J
569	DVUA0075	-1.5221	radical SAM domain-containing protein	R
570	DVU2518	-1.5318	50S ribosomal protein L13	J
571	DVU1782	-1.5428	iron-sulfur cluster-binding protein	C
572	DVU1378	-1.5460	ketol-acid reductoisomerase	EH
573	DVU1329	-1.5509	DNA-directed RNA polymerase subunit alpha	K
574	DVU0138	-1.5510	response regulator	T
575	DVU0684	-1.5655	hflK protein	O
576	DVUA0077	-1.5740	ABC transporter permease	GM

577	DVU3150	-1.5768	30S ribosomal protein S1	J
578	DVU1326	-1.5830	30S ribosomal protein S13	J
579	DVU1581	-1.5832	hypothetical protein	S
580	DVU0839	-1.5903	30S ribosomal protein S16	J
581	DVU2569	-1.5993	peptidyl-prolyl cis-trans isomerase, FKBP-type	O
582	DVU1335	-1.5993	ATP-dependent Clp protease proteolytic subunit	OU
583	DVU1817	-1.6100	cytochrome c-553	C
584	DVUA0005	-1.6408	universal stress protein	T
585	DVU3184	-1.6556	rubredoxin	C
586	DVU1051	-1.6665	cytochrome c-type biogenesis protein CcmE	O
587	DVU1311	-1.6680	50S ribosomal protein L29	J
588	DVU1312	-1.6705	30S ribosomal protein S17	J
589	DVU1918	-1.6727	periplasmic [NiFeSe] hydrogenase large subunit, selenocysteine-containing	C
590	DVU2770	-1.6752	response regulator	T
591	DVU0504	-1.6785	30S ribosomal protein S15	J
592	DVU0265	-1.6851	hypothetical protein	C
593	DVU0459	-1.6881	hypothetical protein	S
594	DVU2470	-1.6919	membrane protein	R
595	DVUA0076	-1.7281	ABC transporter ATP-binding protein	GM
596	DVU1228	-1.7354	thiol peroxidase	O
597	DVU2670	-1.7589	hypothetical protein	D
598	DVU0407	-1.7591	rare lipoprotein A family protein	M
599	DVU2496	-1.7631	lipoprotein	M
600	DVU3080	-1.7672	transcriptional regulator	K
601	DVUA0006	-1.7708	magnesium transporter MgtE	P
602	DVU1792	-1.7731	30S ribosomal protein S21	J
603	DVU0629	-1.7771	TetR family transcriptional regulator	K
604	DVU0683	-1.8176	hflC protein	O
605	DVU1328	-1.8511	30S ribosomal protein S4	J
606	DVU0264	-1.8539	ferredoxin, 4Fe-4S	C
607	DVU1013	-1.8566	TolC family type I secretion outer membrane protein	MU
608	DVU3117	-1.8809	hypothetical protein	C
609	DVU1327	-1.9454	30S ribosomal protein S11	J
610	DVU0943	-1.9468	hypothetical protein	S
611	DVU1325	-1.9562	50S ribosomal protein L36	J
612	DVU0838	-1.9770	hypothetical protein	R
613	DVU1664	-2.0046	ribosome biogenesis GTP-binding protein YsxC	R
614	DVU3084	-2.0121	transcriptional regulator	K
615	DVUA0091	-2.0324	catalase	P
616	DVU2428	-2.0647	lipoprotein	M
617	DVU0262	-2.0849	hypothetical protein	S
618	DVU0266	-2.1045	hypothetical protein	R
619	DVU0263	-2.1825	acidic cytochrome c3	C
620	DVU0260	-2.2116	response regulator	T
621	DVU1904	-2.2640	chemotaxis protein CheW	NT
622	DVU2449	-2.3046	S-adenosylmethionine synthetase	H
623	DVU2298	-2.3973	glycine/betaine/L-proline ABC transporter permease	E
624	DVU2299	-2.4200	glycine betaine/L-proline ABC transporter ATP-binding protein	E
625	DVU3094	-2.4507	rubrerythrin	C
626	DVU1014	-2.5383	hypothetical protein	S
627	DVU2215	-2.6212	RNA-binding protein	K

628	DVU0261	-2.6508	universal stress protein	T
629	DVU3093	-2.6593	rubredoxin-like protein	C
630	DVU1257	-2.6869	RNA-binding protein	K
631	DVU0259	-2.7109	DNA-binding response regulator	T
632	DVU1382	-2.7824	HesB family selenoprotein	R
633	DVU2650	-2.9345	hypothetical protein	S

DvH:	All Significant CCBF	Unique to BF
Up-Expressed	287	238
Down-Expressed	485	360
TOTAL	*1257	*1058

*includes all significant genes without expression cut-off

> 2 LogFC		0
< -2 LogFC		25

Table S6. Co-culture biofilm specific gene expression in *M. maripaludis*.

Methanococcus maripaludis S2

	GeneID	CC Biofilm Log$_2$FC	Product	COG
1	MMP0998	5.6933	hypothetical protein	P
2	MMP0275	3.3326	periplasmic copper-binding protein	P
3	MMP1602	2.6144	hypothetical protein	S
4	MMP0750	2.3699	hypothetical protein	S
5	MMP0775	2.3583	hypothetical protein	S
6	MMP0467	2.3521	hypothetical protein	S
7	MMP0466	2.3463	hypothetical protein	S
8	MMP0745	2.3313	hypothetical protein	R
9	MMP0211	2.3173	hypothetical protein	S
10	MMP0782	2.2911	hypothetical protein	S
11	MMP1483	2.2521	cobalt ABC transporter inner membrane protein	P
12	MMP0518	2.2119	hypothetical protein	S
13	MMP0530	2.1702	hypothetical protein	KV
14	MMP0462	2.1630	hypothetical protein	S
15	MMP1490	2.0987	ATP/GTP-binding motif-containing protein	F
16	MMP0673	2.0951	hypothetical protein	NU
17	MMP1276	2.0773	hypothetical protein	S
18	MMP0434	1.9885	hypothetical protein	S
19	MMP0739	1.9866	Asp/Glu racemase:aspartate racemase	M
20	MMP0747	1.9755	hypothetical protein	S
21	MMP0195	1.9603	hypothetical protein	S
22	MMP1339	1.9491	SAM-binding motif-containing protein	J
23	MMP0999	1.9478	hypothetical protein	S
24	MMP1575	1.9404	6-carboxyhexanoate--CoA ligase	H
25	MMP0744	1.9207	hypothetical protein	R
26	MMP0468	1.9102	hypothetical protein	S
27	MMP0749	1.9019	hypothetical protein	S
28	MMP0077	1.9002	radical SAM domain-containing protein	O
29	MMP0217	1.8885	transcriptional repressor-like protein	K
30	MMP0471	1.8753	hypothetical protein	K
31	MMP1124	1.8660	thiamine-monophosphate kinase	H
32	MMP1338	1.8610	hypothetical protein	S
33	MMP0089	1.8535	siroheme synthase	H
34	MMP0438	1.8495	hypothetical protein	C
35	MMP0662	1.8469	hypothetical protein	T
36	MMP0513	1.8380	molybdopterin biosynthesis moeA protein	H
37	MMP0380	1.8348	DNA polymerase B protein	L
38	MMP1110	1.8301	hypothetical protein	S
39	MMP0533	1.7858	hypothetical protein	RX
40	MMP1279	1.7746	camphor resistance protein CrcB	D
41	MMP0364	1.7555	hypothetical protein	NU
42	MMP0454	1.7489	hypothetical protein	R
43	MMP0892	1.7390	GCN5-like N-acetyltransferase	J
44	MMP0047	1.7320	radical SAM domain-containing protein	C
45	MMP1576	1.7255	hypothetical protein	S
46	MMP0408	1.7183	H+-transporting two-sector ATPase subunit A	S
47	MMP0143	1.7181	hypothetical protein	S
48	MMP1664	1.7133	hypothetical protein	S
49	MMP0757	1.7050	hypothetical protein	S
50	MMP0881	1.7044	hypothetical protein	S
51	MMP0460	1.6995	hypothetical protein	K

52	MMP0573	1.6952	molybdopterin-guanine dinucleotide biosynthesis protein A	H
53	MMP1678	1.6942	endonuclease IV	L
54	MMP0767	1.6907	hypothetical protein	S
55	MMP1649	1.6900	ABC transporter ATPase	E
56	MMP0754	1.6875	hypothetical protein	S
57	MMP1226	1.6872	geranylgeranyl reductase	C
58	MMP1203	1.6758	cobalt-precorrin-6A synthase	H
59	MMP0790	1.6747	hypothetical protein	S
60	MMP1103	1.6741	hypothetical protein	S
61	MMP0714	1.6736	indolepyruvate oxidoreductase subunit beta	C
62	MMP1393	1.6724	hypothetical protein	S
63	MMP0966	1.6717	uroporphyrin-III C-methyltransferase	H
64	MMP0990	1.6692	hypothetical protein	S
65	MMP1590	1.6563	ExsB family protein	R
66	MMP0520	1.6557	HAD superfamily ATPase	P
67	MMP0519	1.6522	hypothetical protein	S
68	MMP1221	1.6494	SAM-binding motif-containing protein	H
69	MMP0616	1.6349	OB-fold nucleic acid binding domain-containing protein	R
70	MMP0337	1.6263	hypothetical protein	S
71	MMP0461	1.6245	hypothetical protein	S
72	MMP0191	1.6192	hypothetical protein	R
73	MMP1102	1.6077	phospholipase D/transphosphatidylase	R
74	MMP0863	1.6075	CBS domain-containing protein	R
75	MMP0005	1.5923	hypothetical protein	S
76	MMP0090	1.5913	glycosyl transferase	M
77	MMP0773	1.5793	hypothetical protein	U
78	MMP0140	1.5786	(NiFe) hydrogenase maturation protein HypF	O
79	MMP1232	1.5778	PP-loop domain-containing protein	D
80	MMP0516	1.5756	quinolinate phosphoribosyl transferase	H
81	MMP0900	1.5740	rhodanese domain-containing protein	R
82	MMP0208	1.5704	hypothetical protein	R
83	MMP1000	1.5674	hypothetical protein	S
84	MMP0185	1.5605	5'-methylthioadenosine phosphorylase	F
85	MMP0488	1.5590	low molecular weight phosphotyrosine protein phosphatase	T
86	MMP0360	1.5499	hypothetical protein	S
87	MMP0472	1.5447	integrase/recombinase	L
88	MMP0827	1.5432	hypothetical protein	S
89	MMP0365	1.5366	hypothetical protein	S
90	MMP1591	1.5351	cobalamin (vitamin B12) biosynthesis CbiG protein	H
91	MMP1238	1.5288	biotin synthase	H
92	MMP0840	1.5267	TetR family transcriptional regulator	K
93	MMP0766	1.5159	site-specific recombinase	L
94	MMP0675	1.5156	hypothetical protein	S
95	MMP0111	1.5127	hypothetical protein	M
96	MMP0216	1.5109	cation transport ATPase	P
97	MMP0864	1.5086	Na+/H+ exchanger	P
98	MMP0741	1.5024	hypothetical protein	S
99	MMP0274	1.5002	hydrogenase expression/formation protein HypE	O
100	MMP0032	1.5001	transcription regulator ArsR	K
101	MMP0228	1.4971	N(2),N(2)-dimethylguanosine tRNA methyltransferase	J
102	MMP1027	1.4934	hypothetical protein	S
103	MMP1268	1.4840	hypothetical protein	S

104	MMP0474	1.4812	hypothetical protein	S
105	MMP0067	1.4769	nitrogen regulatory protein P-II	E
106	MMP0672	1.4754	binding-protein dependent transport system innermembrane protein	H
107	MMP0551	1.4721	binding-protein dependent transport system innermembrane protein	E
108	MMP0652	1.4685	hypothetical protein	S
109	MMP0762	1.4664	hypothetical protein	NU
110	MMP0850	1.4652	amino acid transporter	E
111	MMP0334	1.4645	TrmH family RNA methyltransferase	J
112	MMP0161	1.4554	2-phosphosulfolactate phosphatase	HR
113	MMP0233	1.4472	hypothetical protein	S
114	MMP0371	1.4422	hypothetical protein	S
115	MMP0473	1.4394	hypothetical protein	S
116	MMP1425	1.4336	tRNA 2'-O-methylase	S
117	MMP0200	1.4287	molybdenum containing formylmethanofuran dehydrogenase subunit E	C
118	MMP0011	1.4278	DNA-cytosine methyltransferase	L
119	MMP0617	1.4203	DNA repair and recombination protein RadB	L
120	MMP0769	1.4162	hypothetical protein	M
121	MMP0019	1.4141	hypothetical protein	S
122	MMP0996	1.4106	hypothetical protein	C
123	MMP0229	1.4100	amino acid ABC transporter ATP-binding protein	E
124	MMP1078	1.4007	hypothetical protein	S
125	MMP0378	1.3986	amidohydrolase	FR
126	MMP1713	1.3941	hypothetical protein	E
127	MMP1581	1.3934	DNA helicase	L
128	MMP0867	1.3910	binding-protein dependent transport system innermembrane protein	E
129	MMP0994	1.3899	hypothetical protein	P
130	MMP1514	1.3897	prephenate dehydrogenase	E
131	MMP0907	1.3872	transcriptional regulator TrmB	K
132	MMP0618	1.3867	hypothetical protein	S
133	MMP0789	1.3840	cytosine permease	F
134	MMP0475	1.3830	hypothetical protein	M
135	MMP1423	1.3815	aldehyde dehydrogenase	M
136	MMP0813	1.3780	hypothetical protein	R
137	MMP0307	1.3750	hypothetical protein	R
138	MMP0033	1.3721	LysR family protein	LO
139	MMP0201	1.3674	molybdenum cofactor biosynthesis protein	H
140	MMP0849	1.3663	L-lysine/ homoserine-homoserine lactone exporterfamily protein	E
141	MMP0449	1.3638	ferredoxin	C
142	MMP0547	1.3636	RecJ-like protein	L
143	MMP1277	1.3624	succinate dehydrogenase flavoprotein subunit	C
144	MMP0564	1.3614	hypothetical protein	R
145	MMP0642	1.3603	hypothetical protein	S
146	MMP0198	1.3577	ABC-type iron(III) transport system ATP binding protein	PH
147	MMP1227	1.3558	cobalt-precorrin-6Y C(5)-methyltransferase	H
148	MMP1574	1.3538	8-amino-7-oxononanoate synthase	H
149	MMP0110	1.3533	ABC transporter:AAA ATPase	E
150	MMP0368	1.3515	hypothetical protein	S
151	MMP1395	1.3514	Hef nuclease	L

152	MMP1243	1.3504	UBA/THIF-type NAD/FAD binding protein	R
153	MMP0435	1.3466	hypothetical protein	J
154	MMP0560	1.3341	SAM-binding motif-containing protein	R
155	MMP1476	1.3249	hypothetical protein	S
156	MMP0381	1.3189	3-isopropylmalate dehydratase small subunit	E
157	MMP0565	1.2939	hypothetical protein	R
158	MMP1674	1.2872	flagellar accessory protein FlaH	NU
159	MMP0759	1.2744	hypothetical protein	R
160	MMP0896	1.2695	polysaccharide biosynthesis protein	R
161	MMP0798	1.2678	hypothetical protein	S
162	MMP0768	1.2662	hypothetical protein	H
163	MMP0988	1.2650	RNA methyltransferase-like protein	J
164	MMP0663	1.2649	sulfate transporter	P
165	MMP1267	1.2647	hypothetical protein	E
166	MMP0703	1.2615	hypothetical protein	S
167	MMP0049	1.2611	carbonic anhydrase	R
168	MMP0862	1.2585	GCN5-like N-acetyltransferase	J
169	MMP1638	1.2529	MoaA/nifB/pqqE family protein	R
170	MMP1195	1.2522	cytoplasmic protein	S
171	MMP1334	1.2329	solute-binding protein/glutamate receptor	R
172	MMP1080	1.2308	group 1 glycosyl transferase	M
173	MMP0423	1.2232	hypothetical protein	S
174	MMP0580	1.2222	anaerobic ribonucleoside-triphosphate reductase activating protein	O
175	MMP0149	1.2204	RNA methylase	L
176	MMP1601	1.2132	RNA methylase	R
177	MMP0484	1.2024	sodium/hydrogen exchanger	P
178	MMP0463	1.2008	hypothetical protein	S
179	MMP1341	1.2007	SMC domain-containing protein	D
180	MMP1123	1.1944	radical SAM domain-containing protein	C
181	MMP0649	1.1915	carbamoyltransferase	O
182	MMP0415	1.1838	O-sialoglycoprotein endopeptidase/protein kinase	O
183	MMP0074	1.1792	hypothetical protein	S
184	MMP0189	1.1777	hypothetical protein	S
185	MMP1389	1.1768	hypothetical protein	G
186	MMP0871	1.1751	hypothetical protein	V
187	MMP1009	1.1679	dihydroorotase	F
188	MMP0595	1.1618	hypothetical protein	E
189	MMP1233	1.1608	formate dehydrogenase accessory protein FdhD	C
190	MMP1170	1.1603	glycosyl transferase	M
191	MMP0147	1.1587	nitrogenase reductase-like protein	P
192	MMP0377	1.1564	isoleucyl-tRNA synthetase-like protein	R
193	MMP1620	1.1562	hypothetical protein	S
194	MMP0976	1.1502	hypothetical protein	S
195	MMP0973	1.1492	hypothetical protein	R
196	MMP1105	1.1479	succinate-CoA ligase (ADP-forming), beta chain	C
197	MMP1055	1.1476	hypothetical protein	S
198	MMP1659	1.1460	aspartate carbamoyltransferase catalytic subunit	F
199	MMP1521	1.1450	hypothetical protein	S
200	MMP1172	1.1427	DNA protection protein DPS	R
201	MMP1478	1.1388	cobyrinic acid a,c-diamide synthase:cobyrinic acid a,c-diamide synthase CbiA	H

202	MMP0205	1.1366	molybdenum ABC transporter periplasmic molybdenum-binding protein	P
203	MMP1552	1.1364	3-octaprenyl-4-hydroxybenzoate carboxy-lyase	H
204	MMP1645	1.1353	aspartate/glutamate/uridylate kinase	R
205	MMP0316	1.1341	indolepyruvate oxidoreductase subunit alpha 1	C
206	MMP0349	1.1240	2-hydroxyglutaryl-CoA dehydratase subunit A-likeprotein	I
207	MMP1258	1.1159	delta-aminolevulinic acid dehydratase	H
208	MMP0268	1.1081	tRNA pseudouridine synthase A	J
209	MMP0954	1.1079	hypothetical protein	S
210	MMP0699	1.1044	MATE efflux family protein	V
211	MMP0529	1.1035	sulfate transporter family protein	P
212	MMP1012	1.0922	exodeoxyribonuclease III Xth	L
213	MMP1087	1.0849	hypothetical protein	R
214	MMP0170	1.0808	RimK family alpha-L-glutamate ligase	HJ
215	MMP1144	1.0802	bacitracin resistance protein BacA	V
216	MMP0332	1.0786	hypothetical protein	RX
217	MMP0764	1.0767	hypothetical protein	S
218	MMP0579	1.0732	hypothetical protein	R
219	MMP0409	1.0717	glucose-methanol-choline oxidoreductase	C
220	MMP0439	1.0702	dihydroorotate dehydrogenase 1B	F
221	MMP1020	1.0695	hypothetical protein	R
222	MMP0975	1.0634	molybdenum ABC transporter solute-binding protein	P
223	MMP0613	1.0599	acetolactate decarboxylase	Q
224	MMP1377	1.0598	hypothetical protein	R
225	MMP0146	1.0506	hypothetical protein	Q
226	MMP1525	1.0454	modulator of DNA gyrase	R
227	MMP0799	1.0443	TetR family transcriptional regulator Member	K
228	MMP0615	1.0350	hypothetical protein	S
229	MMP0561	1.0347	carboxymuconolactone decarboxylase	S
230	MMP0589	1.0322	radical SAM domain-containing protein	C
231	MMP1386	1.0262	hypothetical protein	S
232	MMP0291	1.0260	hydrogenase expression/formation protein-like protein	O
233	MMP1106	1.0170	hypothetical protein	R
234	MMP1501	1.0103	phosphodiesterase	R
235	MMP0315	1.0005	indolepyruvate oxidoreductase subunit B	C
236	MMP1578	0.9984	nicotinamide-nucleotide adenylyltransferase	H
237	MMP1672	0.9952	flagellar protein F	N
238	MMP0783	0.9909	hypothetical protein	R
239	MMP1336	0.9861	translation factor	J
240	MMP0412	0.9800	MiaB-like tRNA modifying protein	J
241	MMP0094	0.9764	pseudouridylate synthase	J
242	MMP1209	0.9739	hypothetical protein	S
243	MMP1354	0.9716	thiamine biosynthesis protein	H
244	MMP0113	0.9650	hypothetical protein	S
245	MMP1604	0.9624	hypothetical protein	S
246	MMP1284	0.9597	DEAD/DEAH box helicase domain-containing protein	R
247	MMP1228	0.9524	hypothetical protein	S
248	MMP1011	0.9517	glutamyl-tRNA synthetase	J
249	MMP1680	0.9504	glucosamine--fructose-6-phosphate aminotransferase	M
250	MMP0812	0.9434	hypothetical protein	M

251	MMP1126	0.9421	proliferating-cell nucleolar antigen	J
252	MMP0711	0.9419	magnesium/cobalt transporter CorA	P
253	MMP0756	0.9416	hypothetical protein	V
254	MMP1701	0.9364	amino acid-binding ACT domain-containing protein	E
255	MMP1092	0.9311	auxin efflux carrier	R
256	MMP0021	0.9284	hypothetical protein	S
257	MMP1219	0.9213	dinG ATP-dependent helicase	KL
258	MMP1008	0.9171	indole-3-glycerol-phosphate synthase	E
259	MMP1077	0.9160	phosphoglucomutase/phosphomannomutase	G
260	MMP1315	0.9111	2-oxoglutarate ferredoxin oxidoreductase subunitgamma	C
261	MMP0418	0.9013	carbohydrate kinase PfkB	G
262	MMP0401	0.9003	methionine synthase	E
263	MMP1679	0.8999	hypothetical protein	S
264	MMP0265	0.8973	hypothetical protein	S
265	MMP0112	0.8964	2,3-bisphosphoglycerate-independent phosphoglycerate mutase 2	G
266	MMP0877	0.8953	quinolinate phosphoribosyl transferase:nicotinate-nucleotide pyrophosphorylase	H
267	MMP1356	0.8895	PP-loop domain-containing protein	D
268	MMP1199	0.8866	phosphate transporter PhoU	P
269	MMP0392	0.8843	phosphoribosylamine--glycine ligase	F
270	MMP0844	0.8786	hypothetical protein	S
271	MMP0007	0.8774	geranylgeranylglyceryl phosphate synthase-like protein	R
272	MMP0088	0.8730	glutamyl-tRNA reductase	H
273	MMP0555	0.8710	preflagellin peptidase	NU
274	MMP0264	0.8682	mechanosensitive ion channel MscS	M
275	MMP0793	0.8619	hypothetical protein	R
276	MMP0526	0.8551	hypothetical protein	S
277	MMP0131	0.8496	L-tyrosine decarboxylase	E
278	MMP0554	0.8494	SAM-binding motif-containing protein	J
279	MMP0947	0.8397	ATP phosphoribosyltransferase	E
280	MMP1201	0.8221	nuclease	L
281	MMP0755	0.8111	ATP/GTP-binding motif-containing protein	V
282	MMP1205	0.8104	3-phosphoshikimate 1-carboxyvinyltransferase	E
283	MMP0571	0.7851	molybdenum cofactor biosynthesis protein A	H
284	MMP1589	0.7765	carbamoyl phosphate synthase small subunit	EF
285	MMP1335	0.7546	mevalonate kinase	I
286	MMP0690	0.7452	polyferredoxin	C
287	MMP0955	0.7401	succinyl-CoA synthetase subunit alpha	C
288	MMP0224	0.7329	glutamate-1-semialdehyde aminotransferase	H
289	MMP0815	0.7326	hypothetical protein	P
290	MMP0030	0.7060	MCM family DNA replication protein	L
291	MMP0706	0.6868	NAD binding site:UDP-glucose/GDP-mannose dehydrogenase	M
292	MMP0915	0.6724	nucleoside triphosphate: 5'-deoxyadenosylcobinamide phosphate nucleotidyltransferase	H
293	MMP0634	0.6673	hypothetical protein	V
294	MMP0116	0.6613	N-acetyl-gamma-glutamyl-phosphate reductase	E
295	MMP0057	0.6213	FO synthase subunit 2	HR

296	MMP0013	-0.7180	argininosuccinate lyase	E
297	MMP1455	-0.7371	transmembrane subunit of a hydrogenase	S
298	MMP0006	-0.7543	3-dehydroquinate synthase	E
299	MMP1428	-0.7762	hypothetical protein	U
300	MMP0968	-0.7949	histidinol dehydrogenase	E
301	MMP1211	-0.8073	hypothetical protein	I
302	MMP1700	-0.8373	SSS sodium solute transporter superfamily	ER
303	MMP1447	-0.8508	Cro repressor family protein	KX
304	MMP1479	-0.8568	hypothetical protein	R
305	MMP1593	-0.8612	hypothetical protein	R
306	MMP0133	-0.8654	inosine-5'-monophosphate dehydrogenase	F
307	MMP0374	-0.8676	hypothetical protein	R
308	MMP1217	-0.8933	hypothetical protein	S
309	MMP0231	-0.9437	cysteine-rich small domain	R
310	MMP0991	-0.9667	hypothetical protein	S
311	MMP0186	-0.9723	hypothetical protein	J
312	MMP1712	-0.9728	LysR family transcriptional regulator	K
313	MMP0040	-1.0113	type II secretion system protein E	U
314	MMP0933	-1.0153	response regulator receiver protein	T
315	MMP0219	-1.0156	manganese-dependent inorganic pyrophosphatase	C
316	MMP1362	-1.0185	DNA-directed RNA polymerase subunit B'	K
317	MMP0680	-1.0225	uracil phosphoribosyltransferase	F
318	MMP0607	-1.0250	hypothetical protein	S
319	MMP1695	-1.0281	F420-non-reducing hydrogenase subunit	C
320	MMP0631	-1.0299	iron dependent repressor	K
321	MMP0971	-1.0304	adenylosuccinate lyase	F
322	MMP0901	-1.0343	ATP/GTP-binding motif-containing protein	R
323	MMP1711	-1.0564	proliferating cell nuclear antigen	L
324	MMP1222	-1.0665	DNA repair and recombination protein RadA	L
325	MMP0064	-1.0794	nitrogen regulatory protein P-II	E
326	MMP0255	-1.0879	isoleucyl-tRNA synthetase-like protein	R
327	MMP1427	-1.0943	hypothetical protein	S
328	MMP0396	-1.1211	phosphopyruvate hydratase	G
329	MMP0370	-1.1267	hypothetical protein	S
330	MMP0302	-1.1356	hypothetical protein	S
331	MMP0442	-1.1376	hypothetical protein	S
332	MMP0237	-1.1409	hypothetical protein	S
333	MMP0073	-1.1413	argininosuccinate synthase	E
334	MMP1240	-1.1474	Sep-tRNA:Cys-tRNA synthetase	R
335	MMP0340	-1.1531	pyruvate carboxylase subunit B	C
336	MMP0695	-1.1570	proteasome subunit beta	O
337	MMP1707	-1.1593	translation initiation factor IF-2 subunit alpha	J
338	MMP0654	-1.1597	ketol-acid reductoisomerase	EH
339	MMP1040	-1.1688	V-type ATP synthase subunit K	C
340	MMP0329	-1.1746	hypothetical protein	S
341	MMP1404	-1.1786	30S ribosomal protein S3P	J
342	MMP1502	-1.1826	hypothetical protein	C
343	MMP0317	-1.1965	hypothetical protein	G
344	MMP1696	-1.2028	F420-non-reducing hydrogenase subunit delta	C
345	MMP1583	-1.2109	S-adenosylmethionine decarboxylase-like protein	E
346	MMP1458	-1.2153	hypothetical protein	C
347	MMP0627	-1.2155	50S ribosomal protein L34e	J
348	MMP0440	-1.2221	DNA-directed RNA polymerase subunit E'	K
349	MMP0667	-1.2229	30S ribosomal protein S2	J

350	MMP1391	-1.2229	aspartate-semialdehyde dehydrogenase	E
351	MMP0689	-1.2312	xanthine/uracil permease	R
352	MMP0621	-1.2328	xylose isomerase domain-containing protein	G
353	MMP1504	-1.2423	pyruvate ferredoxin oxidoreductase subunit beta	C
354	MMP1432	-1.2490	adenylosuccinate synthetase	F
355	MMP0854	-1.2513	nitrogen regulatory protein P-II	E
356	MMP1705	-1.2574	creatininase	R
357	MMP0050	-1.2590	6,7-dimethyl-8-ribityllumazine synthase	H
358	MMP0082	-1.2679	glutamate synthase large subunit	E
359	MMP0923	-1.2690	dihydrodipicolinate reductase	E
360	MMP0873	-1.2770	hypothetical protein	U
361	MMP1367	-1.2852	30S ribosomal protein S12P	J
362	MMP1218	-1.2944	hypothetical protein	S
363	MMP1312	-1.2945	hypothetical protein	S
364	MMP0670	-1.3037	hypothetical protein	GER
365	MMP0385	-1.3073	uridylate kinase	F
366	MMP1319	-1.3073	30S ribosomal protein S13P	J
367	MMP0626	-1.3099	cytidylate kinase	F
368	MMP0737	-1.3144	L-aspartate dehydrogenase	R
369	MMP1328	-1.3247	enolase	G
370	MMP1208	-1.3248	translation initiation factor IF-2 subunit gamma	J
371	MMP1646	-1.3250	hypothetical protein	K
372	MMP1263	-1.3327	hypothetical protein	R
373	MMP0060	-1.3431	50S ribosomal protein LX	J
374	MMP0165	-1.3502	ABC transporter	GM
375	MMP0606	-1.3511	ribosomal RNA methyltransferase RrmJ/FtsJ	J
376	MMP1359	-1.3539	hypothetical protein	S
377	MMP0236	-1.3572	hypothetical protein	R
378	MMP0156	-1.3609	30S ribosomal protein S19e	J
379	MMP1329	-1.3672	ferredoxin	C
380	MMP0765	-1.3720	hypothetical protein	S
381	MMP0620	-1.3762	methyl coenzyme M reductase, component A2	R
382	MMP1381	-1.3780	beta-lactamase-like protein	R
383	MMP1439	-1.3825	cofactor-independent phosphoglycerate mutase	G
384	MMP0059	-1.3841	hypothetical protein	S
385	MMP1246	-1.3894	tungsten containing formylmethanofuran dehydrogenase subunit G	C
386	MMP0341	-1.4077	pyruvate carboxylase subunit A	I
387	MMP1223	-1.4113	hypothetical protein	S
388	MMP1212	-1.4223	acetyl-CoA acetyltransferase	I
389	MMP0625	-1.4231	50S ribosomal protein L14e	J
390	MMP1498	-1.4232	hypothetical protein	S
391	MMP0897	-1.4246	bifunctional ornithine acetyltransferase/N-acetylglutamate synthase	E
392	MMP1363	-1.4255	DNA-directed RNA polymerase subunit A'	K
393	MMP0054	-1.4315	hypothetical protein	J
394	MMP1023	-1.4498	TetR family transcriptional regulator	K
395	MMP0041	-1.4736	transcription initiation factor IIB	K
396	MMP0061	-1.4785	translation initiation factor IF-6	J
397	MMP0668	-1.4790	hypothetical protein	R
398	MMP0576	-1.4914	dihydrodipicolinate synthase	EM
399	MMP0344	-1.4920	hypothetical protein	S
400	MMP0098	-1.5036	ferredoxin	C

401	MMP1704	-1.5138	hypothetical protein	K
402	MMP0540	-1.5142	phosphoribosylaminoimidazole-succinocarboxamide synthase	F
403	MMP0081	-1.5221	glutamate synthase large subunit	E
404	MMP0887	-1.5336	stress responsive alpha-beta barrel domain-containing protein	S
405	MMP0597	-1.5373	fibrillarin	J
406	MMP0194	-1.5488	hypothetical protein	S
407	MMP0044	-1.5512	beta-lactamase domain-containing protein	R
408	MMP1470	-1.5558	prefoldin subunit alpha	O
409	MMP0937	-1.5563	F420-0--gamma-glutamyl ligase	S
410	MMP1579	-1.5660	30S ribosomal protein S15P	J
411	MMP0051	-1.5803	phosphoribosyl-ATP pyrophosphatase	E
412	MMP0163	-1.5882	arsenite-activated ATPase ArsA	P
413	MMP1546	-1.5892	50S ribosomal protein L2P	J
414	MMP1104	-1.5974	aspartate carbamoyltransferase regulatory subunit	F
415	MMP1709	-1.6033	50S ribosomal protein L44e	J
416	MMP0153	-1.6242	trans-homoaconitate synthase	E
417	MMP1563	-1.6253	tetrahydromethanopterin S-methyltransferase subunit B	H
418	MMP1541	-1.6382	hypothetical protein	S
419	MMP1370	-1.6386	elongation factor 1-alpha	J
420	MMP1326	-1.6390	DNA-directed RNA polymerase subunit N	K
421	MMP1444	-1.6455	methionine aminopeptidase	J
422	MMP1310	-1.6457	IMP cyclohydrolase	F
423	MMP0658	-1.6478	MoaA/nifB/pqqE family protein	R
424	MMP1684	-1.6651	metallophosphoesterase	R
425	MMP1403	-1.6701	50S ribosomal protein L22P	J
426	MMP1369	-1.6809	elongation factor EF-2	J
427	MMP1547	-1.6895	30S ribosomal protein S19P	J
428	MMP0480	-1.6908	hypothetical protein	K
429	MMP1721	-1.7075	hypothetical protein	D
430	MMP1368	-1.7089	30S ribosomal protein S7P	J
431	MMP0383	-1.7239	S-layer protein	M
432	MMP1206	-1.7507	glutamine synthetase	E
433	MMP0574	-1.7530	hypothetical protein	S
434	MMP1358	-1.7579	ferredoxin	C
435	MMP1683	-1.7627	hypothetical protein	S
436	MMP1410	-1.7781	50S ribosomal protein L24P	J
437	MMP1433	-1.7843	50S ribosomal protein L11P	J
438	MMP0157	-1.7929	hypothetical protein	R
439	MMP1045	-1.7969	V-type ATP synthase subunit B	C
440	MMP0298	-1.8304	50S ribosomal protein L15e	J
441	MMP0164	-1.8560	sirohydrochlorin cobaltochelatase	H
442	MMP1720	-1.8699	hypothetical protein	S
443	MMP0083	-1.8703	coenzyme F420 hydrogenase/dehydrogenase subunit beta domain-containing protein	C
444	MMP0152	-1.8713	citrate transporter	P
445	MMP1513	-1.8790	alanine dehydrogenase	E
446	MMP1261	-1.9088	hypothetical protein	S
447	MMP1042	-1.9221	V-type ATP synthase subunit C	C
448	MMP0029	-1.9308	hypothetical protein	S
449	MMP1565	-1.9598	tetrahydromethanopterin S-methyltransferase subunit A	H
450	MMP0022	-1.9768	hypothetical protein	S
451	MMP1632	-2.0170	glutamate-binding protein	ET
452	MMP1043	-2.0210	V-type ATP synthase subunit F	C

453	MMP1411	-2.0419	30S ribosomal protein S4e	J
454	MMP0045	-2.0441	bifunctional short chain isoprenyl diphosphate synthase	H
455	MMP1044	-2.0586	V-type ATP synthase subunit A	C
456	MMP1512	-2.0834	alanine racemase	M
457	MMP0250	-2.0889	RNA-associated protein	J
458	MMP0158	-2.1360	hypothetical protein	J
459	MMP0303	-2.1461	rubredoxin-type Fe(Cys)4 protein	C
460	MMP1320	-2.1861	30S ribosomal protein S4P	J
461	MMP1416	-2.1964	50S ribosomal protein L32e	J
462	MMP1046	-2.2069	V-type ATP synthase subunit D	C
463	MMP0669	-2.2109	30S ribosomal protein S3Ae	J
464	MMP1325	-2.2135	30S ribosomal protein S9P	J
465	MMP1137	-2.2155	Lrp/AsnC family transcriptional regulator	K
466	MMP1708	-2.2330	30S ribosomal protein S27e	J
467	MMP1556	-2.2367	methyl-coenzyme M reductase I, protein D	H
468	MMP0166	-2.2384	MATE family drug/sodium antiporter	V
469	*MMP0686*	-2.2588	fructose-bisphosphate aldolase	G
470	MMP1259	-2.2661	FAD-dependent pyridine nucleotide-disulfide oxidoreductase	R
471	MMP0251	-2.2798	proteasome subunit alpha	O
472	MMP1566	-2.3078	tetrahydromethanopterin S-methyltransferase subunit G	H
473	MMP0025	-2.3230	hypothetical protein	S
474	MMP1260	-2.3519	hypothetical protein	P
475	MMP1321	-2.3567	30S ribosomal protein S11P	J
476	MMP1324	-2.3718	50S ribosomal protein L13P	J
477	MMP1247	-2.3872	tungsten containing formylmethanofuran dehydrogenase subunit D	C
478	MMP0962	-2.3974	zinc finger protein	S
479	MMP0168	-2.4002	ParR family transcriptional regulator	K
480	MMP1609	-2.4071	formylmethanofuran--tetrahydromethanopterin formyltransferase	C
481	MMP1418	-2.4293	50S ribosomal protein L18P	J
482	MMP1322	-2.4296	DNA-directed RNA polymerase subunit D	K
483	MMP1558	-2.4314	methyl-coenzyme M reductase I subunit gamma	H
484	MMP0961	-2.4368	hypothetical protein	S
485	MMP0407	-2.5039	hypothetical protein	R
486	MMP1047	-2.5075	hypothetical protein	S
487	MMP0585	-2.5161	UspA domain-containing protein	T
488	MMP0260	-2.5163	50S ribosomal protein L1P	J
489	MMP1248	-2.5558	tungsten containing formylmethanofuran dehydrogenase subunit A	C
490	MMP1559	-2.5733	methyl-coenzyme M reductase I subunit alpha	H
491	MMP1174	-2.5809	peroxiredoxin	O
492	MMP1413	-2.5813	30S ribosomal protein S14P	J
493	MMP0372	-2.5854	F420-dependent methylenetetrahydromethanopterin dehydrogenase	C
494	MMP1414	-2.6143	30S ribosomal protein S8P	J
495	MMP1417	-2.6187	50S ribosomal protein L19e	J
496	MMP1323	-2.6254	50S ribosomal protein L18e	J
497	MMP1412	-2.6311	50S ribosomal protein L5P	J
498	MMP0159	-2.6541	50S ribosomal protein L39e	J
499	MMP0639	-2.6544	50S ribosomal protein L24e	J
500	MMP0181	-2.6591	hypothetical protein	M

501	MMP1249	-2.6690	tungsten containing formylmethanofuran dehydrogenase subunit C	C
502	MMP0248	-2.6769	DNA-directed RNA polymerase-like protein	K
503	MMP1188	-2.7398	hypothetical protein	S
504	MMP0259	-2.7677	acidic ribosomal protein P0	J
505	MMP0640	-2.7762	30S ribosomal protein S28e	J
506	MMP0182	-2.7841	hypothetical protein	S
507	MMP1635	-2.7942	redox-active disulfide protein 1	C
508	MMP1158	-2.8084	hypothetical protein	S
509	MMP1415	-2.8501	50S ribosomal protein L6P	J
510	MMP0651	-2.8716	acetolactate synthase 3 regulatory subunit	E
511	MMP0249	-2.8724	50S ribosomal protein L37Ae	J
512	MMP1347	-2.8826	histone B	B
513	MMP0575	-2.9084	aspartyl/glutamyl-tRNA amidotransferase subunit C	J
514	MMP1156	-2.9150	carboxymuconolactone decarboxylase	S
515	MMP1155	-2.9187	heterosulfide reductase subunit B1	C
516	MMP0823	-2.9767	coenzyme F420-non-reducing hydrogenase subunit alpha	C
517	MMP1054	-2.9852	heterodisulfide reductase subunit C2	C
518	MMP1160	-3.0832	hypothetical protein	C
519	MMP0258	-3.1408	50S ribosomal protein L12P	J
520	MMP0630	-3.1607	ferrous iron transporter	P
521	MMP0127	-3.2063	H(2)-dependent methylenetetrahydromethanopterin dehydrogenase	C
522	MMP0817	-3.3086	coenzyme F420-reducing hydrogenase subunit beta	C
523	MMP1053	-3.3131	heterodisulfide reductase subunit B2	C
524	MMP1637	-3.4793	hypothetical protein	S
525	MMP0709	-3.5657	hypothetical protein	R
526	MMP0822	-3.6208	coenzyme F420-non-reducing hydrogenase subunit gamma	C
527	MMP1421	-3.6697	50S ribosomal protein L15P	J
528	MMP1419	-3.6698	30S ribosomal protein S5P	J
529	MMP0058	-3.7993	methylenetetrahydromethanopterin reductase	C
530	MMP0824	-4.0296	coenzyme F420-non-reducing hydrogenase subunit beta	C
531	MMP0692	-4.0390	hypothetical protein	M
532	MMP1136	-4.0834	rubrerythrin	C
533	MMP1420	-4.2399	50S ribosomal protein L30P	J
534	MMP1302	-4.6791	hypothetical protein	R
535	MMP0825	-5.1294	heterodisulfide reductase subunit A	C

Mmp:	All Significant CCBF	Unique to BF
Up-Expressed	336	285
Down-Expressed	434	238
TOTAL	*787	*535

*includes all significant genes without expression cut-off

> 2 LogFC		28
< -2 LogFC		90

CHAPTER THREE

ACTIVITY PARTITIONING IN AN ARCHAEAL-BACTERIAL BIOFILM

Contribution of Authors and Co-Authors

Manuscript in Chapter 3

Author: Laura B. Camilleri

Contributions: Developed experimental design, performed experiments, analyzed data, wrote and revised the manuscript.

Co-Author: B.P. Bowen

Contributions: Determined deuterated fraction of proteome.

Co-Author: C.J. Petzold

Contributions: Performed proteomic analysis.

Co-Author: T.R. Northen

Contributions: P.I. for proteomic analysis.

Co-Author: Matthew W. Fields

Contributions: Developed experimental design, analyzed data, wrote and revised the manuscript.

Manuscript Information

Laura B. Camilleri, B.P. Bowen, C.J. Petzold, T.R. Northen, and M.W. Fields

Letters in Applied Microbiology

Status of Manuscript:
__x__ Prepared for submission to a peer-reviewed journal
_____ Officially submitted to a peer-reviewed journal
_____ Accepted by a peer-reviewed journal
_____ Published in a peer-reviewed journal

ABSTRACT

In the absence of sulfate as an electron acceptor and the addition of the hydrogenotrophic methanogen, *Desulfovibrio vulgaris* Hildenborough and *Methanococcus maripaludis* can form a cooperative syntrophic relationship. The syntrophy between sulfate-reducing bacteria and methanogenic archaea is of interest because both these guilds play crucial roles in many different anaerobic environments. In monocultures, only *D. vulgaris* Hildenborough readily forms biofilm; however, the co-culture biofilm is evenly interspersed with *M. maripaludis*, and is thicker and filled with topographical features such as ridges, spires, and valleys. To better understand the interactions between *M. maripaludis* and *D. vulgaris* Hildenborough and the impact on function, deuterium-labeled proteomics and BONCAT microscopy were used to delineate activity states of the two biofilm populations. Deuterium-labeled proteins were observed in both populations, and the *D. vulgaris* labeled proteins were enriched for carbon oxidation and electron transfer while the *M. maripaludis* proteins were strongly enriched in carbon dioxide processing and methane generation. Interestingly, BONCAT labeling was observed for both organisms grown as monocultures; however, under co-culture biofilm conditions, only *D. vulgaris* was detected to be BONCAT active, yet methane was being actively produced. The data suggest that during co-culture growth, *D. vulgaris* and *M. maripaludis* have altered levels of respective cellular activity that results in streamlined specialization with respect to lactate-oxidation and methane-generation. The results suggest that an interdomain mutualistic biofilm partitions activity to optimize carbon processing and energy conservation and could have implications for bacterial-archaeal interactions that have evolved at the lower limits of thermodynamic energy conservation.

INTRODUCTION

Communities of microorganisms are believed to primarily exist in the environment adhered to a surface or as an aggregation referred to as a biofilm due to the intrinsic biotic and abiotic advantages conferred by this mode of growth. Biofilms are typically complex webs of multiple species that communicate by chemical signaling and can structure themselves depending on the synergistic and antagonistic interactions of the members (Momeni et al., 2013). Biofilms are heterogenous, yet structured, microbial communities that can represent relevant systems to understand emergent properties of metabolic interactions. A growing interest in biofilm science is the consequence of dynamic biofilm behavior in relation to metabolic and cross species interactions, namely structure-function relationships at different spatial and temporal scales.

The structure and function of multispecies biofilms can be more complex than monoculture biofilms. We have recently shown that the structure of a mixed biofilm community is dependent upon the nature of the interactions (*i.e.*, cooperative or competitive) and that the degree of intermixing of two-member communities is greater under cooperation versus competition (Momeni et al., 2013). Despite the ubiquity of biofilms and importance of anaerobes, little work has been done to understand how biofilm structure affects function in anaerobic microbial communities (Bernstein et al., 2012; Brenner & Arnold, 2011; Nielsen et al., 2000; Raskin et al., 1996). While interactions between SRB and methanogens have been studied for decades, very little has been done to characterize the emergent properties of interactive populations in anaerobic biofilms, particularly in the context of interdomain, linked metabolism and activity.

Experiments that aim to assess microbial community activity can use a variety of -omic techniques, and a dependable marker of microbial activity is protein expression, as it has been reported that mRNA and protein expression of the same gene can be uncorrelated (Binder & Liu, 1998; Bollmann et al., 2005; Foster et al., 2009; Morgenroth et al., 2000; Oda et al., 2000; Schmid et al., 2001; Taniguchi et al., 2010; Wagner et al., 1995). Traditional methods of measuring protein synthesis require the use of stable isotope labeling, which is an indirect measure of overall cellular activity, and can sometimes be limited by available substrates. Protein synthesis can also be measured using deuterium oxide (^2H_2O). Deuterons (^2H) can rapidly replace protons (H) of active or newly synthesized proteins and provide a mass shift that is readily measured by peptide identifications by liquid chromatography-mass spectrometry (LC-MS). Additionally, deuterium oxide is generally regarded as being less harmful as routine enrichments of 5% heavy water in rodents provided no change in normal physiology, making it ideal for *in situ* incubations (Busch et al., 2007; De Riva et al., 2010).

A newer method for analyzing functional protein synthesis is to utilize bioorthogonal noncanonical amino acid tagging or BONCAT (Hatzenpichler et al., 2016). Bioorthogonal compounds are analogs of native biomolecules (*e.g.*, amino acids, nucleotides, lipids) with a functional group that can be conjugated to fluorescence dyes via click chemistry. Homopropargylglycine (HPG) is a bioorthogonal surrogate for the amino acid methionine and is advantageous because no genetic modification of the host cell is needed. After cells are exposed, a selective click chemistry detectable reaction allows direct microscopic visualization of new protein synthesis that occurred during the incubation (Dieterich et al., 2006; Hatzenpichler et al., 2014).

Previously, an archaeal-bacterial biofilm between *Methanococcus maripaludis* S2 (Mmp) and *Desulfovibrio vulgaris* Hildenborough (DvH) optimized carrying capacity as defined by biomass yield per mass flux of lactate or methane (Brileya et al., 2014b). Previous results suggest that the multispecies biofilm creates an environment conducive to resource sharing that increases the carrying capacity for cooperative populations, but it is unknown how this is accomplished. Due to the unique physiology of the biofilm and the physical facilitation of interactions between the two species from close proximity, we wanted to determine the respective metabolic activity of the two populations during biofilm establishment. Here we explore an alternate approach with the use of heavy water (deuterium oxide; ^2H_2O) for nonspecific protein labeling in which rates of activity within the syntrophic co-culture were extrapolated, as well as the first use of BONCAT (to the authors' knowledge) in a co-culture biofilm to visualize translational activity within the system.

MATERIALS AND METHODS

Culture Conditions

Desulfovibrio vulgaris Hildenborough and *Methanococcus maripaludis* S2 were anaerobically cultivated as previously described in co-culture medium (CCM) with 80%

N_2: 20% CO_2 sparged headspace at 30°C and shaking at 125 rpm (Brileya et al., 2014b). Addition of 30 mM sulfate to serum bottles was used for batch, planktonic, monocultures of *D. vulgaris* Hildenborough. Whereas, addition of 30 mM acetate instead of lactate, along with an over pressurization of 80% H_2: 20% CO_2 gas to 200 kPa, was used for batch, planktonic, monocultures of *M. maripaludis* grown in serum bottles. Glass slides were used to cultivate co-culture biofilm on in a modified, continuously stirred, 1 L CDC reactor and samples were analyzed for optical density, protein, lactate, and acetate as previously described (Brileya et al., 2014b; Clark et al., 2006, 2012).

Deuterium Oxide Addition

The culture medium and individual reactors were enriched to a final concentration (vol/vol) of 5% deuterium oxide (^2H_2O) by the addition of 99% (mol/mol) ^2H_2O (Cambridge Isotope Laboratories) (Figure 1). The continuously stirred biofilm reactor system containing the co-culture was destructively harvested from replicate reactors. Samples were collected before enrichment for a base deuterium level (Time 0), 24 hours after deuterium oxide addition, and 48 hours post-addition. The biofilm samples were similarly collected for two separate deuterium addition experiments, for the early stage of initial biofilm development at 96 hours and the late stage in which acetate and methane generation was in steady state (312 h). Samples were collected from the planktonic portion of the reactors and sent to Metabolic Solutions Inc. for deuterium concentration analysis.

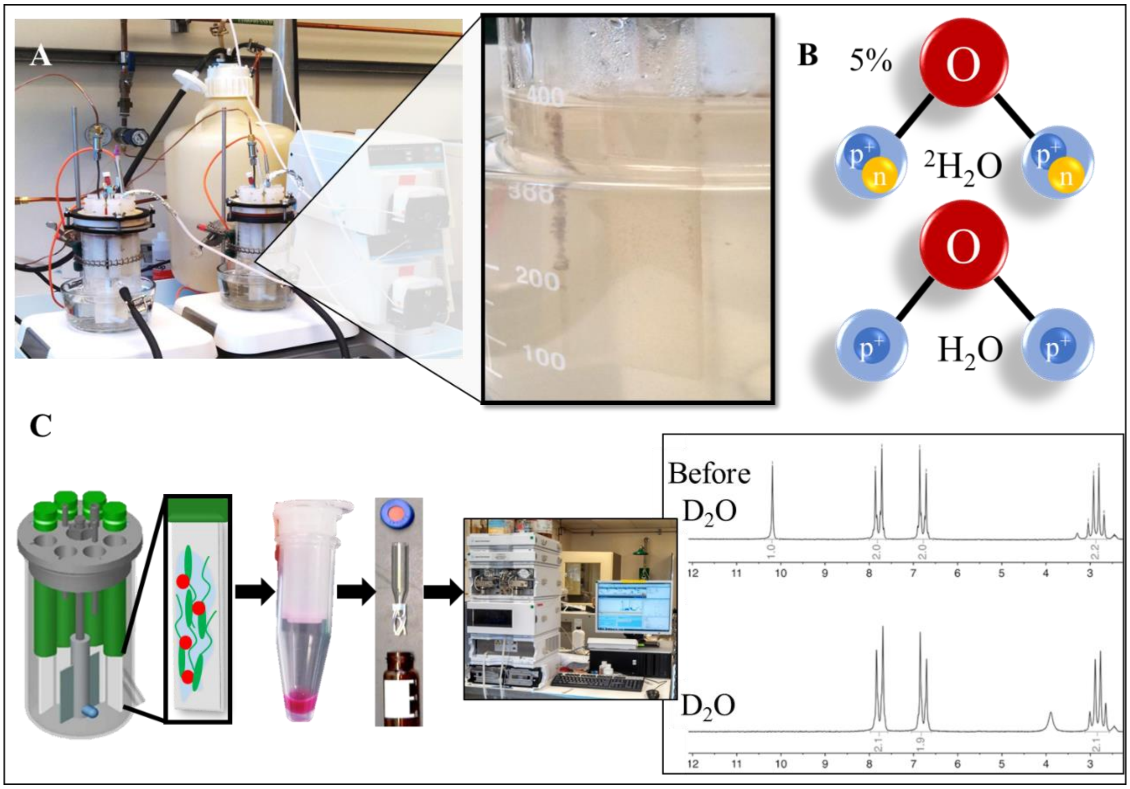

Figure 1. Deuterium oxide workflow for the co-culture biofilm reactors. (A) Anaerobic co-culture biofilm reactor setup with glass slides for biofilm attachment (B) Deuterium oxide (D_2O or ^2H_2O) was added at 5% (vol/vol) during the Early Stage (96 h) and Late Stage (312 h) biofilm development (C) Co-culture biofilm was harvested at 24 and 48 hours after D_2O addition, methanol extracted, and ran on LC-MS. The methanol extracted pellet was analyzed for proteomics and mass shifts were tracked.

Deuterium Proteomic Analysis

For proteomic analysis, pellets from the co-culture experiments were prepared as described previously (González Fernández-Niño et al., 2015). Briefly, chloroform/methanol precipitation was used to lyse co-culture cell pellets and extract proteins. The protein pellet was resuspended in 100 mM AMBIC with 20% acetonitrile and reduced with tris(2-carboxyethyl)phosphine (TCEP) for 30 mins, followed by addition of iodoacetamide (IAA; final conc. 10 mM) for 30 mins in the dark, and then digested overnight with MS-grade trypsin (1:50 w/w trypsin: protein) at 37°C. Peptides were stored at -20°C until analysis.

Identification of peptides and determination of the peptide retention times (RT) from the co-culture samples were analyzed on an Agilent 1290 UHPLC - 6550 QTOF liquid chromatography mass spectrometer (LC-MS/MS; Agilent Technologies) system in Auto-MS/MS mode and the operating parameters for the LC-MS/MS system were described previously (González Fernández-Niño et al., 2015). Forty (40) µg of peptides were separated on a Sigma-Aldrich Ascentis Express Peptide ES-C18 column (2.1 mm x 100 mm, 2.7 µm particle size, operated at 60°C) and a flow rate of 0.4 mL/min. The chromatography gradient conditions were as follows: from the initial starting condition (95% buffer A (100% water, 0.1% formic acid) and 5% buffer B (100% acetonitrile, 0.1% formic acid)) the buffer B composition was increased to 35% over 120 min; then buffer B was increased to 80% over 3 min and held for 7 min, followed by a ramp back down to 5% B over 1 min where it was held for 6 min to re-equilibrate the column to the original conditions. Data were analyzed with the Mascot search engine version 2.3.02 (Matrix Science), the data were searched against a combined *Desulfovibrio vulgaris* Hildenborough and *Methanococcus maripaludis* database that also includes common lab contaminants. The Mascot results were curated and validated by using Scaffold (Proteome Software Inc., Seattle, WA) as described previously (González Fernández-Niño et al., 2015). For co-culture samples labeled with D_2O, accurate quantification of incorporation of the deuterium atoms in the peptides was achieved by operating the Agilent 1290 UHPLC - 6550 QTOF in MS mode with identical chromatography conditions to the shotgun proteomic analysis described above. Peptides were identified by matching the accurate mass of the mono-isotopic peptide ion and RT with the identified peptides from the shotgun proteomic analysis.

Bioorthogonal Noncanonical Amino Acid Tagging (BONCAT) and rRNA-targeted FISH

All BONCAT experiments were conducted either in triplicate batch conditions or duplicate continuously stirred reactor conditions. The L-methionine surrogate L-homopropargylglycine (HPG) was used for BONCAT labeling and added post-inoculation (9 h) for batch co-cultures and 312 hours for the biofilm reactors. A separate co-culture was also used for a short-term (2 min) incubation of an actively growing sub-sample with 50 µM HPG to check for labeling. The planktonic batch co-culture samples with 50 µM HPG were collected before addition (T=0), 4 h, 12 h, 16 h, 18 h, 24 h, 48 h, and 96 h after addition then fixed and stored at 4°C until microscopy was done. The co-culture biofilm had samples harvested before 50 µM HPG addition for a T=0, 24 h, 48 h, and 72 h before being fixed and stored. After harvesting, samples were fixed in 4% paraformaldehyde, according to the fluorescence *in situ* hybridization (FISH) and 3D-FISH protocols to visualize the intact or scraped biofilm as previously described (Brileya et al., 2014a; Brileya et al., 2014b). Absorbance readings (600 nm) were taken over time from planktonic cultures incubated with HPG concentrations of 50 µM and 200 µM for batch mono- and co- cultures. Additionally, the uridine analogue 5-ethynyl-2’-deoxyuridine (EdU) was tested as a proxy for DNA synthesis in mono- and co-cultures.

To fluorescently label the respective populations undergoing active protein synthesis, the BONCAT-FISH protocol using the domain specific FISH probes EUB338-Cy3 and ARCH915-Cy5 and Cu(I)-catalyzed conjugation of HPG with an azide dye was used (Brileya et al., 2014b; Hatzenpichler & Orphan, 2015). BONCAT-FISH was performed following the protocol of Hatzenpichler and Orphan (Hatzenpichler & Orphan, 2015) and Hatzenpichler et al. (Hatzenpichler et al., 2014). Fixed biomass was immobilized on Teflon-coated glass slides and dried at 46°C. An increasing ethanol series [50%, 80%, and 96% ethanol in double-distilled water (ddH_2O)] was performed, and the slides were air dried. Solutions were prepared as described (Hatzenpichler & Orphan, 2015), and the reagents were always freshly mixed. This solution contained 5 mM sodium ascorbate (Sigma-Aldrich), 5 mM amino-guanidine hydrochloride (Sigma-Aldrich), 500 µM Tris[(1-hydroxypropyl-1H-1,2,3-triazol-4-yl)methyl]amine (THPTA; Click Chemistry Tools), 100 µM CuSO4 (Sigma-Aldrich), and 2 µM of azide-modified dye carboxyrhodamine 110 (CR-110; Click Chemistry Tools) in 0.2-µm-filtered 1× PBS, pH 7.4; 20 µL of this solution was applied on top of the biomass, and the glass slides were incubated for 45 min at room temperature (RT) in a dark humid chamber. Afterward, slides were washed three times in 1× PBS and an increasing ethanol series (50%, 80%, and 96%), before beginning the FISH protocol (Brileya et al., 2014b). The samples were mounted with Citifluor AF-1 antifading solution (Electron Microscopy Sciences) and were analyzed with a Leica TCS SP5 II inverted confocal laser scanning microscope with 488, 561, and 633 nm lasers and appropriate filter sets.

RESULTS

Biofilm Growth

Under the tested growth conditions, the continuous culture biofilm reactor displayed exponential growth in the planktonic phase for the first approximate 150 h as lactate is consumed and equimolar levels of acetate were produced (Figure 2). The lactate and acetate level approach steady-state levels at approximately 245 h. As previously reported, the biofilm is considered at an early stage of development between 50 and 150 h, intermediate between 150 h and 250 h, and mature or late biofilm after 250 h (Brileya et al., 2014b). For the labeled proteomics samples, biofilm samples were harvested at 96 h (“early”) and 312 h (“late”).

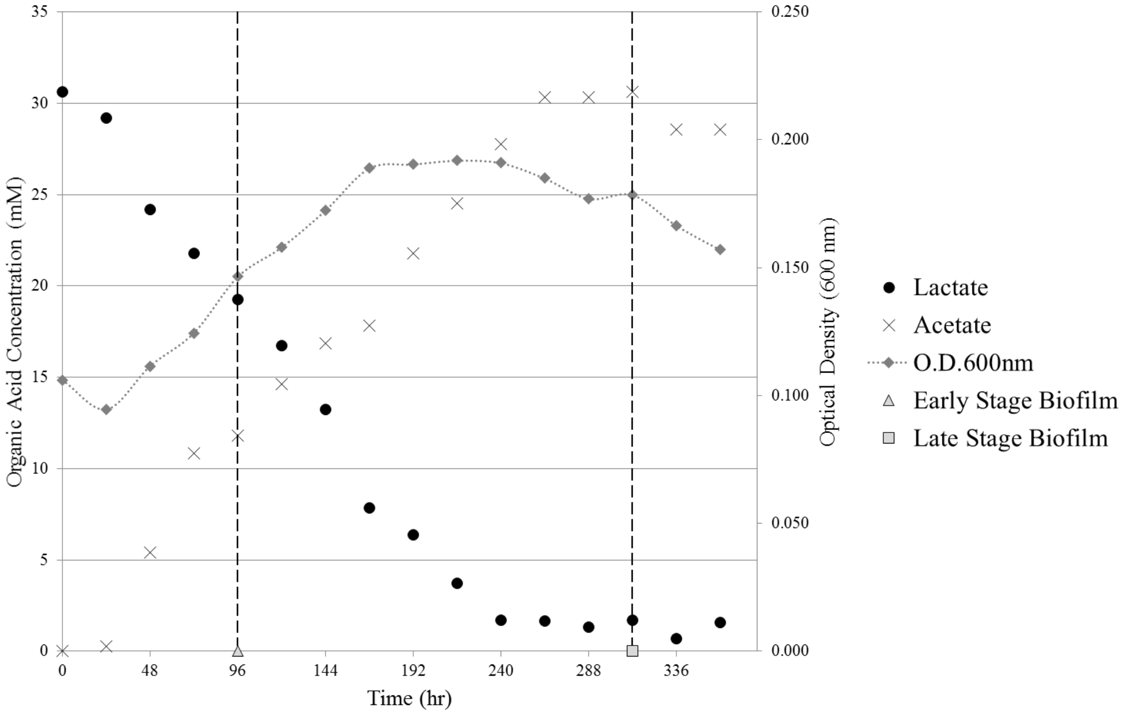

Figure 2. Co-culture biofilm reactor sample analysis over time. Planktonic samples were collected every 24 h for organic acid quantification (Lactate and Acetate) and planktonic optical density (O.D.$_{600nm}$). Typical lactate consumption followed by proportional acetate production is depicted. Deuterium oxide (D_2O or ^2H_2O) was added to the respective co-culture reactors during Early Stage biofilm development at 96 h (shown by the dotted line) as lactate is being depleted, and Late Stage biofilm development at 312 h (shown by the dotted line) when the reactor stabilizes.

Deuterated Proteomics

The deuterated peptides identified in *D. vulgaris* could be assigned to 184 different proteins, whereas only 23 proteins could be assigned to *M. maripaludis*. Among the identified polypeptides in *D. vulgaris* were putative proteins involved in carbon utilization that included acetate kinase (DVU3030), acetolactate synthase (DVU1612), alcohol dehydrogenase (DVU2201 and DVU2405), and lactate permease (DVU3026) (Figure 3). Putative proteins in energy conservation included adenylate kinase

(DVU1932), adenylyl sulfate reductase (DVU0846-7), carbon monoxide induced hydrogenase (DVU2291, DVU2287-8, DVU2401, DVU2399), cytochrome c nitrite reductase (DVU0625), dissimilatory sulfite reductase (DVU0402-4, DVU2776, DVU1289), formate dehydrogenase (DVU0577), heterodisulfide reductase (DVU2402-4), NiFe hydrogenase (DVU1922), NiFeSe hydrogenase (DVU1918). Putative proteins involved in general stress response included carbon starvation protein (DVU0598), chemotaxis proteins (DVU2072, DVU0992, DVU1904), and universal stress proteins (DVU0423, DVU2100, DVU1030, DVU0893). Presumptive proteins with unknown function included conserved hypotheticals (DVU2077, DVUA0116, DVU2398, DVU3032, DVU0797, DVU2938). In addition, specific to amino acid production and/or utilization, labeled polypeptides were detected for 23 presumptive proteins (Table 1). These included putative transporters/porins (n=10) or enzymes involved in biosynthesis/utilization (n=13).

Organism	GeneID	Description
Desulfovibrio vulgaris Hildenborough		
	DVU0107, DVU0169, DVU0386, DVU0547, DVU0675, DVU0712, DVU0716, DVU0966, DVU1238, DVU2297	ABC-type amino acid transport/signal transduction systems
	DVU1377	acetolactate synthase, small subunit (TIGR)
	DVU3048	aspartate-semialdehyde dehydrogenase (TIGR)
	DVU2982	3-isopropylmalate dehydratase, large subunit, putative (TIGR)
	DVU1203	serine hydroxymethyltransferase (TIGR)
	DVU1425-6	glycine cleavage system protein (TIGR)
	DVU0278	glyoxalase family protein (TIGR)
	DVU0418	saccharopine dehydrogenase (TIGR)
	DVU1378	ketol-acid reductoisomerase (TIGR)
	DVU3373	dihydroxy-acid dehydratase (TIGR)
	DVU3197	branched-chain amino acid aminotransferase (TIGR)
	DVU1655	aminotransferase, classes I and II (TIGR)
	DVU1612	ACT domain protein

Table 1. Deuterated amino acid peptides identified from the co-culture biofilm. *D. vulgaris* peptides that were deuterium labeled in the co-culture biofilm and function in amino acid production, utilization, or transport.

M. maripaludis had a more limited array of polypeptides that were identified (Table 2). This could be due to a dilution bias from the higher ratio of *D. vulgaris* to *M. maripaludis* present and/or different synthesis rates/protein half-lives. Similar to previous results, the “early” biofilm (96 h) had a population ratio that was approximately 4:1 (DvH: Mmp) and approximately 2.3:1 (DvH: Mmp) at the “late” biofilm time point (312 h). The labeled putative proteins for *M. maripaludis* that were identified were predominantly involved with carbon and electron flow for methanogenesis and included coenzyme F420 reducing hydrogenases, methylenetetrahydromethanopterin dehydrogenases (MMP0058, MMP1382, MMP1384, MMP0372), formate transporter

(MMP1301), methyl coenzyme M reductase I (MMP1559, MMP1555, MMP1558), and methyltetrahydromethanopterin methyltransferase (MMP1565-7) (Figure 3). Similar to *D. vulgaris*, several labeled polypeptides were predicted to be involved with amino acid metabolism and included alanine dehydrogenase (MMP1513) and a GMP synthase (glutamine hydrolyzing, MMP0894). In addition, *M. maripaludis* had several putative proteins predicted to be involved in DNA- and protein-processing including archaeal histones A and B (MMP0386, MMP1347) and proteasome subunit A (MMP0251).

Organism	GeneID	Description
Methanococcus maripaludis S2		
	MMP1045	A1A0 ATPase, subunit B (NCBI)
	MMP1513	alanine dehydrogenase (NCBI)
	MMP0386	archaeal histone A (NCBI)
	MMP1347	archaeal histone B (NCBI)
	MMP1515	Chaperonin GroEL (thermosome, HSP60 family) (NCBI)
	MMP0058	coenzyme F420-dependent N5,N10-methylenetetrahydromethanopterin reductase (NCBI)
	MMP1382	coenzyme F420-reducing hydrogenase subunit alpha (NCBI)
	MMP1384	coenzyme F420-reducing hydrogenase subunit gamma (NCBI)
	MMP0372	F420-dependent methylenetetrahydromethanopterin dehydrogenase (NCBI)
	MMP1301	Formate transporter (NCBI)
	MMP0894	GMP synthase (glutamine-hydrolyzing). (NCBI)
	MMP0258	LSU ribosomal protein L12A (NCBI)
	MMP1559	Methyl-coenzyme M reductase I, alpha subunit (NCBI)
	MMP1555	Methyl-coenzyme M reductase I, beta subunit (NCBI)
	MMP1558	Methyl-coenzyme M reductase I, gamma subunit (NCBI)
	MMP1565	N5-methyltetrahydromethanopterin: methyltransferase, subunit A and F related protein (NCBI)
	MMP1566	N5-methyltetrahydromethanopterin: methyltransferase, subunit G (NCBI)
	MMP1567	N5-methyltetrahydromethanopterin: methyltransferase, subunit H (NCBI)
	MMP0251	proteasome, subunit alpha (NCBI)
	MMP0383	S-layer protein (NCBI)
	MMP0443	SSU ribosomal protein S24E (NCBI)
	MMP1370	translation elongation factor EF-1, subunit alpha (NCBI)

Table 2. Deuterated peptides from *M. maripaludis* that were identified as being actively made (labeled) in the co-culture biofilm.

The incorporated deuterium amount was calculated for *M. maripaludis* and *D. vulgaris* Hildenborough for the early stage and late stage biofilm samples, as previously defined by flux of lactate to methane. Overall, the fraction of newly synthesized proteins for key metabolic enzymes identified for *M. maripaludis* showed a much higher level of deuterium incorporation as compared to *D. vulgaris* Hildenborough during the late stage biofilm (Figure 3). Additionally, there was a significant increase in the total amount of deuterium that was incorporated into newly made proteins for *M. maripaludis* in the late stage biofilm development as compared to the early stage biofilm. This is not surprising since the biofilm formation is initiated by *D. vulgaris* Hildenborough and the methanogen incorporates into the biofilm until the biofilm community ratio becomes stable and more even compared to early biofilm development stages (Brileya et al., 2014b).

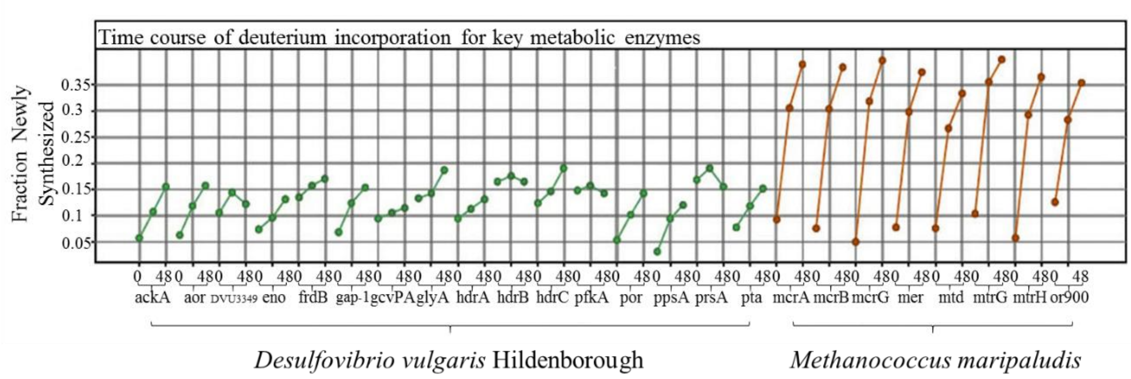

Figure 3. Deuterium incorporation for key proteins over 48 h. The deuterium incorporation for the fraction of newly synthesized proteins as defined by percent deuterium incorporation (x-axis) at time 0 h, 24 h, and 48 h related to peptides for energy production for both *D. vulgaris* and *M. maripaludis* in the late stage of co-culture biofilm development is depicted. *M. maripaludis* has greater deuterium incorporation overall as compared to *D. vulgaris* in the late stage.

D. vulgaris Hildenborough exhibited relatively similar levels of deuterium incorporation for both the early and late stage biofilm development overall. Interestingly, the two organisms show similar deuterium half-saturation times during the early stage biofilm sampling (Figure 3 and 4). During the late stage biofilm, *M. maripaludis* retained a deuterium half-saturation time of around 50 hours, but *D. vulgaris* Hildenborough had a markedly increased half-saturation time of approximately 300 hours. These results suggested that the activity of *D. vulgaris* Hildenborough was slower in the mature biofilm while the methanogen appeared to be at least maintaining protein synthesis, albeit for a select group of detected proteins. To test the accuracy of this hypothesis we employed the use of BONCAT for planktonic batch mono- and co-cultures as well as a co-culture biofilm reactor system to ascertain translational activity for both populations.

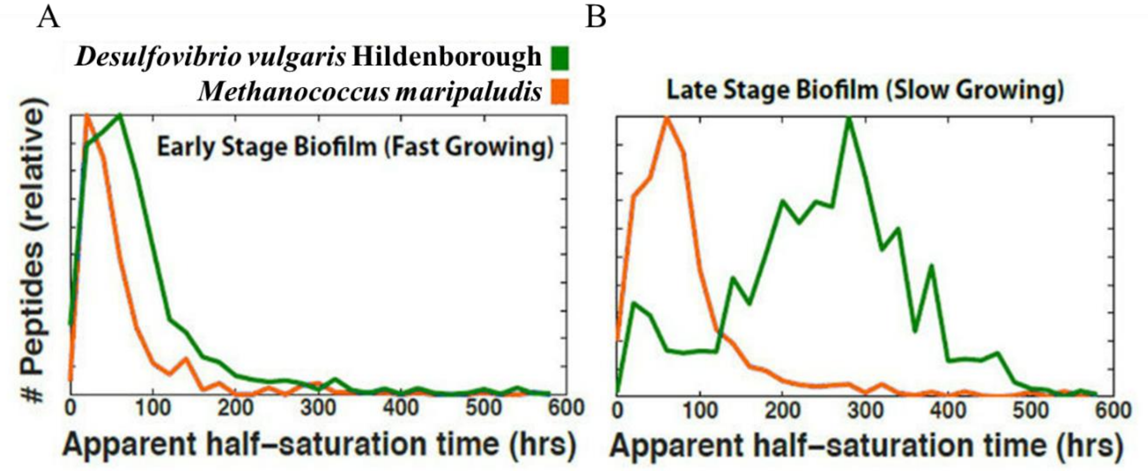

Figure 4. Deuterium incorporation in newly made peptides for each organism in the co-culture biofilm plotted as a rate. (A) The time required for 50% deuterium incorporation to occur in *M. maripaludis* and *D. vulgaris* peptides was less than ~100 h in early stage co-culture biofilm development. (B) In the late stage biofilm, *D. vulgaris* increases peptide deuterium incorporation to ~300 h while *M. maripaludis* stays around ~100 h.

BONCAT – FISH of mono- and co-cultures

Based on previous results with HPG, cells grown with 50 µM HPG were visualized after click chemistry preparations (Hatzenpichler et al., 2014). Monoculture *D. vulgaris* cells could be visualized with BONCAT labeling, and the majority of cells were labeled (Figure 5A). In addition, BONCAT labeled *D. vulgaris* cells could then be visualized with FISH probes (Figure 5B). Likewise, monoculture *M. maripaludis* cells could be visualized with BONCAT labeling (50 µM HPG) and almost all cells were BONCAT positive (Figure 6A). BONCAT labeled *M. maripaludis* cells could also be visualized with FISH (Figure 6B). However, when the batch co-culture was tested, the *D. vulgaris* cells were observed to be BONCAT active, but BONCAT labeling of *M. maripaludis* was not observed even after 96 hours of incubation, although methane was still being produced (Figure 7). Moreover, we then tested a mature co-culture biofilm and a similar result was observed (Figure 8). The *D. vulgaris* cells were HPG active while the *M. maripaludis* cells were not observed to be BONCAT-active (Figure 8B). As previously demonstrated, SSU rRNA gene FISH probes were able to label *M. maripaludis* cells in the co-culture biofilm and the co-culture biofilm reactor was actively producing methane. These results indicated that *M. maripaludis* cells did have some level of metabolic activity; however, HPG-based translational activity was below a detectable limit, *M. maripaludis* was not utilizing the HPG at the same rate as monoculture conditions, and/or competition for HPG between the populations was limiting uptake by *M. maripaludis.*

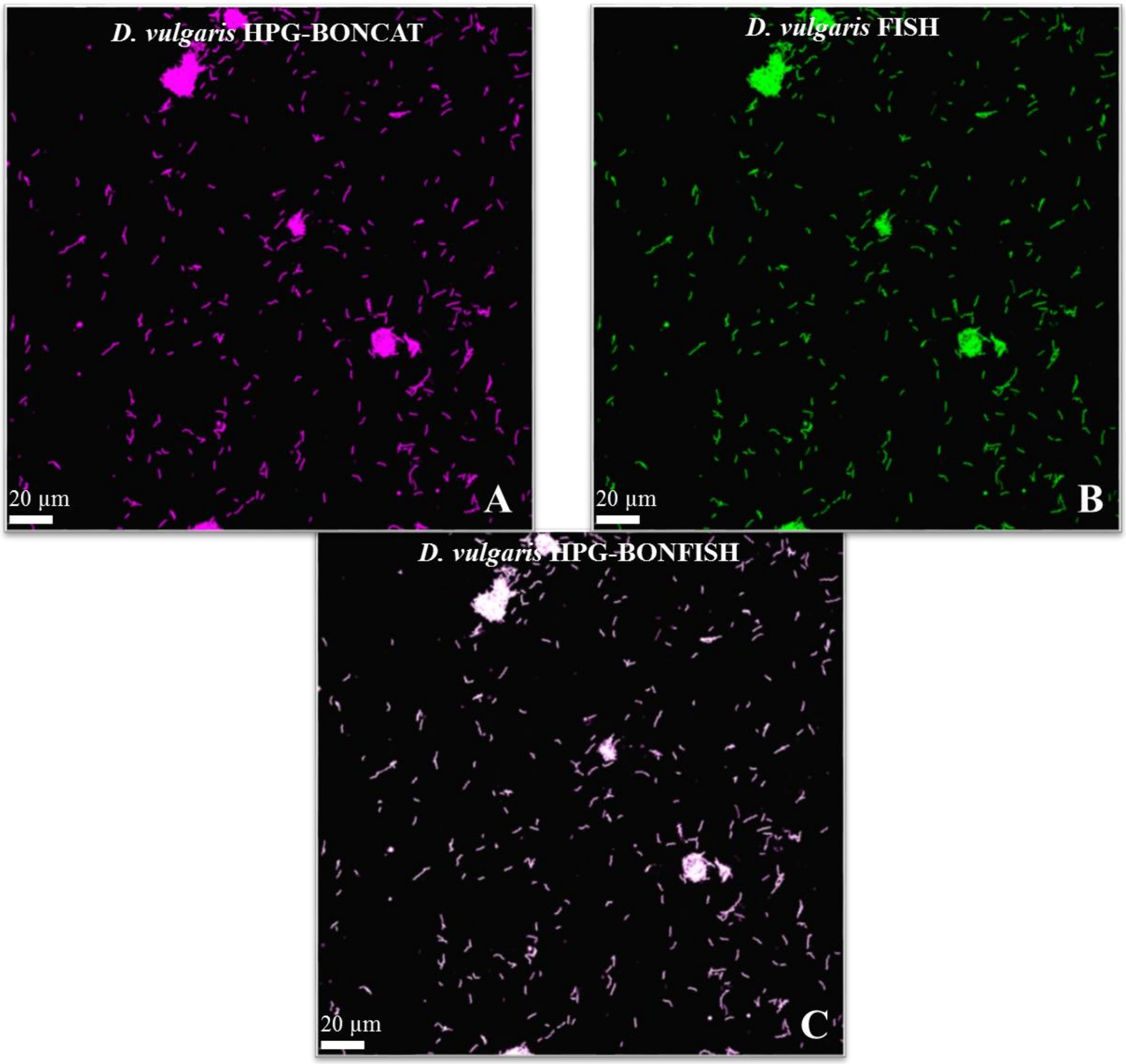
D. vulgaris HPG-BONCAT
20 µm
A
D. vulgaris FISH
20 µm
B
D. vulgaris HPG-BONFISH
20 µm
C

Figure 5. Monoculture batch BONCAT and FISH images for *D. vulgaris* Hildenborough. The methionine surrogate HPG was incubated with batch planktonic *D. vulgaris* (A) *D. vulgaris* showed complete BONCAT labeling (Purple) (B) *D. vulgaris* EUB338-FISH labeled (Green) (C) *D. vulgaris* overlay of BONCAT and FISH (BONFISH).

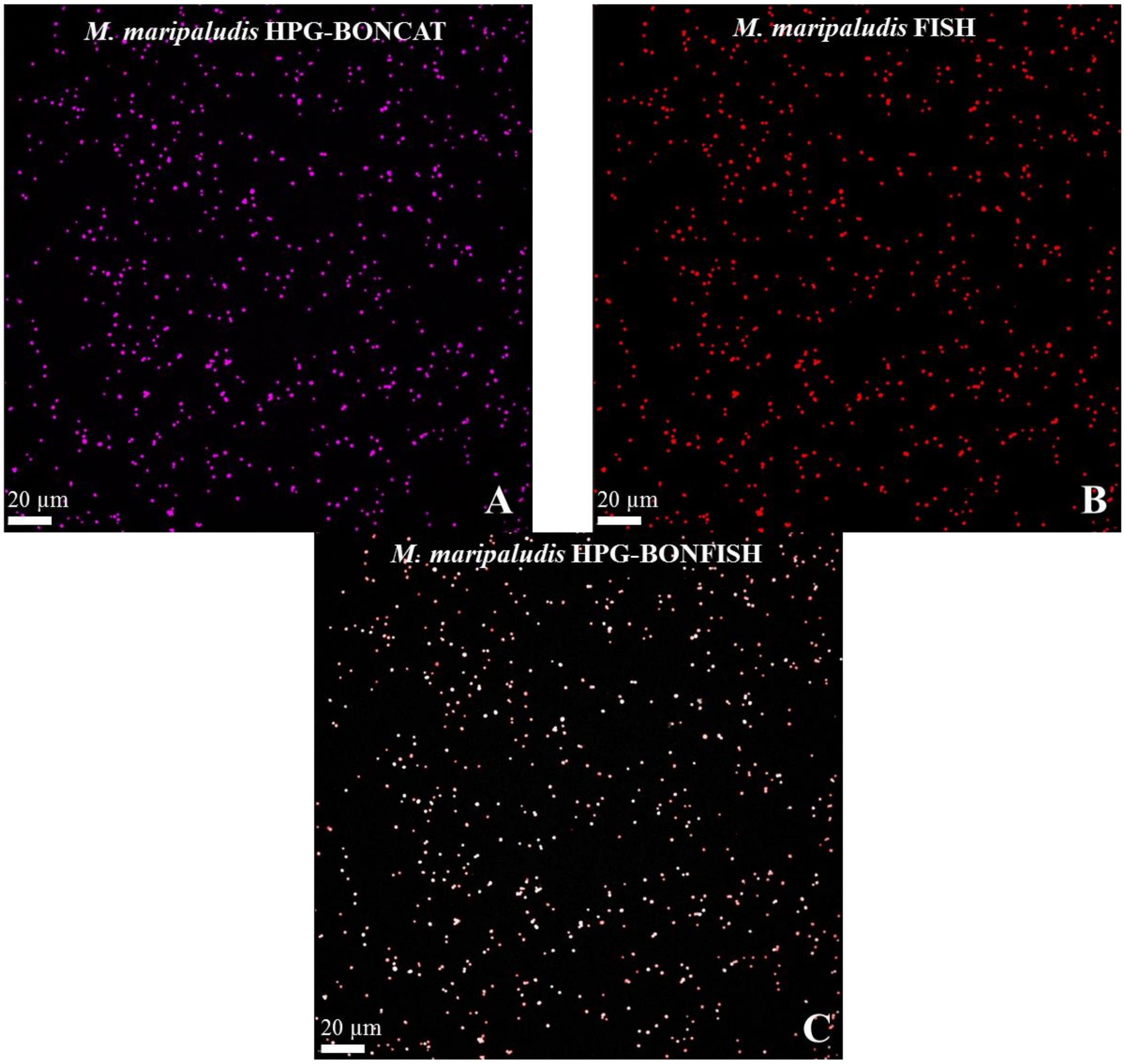
M. maripaludis HPG-BONCAT
20 µm
A
M. maripaludis FISH
20 µm
B
M. maripaludis HPG-BONFISH
20 µm
C

Figure 6. Monoculture batch BONCAT and FISH images for *M. maripaludis*. The methionine surrogate HPG was incubated with batch planktonic *M. maripaludis* (A) *M. maripaludis* showed complete BONCAT labeling (Purple) (B) *M. maripaludis* ARCH915-FISH labeled (Red) (C) *M. maripaludis* overlay of BONCAT and FISH (BONFISH).

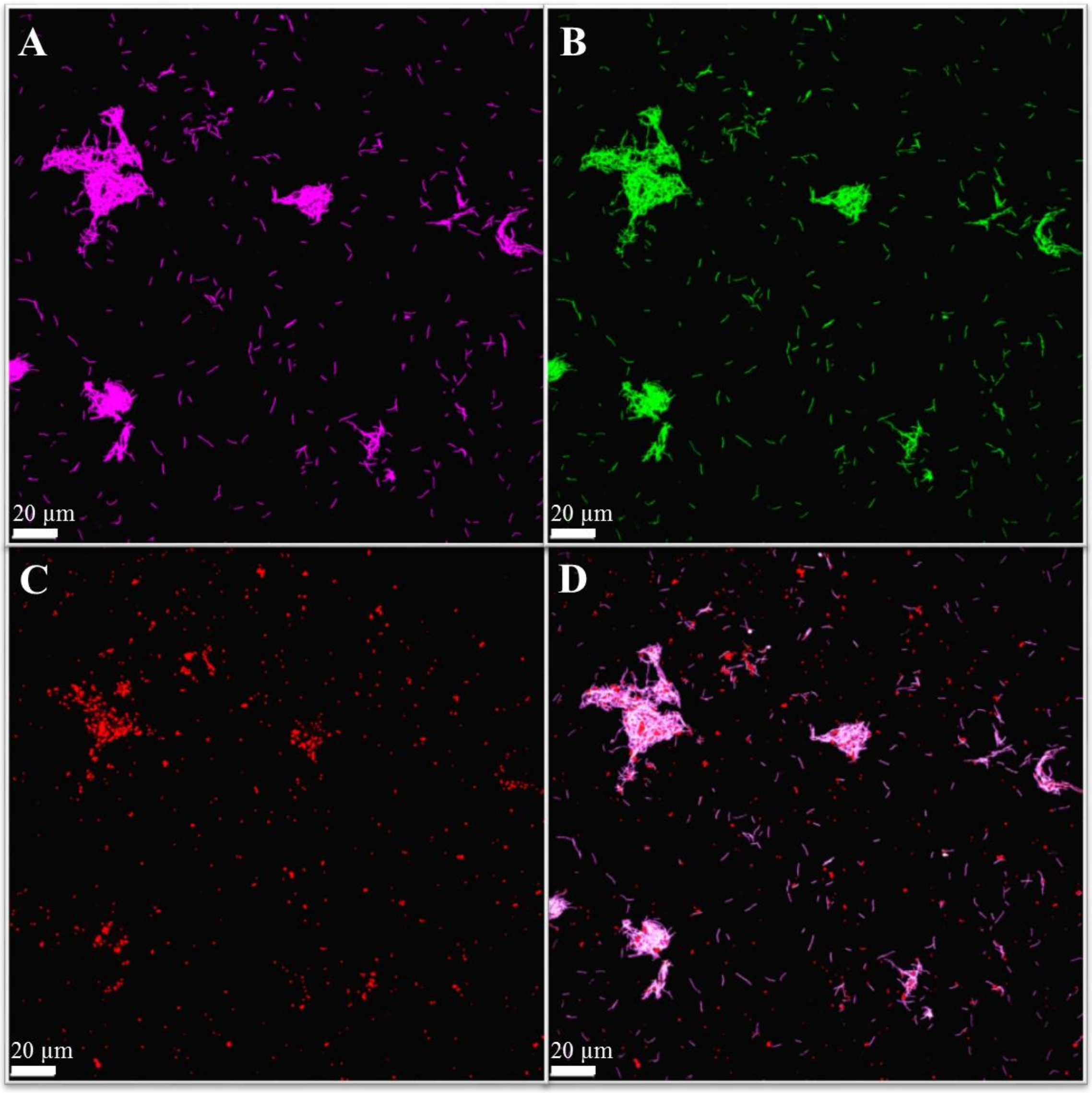

Figure 7. Co-culture Planktonic BONCAT and FISH labeling images. The methionine surrogate HPG was incubated with a planktonic batch co-culture of *M. maripaludis* and *D. vulgaris* Hildenborough then FISH labeled. Pictured is the (A) BONCAT labeling (Purple) (B) FISH labeled *D. vulgaris* (Green) (C) FISH labeled *M. maripaludis* (Red) and (D) Overlay of FISH and BONCAT images.

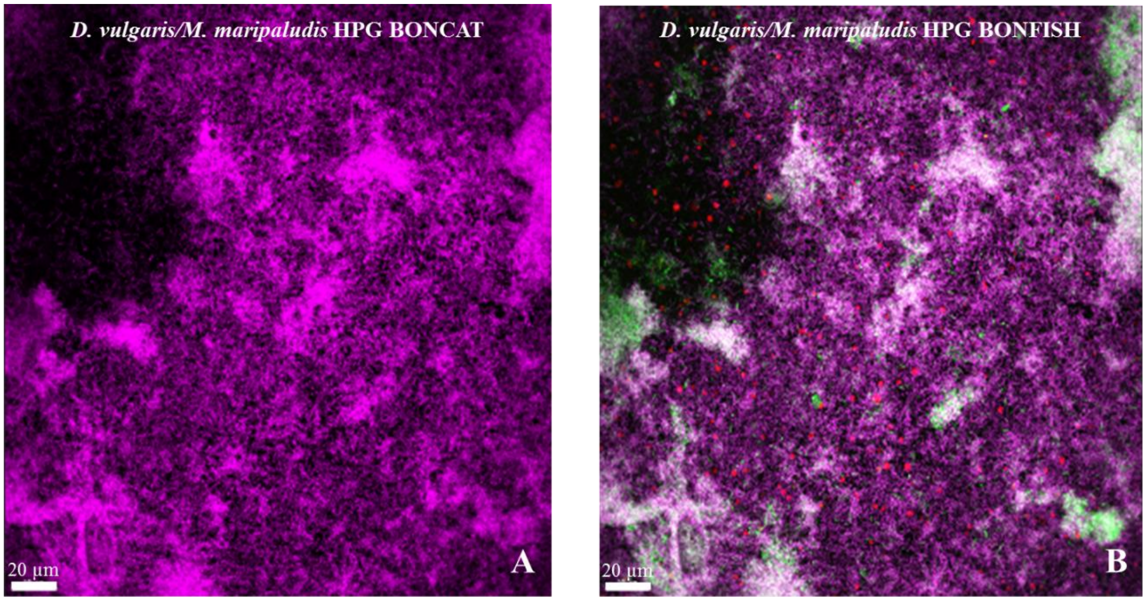
D. vulgaris/M. maripaludis HPG BONCAT
20 µm
A
D. vulgaris/M. maripaludis HPG BONFISH
20 µm
B

Figure 8. Co-culture biofilm BONCAT and FISH labeling images. The methionine surrogate HPG was incubated in a co-culture biofilm reactor system of *M. maripaludis* and *D. vulgaris* Hildenborough then FISH labeled. (A) The HPG BONCAT labeling (Purple) for the co-culture biofilm. (B) The overlay (BONFISH) of the FISH labeled *M. maripaludis* (Red) and FISH labeled *D. vulgaris* (Green) overlaid with the BONCAT labeling (Purple) images.

Growth was monitored using absorbance readings (600 nm) over time to assess HPG toxicity and sensitivity for the individual mono- cultures grown in batch mode. *M. maripaludis* demonstrated no deviation in batch planktonic growth from the control for levels of 50 µM and 200 µM HPG (Figure 9A). However, *D. vulgaris* Hildenborough exhibited a decrease in growth rate and biomass yield that correlated with increasing HPG concentrations (16% decrease with 50 µM HPG and 33% decrease with 200 µM HPG in growth rate) (Figure 9B). However, it should be noted that at these HPG levels, *D. vulgaris* cells are still BONCAT labeled. The co-culture growth was also impacted with 50 and 200 µM HPG, and the growth rate was reduced approximately 27% by both concentrations (Figure 9C). It is important to mention that the predicted proteome of *D.*

vulgaris Hildenborough contains twice the amount of methionine as *M. maripaludis* based upon predicted amino acid content from the genome, and therefore, could account for the greater physiological impact observed. Interestingly, both cultures would fail to grow in the presence of HPG if the incubation was not started until at least nine hours post culture inoculation which is most likely related to a tolerance threshold ratio of HPG:biomass.

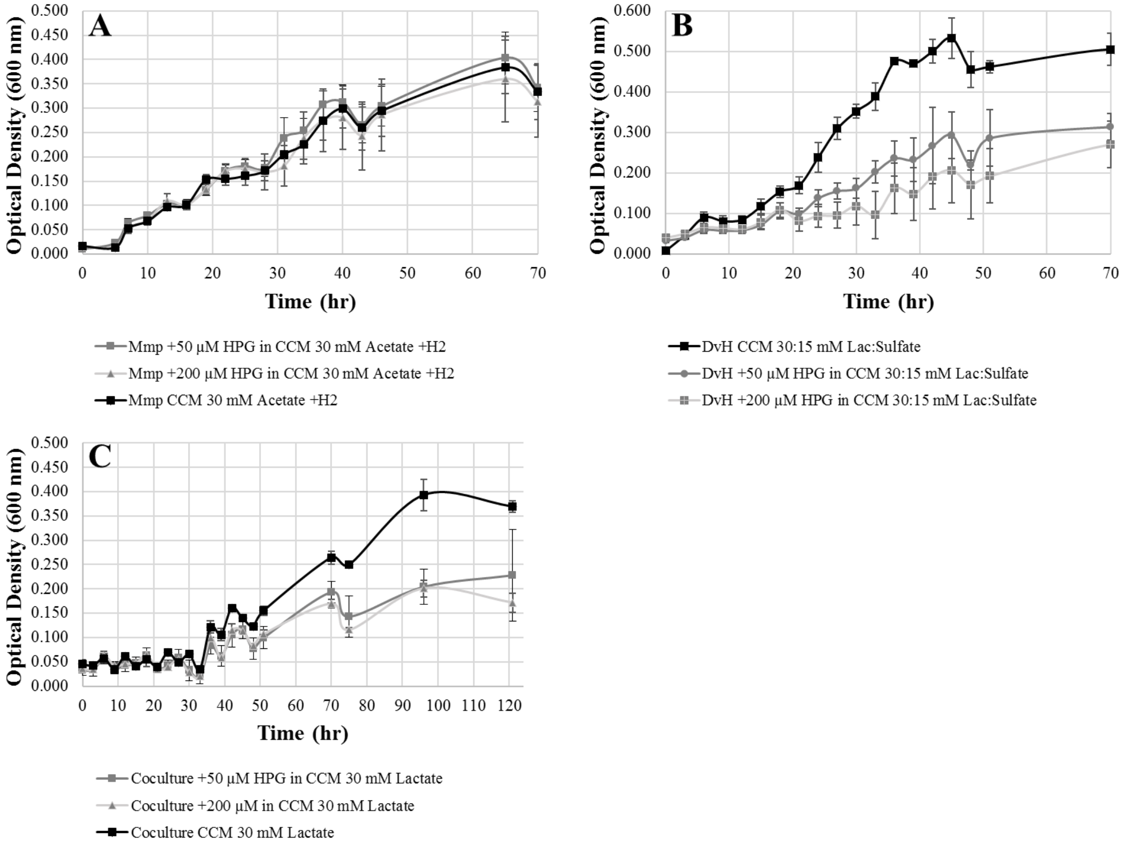

Figure 9. Culture absorbance readings (600 nm) with HPG were taken over time. The methionine surrogate HPG was incubated with the following cultures after 9 h. (A) *M. maripaludis* (Mmp) had no growth effect from 50 µM HPG in CCM with 30 mM Acetate and 80%:20% H_2:CO_2 and all cells were BONCAT labeled. (B) *D. vulgaris* Hildenborough (DvH) in CCM with 30 mM lactate and 15 mM sulfate experienced slower growth rates as compared to the control although BONCAT still illuminated the culture. (C) Co-cultures of planktonic *D. vulgaris* and *M. maripaludis* also had slower growth rates as compared to the CCM control and only DvH was BONCAT labeled.

Currently, there is not a reliable method for quantification of HPG; therefore, spent medium of the monocultures and co-cultures incubated with HPG were filter sterilized and re-incubated with fresh *D. vulgaris* or *M. maripaludis* cultures to observe if remaining HPG levels were adequate for labeling. Monoculture *D. vulgaris* was labeled in spent medium of *D. vulgaris* or *M. maripaludis* incubated with 50 µM HPG (Figure 10), and *M. maripaludis* was labeled in the spent medium of either *D. vulgaris, M. maripaludis,* or co-culture (Figure 11). These results indicated that in both monoculture and co-culture conditions the HPG levels were not being depleted and could not explain the inability to have BONCAT-labeled *M. maripaludis* cells in co-culture. Since HPG caused a 16% decrease in *D. vulgaris* growth rate that could impact co-culture metabolic interactions, an actively growing co-culture sub-sample was incubated short-term (2 min) with HPG. Preliminary experiments showed that both *D. vulgaris* and *M. maripaludis* monocultures could be labeled with short-term incubations (2 min) (data not shown). For the co-culture sub-sample, the *D. vulgaris* cells were BONCAT-positive but *M. maripaludis* cells were not (Figure 12).

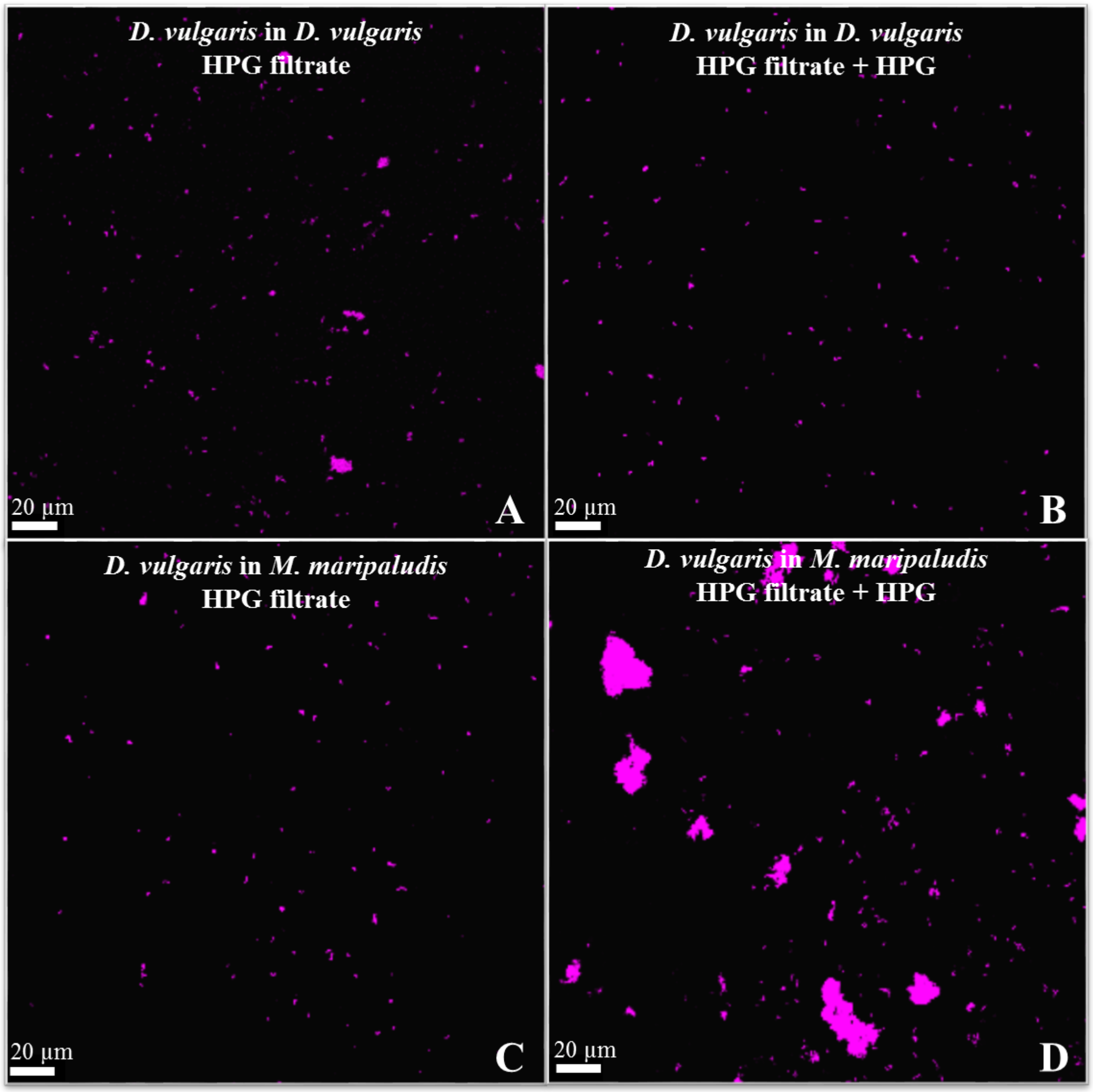
D. vulgaris in D. vulgaris HPG filtrate
20 µm
A
D. vulgaris in D. vulgaris HPG filtrate + HPG
20 µm
B
D. vulgaris in M. maripaludis HPG filtrate
20 µm
C
D. vulgaris in M. maripaludis HPG filtrate + HPG
20 µm
D

Figure 10. Spent media filtrate incubations were used to determine HPG was not being depleted. (A) *D. vulgaris* Hildenborough was grown with 50 µM HPG before being filtered and re-inoculated with a fresh culture of *D. vulgaris* and BONCAT labeled (Purple). (B) The spent HPG filtrate from *D. vulgaris* was supplemented with an additional 50 µM HPG before being inoculated with *D. vulgaris* and BONCAT labeled (Purple). (C) *M. maripaludis* was grown with 50 µM HPG before being filtered and inoculated with a fresh culture of *D. vulgaris* and BONCAT labeled (Purple). (D) The spent HPG filtrate from *M. maripaludis* was supplemented with an additional 50 µM HPG before being inoculated with *D. vulgaris* and BONCAT labeled.

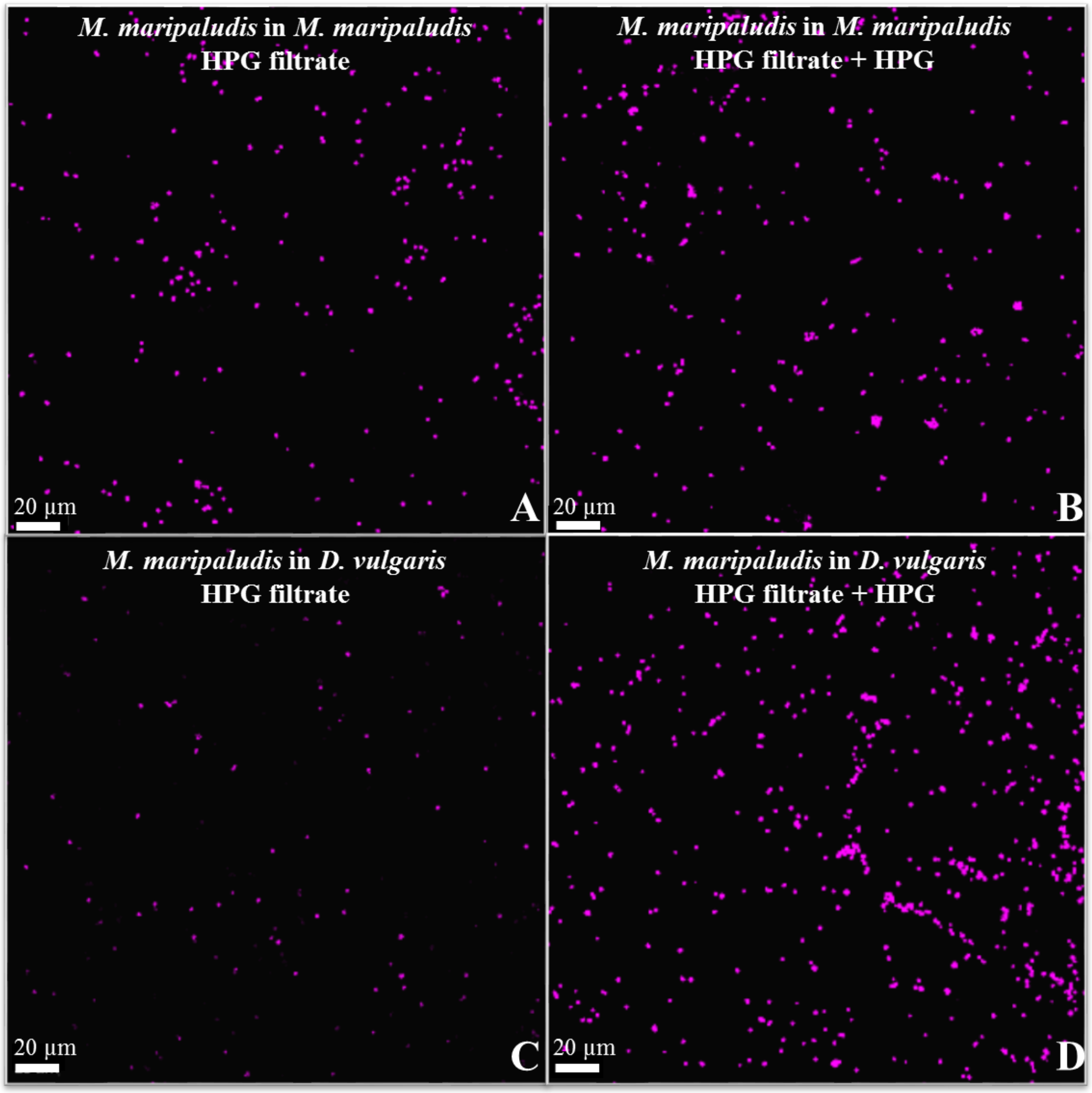
M. maripaludis in *M. maripaludis*
HPG filtrate
20 µm
A
M. maripaludis in *M. maripaludis*
HPG filtrate + HPG
20 µm
B
M. maripaludis in *D. vulgaris*
HPG filtrate
20 µm
C
M. maripaludis in *D. vulgaris*
HPG filtrate + HPG
20 µm
D

Figure 11. Spent media filtrate incubations were used to determine HPG was not being depleted. (A) Batch planktonic *M. maripaludis* was grown with 50 µM HPG before being filtered and re-inoculated with a fresh culture of *M. maripaludis* and BONCAT labeled (purple). (B) The spent HPG filtrate from *M. maripaludis* was supplemented with an additional 50 µM HPG before being inoculated with *M. maripaludis* and BONCAT labeled (Purple). (C) *D. vulgaris* was grown with 50 µM HPG before being filtered and inoculated with a fresh culture of *M. maripaludis* and BONCAT labeled (purple). (D) The spent HPG filtrate from *D. vulgaris* was supplemented with an additional 50 µM HPG before being inoculated with *M. maripaludis* and BONCAT labeled.

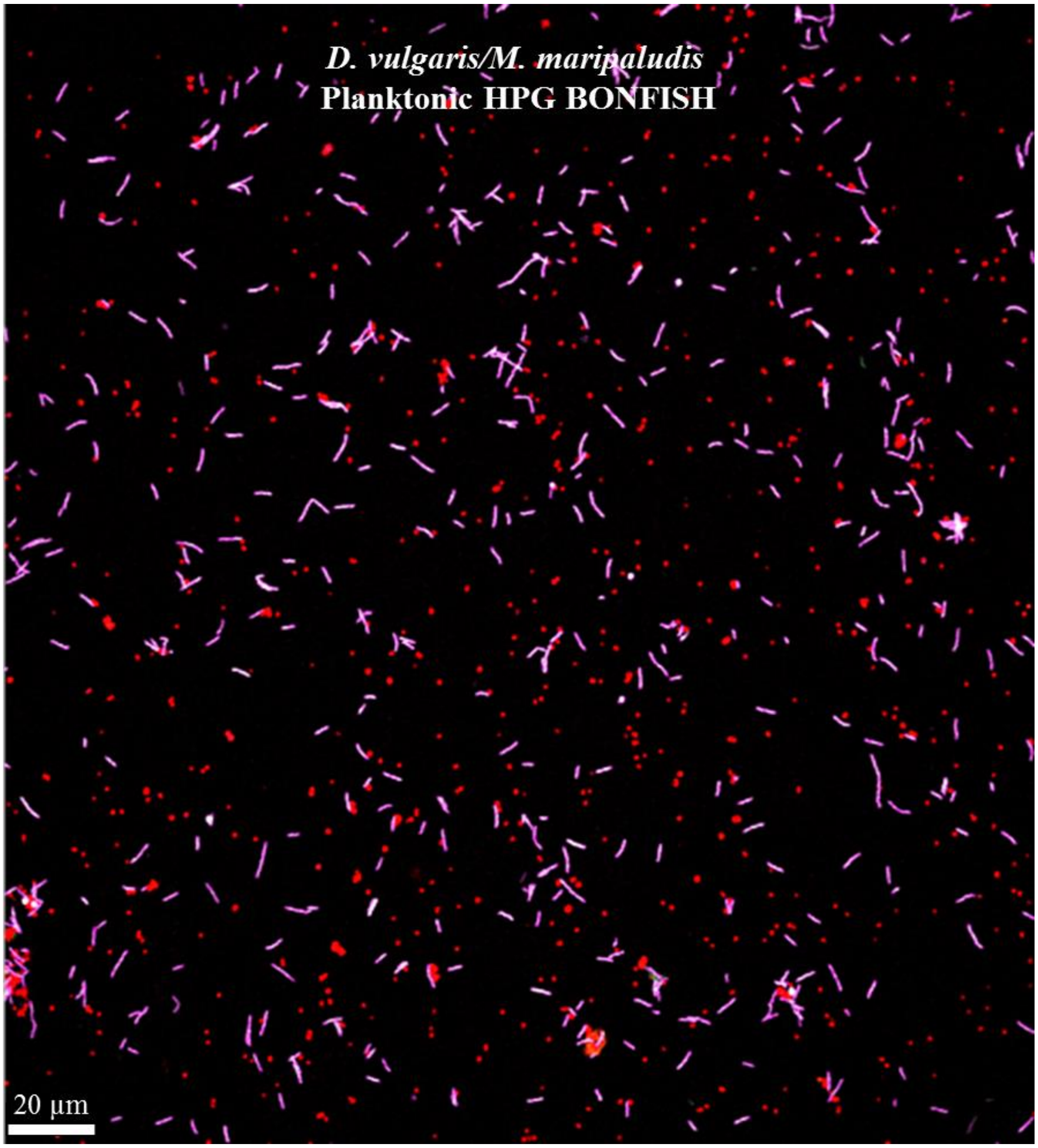
D. vulgaris/M. maripaludis
Planktonic HPG BONFISH
20 µm

Figure 12. Co-culture planktonic HPG BONFISH labels *D. vulgaris* Hildenborough. A short term (2 min) incubation using the methionine surrogate HPG (50 µM) was added to a planktonic co-culture of *M. maripaludis* and *D. vulgaris* Hildenborough then FISH labeled. Pictured is the overlay of the FISH labeled *M. maripaludis* (Red) and FISH labeled *D. vulgaris* (Green) overlaid with the BONCAT labeling (Purple). *M. maripaludis* is clearly not BONCAT labeled (Purple) in co-culture.

The HPG molecule assesses activity as translational activity via incorporation into a growing polypeptide; therefore, a different analog was used to target a different cellular process. The uridine analogue 5-ethynyl-2'-deoxyuridine (EdU) was tested as a proxy for DNA synthesis in the monoculture and co-cultures. In the presence of EdU, both the *D. vulgaris* and *M. maripaludis* monocultures were labeled (Figure 13A-C and 13D-E, respectively). In co-culture, both populations were labeled, but at a lower level possibly as a consequence of slower growth of the co-culture as well as lower overall incorporation based upon DNA per cell (Figure 13G-H).

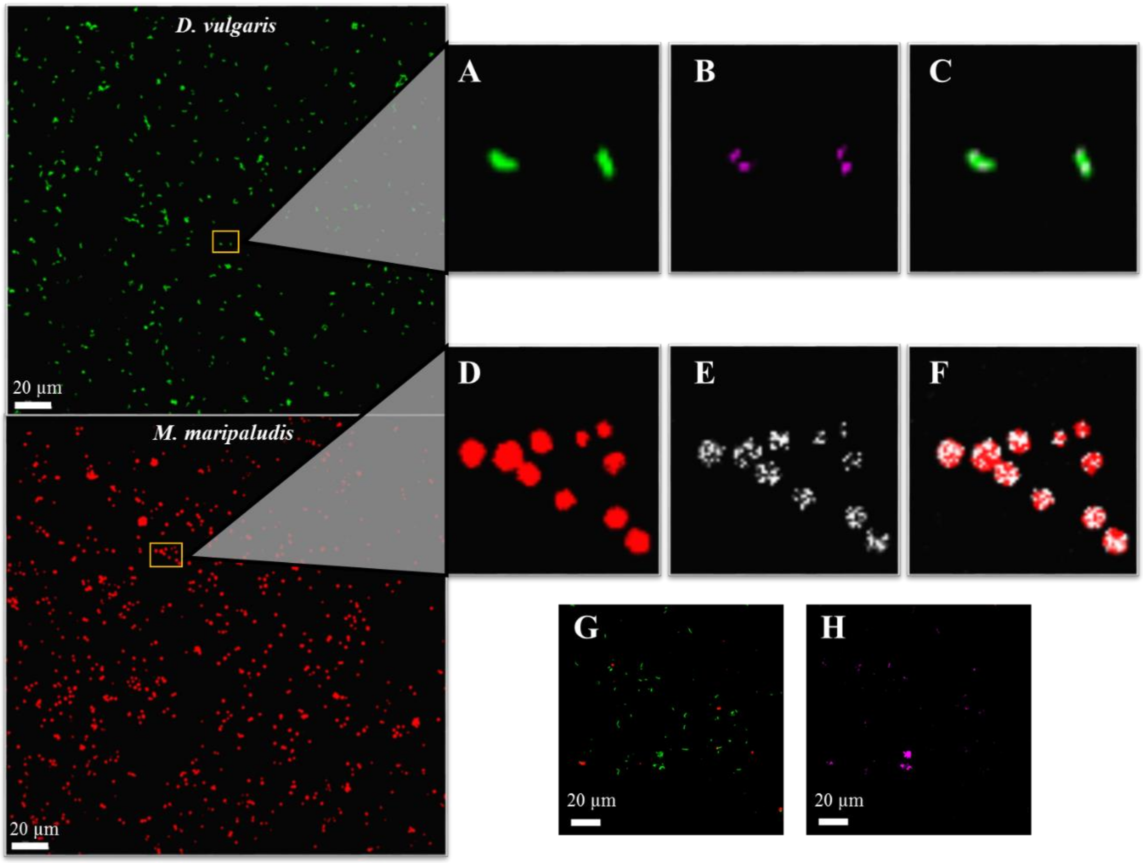

Figure 13. Monoculture EdU labeling was used to test DNA synthesis activity. Batch planktonic monocultures of *M. maripaludis* and *D. vulgaris* Hildenborough were incubated with EdU and then FISH labeled. (A) FISH labeled *D. vulgaris* (Green) (B) EdU (Purple) labeled *D. vulgaris* (C) EdU-FISH overlay for *D. vulgaris* (D) FISH labeled *M. maripaludis* (Red) (E) EdU (White) labeled *M. maripaludis* (F) EdU-FISH overlay for *M. maripaludis*. (G) The co-culture of *D. vulgaris* (Green) and *M. maripaludis* (Red) was also FISH labeled and (H) *D. vulgaris* and *M. maripaludis* are both EdU labeled (Purple).

DISCUSSION

Mutually beneficial interactions in natural systems are ubiquitous, but little is known about the underlying mechanisms that contribute to minimizing costs and maximizing benefits. Developing a tractable, relevant system for understanding the physiological characteristics of cooperative behavior is crucial to understanding many bio-systems under natural conditions. Inhabitants of anaerobic ecosystems are assumed to function at the thermodynamic limit for energy generation and biomass production given system constraints (Bryant et al., 1977; Kato & Watanabe, 2010; McInerney et al., 2009; Thauer et al., 2008). When one metabolism is obligately coupled to another through interspecies H_2, formate, or electron transfer, organisms must persist by sharing the overall free energy of the reaction (Kato & Watanabe, 2010). Therefore, syntrophic physiology plays an important role in microbial communities dominated by fluctuations in nutrient availability and stress, where community interactions are thought to provide stability (Hansen et al., 2007). The syntrophy between sulfate-reducing bacteria (SRB) and methanogenic archaea is of interest because both these guilds play crucial roles in many different anaerobic environments. Despite the ubiquity of biofilms and importance of anaerobes, little work has been done to understand how species interactions affect function in anaerobic microbial communities (Bernstein et al., 2012; Brenner & Arnold, 2011; Nielsen et al., 2000; Raskin et al., 1996), and while interactions between SRB and methanogens have been studied, very little has been done to characterize the emergent properties of interactive populations in anaerobic biofilms.

Previous research has shown that a *D. vulgaris* and *M. maripaludis* co-culture biofilm has a unique structure compared to monoculture conditions that contributes to an increased level of *M. maripaludis* in the biofilm as well as methane generation (Brileya et al., 2014b). Recent gene expression data demonstrated that *M. maripaludis* had a much broader change in expression as compared to *D. vulgaris* Hildenborough in a co-culture biofilm (Camilleri et al., in prep). The research aim for the current study was to utilize a combination of methodologies to determine if there was differential protein expression and overall activity for a bacterium and archaeon in a syntrophic mutualism.

Deuterium labeling results from the co-culture biofilm demonstrated that the newly synthesized proteins for both organisms were enriched in energy production, membrane proteins, and amino acid production/utilization. The most unexpected result was the apparent slowing of *D. vulgaris* protein synthesis (as determined by the deuterium half-saturation time) during the late stage biofilm development. One explanation for this observation is that as the biofilm matures, the metabolic activity of *D. vulgaris* is dictated by the coupled metabolic rate. This could mean that *D. vulgaris* is slowing overall metabolism as the biofilm is established and the metabolic interaction with *M. maripaludis* is maximized. For *M. maripaludis*, the deuterium half-saturation time was similar between the early and late biofilm samples. This result indicated that overall activity level did not change as *M. maripaludis* incorporated into the biofilm and methane levels stabilized. Hence, the bacterium and archaeon had different cellular activity states although the two populations were metabolically linked and sharing the conserved energy from the coupled reactions of incomplete lactate oxidation to acetate/H_2 ($\Delta G^{\circ\prime}$= -48.7 kJ/mol) and hydrogenotrophic methanogenesis ($\Delta G^{\circ\prime}$= -32.7 kJ/mol) (Conrad, 1999).

The deuterated proteins identified in the co-culture biofilm may also be an indication of metabolic modulation for each respective population. *M. maripaludis* had labeled proteins enriched in methanogenesis and could indicate that the syntrophy affords the opportunity to focus protein investment into methane production for the methanogen which is the “terminal” electron-accepting reaction for the co-culture. Stream-lined production for enzymes involved in methanogenesis is beneficial to both populations in terms of energy conservation for the couple between lactate oxidation and CO_2-reduction. An increase in CO_2-reduction consumes cross-fed electrons from *D. vulgaris* driven by lactate oxidation. Coinciding with this observation, labeled *D. vulgaris* proteins were enriched in the functions of lactate-oxidation and electron-transfer. The term ‘obligately mutualistic metabolism’ was proposed by Morris et al. (Morris et al., 2013) to emphasize the benefit to both partners by somehow optimizing output (*i.e*., biomass, products) with minimal energy resources. Earlier work has shown that *D. vulgaris* has an increased growth yield when co-cultured with a methanogen (Traore et al., 1983), and our results demonstrate a mechanism via streamlined protein expression. The notion of comparative advantages, similar to economics, can help explain resource costs and required goods when metabolites are shared for mutual benefit (D’Souza et al., 2018; Ferenci, 2016; Hammerstein & Noë, 2016; Lilja & Johnson, 2016; Tasoff et al., 2015).

Recently, a constructed co-culture was shown to re-direct overall metabolic flux to facilitate cell growth and activity (Wang et al., 2019); therefore, the notion for two microorganisms that can co-occur in natural environments to be able to coordinate metabolism to lower individual costs would be expected – particularly in a biofilm where close proximity would help ensure mutual benefit. Moreover, recent studies have estimated metabolic dependencies (*e.g*., amino acids) from co-occurring communities as major drivers for microbial community architecture (Zelezniak et al., 2015). In the presented study, both organisms had labeled polypeptides annotated to be involved in amino acid utilization and/or production, particularly *D. vulgaris* (Table 1). Previous work has demonstrated that *D. vulgaris* can produce and excrete certain amino acids (He et al., 2010), and previous co-culture work with *D. vulgaris* and *M. maripaludis* has predicted the exchange of alanine (Walker et al., 2012). Our recent transcriptomic work and metabolic model work has suggested the exchange of other amino acids in addition to alanine (Camilleri et al., in prep), and it has been proposed that trading metabolites could increase resource efficiency by separating metabolic pathways in different cells (Lilja & Johnson, 2016). In addition, metabolite leakage occurs between different organisms and enables metabolic interdependence, and this has been proposed to then cause changes in metabolic fluxes and leakage of other metabolites for surrounding cells (D'Souza et al., 2018).

Although, in the case of *D. vulgaris* and *M. maripaludis*, resources might be shared in the context of a "forced trade" because *D. vulgaris* serves as the "electron-donor" to *M. maripaludis* which then serves as the "electron-acceptor" for *D. vulgaris*. Both organisms appear to have a streamlined metabolic flux in terms of lactate and methane processing, and the BONCAT data indicated that translational activity was very different between *D. vulgaris* and *M. maripaludis* when in co-culture. In planktonic monocultures, the microorganisms were both translationally active as evidenced by HPG incorporation. Surprisingly, the planktonic and biofilm co-culture only demonstrated HPG-BONCAT labeling of *D. vulgaris*. Despite the BONCAT results indicating that the methanogen was not active, methane was being actively produced, low levels of DNA synthesis activity were detected by EdU labeling, and *M. maripaludis* remained detectable via FISH (rRNA gene). Initially this anomaly was believed to be from HPG depletion due to a possibly higher uptake rate in the SRB than the methanogen, as the predicted methionine content of *D. vulgaris* is double that of *M. maripaludis*. However, *M. maripaludis* incubated in spent HPG medium could still be labeled under the monoculture condition. These results suggest that *M. maripaludis* experienced metabolic modulation when in co-culture with *D. vulgaris* based upon the different responses between mono- and co-cultures. The lack of HPG-BONCAT labeling could indicate that *M. maripaludis* is obtaining methionine/precursors through a metabolic exchange with *D. vulgaris* and/or that *M. maripaludis* is focused on energy generation with limited protein turnover.

Alternatively, an autophagy state could also play a role in which *M. maripaludis* has an altered internal recycling of resources (*e.g.*, amino acids) that coincides with slower biomass generation. Intracellular protein degradation was first reported in eukaryotes but is also observed in archaea (and some bacteria) where cells can use autophagy-like responses to re-allocate resources to synthesize needed cellular components (Maupin-Furlow, 2012; Starokadomskyy & Dmytruk, 2013; Stryeck et al., 2017). Recent work has demonstrated the existence of signal-guided proteolysis in archaea related to the ubiquitin-proteasome in eukaryotes (Fu et al., 2016). The *M. maripaludis* putative protein, MMP0251, was detected via deuterium proteomics and is annotated as *psm*A, a proteasome subunit. The potential role of targeted protein turnover in *M. maripaludis* under different growth conditions is unknown, but an autophagy-like state could also contribute to the methanogen being “active” but not detectable via HPG in co-culture. This could also coincide with a re-formatting of available resource to proteins directly involved in methanogenesis.

Overall, the results demonstrate that in an interdomain co-culture biofilm, metabolic flux is streamlined for lactate oxidation and CO_2-reduction, and other metabolites in addition to H_2 may be shared. In the mature co-culture biofilm, the bacterium and archaeon appear to have different “basal metabolic rates” in that *D. vulgaris* has a more focused metabolism on lactate oxidation and carbon processing while *M. maripaludis* has a more focused metabolism on CO_2-reduction and electron consumption. The two organisms appear to have different cellular mechanisms to achieve the observed mutualism in a low-energy environment via function partitioning. Being in close proximity (i.e., biofilm) allows for close-range sharing of metabolites and provides a more homeostatic environment that allows for the expression of fewer proteins in a more consistent fashion that would contribute to improved cost-benefit investment ratios.

In addition to the applied microbiology context of improved understanding of metabolic interactions, fundamentally, this unique bacterial-archaeal biofilm represents interdomain interactions that could have contributed to evolutionary processes that lead to the development of eukaryotic life (Hooper & Burstein, 2014; Wrede et al., 2012). Given the recent arguments for the plausibility of symbiogenetic scenario for the origin of eukaryotes from bacteria and archaea (Koonin, 2015), it could be argued that interdomain biofilms would have provided intimate co-localization where metabolic interactions would have been forged and selected. Future work should focus on the emergent properties of metabolic interactions in biofilms.

Acknowledgments. This material by ENIGMA- Ecosystems and Networks Integrated with Genes and Molecular Assemblies (http://enigma.lbl.gov), a Scientific Focus Area Program at Lawrence Berkeley National Laboratory is based upon work supported by the U.S. Department of Energy, Office of Science, Office of Biological & Environmental Research under contract number DE-AC02-05CH11231.

REFERENCES CITED

Bernstein, H. C., Paulson, S. D., & Carlson, R. P. (2012). Synthetic Escherichia coli consortia engineered for syntrophy demonstrate enhanced biomass productivity. *Journal of Biotechnology*, *157*(1), 159–166. http://doi.org/10.1016/j.jbiotec.2011.10.001

Binder, B. J., & Liu, Y. C. (1998). Growth rate regulation of rRNA content of a marine Synechococcus (Cyanobacterium) strain. *Applied and Environmental Microbiology*, *64*(9), 3346–3351.

Bollmann, A., Schmidt, I., Saunders, A. M., & Nicolaisen, M. H. (2005). Influence of Starvation on Potential Ammonia-Oxidizing Activity and amoA mRNA Levels of Nitrosospira briensis. *Applied and Environmental Microbiology*, *71*(3), 1276–1282. http://doi.org/10.1128/AEM.71.3.1276

Brenner, K., & Arnold, F. H. (2011). Self-Organization, Layered Structure, and Aggregation Enhance Persistence of a Synthetic Biofilm Consortium. *PLoS ONE*, *6*(2), e16791. http://doi.org/10.1371/journal.pone.0016791

Brileya, K. A., Camilleri, L. B., & Fields, M. W. (2014a). 3D-Fluorescence In Situ Hybridization of Intact, Anaerobic Biofilm. In L. Sun & W. Shou (Eds.), *Engineering and Analyzing Multicellular Systems* (Vol. 1151, pp. 189–197). New York, NY: Springer New York. http://doi.org/10.1007/978-1-4939-0554-6

Brileya, K. A., Camilleri, L. B., Zane, G. M., Wall, J. D., & Fields, M. W. (2014b). Biofilm growth mode promotes maximum carrying capacity and community stability during product inhibition syntrophy. *Frontiers in Microbiology*, *5*(12), 693. http://doi.org/10.3389/fmicb.2014.00693

Bryant, M. P., Campbell, L. L., Reddy, C. A., & Crabill, M. R. (1977). Growth of Desulfovibrio in lactate or ethanol media low in sulfate in association with H2-utilizing methanogenic bacteria. *Applied and Environmental Microbiology*, *33*(5), 1162–9. Retrieved from http://www.ncbi.nlm.nih.gov/pubmed/879775

Busch, R., Neese, R. A., Awada, M., Hayes, G. M., & Hellerstein, M. K. (2007). Measurement of cell proliferation by heavy water labeling. *Nature Protocols*, *2*(12), 3045–3057. http://doi.org/10.1038/nprot.2007.420

Clark, M. E., He, Q., He, Z., Huang, K. H., Alm, E. J., Wan, X.-F., … Fields, M. W. (2006). Temporal transcriptomic analysis as Desulfovibrio vulgaris Hildenborough transitions into stationary phase during electron donor depletion. *Applied and Environmental Microbiology*, *72*(8), 5578–88. http://doi.org/10.1128/AEM.00284-06

Clark, M. E., He, Z., Redding, A. M., Joachimiak, M. P., Keasling, J. D., Zhou, J. Z., … Fields, M. W. (2012). Transcriptomic and proteomic analyses of Desulfovibrio vulgaris biofilms: carbon and energy flow contribute to the distinct biofilm growth state. *BMC Genomics*, *13*(1), 138. http://doi.org/10.1186/1471-2164-13-138

Conrad, R. (1999). Contribution of hydrogen to methane production and control of hydrogen concentrations in methanogenic soils and sediments. *FEMS Microbiology Ecology*, *28*(3), 193–202. http://doi.org/10.1016/S0168-6496(98)00086-5

D’Souza, G., Shitut, S., Preussger, D., Yousif, G., Waschina, S., & Kost, C. (2018). Ecology and evolution of metabolic cross-feeding interactions in bacteria. *Natural Product Reports*, *35*(5), 455–488. http://doi.org/10.1039/C8NP00009C

De Riva, A., Deery, M. J., McDonald, S., Lund, T., & Busch, R. (2010). Measurement of protein synthesis using heavy water labeling and peptide mass spectrometry: Discrimination between major histocompatibility complex allotypes. *Analytical Biochemistry*, *403*(1–2), 1–12. http://doi.org/10.1016/j.ab.2010.04.018

Dieterich, D. C., Link, A. J., Graumann, J., Tirrell, D. A., & Schuman, E. M. (2006). Selective identification of newly synthesized proteins in mammalian cells using bioorthogonal noncanonical amino acid tagging (BONCAT). *Proceedings of the National Academy of Sciences of the United States of America*, *103*(25), 9482–7. http://doi.org/10.1073/pnas.0601637103

Ferenci, T. (2016). Trade-off Mechanisms Shaping the Diversity of Bacteria. *Trends in Microbiology*, *24*(3), 209–223. http://doi.org/10.1016/j.tim.2015.11.009

Foster, R. A., Subramaniam, A., & Zehr, J. P. (2009). Distribution and activity of diazotrophs in the Eastern Equatorial Atlantic. *Environmental Microbiology*, *11*(4), 741–750. http://doi.org/10.1111/j.1462-2920.2008.01796.x

Fu, X., Liu, R., Sanchez, I., Silva-Sanchez, C., Hepowit, N. L., Cao, S., … Maupin-Furlow, J. (2016). Ubiquitin-Like Proteasome System Represents a Eukaryotic-Like Pathway for Targeted Proteolysis in Archaea. *MBio*, *7*(4), 1–14. http://doi.org/10.1128/mBio.01192-16

González Fernández-Niño, S. M., Smith-Moritz, A. M., Chan, L. J. G., Adams, P. D., Heazlewood, J. L., & Petzold, C. J. (2015). Standard Flow Liquid Chromatography for Shotgun Proteomics in Bioenergy Research. *Frontiers in Bioengineering and Biotechnology*, *3*(April), 1–7. http://doi.org/10.3389/fbioe.2015.00044

Hammerstein, P., & Noë, R. (2016). Biological trade and markets. *Philosophical Transactions of the Royal Society B: Biological Sciences*, *371*(1687), 20150101. http://doi.org/10.1098/rstb.2015.0101

Hansen, S. K., Rainey, P. B., Haagensen, J. A. J., & Molin, S. (2007). Evolution of species interactions in a biofilm community. *Nature*, *445*(7127), 533–536. http://doi.org/10.1038/nature05514

Hatzenpichler, R., Connon, S. A., Goudeau, D., Malmstrom, R. R., Woyke, T., & Orphan, V. J. (2016). Visualizing in situ translational activity for identifying and sorting slow-growing archaeal−bacterial consortia. *Proceedings of the National Academy of Sciences*, *113*(28), E4069–E4078. http://doi.org/10.1073/pnas.1603757113

Hatzenpichler, R., & Orphan, V. J. (2015). Detection of Protein-Synthesizing Microorganisms in the Environment via Bioorthogonal Noncanonical Amino Acid Tagging (BONCAT). In T. McGenity, K. Timmis, & B. Nogales (Eds.), *Hydrocarbon and Lipid Microbiology Protocols* (Springer P, pp. 145–157). Springer Berlin Heidelberg. http://doi.org/https://doi.org/10.1007/8623_2015_61

Hatzenpichler, R., Scheller, S., Tavormina, P. L., Babin, B. M., Tirrell, D. A., & Orphan, V. J. (2014). In situ visualization of newly synthesized proteins in environmental microbes using amino acid tagging and click chemistry. *Environmental Microbiology*, *16*(8), 2568–90. http://doi.org/10.1111/1462-2920.12436

He, Z., Zhou, A., Baidoo, E., He, Q., Joachimiak, M. P., Benke, P., … Zhou, J. (2010). Global Transcriptional, Physiological, and Metabolite Analyses of the Responses of Desulfovibrio vulgaris Hildenborough to Salt Adaptation. *Applied and Environmental Microbiology*, *76*(5), 1574–1586. http://doi.org/10.1128/AEM.02141-09

Hooper, S. L., & Burstein, H. J. (2014). Minimization of extracellular space as a driving force in prokaryote association and the origin of eukaryotes. *Biology Direct*, *9*(1), 24. http://doi.org/10.1186/1745-6150-9-24

Kato, S., & Watanabe, K. (2010). Ecological and Evolutionary Interactions in Syntrophic Methanogenic Consortia. *Microbes and Environments*, *25*(3), 145–151. http://doi.org/10.1264/jsme2.ME10122

Koonin, E. V. (2015). Origin of eukaryotes from within archaea, archaeal eukaryome and bursts of gene gain: eukaryogenesis just made easier? *Philosophical Transactions of the Royal Society B: Biological Sciences*, *370*(1678), 20140333. http://doi.org/10.1098/rstb.2014.0333

Lilja, E. E., & Johnson, D. R. (2016). Segregating metabolic processes into different microbial cells accelerates the consumption of inhibitory substrates. *The ISME Journal*, *10*(7), 1568–1578. http://doi.org/10.1038/ismej.2015.243

Maupin-Furlow, J. (2012). Proteasomes and protein conjugation across domains of life. *Nature Reviews Microbiology*, *10*(2), 100–111. http://doi.org/10.1038/nrmicro2696

McInerney, M. J., Sieber, J. R., & Gunsalus, R. P. (2009). Syntrophy in anaerobic global carbon cycles. *Current Opinion in Biotechnology*, *20*(6), 623–632. http://doi.org/10.1016/j.copbio.2009.10.001

Momeni, B., Brileya, K. A., Fields, M. W., & Shou, W. (2013). Strong inter-population cooperation leads to partner intermixing in microbial communities. *ELife*, *2*, e00230. http://doi.org/10.7554/eLife.00230

Morgenroth, E., Obermayer, A., Arnold, E., Brühl, A., Wagner, M., & Wilderer, P. A. (2000). Effect of long-term idle periods on the performance of sequencing batch reactors. *Water Science and Technology*, *41*(1), 105–113. http://doi.org/10.2166/wst.2000.0018

Morris, B. E. L., Henneberger, R., Huber, H., & Moissl-Eichinger, C. (2013). Microbial syntrophy: interaction for the common good. *FEMS Microbiology Reviews*, *37*(3), 384–406. http://doi.org/10.1111/1574-6976.12019

Nielsen, A. T., Tolker-Nielsen, T., Barken, K. B., & Molin, S. (2000). Role of commensal relationships on the spatial structure of a surface-attached microbial consortium. *Environmental Microbiology*, *2*(1), 59–68. http://doi.org/10.1046/j.1462-2920.2000.00084.x

Oda, Y., Slagman, S. J., Meijer, W. G., Forney, L. J., & Gottschal, J. C. (2000). Influence of growth rate and starvation on fluorescent in situ hybridization of Rhodopseudomonas palustris. *FEMS Microbiology Ecology*, *32*(3), 205–213. http://doi.org/10.1016/S0168-6496(00)00029-5

Raskin, L., Rittmann, B. E., & Stahl, D. A. (1996). Competition and coexistence of sulfate-reducing and methanogenic populations in anaerobic biofilms. *Applied and Environmental Microbiology*, *62*(10), 3847–57. Retrieved from http://www.pubmedcentral.nih.gov/articlerender.fcgi?artid=1388966&tool=pmcentrez&rendertype=abstract

Schmid, M., Schmitz-Esser, S., Jetten, M., & Wagner, M. (2001). 16S-23S rDNA intergenic spacer and 23S rDNA of anaerobic ammonium-oxidizing bacteria: implications for phylogeny and in situ detection. *Environmental Microbiology*, *3*(7), 450–9. Retrieved from http://www.ncbi.nlm.nih.gov/pubmed/11553235

Starokadomskyy, P., & Dmytruk, K. V. (2013). A bird’s-eye view of autophagy. *Autophagy*, *9*(7), 1121–1126. http://doi.org/10.4161/auto.24544

Stryeck, S., Birner-Gruenberger, R., & Madl, T. (2017). Integrative metabolomics as emerging tool to study autophagy regulation. *Microbial Cell*, *4*(8), 240–258. http://doi.org/10.15698/mic2017.08.584

Taniguchi, Y., Choi, P. J., Li, G., Chen, H., Babu, M., Hearn, J., … Xie, X. S. (2010). Quantifying E. coli Proteome and Transcriptome with Single-Molecule Sensitivity in Single Cells. *Most*, *329*(5991), 533–538. http://doi.org/10.1126/science.1188308.

Tasoff, J., Mee, M. T., & Wang, H. H. (2015). An Economic Framework of Microbial Trade. *PLOS ONE*, *10*(7), e0132907. http://doi.org/10.1371/journal.pone.0132907

Thauer, R. K., Kaster, A.-K., Seedorf, H., Buckel, W., & Hedderich, R. (2008). Methanogenic archaea: ecologically relevant differences in energy conservation. *Nature Reviews. Microbiology*, *6*(8), 579–91. http://doi.org/10.1038/nrmicro1931

Traore, A. S., Gaudin, C., Hatchikian, C. E., Gall, J. L. E., & Belaich, J. (1983). Energetics of Growth of a Defined Mixed Culture of Desulfovibrio vulgaris and Methanosarcina barkeri: Maintenance Energy Coefficient of the Sulfate-Reducing Organism in the Absence and Presence of Its Partner. *Journal of Bacteriology*, *155*(3), 1260–1264.

Wagner, M., Rath, G., Amann, R., Koops, H.-P., & Schleifer, K.-H. (1995). In situ Identification of Ammonia-oxidizing Bacteria. *Systematic and Applied Microbiology*, *18*(2), 251–264. http://doi.org/10.1016/S0723-2020(11)80396-6

Walker, C. B., Redding-Johanson, A. M., Baidoo, E. E., Rajeev, L., He, Z., Hendrickson, E. L., … Stahl, D. A. (2012). Functional responses of methanogenic archaea to syntrophic growth. *The ISME Journal*, *6*(11), 2045–2055. http://doi.org/10.1038/ismej.2012.60

Wang, S., Tang, H., Peng, F., Yu, X., Su, H., Xu, P., & Tan, T. (2019). Metabolite-based mutualism enhances hydrogen production in a two-species microbial consortium. *Communications Biology*, *2*(1), 82. http://doi.org/10.1038/s42003-019-0331-8

Wrede, C., Dreier, A., Kokoschka, S., & Hoppert, M. (2012). Archaea in Symbioses. *Archaea*, *2012*, 1–11. http://doi.org/10.1155/2012/596846

Zelezniak, A., Andrejev, S., Ponomarova, O., & Mende, D. R. (2015). Metabolic dependencies drive species co-occurrence in diverse microbial communities. *Proceedings of the National Academy of Sciences*, *112*(20), 201522642. http://doi.org/10.1073/pnas.1522642113

CHAPTER FOUR

METHANOCOCCUS MARIPALUDIS FACTOR CAUSES SLOWED GROWTH IN DESULFOVIBRIO VULGARIS HILDENBOROUGH

Contribution of Authors and Co-Authors

Manuscript in Chapter 4

Author: Laura B. Camilleri

Contributions: Developed experimental design, performed experiments, analyzed data, wrote and revised the manuscript.

Co-Author: Matthew W. Fields

Contributions: Developed experimental design, analyzed data, wrote and revised the manuscript.

Manuscript Information

Laura B. Camilleri and Matthew W. Fields

Letters in Applied Microbiology

Status of Manuscript:
__x_ Prepared for submission to a peer-reviewed journal
____ Officially submitted to a peer-reviewed journal
____ Accepted by a peer-reviewed journal
____ Published in a peer-reviewed journal

ABSTRACT

Syntrophic mutualisms have been studied across the three domains of life and a better understanding of different interactions are demonstrating that microbial interactions can be graduations across the positive (*i.e.*, cooperation) and negative (*i.e.*, competition) spectrum. It is well recognized that sulfate-reducing bacteria can enter into syntrophy with hydrogenotrophic methanogens when sulfate is not present. Previous work has demonstrated that the specific association between *Desulfovibrio vulgaris* Hildenborough and *Methanococcus maripaludis* in a biofilm can enhance the carrying capacity of both populations as defined by mass flux per methane formed. In the co-culture biofilm system, the association through metabolic pairing was tested by stressing the system with sulfate. Expectedly, *D. vulgaris* cell number and biomass increased in the planktonic and biofilm fractions post-sulfate addition, but *M. maripaludis* was observed to not only remain in the planktonic and biofilm fractions but increased in the bio-volume fraction of the biofilm. Post-sulfate addition (100 h), *M. maripaludis* remained viable in the biofilm (10^7 cells/cm^2), and dilution series cultures were methanogenic in the presence of sulfate. In addition, monoculture *M. maripaludis* could tolerate up to 55 mM sulfate with no noticeable impact on growth. When *D. vulgaris* was inoculated into cell-free spent medium from both co-culture and *M. maripaludis* monocultures that was supplemented with lactate and sulfate, growth lagged for up to 10 h, sulfate was reduced more slowly, and H_2 gas was detected. Similar results were observed with *Desulfovibrio alaskensis* G20 but not *Pseudomonas aeruginosa*. A <10 kDa fraction of *M. maripaludis* spent medium demonstrated similar growth lag effects, but a known compound could not be identified via proteomic or metabolomic screens. The results demonstrate that a *M. maripaludis* product can directly and/or indirectly slow the growth of *Desulfovibrio* in the presence of sulfate. The exact mechanism(s) for the metabolic modulation is not known.

INTRODUCTION

Mutualism has conceptually been synonymous with equal reciprocation via cooperation between cross-feeding organisms (*i.e.*, syntrophy). A mutualistic cooperation can ensue with a model co-culture of the sulfate-reducing bacterium, *Desulfovibrio vulgaris* Hildenborough (DvH), and the hydrogenotrophic archaeal methanogen, *Methanococcus maripaludis* S2 (Mmp) when the growth medium contains lactate without sulfate as a terminal electron acceptor. In this scenario, the historical paradigm has been that *Desulfovibrio* will ferment the lactate to produce H_2 gas that is then consumed by *Methanococcus* for CO_2 reduction to CH_4. Because H_2 can be inhibitory to *Desulfovibrio* via feedback inhibition, the syntrophy with *Methanococcus* is beneficial due to the maintenance of a lower partial pressure of H_2 that has been appropriately described as a product inhibition mutualism (Dean, 1985).

Previous work has demonstrated that *Desulfovibrio* monocultures form thin but stable biofilms. *Methanococcus* does not readily form biofilm as a monoculture although it has been shown to form pellicles (Brileya et al., 2013). Upon establishment of a co-culture under no sulfate conditions, *Desulfovibrio* initiates biofilm formation in which *Methanococcus* readily incorporates, most likely driven by hydrogenotaxis (Brileya et al., 2013). Interestingly, the co-culture biofilm has a distinct phenotype with a thicker three-dimensional topography that includes ridges, spires, and valleys that is not observed in the *D. vulgaris* monoculture (Brileya et al., 2014b; Clark et al., 2012). Further investigation into this co-culture system revealed that the biofilm growth mode promoted a stable and more even carrying-capacity with maximal methane flux by unit substrate compared to planktonic-only populations (Brileya et al., 2014b).

Interactions that occur on the microscale can greatly impact overall community function, and impacts include phenotypic heterogeneity, genomic plasticity, and altered carbon flow utilization. A principle in microbial community formation is that interactions can alleviate the constraint on any one individual organism in various ways such as resource sharing and protection that minimizes investment costs for any one population (Carlson et al., 2018). This would imply that persistent mutualistic interactions must be beneficial to some extent but the existence of selected, specific interactions in nature are debated. For example, the origin of microbial community spatial structure has been hypothesized to be a result of passive mutualistic interactions such as would occur from cell leakage or side products that make associations beneficial by chance and not evolution (Marchal et al., 2017). Physical associations mediated through bacterial flagellum in the syntrophic co-culture between *Pelotomaculum thermopropionicum* and *Methanothermobacter thermautotrophicus* was found to enhance mutualism and thus represents a potentially selected and specific interaction phenotype (Shimoyama et al., 2009). It was reported that the presence of the filament cap protein (FLiD) was able to encourage expression of methanogenic genes needed to maintain the syntrophy (Shimoyama et al., 2009). This finding suggests that in addition to the importance of proximity for passive interactions, physical associations can alter metabolisms to better suit the community.

The research presented here aims to further classify the levels of interaction between *Desulfovibrio vulgaris* Hildenborough and *Methanococcus maripaludis* within a co-culture biofilm. Dependent upon environmental conditions (sulfate or no sulfate), the potential interactions could range from competition to cooperation. An improved understanding of factors that drive biofilm community relationships will aid in discernment of environmental observations as well as manipulation of interactions to achieve and/or maintain stable ecosystem function particularly for low energy, anaerobic environments. The presented research provides insight into the metabolic association between *Desulfovibrio vulgaris* Hildenborough in the co-culture biofilm in response to the invasion of *Methanococcus maripaludis* and how metabolic interactions are affected by a stress perturbation of a more thermodynamically favorable electron acceptor such as sulfate.

MATERIALS AND METHODS

Culture Conditions

Desulfovibrio vulgaris Hildenborough and *Methanococcus maripaludis* S2 were anaerobically cultured in coculture media (CCM) with 80% N_2: 20% CO_2 sparged headspace at 30°C and shaking at 125 rpm (Brileya et al., 2014b). Batch, planktonic, monocultures of *D. vulgaris* Hildenborough and *Desulfovibrio alaskensis* G20 were grown in serum bottles or Balch tubes with the addition of 30 mM sulfate. Batch, planktonic, monocultures of *M. maripaludis* were grown in serum bottles or Balch tubes and amended with 30 mM acetate instead of lactate, along with an over pressurization of 80% H_2: 20% CO_2 (200 kPa). Co-culture biofilm was propagated on glass slides in a modified, continuously stirred, 1 L CDC reactor (BioSurface Technologies Corp., Bozeman, MT, USA) and sampled every 24 hours for planktonic optical density (600 nm), protein, and anions (lactate, acetate, sulfate) as previously described (Brileya et al., 2014b; Clark et al., 2006, 2012). Protein quantification was determined from the Quant-iT protein assay with a Qubit fluorometer (Invitrogen) following manufacturer's directions.

Gas Chromatography

Gas analysis was conducted with a 490microGC (Agilent Technologies, Inc., Santa Clara, CA, USA) containing dual channels and thermal conductivity detectors. Helium carrier gas was used for the 10 m Molsieve5A and PoraplotQ columns at 145 kPa and 80°C with injectors at 110°C and the heated sample line at 40°C. Injections made from the reactor headspace were as previously described (Brileya et al., 2014b).

Sulfate Stress

The co-culture biofilm reactor system with *D. vulgaris* Hildenborough and *M. maripaludis* was grown to steady state with daily sampling for lactate, acetate, methane production, and planktonic optical density. At 480 hours, planktonic and biofilm samples were destructively harvested and fixed in 4% paraformaldehyde for a microscopy baseline. The reactors were given 24 hours to equilibrate after the baseline biofilm was harvested, and then at 504 hours 30 mM sodium sulfate (vol/vol) was added to the duplicate reactors and the carboy of media. Planktonic samples were also collected and filtered using a 0.22 µm PTFE syringe filter during sulfate stress to monitor sulfate and lactate concentration using a Dionex ICS-1100 ion chromatography equipped with the AS-DV Carousel and Chromeleon software (Thermo Scientific). Hydrogen sulfide (H_2S) was quantified from planktonic samples using a hydrogen sulfide assay as described (Cord-Ruwisch, 1985). Briefly, a standard curve for sulfide concentrations from 1.5 mM to 50 mM was prepared anaerobically. Samples of 50 µL were added to 4 mL of a copper sulfate solution and the absorbance was measured at 480 nm in a Shimadzu UV-1700 Pharma spec UV-VIS spectrophotometer (Shimadzu Corp., Kyoto, Japan). The co-culture biofilm samples were destructively harvested 24 hours (reactor T=528) and 96 hours (reactor T=600) after sulfate addition. The slides were quantified for protein and image analysis as well as for transfer into batch media. The co-culture biofilm was anaerobically harvested and scraped into 10 mL of the lactate sulfate media in batch Balch tubes. The transferred biofilm was homogenized before being serially diluted and grown planktonically for optical density and gas chromatography analysis.

Cell Counts and Image Analysis of Co-culture Biofilm

Fluorescence *in situ* hybridization (FISH) was accomplished using the domain specific bacterial probe EUB338-Cy3 and archaeal probe ARCH915-Cy5. Fluorescently stained polyacrylamide embedded fixed whole biofilm for 3D-FISH was imaged on a Leica TCS SP5 II upright confocal laser scanning microscope using a 63x 0.9 NA long working distance (2.2 mm) water dipping objective (Leica Microsystems, Exton, PA) as previously described (Brileya et al., 2014a; Brileya et al., 2014b; Daims et al., 2006). Biovolumes of *D. vulgaris* and *M. maripaludis* were determined from measured threshold areas for the two channels, Cy3 and Cy5 respectively, using MetaMorph (Molecular Devices, Sunnyvale, CA, USA). Planktonic samples that were collected for cell counts were fixed in 2% formaldehyde (final concentration) and stained with 0.3 g/L Acridine Orange as described (Brileya et al., 2014b). Integrated morphometry analysis in MetaMorph was used to extrapolate planktonic cell counts for the respective populations.

Spent Filtrate Preparation

Initial growth curves acquired from absorbance measurements (600 nm) were carried out in 40 mL quantities of 0.22 µm (Pall) syringe filtered batch, planktonic, *M. maripaludis* grown in 125 mL serum bottles for 167 hours. Replicate Balch tubes were prepared with the anaerobic filtrate and amended with 30 mM fresh lactate and sulfate or acetate for the respective *D. vulgaris* Hildenborough, *D. alaskensis* G20, or *M. maripaludis* cultures as well as an additional 1X of ammonium chloride, potassium, vitamins, trace minerals, and selenite (Walker et al., 2009). Filtrate was also prepared for 0.22 µM filtered co-culture planktonic reactor samples and *M. maripaludis* cultures. The filtrate was centrifuge filtered at 4700 rpm for 20 minutes at 4°C using manufacturer recommended protocol for the 10 kDa molecular weight cutoff Amicon® Ultra-15 units (Sigma-Aldrich). The samples were then freeze dried using VirTis Genesis Pilot Lyophilizer (SP Scientific, USA). The lyophilized material was resuspended in 3 mL of

HPLC grade methanol and then freeze dried again before being resuspended in fresh CCM media with the necessary substrate amendments. Growth curves of the filtrate preparations were recorded by taking optical density readings (600 nm) on a tube Spectronic 20D+ (Thermo Fisher Scientific) every 2 hours for up to 100 hours.

RESULTS

Sulfate Stress of the Co-culture Biofilm Reactor

As previously shown (Brileya et al., 2014b), the co-culture biofilm reaches a consistent methane flux by approximately 300 h as the biofilm forms and matures (Figure 1). The sulfate addition (504 h) to the co-culture reactors coincided with a subsequent methane burst (~6 h post addition) and a steady increase in optical density (600 nm) readings for the planktonic population (Figure 1). The planktonic cell counts for *D. vulgaris* Hildenborough (DvH) increased 2-fold, while planktonic *M. maripaludis* (Mmp) showed a brief increase in cell counts (up 10,000 cells/ml) followed by a decline that was not statistically significant from the pre-sulfate baseline value of ~5,000 cells/ml (Figure 2). This resulted in the planktonic population ratio of *D. vulgaris* Hildenborough to *M. maripaludis* increasing from 2:1 to 5:1. The co-culture biofilm also did not show a decrease in the *M. maripaludis* population as anticipated, instead the FISH derived biovolume showed a 3-fold increase in the *M. maripaludis* population post-sulfate addition (Figure 2). *D. vulgaris* Hildenborough increased 5-fold in the co-culture biofilm thereby changing the population ratio in the biofilm to 6:1.

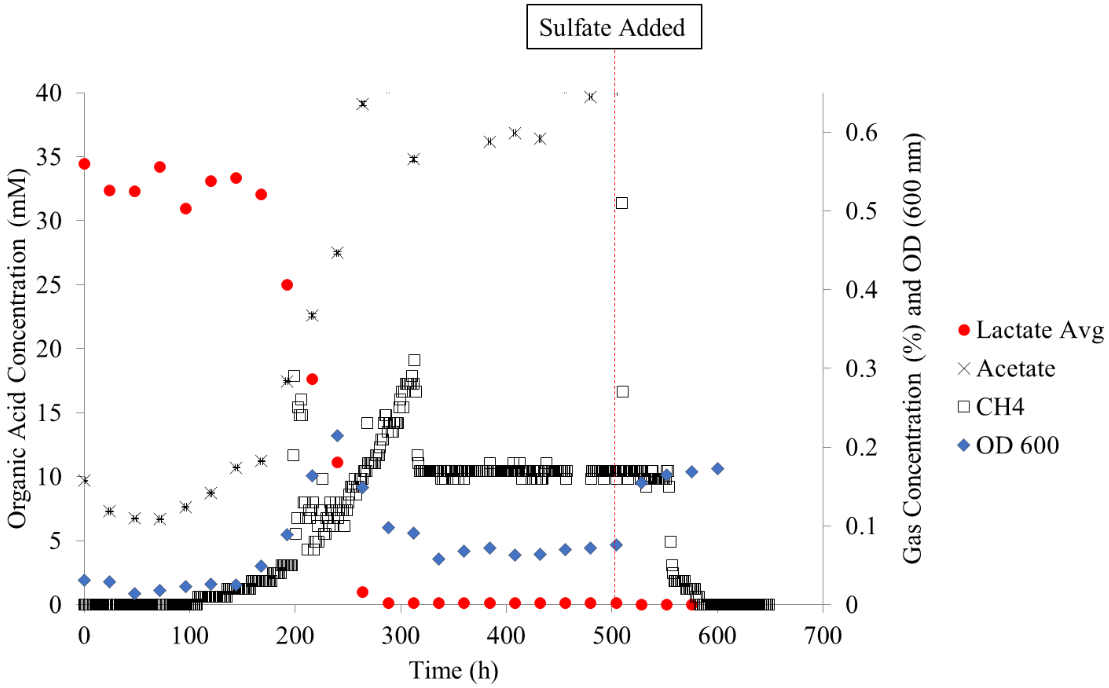

Figure 1. *D. vulgaris* Hildenborough and *M. maripaludis* co-culture biofilm reactor analysis used planktonic samples collected after 48 h incubation every 24 h for organic acid quantification (Lactate and Acetate), planktonic optical density (O.D.$_{600nm}$), and hourly for headspace (CH_4) analysis. Typical lactate consumption followed by proportional acetate production is depicted. Sulfate stress occurred at 504 hours (dotted line) which resulted in a CH_4 burst followed by a sharp decline (attributed to sulfide corrosion of the instrument columns) and increased planktonic growth (O.D.$_{600nm}$).

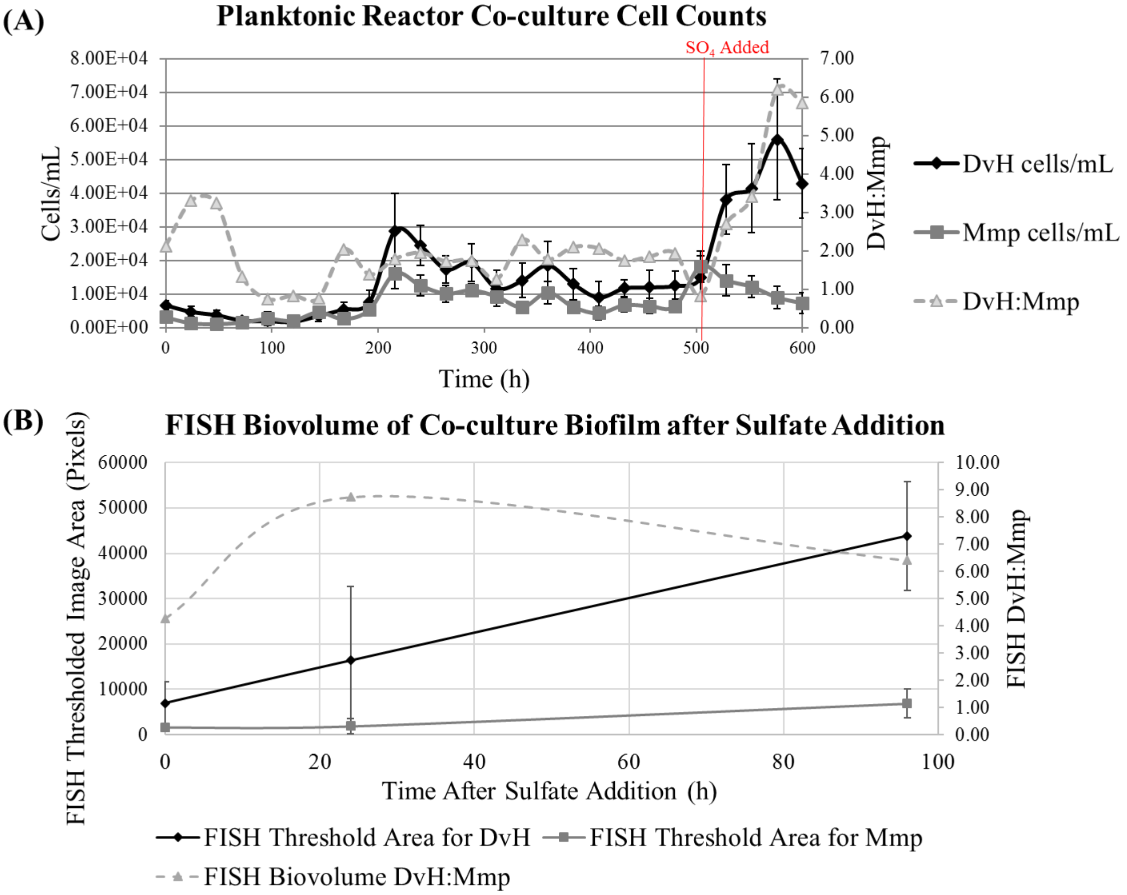

Figure 2. Average cell populations in co-culture before and after sulfate stress. Planktonic samples were collected from the *D. vulgaris* Hildenborough (DvH) and *M. maripaludis* (Mmp) co-culture reactors for cell counts (A) planktonic portion of reactor co-culture before sulfate addition are steady and show an increase in the DvH population as well as a higher DvH to Mmp ratio (DvH:Mmp) post-addition. (B) Biofilm was harvested, and FISH was used to calculate respective culture biovolumes (pixel area) which showed an increase in DvH followed by an increase in Mmp leading to a lower ratio (DvH:Mmp) between the populations.

Interestingly, a sharp decline in methane started approximately 50 hours post-sulfate addition, however, there was ultimately a failure by the gas chromatography instrumentation which is ascribed to be due to the columns becoming contaminated with sulfide from failed guard columns (data not shown). Soluble sulfide levels were 0.1 mM (Figure S1). To ascertain the presence of viable *M. maripaludis* cells, biofilm slides were anaerobically harvested (~100 h post-sulfate addition) from the sulfate stressed reactors and scraped into batch Balch tubes that contained fresh lactate:sulfate medium. After homogenizing the co-culture biofilm in the medium (~1 ml anoxic medium), serial dilutions were performed in the tubes before being incubated. After 200 hours, growth was observed up to 10^7 cells/cm^2 and methane was detected in the headspace of all tubes, as confirmed by single injections made on an alternate gas chromatography instrument (data not shown). The co-culture populations were visualized with FISH probes before the sulfate addition as well as 24 h, 48 h, and 96 h post-sulfate (Figure 3). After the sulfate addition (24 h), the *D. vulgaris* biovolume increased 2.5-fold whereas *M. maripaludis* remained at similar levels. At 48 h post-sulfate addition, the *D. vulgaris* appeared to expand and occupy biofilm space, and by 96 h post-sulfate, the *D. vulgaris* biovolume increased an additional 2.6-fold. Surprisingly, the *M. maripaludis* micro-clusters did not disappear and/or get replaced by growing *D. vulgaris* biomass, but rather expanded with the *D. vulgaris* network (3.5-fold biovolume increase).

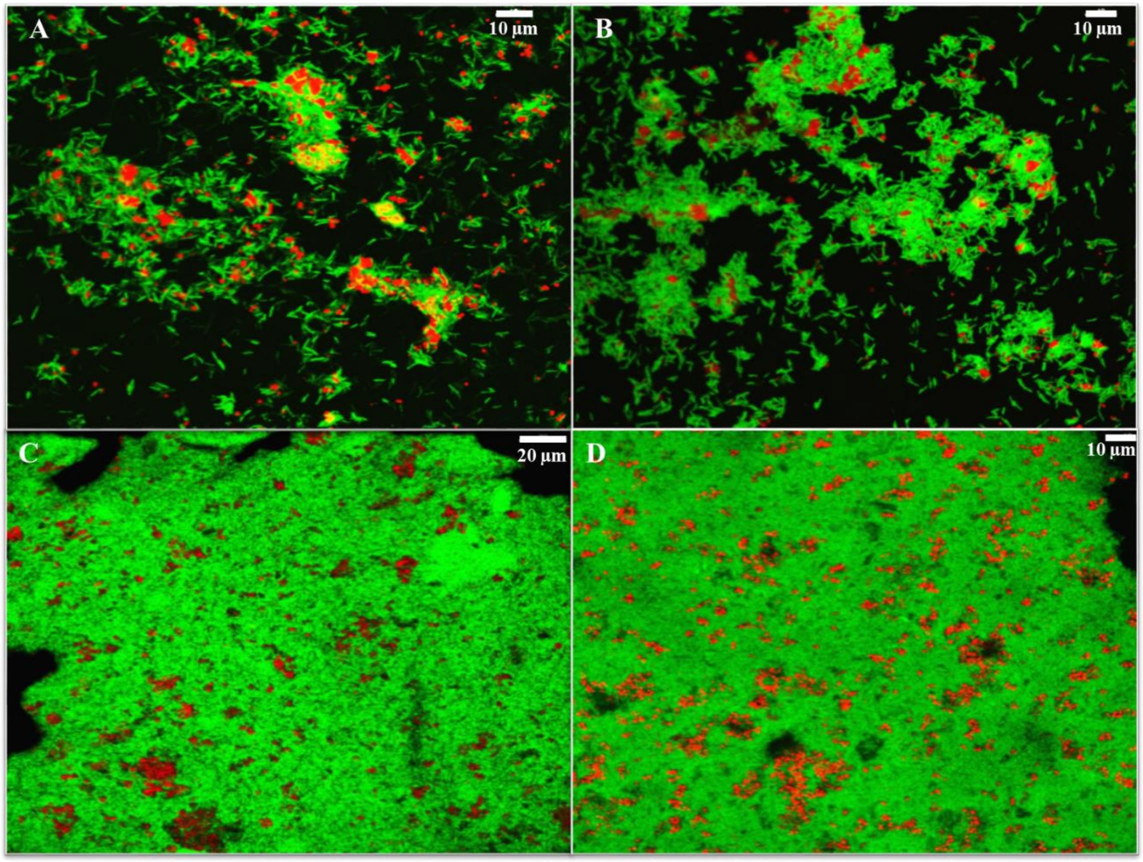

Figure 3. Co-culture biofilm FISH was imaged before and after sulfate addition. Scraped biofilm of *D. vulgaris* Hildenborough (EUB338-Green) and *M. maripaludis* (ARCH915-Red) from the co-culture biofilm reactor were harvested (A) before sulfate stress (B) 24 hours after sulfate stress (C) 48 hours after sulfate stress and (D) 96 hours after sulfate stress.

Growth Effect of Filtered Media

Spent media from the planktonic portion of the co-culture reactors was filtered via centrifugation (filter with 10 kDa molecular weight cut-off) before being lyophilized and resuspended in fresh medium with lactate and sulfate. The *D. vulgaris* culture had a 12-hour growth lag and decreased maximum optical density (600 nm) that was not observed in the control lacking the filtrate (Figure 4A). Once growth initiated in the treated culture, the growth rate was approximately 2-fold lower. The same 10 kDa filtered fraction from the co-culture reactors was prepared for *M. maripaludis* with the appropriate amendments (CCM + H_2/CO_2) and growth effects (rate or yield) were not observed (Figure 4B). These observations led to the hypothesis that a *M. maripaludis* factor could impact *D. vulgaris* growth and therefore prompted further testing using spent medium from batch *M. maripaludis* monocultures.

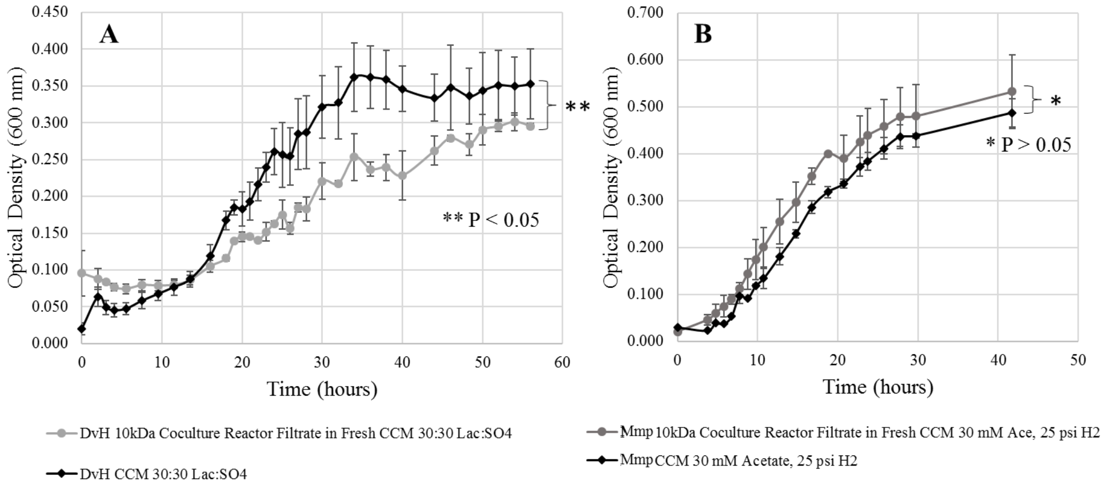

Figure 4. Planktonic samples were collected from the co-culture biofilm reactors and centrifuge filtered to 10 kDa before being lyophilized and resuspended in fresh CCM with 30 mM lactate and sulfate amendments for *D. vulgaris* Hildenborough (DvH), and 30 mM acetate with over-pressurization of H_2 for *M. maripaludis* (Mmp). (A) DvH has a lag time of 13 hours with an incumbered maximum $O.D._{600nm}$ and growth rate (**p-value < 0.05) as compared to the unmodified growth control (black) when grown in the co-culture reactor filtrate. (B) *M. maripaludis* exhibits no statistically significant (*p-value > 0.05) growth impact as compared to the control (black) when grown in the co-culture reactor filtrate.

Further growth experiments were done with the 10 kDa filtered fraction from *M. maripaludis* that was resuspended with fresh medium. Interestingly, the monoculture *D. vulgaris* did not have appreciable growth in the 10 kDa filtrate from the methanogen

(Figure 5A). To determine if the growth effect was unique to *D. vulgaris*, a different sulfate-reducing bacterium, *Desulfovibrio alaskensis* G20, was tested for growth with the 10 kDa filtered fraction from *M. maripaludis* amended with fresh lactate/sulfate medium. The *D. alaskensis* G20 growth rate declined 1.4x and the biomass yield was approximately 1.5x lower (Figure 5B). *Pseudomonas aeruginosa* was tested as a non-sulfate-reducing bacterium (Gram-negative), and growth was not impaired and perhaps had a faster initial growth rate (Figure 5C). Interestingly, *M. maripaludis* incubated in a filtered *D. vulgaris* spent medium did not exhibit significant growth effects (data not shown).

Because the growth of the *Desulfovibrio* species in the methanogen 10 kDa filtrate was most impacted, the utilization of lactate and sulfate along with production of H_2 was determined. However, these growth tests were done with filtrate that was not concentrated as to get some degree of *D. vulgaris* growth. The 10 kDa filtrate was amended with lactate + sulfate for *D. vulgaris* or *D. alaskensis* and amended with lactate-only for the co-culture. The amendment of additional nitrogen, phosphorus, and vitamins to the filtrate did not significantly increase growth or alleviate the growth effect (data not shown). *D. vulgaris* in CCM with 30 mM lactate and 30 mM sulfate had a growth rate of 0.08/h, and used lactate and sulfate at a similar rate of 0.2 mM/h (Figure 6A). *D. vulgaris* also displayed a transient increase in H_2 with a maximum of 0.12%. When *D. vulgaris* was incubated with the *M. maripaludis* filtrate, the growth rate declined to 0.04/h, the lactate and sulfate were utilized at a slower rate (0.068 mM sulfate/h and 0.076 mM lactate/h), and H_2 was only 0.06% (Figure 6B). In addition, the ratio of lactate to sulfate consumed per max biomass for the control was 3.38 (mM/mM/O.D.$_{600nm}$) but was 8.80 for the filtrate treated culture. *D. alaskensis* in CCM with 30 mM lactate and 30 mM sulfate had a growth rate of 0.068/h, used lactate at a rate of 0.43 mM/h and sulfate at a rate of 0.43 mM/h with a transient burst of 0.18% H_2 (Figure 6C). When *D. alaskensis* was incubated with the *M. maripaludis* filtrate, the growth rate was similar, and the lactate and sulfate were utilized at a slower rate (0.3 mM/h), and H_2 was 0.17% (Figure 6B). For *D. alaskensis*, the ratio of lactate to sulfate consumed per max biomass for the control was 2.07 (mM/mM/ O.D.$_{600nm}$) but was 3.15 for the filtrate treated culture. For the co-culture in CCM with 30 mM lactate, the growth rate is 0.04/h and lactate consumption has a k_{max} of 0.05 mM/h (Figure 7). In the presence of *M. maripaludis* 10 kDa filtrate, the co-culture has a slower growth (0.03 vs 0.04/h) and slower lactate consumption (0.03 mM/h). The ratio of lactate consumed to CH_4 produced per unit biomass was approximately 2-fold higher for the filtrate treatment compared to the control (2.91 versus 1.47) (Figure 7).

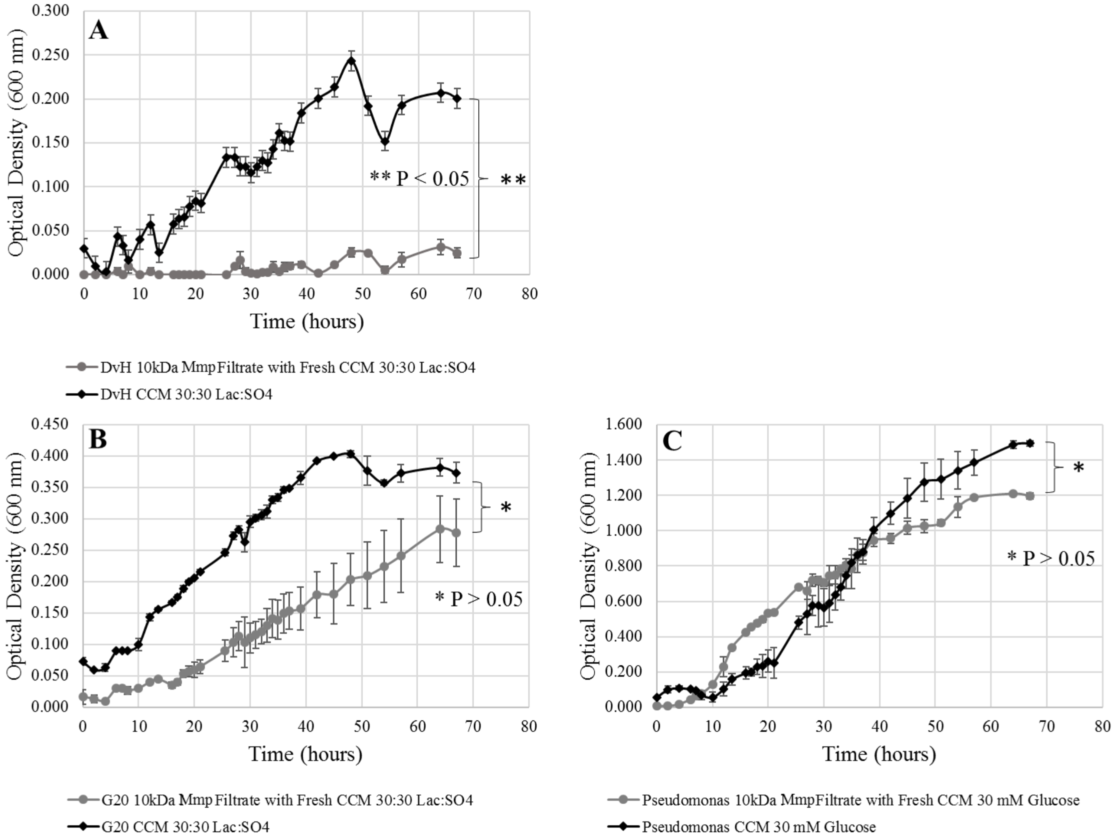

Figure 5. Planktonic samples were collected from *M. maripaludis* (Mmp) spent media and centrifuge filtered to 10 kDa before being lyophilized and resuspended in fresh CCM with 30 mM lactate and sulfate amendments for *D. vulgaris* Hildenborough (DvH) and *D. alaskensis* G20 (G20), and 30 mM glucose for *Pseudomonas aeruginosa*. (A) DvH exhibits no growth (**p-value < 0.05) as compared to the control (black) when grown in the spent *M. maripaludis* filtrate. (B) *D. alaskensis* G20 experiences a reduced growth rate from the control (black) that is not statistically significant (*p-value > 0.05) when grown in the *M. maripaludis* filtrate. (C) *P. aeruginosa* has no statistically significant growth rate deviation (*p-value > 0.05) from the control (black) when grown in the *M. maripaludis* filtrate.

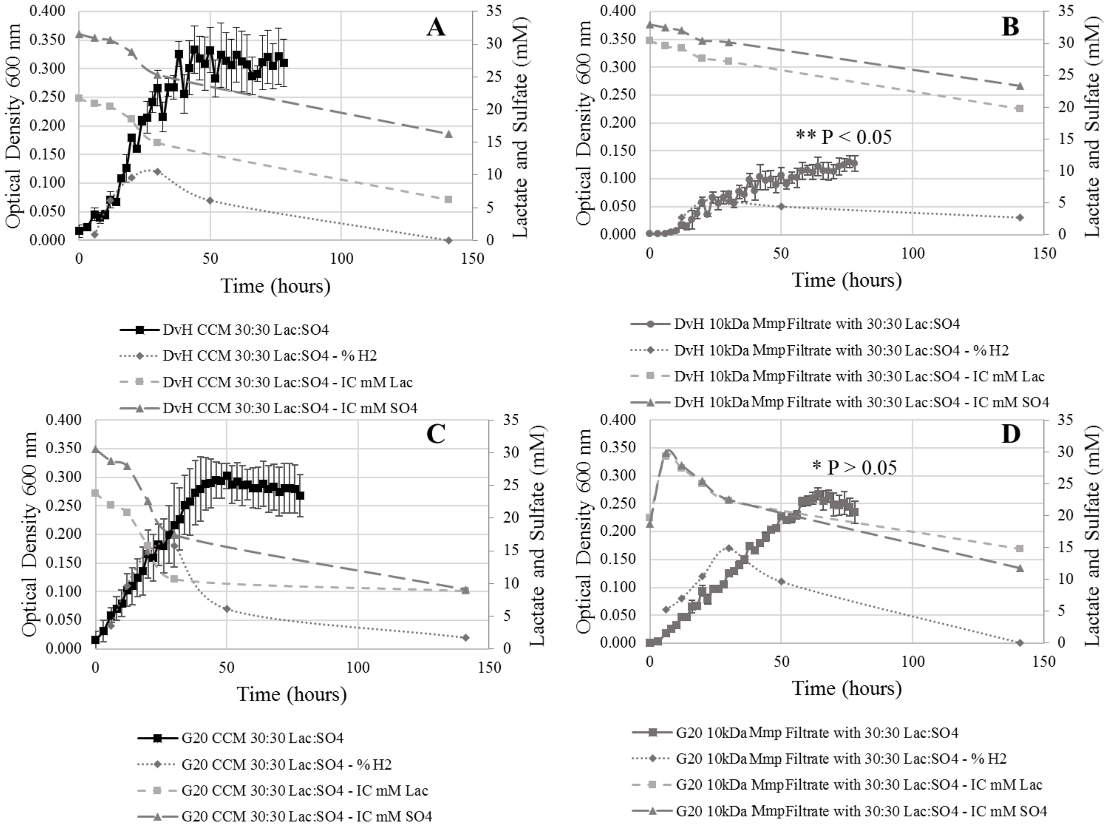

Figure 6. Planktonic samples were collected from *M. maripaludis* (Mmp) spent media and centrifuge filtered to 10 kDa before the addition of 30 mM lactate and sulfate for *D. vulgaris* Hildenborough (DvH) and *D. alaskensis* G20. Samples were collected to determine hydrogen, lactate, and sulfate concentrations over time. (A) *D. vulgaris* Hildenborough in standard CCM media (B) *D. vulgaris* Hildenborough grown in the filtrate has impaired growth as compared to the control in (A) (**p-value < 0.05) and less lactate and sulfate depletion. (C) *D. alaskensis* G20 grown in standard CCM media. (D) *D. alaskensis* G20 grown in the filtrate has a slower rate of growth compared to the control in (C) but not statistically significant (*p-value > 0.05) and only slightly less hydrogen production, optical density, and lactate/sulfate depletion.

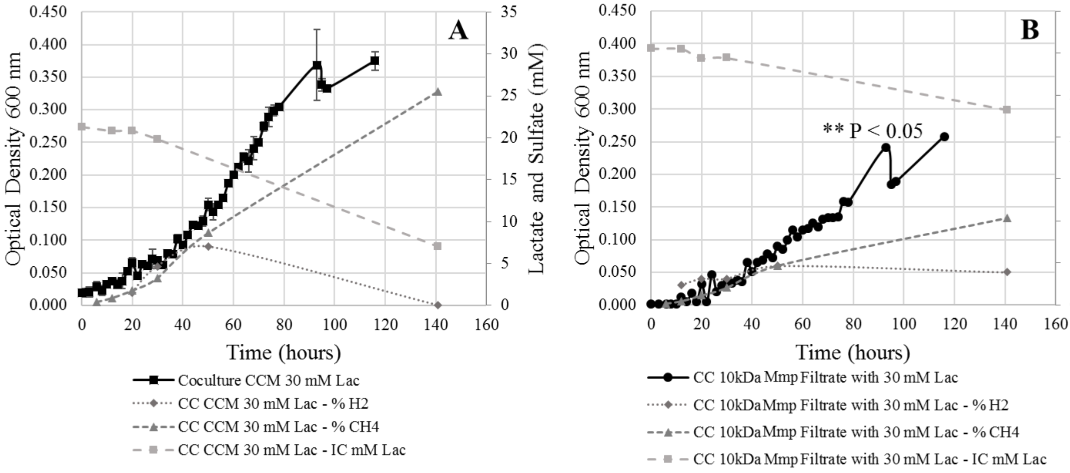

Figure 7. Sulfate and lactate depletion in the presence of filtrate. Planktonic samples were collected from *M. maripaludis* (Mmp) spent media and centrifuge filtered to 10 kDa before the addition of 30 mM lactate for *D. vulgaris* Hildenborough and *M. maripaludis* co-culture (CC) growth. Samples were collected to determine lactate, sulfate, and hydrogen concentrations over time. (A) Co-culture (CC) in standard CCM media (B) Co-culture (CC) grown in the filtrate has impaired growth as compared to the control in (A) (**p-value < 0.05) and less lactate depletion, and less methane accumulation.

DISCUSSION

The results demonstrate that *M. maripaludis* is able to withstand sulfate stress and maintain viability within a co-culture biofilm for ~100 hours post-sulfate addition. The slower growth observed for *D. vulgaris* in co-culture with *M. maripaludis* is dictated by the metabolic pairing through hydrogen oxidation. Previous work showed for the test SRBs and methanogens, that SRBs have a smaller K_S (substrate affinity) for H_2, and thus can outcompete methanogens (Kristjansson et al., 1982). However, recent work demonstrated the co-occurrence of methanogenesis and sulfate-reduction in sulfate-rich estuarine sediments (Sela-Adler et al., 2017). Therefore, methanogens must have direct and/or indirect mechanisms to deal with sulfate stress and maintain metabolic activity, or it is heterogeneity that allows them to co-exist. As outlined by Conrad (Conrad, 1999), the steady-state concentration of H_2 in most methanogenic environments is near the thermodynamic equilibrium that is approximately -23 kJ/mol CH_4, and hydrogenotrophic methanogenesis would be inhibited if H_2 concentrations fall below this limit. For other organisms and/or groups to compete, H_2-consuming reactions with higher affinity for H_2 would take over at least by a rate equal to that of the methanogen (Conrad, 1999).

In a thermodynamic context, the sulfate-reducer should abandon the mutualism with the methanogen in order to utilize the more energetically favorable sulfate, but instead the biofilm maintained both populations and therefore the syntrophic metabolic coupling post-sulfate addition. Instead of a succession occurring (loss of methanogen), the biofilm community appeared stable and increased both members during sulfate exposure. Maintenance of the syntrophy would appear to only benefit the methanogen that is relying on the SRB for energy (*i.e.*, H_2); however metabolic heterogeneity of the SRB (*i.e.*, sulfidogenic vs. syntrophic) population seems likely, particularly as the biofilm increased in biomass/volume and likely experienced increased mass transport limitations for lactate and sulfate. It is well accepted that there is a higher degree of heterogeneity in biofilms compared with planktonic growth modes due to the additional physical and chemical influences (Stewart & Franklin, 2008). Significant single cell gene expression heterogeneity (*e.g.*, ~40 fold) has been reported for *D. vulgaris* in a similar system when grown as a planktonic monoculture or a co-culture with *Methanosarcina barkeri* (Qi et al., 2014), as well as when monoculture *D. vulgaris* is grown as a biofilm (Qi et al., 2016). Metabolic heterogeneity in SRB is advantageous as it increases the chance of survival in the environment where substrates are in constant flux (Plugge et al., 2011). The co-culture biofilm exposed to sulfate (96 h) showed persistence of the methanogenic population; therefore, indicating that a portion of the *D. vulgaris* population maintained a syntrophic metabolism or at least metabolic by-products were available for the methanogen. It is possible that portions of the internal biofilm were experiencing sulfate limitation (or *D. vulgaris* cell death and lysis) and could sustain localized clusters of the methanogen; however, that would not explain the observation of CH_4 in the batch, planktonic culture tubes with lactate and sulfate.

The persistence of the syntrophic metabolic coupling in the biofilm was hypothesized to be attributed to *M. maripaludis* exerting influence over *D. vulgaris* to ensure a continued partnership. Namely, if growth could be slowed enough so that *M. maripaludis* could still compete for H_2 and/or maintain other metabolic interactions, the methanogen could prolong persistence. The *M. maripaludis* filtrate had a detrimental impact on *D. vulgaris* growth, and to a lesser extent on *D. alaskensis* but not the unrelated Gram-negative bacterium, *P. aeruginosa*. *M. maripaludis* was also not significantly influenced when grown in filtrates of *D. vulgaris*, thereby indicating the methanogen as the source of the growth effects when the co-culture filtrates were tested. Moreover, dependent upon how the filtrate was processed (filtered through 0.22 µm or concentrated through 10 kDa filtration and lyophilization), the spent fraction inhibited or slowed growth in *D. vulgaris*.

Nutrient amendment did not alleviate the decline in growth, and moreover, micro-nutrient depletion could not explain the lack of growth for *D. vulgaris* in the 10 kDa *M. maripaludis* filtrate experiments because the samples were resuspended in fresh medium. Additionally, both *D. alaskensis* G20 and *P. aeruginosa* were able to grow in the 10 kDa *M. maripaludis* filtrate which indicates that the preparation itself is likely not the reason for the growth impact on *D. vulgaris*. A metabolomic screen of the 10 kDa fraction did not return any substantial targets on known antimicrobial molecules/metabolites; however, little is known about anti-microbials in archaea. Current findings report only 5 known archaeocins compared to 338 bacteriocins in bacteria (G. Wang et al., 2009, 2016; Z. Wang, 2004). Without knowing the potential class of compound(s), it is difficult to quantify it much less elucidate the mechanism. Future work is needed to prepare different fractions from different growth conditions to screen for the unknown metabolite.

The ability of *M. maripaludis* to endure sulfate stress when metabolically coupled to *D. vulgaris* was demonstrated here and could ultimately be explained by a metabolic modulation that causes *D. vulgaris* to alter the ratio of lactate oxidized to sulfate reduced. An increase in lactate oxidized with a decrease in sulfate reduced and decrease in biomass biosynthesis could contribute to the maintenance of H_2 levels (and/or other metabolites) that would sustain the methanogen in the presence of sulfate. The data suggests that the interplay between SRBs and methanogens is not an “all-or-none” scenario, but rather a spectrum dictated by utilization and production rates in local proximities that ultimately dictate local metabolic flux. Moreover, the results suggest that *M. maripaludis* directly and/or indirectly (*i.e.*, metabolic modulation) influences the ability of *Desulfovibrio* to oxidize lactate and produce subsequent by-products. It is unclear if the symbiosis is maintained by proximity in the biofilm thereby syncing metabolisms, targeted metabolic modulation, and/or if there is protein mediated communication occurring similar to the flagellar cap protein (FliD) interaction that was reported by Shimoyama (Shimoyama et al., 2009). The potential for *M. maripaludis* filtrate to negatively influence *D. vulgaris* growth in monoculture represents the complexity of interactions that can occur between these two organisms and should be further assessed to determine the potential role it could play in syntrophy.

Acknowledgments. This material by ENIGMA- Ecosystems and Networks Integrated with Genes and Molecular Assemblies (http://enigma.lbl.gov), a Scientific Focus Area Program at Lawrence Berkeley National Laboratory is based upon work supported by the U.S. Department of Energy, Office of Science, Office of Biological & Environmental Research under contract number DE-AC02-05CH11231.

REFERENCES CITED

Brileya, K. A., Camilleri, L. B., & Fields, M. W. (2014a). 3D-Fluorescence In Situ Hybridization of Intact, Anaerobic Biofilm. In L. Sun & W. Shou (Eds.), *Engineering and Analyzing Multicellular Systems* (Vol. 1151, pp. 189–197). New York, NY: Springer New York. http://doi.org/10.1007/978-1-4939-0554-6

Brileya, K. A., Camilleri, L. B., Zane, G. M., Wall, J. D., & Fields, M. W. (2014b). Biofilm growth mode promotes maximum carrying capacity and community stability during product inhibition syntrophy. *Frontiers in Microbiology*, *5*(12), 693. http://doi.org/10.3389/fmicb.2014.00693

Brileya, K. A., Connolly, J. M., Downey, C., Gerlach, R., & Fields, M. W. (2013). Taxis toward hydrogen gas by Methanococcus maripaludis. *Scientific Reports*, *3*, 3140. http://doi.org/10.1038/srep03140

Carlson, R. P., Beck, A. E., Phalak, P., Fields, M. W., Gedeon, T., Hanley, L., … Heys, J. J. (2018). Competitive resource allocation to metabolic pathways contributes to overflow metabolisms and emergent properties in cross-feeding microbial consortia. *Biochemical Society Transactions*, *46*(2), 269–284. http://doi.org/10.1042/BST20170242

Clark, M. E., He, Q., He, Z., Huang, K. H., Alm, E. J., Wan, X.-F., … Fields, M. W. (2006). Temporal transcriptomic analysis as Desulfovibrio vulgaris Hildenborough transitions into stationary phase during electron donor depletion. *Applied and Environmental Microbiology*, *72*(8), 5578–88. http://doi.org/10.1128/AEM.00284-06

Clark, M. E., He, Z., Redding, A. M., Joachimiak, M. P., Keasling, J. D., Zhou, J. Z., … Fields, M. W. (2012). Transcriptomic and proteomic analyses of Desulfovibrio vulgaris biofilms: carbon and energy flow contribute to the distinct biofilm growth state. *BMC Genomics*, *13*(1), 138. http://doi.org/10.1186/1471-2164-13-138

Conrad, R. (1999). Contribution of hydrogen to methane production and control of hydrogen concentrations in methanogenic soils and sediments. *FEMS Microbiology Ecology*, *28*(3), 193–202. http://doi.org/10.1016/S0168-6496(98)00086-5

Cord-Ruwisch, R. (1985). A quick method for the determination of dissolved and precipitated sulfides in cultures of sulfate-reducing bacteria. *Journal of Microbiological Methods*, *4*, 33–36.

Daims, H., Lücker, S., & Wagner, M. (2006). Daime, a novel image analysis program for microbial ecology and biofilm research. *Environmental Microbiology*, *8*(2), 200–213. http://doi.org/10.1111/j.1462-2920.2005.00880.x

Dean, A. M. (1985). The dynamics of microbial commensalisms and mutualisms. In D. H. Boucher (Ed.), *The Biology of Mutualism* (pp. 270–300). Oxford: Oxford University Press. Retrieved from https://books.google.com/books?hl=en&lr=&id=dWuQS_3F2P0C&oi=fnd&pg=PA270&ots=_vLqPPvfaW&sig=kQJWc5rcE0FIzy8fpfml3ZWn3-k#v=onepage&q&f=false

Kristjansson, J. K., Schönheit, P., & Thauer, R. K. (1982). Different Ks values for hydrogen of methanogenic bacteria and sulfate reducing bacteria: An explanation for the apparent inhibition of methanogenesis by sulfate. *Archives of Microbiology*, *131*(3), 278–282. http://doi.org/10.1007/BF00405893

Marchal, M., Goldschmidt, F., Derksen-Müller, S. N., Panke, S., Ackermann, M., & Johnson, D. R. (2017). A passive mutualistic interaction promotes the evolution of spatial structure within microbial populations. *BMC Evolutionary Biology*, *17*(1), 106. http://doi.org/10.1186/s12862-017-0950-y

Plugge, C. M., Zhang, W., Scholten, J. C. M., & Stams, A. J. M. (2011). Metabolic Flexibility of Sulfate-Reducing Bacteria. *Frontiers in Microbiology*, *2*(5), 81. http://doi.org/10.3389/fmicb.2011.00081

Qi, Z., Chen, L., & Zhang, W. (2016). Comparison of Transcriptional Heterogeneity of Eight Genes between Batch Desulfovibrio vulgaris Biofilm and Planktonic Culture at a Single-Cell Level. *Frontiers in Microbiology*, *7*(4), 1–14. http://doi.org/10.3389/fmicb.2016.00597

Qi, Z., Pei, G., Chen, L., & Zhang, W. (2014). Single-cell analysis reveals gene-expression heterogeneity in syntrophic dual-culture of Desulfovibrio vulgaris with Methanosarcina barkeri. *Scientific Reports*, *4*, 7478. http://doi.org/10.1038/srep07478

Sela-Adler, M., Ronen, Z., Herut, B., Antler, G., Vigderovich, H., Eckert, W., & Sivan, O. (2017). Co-existence of Methanogenesis and Sulfate Reduction with Common Substrates in Sulfate-Rich Estuarine Sediments. *Frontiers in Microbiology*, *8*(5), 1–11. http://doi.org/10.3389/fmicb.2017.00766

Shimoyama, T., Kato, S., Ishii, S., & Watanabe, K. (2009). Flagellum Mediates Symbiosis. *Science*, *323*(5921), 1574–1574. http://doi.org/10.1126/science.1170086

Stewart, P. S., & Franklin, M. J. (2008). Physiological heterogeneity in biofilms. *Nature Reviews. Microbiology*, *6*(3), 199–210. http://doi.org/10.1038/nrmicro1838

Walker, C. B., He, Z., Yang, Z. K., Ringbauer, J. A, He, Q., Zhou, J., … Stahl, D. A. (2009). The electron transfer system of syntrophically grown Desulfovibrio vulgaris. *Journal of Bacteriology*, *191*(18), 5793–801. http://doi.org/10.1128/JB.00356-09

Wang, G., Li, X., & Wang, Z. (2009). APD2: the updated antimicrobial peptide database and its application in peptide design. *Nucleic Acids Research, 37*(Database issue), D933-7. http://doi.org/10.1093/nar/gkn823

Wang, G., Li, X., & Wang, Z. (2016). APD3: the antimicrobial peptide database as a tool for research and education. *Nucleic Acids Research*, *44*(D1), D1087-93. http://doi.org/10.1093/nar/gkv1278

Wang, Z. (2004). APD: the Antimicrobial Peptide Database. *Nucleic Acids Research*, *32*(90001), 590D–592. http://doi.org/10.1093/nar/gkh025

SUPPLEMENTAL FIGURES

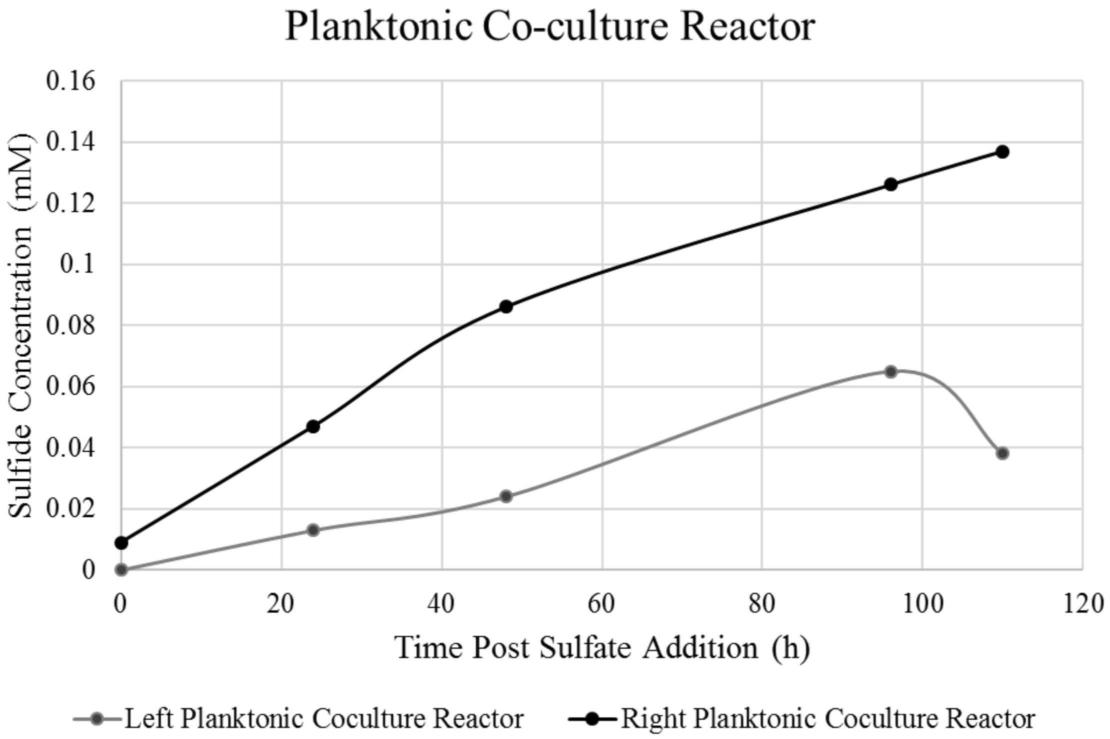

Figure S1. Sulfide concentration in planktonic portion of co-culture reactor replicates (Left and Right) post-sulfate addition. Planktonic samples were collected from the *D. vulgaris* Hildenborough (DvH) and *M. maripaludis* (Mmp) co-culture reactors for sulfide analysis.

CHAPTER FIVE

GROWTH EFFECTS OF SULFOPYRUVATE AND SULFOACETATE ON THE SULFATE-REDUCING BACTERIUM, DESULFOVIBRIO VULGARIS HILDENBOROUGH, AND THE METHANOGENIC ARCHAEON METHANOCOCCUS MARIPALUDIS S2

Contribution of Authors and Co-Authors

Manuscript in Chapter 5

Author: Laura B. Camilleri

Contributions: Developed experimental design, performed experiments, analyzed data, wrote and revised the manuscript.

Co-Author: Matthew W. Fields

Contributions: Developed experimental design, analyzed data, wrote and revised the manuscript.

Manuscript Information

Laura B. Camilleri and Matthew W. Fields

Scientific Reports

Status of Manuscript:
_____ Prepared for submission to a peer-reviewed journal
__x_ Officially submitted to a peer-reviewed journal
_____ Accepted by a peer-reviewed journal
_____ Published in a peer-reviewed journal

ABSTRACT

Sulfonates contribute immensely to the global sulfur cycle and are observed in numerous naturally occurring compounds including S-containing amino acids cysteine and methionine, neurotransmitters in eukaryotes, and CoM in methanogens. While a small number of microorganisms have been reported to utilize sulfonates directly as a sole carbon and/or energy source, little is known about the cycling of sulfonates in bacteria and the potential impacts on physiology. Given the fundamental and applied interests in sulfate-reducing bacteria and archaeal methanogens and their interactions, sulfopyruvate and sulfoacetate utilization was tested in the sulfate-reducing bacterium *Desulfovibrio vulgaris* Hildenborough and the hydrogenotrophic methanogen *Methanococcus maripaludis*. Both sulfopyruvate and sulfoacetate did not support growth of either microorganism as the sole carbon and energy source. When lactate and sulfate were provided for growth in the presence of sulfopyruvate (10 mM), *D. vulgaris* did not grow. However, in the presence of sulfoacetate (30 mM) with lactate and sulfate, *D. vulgaris* had slightly inhibited growth. For *M. maripaludis,* sulfopyruvate (10 mM) caused an extended growth lag in the presence of H_2 and CO_2, and sulfoacetate (30 mM) inhibited growth. Sulfoacetate (30 mM) had a similar inhibitory effect on growth of a sulfate-free co-culture of *D. vulgaris* and *M. maripaludis*. However, for both *D. vulgaris* and *M. maripaludis* monocultures, lower levels of sulfoacetate (0.1 or 1 mM) had small stimulatory effects on growth. The results demonstrate that sulfoacetate can be an inhibitor of *D. vulgaris* and *M. maripaludis* growth at high concentrations but promote growth at lower concentrations and could play a role in metabolic interactions between SRBs and methanogens.

INTRODUCTION

Sulfonates are ubiquitous in nature and encompass a variety of compounds, many of which are natural products. Sulfonates can be found in capnine (a bacterial sulfolipid), bacterial siderophores (petrobactinsulfonate), endospores (sulfolactate), as well as plant sulfolipids (sulfoquinovose), and sulfur (Cook et al., 2008). Sulfoacetate has largely been associated with algae and plants as a degradation product of sulfoquinovose and various pathways such as the degradation of taurine (2-aminoethanesulfonate) can be interconverted with sulfoacetate (Denger et al., 2004). Different sulfonates can be nutritionally important to organisms as it can provide a sole source of nitrogen and carbon thereby providing an important link between the N, C, and S cycles (Denger et al., 2009; Krejčík et al., 2008). Since sulfonates carry a negative charge and can release 500-fold more sulfur than needed for growth, ABC transporters are common along with a sulfonate anion exporter (DUF81) to prevent osmotic stress (Cook et al., 2008; Weinitschke et al., 2007).

Recent studies have reported bacteria such as *Cupriavidus necator, Rhodopseudomonas palustris*, *Roseovarius nubinhibens* ISM, *Neptuniibacter caesariensis* MED92, and *Desulfovibrio* strain IC1 can grow with sulfonates at concentrations of 10-20 mM (Denger et al., 2009, 2004; Krejčík et al., 2008; Weinitschke et al., 2007). Sulfate-reducing bacteria (SRB) such as *Desulfovibrio* strain IC1 have also been shown to specifically utilize sulfonates such as isethionate (2-hydroxy-ethanesulfonate) as terminal electron acceptors (Lie et al., 1996). Much of our knowledge about sulfonates is derived from the characterization of methanogenesis in which it was discovered that archaeal methanogens require the sulfonate, coenzyme M (2-mercaptoethanesulfonic acid), in the terminal step to methane formation (Graupner et al., 2000; White, 1986, 2017). Desulfonation reactions are known to generate sulfite (with the exception of C_2 sulfonates like taurine) which is toxic to all cells due to its nucleophilic reactivity and inhibits methanogenesis at levels exceeding 40 mM (Balderston & Payne, 1976; Becker & Ragsdale, 1998; Johnson & Mukhopadhyay, 2008; Mahlert et al., 2002; Weinitschke et al., 2007). Structural analogs of coenzyme M such as 2-bromoethanesulfonate (BES) are common inhibitors for methanogenesis when used at concentrations around 50 mM, and higher concentrations are needed specifically for hydrogenotrophic methanogens (Gunsalus et al., 1978; Liu et al., 2011; Zinder et al., 1984).

Hydrogenotrophic methanogenesis and sulfate reduction are considered ancient, anaerobic metabolisms (Leigh, 2001; Teske et al., 2003). In a co-culture biofilm reactor system between the hydrogenotrophic methanogen, *Methanococcus maripaludis* S2, and the SRB *Desulfovibrio vulgaris* Hildenborough, it was found that one of the most up-expressed co-culture biofilm genes encoded a putative membrane protein proposed to function as an anionic (sulfoacetate) exporter (DUF81 domain, DVU0149) (Camilleri et al., in prep). Given the potential role of sulfonates for S-cycling in sulfate-reducing bacteria and the role of sulfonates as metabolic precursors for the biosynthesis of coenzyme M in methanogens, the potential growth effects of sulfonates on *M. maripaludis* S2 and *D. vulgaris* Hildenborough were explored.

MATERIALS AND METHODS

Culture Conditions

Batch, planktonic, monocultures of *Desulfovibrio vulgaris* Hildenborough were grown in anaerobic Balch tubes of coculture media (CCM) containing 30 mM lactate and 15 mM sulfate with 80% N_2: 20% CO_2 headspace at 30°C with shaking at 125 rpm. Batch, planktonic, monocultures of *Methanococcus maripaludis* S2 were grown similarly in anaerobic Balch tubes and amended with 30 mM acetate, instead of lactate and sulfate, and over pressurized with 80% H_2: 20% CO_2 gas to 200 kPa (Brileya et al., 2014; Walker et al., 2009). All growth curves had absorbance readings (600 nm) measured using Unico 1100RS spectrophotometer (United Products and Instruments, Inc).

Sulfonate Compound Addition

The effect of sulfonate amendments was tested using 30 mM, 1 mM, 0.1 mM, 0.01 mM sulfoacetate and 10 mM sulfopyruvate (Sigma-Aldrich). The solubility of sulfopyruvate is 12.9 mg/mL in water therefore the base coculture media was modified to contain less water in order to add larger volumes of the amendments. This modified CCM was also used for the growth controls. For *D. vulgaris* Hildenborough, the control growth was tested with 30 mM formate, 10 mM pyruvate, or 30 mM lactate with and without sulfate additions. Sulfoacetate and sulfopyruvate were also tested with and without sulfate amendments. *M. maripaludis* was grown with 30 mM formate, 10 mM pyruvate, or 30 mM acetate with and without hydrogen gas over pressurization.

RESULTS AND DISCUSSION

Desulfovibrio vulgaris growth

D. vulgaris Hildenborough exhibited no growth on formate unless sulfate was present in CCM, and the pyruvate with sulfate amendment had no deviation in growth from the control (Figure 1). *D. vulgaris* cultures could slowly ferment media with pyruvate only or formate and sulfate (Figure 1) . The addition of sulfopyruvate did not result in growth regardless of sulfate or lactate addition (data not shown). However, slightly impeded growth was observed in the presence of sulfoacetate if lactate and sulfate were added. These results indicated that *D. vulgaris* could not desulfonate either sulfopyruvate or sulfoacetate in order to utilize the associated sulfite and/or organic carbon as electron acceptors or electron donors, respectively. The currently annotated genome of *D. vulgaris* does not indicate the presence of a known desulfonase despite the presence of several genes that are predicted to encode sulfonate transporters.

When lactate and sulfate were provided as typical electron donor and electron acceptor, respectively, growth was almost completely inhibited in the presence of 30 mM sulfoacetate (Figure 2). Interestingly, when sulfoacetate was provided at a reduced level (1 mM and 0.1 mM) with lactate and sulfate in the tested growth medium, growth was enhanced for *D. vulgaris* in that the growth rate was increased and the $O.D._{600nm}$ was increased as compared to the lactate with sulfate control (Figure 2). The results demonstrated that sulfoacetate inhibited *D. vulgaris* at high levels (30 mM), but at low levels (1 mM and 0.1 mM) growth increased by ~2-fold as compared to the control growth.

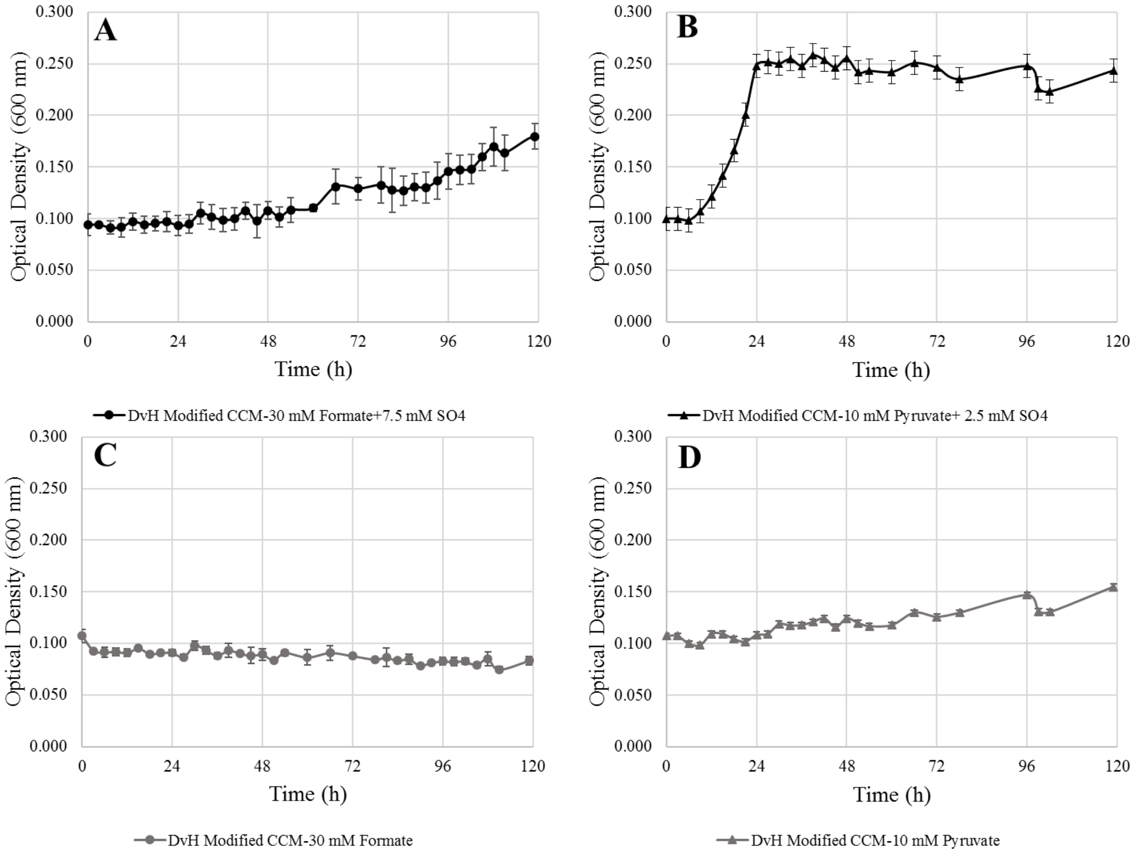

Figure 1. *D. vulgaris* growth on formate and pyruvate utilizing absorbance readings (600 nm) over time. (A) *D. vulgaris* Hildenborough (DvH) growth on formate with sulfate (30 mM: 7.5 mM), (B) pyruvate with sulfate (10 mM: 2.5 mM), (C) formate (30 mM) alone, and (D) pyruvate as the sole source of carbon and energy (10 mM).

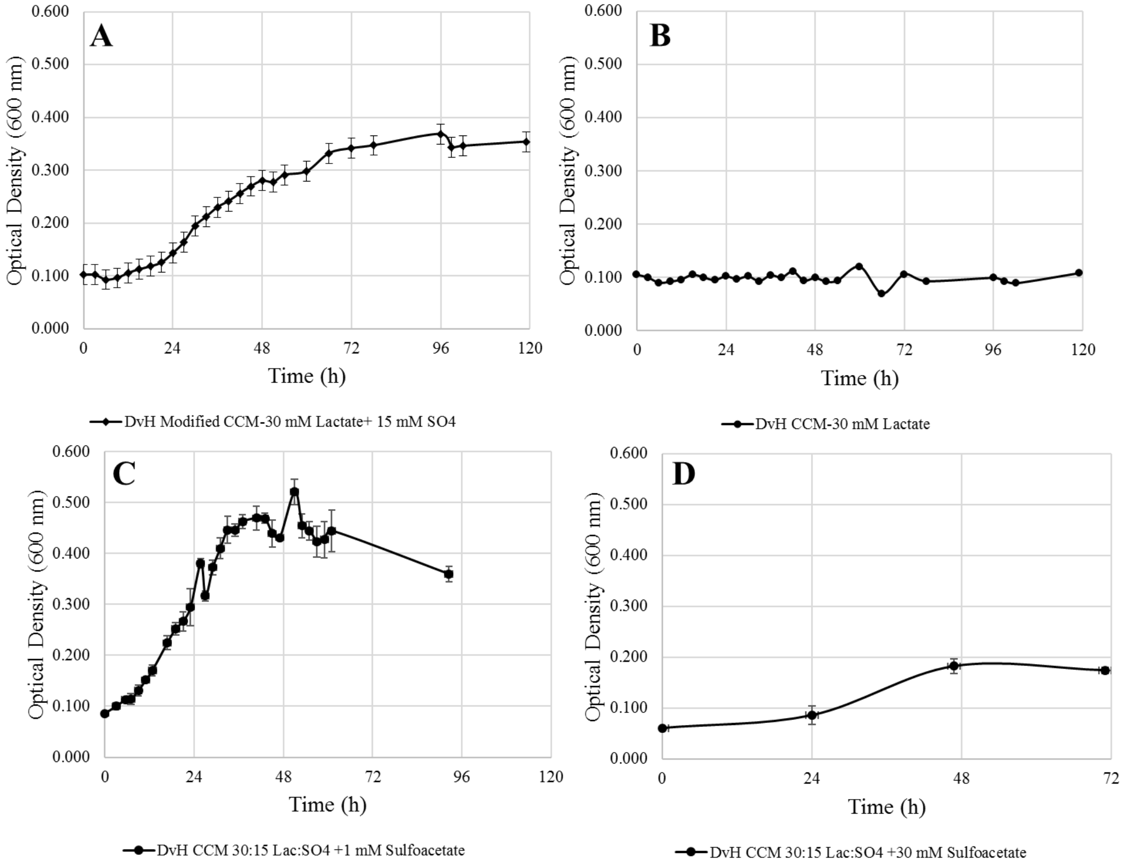

Figure 2. *D. vulgaris* growth on lactate and sulfoacetate utilizing absorbance readings (600 nm) over time. (A) *D. vulgaris* Hildenborough (DvH) growth in CCM with 30 mM lactate and 15 mM sulfate, (B) lactate (30 mM) alone (C) lactate and sulfate (30 mM: 15 mM) in the presence of 1 mM sulfoacetate, and (D) lactate and sulfate (30 mM: 15 mM) in the presence of 30 mM sulfoacetate.

In *D. vulgaris*, sulfopyruvate and sulfoacetate may be involved in the degradation of sulfur-containing amino acids cysteine and methionine. A complete pathway for cysteine to sulfolactate/sulfoacetate/sulfopyruvate is not predicted in *D. vulgaris* Hildenborough, and the genome annotation does not contain an identified enzyme to catalyze the conversion of sulfopyruvate to sulfolactate. The commonly identified enzymes with this activity include sulfolactate dehydrogenase (R and S) and malate dehydrogenase. The *D. vulgaris* Hildenborough genome has multiple genes that are annotated as presumptive lactate/malate dehydrogenases (NAD^+-linked – DVU0339 and DVU1412; FMN-linked – DVU2784). Sequence comparisons and biochemical studies have recently expanded the functionality of previously annotated malate and lactate dehydrogenases to have other activities such as sulfolactate dehydrogenase (Muramatsu et al., 2005); however, the potential role of DVU0339, DVU1412, and DVU2784 in conversion of sulfopyruvate to sulfolactate is unknown.

Other members of the *Desulfovibrio* family have demonstrated growth capabilities on sulfonate compounds such as cysteate or isethionate, as is the case with *Desulfovibrio desulfuricans* IC1 (Lie et al., 1996). Cysteate can be a product from cysteine degradation and can be converted to 3-sulfopyruvate by cysteine lyase. However, cysteine lyase has not been identified in the *D. vulgaris* Hildenborough genome via annotation. The *D. vulgaris* Hildenborough genome has five genes (DVU0494, 0841, 1655, 3121, and 3223) annotated as aspartate aminotransferases (EC 2.6.1.1) that could convert cysteate to 3-sulfopyruvate, but the exact roles for these presumptive proteins is not known. The results suggested that although sulfoacetate could not be used as a sole source of carbon and/or energy, low levels might serve as a co-metabolite. Previous work has shown that BES can serve as an alternative electron acceptor for sulfate-reducing bacteria (Ye et al., 1999) which could be beneficial at low levels but detrimental at high levels dependent upon electrogenic flow and/or enzyme-ligand interactions. It is also possible that sulfoacetate would impact precursor cycling between C and S compounds, but further work is needed to elucidate the possible role(s) of sulfoacetate in *D. vulgaris* metabolism.

Methanococcus maripaludis growth

M. maripaludis is routinely grown in CCM with H_2:CO_2 with and without acetate (30 mM), and the growth rate is similar for both conditions (0.037 h^{-1} versus 0.035 h^{-1}) (Figure 3). *M. maripaludis* displays little growth when provided with formate only (30 mM) and did not grow with pyruvate (10 mM) as the sole source of carbon and energy (Figure 4). *M. maripaludis* could grow in the presence of pyruvate when combined with H_2:CO_2 and the growth rate was slightly slower than the control (0.032 h^{-1}) (Figure 4). *M. maripaludis* could not grow with sulfopyruvate or sulfoacetate as the sole source of carbon and energy (data not shown). Growth was restored on sulfopyruvate when H_2:CO_2 was provided; however, there was a significant lag-phase (50 h) and the growth rate declined to 0.020 h^{-1} (almost 2-fold lower than the control) (Figure 5). Sulfoacetate completely inhibited *M. maripaludis* growth at 30 mM; however, similar to *D. vulgaris* growth, *M. maripaludis* displayed an increased growth rate in the presence of lower sulfoacetate levels (Figure 5). At 1 mM sulfoacetate, the growth was 0.055 h^{-1} and at 0.1

mM sulfoacetate the growth rate was 0.078 h^{-1}. These results demonstrated that sulfoacetate inhibited *M. maripaludis* at high levels (30 mM), but at low levels (1 mM and 0.1 mM) increased the growth rate by 1.5- to 2-fold as compared to the control. These results suggested that although sulfopyruvate and sulfoacetate could not be used as a sole source of carbon and/or energy by *M. maripaludis*, low levels might serve as a co-metabolite, perhaps for coenzyme biosynthesis.

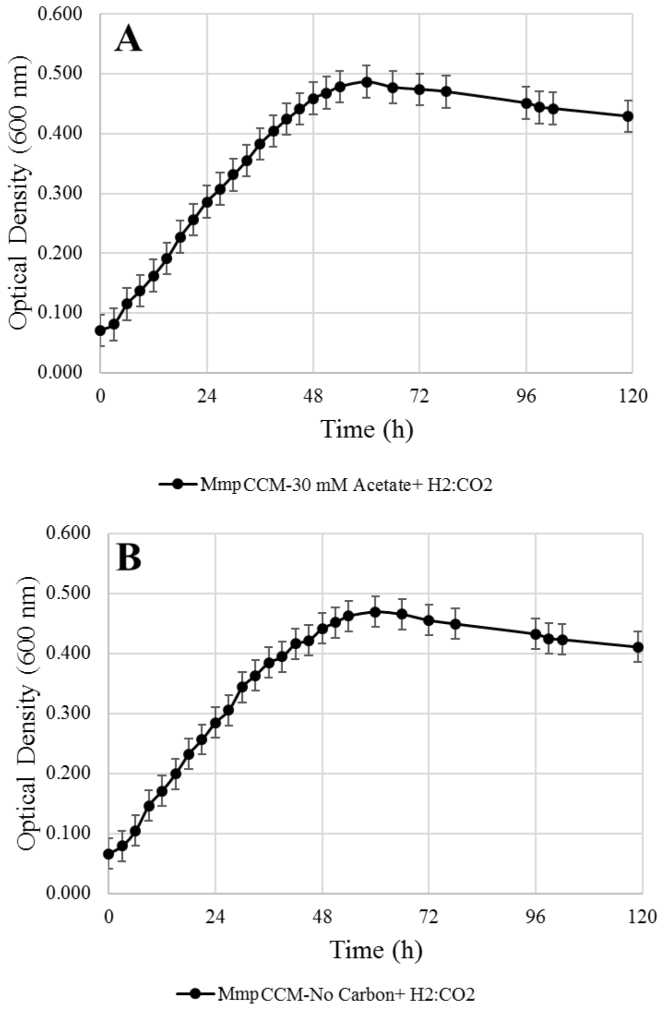

Figure 3. *M. maripaludis* (Mmp) growth utilizing absorbance readings (600 nm) over time with H_2:CO_2 (80%:20%) with acetate (30 mM) and without acetate.

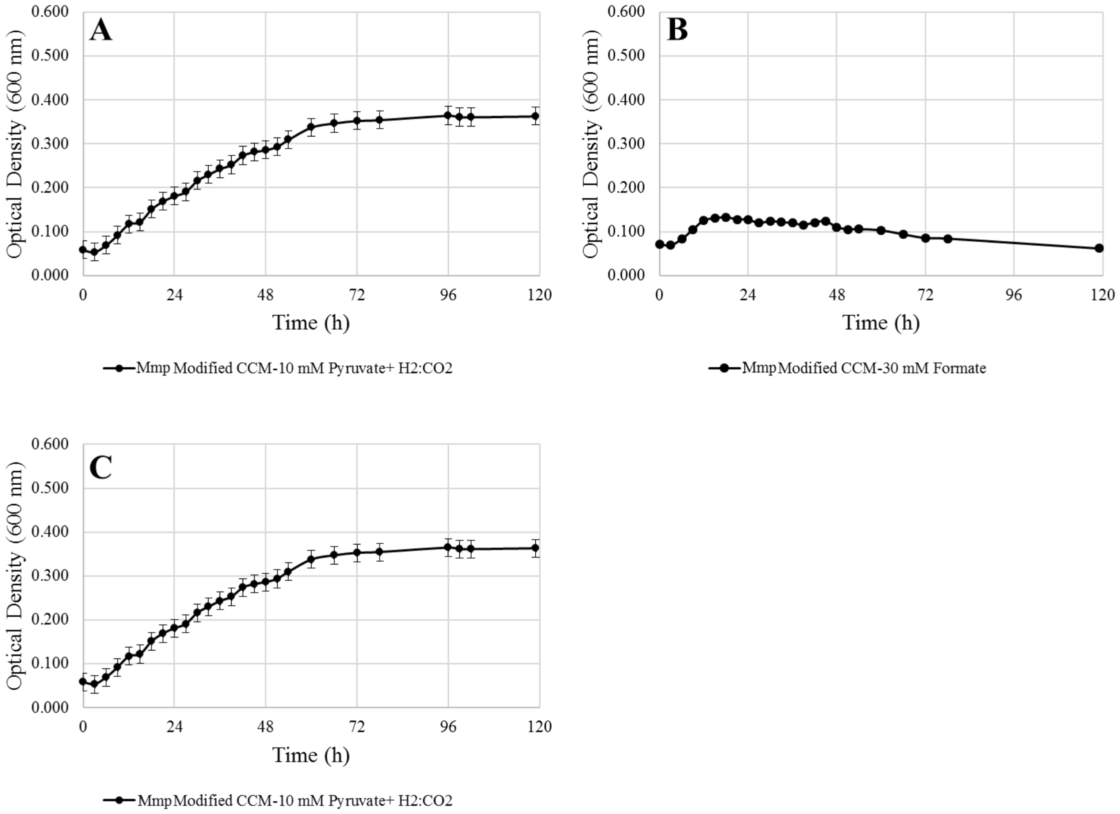

Figure 4. *M. maripaludis* (Mmp) growth on formate and pyruvate utilizing absorbance readings (600 nm) over time. (A) *M. maripaludis* growth on pyruvate (10 mM) with H_2:CO_2, (B) formate (30 mM) alone, and (C) pyruvate (10 mM) alone.

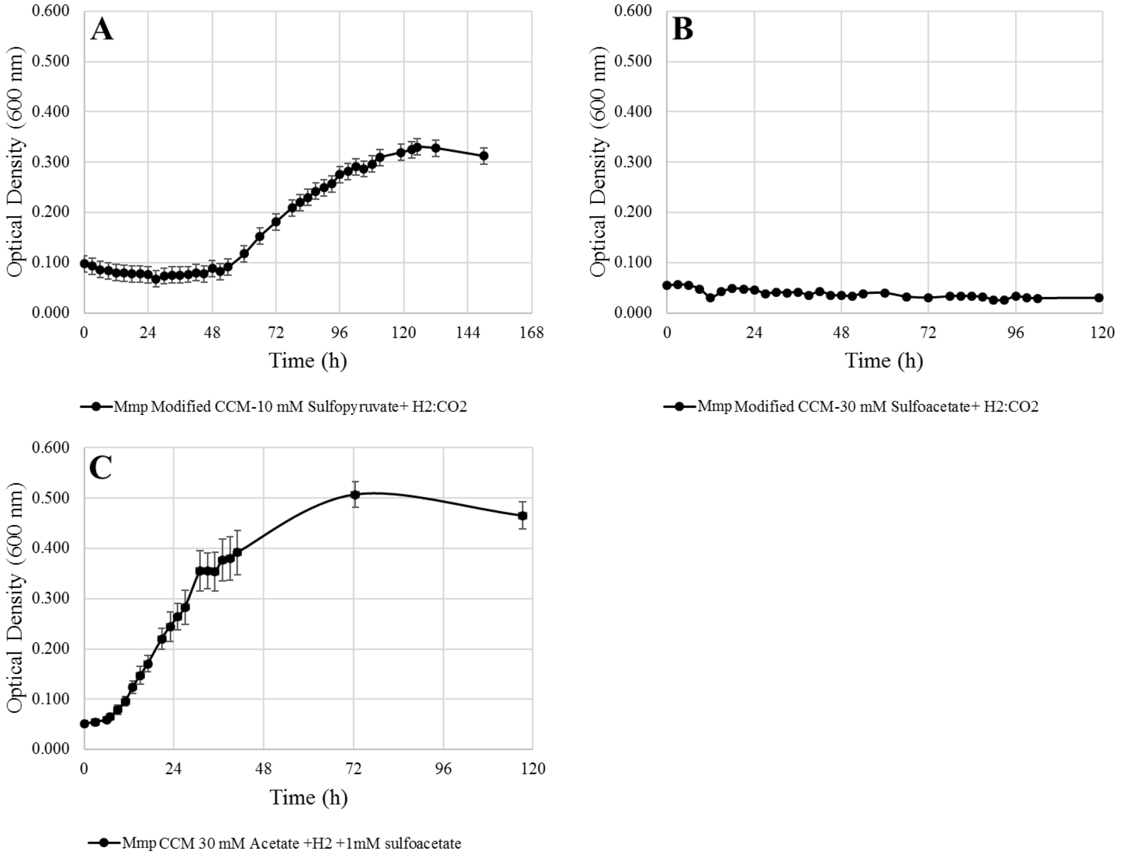

Figure 5. *M. maripaludis* (Mmp) growth with sulfopyruvate and sulfoacetate utilizing absorbance readings (600 nm) over time. (A) *M. maripaludis* growth on H_2:CO_2 in presence of sulfopyruvate (10 mM) with extended lag-phase, (B) growth was not observed with H_2:CO_2 in presence of sulfoacetate (30 mM), and (C) growth was observed with H_2:CO_2 in presence of 1 mM sulfoacetate.

When considering the presumptive CoM biosynthesis pathway, *M. maripaludis* is predicted to have *com*A (MMP0273), *com*B (MMP0161), *com*C (MMP1133), and *com*DE (MMP0411/1689). These genes presumptively encode the following proteins: phospho-3-sulfolactate synthase, phosphosulfolactate phosphatase, sulfolactate dehydrogenase, and sulfopyruvate decarboxylase. The enzyme for the last predicted step for the conversion of sulfoacetaldehyde to CoM is currently unknown. It is possible that sulfoacetate is an inhibitor of one of these enzymatic steps. Sulfopyruvate is a potential product of the presumptive ComC, a potential substrate for the presumptive ComDE, and may be one of the mechanisms of growth stimulation at low levels. The mechanism of inhibition at higher levels is also unknown but may be the consequence of interactions with other enzymes (*e.g.*, gluconeogenesis). The methanogenic inhibitor, bromoethanesulfonic acid (BES), acts as an analog of CoM that is thought to compete and prevent the last step of methyl reduction (Gunsalus et al., 1978; Ungerfeld et al., 2004). Typically, millimolar levels of BES are needed, and acclimation to the inhibitor occurs commonly (Zinder et al., 1984). Given structural similarities of sulfopyruvate and sulfoacetate with CoM precursors and differences relative to BES (Figure 6), the mode of inhibition may be different. However, BES has previously been shown to impact nonmethanogenic cultures, demonstrating unknown impacts on different physiologies (Löffler et al., 1997). Further work is needed to elucidate the mechanism(s) of inhibition that could help with control of methane emissions in different environments.

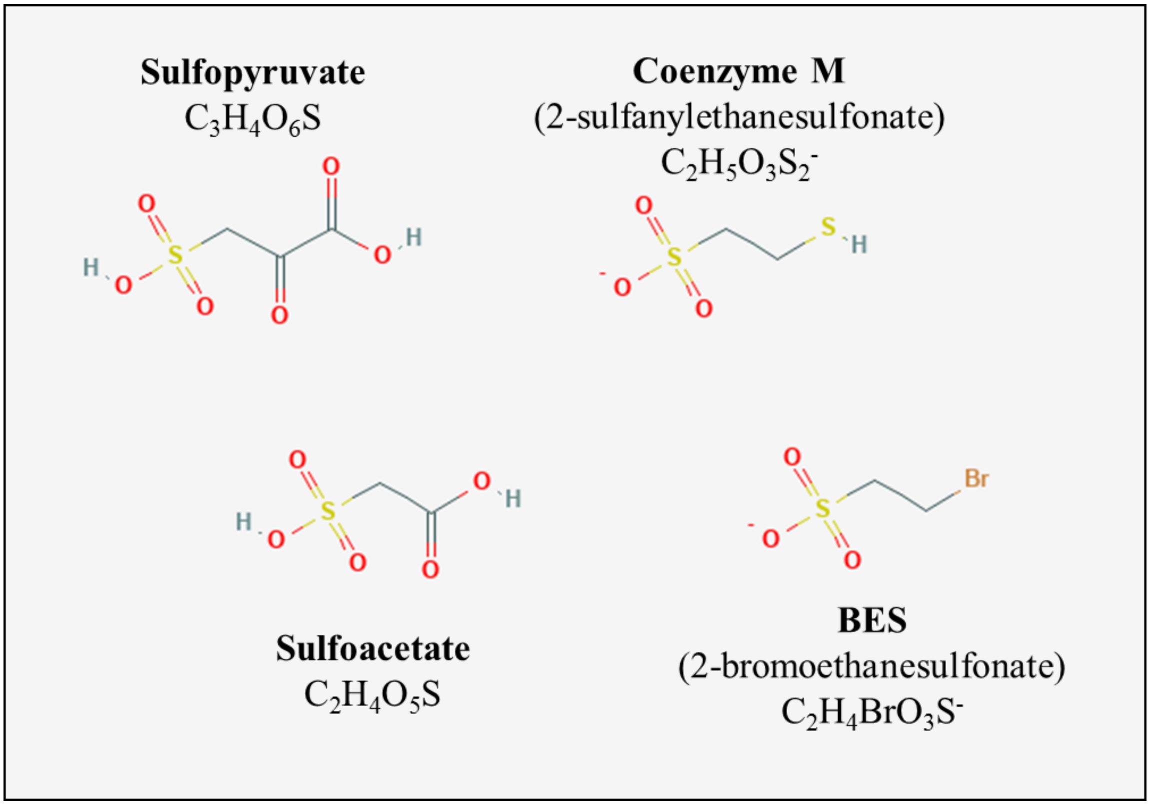
Sulfopyruvate
$C_3H_4O_6S$
Coenzyme M
(2-sulfanylethanesulfonate)
$C_2H_5O_3S_2^-$
Sulfoacetate
$C_2H_4O_5S$
BES
(2-bromoethanesulfonate)
$C_2H_4BrO_3S^-$

Figure 6. Structural comparison of sulfopyruvate, sulfoacetate, coenzyme M, and the methanogenic inhibitor 2-bromoethanesulfonate.

CONCLUSION

The growth of SRBs and the associated sulfide production has detrimental impacts on many different environments and industries globally, including water distribution, oil and gas, and infrastructure. Methane emissions are a major concern for many environments including agriculture, waste-stream management, and oil and gas, but also in industries where methane can be collected as a potential fuel. New methods are needed to assist in the control of both sulfide production and methanogenesis, and the presented results demonstrated that sulfonates can both stimulate and inhibit the growth of the sulfide-producing bacterium, *D. vulgaris*, and the methanogen, *M. maripaludis*. Future work is needed to elucidate modes of action for sulfopyruvate and sulfoacetate.

Acknowledgments. This material by ENIGMA- Ecosystems and Networks Integrated with Genes and Molecular Assemblies (http://enigma.lbl.gov), a Scientific Focus Area Program at Lawrence Berkeley National Laboratory is based upon work supported by the U.S. Department of Energy, Office of Science, Office of Biological & Environmental Research under contract number DE-AC02-05CH11231.

REFERENCES CITED

Balderston, W. L., & Payne, W. J. (1976). Inhibition of methanogenesis in salt marsh sediments and whole-cell suspensions of methanogenic bacteria by nitrogen oxides. *Applied and Environmental Microbiology*, *32*(2), 264–9. Retrieved from http://www.ncbi.nlm.nih.gov/pubmed/970945

Becker, D. F., & Ragsdale, S. W. (1998). Activation of Methyl-SCoM Reductase to High Specific Activity after Treatment of Whole Cells with Sodium Sulfide. *Biochemistry*, *37*(8), 2639–2647. http://doi.org/10.1021/bi972145x

Brileya, K. A., Camilleri, L. B., Zane, G. M., Wall, J. D., & Fields, M. W. (2014). Biofilm growth mode promotes maximum carrying capacity and community stability during product inhibition syntrophy. *Frontiers in Microbiology*, *5*(12), 693. http://doi.org/10.3389/fmicb.2014.00693

Cook, A. M., Smits, T. H. M., & Denger, K. (2008). Sulfonates and Organotrophic Sulfite Metabolism. In C. Dahl & C. G. Friedrich (Eds.), *Microbial Sulfur Metabolism* (pp. 170–183). Springer-Verlag Berlin Heidelberg. http://doi.org/10.1007/978-3-540-72682-1

Denger, K., Mayer, J., Buhmann, M., Weinitschke, S., Smits, T. H. M., & Cook, A. M. (2009). Bifurcated Degradative Pathway of 3-Sulfolactate in Roseovarius nubinhibens ISM via Sulfoacetaldehyde Acetyltransferase and (S)-Cysteate Sulfolyase. *Journal of Bacteriology*, *191*(18), 5648–5656. http://doi.org/10.1128/JB.00569-09

Denger, K., Weinitschke, S., Hollemeyer, K., & Cook, A. M. (2004). Sulfoacetate generated by Rhodopseudomonas palustris from taurine. *Archives of Microbiology*, *182*(2–3), 254–8. http://doi.org/10.1007/s00203-004-0678-0

Graupner, M., Xu, H., & White, R. H. (2000). Identification of an Archaeal 2-Hydroxy Acid Dehydrogenase Catalyzing Reactions Involved in Coenzyme Biosynthesis in Methanoarchaea. *Journal of Bacteriology*, *182*(13), 3688–3692. http://doi.org/10.1128/JB.182.13.3688-3692.2000

Gunsalus, R. P., Romesser, J. A., & Wolfe, R. S. (1978). Preparation of coenzyme M analogs and their activity in the methyl coenzyme M reductase system of Methanobacterium thermoautotrophicum. *Biochemistry*, *17*(12), 2374–2377. http://doi.org/10.1021/bi00605a019

Johnson, E. F., & Mukhopadhyay, B. (2008). A Novel Coenzyme F420 Dependent Sulfite Reductase and a Small Sulfite Reductase in Methanogenic Archaea. In C. Dahl & C. G. Friedrich (Eds.), *Microbial Sulfur Metabolism* (pp. 202–216). Berlin, Heidelberg: Springer Berlin Heidelberg. http://doi.org/10.1007/978-3-540-72682-1

Krejčík, Z., Denger, K., Weinitschke, S., Hollemeyer, K., Pačes, V., Cook, A. M., & Smits, T. H. M. (2008). Sulfoacetate released during the assimilation of taurine-nitrogen by Neptuniibacter caesariensis: purification of sulfoacetaldehyde dehydrogenase. *Archives of Microbiology*, *190*(2), 159–168. http://doi.org/10.1007/s00203-008-0386-2

Leigh, J. A. (2001). Evolution of Energy Metabolism. In J. T. Staley & A. Reysenbach (Eds.), *Biodiversity of Microbial Life: Foundation of Earth's Biosphere* (Wiley Seri). New York: John Wiley & Sons, Inc.

Lie, T. J., Pitta, T., Leadbetter, E. R., Godchaux, W., & Leadbetter, J. R. (1996). Sulfonates: novel electron acceptors in anaerobic respiration. *Archives of Microbiology*, *166*(3), 204–10. http://doi.org/10.1007/s002030050376

Liu, H., Wang, J., Wang, A., & Chen, J. (2011). Chemical inhibitors of methanogenesis and putative applications. *Applied Microbiology and Biotechnology*, *89*(5), 1333–1340. http://doi.org/10.1007/s00253-010-3066-5

Löffler, F. E., Ritalahti, K. M., & Tiedje, J. M. (1997). Dechlorination of chloroethenes is inhibited by 2-bromoethanesulfonate in the absence of methanogens. Applied and Environmental Microbiology, 63(12), 4982–4985.

Mahlert, F., Bauer, C., Jaun, B., Thauer, R. K., & Duin, E. C. (2002). The nickel enzyme methyl-coenzyme M reductase from methanogenic archaea: In vitro induction of the nickel-based MCR-ox EPR signals from MCR-red2. *JBIC Journal of Biological Inorganic Chemistry*, *7*(4–5), 500–513. http://doi.org/10.1007/s00775-001-0325-z

Muramatsu, H., Mihara, H., Kakutani, R., Yasuda, M., Ueda, M., Kurihara, T., & Esaki, N. (2005). The Putative Malate/Lactate Dehydrogenase from Pseudomonas putida Is an NADPH-dependent Δ 1 -Piperideine-2-carboxylate/Δ 1 -Pyrroline-2-carboxylate Reductase Involved in the Catabolism of d-Lysine and d-Proline. *Journal of Biological Chemistry*, *280*(7), 5329–5335. http://doi.org/10.1074/jbc.M411918200

Teske, A., Dhillon, A., & Sogin, M. L. (2003). Genomic Markers of Ancient Anaerobic Microbial Pathways: Sulfate Reduction, Methanogenesis, and Methane Oxidation. *The Biological Bulletin*, *204*(2), 186–191. http://doi.org/10.2307/1543556

Ungerfeld, E. M., Rust, S. R., Boone, D. R., & Liu, Y. (2004). Effects of several inhibitors on pure cultures of ruminal methanogens. *Journal of Applied Microbiology*, *97*(3), 520–526. http://doi.org/10.1111/j.1365-2672.2004.02330.x

Walker, C. B., He, Z., Yang, Z. K., Ringbauer, J. a, He, Q., Zhou, J., … Stahl, D. A. (2009). The electron transfer system of syntrophically grown Desulfovibrio vulgaris. *Journal of Bacteriology*, *191*(18), 5793–801. http://doi.org/10.1128/JB.00356-09

Weinitschke, S., Denger, K., Cook, A. M., & Smits, T. H. M. (2007). The DUF81 protein TauE in Cupriavidus necator H16, a sulfite exporter in the metabolism of C2 sulfonates. *Microbiology*, *153*(9), 3055–3060. http://doi.org/10.1099/mic.0.2007/009845-0

White, R. H. (1986). Intermediates in the biosynthesis of coenzyme M (2-mercaptoethanesulfonic acid). *Biochemistry*, *25*(18), 5304–5308. http://doi.org/10.1021/bi00366a047

White, R. H. (2017). Identification and Biosynthesis of 1-Mercaptoethanesulfonic Acid (1-MES), an Analogue of Coenzyme M, Found Widely in the Methanogenic Archaea. *Biochemistry*, *56*(46), 6137–6144. http://doi.org/10.1021/acs.biochem.7b00971

Ye, D., Quensen, J. F. I., Tiedje, J. M., & Boyd, S. A. (1999). 2-Bromoethanesulfonate, Sulfate, Molybdate, and Ethanesulfonate Inhibit Anaerobic Dechlorination of Polychlorobiphenyls by Pasteurized Microorganisms. Society, 65(1), 327–329. Retrieved from https://aem.asm.org/content/65/1/327

Zinder, S. H., Anguish, T., & Cardwell, S. C. (1984). Selective inhibition by 2-bromoethanesulfonate of methanogenesis from acetate in a thermophilic anaerobic digestor. *Applied and Environmental Microbiology*, *47*(6), 1343–5. Retrieved from http://www.ncbi.nlm.nih.gov/pubmed/16346572

CHAPTER SIX

EPILOGUE

The central theme iterated throughout this dissertation is that the proximity of two interdomain organisms, within an anaerobic co-culture biofilm, can facilitate unique carbon and electron cycling thereby promoting community stability. An integrated understanding of the interactions between microbial communities and ecosystem function is still deficient due to the metabolic plasticity of microorganisms and the inherent complexity associated with studying interactions between populations. Technological advances have made genomic sequencing, transcriptomics, proteomics, and metabolomics commonplace tools for evaluating microorganisms. However, with a vast world of undiscovered microorganisms, and an even larger amount uncultured, a majority of research is still directed toward single species studies. Pure culture studies are essential to curate functional genomic annotations, as well as to discern physiological characteristics, however pure cultures are often not representative of environmental conditions. This is further exemplified by the standard of microbiology laboratory cultivations being conducted for the planktonic mode of growth due to ease of cultivation, despite the paradigm that 99% of microorganisms grow as a biofilm in the environment (Costerton et al., 1987). The research presented here utilizes well studied, genetically tractable, model organisms in order to assess the dynamic interactions of an anaerobic, co-culture biofilm.

Previous work (discussed in Chapter 1) established that metabolic coupling between the sulfate-reducing bacterium (SRB), *Desulfovibrio vulgaris* Hildenborough, and the archaeal hydrogenotrophic methanogen, *Methanococcus maripaludis* S2 could be accomplished through a product inhibition syntrophy (Dean, 1985). In the environment, SRB will outcompete methanogens for free molecular hydrogen (H_2) and other organic substrates in order to gain energy through sulfate reduction. When laboratory cultivations of *D. vulgaris* Hildenborough are performed with lactate and without sulfate amendments, the accumulation of acetate and H_2 products become inhibitory. Therefore, the addition of *M. maripaludis* S2 establishes a beneficial cross-feeding where interspecies H_2 transfer from the SRB along with carbon dioxide reduction produces CH_4 as part of its central energy metabolism, methanogenesis.

This syntrophic mutualism has been studied for the planktonic growth mode, however little work has been done to characterize the co-culture within the biofilm growth mode. Previous studies reported that the co-culture biofilm was initially established by *D. vulgaris*, which produces phenotypically thin biofilms in monoculture (Brileya et al., 2014). As the co-culture biofilm matured, thicker phenotypic features were observed along with an even pattern of intermixing among the *D. vulgaris* and *M. maripaludis* populations which has been previously correlated with cooperative interactions (Momeni et al., 2013). One of the most significant findings published for this co-culture biofilm system was the demonstration of an enhanced system carrying capacity as determined by mass flux to CH_4 (See Appendix D and E) (Brileya et al., 2014).

A systems biology approach was taken for this dissertation to study the complex syntrophic interactions between the sulfate-reducing bacterium, *Desulfovibrio vulgaris* Hildenborough, and the archaeal hydrogenotrophic methanogen, *Methanococcus maripaludis* S2. In Chapter 2, the hypothesis that the enhanced carrying capacity of the co-culture biofilm system was due to unique carbon and electron cycling facilitated by the proximity of the populations within the biofilm, was tested utilizing RNA-Seq transcriptomics. The expression profiles compared *D. vulgaris* in a planktonic monoculture against (1) *D. vulgaris* in a co-culture biofilm and (2) co-culture planktonic growth mode; and *M. maripaludis* in a planktonic monoculture against (1) *M. maripaludis* in a co-culture biofilm and (2) co-culture planktonic growth mode. Additionally, expression of the co-culture biofilm was compared to the planktonic co-culture.

As expected, a unique set of genes were differentially expressed supporting the hypothesis that the co-culture biofilm is phenotypically distinct from the co-culture planktonic growth mode. Since the biofilm establishment was attributed to *D. vulgaris*, it was anticipated that the most expression changes would occur between its different growth modes. Instead, the results revealed that *M. maripaludis* had the largest fold changes in addition to a set of 25 genes that showed statistically significant differential expression for the co-culture biofilm and planktonic growth modes. This could indicate that *M. maripaludis* modulates its metabolism intentionally in order to syntrophically associate within the SRB biofilm, or modulation could be a result of the syntrophic coupling. Support for this hypothesis can be extrapolated if H_2 utilization is considered.

The expression of central methanogenesis genes for *M. maripaludis* (MMP1297-1302, MMP0372, MMP0058, MMP1382-85) in the planktonic co-culture were shown to be significantly up expressed, whereas the same genes in the co-culture biofilm were significantly down expressed. Functional transcriptomic studies have demonstrated that additional mRNA is produced in *M. maripaludis* under H_2 limitation (Hendrickson et al., 2007; Wood et al., 2003). Furthermore, *D. vulgaris* exhibited down expression of the low affinity NiFeSe hydrogenases and increased expression of the high affinity NiFe hydrogenases in the co-culture biofilm indicating H_2 abundance (Krumholz et al., 2015). Therefore, it can be inferred that the co-culture biofilm system alleviates H_2 limitation likely as a result of the close proximity between the interacting populations.

Unfortunately, overall analysis was somewhat limited as it revealed that the vast majority of the most expressed genes found to be unique for the co-culture biofilm were annotated as hypothetical with no matching homologs in the databases. This is an important reminder that despite all the biology that has been done with these model organisms, there is still much that is unknown. The significantly up or down expressed genes that were functionally annotated were central to membrane protein changes, lactate permeases, and electron cycling. To further understand how these expression changes may contribute to potential investment strategies governing metabolic interactions between these two organisms, a metabolic model was constructed. The amino acids alanine, cysteine, glycine, and serine were identified in *M. maripaludis* as potential energy sources that could reduce the requirement for H_2 and/or CO_2. Although the expression data did not identify these as significantly expressed within the co-culture biofilm, previous studies identified alanine as an important syntrophic metabolite in planktonic co-cultures (Walker et al., 2009). This iterates the fact that cellular interactions and mass transport within the biofilm can be significantly different. Proximity is likely facilitating metabolic exchanges thereby contributing to the efficiency of the system, but the lack of functional annotations prevented transcriptomic identification of the full spectrum of interactions occurring.

Transcriptomics alone is not an accurate proxy for activity, and interpretation should always be completed with a combination of other methods, namely proteomics (Arnold et al., 2018; Bollmann et al., 2005; Gedeon & Bokes, 2012; Hendrickson et al., 2000; Taniguchi et al., 2010). Chapter 3 assessed proteomic activity within the co-culture biofilm by using deuterium oxide (^2H_2O) incorporation as a proxy for newly synthesized proteins. Again, the importance of conserved hypotheticals (such as DVU2077, DVUA0116, DVU2398, DVU3032, DVU0797, DVU0799, DVU2938) within the co-culture biofilm was emphasized as they were numerous among the proteins identified. The proteins labeled for *D. vulgaris* that were assigned functional annotations were linked to lactate processing, membrane proteins, and electron cycling. *M. maripaludis* presented proteins central to methanogenesis, alanine dehydrogenase (MMP1513), S-layer (MMP0383), formate/nitrate transport (MMP1301), and electron cycling (MMP0916) as actively synthesized within the co-culture biofilm.

The deuterated proteins identified appeared to corroborate the main findings of the transcriptomic work demonstrating unique carbon and electron cycling (among an abundance of hypotheticals) within the co-culture biofilm. The most surprising finding from this study was the apparent “slowing,” as determined by the apparent half-saturation of deuterium in the fraction of newly synthesized proteins, of *D. vulgaris* proteomic activity during biofilm maturation in the late stage. This prompted a re-analysis of the theoretical framework of what a syntrophic mutualism meant within this system. If the resource ratio is considered, then the rate of growth for an individual microorganism is a function of the rate of consumption of available resources in the environment with consideration to competition with other microorganisms (Archetti *et al.*, 2011; de Mazancourt & Schwartz, 2010; Miller *et al.*, 2005; Pande *et al.*, 2016). Within the co-culture biofilm it was postulated that *D. vulgaris* would be the driver of the syntrophy with *M. maripaludis* since it is the source (*i.e.*, lactate oxidation) of H_2 for the methanogen. The deuterium results could be interpreted as a consequence of *D. vulgaris* being constrained within the co-culture biofilm system due to a slower rate of H_2 utilization by *M. maripaludis,* whom maintained a similar deuterium incorporation rate (*i.e.*, activity) for both the early and late stage biofilm development, or as a result of an antagonistic interaction.

The function of syntrophy within this mutualism in the context of environmental stability was therefore challenged in Chapter 4. Previous studies have reported that sulfate concentrations will inhibit methanogenesis and divert resources towards sulfate reduction (Kristjansson et al., 1982; Mountfort & Asher, 1981; Mountfort et al., 1980). This has been used to describe thermodynamic constraints that determine the segregation of sulfate-reduction from methanogenesis within biochemical depth profiles in the environment, yet sulfate-reduction and methanogenesis have been reported to co-exist

(Oremland & Taylor, 1978). It was hypothesized that if *D. vulgaris* was experiencing a metabolic constraint as a result of syntrophy, then amendment of a more preferred electron acceptor (*i.e.*, sulfate) would cause metabolic uncoupling followed by a washout of *M. maripaludis* in the co-culture biofilm system. Surprisingly, sulfate perturbation resulted in an increase in abundance for both populations in the co-culture biofilm (albeit more so for *D. vulgaris*), without the elimination of *M. maripaludis*. As part of the work to elucidate functional annotations for the hypothetical genes discussed in Chapter 2 and 3, it was discovered that partial hits were related to defense categories (*i.e.*, beta-lactamases) and a DUF81 protein domain which has been resolved to function as a sulfonate (specifically sulfoacetate) transporter. This information taken in context with the sulfate perturbation led to the hypothesis that *M. maripaludis* was influencing the metabolic behavior of *D. vulgaris* in order to maintain the syntrophy. Although initial screening did not identify any antimicrobial peptides in preparations of *M. maripaludis*, the filtered spent media from its monocultures had a negative impact on *D. vulgaris* planktonic growth. This growth inhibition was not observed to the same degree for an alternate SRB, *Desulfovibrio alaskensis* G20, even though a slightly slower growth rate was observed. Further investigation of the filtrate growth inhibition resulted in the finding that supplementation with trace nutrients could partially restore *D. vulgaris* growth planktonically.

The implications for this observation could influence how this mutualism is regarded. For instance, the apparent slowing of deuterated protein synthesis (Chapter 3) in the late stage biofilm could be a result of the methanogen consuming, and therefore competing, for a trace nutrient that is essential for both populations. It has been postulated that a common substrate that SRBs and methanogens compete for is what controls the rate of methanogenesis (Sela-Adler et al., 2017). This scenario would expectedly result in the demise of the co-culture biofilm with the addition of sulfate to ease energetic burdens, however this was not observed. Alternatively, the co-culture biofilm may be able to overcome metabolic constraints observed on the planktonic culture through metabolic coupling and nutrient concentration.

As mentioned briefly before, the *D. vulgaris* hypothetical protein DVU0149 was found to contain a conserved region annotated as DUF81. This has been resolved to be a TauE/SafE exporter of the sulfonate, sulfoacetate (Weinitschke *et al.*, 2007) and was the focus of Chapter 5. Sulfonates are charged and require transporters in order to be moved across the cell membrane. They are also ubiquitous in nature and can function as sole carbon sources, electron acceptors, or sulfur sources, in addition to being necessary components of methanogenic coenzyme M synthesis (Cook *et al.*, 2008; Denger *et al.*, 2014; Felux *et al.*, 2015; Graupner *et al.*, 2000; Harwood *et al.*, 2003; Krejčík *et al.*, 2008; Lie *et al.*, 1996). Since various pathways (*e.g.* cysteine degradation) can produce sulfoacetate and *D. vulgaris* had increased expression for the TauE/SafE exporter, the apparent significance to both methanogens (*i.e.*, coenzyme M synthesis) and sulfate-reducing bacteria (*i.e.*, potential electron acceptor, sulfoglycolysis, cysteine degradation) prompted further exploration of sulfoacetate and sulfopyruvate as potential syntrophic metabolites. The monoculture studies revealed that both substrates were unable to be utilized as sole energy sources and were inhibitory to both *D. vulgaris* and *M.*

maripaludis. However, at 1 mM concentrations of sulfoacetate both cultures were able to grow normally in planktonic monocultures with respective electron donors present. Therefore, future work should be directed toward continued growth studies utilizing sulfonates, and eventual stress perturbations to the co-culture biofilm system with sulfonates.

There are many forms of mutualism that encompass varying degrees of benefits to the partners involved (Faust & Raes, 2012). However, the results depicted from the sulfate stress questioned the differentiation between this mutualism and parasitism. A factor that commonly muddles the characterization of a mutualism is the fact that the same interaction within a different environment may be defined differently, and can therefore be termed conditional mutualism. It has been suggested that parasitic precursors led to the evolution of mutualism, and the syntrophy presented here may be a candidate for this ecological theory to be tested in the future (de Mazancourt *et al.*, 2005; de Mazancourt & Schwartz, 2010).

Sulfate-reducing bacteria and methanogens have evolved occupying and competing for similar niche space and substrates. Therefore, it is likely that conditional mutualisms have arisen in order for survival in environmental spaces that are at the lower thermodynamic limit for life. Appendix A denotes the characterization of *Pelosinus fermentans* JBW45, an environmental isolate that was obtained while screening specifically for sulfate-reducing bacteria in a field stimulated site. The pertinent finding was *P. fermentans* physiological capacity to produce methane under substrate limitation. It has been demonstrated previously that sulfate-reducing bacteria can function as “mini-methane" makers on various substrates such as benzoate, methionine, and pyruvate (Postgate, 1969; Rimbault et al., 1988; Schauder et al., 1986; Shcherbakova & Vaĭnshteĭn, 2000). The ecological relevance for mini-methane production from pathways that differ from known methanogens, in SRBs and other microorganisms, is the possibility for this pathway to be reversible. In the zones of methanogenesis and sulfate-reduction, methane oxidation by sulfate-reducers or other microorganisms within these guilds would play a significant ecological role.

In conclusion, the work presented throughout this dissertation has emphasized the distinctive phenotypic and physiological characteristics of an interdomain co-culture biofilm. The unique carbon and electron cycling for the biofilm growth mode is believed to promote community stability. Furthermore, the proximity of the microorganisms allows for enhanced metabolic coupling from lactate oxidation to CO_2-reduction. The localization of metabolites within the biofilm community are purported to decrease individual costs and improve overall benefits from investment. Further research is needed to elucidate mechanisms of interactions as well as potential antagonisms that may influence the syntrophy.

REFERENCES CITED

Archetti, M., Scheuring, I., Hoffman, M., Frederickson, M. E., Pierce, N. E., & Yu, D. W. (2011). Economic game theory for mutualism and cooperation. *Ecology Letters*, *14*(12), 1300–1312. http://doi.org/10.1111/j.1461-0248.2011.01697.x

Bollmann, A., Schmidt, I., Saunders, A. M., & Nicolaisen, M. H. (2005). aInfluence of Starvation on Potential Ammonia-Oxidizing Activity and. *Applied and Environmental Microbiology*, *71*(3), 1276–1282. http://doi.org/10.1128/AEM.71.3.1276

Brileya, K. A., Camilleri, L. B., Zane, G. M., Wall, J. D., & Fields, M. W. (2014). Biofilm growth mode promotes maximum carrying capacity and community stability during product inhibition syntrophy. *Frontiers in Microbiology*, *5*(12), 693. http://doi.org/10.3389/fmicb.2014.00693

Cook, A. M., Smits, T. H. M., & Denger, K. (2008). Sulfonates and Organotrophic Sulfite Metabolism. In C. Dahl & C. G. Friedrich (Eds.), *Microbial Sulfur Metabolism* (pp. 170–183). Springer-Verlag Berlin Heidelberg. http://doi.org/10.1007/978-3-540-72682-1

Costerton, J. W., Cheng, K. J., Geesey, G. G., Ladd, T. I., Nickel, J. C., Dasgupta, M., & Marrie, T. J. (1987). Bacterial Biofilms in Nature and Disease. *Ann. Rev. Microbiol.*, *41*, 435–464. http://doi.org/10.1146/annurev.mi.41.100187.002251

de Mazancourt, C., Loreau, M., & Dieckmann, U. (2005). Understanding mutualism when there is adaptation to the partner. *Journal of Ecology*, *93*(2), 305–314. http://doi.org/10.1111/j.1365-2745.2004.00952.x

de Mazancourt, C., & Schwartz, M. W. (2010a). A resource ratio theory of cooperation. *Ecology Letters*, *13*(3), 349–59. http://doi.org/10.1111/j.1461-0248.2009.01431.x

de Mazancourt, C., & Schwartz, M. W. (2010b). A resource ratio theory of cooperation. *Ecology Letters*, *13*(3), 349–359. http://doi.org/10.1111/j.1461-0248.2009.01431.x

Dean, A. M. (1985). The dynamics of microbial commensalisms and mutualisms. In D. H. Boucher (Ed.), *The Biology of Mutualism* (pp. 270–300). Oxford: Oxford University Press. Retrieved from https://books.google.com/books?hl=en&lr=&id=dWuQS_3F2P0C&oi=fnd&pg=PA270&ots=_vLqPPvfaW&sig=kQJWc5rcE0FIzy8fpfml3ZWn3-k#v=onepage&q&f=false

Denger, K., Weinitschke, S., Hollemeyer, K., & Cook, A. M. (2014). Sulfoacetate generated by Rhodopseudomonas palustris from taurine. http:/doi.org/10.1007/s00203-004-0678-0

Faust, K., & Raes, J. (2012). Microbial interactions: from networks to models. *Nature Reviews Microbiology*, *10*(8), 538–550. http://doi.org/10.1038/nrmicro2832

Felux, A.-K., Spiteller, D., Klebensberger, J., & Schleheck, D. (2015). Entner–Doudoroff pathway for sulfoquinovose degradation in Pseudomonas putida SQ1. *Proceedings of the National Academy of Sciences*, *112*(31), E4298–E4305. http://doi.org/10.1073/pnas.1507049112

Gedeon, T., & Bokes, P. (2012). Delayed protein synthesis reduces the correlation between mRNA and protein fluctuations. *Biophysical Journal*, *103*(3), 377–385. http://doi.org/10.1016/j.bpj.2012.06.025

Graupner, M., Xu, H., & White, R. H. (2000). Identification of the gene encoding sulfopyruvate decarboxylase, an enzyme involved in biosynthesis of coenzyme M. *Journal of Bacteriology*, *182*(17), 4862–4867. http://doi.org/10.1128/JB.182.17.4862-4867.2000

Harwood, J. L., Ellis, A. J., White, G. F., Roy, A. B., & Hewlins, M. J. E. (2003). Glycolytic Breakdown of Sulfoquinovose in Bacteria: a Missing Link in the Sulfur Cycle. *Applied and Environmental Microbiology*, *69*(11), 6434–6441. http://doi.org/10.1128/aem.69.11.6434-6441.2003

Hendrickson, E. L., Haydock, A. K., Moore, B. C., Whitman, W. B., & Leigh, J. A. (2007). Functionally distinct genes regulated by hydrogen limitation and growth rate in methanogenic Archaea. *Proceedings of the National Academy of Sciences of the United States of America.*, *104*(21), 8930–8934. http://doi.org/10.1073/pnas.0701157104

Krejčík, Z., Denger, K., Weinitschke, S., Hollemeyer, K., Pačes, V., Cook, A. M., & Smits, T. H. M. (2008). Sulfoacetate released during the assimilation of taurine-nitrogen by Neptuniibacter caesariensis: Purification of sulfoacetaldehyde dehydrogenase. *Archives of Microbiology*, *190*(2), 159–168. http://doi.org/10.1007/s00203-008-0386-2

Kristjansson, J. K., Schönheit, P., & Thauer, R. K. (1982). Different Ks values for hydrogen of methanogenic bacteria and sulfate reducing bacteria: An explanation for the apparent inhibition of methanogenesis by sulfate. *Archives of Microbiology*, *131*(3), 278–282. http://doi.org/10.1007/BF00405893

Krumholz, L. R., Bradstock, P., Sheik, C. S., Diao, Y., Gazioglu, O., Gorby, Y., & McInerney, M. J. (2015). Syntrophic Growth of Desulfovibrio alaskensis Requires Genes for H 2 and Formate Metabolism as Well as Those for Flagellum and Biofilm Formation. *Applied and Environmental Microbiology*, *81*(7), 2339–2348. http://doi.org/10.1128/AEM.03358-14

Lie, T. J., Pitta, T., Leadbetter, E. R., Godchaux, W., & Leadbetter, J. R. (1996). Sulfonates: novel electron acceptors in anaerobic respiration. *Archives of Microbiology*, *166*(3), 204–10. http://doi.org/10.1007/s002030050376

Miller, T., Burns, J., Munguia, P., Walters, E., Kneitel, J., Richards, P., … Buckley, H. (2005). A Critical Review of Twenty Years' Use of the Resource-Ratio Theory. *American Naturalist*, *165*(4), 439–448. Retrieved from isi:000227517000006%5Cnpapers2://publication/uuid/F528658C-E918-41E4-B25C-60C38CAB51F9

Momeni, B., Brileya, K. A., Fields, M. W., & Shou, W. (2013). Strong inter-population cooperation leads to partner intermixing in microbial communities. *ELife*, *2*, e00230. http://doi.org/10.7554/eLife.00230

Morgenroth, E., Obermayer, A., Arnold, E., Brühl, A., Wagner, M., & Wilderer, P. A. (2000). Effect of long-term idle periods on the performance of sequencing batch reactors. *Water Science and Technology*, *41*(1), 105–113. http://doi.org/10.2166/wst.2000.0018

Mountfort, D. O., & Asher, R. A. (1981). Role of Sulfate Reduction Versus Methanogenesis in Terminal Carbon Flow in Polluted Intertidal Sediment of Waimea Inlet, Nelson, New Zealand. *Applied and Environmental Microbiology*, *42*(2), 252–258. Retrieved from http://aem.asm.org/cgi/reprint/42/2/252

Mountfort, D. O., Asher, R. A., Mays, E. L., & Tiedje, J. M. (1980). Carbon and electron flow in mud and sandflat intertidal sediments at Delaware inlet, Nelson, New Zealand. *Applied and Environmental Microbiology*, *39*(4), 686–94. Retrieved from http://www.ncbi.nlm.nih.gov/pubmed/16345535%0Ahttp://www.pubmedcentral.nih.gov/articlerender.fcgi?artid=PMC291405

Oda, Y., Slagman, S. J., Meijer, W. G., Forney, L. J., & Gottschal, J. C. (2000). Influence of growth rate and starvation on fluorescent in situ hybridization of Rhodopseudomonas palustris. *FEMS Microbiology Ecology*, *32*(3), 205–213. http://doi.org/10.1016/S0168-6496(00)00029-5

Oremland, R. S., & Taylor, B. F. (1978). Sulfate reduction and methanogenesis in marine sediments. *Geochimica et Cosmochimica Acta*, *42*(2), 209–214. http://doi.org/10.1016/0016-7037(78)90133-3

Pande, S., Kaftan, F., Lang, S., Svatoš, A., Germerodt, S., & Kost, C. (2016). Privatization of cooperative benefits stabilizes mutualistic cross-feeding interactions in spatially structured environments. *The ISME Journal*, *10*(6), 1413–1423. http://doi.org/10.1038/ismej.2015.212

Postgate, J. R. (1969). Methane as a Minor Product of Pyruvate Metabolism by Sulphate-reducing and Other Bacteria. *Journal of General Microbiology*, (57), 293–302.

Rimbault, A., Niel, P., Virelizier, H., Christian, J., Leluan, G., Niel, I. P., … Etiudes, S. (1988). l-Methionine , a Precursor of Trace Methane in Some Proteolytic Clostridia L-Methionine , Precursor of Trace Methane in Some Proteolytic Clostridia, *54*(6).

Schauder, R., Eikmanns, B., Thauer, R. K., Widdel, F., & Fuchs, G. (1986). Acetate oxidation to CO2 in anaerobic bacteria via a novel pathway not involving reactions of the citric acid cycle. *Archives of Microbiology*, *145*(2), 162–172. http://doi.org/10.1007/BF00446775

Sela-Adler, M., Ronen, Z., Herut, B., Antler, G., Vigderovich, H., Eckert, W., & Sivan, O. (2017). Co-existence of Methanogenesis and Sulfate Reduction with Common Substrates in Sulfate-Rich Estuarine Sediments. *Frontiers in Microbiology*, *8*(5), 1–11. http://doi.org/10.3389/fmicb.2017.00766

Shcherbakova, V. A., & Vaĭnshteĭn, M. B. (2000). Methane production by the sulfate-reducing bacterium Desulfosarcina variabilis. *Microbiology*, *69*(3), 277–280. Retrieved from http://www.ncbi.nlm.nih.gov/pubmed/10920802

Taniguchi, Y., Choi, P. J., Li, G., Chen, H., Babu, M., Hearn, J., … Xie, X. S. (2010). Quantifying E. coli Proteome and Transcriptome with Single-Molecule Sensitivity in Single Cells. *Most*, *329*(5991), 533–538. http://doi.org/10.1126/science.1188308.

Walker, C. B., He, Z., Yang, Z. K., Ringbauer, J. A, He, Q., Zhou, J., … Stahl, D. A. (2009). The electron transfer system of syntrophically grown Desulfovibrio vulgaris. *Journal of Bacteriology*, *191*(18), 5793–801. http://doi.org/10.1128/JB.00356-09

Weinitschke, S., Denger, K., Cook, A. M., & Smits, T. H. M. (2007). The DUF81 protein TauE in Cupriavidus necator H16, a sulfite exporter in the metabolism of C2 sulfonates. *Microbiology*, *153*(9), 3055–3060. http://doi.org/10.1099/mic.0.2007/009845-0

Wood, G. E., Haydock, A. K., John, A., & Leigh, J. A. (2003). Function and Regulation of the Formate Dehydrogenase Genes of the Methanogenic Archaeon Methanococcus maripaludis Function and Regulation of the Formate Dehydrogenase Genes of the Methanogenic Archaeon Methanococcus maripaludis, *185*(8), 2548–2554. http://doi.org/10.1128/JB.185.8.2548

REFERENCES CITED

REFERENCES CITED

Anders, S., Pyl, P. T., & Huber, W. (2015). HTSeq--a Python framework to work with high-throughput sequencing data. *Bioinformatics*, *31*(2), 166–169. http://doi.org/10.1093/bioinformatics/btu638

Archetti, M., Scheuring, I., Hoffman, M., Frederickson, M. E., Pierce, N. E., & Yu, D. W. (2011). Economic game theory for mutualism and cooperation. *Ecology Letters*, *14*(12), 1300–1312. http://doi.org/10.1111/j.1461-0248.2011.01697.x

Arkin, A. P., Cottingham, R. W., Henry, C. S., Harris, N. L., Stevens, R. L., Maslov, S., … Yu, D. (2018). KBase: The United States Department of Energy Systems Biology Knowledgebase. *Nature Biotechnology*, *36*(7), 566–569. http://doi.org/10.1038/nbt.4163

Baker, G. C., Smith, J. J., & Cowan, D. A. (2003). Review and re-analysis of domain-specific 16S primers. *Journal of Microbiological Methods*, *55*(3), 541–555. http://doi.org/10.1016/j.mimet.2003.08.009

Balderston, W. L., & Payne, W. J. (1976). Inhibition of methanogenesis in salt marsh sediments and whole-cell suspensions of methanogenic bacteria by nitrogen oxides. *Applied and Environmental Microbiology*, *32*(2), 264–9. Retrieved from http://www.ncbi.nlm.nih.gov/pubmed/970945

Bassler, B. L. (1999). How bacteria talk to each other: regulation of gene expression by quorum sensing. *Current Opinion in Microbiology*, *2*(2), 582–587.

Becker, D. F., & Ragsdale, S. W. (1998). Activation of Methyl-SCoM Reductase to High Specific Activity after Treatment of Whole Cells with Sodium Sulfide. *Biochemistry*, *37*(8), 2639–2647. http://doi.org/10.1021/bi972145x

Beech, I. B., Sunner, J. A., & Hiraoka, K. (2005). Microbe-surface interactions in biofouling and biocorrosion processes. *International Microbiology*, *8*(3), 157–68. http://doi.org/16200494

Beller, H. R., Han, R., Karaoz, U., Lim, H., & Brodie, E. L. (2013). Genomic and Physiological Characterization of the Chromate-Reducing, Aquifer-Derived Firmicute Pelosinus sp. Strain HCF1. *Applied and Environmental Microbiology*, *79*(1), 63–73. http://doi.org/10.1128/AEM.02496-12

Bernstein, H. C., Paulson, S. D., & Carlson, R. P. (2012). Synthetic Escherichia coli consortia engineered for syntrophy demonstrate enhanced biomass productivity. *Journal of Biotechnology*, *157*(1), 159–166. http://doi.org/10.1016/j.jbiotec.2011.10.001

Bhide, J. V., Dhakephalkar, P. K., & Paknikar, K. M. (1996). Microbiological process for the removal of Cr(VI) from chromate-bearing cooling tower effluent. *Biotechnology Letters*, *18*(6), 667–672. http://doi.org/10.1007/BF00130763

Binder, B. J., & Liu, Y. C. (1998). Growth rate regulation of rRNA content of a marine Synechococcus (Cyanobacterium) strain. *Applied and Environmental Microbiology*, *64*(9), 3346–3351.

Bolger, A. M., Lohse, M., & Usadel, B. (2014). Trimmomatic: a flexible trimmer for Illumina sequence data. *Bioinformatics*, *30*(15), 2114–2120. http://doi.org/10.1093/bioinformatics/btu170

Bollmann, A., Schmidt, I., Saunders, A. M., & Nicolaisen, M. H. (2005). Influence of Starvation on Potential Ammonia-Oxidizing Activity and amoA mRNA Levels of Nitrosospira briensis. *Applied and Environmental Microbiology*, *71*(3), 1276–1282. http://doi.org/10.1128/AEM.71.3.1276

Bowen De León, K., Utturkar, S. M., Camilleri, L. B., Elias, D. A., Arkin, A. P., Fields, M. W., … Wall, J. D. (2015). Complete Genome Sequence of Pelosinus fermentans JBW45, a Member of a Remarkably Competitive Group of Negativicutes in the Firmicutes Phylum. *Genome Announcements*, *3*(5), 3–4. http://doi.org/10.1128/genomeA.01090-15

Bowen De León, K., Young, M. L., Camilleri, L. B., Brown, S. D., Skerker, J. M., Deutschbauer, A. M., … Fields, M. W. (2012). Draft Genome Sequence of Pelosinus fermentans JBW45, Isolated during In Situ Stimulation for Cr(VI) Reduction. *Journal of Bacteriology*, *194*(19), 5456–5457. http://doi.org/10.1128/JB.01224-12

Brady, D., & Duncan, J. R. (1994). Bioaccumulation of metal cations by Saccharomyces cerevisiae. *Applied Microbiology and Biotechnology*, *41*(1), 149–154. http://doi.org/10.1007/s002530050123

Braissant, O., Decho, A. W., Dupraz, C., Glunk, C., Przekop, K. M., & Visscher, P. T. (2007). Exopolymeric substances of sulfate-reducing bacteria: Interactions with calcium at alkaline pH and implication for formation of carbonate minerals. *Geobiology*, *5*(4), 401–411. http://doi.org/10.1111/j.1472-4669.2007.00117.x

Branda, S. S., Vik, S., Friedman, L., & Kolter, R. (2005). Biofilms: the matrix revisited. *Trends in Microbiology*, *13*(1), 20–6. http://doi.org/10.1016/j.tim.2004.11.006

Brenner, K., & Arnold, F. H. (2011). Self-Organization, Layered Structure, and Aggregation Enhance Persistence of a Synthetic Biofilm Consortium. *PLoS ONE*, *6*(2), e16791. http://doi.org/10.1371/journal.pone.0016791

Brileya, K. A., Camilleri, L. B., & Fields, M. W. (2014a). 3D-Fluorescence In Situ Hybridization of Intact, Anaerobic Biofilm. In L. Sun & W. Shou (Eds.), *Engineering and Analyzing Multicellular Systems* (Vol. 1151, pp. 189–197). New York, NY: Springer New York. http://doi.org/10.1007/978-1-4939-0554-6

Brileya, K. A., Camilleri, L. B., Zane, G. M., Wall, J. D., & Fields, M. W. (2014b). Biofilm growth mode promotes maximum carrying capacity and community stability during product inhibition syntrophy. *Frontiers in Microbiology*, *5*(12), 693. http://doi.org/10.3389/fmicb.2014.00693

Brileya, K. A., Connolly, J. M., Downey, C., Gerlach, R., & Fields, M. W. (2013). Taxis toward hydrogen gas by Methanococcus maripaludis. *Scientific Reports*, *3*, 3140. http://doi.org/10.1038/srep03140

Brown, S. D., Podar, M., Klingeman, D. M., Johnson, C. M., Yang, Z. K., Utturkar, S. M., … Elias, D. A. (2012). Draft Genome Sequences for Two Metal-Reducing Pelosinus fermentans Strains Isolated from a Cr(VI)-Contaminated Site and for Type Strain R7. *Journal of Bacteriology*, *194*(18), 5147–5148. http://doi.org/10.1128/JB.01174-12

Brown, S. D., Utturkar, S. M., Magnuson, T. S., Ray, A. E., Poole, F. L., Lancaster, W. A., … Elias, D. A. (2014). Complete Genome Sequence of Pelosinus sp. Strain UFO1 Assembled Using Single-Molecule Real-Time DNA Sequencing Technology. *Genome Announcements*, *2*(5), 2–3. http://doi.org/10.1128/genomeA.00881-14

Bryant, M. P., Campbell, L. L., Reddy, C. A., & Crabill, M. R. (1977). Growth of Desulfovibrio in lactate or ethanol media low in sulfate in association with H2-utilizing methanogenic bacteria. *Applied and Environmental Microbiology*, *33*(5), 1162–9. Retrieved from http://www.ncbi.nlm.nih.gov/pubmed/879775

Burmølle, M., Ren, D., Bjarnsholt, T., & Sørensen, S. J. (2014). Interactions in multispecies biofilms: do they actually matter? *Trends in Microbiology*, *22*(2), 84–91. http://doi.org/10.1016/j.tim.2013.12.004

Busch, R., Neese, R. A., Awada, M., Hayes, G. M., & Hellerstein, M. K. (2007). Measurement of cell proliferation by heavy water labeling. *Nature Protocols*, *2*(12), 3045–3057. http://doi.org/10.1038/nprot.2007.420

Carlson, R. P., Beck, A. E., Phalak, P., Fields, M. W., Gedeon, T., Hanley, L., … Heys, J. J. (2018). Competitive resource allocation to metabolic pathways contributes to overflow metabolisms and emergent properties in cross-feeding microbial consortia. *Biochemical Society Transactions*, *46*(2), 269–284. http://doi.org/10.1042/BST20170242

Clark, M. E., Edelmann, R. E., Duley, M. L., Wall, J. D., & Fields, M. W. (2007). Biofilm formation in Desulfovibrio vulgaris Hildenborough is dependent upon protein filaments. *Environmental Microbiology*, *9*(11), 2844–54. http://doi.org/10.1111/j.1462-2920.2007.01398.x

Clark, M. E., He, Q., He, Z., Huang, K. H., Alm, E. J., Wan, X.-F., … Fields, M. W. (2006). Temporal transcriptomic analysis as Desulfovibrio vulgaris Hildenborough transitions into stationary phase during electron donor depletion. *Applied and Environmental Microbiology*, *72*(8), 5578–88. http://doi.org/10.1128/AEM.00284-06

Clark, M. E., He, Z., Redding, A. M., Joachimiak, M. P., Keasling, J. D., Zhou, J. Z., … Fields, M. W. (2012). Transcriptomic and proteomic analyses of Desulfovibrio vulgaris biofilms: carbon and energy flow contribute to the distinct biofilm growth state. *BMC Genomics*, *13*(1), 138. http://doi.org/10.1186/1471-2164-13-138

Conrad, R. (1999). Contribution of hydrogen to methane production and control of hydrogen concentrations in methanogenic soils and sediments. *FEMS Microbiology Ecology*, *28*(3), 193–202. http://doi.org/10.1016/S0168-6496(98)00086-5

Conway de Macario, E., & Macario, A. J. L. (2009). Methanogenic archaea in health and disease: A novel paradigm of microbial pathogenesis. *International Journal of Medical Microbiology*, *299*(2), 99–108. http://doi.org/10.1016/j.ijmm.2008.06.011

Cook, A. M., Smits, T. H. M., & Denger, K. (2008). Sulfonates and Organotrophic Sulfite Metabolism. In C. Dahl & C. G. Friedrich (Eds.), *Microbial Sulfur Metabolism* (pp. 170–183). Springer-Verlag Berlin Heidelberg. http://doi.org/10.1007/978-3-540-72682-1

Cord-Ruwisch, R. (1985). A quick method for the determination of dissolved and precipitated sulfides in cultures of sulfate-reducing bacteria. *Journal of Microbiological Methods*, *4*, 33–36.

Corral-Lugo, A., Daddaoua, A., Ortega, A., Espinosa-Urgel, M., & Krell, T. (2016). So different and still so similar: The plant compound rosmarinic acid mimics bacterial homoserine lactone quorum sensing signals. *Communicative and Integrative Biology*, *9*(2), 1–4. http://doi.org/10.1080/19420889.2016.1156832

Costa, M., & Klein, C. B. (2006). Toxicity and Carcinogenicity of Chromium Compounds in Humans. *Critical Reviews in Toxicology*, *36*(2), 155–163. http://doi.org/10.1080/10408440500534032

Costerton, J. W. (1999). Introduction to biofilm. *International Journal of Antimicrobial Agents*, *11*, 217–221.

Costerton, J. W. (2007). *The Biofilm Primer*. (J. W. Costerton, Ed.) (Vol. 1). Springer Berlin Heidelberg. http://doi.org/10.1007/b136878

Costerton, J. W., Cheng, K. J., Geesey, G. G., Ladd, T. I., Nickel, J. C., Dasgupta, M., & Marrie, T. J. (1987). Bacterial Biofilms in Nature and Disease. *Ann. Rev. Microbiol.*, *41*, 435–464. http://doi.org/10.1146/annurev.mi.41.100187.002251

Costerton, W. J., & Wilson, M. (2004). Introducing Biofilms. *Biofilms*, *1*(1), 1–4. http://doi.org/10.1017/S1479050504001164

D'Souza, G., Shitut, S., Preussger, D., Yousif, G., Waschina, S., & Kost, C. (2018). Ecology and evolution of metabolic cross-feeding interactions in bacteria. *Natural Product Reports*, *35*(5), 455–488. http://doi.org/10.1039/C8NP00009C

Daims, H., Lücker, S., & Wagner, M. (2006). Daime, a novel image analysis program for microbial ecology and biofilm research. *Environmental Microbiology*, *8*(2), 200–213. http://doi.org/10.1111/j.1462-2920.2005.00880.x

de Mazancourt, C., Loreau, M., & Dieckmann, U. (2005). Understanding mutualism when there is adaptation to the partner. *Journal of Ecology*, *93*(2), 305–314. http://doi.org/10.1111/j.1365-2745.2004.00952.x

de Mazancourt, C., & Schwartz, M. W. (2010). A resource ratio theory of cooperation. *Ecology Letters*, *13*(3), 349–359. http://doi.org/10.1111/j.1461-0248.2009.01431.x

De Riva, A., Deery, M. J., McDonald, S., Lund, T., & Busch, R. (2010). Measurement of protein synthesis using heavy water labeling and peptide mass spectrometry: Discrimination between major histocompatibility complex allotypes. *Analytical Biochemistry*, *403*(1–2), 1–12. http://doi.org/10.1016/j.ab.2010.04.018

Dean, A. M. (1985). The dynamics of microbial commensalisms and mutualisms. In D. H. Boucher (Ed.), *The Biology of Mutualism* (pp. 270–300). Oxford: Oxford University Press. Retrieved from https://books.google.com/books?hl=en&lr=&id=dWuQS_3F2P0C&oi=fnd&pg=PA270&ots=_vLqPPvfaW&sig=kQJWc5rcE0FIzy8fpfml3ZWn3-k#v=onepage&q&f=false

Decho, A. W. (2000). Exopolymer Microdomains as a Structuring Agent for Heterogeneity Within Microbial Biofilms. In R. E. Riding & S. M. Awramik (Eds.), *Microbial Sediments* (pp. 9–15). Berlin, Heidelberg: Springer-Verlag Berlin Heidelberg. http://doi.org/10.1007/978-3-662-04036-2_2

Decho, A. W., Norman, R. S., & Visscher, P. T. (2010). Quorum sensing in natural environments: emerging views from microbial mats. *Trends in Microbiology*, *18*(2), 73–80. http://doi.org/10.1016/j.tim.2009.12.008

Denger, K., Mayer, J., Buhmann, M., Weinitschke, S., Smits, T. H. M., & Cook, A. M. (2009). Bifurcated Degradative Pathway of 3-Sulfolactate in Roseovarius nubinhibens ISM via Sulfoacetaldehyde Acetyltransferase and (S)-Cysteate Sulfolyase. *Journal of Bacteriology*, *191*(18), 5648–5656. http://doi.org/10.1128/JB.00569-09

Denger, K., Weinitschke, S., Hollemeyer, K., & Cook, A. M. (2004). Sulfoacetate generated by Rhodopseudomonas palustris from taurine. *Archives of Microbiology*, *182*(2–3), 254–8. http://doi.org/10.1007/s00203-004-0678-0

Denger, K., Weinitschke, S., Hollemeyer, K., & Cook, A. M. (2014). aSulfoacetate generated by Rhodopseudomonas palustris from taurine, (November). http://doi.org/10.1007/s00203-004-0678-0

Dieterich, D. C., Link, A. J., Graumann, J., Tirrell, D. A., & Schuman, E. M. (2006). Selective identification of newly synthesized proteins in mammalian cells using bioorthogonal noncanonical amino acid tagging (BONCAT). *Proceedings of the National Academy of Sciences of the United States of America*, *103*(25), 9482–7. http://doi.org/10.1073/pnas.0601637103

Dunne, W. M. J. (2002). Bacterial adhesion: seen any good biofilms lately? *Clinical Microbiology Reviews*, *15*(2), 155–166. http://doi.org/10.1128/CMR.15.2.155

Eberhard, A., Burlingame, A. L., Eberhard, C., Kenyon, G. L., Nealson, K. H., & Oppenheimer, N. J. (1981). Structural Identification of Autoinducer of Photobacterium fischeri Luciferase. *Biochemistry*, *20*(9), 2444–2449. http://doi.org/10.1021/bi00512a013

Engebrecht, J., Nealson, K., & Silverman, M. (1983). Bacterial Bioluminescence: Isolation and Genetic Analysis of Functions from Vibrio fischeri. *Cell*, *32*(3), 773–781. http://doi.org/10.1016/0092-8674(83)90063-6

Faust, K., & Raes, J. (2012). Microbial interactions: from networks to models. *Nature Reviews Microbiology*, *10*(8), 538–550. http://doi.org/10.1038/nrmicro2832

Felux, A.-K., Spiteller, D., Klebensberger, J., & Schleheck, D. (2015). Entner–Doudoroff pathway for sulfoquinovose degradation in Pseudomonas putida SQ1. *Proceedings of the National Academy of Sciences*, *112*(31), E4298–E4305. http://doi.org/10.1073/pnas.1507049112

Ferenci, T. (2016). Trade-off Mechanisms Shaping the Diversity of Bacteria. *Trends in Microbiology*, *24*(3), 209–223. http://doi.org/10.1016/j.tim.2015.11.009

Ferrera, I., Longhorn, S., Banta, A. B., Liu, Y., Preston, D., & Reysenbach, A.-L. (2007). Diversity of 16S rRNA gene, ITS region and aclB gene of the Aquificales. *Extremophiles*, *11*(1), 57–64. http://doi.org/10.1007/s00792-006-0009-2

Fields, M. W., Yan, T., Rhee, S., Carroll, S. L., Jardine, P. M., Watson, D. B., … Zhou, J. (2005). Impacts on microbial communities and cultivable isolates from groundwater contaminated with high levels of nitric acid - uranium waste. *FEMS Microbiology Ecology*, *53*(3), 417–428. http://doi.org/10.1016/j.femsec.2005.01.010

Flemming, H. C. (1996). Economical and Technical Overview. In E. Heitz, H. C. Flemming, & W. Sand (Eds.), *Microbially Influenced Corrosion of Materials* (pp. 6–14). New York: Springer-Verlag.

Flemming, H. C., & Wingender, J. (2010). The biofilm matrix. *Nature Reviews. Microbiology*, *8*(9), 623–33. http://doi.org/10.1038/nrmicro2415

Flemming, H. C., & Wuertz, S. (2019). Bacteria and archaea on Earth and their abundance in biofilms. *Nature Reviews Microbiology*, *17*(4), 247–260. http://doi.org/10.1038/s41579-019-0158-9

Fondi, M., & Liò, P. (2015). Multi -omics and metabolic modelling pipelines: Challenges and tools for systems microbiology. *Microbiological Research*, *171*, 52–64. http://doi.org/10.1016/j.micres.2015.01.003

Foster, R. A., Subramaniam, A., & Zehr, J. P. (2009). Distribution and activity of diazotrophs in the Eastern Equatorial Atlantic. *Environmental Microbiology*, *11*(4), 741–750. http://doi.org/10.1111/j.1462-2920.2008.01796.x

Fu, X., Liu, R., Sanchez, I., Silva-Sanchez, C., Hepowit, N. L., Cao, S., … Maupin-Furlow, J. (2016). Ubiquitin-Like Proteasome System Represents a Eukaryotic-Like Pathway for Targeted Proteolysis in Archaea. *MBio*, *7*(4), 1–14. http://doi.org/10.1128/mBio.01192-16

Fuqua, W. C., Winans, S. C., & Greenberg, E. P. (1994). Quorum Sensing in Bacteria: the LuxR-LuxI Family of Cell Density-Responsive Transcriptional Regulators. *Journal of Bacteriology*, *176*(2), 269–275. http://doi.org/10.1128/jb.176.2.269-275.1994

Gadd, G. M. (1990). Heavy metal accumulation by bacteria and other microorganisms. *Experientia*, *46*(8), 834–840. http://doi.org/10.1007/BF01935534

Gadd, G. M., & White, C. (1993). Microbial treatment of metal pollution - a working biotechnology? *Trends in Biotechnology*, *11*(8), 353–359. http://doi.org/10.1016/0167-7799(93)90158-6

Gedeon, T., & Bokes, P. (2012). Delayed protein synthesis reduces the correlation between mRNA and protein fluctuations. *Biophysical Journal*, *103*(3), 377–385. http://doi.org/10.1016/j.bpj.2012.06.025

Geesey, G. G., Mutch, R., Costerton, J. W., & Green, R. B. (1978). Sessile Bacteria: An Important Component of the Microbial Population in Small Mountain Streams. *Limnology and Oceanography*, *23*(6), 1214–1223. Retrieved from https://www.jstor.org/stable/2835675

Gerstl, M. P., Jungreuthmayer, C., & Zanghellini, J. (2015a). tEFMA: computing thermodynamically feasible elementary flux modes in metabolic networks. *Bioinformatics*, *31*(13), 2232–2234. http://doi.org/10.1093/bioinformatics/btv111

Gerstl, M. P., Ruckerbauer, D. E., Mattanovich, D., Jungreuthmayer, C., & Zanghellini, J. (2015b). Metabolomics integrated elementary flux mode analysis in large metabolic networks. *Scientific Reports*, *5*(1), 8930. http://doi.org/10.1038/srep08930

González Fernández-Niño, S. M., Smith-Moritz, A. M., Chan, L. J. G., Adams, P. D., Heazlewood, J. L., & Petzold, C. J. (2015). Standard Flow Liquid Chromatography for Shotgun Proteomics in Bioenergy Research. *Frontiers in Bioengineering and Biotechnology*, *3*(April), 1–7. http://doi.org/10.3389/fbioe.2015.00044

Graupner, M., Xu, H., & White, R. H. (2000). Identification of an Archaeal 2-Hydroxy Acid Dehydrogenase Catalyzing Reactions Involved in Coenzyme Biosynthesis in Methanoarchaea. *Journal of Bacteriology*, *182*(13), 3688–3692. http://doi.org/10.1128/JB.182.13.3688-3692.2000

Graupner, M., Xu, H., & White, R. H. (2000). Identification of the gene encoding sulfopyruvate decarboxylase, an enzyme involved in biosynthesis of coenzyme M. *Journal of Bacteriology*, *182*(17), 4862–4867. http://doi.org/10.1128/JB.182.17.4862-4867.2000

Gross, R., Hauer, B., Otto, K., & Schmid, A. (2007). Microbial biofilms: New catalysts for maximizing productivity of long-term biotransformations. *Biotechnology and Bioengineering*, *98*(6), 1123–1134. http://doi.org/10.1002/bit.21547

Gross, S. M., Martin, J. A., Simpson, J., Abraham-Juarez, M., Wang, Z., & Visel, A. (2013). De novo transcriptome assembly of drought tolerant CAM plants, Agave deserti and Agave tequilana. *BMC Genomics*, *14*(1), 563. http://doi.org/10.1186/1471-2164-14-563

Gunsalus, R. P., Romesser, J. A., & Wolfe, R. S. (1978). Preparation of coenzyme M analogs and their activity in the methyl coenzyme M reductase system of Methanobacterium thermoautotrophicum. *Biochemistry*, *17*(12), 2374–2377. http://doi.org/10.1021/bi00605a019

Gutleben, J., Chaib De Mares, M., van Elsas, J. D., Smidt, H., Overmann, J., & Sipkema, D. (2018). The multi-omics promise in context: from sequence to microbial isolate. *Critical Reviews in Microbiology*, *44*(2), 212–229. http://doi.org/10.1080/1040841X.2017.1332003

Hall-Stoodley, L., Costerton, J. W., & Stoodley, P. (2004). Bacterial biofilms: from the natural environment to infectious diseases. *Nature Reviews Microbiology*, *2*(2), 95–108. http://doi.org/10.1038/nrmicro821

Hamilton, S., Bongaerts, R. J., Mulholland, F., Cochrane, B., Porter, J., Lucchini, S., … Hinton, J. C. (2009). The transcriptional programme of Salmonella enterica serovar Typhimurium reveals a key role for tryptophan metabolism in biofilms. *BMC Genomics*, *10*(1), 599. http://doi.org/10.1186/1471-2164-10-599

Hamilton, W. A. (2003). Microbially Influenced Corrosion as a Model System for the Study of Metal Microbe Interactions: A Unifying Electron Transfer Hypothesis. *Biofouling*, *19*(1), 65–76. http://doi.org/10.1080/0892701021000041078

Hammerstein, P., & Noë, R. (2016). Biological trade and markets. *Philosophical Transactions of the Royal Society B: Biological Sciences*, *371*(1687), 20150101. http://doi.org/10.1098/rstb.2015.0101

Hammerstein, P., & Selten, R. (1994). Game theory and evolutionary biology. In R. J. Aumann & S. Hart (Eds.), *Handbook of Game Theory with Economic Applications* (Vol. 2, pp. 929–993). Elsevier Science B.B. http://doi.org/10.1016/S1574-0005(05)80060-8

Hansen, S. K., Rainey, P. B., Haagensen, J. A. J., & Molin, S. (2007). Evolution of species interactions in a biofilm community. *Nature*, *445*(7127), 533–536. http://doi.org/10.1038/nature05514

Harwood, J. L., Ellis, A. J., White, G. F., Roy, A. B., & Hewlins, M. J. E. (2003). Glycolytic Breakdown of Sulfoquinovose in Bacteria: a Missing Link in the Sulfur Cycle. *Applied and Environmental Microbiology*, *69*(11), 6434–6441. http://doi.org/10.1128/aem.69.11.6434-6441.2003

Hatchikian, C. E. (1975). Purification and Properties of Thiosulfate Reductase from Desulfovibrio gigas. *Archives of Microbiology*, (105), 249–256. http://doi.org/10.1093/oxfordjournals.jbchem.a135144

Hatzenpichler, R., Connon, S. A., Goudeau, D., Malmstrom, R. R., Woyke, T., & Orphan, V. J. (2016). Visualizing in situ translational activity for identifying and sorting slow-growing archaeal−bacterial consortia. *Proceedings of the National Academy of Sciences*, *113*(28), E4069–E4078. http://doi.org/10.1073/pnas.1603757113

Hatzenpichler, R., & Orphan, V. J. (2015). Detection of Protein-Synthesizing Microorganisms in the Environment via Bioorthogonal Noncanonical Amino Acid Tagging (BONCAT). In T. McGenity, K. Timmis, & B. Nogales (Eds.), *Hydrocarbon and Lipid Microbiology Protocols* (Springer P, pp. 145–157). Springer Berlin Heidelberg. http://doi.org/https://doi.org/10.1007/8623_2015_61

Hatzenpichler, R., Scheller, S., Tavormina, P. L., Babin, B. M., Tirrell, D. A., & Orphan, V. J. (2014). In situ visualization of newly synthesized proteins in environmental microbes using amino acid tagging and click chemistry. *Environmental Microbiology*, *16*(8), 2568–90. http://doi.org/10.1111/1462-2920.12436

He, Z., Zhou, A., Baidoo, E., He, Q., Joachimiak, M. P., Benke, P., … Zhou, J. (2010). Global Transcriptional, Physiological, and Metabolite Analyses of the Responses of Desulfovibrio vulgaris Hildenborough to Salt Adaptation. *Applied and Environmental Microbiology*, *76*(5), 1574–1586. http://doi.org/10.1128/AEM.02141-09

Heidelberg, J. F., Seshadri, R., Haveman, S. a, Hemme, C. L., Paulsen, I. T., Kolonay, J. F., … Fraser, C. M. (2004). The genome sequence of the anaerobic, sulfate-reducing bacterium Desulfovibrio vulgaris Hildenborough. *Nature Biotechnology*, *22*(5), 554–559. http://doi.org/10.1038/nbt959

Hendrickson, E. L., Haydock, A. K., Moore, B. C., Whitman, W. B., & Leigh, J. A. (2007). Functionally distinct genes regulated by hydrogen limitation and growth rate in methanogenic Archaea. *Proceedings of the National Academy of Sciences of the United States of America.*, *104*(21), 8930–8934. http://doi.org/10.1073/pnas.0701157104

Holman, H.-Y. N., Wozei, E., Lin, Z., Comolli, L. R., Ball, D. A., Borglin, S., … Downing, K. H. (2009). Real-time molecular monitoring of chemical environment in obligate anaerobes during oxygen adaptive response. *Proceedings of the National Academy of Sciences*, *106*(31), 12599–12604. http://doi.org/10.1073/pnas.0902070106

Hooper, S. L., & Burstein, H. J. (2014). Minimization of extracellular space as a driving force in prokaryote association and the origin of eukaryotes. *Biology Direct*, *9*(1), 24. http://doi.org/10.1186/1745-6150-9-24

Jarrell, K. F., Walters, A. D., Bochiwal, C., Borgia, J. M., Dickinson, T., & Chong, J. P. J. (2011). Major players on the microbial stage: why archaea are important. *Microbiology*, *157*(4), 919–936. http://doi.org/10.1099/mic.0.047837-0

Ji, G., Beavis, R., & Novick, R. P. (1997). Bacterial Interference Caused by Autoinducing Peptide Variants. *Science*, *276*(5321), 2027–2030. Retrieved from https://www.jstor.org/stable/2892976

Johnson, E. F., & Mukhopadhyay, B. (2008). A Novel Coenzyme F420 Dependent Sulfite Reductase and a Small Sulfite Reductase in Methanogenic Archaea. In C. Dahl & C. G. Friedrich (Eds.), *Microbial Sulfur Metabolism* (pp. 202–216). Berlin, Heidelberg: Springer Berlin Heidelberg. http://doi.org/10.1007/978-3-540-72682-1

Jones, W. J., Nagle, D. P., & Whitman, W. B. (1987). Methanogens and the diversity of archaebacteria. *Microbiological Reviews*, *51*(1), 135–77. Retrieved from http://www.pubmedcentral.nih.gov/articlerender.fcgi?artid=373095&tool=pmcentrez&rendertype=abstract

Kato, S., & Watanabe, K. (2010). Ecological and Evolutionary Interactions in Syntrophic Methanogenic Consortia. *Microbes and Environments*, *25*(3), 145–151. http://doi.org/10.1264/jsme2.ME10122

Keller, L., & Surette, M. G. (2006). Communication in bacteria: An ecological and evolutionary perspective. *Nature Reviews Microbiology*, *4*(4), 249–258. http://doi.org/10.1038/nrmicro1383

Kolter, R. (2005). Surfacing views of biofilm biology. *Trends in Microbiology*, *13*(1), 1–2. http://doi.org/10.1016/j.tim.2004.11.003

Konhauser, K. O. (2006). *Introduction to Geomicrobiology* (illustrate, Vol. 10). Wiley.

Koonin, E. V. (2015). Origin of eukaryotes from within archaea, archaeal eukaryome and bursts of gene gain: eukaryogenesis just made easier? *Philosophical Transactions of the Royal Society B: Biological Sciences*, *370*(1678), 20140333. http://doi.org/10.1098/rstb.2014.0333

Kratochvil, D., & Volesky, B. (1998). Advances in the biosorption of heavy metals. *Trends in Biotechnology*, *16*(7), 291–300. http://doi.org/10.1016/S0167-7799(98)01218-9

Kreft, J.-U., Hartmann, A., Müller, J., Kuttler, C., Rothballer, M., & Hense, B. A. (2007). Does efficiency sensing unify diffusion and quorum sensing? *Nature Reviews Microbiology*, *5*(3), 230–239. http://doi.org/10.1038/nrmicro1600

Krejčík, Z., Denger, K., Weinitschke, S., Hollemeyer, K., Pačes, V., Cook, A. M., & Smits, T. H. M. (2008). Sulfoacetate released during the assimilation of taurine-nitrogen by Neptuniibacter caesariensis: purification of sulfoacetaldehyde dehydrogenase. *Archives of Microbiology*, *190*(2), 159–168. http://doi.org/10.1007/s00203-008-0386-2

Kristjansson, J. K., Schönheit, P., & Thauer, R. K. (1982). Different Ks values for hydrogen of methanogenic bacteria and sulfate reducing bacteria: An explanation for the apparent inhibition of methanogenesis by sulfate. *Archives of Microbiology*, *131*(3), 278–282. http://doi.org/10.1007/BF00405893

Krumholz, L. R., Bradstock, P., Sheik, C. S., Diao, Y., Gazioglu, O., Gorby, Y., & McInerney, M. J. (2015). Syntrophic Growth of Desulfovibrio alaskensis Requires Genes for H 2 and Formate Metabolism as Well as Those for Flagellum and Biofilm Formation. *Applied and Environmental Microbiology*, *81*(7), 2339–2348.

Krzmarzick, M. J., Miller, H. R., Yan, T., & Novak, P. J. (2014). Novel Firmicutes Group Implicated in the Dechlorination of Two Chlorinated Xanthones, Analogues of Natural Organochlorines. *Applied and Environmental Microbiology*, *80*(3), 1210–1218. http://doi.org/10.1128/AEM.03472-13

Kurczy, M. E., Zhu, Z.-J., Ivanisevic, J., Schuyler, A. M., Lalwani, K., Santidrian, A. F., … Siuzdak, G. (2015). Comprehensive bioimaging with fluorinated nanoparticles using breathable liquids. *Nature Communications*, *6*(1), 5998. http://doi.org/10.1038/ncomms6998

Langmead, B., & Salzberg, S. L. (2012). Fast gapped-read alignment with Bowtie 2. *Nature Methods*, *9*(4), 357–359. http://doi.org/10.1038/nmeth.1923

Lawrence, J. R., Swerhone, G. D. W., Kuhlicke, U., & Neu, T. R. (2007). In situ evidence for microdomains in the polymer matrix of bacterial microcolonies. *Canadian Journal of Microbiology*, *53*(3), 450–458. http://doi.org/10.1139/W06-146

Leigh, J. A. (2001). Evolution of Energy Metabolism. In J. T. Staley & A. Reysenbach (Eds.), *Biodiversity of Microbial Life: Foundation of Earth's Biosphere* (Wiley Seri). New York: John Wiley & Sons, Inc.

Leloup, J., Fossing, H., Kohls, K., Holmkvist, L., Borowski, C., & Jørgensen, B. B. (2009). Sulfate-reducing bacteria in marine sediment (Aarhus Bay, Denmark): abundance and diversity related to geochemical zonation. *Environmental Microbiology*, *11*(5), 1278–1291. http://doi.org/10.1111/j.1462-2920.2008.01855.x

Lenhart, K., Bunge, M., Ratering, S., Neu, T. R., Schüttmann, I., Greule, M., … Keppler, F. (2012). Evidence for methane production by saprotrophic fungi. *Nature Communications*, *3*, 1046. http://doi.org/10.1038/ncomms2049

Lie, T. J., Pitta, T., Leadbetter, E. R., Godchaux, W., & Leadbetter, J. R. (1996). Sulfonates: novel electron acceptors in anaerobic respiration. *Archives of Microbiology*, *166*(3), 204–10. http://doi.org/10.1007/s002030050376

Lilja, E. E., & Johnson, D. R. (2016). Segregating metabolic processes into different microbial cells accelerates the consumption of inhibitory substrates. *The ISME Journal*, *10*(7), 1568–1578. http://doi.org/10.1038/ismej.2015.243

Little, B. J., & Lee, J. S. (2007). Microbiologically Influenced Corrosion. In R. W. Revie (Ed.), *Wiley Series in Corrosion*. Hoboken, New Jersey: John Wiley & Sons, Inc. Retrieved from cfm.mines.edu/research.html

Liu, H., Wang, J., Wang, A., & Chen, J. (2011). Chemical inhibitors of methanogenesis and putative applications. *Applied Microbiology and Biotechnology*, *89*(5), 1333–1340. http://doi.org/10.1007/s00253-010-3066-5

Löffler, F. E., Ritalahti, K. M., & Tiedje, J. M. (1997). Dechlorination of chloroethenes is inhibited by 2-bromoethanesulfonate in the absence of methanogens. Applied and Environmental Microbiology, 63(12), 4982–4985.

Lohner, S. T., Deutzmann, J. S., Logan, B. E., Leigh, J., & Spormann, A. M. (2014). Hydrogenase-independent uptake and metabolism of electrons by the archaeon Methanococcus maripaludis. *The ISME Journal*, *8*(8), 1673–1681. http://doi.org/10.1038/ismej.2014.82

Loverdo, C., Bénichou, O., Moreau, M., & Voituriez, R. (2008). Enhanced reaction kinetics in biological cells. *Nature Physics*, *4*(2), 134–137. http://doi.org/10.1038/nphys830

Lupton, F. S., Conrad, R., & Zeikus, J. G. (1984). Physiological Function of Hydrogen Metabolism During Growth of Sulfidogenic Bacteria on Organic Substrates. *Journal of Bacteriology*, *159*(3), 843–849.

Luton, P. E., Wayne, J. M., Sharp, R. J., & Riley, P. W. (2002). The mcrA gene as an alternative to 16S rRNA in the phylogenetic analysis of methanogen populations in landfill. *Microbiology*, *148*(11), 3521–30. http://doi.org/10.1099/00221287-148-11-3521

Lyon, G. J., Wright, J. S., Muir, T. W., & Novick, R. P. (2002). Key Determinants of Receptor Activation in the agr Autoinducing Peptides of Staphylococcus aureus †. *Biochemistry*, *41*(31), 10095–10104. http://doi.org/10.1021/bi026049u

Mahlert, F., Bauer, C., Jaun, B., Thauer, R. K., & Duin, E. C. (2002). The nickel enzyme methyl-coenzyme M reductase from methanogenic archaea: In vitro induction of the nickel-based MCR-ox EPR signals from MCR-red2. *JBIC Journal of Biological Inorganic Chemistry*, *7*(4–5), 500–513. http://doi.org/10.1007/s00775-001-0325-z

Marchal, M., Goldschmidt, F., Derksen-Müller, S. N., Panke, S., Ackermann, M., & Johnson, D. R. (2017). A passive mutualistic interaction promotes the evolution of spatial structure within microbial populations. *BMC Evolutionary Biology*, *17*(1), 106. http://doi.org/10.1186/s12862-017-0950-y

Matz, C. (2011). Competition, Communication, Cooperation: Molecular Crosstalk in Multi-species Biofilms. In H. C. Flemming, J. Wingender, & U. Szewzyk (Eds.), *Biofilm Highlights* (Springer S, Vol. 5, pp. 29–40). Springer Berlin Heidelberg. http://doi.org/10.1007/978-3-642-19940-0

Maupin-Furlow, J. (2012). Proteasomes and protein conjugation across domains of life. *Nature Reviews Microbiology*, *10*(2), 100–111. http://doi.org/10.1038/nrmicro2696

Mayville, P., Ji, G., Beavis, R., Yang, H., Goger, M., Novick, R. P., & Muir, T. W. (1999). Structure-activity analysis of synthetic autoinducing thiolactone peptides from Staphylococcus aureus responsible for virulence. *Proceedings of the National Academy of Sciences of the United States of America*, *96*(4), 1218–23. Retrieved from http://www.pubmedcentral.nih.gov/articlerender.fcgi?artid=15443&tool=pmcentrez

McInerney, M. J., & Bryant, M. P. (1981). Anaerobic degradation of lactate by syntrophic associations of Methanosarcina barkeri and Desulfovibrio species and effect of H2 on acetate degradation. *Applied and Environmental Microbiology*, *41*(2), 346–354.

McInerney, M. J., Sieber, J. R., & Gunsalus, R. P. (2009). Syntrophy in anaerobic global carbon cycles. *Current Opinion in Biotechnology*, *20*(6), 623–632. http://doi.org/10.1016/j.copbio.2009.10.001

Michel, C., Brugna, M., Aubert, C., Bernadac, A., & Bruschi, M. (2001). Enzymatic reduction of chromate: comparative studies using sulfate-reducing bacteria. *Applied Microbiology and Biotechnology*, *55*(1), 95–100. http://doi.org/10.1007/s002530000467

Miller, T., Burns, J., Munguia, P., Walters, E., Kneitel, J., Richards, P., … Buckley, H. (2005). A Critical Review of Twenty Years' Use of the Resource-Ratio Theory. *American Naturalist*, *165*(4), 439–448. Retrieved from isi:000227517000006%5Cnpapers2://publication/uuid/F528658C-E918-41E4-B25C-60C38CAB51F9

Moe, W. M., Stebbing, R. E., Rao, J. U., Bowman, K. S., Nobre, M. F., da Costa, M. S., & Rainey, F. A. (2012). Pelosinus defluvii sp. nov., isolated from chlorinated solvent-contaminated groundwater, emended description of the genus Pelosinus and transfer of Sporotalea propionica to Pelosinus propionicus comb. nov. *International Journal of Systematic and Evolutionary Microbiology*, *62*(Pt 6), 1369–76. http://doi.org/10.1099/ijs.0.033753-0

Momeni, B., Brileya, K. A., Fields, M. W., & Shou, W. (2013). Strong inter-population cooperation leads to partner intermixing in microbial communities. *ELife*, *2*, e00230. http://doi.org/10.7554/eLife.00230

Morgenroth, E., Obermayer, A., Arnold, E., Brühl, A., Wagner, M., & Wilderer, P. A. (2000). Effect of long-term idle periods on the performance of sequencing batch reactors. *Water Science and Technology*, *41*(1), 105–113. http://doi.org/10.2166/wst.2000.0018

Morris, B. E. L., Henneberger, R., Huber, H., & Moissl-Eichinger, C. (2013). Microbial syntrophy: interaction for the common good. *FEMS Microbiology Reviews*, *37*(3), 384–406. http://doi.org/10.1111/1574-6976.12019

Mountfort, D. O., & Asher, R. A. (1981). Role of Sulfate Reduction Versus Methanogenesis in Terminal Carbon Flow in Polluted Intertidal Sediment of Waimea Inlet, Nelson, New Zealand. *Applied and Environmental Microbiology*, *42*(2), 252–258. Retrieved from http://aem.asm.org/cgi/reprint/42/2/252

Mountfort, D. O., Asher, R. A., Mays, E. L., & Tiedje, J. M. (1980). Carbon and electron flow in mud and sandflat intertidal sediments at Delaware inlet, Nelson, New Zealand. *Applied and Environmental Microbiology*, *39*(4), 686–94. Retrieved from http://www.ncbi.nlm.nih.gov/pubmed/16345535%0Ahttp://www.pubmedcentral.nih.gov/articlerender.fcgi?artid=PMC291405

Muramatsu, H., Mihara, H., Kakutani, R., Yasuda, M., Ueda, M., Kurihara, T., & Esaki, N. (2005). The Putative Malate/Lactate Dehydrogenase from Pseudomonas putida Is an NADPH-dependent Δ 1 -Piperideine-2-carboxylate/Δ 1 -Pyrroline-2-carboxylate Reductase Involved in the Catabolism of d-Lysine and d-Proline. *Journal of Biological Chemistry*, *280*(7), 5329–5335. http://doi.org/10.1074/jbc.M411918200

Nadell, C. D., Xavier, J. B., Levin, S. A., & Foster, K. R. (2008). The evolution of quorum sensing in bacterial biofilms. *PLoS Biology*, *6*(1), e14. http://doi.org/10.1371/journal.pbio.0060014

Nealson, K. H., Platt, T., & Hastings, J. W. (1970). Cellular control of the synthesis and activity of the bacterial luminescent system. *Journal of Bacteriology*, *104*(1), 313–322.

Nielsen, A. T., Tolker-Nielsen, T., Barken, K. B., & Molin, S. (2000). Role of commensal relationships on the spatial structure of a surface-attached microbial consortium. *Environmental Microbiology*, *2*(1), 59–68. http://doi.org/10.1046/j.1462-2920.2000.00084.x

Oda, Y., Slagman, S. J., Meijer, W. G., Forney, L. J., & Gottschal, J. C. (2000). Influence of growth rate and starvation on fluorescent in situ hybridization of Rhodopseudomonas palustris. *FEMS Microbiology Ecology*, *32*(3), 205–213. http://doi.org/10.1016/S0168-6496(00)00029-5

Odom, J. M., & Peck, H. D. (1981). Hydrogen cycling as a general mechanism for energy coupling in the sulfate-reducing bacteria, Desulfovibrio sp. *FEMS Microbiology Letters*, *12*, 47–50.

Or, D., Smets, B. F., Wraith, J. M., Dechesne, A., & Friedman, S. P. (2007). Physical constraints affecting bacterial habitats and activity in unsaturated porous media – a review. *Advances in Water Resources*, *30*(6–7), 1505–1527. http://doi.org/10.1016/j.advwatres.2006.05.025

Oremland, R. S., & Taylor, B. F. (1978). Sulfate reduction and methanogenesis in marine sediments. *Geochimica et Cosmochimica Acta*, *42*(2), 209–214. http://doi.org/10.1016/0016-7037(78)90133-3

Pande, S., Kaftan, F., Lang, S., Svatoš, A., Germerodt, S., & Kost, C. (2016). Privatization of cooperative benefits stabilizes mutualistic cross-feeding interactions in spatially structured environments. *The ISME Journal*, *10*(6), 1413–1423.

Pankhania, I. P., Spormann, A. M., Hamilton, W. A., & Thauer, R. K. (1988). Lactate conversion to acetate, CO2 and H2 in cell suspensions of Desulfovibrio vulgaris (Marburg): indications for the involvement of an energy driven reaction. *Archives of Microbiology*, *150*(1), 26–31. http://doi.org/10.1007/BF00409713

Payne, D. E., & Boles, B. R. (2016). Emerging interactions between matrix components during biofilm development. *Current Genetics*, *62*(1), 137–141. http://doi.org/10.1007/s00294-015-0527-5

Payne, R. B., Gentry, D. M., Rapp-Giles, B. J., Casalot, L., & Wall, J. D. (2002). Uranium Reduction by Desulfovibrio desulfuricans Strain G20 and a Cytochrome c3 Mutant. *Applied and Environmental Microbiology*, *68*(6), 3129–3132. http://doi.org/10.1128/AEM.68.6.3129-3132.2002

Peck, H. D. (1960). Evidence for oxidative phosphorylation during the reduction of sulfate with hydrogen by Desulfovibrio desulfuricans. *The Journal of Biological Chemistry*, *235*(9), 2734–2738.

Petersen, J. M., Zielinski, F. U., Pape, T., Seifert, R., Moraru, C., Amann, R., … Dubilier, N. (2011). Hydrogen is an energy source for hydrothermal vent symbioses. *Nature*, *476*(7359), 176–180. http://doi.org/10.1038/nature10325

Plugge, C. M., Scholten, J. C. M., Culley, D. E., Nie, L., Brockman, F. J., & Zhang, W. (2010). Global transcriptomics analysis of the Desulfovibrio vulgaris change from syntrophic growth with Methanosarcina barkeri to sulfidogenic metabolism. *Microbiology*, *156*(Pt 9), 2746–56. http://doi.org/10.1099/mic.0.038539-0

Plugge, C. M., Zhang, W., Scholten, J. C. M., & Stams, A. J. M. (2011). Metabolic Flexibility of Sulfate-Reducing Bacteria. *Frontiers in Microbiology*, *2*(5), 81. http://doi.org/10.3389/fmicb.2011.00081

Postgate, J. R. (1969). Methane as a Minor Product of Pyruvate Metabolism by Sulphate-reducing and Other Bacteria. *Journal of General Microbiology*, *57*(3), 293–302. http://doi.org/10.1099/00221287-57-3-293

Postgate, J. R. (1979). *The Sulphate-Reducing Bacteria*. Cambridge University Press.

Prosser, J. I., Bohannan, B. J. M., Curtis, T. P., Ellis, R. J., Firestone, M. K., Freckleton, R. P., … Young, J. P. W. (2007). The role of ecological theory in microbial ecology. *Nature Reviews Microbiology*, *5*(5), 384–392. http://doi.org/10.1038/nrmicro1643

Qi, Z., Chen, L., & Zhang, W. (2016). Comparison of Transcriptional Heterogeneity of Eight Genes between Batch Desulfovibrio vulgaris Biofilm and Planktonic Culture at a Single-Cell Level. *Frontiers in Microbiology*, *7*(4), 1–14. http://doi.org/10.3389/fmicb.2016.00597

Qi, Z., Pei, G., Chen, L., & Zhang, W. (2014). Single-cell analysis reveals gene-expression heterogeneity in syntrophic dual-culture of Desulfovibrio vulgaris with Methanosarcina barkeri. *Scientific Reports*, *4*, 7478. http://doi.org/10.1038/srep07478

Rabus, R., Hansen, T. A., & Widdel, F. (2013). *The Prokaryotes*. (E. Rosenberg, E. F. DeLong, S. Lory, E. Stackebrandt, & F. Thompson, Eds.). Springer Berlin Heidelberg. http://doi.org/10.1007/978-3-642-30141-4

Rabus, R., Venceslau, S. S., Wohlbrand, L., Voordouw, G., & Wall, J. D. (2015). A Post-Genomic View of the Ecophysiology, Catabolism and Biotechnological Relevance of Sulphate-Reducing Prokaryotes. In R. K. Poole (Ed.), *Advances in Microbial Physiology* (pp. 55–321). Elsevier. Retrieved from https://doi.org/10.1016/bs.ampbs.2015.05.002

Raskin, L., Rittmann, B. E., & Stahl, D. A. (1996). Competition and coexistence of sulfate-reducing and methanogenic populations in anaerobic biofilms. *Applied and Environmental Microbiology*, *62*(10), 3847–57. Retrieved from http://www.pubmedcentral.nih.gov/articlerender.fcgi?artid=1388966&tool=pmcentrez&rendertype=abstract

Ray, A. E., Connon, S. A., Neal, A. L., Fujita, Y., Cummings, D. E., Ingram, J. C., & Magnuson, T. S. (2018). Metal Transformation by a Novel Pelosinus Isolate From a Subsurface Environment. *Frontiers in Microbiology*, *9*(8), 1–12. http://doi.org/10.3389/fmicb.2018.01689

Reysenbach, A. L., Longnecker, K., & Kirshtein, J. (2000). Novel bacterial and archaeal lineages from an in situ growth chamber deployed at a Mid-Atlantic Ridge hydrothermal vent. *Applied and Environmental Microbiology*, *66*(9), 3798–806. http://doi.org/10.1128/AEM.66.9.3798-3806.2000.Updated

Rimbault, A., Niel, P., Virelizier, H., Christian, J., Leluan, G., Niel, I. P., … Etiudes, S. (1988). l-Methionine , a Precursor of Trace Methane in Some Proteolytic Clostridia L-Methionine , Precursor of Trace Methane in Some Proteolytic Clostridia, *54*(6).

Robinson, M. D., McCarthy, D. J., & Smyth, G. K. (2010). edgeR: a Bioconductor package for differential expression analysis of digital gene expression data. *Bioinformatics*, *26*(1), 139–140. http://doi.org/10.1093/bioinformatics/btp616

Schauder, R., Eikmanns, B., Thauer, R. K., Widdel, F., & Fuchs, G. (1986). Acetate oxidation to CO2 in anaerobic bacteria via a novel pathway not involving reactions of the citric acid cycle. *Archives of Microbiology*, *145*(2), 162–172. http://doi.org/10.1007/BF00446775

Schmid, M., Schmitz-Esser, S., Jetten, M., & Wagner, M. (2001). 16S-23S rDNA intergenic spacer and 23S rDNA of anaerobic ammonium-oxidizing bacteria: implications for phylogeny and in situ detection. *Environmental Microbiology*, *3*(7), 450–9. Retrieved from http://www.ncbi.nlm.nih.gov/pubmed/11553235

Schooling, S. R., & Beveridge, T. J. (2006). Membrane Vesicles: an Overlooked Component of the Matrices of Biofilms. *Journal of Bacteriology*, *188*(16), 5945–5957. http://doi.org/10.1128/JB.00257-06

Sela-Adler, M., Ronen, Z., Herut, B., Antler, G., Vigderovich, H., Eckert, W., & Sivan, O. (2017). Co-existence of Methanogenesis and Sulfate Reduction with Common Substrates in Sulfate-Rich Estuarine Sediments. *Frontiers in Microbiology*, *8*(5), 1–11. http://doi.org/10.3389/fmicb.2017.00766

Shcherbakova, V. A., & Vaĭnshteĭn, M. B. (2000). Methane production by the sulfate-reducing bacterium Desulfosarcina variabilis. *Microbiology*, *69*(3), 277–280. Retrieved from http://www.ncbi.nlm.nih.gov/pubmed/10920802

Shen, Y., & Buick, R. (2004). The antiquity of microbial sulfate reduction, *64*, 243–272. http://doi.org/10.1016/S0012-8252(03)00054-0

Shimoyama, T., Kato, S., Ishii, S., & Watanabe, K. (2009). Flagellum Mediates Symbiosis. *Science*, *323*(5921), 1574–1574. http://doi.org/10.1126/science.1170086

Shirtliff, M. E., Mader, J. T., & Camper, A. K. (2002). Molecular interactions in biofilms. *Chemistry and Biology*, *9*(8), 859–871.

Sisler, F. D., & Zobell, C. E. (1951). Hydrogen utilization by some marine sulfate-reducing bacteria. *Journal of Bacteriology*, *62*(1), 117–27. Retrieved from http://www.ncbi.nlm.nih.gov/pubmed/14861165

Stadtman, T. C., & Barker, H. A. (1951). Studies on the methane fermentation. VIII. Tracer experiments of fatty acid oxidation by methane bacteria. *Journal of Bacteriology*, *61*(1), 67–80. Retrieved from http://www.ncbi.nlm.nih.gov/pubmed/14824080

Stahl, D. A., Hillesland, K. L., & Harcombe, W. (2011). Measuring the Costs of Microbial Mutualism. *Microbe Magazine*, *6*(10), 427–434. http://doi.org/10.1128/microbe.6.427.1

Stams, A. J. M., & Plugge, C. M. (2009). Electron transfer in syntrophic communities of anaerobic bacteria and archaea. *Nature Reviews Microbiology*, *7*(8), 568–577. http://doi.org/10.1038/nrmicro2166

Starokadomskyy, P., & Dmytruk, K. V. (2013). A bird's-eye view of autophagy. *Autophagy*, *9*(7), 1121–1126. http://doi.org/10.4161/auto.24544

Stewart, P. S., & Costerton, J. W. (2001). Antibiotic resistance of bacteria in biofilms. *Lancet*, *358*(9276), 135–8. Retrieved from http://www.ncbi.nlm.nih.gov/pubmed/11463434

Stewart, P. S., & Franklin, M. J. (2008). Physiological heterogeneity in biofilms. *Nature Reviews. Microbiology*, *6*(3), 199–210. http://doi.org/10.1038/nrmicro1838

Stoecker, K., Dorninger, C., Daims, H., & Wagner, M. (2010). Double Labeling of Oligonucleotide Probes for Fluorescence In Situ Hybridization (DOPE-FISH) Improves Signal Intensity and Increases rRNA Accessibility. *Applied and Environmental Microbiology*, *76*(3), 922–926. http://doi.org/10.1128/AEM.02456-09

Stryeck, S., Birner-Gruenberger, R., & Madl, T. (2017). Integrative metabolomics as emerging tool to study autophagy regulation. *Microbial Cell*, *4*(8), 240–258. http://doi.org/10.15698/mic2017.08.584

Stylo, M., Neubert, N., Roebbert, Y., Weyer, S., & Bernier-Latmani, R. (2015). Mechanism of Uranium Reduction and Immobilization in Desulfovibrio vulgaris Biofilms. *Environmental Science & Technology*, *49*(17), 10553–10561. http://doi.org/10.1021/acs.est.5b01769

Taniguchi, Y., Choi, P. J., Li, G., Chen, H., Babu, M., Hearn, J., … Xie, X. S. (2010). Quantifying E. coli Proteome and Transcriptome with Single-Molecule Sensitivity in Single Cells. *Most*, *329*(5991), 533–538. http://doi.org/10.1126/science.1188308.

Tasoff, J., Mee, M. T., & Wang, H. H. (2015). An Economic Framework of Microbial Trade. *PLOS ONE*, *10*(7), e0132907. http://doi.org/10.1371/journal.pone.0132907

Teske, A., Dhillon, A., & Sogin, M. L. (2003). Genomic Markers of Ancient Anaerobic Microbial Pathways: Sulfate Reduction, Methanogenesis, and Methane Oxidation. *The Biological Bulletin*, *204*(2), 186–191. http://doi.org/10.2307/1543556

Thauer, R. K. (2012). The Wolfe cycle comes full circle. *Proceedings of the National Academy of Sciences*, *109*(38), 15084–15085. http://doi.org/10.1073/pnas.12131931

Thauer, R. K., Kaster, A.-K., Seedorf, H., Buckel, W., & Hedderich, R. (2008). Methanogenic archaea: ecologically relevant differences in energy conservation. *Nature Reviews. Microbiology*, *6*(8), 579–91. http://doi.org/10.1038/nrmicro1931

Thorgersen, M. P., Lancaster, W. A., Rajeev, L., Ge, X., Vaccaro, B. J., Poole, F. L., … Adams, M. W. W. (2017). A Highly Expressed High-Molecular-Weight S-Layer Complex of Pelosinus sp. Strain UFO1 Binds Uranium. *Applied and Environmental Microbiology*, *83*(4), 1–10. http://doi.org/10.1128/AEM.03044-16

Tomasz, A. (1965). Control of the competent state in pneumococcus by a hormone-like cell product: An example for a new type of regulatory mechanism in bacteria. *Nature*, *208*(5006), 155–159. http://doi.org/10.1038/208155a0

Traore, A. S., Gaudin, C., Hatchikian, C. E., Gall, J. L. E., & Belaich, J. (1983). Energetics of Growth of a Defined Mixed Culture of Desulfovibrio vulgaris and Methanosarcina barkeri: Maintenance Energy Coefficient of the Sulfate-Reducing Organism in the Absence and Presence of Its Partner. *Journal of Bacteriology*, *155*(3), 1260–1264.

Truper, H. (1984). Phototrophic bacteria and their sulfur metabolism. In A. Müller & B. Krebs (Eds.), *Sulfur: its significance for chemistry, for the geo-, bio- and cosmosphere, and technology* (Vol. 5, pp. 351–365). Amsterdam: Elsevier Science.

Tyagi, M., da Fonseca, M. M. R., & de Carvalho, C. C. C. R. (2011). Bioaugmentation and biostimulation strategies to improve the effectiveness of bioremediation processes. *Biodegradation*, *22*(2), 231–241. http://doi.org/10.1007/s10532-010-9394-4

Ueno, Y., Yamada, K., Yoshida, N., Maruyama, S., & Isozaki, Y. (2006). Evidence from fluid inclusions for microbial methanogenesis in the early Archaean era. *Nature*, *440*(7083), 516–519. http://doi.org/10.1038/nature04584

ul Haq, R., & Shakoori, A. R. (1998). Short communication: Microbiological treatment of industrial wastes containing toxic chromium involving successive use of bacteria, yeast and algae. *World Journal of Microbiology and Biotechnology*, *14*(4), 583–585. http://doi.org/10.1023/A:1008849814190

Ungerfeld, E. M., Rust, S. R., Boone, D. R., & Liu, Y. (2004). Effects of several inhibitors on pure cultures of ruminal methanogens. *Journal of Applied Microbiology*, *97*(3), 520–526. http://doi.org/10.1111/j.1365-2672.2004.02330.x

Valls, M., & de Lorenzo, V. (2002). Exploiting the genetic and biochemical capacities of bacteria for the remediation of heavy metal pollution. *FEMS Microbiology Reviews*, *26*(4), 327–338. http://doi.org/10.1111/j.1574-6976.2002.tb00618.x

Voordouw, G. (2002). Carbon Monoxide Cycling by Desulfovibrio vulgaris Hildenborough, *184*(21), 5903–5911. http://doi.org/10.1128/JB.184.21.5903

Wagner, M., Rath, G., Amann, R., Koops, H.-P., & Schleifer, K.-H. (1995). In situ Identification of Ammonia-oxidizing Bacteria. *Systematic and Applied Microbiology*, *18*(2), 251–264. http://doi.org/10.1016/S0723-2020(11)80396-6

Walker, C. B., He, Z., Yang, Z. K., Ringbauer, J. a, He, Q., Zhou, J., … Stahl, D. A. (2009). The electron transfer system of syntrophically grown Desulfovibrio vulgaris. *Journal of Bacteriology*, *191*(18), 5793–801. http://doi.org/10.1128/JB.00356-09

Walker, C. B., Redding-Johanson, A. M., Baidoo, E. E., Rajeev, L., He, Z., Hendrickson, E. L., … Stahl, D. A. (2012). Functional responses of methanogenic archaea to syntrophic growth. *The ISME Journal*, *6*(11), 2045–2055. http://doi.org/10.1038/ismej.2012.60

Wang, G., Li, X., & Wang, Z. (2009). APD2: the updated antimicrobial peptide database and its application in peptide design. *Nucleic Acids Research*, *37*(Database issue), D933-7. http://doi.org/10.1093/nar/gkn823

Wang, G., Li, X., & Wang, Z. (2016). APD3: the antimicrobial peptide database as a tool for research and education. *Nucleic Acids Research*, *44*(D1), D1087-93. http://doi.org/10.1093/nar/gkv1278

Wang, S., Tang, H., Peng, F., Yu, X., Su, H., Xu, P., & Tan, T. (2019). Metabolite-based mutualism enhances hydrogen production in a two-species microbial consortium. *Communications Biology*, *2*(1), 82. http://doi.org/10.1038/s42003-019-0331-8

Wang, Z. (2004). APD: the Antimicrobial Peptide Database. *Nucleic Acids Research*, *32*(90001), 590D–592. http://doi.org/10.1093/nar/gkh025

Weinitschke, S., Denger, K., Cook, A. M., & Smits, T. H. M. (2007). The DUF81 protein TauE in Cupriavidus necator H16, a sulfite exporter in the metabolism of C2 sulfonates. *Microbiology*, *153*(9), 3055–3060. http://doi.org/10.1099/mic.0.2007/009845-0

White, R. H. (1986). Intermediates in the biosynthesis of coenzyme M (2-mercaptoethanesulfonic acid). *Biochemistry*, *25*(18), 5304–5308. http://doi.org/10.1021/bi00366a047

White, R. H. (2017). Identification and Biosynthesis of 1-Mercaptoethanesulfonic Acid (1-MES), an Analogue of Coenzyme M, Found Widely in the Methanogenic Archaea. *Biochemistry*, *56*(46), 6137–6144. http://doi.org/10.1021/acs.biochem.7b00971

Whiteley, M., Diggle, S. P., & Greenberg, E. P. (2017). Progress in and promise of bacterial quorum sensing research. *Nature*, *551*(7680), 313–320. http://doi.org/10.1038/nature24624

Whiteley, M., Lee, K. M., & Greenberg, E. P. (1999). Identification of genes controlled by quorum sensing in Pseudomonas aeruginosa. *Proceedings of the National Academy of Sciences*, *96*(24), 13904–13909. Retrieved from http://www.pnas.org/content/96/24/13904.full%5Cnpapers3://publication/uuid/831AA5C7-E5F1-44A1-914F-4B3548AC317E

Widdel, F. (1988). Microbiology and ecology of sulphate- and sulfur-reducing bacteria. In A. J. B. Zehnder (Ed.), *Biology of Anaerobic Microorganisms* (99th ed., pp. 469–585). New York: Wiley.

Wingett, S. W., & Andrews, S. (2018). FastQ Screen: A tool for multi-genome mapping and quality control. *F1000Research*, *7*(0), 1338. http://doi.org/10.12688/f1000research.15931.1

Wood, G. E., Haydock, A. K., John, A., & Leigh, J. A. (2003). Function and Regulation of the Formate Dehydrogenase Genes of the Methanogenic Archaeon Methanococcus maripaludis Function and Regulation of the Formate Dehydrogenase Genes of the Methanogenic Archaeon Methanococcus maripaludis, *185*(8), 2548–2554. http://doi.org/10.1128/JB.185.8.2548

Wrede, C., Dreier, A., Kokoschka, S., & Hoppert, M. (2012). Archaea in Symbioses. *Archaea*, *2012*, 1–11. http://doi.org/10.1155/2012/596846

Wyndham, R. C., & Costerton, J. W. (1981). Heterotrophic potentials and hydrocarbon biodegradation potentials of sediment microorganisms within the athabasca oil sands deposit. *Applied and Environmental Microbiology*, *41*(3), 783–90. Retrieved from http://www.pubmedcentral.nih.gov/articlerender.fcgi?artid=243775&tool=pmcentrez&rendertype=abstract

Ye, D., Quensen, J. F. I., Tiedje, J. M., & Boyd, S. A. (1999). 2-Bromoethanesulfonate, Sulfate, Molybdate, and Ethanesulfonate Inhibit Anaerobic Dechlorination of Polychlorobiphenyls by Pasteurized Microorganisms. Society, 65(1), 327–329. Retrieved from https://aem.asm.org/content/65/1/327

Yvon-Durocher, G., Allen, A. P., Bastviken, D., Conrad, R., Gudasz, C., St-Pierre, A., … del Giorgio, P. A. (2014). Methane fluxes show consistent temperature dependence across microbial to ecosystem scales. *Nature*, *507*(7493), 488–491. http://doi.org/10.1038/nature13164

Zelezniak, A., Andrejev, S., Ponomarova, O., & Mende, D. R. (2015). Metabolic dependencies drive species co-occurrence in diverse microbial communities. *Proceedings of the National Academy of Sciences*, *112*(20), 201522642. http://doi.org/10.1073/pnas.1522642113

Zhang, W., Li, F., & Nie, L. (2010). Integrating multiple ' omics ' analysis for microbial biology : application and methodologies. *Microbiology*, *156*, 287–301. http://doi.org/10.1099/mic.0.034793-0

Zinder, S. H., Anguish, T., & Cardwell, S. C. (1984). Selective inhibition by 2-bromoethanesulfonate of methanogenesis from acetate in a thermophilic anaerobic digestor. *Applied and Environmental Microbiology*, *47*(6), 1343–5. Retrieved from http://www.ncbi.nlm.nih.gov/pubmed/16346572

APPENDICES

APPENDIX A

METHANE PRODUCTION IN PELOSINUS FERMENTANS JBW45

Contribution of Authors and Co-Authors

Manuscript in Appendix A

Author: Laura B. Camilleri

Contributions: Developed experimental design, performed experiments, analyzed data, wrote and revised the manuscript.

Co-Author: Matthew W. Fields

Contributions: Developed experimental design, analyzed data, wrote and revised the manuscript.

Manuscript Information

Laura B. Camilleri and M.W. Fields

Letters in Applied Microbiology

Status of Manuscript:
__x__ Prepared for submission to a peer-reviewed journal
_____ Officially submitted to a peer-reviewed journal
_____ Accepted by a peer-reviewed journal
_____ Published in a peer-reviewed journal

ABSTRACT

Many contaminated heavy metal or chlorinated solvent subsurface sites have been stimulated for sulfate-reducing bacteria due to their widely documented ability to immobilize toxic metals and function in bioremediation. However, multiple locations that have undergone nutrient addition *in situ* have reported prominent members of the microbial communities belonging to the *Pelosinus* spp. This presents a challenge for stimulation in the environment as it can lead to enrichment of untargeted organisms that may counteract bioremediation efforts. Similar to other reports, after a polylactate compound was used to stimulate microbial populations within the chromium contaminated Hanford Nuclear Reservation 100-H site, *Pelosinus* spp. were found to increase in relative abundance. Enrichments recovered the isolate *Pelosinus fermentans* JBW45, a strictly anaerobic isolate that seemed to outcompete sulfate-reducing bacteria under the tested conditions. *P. fermentans* JBW45 belongs to a poorly characterized genus of fermentative bacteria that appear to have widespread ecological implications. Other reported isolates have been found to function in Fe(III) reduction, and *Pelosinus* sp. strain UFO1 has been recently documented to bind uranium. The genome sequence for this isolate was previously reported; here we detail some of *P. fermentans* JBW45 metabolic characteristics. Fermentative growth of *P. fermentans* was observed on glycerol, fructose, glucose, sucrose, lactate, and pyruvate. This bacterium also demonstrated unexpected physiologies such as hydrogen and methane production depending on the fermented carbon source. Methanogenic contaminants were ruled out by PCR, and no homologies were found for central genes to existing methanogenesis pathways. Based upon previous reports, it appears that *Pelosinus fermentans* JBW45 functions as a "mini-methane" producer under nutrient limiting conditions.

.

INTRODUCTION

Advances in technology have allowed insight into metabolic potential of organisms as well as the range of community members present in various environments, some of which we can harness for genetic and biochemical exploitation (Valls & de Lorenzo, 2002). In addition to numerous industrial applications, microorganisms can be used to remediate sites contaminated with heavy metals such as Cr(VI), a highly toxic and carcinogenic metal (Costa & Klein, 2006). Microbial ecosystems are comprised of vast and complex biogeochemistry. Bioremediation efforts favor *in situ* methods for immobilization through the use of remediating bacteria since it is considered to be more cost effective (Tyagi et al., 2011). Remediation of heavy metals can include biosorption by the cellular mass, active transport, entrapment into cellular capsules, precipitation, and oxidation-reduction reactions (Bhide et al., 1996; Brady & Duncan, 1994; Gadd, 1990; Gadd & White, 1993; Kratochvil & Volesky, 1998; ul Haq & Shakoori, 1998). The capability of microorganisms to carry out certain metabolic strategies allows for the development of new approaches to influence ecosystems.

Pelosinus fermentans JBW45 is a previously reported anaerobic bacterial isolate obtained from Cr(VI)-contaminated groundwater at the Hanford Nuclear Reservation 100-H site (Washington, USA) after stimulation with a polylactate compound (Bowen De León et al., 2012, 2015). Enrichment at this site was specifically directed toward sulfate-reducing bacteria due to their ability to reduce heavy metals (*e.g.,* chromium), however, the predominant population observed was determined to belong to *Pelosinus* spp. This observation has been described for many other contaminated sites (Beller et al., 2013; Brown et al., 2012, 2014; Krzmarzick et al., 2014; Moe et al., 2012). Other *Pelosinus fermentans* strains have demonstrated various heavy metal-reducing characteristics, therefore further physiological characterization was investigated for the isolate *P. fermentans* str. JBW45 (Ray et al., 2018; Thorgersen et al., 2017).

MATERIALS AND METHODS

Culture Conditions

Pelosinus fermentans JBW45 was anaerobically cultured in standard lactate-sulfate media (LS4D) with 60 mM sodium lactate and 30 mM sodium sulfate in Balch tubes or serum bottles with N_2 headspace. Modified LS4D media (4D) withheld the lactate and sulfate in order to add alternative electron donors and acceptors at varying concentrations (Clark et al., 2006). The bicarbonate buffered co-culture medium (CCM) with 30 mM lactate and 80% N_2:20% CO_2 headspace was also used for cultivation and modified similarly without lactate addition to test alternative electron donors and acceptors (Walker et al., 2009). H_2 addition was accomplished with pressurization to 200 kPa with 80% H_2:20% CO_2. Sterile anaerobic stock solutions were prepared for various electron donors and acceptors in concentrations that allowed for uniform volume amendments to the different test culture conditions. The following substrates were tested: 2 and 10 mM Sodium Acetate, 20 mM Sodium Formate, 10 mM Sodium Lactate, 5 mM Sodium Sulfate, 8 mM Sodium Nitrate, 10 mM Fructose, 10 mM Glucose, 10 mM

Sucrose, 10 mM Sodium Pyruvate, 10 mM Methionine, 10 mM Methanethiol, 10 mM Dimethyl Sulfide (DMS), 10 mM Dimethyl Disulfide (DMDS), 5 µM Methylphosphonate, 5 mM Bromoethanesulfonate (BES), 258 and 6.5 mM Glycerol. The cultures were grown at more environmentally relevant temperatures of 23°C in the dark. Growth curves were acquired by recording optical density readings (600 nm) on a tube Spectronic 20D+ (Thermo Fisher Scientific).

Cell Imaging

Planktonic samples were collected and fixed in 2% formaldehyde (final concentration) and stained with 0.3 g/L Acridine Orange as described (Brileya et al., 2014). Traditional Gram staining and spore staining were also conducted. Fluorescence *in situ* hybridization was performed on planktonic cultures. Samples were fixed in 4% paraformaldehyde for 3 hours at 4°C, then 10 µL was placed into a well on a Teflon coated slide (Paul Marienfeld GmbH & Co. KG, Lauda-Königshofen, Germany). The sample was dehydrated and hybridized in buffer solution containing 180 µL 5 M NaCl, 20 µL1 M Tris HCl, 449 µL double deionized (dd) H_2O, 1 µL 10% SDS and 350 µL deionized formamide (final concentration 35%) with 3 ng each of probes EUB338 (GCT GCC TCC CGT AGG AGT) double labeled with Cy3, and ARCH915 (GTG CTC CCC CGC CAA TTC CT) double labeled with Cy5, for 4 hours at 46°C in a humid chamber (Stoecker et al., 2010). Samples were washed in prewarmed washing buffer containing 700 µL 5 M NaCl, 1 mL 1 M Tris HCl, 500 µL 0.5 M EDTA, and raised to 50 mL with ddH2O, at 47°C for 10 min, then dipped in ice cold ddH2O and quickly dried with compressed air. Samples were mounted with Citifluor AF1 antifadent (Citifluor Ltd., Leicester, UK) for imaging using a Leica TCS SP5 II inverted confocal laser scanning microscope with 488, 561, and 633 nm lasers and appropriate filter sets for Cy3 and Cy5.

Electron Microscopy

The Zeiss Supra55VP FE-SEM was used to image samples of *P. fermentans* JBW45. The samples were fixed in 2% paraformaldehyde, 2.5% glutaraldehyde and 0.05 M Na-cacodylate overnight at room temperature. Samples were dehydrated in increasing amounts of ethanol (25%, 50%, 75%, 95%, 100% ethanol) for 20 minutes each. The samples were mounted on stubs with double-sided carbon tape and viewed at 1.0 kV.

Gas Chromatography

Gas analysis was conducted with a 490microGC (Agilent Technologies, Inc., Santa Clara, CA, USA) containing dual channels and thermal conductivity detectors. Helium carrier gas was used for the 10 m Molsieve5A and PoraplotQ columns at 145 kPa and 80°C with injectors at 110°C and the heated sample line at 40°C. Samples were collected from the headspace and manually injected for analysis.

Polymerase Chain Reaction

DNA was extracted from *P. fermentans* JBW45 using the Wizard® Genomic DNA Purification Kit (Promega Corporation, Madison, WI, USA) as per manufacturer protocol for Gram positive and negative bacteria with the recommended lysis using 10 mg/mL lysozyme. DNA concentrations were determined using the Qubit® dsDNA BR Assay Kit and fluorometer (Life Technologies, Carlsbad, California, USA). PCR amplification was performed with primers McrA Forward (5’GGTGGTGTMGGATTCACACARTAYGCWACAGC-3’) and McrA Reverse (5’TTCATTGCRTAGTTWGGRTAGTT-3’) (Luton et al., 2002), and Archaeal 16S 21F (5’-TTCYGGTTGATCCYGCCRGA-3’), and Archaeal 16S 1492R (5’-CGGTTACCTTGTTACGACTT-3’) (Baker et al., 2003). PCR cycles were optimized to minimize PCR-induced artifacts. Each 20 µL PCR reaction mixture contained 50 mM KCl, 10 mM Tris–HCl pH 9.0 and 0.1% Triton X-100, 1.8 mM $MgCl_2$, 80 ng bovine serum albumin, 0.25 mM 4 × dNTPs, 10 pmol each primer, 2.5 U Taq polymerase, and 1 µl purified DNA (5–10 ng) (Fields et al., 2005). The PCR parameters for the McrA primers were as follows: 95°C for 2 min; 95°C for 30 s, 54°C for 30 s, 72°C for 30 s, 30 cycles; 72°C for 5 min. The PCR parameters for the Archaeal 16S primers were as follows: 94°C for 5 min; 94°C for 30 s, 52°C for 30 s, 72°C for 2 min, 30 cycles; 72°C for 7 min. PCR products were analyzed on 0.8% (w/v) TAE agarose gels.

Gas Chromatography – Mass Spectrometry

Methane production was tested by cultivating *P. fermentans* JBW45 with 13% $^{13}CO_2$ in the headspace (99%, Cambridge Isotope Laboratories, Inc., MA) and incubating for 100 hours. The headspace was sampled and 100 µL was manually injected onto Agilent 6890 GC 5973 electron impact ionization mass selective detector (Agilent Technologies, Palo Alto, CA, USA) interfaced with Agilent Enhanced ChemStation software and operated in scan mode. A GS-Carbonplot column (60 m × 0.320 mm i.d. × 1.50 μm film thickness) was used for analysis. The following parameters were used: 100 μL manual injection with 30:1 split ratio, constant flow at 1 mL/min, injector temperature 185ºC, constant interface temperature 60ºC, and scan range m/z 2-100. The carrier gas was ultra-high purity helium. The areas obtained from extracted ion chromatograms were used for analysis. For methane, m/z = 16 and 17 were used. For CO_2, m/z = 44 and 45 were used for deconvolution. Standards were run and analyzed to deconvolute this data for the determination of the fraction of ^{13}C in CH_4 and CO_2.

RESULTS

Pelosinus fermentans JBW45 is a strictly anaerobic bacillus with a fermentative metabolism (Figure 1 and 2). It stained Gram-variable and was found to produce spores (data not shown). Growth was originally observed without deference to substrate concentration. Further investigation revealed that *P. fermentans* JBW45 was using the residual glycerol from the freezer stock to support its growth (Figure 3). Subsequent growth measurements were properly passaged so that the maximum amount of glycerol carried over would be 1.49 g/L. *P. fermentans* grew with a doubling time of 4-12 hours on fructose, glucose, sucrose, and pyruvate (Figure 4). Growth also proceeded on lactate with and without nitrate present, however no growth was observed with lactate and sulfate (Figure 5). The culture was unable to grow aerobically or anaerobically with acetate even if formate was added (Figure 6).

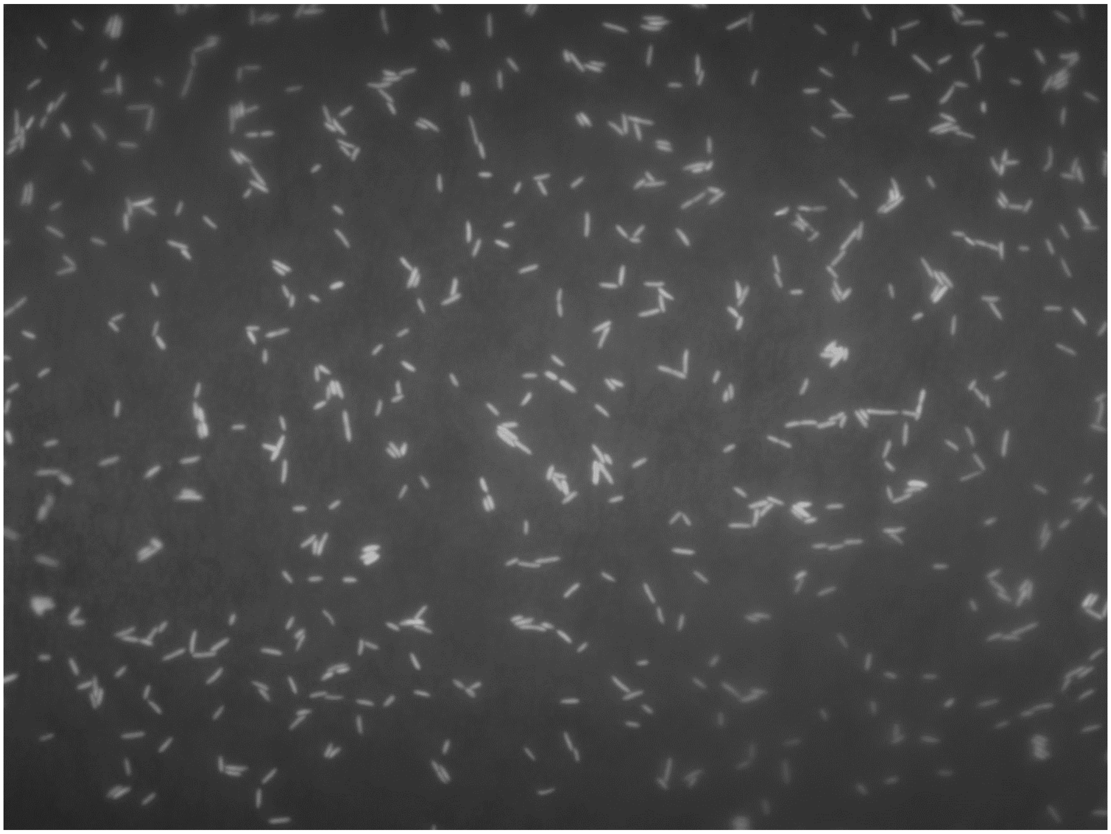

Figure 1. Acridine orange stained *P. fermentans* JBW45 rod shaped cells imaged on a Nikon Eclipse E-800 epi-fluorescent microscope (100x). Cells were measured to be 2-3 µm long.

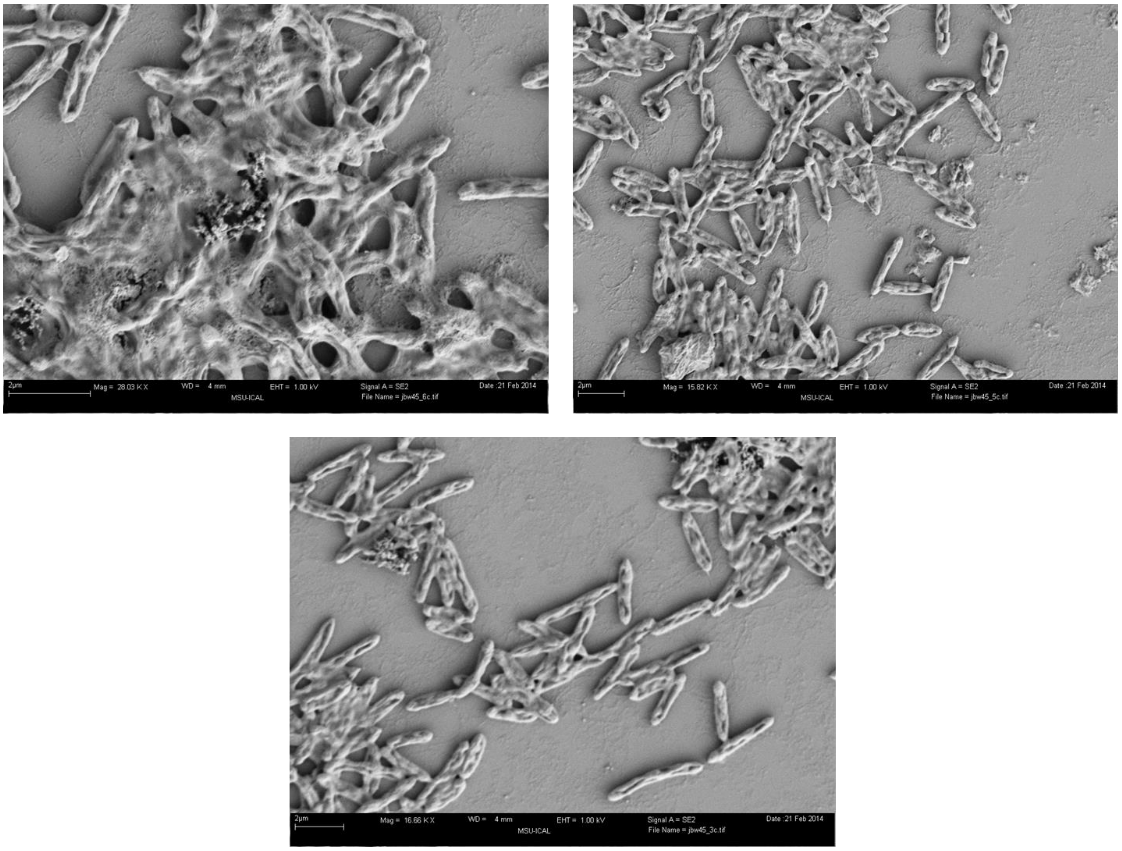
2µm
Mag = 28.03 K X
WD = 4 mm
EHT = 1.00 kV
Signal A = SE2
Date :21 Feb 2014
MSU-ICAL
File Name = jbw45_6c.tif
2µm
Mag = 15.82 K X
WD = 4 mm
EHT = 1.00 kV
Signal A = SE2
Date :21 Feb 2014
MSU-ICAL
File Name = jbw45_5c.tif
2µm
Mag = 16.66 K X
WD = 4 mm
EHT = 1.00 kV
Signal A = SE2
Date :21 Feb 2014
MSU-ICAL
File Name = jbw45_3c.tif

Figure 2. Field Emission Scanning Electron Microscope image of *P. fermentans* JBW45 grown in CCM with lactate. Extracellular polymeric substances (EPS) appear to be surrounding the cells and round intracellular nodules are likely spores.

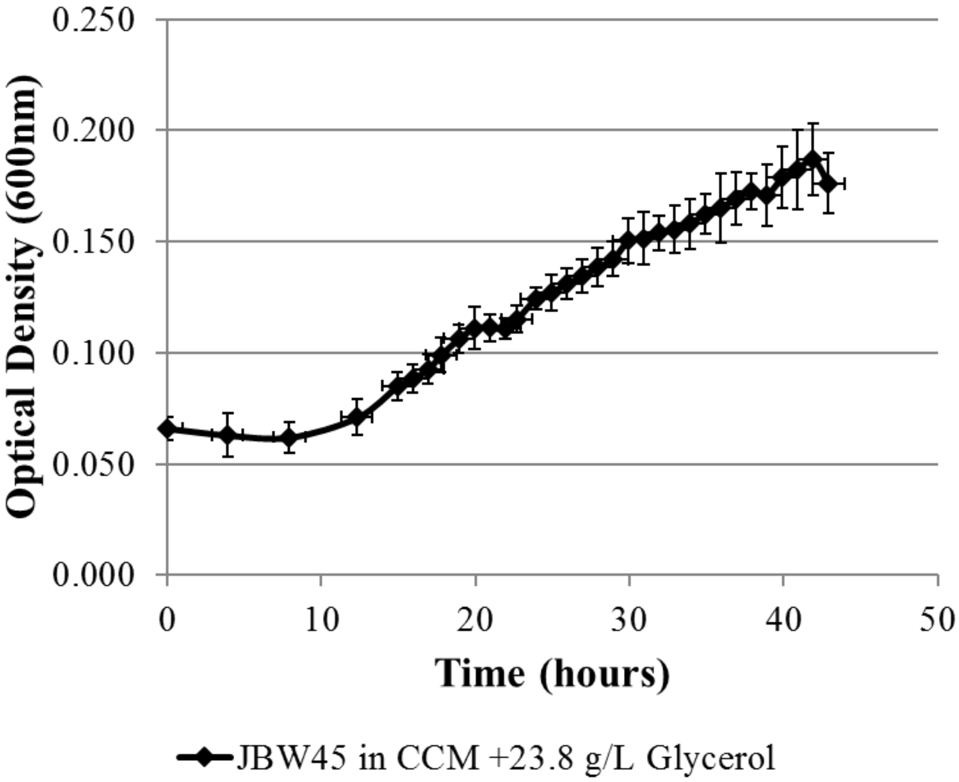

Figure 3. *Pelosinus fermentans* JBW45 was shown to grow to a maximum optical density (600 nm) of 0.182 with 0.258 M glycerol.

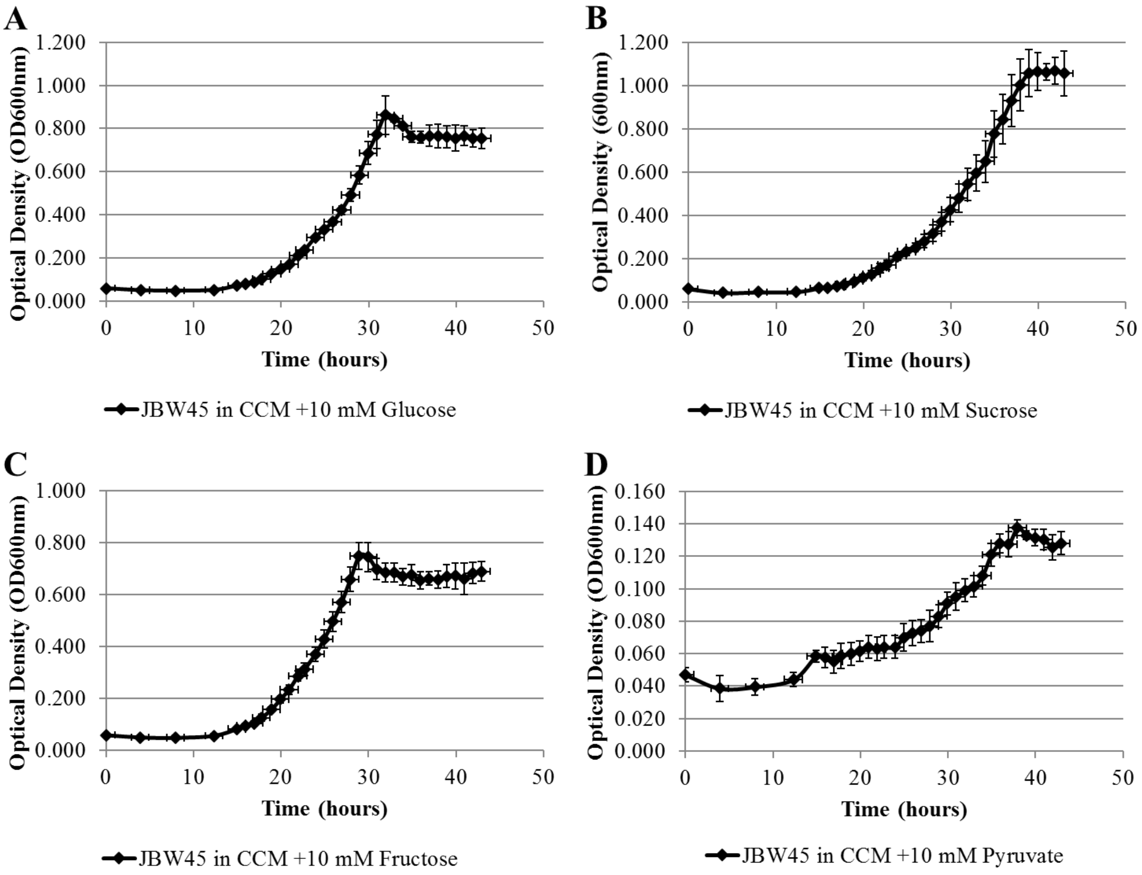

Figure 4. *Pelosinus fermentans* JBW45 anaerobic growth utilizing absorbance readings (600 nm) over time on (A) 10 mM glucose, (B) 10 mM sucrose, (C) 10 mM fructose, and (D) 10 mM pyruvate.

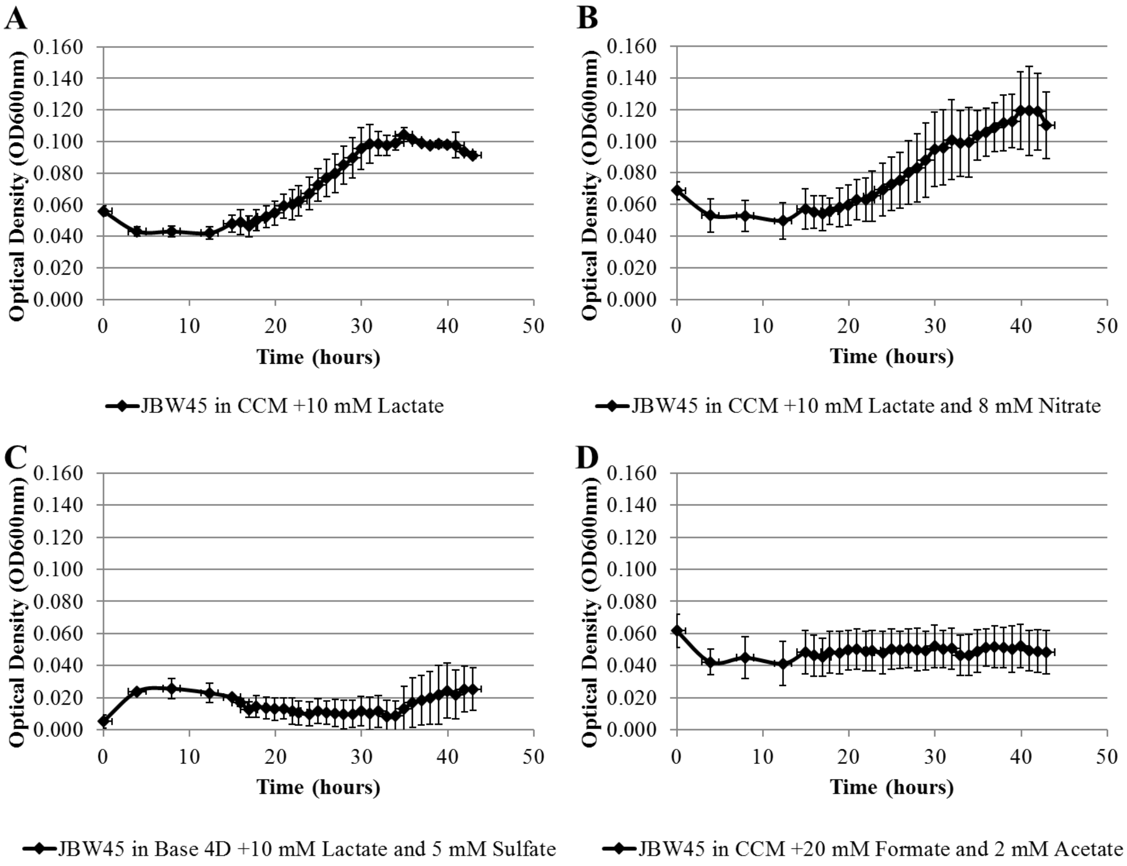

Figure 5. *Pelosinus fermentans* JBW45 growth utilizing absorbance readings (600 nm) over time on (A) 10 mM lactate and (B) 10 mM lactate and 8 mM nitrate, but did not grow on (C) 10 mM lactate and 5 mM sulfate, or (D) 20 mM formate and 2 mM acetate.

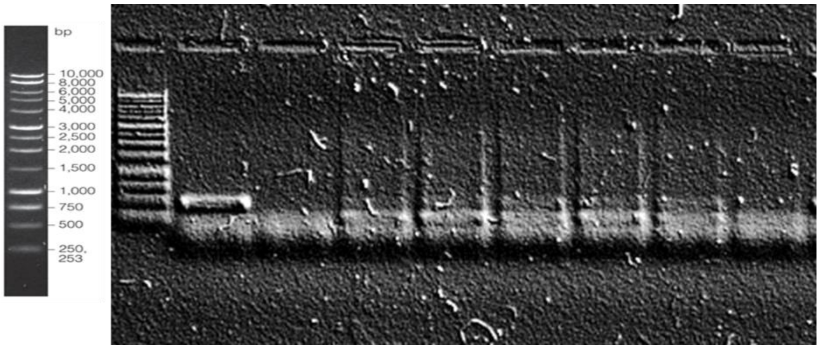
bp
10,000
8,000
6,000
5,000
4,000
3,000
2,500
2,000
1,500
1,000
750
500
250,
253

Figure 6. Gel electrophoresis image of *P. fermentans* JBW45 grown with different carbon sources and amplified using PCR primer McrA to detect archaeal contaminants and/or presence of the methanogenesis gene, Methyl Coenzyme M reductase A. Lanes from left to right: hyperladder, positive control with expected 500 bp band, negative no template control, *P. fermentans* JBW45 in CCM-Lactate, *P. fermentans* JBW45 in CCM-Pyruvate, *P. fermentans* JBW45 in CCM-Acetate+BES, *P. fermentans* JBW45 in CCM-Fructose, *P. fermentans* JBW45 in CCM- no carbon, *P. fermentans* JBW45 in CCM-Acetate.

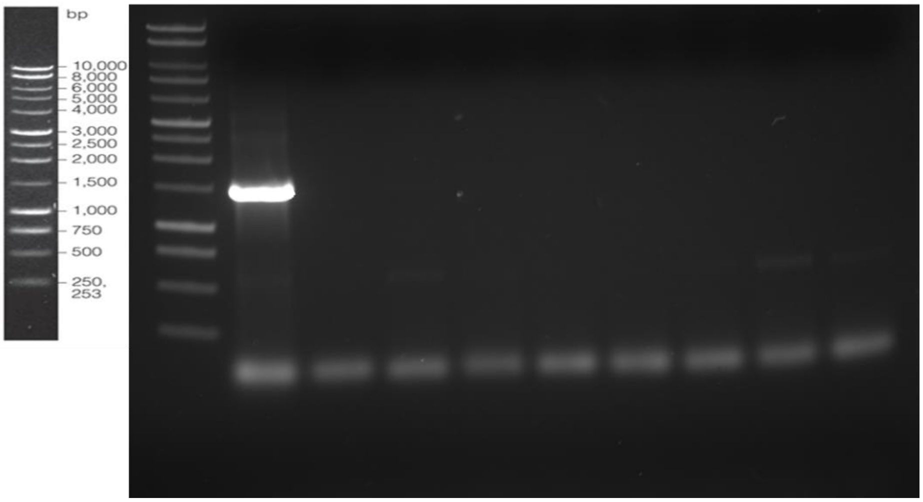
bp
10,000
8,000
6,000
5,000
4,000
3,000
2,500
2,000
1,500
1,000
750
500
250,
253

Figure 7. Gel electrophoresis image of *P. fermentans* JBW45 grown with different carbon sources (in triplicate) and amplified using PCR primer Arch30 to detect archaeal contaminants. Lanes from left to right: hyperladder, positive control with expected 1500 bp band, negative no template control, *P. fermentans* JBW45 4D+Fructose, *P. fermentans* JBW45 CCM-A, *P. fermentans* JBW45 CCM-B, *P. fermentans* JBW45 CCM-C, *P. fermentans* JBW45 Pyruvate-A, *P. fermentans* JBW45 Pyruvate-B, *P. fermentans* JBW45 Pyruvate-C.

Routine incubations would sometimes result in the stoppers bulging, therefore the headspace was analyzed and H_2 was detected. Headspace analysis was performed routinely and revealed the capacity for *P. fermentans* JBW45 to produce methane (observed from 0.01% to 10%) in addition to hydrogen depending upon the growth conditions (Figure S1). Interestingly, it was observed that methane accumulated in the headspace under nutrient limiting conditions. The methane producing cultures were subsequently harvested for DNA extraction and tested for archaeal contamination with primers for the methyl coenzyme M reductase gene (McrA) (Figure 7) and a conserved archaeal 16S region (Figure 8). The PCR protocol was optimized to prevent artifacts, and both sets of primers showed no products of the target size in the samples. Fluorescence *in situ* hybridization was also carried out on the culture and no affinity for the archaeal FISH probe (ARCH915) was demonstrated (Figure 9). To further explore the potential for methanogenesis, *P. fermentans* JBW45 was grown with an over-pressurization of H_2 and an added 13% $^{13}CO_2$ in the headspace. After the incubation, samples from the headspace were analyzed using GC-MS. Preliminary analysis revealed ion peaks at m/z of 16, 17, 44, and 45 which correlates with CH_4, $^{13}CH_4$, CO_2, and $^{13}CO_2$ respectively (Figure S2). In an effort to stimulate methane production, a variety of conditions were tested. *P. fermentans* JBW45 could not grow with acetate and H_2, or H_2 alone, or with lactate and methionine, or methionine alone (Figure S3). Additionally, dimethyl sulfide, dimethyl disulfide, and methanethiol could not support growth (data not shown), however methylphosphonate resulted in growth but not methane production under the tested conditions (Figure S4). The culture was also grown in the presence of BES, a known hydrogenotrophic methanogen inhibitor, and while no methane was recovered in the headspace, growth still occurred (Figure S5).

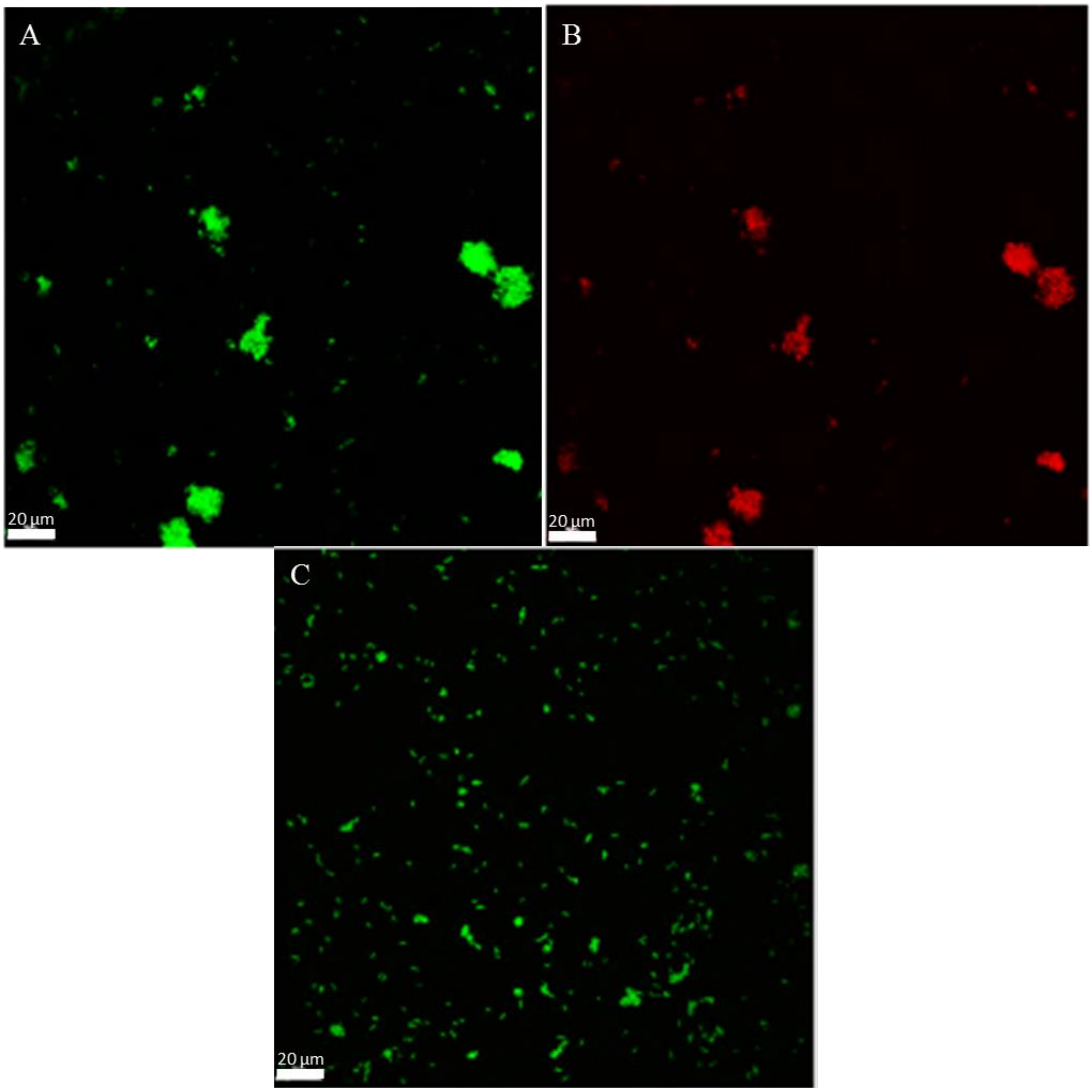

Figure 8. Confocal image of *P. fermentans* JBW45 and a control using FISH probes EUB338 (Green) and ARCH915 (Red). (A) A positive control containing sites for both probes is shown demonstrating EUB338 probe presence as well as (B) ARCH915 positive control. (C) An overlay of both channels representing EUB338 (Green) and ARCH915 (Red) in *P. fermentans* JBW45 is shown clearly demonstrating no ARCH915 signal.

Bioinformatic analysis revealed the capacity for heavy metal tolerance as supported by the presence of chromate transporters, arsenic related genes, and cytochrome c genes (Table 1). There are also numerous hydrogenase, ferredoxin, flavoprotein, and pyruvate-formate lyase genes. The predicted annotations also show sulfate permeases, sulfite transporters and reductases, sporulation proteins, lactate permease and dehydrogenases, nitrate transporters, nitrogenases, and glycerol uptake genes in addition to multiple antimicrobial related proteins.

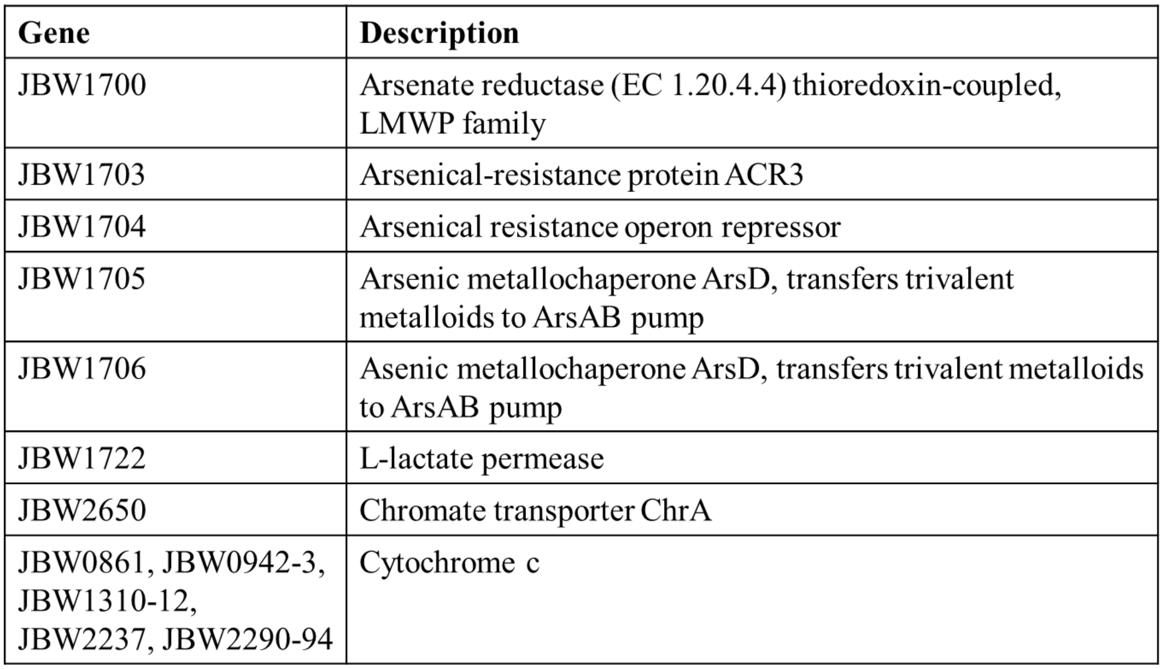

Gene	**Description**
JBW1700	Arsenate reductase (EC 1.20.4.4) thioredoxin-coupled, LMWP family
JBW1703	Arsenical-resistance protein ACR3
JBW1704	Arsenical resistance operon repressor
JBW1705	Arsenic metallochaperone ArsD, transfers trivalent metalloids to ArsAB pump
JBW1706	Asenic metallochaperone ArsD, transfers trivalent metalloids to ArsAB pump
JBW1722	L-lactate permease
JBW2650	Chromate transporter ChrA
JBW0861, JBW0942-3, JBW1310-12, JBW2237, JBW2290-94	Cytochrome c

Table 1. *Pelosinus fermentans* JBW45 gene annotations for heavy metal tolerance as supported by the presence of chromate transporters, arsenic related genes, and cytochrome c genes.

DISCUSSION

The purpose of this project was to analyze the predominant environmental field isolate from Hanford, Washington, after stimulation with a polylactate compound in order to characterize the isolate's physiology and determine how it may influence the ecosystem. The most unexpected discovery with the physiology of *Pelosinus fermentans* JBW45 was the production of methane gas. The ability of sulfate reducing bacteria (SRB) to produce methane has been described since 1951 and has been a source of skepticism due to the difficulty for reproducibility (Postgate, 1969; Sisler & Zobell, 1951). Methanogenic archaea are known to associate with sulfate reducing bacteria and the first response is to regard the results as products of contamination (Stadtman & Barker, 1951). The molecular methods utilized here have ruled out the likelihood of a methanogenic contaminant and lend support to *P. fermentans* JBW45 producing methane on its own.

Unlike what was reported by Postgate in 1969, pyruvate did not yield higher methane concentrations. Instead, only surplus amounts of hydrogen were detected in the headspace. However, there have been reports of SRB with CO dehydrogenase genes forming methane during acetate oxidation to CO_2 via the C_1-pathway (Schauder et al., 1986). Furthermore, mini-methane production was shown to be stimulated by substrate deficiency and incubations beyond 168 hours (Shcherbakova & Vaĭnshteĭn, 2000). *P. fermentans* has a predicted CO dehydrogenase gene (JBW4427-8) and more methane was observed in cultures that were incubated beyond 100 hours (data not shown) which is consistent with previous reports for SRB. The role that *Pelosinus* spp. and sulfate reducing bacteria play in contributing to methane production within ecosystems should be given attention as variation among strains may be capable of producing levels of CH_4 that go beyond what is consistent for mini-methanogenesis.

With advances in molecular technology central dogmas within microbiology are being challenged. Methanogenesis is no longer reserved for only the methanogenic archaea but has also been reported in fungi (Lenhart et al., 2012), and could indicate a metabolic link between domains (Rabus et al., 2013). This data is also significant for consideration of future bioremediation efforts. While *P. fermentans* JBW45 appears to have the metabolic capacity to reduce heavy metals, stimulation efforts utilizing amendments must consider the role ecological competition has on the desired outcome.

Acknowledgments. This material by ENIGMA- Ecosystems and Networks Integrated with Genes and Molecular Assemblies (http://enigma.lbl.gov), a Scientific Focus Area Program at Lawrence Berkeley National Laboratory is based upon work supported by the U.S. Department of Energy, Office of Science, Office of Biological & Environmental Research under contract number DE-AC02-05CH11231.

REFERENCES CITED

Baker, G. C., Smith, J. J., & Cowan, D. A. (2003). Review and re-analysis of domain-specific 16S primers. *Journal of Microbiological Methods*, *55*(3), 541–555. http://doi.org/10.1016/j.mimet.2003.08.009

Beller, H. R., Han, R., Karaoz, U., Lim, H., & Brodie, E. L. (2013). Genomic and Physiological Characterization of the Chromate-Reducing, Aquifer-Derived Firmicute Pelosinus sp. Strain HCF1. *Applied and Environmental Microbiology*, *79*(1), 63–73. http://doi.org/10.1128/AEM.02496-12

Bhide, J. V., Dhakephalkar, P. K., & Paknikar, K. M. (1996). Microbiological process for the removal of Cr(VI) from chromate-bearing cooling tower effluent. *Biotechnology Letters*, *18*(6), 667–672. http://doi.org/10.1007/BF00130763

Bowen De León, K., Utturkar, S. M., Camilleri, L. B., Elias, D. A., Arkin, A. P., Fields, M. W., … Wall, J. D. (2015). Complete Genome Sequence of Pelosinus fermentans JBW45, a Member of a Remarkably Competitive Group of Negativicutes in the Firmicutes Phylum. *Genome Announcements*, *3*(5), 3–4. http://doi.org/10.1128/genomeA.01090-15

Bowen De León, K., Young, M. L., Camilleri, L. B., Brown, S. D., Skerker, J. M., Deutschbauer, A. M., … Fields, M. W. (2012). Draft Genome Sequence of Pelosinus fermentans JBW45, Isolated during In Situ Stimulation for Cr(VI) Reduction. *Journal of Bacteriology*, *194*(19), 5456–5457. http://doi.org/10.1128/JB.01224-12

Brady, D., & Duncan, J. R. (1994). Bioaccumulation of metal cations by Saccharomyces cerevisiae. *Applied Microbiology and Biotechnology*, *41*(1), 149–154. http://doi.org/10.1007/s002530050123

Brileya, K. A., Camilleri, L. B., Zane, G. M., Wall, J. D., & Fields, M. W. (2014). Biofilm growth mode promotes maximum carrying capacity and community stability during product inhibition syntrophy. *Frontiers in Microbiology*, *5*(12), 693. http://doi.org/10.3389/fmicb.2014.00693

Brown, S. D., Podar, M., Klingeman, D. M., Johnson, C. M., Yang, Z. K., Utturkar, S. M., … Elias, D. A. (2012). Draft Genome Sequences for Two Metal-Reducing Pelosinus fermentans Strains Isolated from a Cr(VI)-Contaminated Site and for Type Strain R7. *Journal of Bacteriology*, *194*(18), 5147–5148. http://doi.org/10.1128/JB.01174-12

Brown, S. D., Utturkar, S. M., Magnuson, T. S., Ray, A. E., Poole, F. L., Lancaster, W. A., … Elias, D. A. (2014). Complete Genome Sequence of Pelosinus sp. Strain UFO1 Assembled Using Single-Molecule Real-Time DNA Sequencing Technology. *Genome Announcements*, *2*(5), 2–3. http://doi.org/10.1128/genomeA.00881-14

Clark, M. E., He, Q., He, Z., Huang, K. H., Alm, E. J., Wan, X.-F., … Fields, M. W. (2006). Temporal transcriptomic analysis as Desulfovibrio vulgaris Hildenborough transitions into stationary phase during electron donor depletion. *Applied and Environmental Microbiology*, *72*(8), 5578–88. http://doi.org/10.1128/AEM.00284-06

Costa, M., & Klein, C. B. (2006). Toxicity and Carcinogenicity of Chromium Compounds in Humans. *Critical Reviews in Toxicology*, *36*(2), 155–163. http://doi.org/10.1080/10408440500534032

Fields, M. W., Yan, T., Rhee, S., Carroll, S. L., Jardine, P. M., Watson, D. B., … Zhou, J. (2005). Impacts on microbial communities and cultivable isolates from groundwater contaminated with high levels of nitric acid - uranium waste. *FEMS Microbiology Ecology*, *53*(3), 417–428. http://doi.org/10.1016/j.femsec.2005.01.010

Gadd, G. M. (1990). Heavy metal accumulation by bacteria and other microorganisms. *Experientia*, *46*(8), 834–840. http://doi.org/10.1007/BF01935534

Gadd, G. M., & White, C. (1993). Microbial treatment of metal pollution - a working biotechnology? *Trends in Biotechnology*, *11*(8), 353–359. http://doi.org/10.1016/0167-7799(93)90158-6

Kratochvil, D., & Volesky, B. (1998). Advances in the biosorption of heavy metals. *Trends in Biotechnology*, *16*(7), 291–300. http://doi.org/10.1016/S0167-7799(98)01218-9

Krzmarzick, M. J., Miller, H. R., Yan, T., & Novak, P. J. (2014). Novel Firmicutes Group Implicated in the Dechlorination of Two Chlorinated Xanthones, Analogues of Natural Organochlorines. *Applied and Environmental Microbiology*, *80*(3), 1210–1218. http://doi.org/10.1128/AEM.03472-13

Lenhart, K., Bunge, M., Ratering, S., Neu, T. R., Schüttmann, I., Greule, M., … Keppler, F. (2012). Evidence for methane production by saprotrophic fungi. *Nature Communications*, *3*, 1046. http://doi.org/10.1038/ncomms2049

Luton, P. E., Wayne, J. M., Sharp, R. J., & Riley, P. W. (2002). The mcrA gene as an alternative to 16S rRNA in the phylogenetic analysis of methanogen populations in landfill. *Microbiology*, *148*(11), 3521–30. http://doi.org/10.1099/00221287-148-11-3521

Moe, W. M., Stebbing, R. E., Rao, J. U., Bowman, K. S., Nobre, M. F., da Costa, M. S., & Rainey, F. a. (2012). Pelosinus defluvii sp. nov., isolated from chlorinated solvent-contaminated groundwater, emended description of the genus Pelosinus and transfer of Sporotalea propionica to Pelosinus propionicus comb. nov. *International Journal of Systematic and Evolutionary Microbiology*, *62*(Pt 6), 1369–76. http://doi.org/10.1099/ijs.0.033753-0

Postgate, J. R. (1969). Methane as a Minor Product of Pyruvate Metabolism by Sulphate-reducing and Other Bacteria. *Journal of General Microbiology*, *57*(3), 293–302. http://doi.org/10.1099/00221287-57-3-293

Rabus, R., Hansen, T. A., & Widdel, F. (2013). *The Prokaryotes*. (E. Rosenberg, E. F. DeLong, S. Lory, E. Stackebrandt, & F. Thompson, Eds.). Springer Berlin Heidelberg. http://doi.org/10.1007/978-3-642-30141-4

Ray, A. E., Connon, S. A., Neal, A. L., Fujita, Y., Cummings, D. E., Ingram, J. C., & Magnuson, T. S. (2018). Metal Transformation by a Novel Pelosinus Isolate From a Subsurface Environment. *Frontiers in Microbiology*, *9*(8), 1–12. http://doi.org/10.3389/fmicb.2018.01689

Schauder, R., Eikmanns, B., Thauer, R. K., Widdel, F., & Fuchs, G. (1986). Acetate oxidation to CO2 in anaerobic bacteria via a novel pathway not involving reactions of the citric acid cycle. *Archives of Microbiology*, *145*(2), 162–172. http://doi.org/10.1007/BF00446775

Shcherbakova, V. A., & Vaĭnshteĭn, M. B. (2000). Methane production by the sulfate-reducing bacterium Desulfosarcina variabilis. *Microbiology*, *69*(3), 277–280. Retrieved from http://www.ncbi.nlm.nih.gov/pubmed/10920802

Sisler, F. D., & Zobell, C. E. (1951). Hydrogen utilization by some marine sulfate-reducing bacteria. *Journal of Bacteriology*, *62*(1), 117–27. Retrieved from http://www.ncbi.nlm.nih.gov/pubmed/14861165

Stadtman, T. C., & Barker, H. A. (1951). Studies on the methane fermentation. VIII. Tracer experiments of fatty acid oxidation by methane bacteria. *Journal of Bacteriology*, *61*(1), 67–80. Retrieved from http://www.ncbi.nlm.nih.gov/pubmed/14824080

Stoecker, K., Dorninger, C., Daims, H., & Wagner, M. (2010). Double Labeling of Oligonucleotide Probes for Fluorescence In Situ Hybridization (DOPE-FISH) Improves Signal Intensity and Increases rRNA Accessibility. *Applied and Environmental Microbiology*, *76*(3), 922–926. http://doi.org/10.1128/AEM.02456-09

Thorgersen, M. P., Lancaster, W. A., Rajeev, L., Ge, X., Vaccaro, B. J., Poole, F. L., … Adams, M. W. W. (2017). A Highly Expressed High-Molecular-Weight S-Layer Complex of Pelosinus sp. Strain UFO1 Binds Uranium. *Applied and Environmental Microbiology*, *83*(4), 1–10. http://doi.org/10.1128/AEM.03044-16

Tyagi, M., da Fonseca, M. M. R., & de Carvalho, C. C. C. R. (2011). Bioaugmentation and biostimulation strategies to improve the effectiveness of bioremediation processes. *Biodegradation*, *22*(2), 231–241. http://doi.org/10.1007/s10532-010-9394-4

ul Haq, R., & Shakoori, A. R. (1998). Short communication: Microbiological treatment of industrial wastes containing toxic chromium involving successive use of bacteria, yeast and algae. *World Journal of Microbiology and Biotechnology*, *14*(4), 583–585. http://doi.org/10.1023/A:1008849814190

Valls, M., & de Lorenzo, V. (2002). Exploiting the genetic and biochemical capacities of bacteria for the remediation of heavy metal pollution. *FEMS Microbiology Reviews*, *26*(4), 327–338. http://doi.org/10.1111/j.1574-6976.2002.tb00618.x

Walker, C. B., He, Z., Yang, Z. K., Ringbauer, J. a, He, Q., Zhou, J., … Stahl, D. A. (2009). The electron transfer system of syntrophically grown Desulfovibrio vulgaris. *Journal of Bacteriology*, *191*(18), 5793–801. http://doi.org/10.1128/JB.00356-09

SUPPLEMENTAL FIGURES

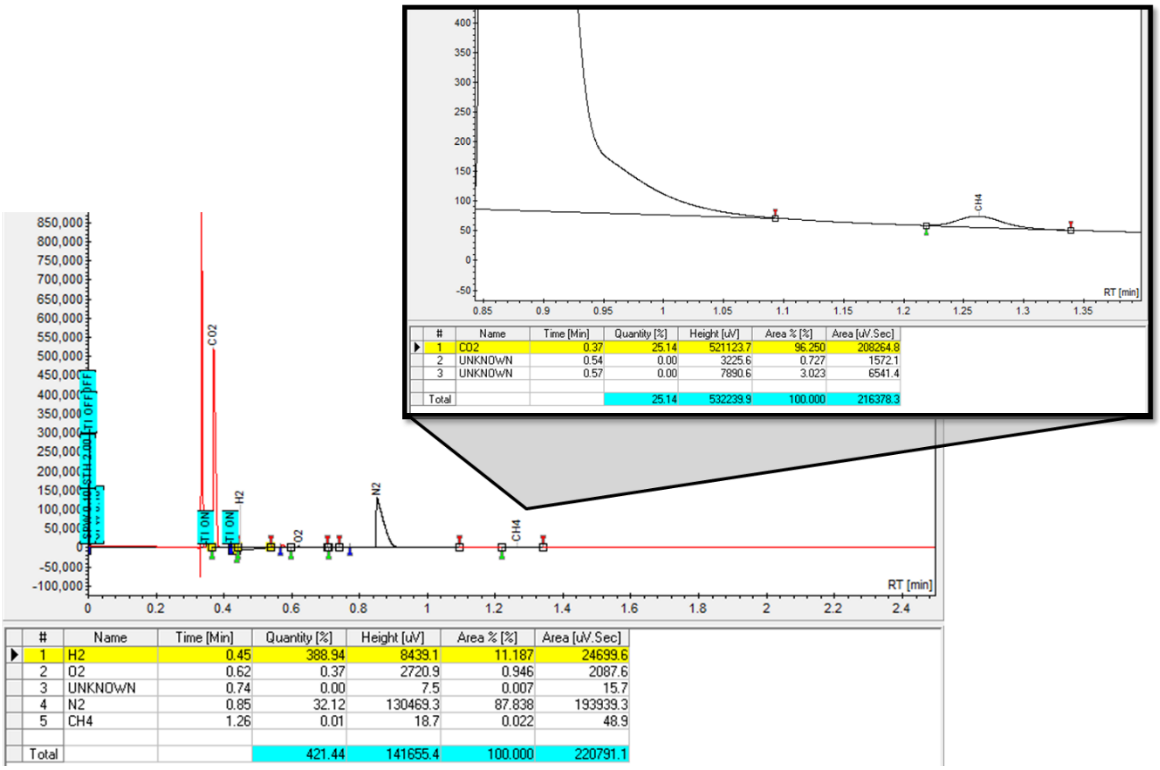
400
350
300
250
200
150
100
50
0
-50
CH4
RT [min]
0.85
0.9
0.95
1
1.05
1.1
1.15
1.2
1.25
1.3
1.35
850,000
800,000
750,000
700,000
650,000
600,000
550,000
500,000
450,000
400,000
350,000
300,000
250,000
200,000
150,000
100,000
50,000
0
-50,000
-100,000
CO2
H2
O2
N2
CH4
TI ON
TI ON
TI OFF
RT [min]
0
0.2
0.4
0.6
0.8
1
1.2
1.4
1.6
1.8
2
2.2
2.4

#	Name	Time [Min]	Quantity [%]	Height [uV]	Area % [%]	Area [uV.Sec]
1	CO2	0.37	25.14	521123.7	96.250	208264.8
2	UNKNOWN	0.54	0.00	3225.6	0.727	1572.1
3	UNKNOWN	0.57	0.00	7890.6	3.023	6541.4
Total			25.14	532239.9	100.000	216378.3

#	Name	Time [Min]	Quantity [%]	Height [uV]	Area % [%]	Area [uV.Sec]
1	H2	0.45	388.94	8439.1	11.187	24699.6
2	O2	0.62	0.37	2720.9	0.946	2087.6
3	UNKNOWN	0.74	0.00	7.5	0.007	15.7
4	N2	0.85	32.12	130469.3	87.838	193939.3
5	CH4	1.26	0.01	18.7	0.022	48.9
Total			421.44	141655.4	100.000	220791.1

Figure S1. *Pelosinus fermentans* JBW45 headspace analysis using gas chromatography demonstrating 0.01% methane peak.

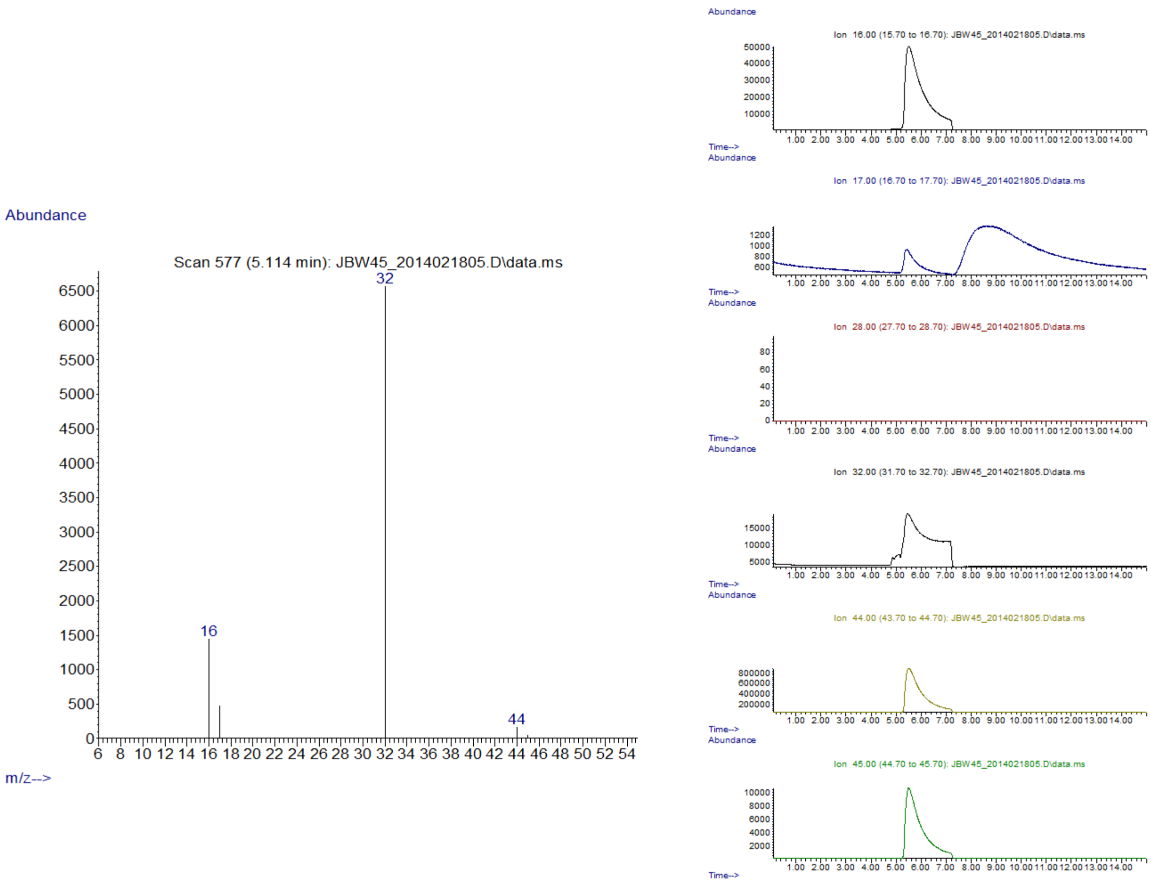

Figure S2. Headspace gas analysis of *Pelosinus fermentans* JBW45 cultures using GC-MS after preliminary $^{13}CO_2$ incubations in CCM with 30 mM lactate and 80%:20% H_2:CO_2. Peaks corresponding to CH_4 (m/z=16), $^{13}CH_4$ (m/z=17), CO_2 (m/z=44), and $^{13}CO_2$ (m/z=45) are depicted.

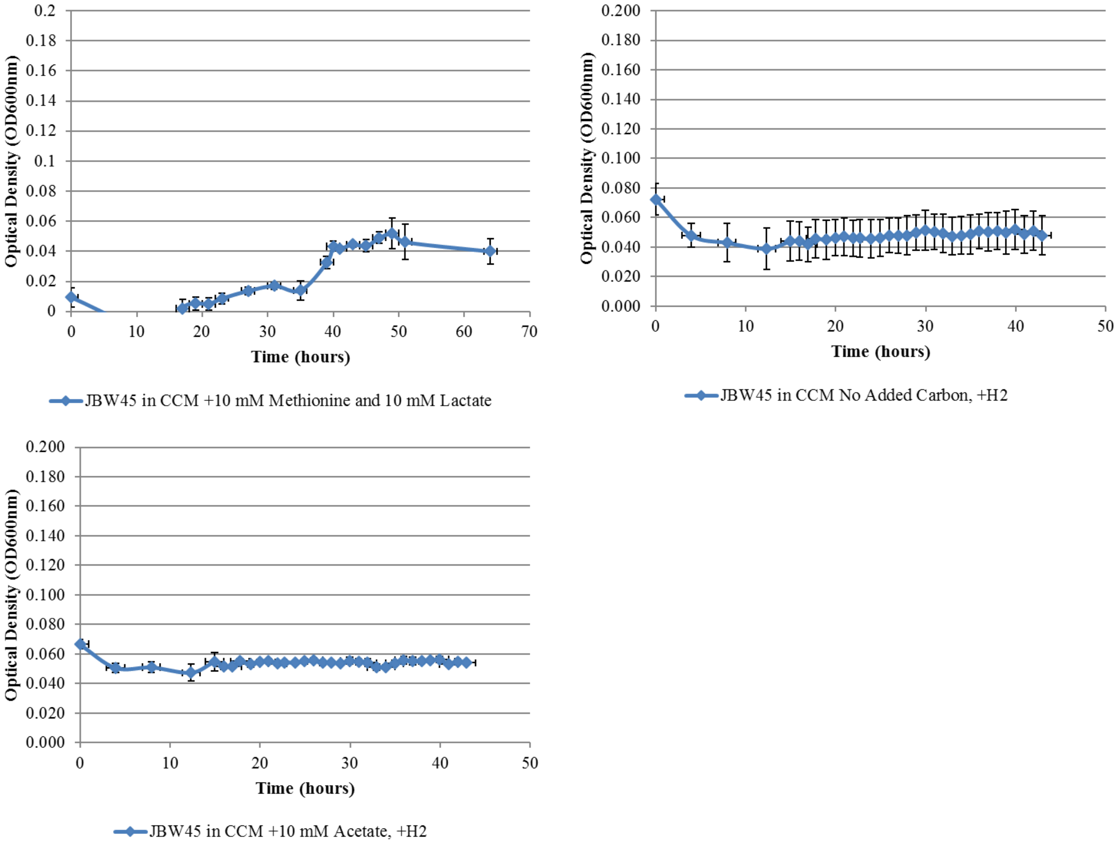

Figure S3. *Pelosinus fermentans* JBW45 did not exhibit growth with 10 mM methionine and 10 mM lactate, H_2 only, or 10 mM acetate with H_2:CO_2 (80%:20%).

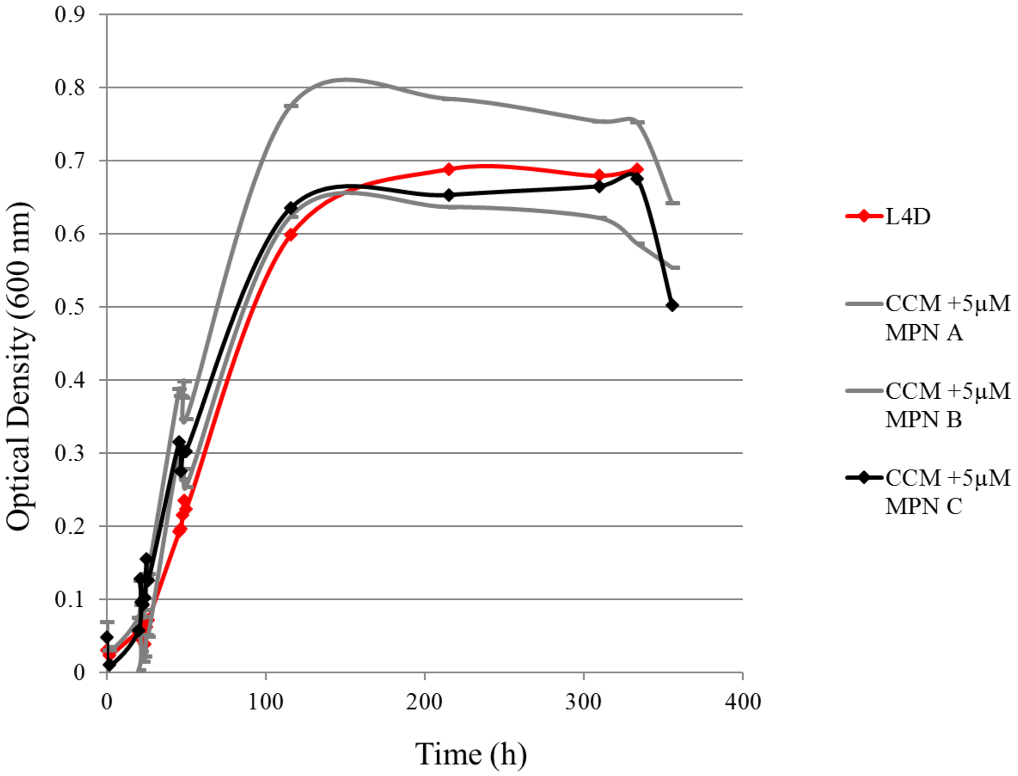

Figure S4. *Pelosinus fermentans* JBW45 growth on CCM with 5 µM methylphosphonate and the control in L4D media utilizing absorbance readings (600 nm) over time.

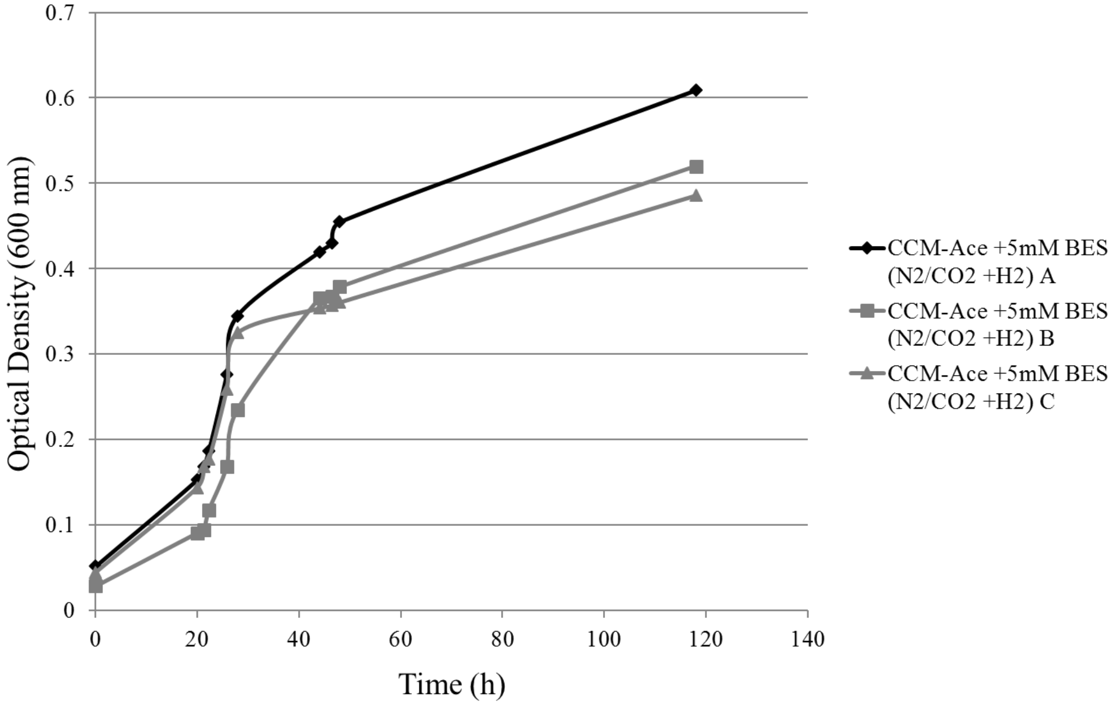

Figure S5. *Pelosinus fermentans* JBW45 growth on CCM with glycerol and 5 mM BES with H_2:CO_2 80%:20% in the headspace.

APPENDIX B

DRAFT GENOME SEQUENCE OF PELOSINUS FERMENTANS JBW45 ISOLATED DURING IN SITU STIMULATION FOR Cr(VI) REDUCTION

Contribution of Authors and Co-Authors

Manuscript in Appendix B

Author: Kara Bowen De León

Contributions: Isolation, sequencing preparation, data analysis, and manuscript preparation.

Co-Author: Mary Lynn Young

Contributions: Laboratory experiments and data analysis.

Co-Author: Laura B. Camilleri

Contributions: Data analysis.

Co-Author: Steven D. Brown

Contributions: Data analysis and submissions to databases.

Co-Author: Jeffrey M. Skerker

Contributions: Data analysis.

Co-Author: Adam M. Deutschbauer

Contributions: Principle investigator for sequence analysis.

Co-Author: Adam P. Arkin

Contributions: Principle investigator for genome sequencing.

Co-Author: Matthew W. Fields

Contributions: Principle investigator of laboratory experiments and genome analysis, manuscript revisions.

Manuscript Information Page

Kara Bowen De León, Mary Lynn Young, Laura B. Camilleri, Steven D. Brown, Jeffrey M. Skerker, Adam M. Deutschbauer, Matthew W. Fields

Journal of Bacteriology

Status of Manuscript:
____ Prepared for submission to a peer-reviewed journal
____ Officially submitted to a peer-review journal
____ Accepted by a peer-reviewed journal
__X_ Published in a peer-reviewed journal

Copyright ©2012 American Society for Microbiology, Journal of Bacteriology, Volume 194, Number 19, 2012, pgs 5456-5457, doi:10.1128/JB.01224-12.

JB
Journals.ASM.org

GENOME ANNOUNCEMENT

Draft Genome Sequence of *Pelosinus fermentans* JBW45, Isolated during *In Situ* Stimulation for Cr(VI) Reduction

Kara Bowen De León,[a,b] Mary Lynn Young,[b] Laura B. Camilleri,[a,b] Steven D. Brown,[c] Jeffrey M. Skerker,[d] Adam M. Deutschbauer,[d] Adam P. Arkin,[d,e] and Matthew W. Fields[a,b]

Department of Microbiology, Montana State University, Bozeman, Montana, USA[a]; Center for Biofilm Engineering, Montana State University, Bozeman, Montana, USA[b]; Biosciences Division, Oak Ridge National Laboratory, Oak Ridge, Tennessee, USA[c]; Physical Biosciences Division, Lawrence Berkeley National Laboratory, Berkeley, California, USA[d]; and Department of Bioengineering, University of California, Berkeley, California, USA[e]

Pelosinus fermentans **JBW45 is an anaerobic, lactate-fermenting bacterium isolated from Cr(VI)-contaminated groundwater at the Hanford Nuclear Reservation 100-H site (Washington) that was collected after stimulation with a polylactate compound. The genome sequence of this organism will provide insight into the metabolic potential of a predominant population during stimulation for metal-reducing conditions.**

The Hanford Nuclear Reservation 100-H site in Eastern Washington is a Cr(VI)-contaminated site designated by the Department of Energy (DOE) as a field study site for bioremediation. A previous injection of hydrogen release compound (HRC) in 2004 resulted in Cr(VI) reduction to below background levels for >3 years (4, 5). After a second injection (in 2008), enrichments were made with groundwater 24 h after HRC addition from the injection well as part of an ongoing effort to characterize the stimulated microbial populations. *Pelosinus fermentans* JBW45 was isolated in anaerobic LS4D medium (2) (modified to 2.5 μM resazurin and 130 μM riboflavin in modified Thauer's vitamins stock [3]), with subsequent dilution to extinction and isolation on LS4D plates. While LS4D is traditionally used to cultivate sulfate-reducing bacteria (SRB), sulfide production decreased and eventually disappeared during the isolation process, and these results suggest that the isolate outcompeted SRB under the tested conditions. This is an important consideration at the field site, where SRB are targeted due to heavy metal reduction capabilities. *Pelosinus* increased in relative abundance during the 2008 *in situ* stimulation (K. Bowen De León and M. W. Fields, unpublished data) and also became a predominant member in lab-scale microcosms injected with 100-H groundwater (8).

Draft genome sequence data for *P. fermentans* JBW45 were generated using an Illumina (1) HiSeq2000 instrument from a paired-end DNA library with an approximate insert size of 500 bp. The Illumina sequence data were trimmed for quality (CLC Genomics Workbench version 4.7.1) and assembled with Velvet (version 1.2.01) (10) into 98 contigs greater than 500 bp (approximately 600X genome coverage). The N_{50} was 155,254 bp, the mean size was 53,854 bp, and the largest contig was 476,917 bp. The estimated draft genome sequence was approximately 5.3 Mb, with a G+C content of 39.3%. The draft genome sequence was annotated at Oak Ridge National Laboratory (ORNL) using an automated annotation pipeline based on the Prodigal gene prediction algorithm (6). A total of 4,765 candidate protein-coding gene models were predicted, with a gene coding density of 85.9%.

The small-subunit (SSU) rRNA gene sequence of the isolate has 99% identity to those of *Pelosinus fermentans* strain DSM 17108 (GenBank accession number JF749997) and *Sporotalea propionica* strains TM1 and DSM 13327 (GenBank accession numbers FN689723 and JF749993, respectively). Because of the similarity of the *Pelosinus* and *Sporotalea* SSU rRNA gene sequences and the almost concurrent publications of the isolations, it has been proposed that *Sporotalea* be renamed to *Pelosinus* (7). Isolate JBW45 has an intervening sequence near the 5′ end of the SSU rRNA gene sequence that is similar to those previously reported in *Pelosinus* species (7, 9). Furthermore, *Pelosinus fermentans* strains with 99 to 100% SSU rRNA gene similarity have been shown to have differing heavy metal-reducing characteristics (8). The genome sequence of this organism will provide insight into the metabolic strategies of a predominant population during stimulation for heavy metal reduction and allow for genome-wide comparisons to other *Pelosinus* species.

Nucleotide sequence accession numbers. This whole-genome shotgun project has been deposited at DDBJ/EMBL/GenBank under the accession number AKVO00000000. The version described in this paper is the first version, AKVO01000000. The Illumina data set has been deposited in the National Center for Biotechnology Information (NCBI) Sequence Read Archive (SRA) under accession number SRA052951.

ACKNOWLEDGMENTS

We thank Sagar M. Utturkar (University of Tennessee) and Miriam L. Land (ORNL) for assistance with assembly and annotation, respectively. This research was conducted by the Ecosystems and Networks Integrated with Genes and Molecular Assemblies (ENIGMA) scientific focus area.

This research was funded by the U.S. Department of Energy Office of Biological and Environmental Research Division under contract no. DE-AC02-05CH11231 to Lawrence Berkeley National Laboratory. K. Bowen De León was supported by the Montana State University Molecular Biosciences Program. K. Bowen De León and L. Camilleri were supported by the NSF-IGERT Program in Geobiological Systems (DGE0654336) at Montana State University.

Oak Ridge National Laboratory is managed by UT-Battelle, LLC, for the U.S. Department of Energy under contract no. DE-AC05-00OR22725.

Received 6 July 2012 Accepted 17 July 2012

Address correspondence to Matthew W. Fields, matthew.fields@biofilm.montana.edu.

Copyright © 2012, American Society for Microbiology. All Rights Reserved.

doi:10.1128/JB.01224-12

REFERENCES

1. **Bennett S.** 2004. Solexa Ltd. Pharmacogenomics **5**:433–438.
2. **Borglin S, Joyner D, Jacobsen J, Mukhopadhyay A, Hazen TC.** 2009. Overcoming the anaerobic hurdle in phenotypic microarrays: generation and visualization of growth curve data for *Desulfovibrio vulgaris* Hildenborough. J. Microbiol. Methods **76**:159–168.
3. **Brandis A, Thauer RK.** 1981. Growth of *Desulfovibrio* species on hydrogen and sulphate as sole energy-source. J. Gen. Microbiol. **126**:249–252.
4. **Faybishenko B, et al.** 2008. *In situ* long-term reductive bioimmobilization of Cr(VI) in groundwater using hydrogen release compound. Environ. Sci. Technol. **42**:8478–8485.
5. **Hubbard SS, et al.** 2008. Geophysical monitoring of hydrological and biogeochemical transformations associated with Cr(VI) bioremediation. Environ. Sci. Technol. **42**:3757–3765.
6. **Hyatt D, et al.** 2010. Prodigal: prokaryotic gene recognition and translation initiation site identification. BMC Bioinformatics **11**:119.
7. **Moe WM, et al.** 2011. *Pelosinus defluvii* sp. nov., isolated from chlorinated solvent contaminated groundwater, emended description of the genus *Pelosinus*, and transfer of *Sporotalea propionica* to *Pelosinus propionicus* comb. nov. Int. J. Syst. Evol. Microbiol. **62**:1369–1376.
8. **Mosher JJ, et al.** 2012. Microbial community succession during lactate amendment and electron acceptor limitation reveals a predominance of metal-reducing *Pelosinus* spp. Appl. Environ. Microbiol. **78**:2082–2091.
9. **Ray AE, et al.** 2010. Intragenomic heterogeneity of the 16S rRNA gene in strain UFO1 caused by a 100-bp insertion in helix 6. FEMS Microbiol. Ecol. **72**:343–353.
10. **Zerbino DR, Birney E.** 2008. Velvet: algorithms for de novo short read assembly using de Bruijn graphs. Genome Res. **18**:821–829.

APPENDIX C

COMPLETE GENOME SEQUENCE OF PELOSINUS FERMENTANS JBW45, A MEMBER OF A REMARKABLY COMPETITIVE GROUP OF NEGATIVICUTES IN THE FIRMICUTES PHYLUM

Contribution of Authors and Co-Authors

Manuscript in Appendix C

Author: Kara Bowen De León

Contributions: Isolation, sequencing preparation, data analysis, and manuscript preparation.

Co-Author: Sagar M. Utturkar

Contributions: Assembly and data analysis.

Co-Author: Laura B. Camilleri

Contributions: Data analysis.

Co-Author: Dwayne A. Elias

Contributions: Data analysis.

Co-Author: Adam P. Arkin

Contributions: Principle investigator for genome sequencing.

Co-Author: Matthew W. Fields

Contributions: Principle investigator of laboratory experiments and genome analysis, manuscript revisions.

Co-Author: Steven D. Brown

Contributions: Data analysis and submissions to databases.

Co-Author: Judy D. Wall

Contributions: Principle investigator for sequence analysis.

Manuscript Information Page

Kara Bowen De León, Sagar M. Utturkar, Laura B. Camilleri, Dwayne A. Elias, Adam P. Arkin, Matthew W. Fields, Steven D. Brown, Judy D. Wall

Genome Announcements

Status of Manuscript:
____ Prepared for submission to a peer-reviewed journal
____ Officially submitted to a peer-review journal
____ Accepted by a peer-reviewed journal
__X_ Published in a peer-reviewed journal

American Society for Microbiology
Genome Announcements, Volume 3, Issue 5, 2015, pgs e01090-15, doi:10.1128/genomeA.01090-15.

genomeA
Journals.ASM.org

Complete Genome Sequence of *Pelosinus fermentans* JBW45, a Member of a Remarkably Competitive Group of *Negativicutes* in the *Firmicutes* Phylum

Kara B. De León,[a] Sagar M. Utturkar,[b] Laura B. Camilleri,[c,d] Dwayne A. Elias,[e] Adam P. Arkin,[f,g] Matthew W. Fields,[c,d] Steven D. Brown,[b,e] Judy D. Wall[a]

Division of Biochemistry, University of Missouri, Columbia, Missouri, USA[a]; Graduate School of Genome Science and Technology, University of Tennessee, Knoxville, Tennessee, USA[b]; Department of Microbiology and Immunology, Montana State University, Bozeman, Montana, USA[c]; Center for Biofilm Engineering, Montana State University, Bozeman, Montana, USA[d]; Biosciences Division, Oak Ridge National Laboratory, Oak Ridge, Tennessee, USA[e]; Physical Biosciences Division, Lawrence Berkeley National Laboratory, Berkeley, California, USA[f]; Department of Bioengineering, University of California, Berkeley, California, USA[g]

K.B.D.L. and S.M.U. contributed equally to this work.

The genome of *Pelosinus fermentans* JBW45, isolated from a chromium-contaminated site in Hanford, Washington, USA, has been completed with PacBio sequencing. Nine copies of the rRNA gene operon and multiple transposase genes with identical sequences resulted in breaks in the original draft genome and may suggest genomic instability of JBW45.

Received 7 August 2015 **Accepted** 11 August 2015 **Published** 24 September 2015

Citation De León KB, Utturkar SM, Camilleri LB, Elias DA, Arkin AP, Fields MW, Brown SD, Wall JD. 2015. Complete genome sequence of *Pelosinus fermentans* JBW45, a member of a remarkably competitive group of *Negativicutes* in the *Firmicutes* phylum. Genome Announc 3(5):e01090-15. doi:10.1128/genomeA.01090-15.

Copyright © 2015 De León et al. This is an open-access article distributed under the terms of the Creative Commons Attribution 3.0 Unported license.

Address correspondence to Judy D. Wall, wallj@missouri.edu.

Pelosinus fermentans JBW45 was isolated from groundwater stimulated for hexavalent-chromium reduction by injection of a polylactate compound (1). *Pelosinus* spp. are found in sites contaminated by heavy metals, explosives, and chlorinated solvents, at low or below-detection levels, but become dominant following nutrient addition *in vitro* (2–14) or *in situ* (1, 15, 16). A strict anaerobe, JBW45 likely resides in sediment-associated, anaerobic microsites (6). Although *Pelosinus* strains have been seen to form spores (17, 18), spore formation has not been documented for JBW45.

Previous genome sequencing of JBW45 with Illumina technology resulted in 98 contigs (1). Draft genome sequences for three other *Pelosinus* spp. from Hanford (A11, B4, and HCF1) and the type strain R7 from Russian kaolin clays are similar to each other but show little synteny with JBW45 or the completed genome of *Pelosinus* sp. UFO1, isolated from Oak Ridge, Tennessee, USA (19–21).

The complete genome sequence of JBW45 was determined with a Pacific Biosciences (PacBio, Menlo Park, California, USA) RSII instrument with P4-C2 chemistry as described previously (22). Two single-molecule real-time (SMRT) cells yielded 1,345,758,432 bases in 202,124 reads with a mean and maximum read length of 6,656 and 35,018 bases, respectively. SMRT analysis version 2.2 and HGAP version 3.0 (PacBio) were used for sequence assembly, which was improved with Pilon (23) and annotated as described previously (1). A single contig with 32-kb overlapping ends was generated, differing only by the presence of a putative transposase gene (JBW_01610). PCR across this region showed the transposase present in 4 of 14 JBW45 colonies, suggesting that the transposase may be actively moving and possibly contributing to evolutionary plasticity (24). Six identical copies (49.6% G+C content) were found in the completed JBW45 genome. This transposase was not found in the completed UFO1 genome. A similar gene (82 to 83% identity) was found as the only gene on a small contig in the draft genomes of A11, B4, HCF1, and R7. JBW45 contains 18 other genes annotated as transposases, many of which occur multiple times in the genome. Transposase and rRNA operon sequences resulted in breaks in assembly of the original JBW45 genome, underscoring the value of longer sequencing technologies, which is consistent with other reports (22, 25, 26).

The final assembly was circularized, resulting in a 5,380,816-bp chromosome with a G+C content of 39.5% and 250-fold sequence coverage. A total of 4,743 protein-coding, 77 tRNA, and 28 rRNA (ten 5S, nine 23S, and nine 16S) genes were identified. Four of the 16S rRNA genes contained a 100-bp insertion, which is consistent with previous findings of intragenomic 16S rRNA gene heterogeneity in UFO1 (21, 27). The average number of bacterial rRNA operons is four (28); however, UFO1 contains fifteen 16S rRNA genes (21). A higher number of rRNA operons may allow rapid adaptation and recovery from the stationary phase (29, 30). This may provide *Pelosinus* spp. with a competitive advantage upon nutrient stimulation.

Nucleotide sequence accession numbers. This whole-genome shotgun project has been deposited in DDBJ/ENA/GenBank under the accession number CP010978. The version described in this paper is the first version, CP010978.1.

ACKNOWLEDGMENTS

PacBio sequencing was performed at the University of Maryland Institute for Genome Sciences. Microbial sequence and data analysis was supported by ENIGMA—Ecosystems and Networks Integrated with Genes and Molecular Assemblies (http://enigma.lbl.gov), a Scientific Focus Area Program at Lawrence Berkeley National Laboratory for the U.S. Department of Energy, Office of Science, Office of Biological and Environmental Research under contract number DE-AC02-05CH11231. Microbial genome sequence assembly, annotation, and analysis by ENIGMA were supported by Oak Ridge National Laboratory, managed by UT-Battelle, LLC, for the U.S. Department of Energy under contract no. DE-AC05-00OR22725.

REFERENCES

1. **Bowen De León K, Young ML, Camilleri LB, Brown SD, Skerker JM, Deutschbauer AM, Arkin AP, Fields MW.** 2012. Draft genome sequence of *Pelosinus fermentans* JBW45, isolated during *in situ* stimulation for Cr(VI) reduction. J Bacteriol **194:**5456–5457. http://dx.doi.org/10.1128/JB.01224-12.
2. **Beller HR, Yang L, Varadharajan C, Han R, Lim HC, Karaoz U, Molins S, Marcus MA, Brodie EL, Steefel CI, Nico PS.** 2014. Divergent aquifer biogeochemical systems converge on similar and unexpected Cr(VI) reduction products. Environ Sci Technol **48:**10699–10706. http://dx.doi.org/10.1021/es5016982.
3. **Burkhardt E-M, Akob DM, Bischoff S, Sitte J, Kostka JE, Banerjee D, Scheinost AC, Küsel K.** 2010. Impact of biostimulated redox processes on metal dynamics in an iron-rich creek soil of a former uranium mining area. Environ Sci Technol **44:**177–183. http://dx.doi.org/10.1021/es902038e.
4. **Fahrenfeld N, Zoeckler J, Widdowson MA, Pruden A.** 2013. Effect of biostimulants on 2,4,6-trinitrotoluene (TNT) degradation and bacterial community composition in contaminated aquifer sediment enrichments. Biodegradation **24:**179–190. http://dx.doi.org/10.1007/s10532-012-9569-2.
5. **Fuller ME, McClay K, Higham M, Hatzinger PB, Steffan RJ.** 2010. Hexahydro-1,3,5-trinitro-1,3,5-triazine (RDX) bioremediation in groundwater: are known RDX-degrading bacteria the dominant players? Biorcm J **14:**121–134. http://dx.doi.org/10.1080/10889868.2010.495367.
6. **Hansel CM, Fendorf S, Jardine PM, Francis CA.** 2008. Changes in bacterial and archaeal community structure and functional diversity along a geochemically variable soil profile. Appl Environ Microbiol **74:**1620–1633. http://dx.doi.org/10.1128/AEM.01787-07.
7. **Krzmarzick MJ, Miller HR, Yan T, Novak PJ.** 2014. Novel *Firmicutes* group implicated in the dechlorination of two chlorinated xanthones, analogues of natural organochlorines. Appl Environ Microbiol **80:**1210–1218. http://dx.doi.org/10.1128/AEM.03472-13.
8. **Martins M, Faleiro ML, da Costa AM, Chaves S, Tenreiro R, Matos AP, Costa MC.** 2010. Mechanism of uranium (VI) removal by two anaerobic bacterial communities. J Hazard Mater **184:**89–96. http://dx.doi.org/10.1016/j.jhazmat.2010.08.009.
9. **Men Y, Lee PKH, Harding KC, Alvarez-Cohen L.** 2013. Characterization of four TCE-dechlorinating microbial enrichments grown with different cobalamin stress and methanogenic conditions. Appl Microbiol Biotechnol **97:**6439–6450. http://dx.doi.org/10.1007/s00253-013-4896-8.
10. **Miura T, Yamazoe A, Ito M, Ohji S, Hosoyama A, Takahata Y, Fujita N.** 2015. The impact of injections of different nutrients on the bacterial community and its dechlorination activity in chloroethene-contaminated groundwater. Microbes Environ **30:**164–171. http://dx.doi.org/10.1264/jsme2.ME14127.
11. **Mosher JJ, Phelps TJ, Podar M, Hurt RA, Jr, Campbell JH, Drake MM, Moberly JG, Schadt CW, Brown SD, Hazen TC, Arkin AP, Palumbo AV, Faybishenko BA, Elias DA.** 2012. Microbial community succession during lactate amendment and electron acceptor limitation reveals a predominance of metal-reducing *Pelosinus* spp. Appl Environ Microbiol **78:**2082–2091. http://dx.doi.org/10.1128/AEM.07165-11.
12. **Newsome L, Morris K, Trivedi D, Atherton N, Lloyd JR.** 2014. Microbial reduction of uranium(VI) in sediments of different lithologies collected from Sellafield. Appl Geochem **51:**55–64. http://dx.doi.org/10.1016/j.apgeochem.2014.09.008.
13. **Penny C, Gruffaz C, Nadalig T, Cauchie H-M, Vuilleumier S, Bringel F.** 2015. Tetrachloromethane-degrading bacterial enrichment cultures and isolates from a contaminated aquifer. Microorganisms **3:**327–343. http://dx.doi.org/10.3390/microorganisms3030327.
14. **Somenahally AC, Mosher JJ, Yuan T, Podar M, Phelps TJ, Brown SD, Yang ZK, Hazen TC, Arkin AP, Palumbo AV, Van Nostrand JD, Zhou J, Elias DA.** 2013. Hexavalent chromium reduction under fermentative conditions with lactate stimulated native microbial communities. PLoS One **8:**e83909. http://dx.doi.org/10.1371/journal.pone.0083909.
15. **Chourey K, Nissen S, Vishnivetskaya T, Shah M, Pfiffner S, Hettich RL, Löffler FE.** 2013. Environmental proteomics reveals early microbial community responses to biostimulation at a uranium- and nitrate-contaminated site. Proteomics **13:**2921–2930. http://dx.doi.org/10.1002/pmic.201300155.
16. **Gihring TM, Zhang G, Brandt CC, Brooks SC, Campbell JH, Carroll S, Criddle CS, Green SJ, Jardine P, Kostka JE, Lowe K, Mehlhorn TL, Overholt W, Watson DB, Yang Z, Wu W-M, Schadt CW.** 2011. A limited microbial consortium is responsible for extended bioreduction of uranium in a contaminated aquifer. Appl Environ Microbiol **77:**5955–5965. http://dx.doi.org/10.1128/AEM.00220-11.
17. **Moe WM, Stebbing RE, Rao JU, Bowman KS, Nobre MF, da Costa MS, Rainey FA.** 2012. *Pelosinus defluvii* sp. nov., isolated from chlorinated solvent-contaminated groundwater, emended description of the genus *Pelosinus*, and transfer of *Sporotalea propionica* to *Pelosinus propionicus* comb. nov. Int J Syst Evol Microbiol **62:**1369–1376. http://dx.doi.org/10.1099/ijs.0.033753-0.
18. **Shelobolina ES, Nevin KP, Blakeney-Hayward JD, Johnsen CV, Plaia TW, Krader P, Woodard T, Holmes DE, VanPraagh CG, Lovley DR.** 2007. *Geobacter pickeringii* sp. nov., *Geobacter argillaceus* sp. nov. and *Pelosinus fermentans* gen. nov., sp. nov., isolated from subsurface kaolin lenses. Int J Syst Evol Microbiol **57:**126–135. http://dx.doi.org/10.1099/ijs.0.64221-0.
19. **Beller HR, Han R, Karaoz U, Lim H, Brodie EL.** 2013. Genomic and physiological characterization of the chromate-reducing, aquifer-derived firmicute *Pelosinus* sp. strain HCF1. Appl Environ Microbiol **79:**63–73. http://dx.doi.org/10.1128/AEM.02496-12.
20. **Brown SD, Podar M, Klingeman DM, Johnson CM, Yang ZK, Utturkar SM, Land ML, Mosher JJ, Hurt RA, Jr, Phelps TJ, Palumbo AV, Arkin AP, Hazen TC, Elias DA.** 2012. Draft genome sequences for two metal-reducing *Pelosinus fermentans* strains isolated from a Cr(VI)-contaminated site and for type strain R7. J Bacteriol **194:**5147–5148. http://dx.doi.org/10.1128/JB.01174-12.
21. **Brown SD, Utturkar SM, Magnuson TS, Ray AE, Poole FL, Lancaster WA, Thorgersen MP, Adams MWW, Elias DA.** 2014. Complete genome sequence of *Pelosinus* sp. strain ufo1 assembled using single-molecule real-time DNA sequencing technology. Genome Announc 2(5):e00881-14. http://dx.doi.org/10.1128/genomeA.00881-14.
22. **Brown SD, Nagaraju S, Utturkar S, De Tissera S, Segovia S, Mitchell W, Land ML, Dassanayake A, Köpke M.** 2014. Comparison of single-molecule sequencing and hybrid approaches for finishing the genome of *Clostridium autoethanogenum* and analysis of CRISPR systems in industrial relevant Clostridia. Biotechnol Biofuels **7:**40. http://dx.doi.org/10.1186/1754-6834-7-40.
23. **Walker BJ, Abeel T, Shea T, Priest M, Abouelliel A, Sakthikumar S, Cuomo CA, Zeng Q, Wortman J, Young SK, Earl AM.** 2014. Pilon: an integrated tool for comprehensive microbial variant detection and genome assembly improvement. PLoS One **9:**e112963. http://dx.doi.org/10.1371/journal.pone.0112963.
24. **Darmon E, Leach DRF.** 2014. Bacterial genome instability. Microbiol Mol Biol Rev **78:**1–39. http://dx.doi.org/10.1128/MMBR.00035-13.
25. **Treangen TJ, Salzberg SL.** 2012. Repetitive DNA and next-generation sequencing: computational challenges and solutions. Nat Rev Genet **13:**36–46. http://dx.doi.org/10.1038/nrg3117.
26. **Utturkar SM, Klingeman DM, Land ML, Schadt CW, Doktycz MJ, Pelletier DA, Brown SD.** 2014. Evaluation and validation of *de novo* and hybrid assembly techniques to derive high-quality genome sequences. Bioinformatics **30:**2709–2716. http://dx.doi.org/10.1093/bioinformatics/btu391.
27. **Ray AE, Connon SA, Sheridan PP, Gilbreath J, Shields M, Newby DT, Fujita Y, Magnuson TS.** 2010. Intragenomic heterogeneity of the 16S rRNA gene in strain UFO1 caused by a 100-bp insertion in helix 6. FEMS Microbiol Ecol **72:** 343–353. http://dx.doi.org/10.1111/j.1574-6941.2010.00868.x.
28. **Stoddard SF, Smith BJ, Hein R, Roller BRK, Schmidt TM.** 2015. *rrn*DB: improved tools for interpreting rRNA gene abundance in bacteria and archaea and a new foundation for future development. Nucleic Acids Res **43:**D593–D598. http://dx.doi.org/10.1093/nar/gku1201.
29. **Condon C, Liveris D, Squires C, Schwartz I, Squires CL.** 1995. rRNA operon multiplicity in *Escherichia coli* and the physiological implications of *rrn* inactivation. J Bacteriol **177:**4152–4156.
30. **Klappenbach JA, Dunbar JM, Schmidt TM.** 2000. rRNA operon copy number reflects ecological strategies of bacteria. Appl Environ Microbiol **66:**1328–1333. http://dx.doi.org/10.1128/AEM.66.4.1328-1333.2000.

APPENDIX D

BIOFILM GROWTH MODE PROMOTES MAXIMUM CARRYING CAPACITY AND COMMUNITY STABILITY DURING PRODUCT INHIBITION SYNTROPHY

Contribution of Authors and Co-Authors

Manuscript in Appendix D

Author: Kristen A. Brileya

Contributions: Developed experimental design, performed experiments, analyzed data, wrote and revised the manuscript.

Co-Author: Laura B. Camilleri

Contributions: Developed experimental design, performed experiments, analyzed data, revised the manuscript.

Co-Author: Matthew W. Fields

Contributions: Developed experimental design, analyzed data, wrote and revised the manuscript.

Manuscript Information Page

Kristen A. Brileya, Laura B. Camilleri, Matthew W. Fields

Frontiers in Microbiology

Status of Manuscript:
____ Prepared for submission to a peer-reviewed journal
____ Officially submitted to a peer-review journal
____ Accepted by a peer-reviewed journal
__X_ Published in a peer-reviewed journal

Frontiers in Microbiology, 2014; 5: 693. Doi: 10.3389/fmicb.2014.00693

frontiers in
MICROBIOLOGY

ORIGINAL RESEARCH ARTICLE
published: 15 December 2014
doi: 10.3389/fmicb.2014.00693

Biofilm growth mode promotes maximum carrying capacity and community stability during product inhibition syntrophy

Kristen A. Brileya[1,2], Laura B. Camilleri[1,2], Grant M. Zane[3], Judy D. Wall[3] and Matthew W. Fields[1,2,4,5,6]*

[1] *Department of Microbiology and Immunology, Montana State University, Bozeman, MT, USA*
[2] *Center for Biofilm Engineering, Montana State University, Bozeman, MT, USA*
[3] *Division of Biochemistry, University of Missouri, Columbia, MO, USA*
[4] *Thermal Biology Institute, Montana State University, Bozeman, MT, USA*
[5] *Ecosystems and Networks Integrated with Genes and Molecular Assemblies, Berkeley, CA, USA*
[6] *National Center for Genome Resources, Santa Fe, NM, USA*

Edited by:
Joerg Graf, University of Connecticut, USA

Reviewed by:
Seana Kelyn Davidson, University of Washington, USA
Masanori Toyofuku, University of Tsukuba, Japan

**Correspondence:*
Matthew W. Fields, Center for Biofilm Engineering, Montana State University, 366 EPS Building, Bozeman, MT 59717, USA
e-mail: matthew.fields@biofilm.montana.edu

Sulfate-reducing bacteria (SRB) can interact syntrophically with other community members in the absence of sulfate, and interactions with hydrogen-consuming methanogens are beneficial when these archaea consume potentially inhibitory H_2 produced by the SRB. A dual continuous culture approach was used to characterize population structure within a syntrophic biofilm formed by the SRB *Desulfovibrio vulgaris* Hildenborough and the methanogenic archaeum *Methanococcus maripaludis*. Under the tested conditions, monocultures of *D. vulgaris* formed thin, stable biofilms, but monoculture *M. maripaludis* did not. Microscopy of intact syntrophic biofilm confirmed that *D. vulgaris* formed a scaffold for the biofilm, while intermediate and steady-state images revealed that *M. maripaludis* joined the biofilm later, likely in response to H_2 produced by the SRB. Close interactions in structured biofilm allowed efficient transfer of H_2 to *M. maripaludis,* and H_2 was only detected in cocultures with a mutant SRB that was deficient in biofilm formation (*,0,pilA*). *M. maripaludis* produced more carbohydrate (uronic acid, hexose, and pentose) as a monoculture compared to total coculture biofilm, and this suggested an altered carbon flux during syntrophy. The syntrophic biofilm was structured into ridges (~300 × 50 μm) and models predicted lactate limitation at ~50 μm biofilm depth. The biofilm had structure that likely facilitated mass transfer of H_2 and lactate, yet maximized biomass with a more even population composition (number of each organism) when compared to the bulk-phase community. Total biomass protein was equivalent in lactate-limited and lactate-excess conditions when a biofilm was present, but in the absence of biofilm, total biomass protein was significantly reduced. The results suggest that multispecies biofilms create an environment conducive to resource sharing, resulting in increased biomass retention, or carrying capacity, for cooperative populations.

Keywords: anaerobic, carrying capacity, hydrogen transfer, population intermixing, sulfate-reducing bacteria

INTRODUCTION

Symbiosis (“living together”) and specifically mutualism, whereby both parties incur a benefit from living together, is widespread throughout the biosphere with well-studied examples in and across all three domains of life (Yeoh et al., 1968; Boucher, 1988; Kato et al., 2011; Moissl-Eichinger and Huber, 2011; Plugge et al., 2011; Gokhale and Traulsen, 2012; Sieber et al., 2012). In communities of bacteria and archaea, mutualism is typically referred to as syntrophy (“eating together”) where by-products of one metabolism serve as substrates for another metabolism (Sieber et al., 2012). The syntrophy between sulfate-reducing bacteria (SRB) and methanogenic archaea is of interest because these guilds both play crucial roles in many different anaerobic environments. SRB link the carbon, sulfur, and nitrogen biogeochemical cycles via carbon-oxidation and sulfate reduction (Purdy et al., 2002; Canfield et al., 2010) and also contribute to redox gradients of microbial ecosystems via the production of sulfide compounds (Moreau et al., 2010; Xie et al., 2013). Methanogenic archaea are responsible for the three largest sources of methane flux to the atmosphere (wetlands, ruminants, and rice cultivation) and form the basis of most anaerobic environments (natural and man-made) that convert CO_2, H_2, and/or acetate/methyl-groups to methane (Thauer et al., 2008; Neef et al., 2010; van Groenigen et al., 2012; Schlesinger and Bernhardt, 2013).

The nature of SRB-methanogen interactions is complex and fluctuates based on substrate flux and availability (Leloup et al., 2009; Stams and Plugge, 2009; Plugge et al., 2011). In the presence of sulfate, methanogens are typically outcompeted by SRB using H_2, formate, and acetate as electron donors for sulfate reduction (Plugge et al., 2011). SRB can alternatively form mutualistic partnerships with hydrogenotrophic methanogens in the absence of sulfate by proton reduction to form H_2 gas. The reaction is kept favorable when hydrogenotrophic methanogens consume H_2, keeping the partial pressure low and thereby eliminating the inhibitory effect of this end-product on the SRB (Figure S1A; McInerney et al., 2009; Stams and Plugge, 2009). Inhabitants of anaerobic ecosystems are assumed to function at the thermodynamic limit for energy generation and biomass production given system constraints (Bryant et al., 1977; Thauer et al., 2008; McInerney et al., 2009; Kato and Watanabe, 2010). When one metabolism is obligately coupled to another through interspecies H_2, formate, or electron transfer, organisms must persist by sharing the overall free energy of the reaction (Kato and Watanabe, 2010). Therefore, syntrophic physiology plays an important role in microbial communities dominated by fluctuations in nutrient availability and stress, where community interactions are thought to provide stability (Hansen et al., 2007).

It is well-accepted that microorganisms can exist attached to surfaces and each other, often surrounded by extracellular polymeric substances (EPS; Hall-Stoodley et al., 2004; Gross et al., 2007; Stewart and Franklin, 2008). Biofilms have been described from environments where there are liquid–solid or liquid–gas interfaces that include terrestrial and deep-sea hydrothermal features, riparian zones, ship hulls, metal pipes, saturated soils, and the human body (Hall-Stoodley et al., 2004), but much of the work to identify the driving force and genetic control over biofilm formation has been done with pure culture studies (e.g., Gross et al., 2007; Stewart and Franklin, 2008; Perez-Osorio et al., 2010; Clark et al., 2012).

The structure and function of multispecies biofilms can be more complex than monocultures, and biofilm structure from several environments has been characterized with confocal scanning laser microscopy (CSLM) using fluorescence *in situ* hybridization (FISH) and immunofluorescence (Møller et al., 1998; Hall-Stoodley et al., 2006; Al-Ahmad et al., 2009; Stams and Plugge, 2009; Jakubovics, 2010; Zijnge et al., 2010). We have recently shown that the structure of a mixed biofilm community is dependent upon the nature of the interactions (i.e., cooperative or competitive) and that the degree of intermixing of two-member communities is greater during cooperation versus competition (Momeni et al., 2013). The dependence of biofilm structure on function has also been demonstrated in a dual culture system where commensal biofilm cells interacted closely in mixed microcolonies, while non-commensals formed separate non-interacting biofilm micro-colonies (Nielsen et al., 2000). Despite the ubiquity of biofilms and importance of anaerobes, little work has been done to understand how biofilm structure affects function in anaerobic microbial communities (Raskin et al., 1996; Nielsen et al., 2000; Brenner and Arnold, 2011; Bernstein et al., 2012).

While interactions between SRB and methanogens have been studied, very little has been done to characterize the emergent properties of interactive populations in anaerobic biofilms. The purpose of this work was to characterize the relationship between biofilm structure and function in biofilm formed by a SRB and a hydrogenotrophic methanogen cultured syntrophically under nutrient limitation and nutrient excess conditions (i.e., carbon source and electron donor/acceptor). We hypothesized that a biofilm would be functionally more efficient in terms of product formation (i.e., CH_4) compared to populations in the bulk aqueous phase. A system was developed for anaerobic continuous culture where biofilm and planktonic growth phases could be monitored to determine the difference in biomass yield per mass flux of lactate and methane under varying conditions. To compare the biomass yield of biofilm to the biomass yield of planktonic cocultures, we removed the biofilm from a series of reactors, and in another experiment, used a biofilm deficient mutant coculture.

MATERIALS AND METHODS

CULTURE CONDITIONS

Desulfovibrio vulgaris ATCC 29579 and *Methanococcus maripaludis* S2 (DSM 14266) were continuously cultured in modified 1L CDC reactors (BioSurface Technologies Corp., Bozeman, MT, USA) for anaerobic biofilm growth (Figure S1B). Biofilm coupon holders were modified to hold glass microscope slides cut to 7.6 cm X.8 cm as previously described (Clark et al., 2012). Both monocultures and cocultures were grown in coculture medium (CCM), a bicarbonate buffered, basal salts medium without choline chloride (Walker et al., 2009). Monoculture *D. vulgaris* medium was supplemented with 25 mM sodium sulfate, or grown in standard lactate-sulfate medium (LS4D) with 30 mM lactate and 25 mM sodium sulfate as previously described Clark et al. (2006). Headspace (290 mL) was purged at 20 mL/min with anoxic 80% N_2:20% CO_2 (v/v) for coculture and monoculture *D. vulgaris* or 80% H_2:20% CO_2 for monoculture *M. maripaludis* through a 0–20 SCCM mass controller (Alicat Scientific, Tucson, AZ, USA). Reactors were maintained at 30°C with stirring at 80 rpm. The reactor aqueous phase (375 mL) was inoculated with 20 mL of mid-exponential phase planktonic cultures grown from glycerol freezer (–80°C) stocks in 40 mL of CCM in 125 mL serum bottles. Fresh CCM in a 20 L glass carboy was continuously sparged with sterile anoxic 80% N_2:20% CO_2 and supplied at a dilution rate of $0.017\ h^{-1}$ starting after 48 h of batch growth by a Masterflex L/S pump (Cole-Parmer Instruments Co., Vernon Hills, IL, USA). Batch monoculture *M. maripaludis* was grown in Balch tubes in 5 mL of CCM with 30 mM acetate in lieu of lactate, prepared under 80% N_2:20% CO_2, and then pressurized after autoclaving to 200 kPa with 80% H_2:20% CO_2.

GAS CHROMATOGRAPHY

Gas measurements were made by automated injections (250 ms) of reactor headspace via a 16-port stream selector (Vici-Valco Instruments Co. Inc., Houston, TX, USA) to a 490microGC (Agilent Technologies Inc., Santa Clara, CA, USA) equipped with dual channels and dual thermal conductivity detectors. Molsieve5A and PoraplotQ (both 10 m) columns were run with Helium carrier gas at 145 kPa and 80°C with injectors at 110°C and heated sample line at 40°C. The CDC reactor lids were fitted with stainless steel fittings (Swagelok, Idaho Falls, ID, USA) to accommodate 1/16" PEEK tubing to the stream selector. Scotty calibration gasses were used as standards (Air Liquide America Specialty Gases, Plumsteadville, PA, USA).

FLUORESCENCE *IN SITU* HYBRIDIZATION

Fluorescence *in situ* hybridization was used on scraped biofilms to determine relative biovolume of each cell type. Whole biofilm on the glass coupon was fixed in 4% paraformaldehyde in a 50 mL conical tube for 3 h at 4°C, then scraped into a well on a Teflon coated slide (Paul Marienfeld GmbH & Co. KG, Lauda-Königshofen, Germany). Dried biofilm was dehydrated and hybridized in buffer solution containing 180 μL 5 M NaCl, 20 μL 1 M Tris HCl, 449 μL double deionized (dd) H_2O, 1 μL 10% SDS and 350 μL deionized formamide (final concentration 35%) with 3 ng each of probes EUB338 (GCT GCC TCC CGT AGG AGT) double labeled with Cy3 and ARCH915 (GTG CTC CCC CGC CAA TTC CT) double labeled with Cy5 for 4 h at 46°C in a humid chamber (Stoecker et al., 2010). Samples were washed in prewarmed washing buffer containing 700 μL 5 M NaCl, 1 mL 1 M TrisHCl, 500 μL 0.5 M EDTA and raised to 50 mL with ddH_2O, at 47°C for 10 min, then dipped in ice cold ddH_2O and quickly dried with compressed air. Samples were mounted with Citifluor AF1 antifadent (Citifluor Ltd., Leicester, UK) for CLSM. 3D-FISH (Daims et al., 2006) was used to determine colocalization patterns on intact, unscraped biofilm. For 3D-FISH, whole fixed biofilm on the glass coupons was embedded in polyacrylamide prior to dehydration (Daims et al., 2006; Brileya et al., 2014).

CONFOCAL LASER SCANNING MICROSCOPY

Fluorescently labeled biofilm was imaged using a Leica TCS SP5 II inverted confocal laser scanning microscope with 488, 561, and 633 nm lasers and appropriate filter sets for Cy3 and Cy5. Polyacrylamide-embedded whole biofilm for 3D-FISH and fluorescently stained hydrated biofilm were imaged on a Leica TCS SP5 II upright confocal laser scanning microscope using a 63x 0.9 NA long working distance (2.2 mm) water dipping objective (Leica Microsystems, Exton, PA, USA).

5-CYANO-2,3-DITOLYL TETRAZOLIUM CHLORIDE (CTC) STAINING

Biofilm metabolic potential was assessed using the redox stain 5-cyano-2,3-ditolyl tetrazolium chloride (CTC). Whole hydrated biofilm coupons were removed in an anaerobic chamber and incubated in freshly prepared anoxic 0.05% CTC solution for 2 h as in Stewart et al. (1994). The reaction was stopped with 5% formaldehyde and rinsed with ddH_2O. Hydrated biofilm was stained with 1 μg/mL DAPI for 20 min in the dark and rinsed with ddH_2O before CLSM.

CELL COUNTS AND BIOFILM RELATIVE ABUNDANCE

One milliliter of planktonic phase was fixed in formaldehyde (final concentration 2%) overnight then diluted as necessary and stained for 20 min in the dark with an equal volume of filtered 0.3g/L Acridine Orange. Stained samples were collected through a filter chimney on a black polycarbonate track-etched isopore filter (EMD Millipore Corp., Billerica, MA, USA) and imaged on a Nikon Eclipse E800 microscope with a mercury bulb for fluorescence. At least ten random fields of view were analyzed and cells were counted via integrated morphometry analysis in MetaMorph version 7.6 (Molecular Devices, Sunnyvale, CA, USA).

Biofilm relative abundance (biovolume) was determined using thirty CLSM images per sample, captured from random locations in x, y, and z planes. MetaMorph was used to measure the thresholded area of the two channels in each image.

PROTEIN NORMALIZATION

One *M. maripaludis* cell and one *D. vulgaris* cell are not the same shape or volume, so average biomass (protein) per cell was determined using monocultures. Biological duplicates of each monoculture were grown to late exponential phase in 125 mL serum bottles. One portion was filtered and dried to determine dry weight per cell. The Lowry protein assay was done in triplicate on each culture to determine protein biomass weight per volume. Additionally cells were fixed and stained for counting as described above. Twenty fields of view were analyzed for each culture to determine cell number per volume and area per cell using MetaMorph version 7.6 software (Figure S2). Protein per cell area was observed to be equivalent in both cell types on average, so no correction factor was applied when determining the fraction of biofilm biovolume contributed by *M. maripaludis* and *D. vulgaris*. Total protein per cell was found to be skewed toward one cell of *D. vulgaris* containing more protein than one cell of *M. maripaludis* (Figure S2). Therefore when a total planktonic protein measurement was related to cell counts of each population, a correction factor was also applied where 40% of one protein unit was attributed to *M. maripaludis* and 60% to *D. vulgaris*.

1-D BIOFILM ACCUMULATION MODEL

Diffusion in the biofilm was modeled using a biofilm accumulation model (BAM; Wanner and Gujer, 1986) to predict effects of biofilm thickness, inlet substrate concentration, and volumetric flow rate on methane production and cell ratios. Input parameters are listed in Table S1. Rate coefficients for substrates were K_s 1̲ while stoichiometric coefficients were 1/yield. Yields were calculated based on Gibbs Free Energies for the associated half reactions normalized to one electron. Aqueous diffusion coefficients (D_{aq}) at 25°C for substrates (Stewart, 2003) were corrected to 30°C using D_{30}/D_{25} 1̲.135. D_{aq} of lactate was calculated as in Wilke and Chang (1955):

$$\frac{\underline{D_L\mu}}{T_{abs}} = \frac{-7.4\times10^{-8}(XM)^{0.5}}{V_b^{0.6}}$$

Biofilm accumulation model allows for input of a ratio of the effective diffusion coefficient to the aqueous diffusion coefficient (D_e/D_{aq}) which is then applied to all solutes to account for the decreased diffusion observed in the biofilm matrix compared to water.

ELECTRON MICROSCOPY

Micrographs in **Figures 1A,C,D** and 3 were collected on a Zeiss Supra55VP FE-SEM. Biofilm was fixed in a solution of 2% paraformaldehyde, 2.5% glutaraldehyde and 0.05 M Na-cacodylate overnight at room temperature. Coupons were rinsed and stepwise dehydrated in ethanol before being cut and critical point dried on a Samdri-795 (Tousimis Research Corporation, Rockville, MD, USA). Glass pieces with dry biofilm were mounted on SEM stubs with double-sided carbon tape and silver, then sputter coated with Iridium for 35 s at 35 mA.

Figure 1B was unfixed biofilm scraped directly onto double-sided carbon tape, frozen while hydrated in liquid N_2, splutter-coated with Platinum for 2 min, and imaged using a dual beam focused ion beam (FIB)-FE-SEM (Helios NanoLab, FEI Company, Hilsboro, OR, USA) equipped with a cryostage.

SAMPLE COLLECTION AND ANALYSIS

Reactor outflow was collected on ice and measured daily to monitor flow rate. Samples of the planktonic phase were collected at the outflow for optical density at 600 nm (OD), high performance liquid chromatography (HPLC), protein measurements, and direct cell counts. Filtered samples were analyzed in triplicate with a fucose internal standard, for lactate, acetate, and formate concentrations via HPLC (Agilent 1200 series) equipped with a BioRad Aminex HPX-87H column. Lactate and formate concentration were measured with a VWD detector while acetate concentration was measured with an RID detector. Planktonic cultures were centrifuged at 6,000 *g* for 10 min and the whole cell pellet was analyzed for protein, hexose, pentose, and uronic acid composition. Biofilm samples for these analyses were collected by aseptically replacing a biofilm coupon with a sterile butyl stopper, and scraping the biofilm into sterile water with a spatula. Whole biofilm was analyzed for protein and carbohydrates. Protein concentrations were determined with the Lowry et al. (1951) assay using bovine serum albumin as the standard. Hexose sugars were measured by the colorimetric cysteine–sulfuric acid method with glucose as the standard. Pentose sugars were measured with a colorimetric orcinol-$FeCl_3$ assay with xylose as the standard. A colorimetric carbazole assay was used to measure uronic acid concentration with D-galacturonic acid as the standard (Chaplin and Kennedy, 1994).

RESULTS

BIOFILM STRUCTURE AND COMPOSITION

Monocultures of *D. vulgaris* formed biofilm on silica slides under continuous culture conditions when sulfate was provided as an electron acceptor (**Figures 1A,C**). Monoculture *M. maripaludis* did not form a biofilm on silica slides when grown in continuous culture supplemented with H_2, as observed with protein assay, light microscopy, and scanning electron microscopy. Material was observed on the glass slides but was confirmed to be salts via energy dispersive X-ray spectroscopy and not protein or carbohydrate (data not shown).

When *D. vulgaris* and *M. maripaludis* were cocultivated with lactate (without sulfate and H_2), methane was produced and biofilm was formed. The coculture biofilm had an altered appearance and structure compared to monoculture *D. vulgaris* biofilm (compare **Figures 1A to 1B** and **1C to 1D**) and *M. maripaludis* cells were observed in both the biofilm and planktonic phases. These results indicate that the methanogen was dependent upon *D. vulgaris* under the tested conditions to grow in a biofilm state.

The protein and carbohydrate levels were compared for different growth conditions (cell-associated carbohydrate levels were normalized to protein biomass). As previously reported, *D. vulgaris* does not produce an extensive carbohydrate-rich biofilm on

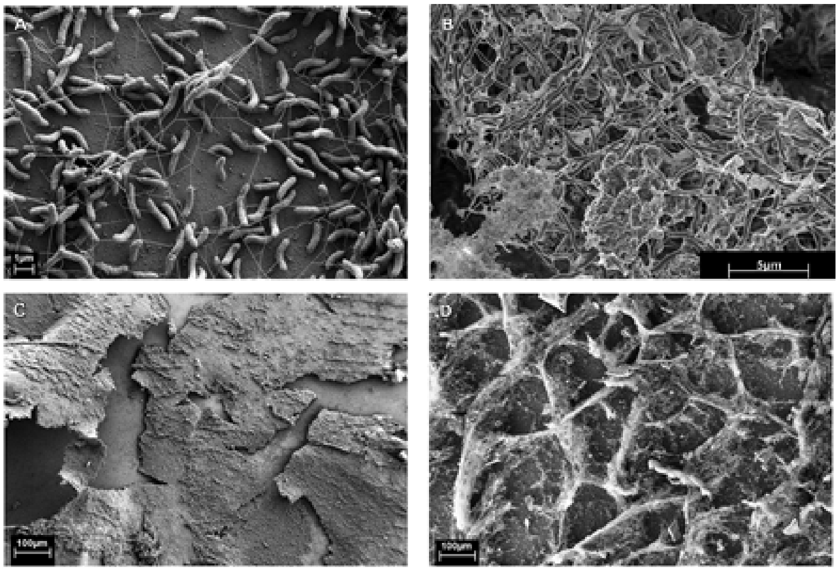

FIGURE 1 | Monocultures of **(A,C)** *Desulfovibrio vulgaris* biofilm from continuous culture (5,420X and 101X, respectively). **(B,D)** Coculture biofilm of *D. vulgaris* and *M. maripaludis* (10,000X and 100X, respectively).

glass slides (Clark et al., 2007), but in CCM, *D. vulgaris* produced slightly increased levels of hexose and pentose equivalents compared to growth in LS4D medium (**Figure 2**). The uronic acid levels were similar for *D. vulgaris* when grown in LS4D or CCM (**Figure 2**) under the tested conditions. In the coculture biofilms, the uronic acid levels were similar while hexose and pentose levels were slightly decreased compared to *D. vulgaris* monocultures in CCM (**Figure 2**). The reported values were lower than previous reports for other monoculture and multispecies biofilm EPS that can constitute as much as 90% of the dry mass of a culture (Flemming and Wingender, 2010; Poli et al., 2010). Lack of extracellular material might present less mass transfer resistance to H_2 diffusion and would therefore be beneficial to both organisms. As noted above, *M. maripaludis* did not form monoculture biofilm under the tested conditions; however, *M. maripaludis* did form a pellicle when grown in static tubes as a monoculture. The *M. maripaludis* pellicle had approximately 10-fold more uronic acid, 7-fold more hexose, and 30-fold more pentose compared to coculture biofilm (**Figure 2**). These results suggest that *M. maripaludis* had altered carbon flow that resulted in less carbon allocation to EPS.

COCULTURE BIOFILM DEVELOPMENT AND STRUCTURE

Coculture biofilm was initiated by *D. vulgaris,* which formed a monolayer during the initial 48 h of batch mode in the continuous culture system (**Figures 3A,D**). At this early time point (0 h, initiation of flow) *D. vulgaris* out-numbered *M. maripaludis* in the biofilm 32:1, while the planktonic phase ratios of *D. vulgaris* to *M. maripaludis* were 2.7:1 (**Table 1**). After 48 h of continuous culture the biofilm grew in ridges, both normal and parallel to flow caused by liquid agitation (**Figures 3B,E**). Cell ratios in the biofilm decreased rapidly to 3.5:1 after 48 h as *M. maripaludis* cells were incorporated into the biofilm and grew, while planktonic ratios increased slightly to an average of 3.2:1. After 240 h, steady-state ratios of cells in the biofilm remained approximately 2.2:1 with similar planktonic ratios of 1.6:1 (**Table 1**). This is in contrast to the published 4:1 ratios observed in planktonic-only reactors for the same syntrophic pair under lactate-excess conditions and our own observation of 6.3:1 in planktonic phase-only reactors (**Table 1**; Stolyar et al., 2007; Walker et al., 2009, 2012). These results indicate that four times more *D. vulgaris* are typically needed to oxidize enough lactate to generate sufficient H_2 for *M. maripaludis* in the bulk aqueous phase; however, in the presence of biofilm, a more even distribution (approximately 2:1) of interacting populations was sustained in both the biofilm and planktonic phases.

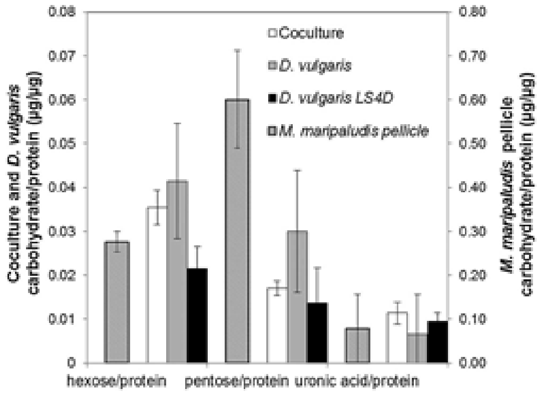

FIGURE 2 | Biofilm carbohydrate composition normalized to protein biomass for hexose, pentose, and uronic acid in continuous culture biofilm (coculture and *D. vulgaris* monoculture, primary axis) and batch *M. maripaludis* pellicle (secondary axis). Error bars represent 95% confidence interval. Coculture in CCM *n* = 6, *D. vulgaris* in CCM *n* = 4, *D. vulgaris* in LS4D *n* = 8, *M. maripaludis* batch pellicle in CCM *n* = 3.

Coculture biofilm macrostructure was observed with both fixed and unfixed, still hydrated biofilm (**Figures 1D** and **3C,F**). The structured biofilm included tall ridges and spires with deep valleys, often 300–400 μm tall, but always with at least one dimension <50 μm as measured by fluorescence microscopy of intact hydrated biofilm or cryosections of frozen hydrated biofilm (**Figure 3F**). Notably, the macrostructure was not observed in *D. vulgaris* monoculture biofilms grown in LS4D medium (Clark et al., 2007) nor in CCM (**Figures 1A,C**). The critical biofilm thickness that would allow for diffusion of 30 mM lactate to the substratum was estimated to be 50 μm, as predicted by a 1D BAM (Figure S3 and Table S1). These results suggest that the macrostructure was influenced by lactate diffusion limitation. Microcolonies of *M. maripaludis* cells were spread throughout a matrix of *D. vulgaris* cells with an intermixed pattern. Cell association in the structured biofilm was observed to be random with no pattern of colocalization detectable (Figure S4). It has recently been shown that increased intermixing is a marker of cooperation (Momeni et al., 2013), so it is reasonable that this cooperative community was highly intermixed.

BIOFILM AND PLANKTONIC COMMUNITY FUNCTION: THE BASE CASE

The base case represents the standard syntrophic system described above that contained a structured biofilm and a planktonic phase in continuous culture. Little, if any previous work has been done to characterize syntrophic interactions with interacting biofilm and planktonic phases, so a baseline understanding of function (CH_4 and H_2 production and lactate consumption) was necessary to determine a basal state under the tested conditions. During the first 100 h of biofilm development, methane levels increased as lactate levels declined with an equimolar increase in acetate (**Figure 4A**). The biofilm population was 78% *D. vulgaris* and 22% *M. maripaludis* (3.5:1) with similar planktonic population distribution (**Table 1**). During the next 50 h, the system approached a steady-state in which all 30 mM of lactate was consumed, and both organisms in both phases of the reactor increased rapidly in number. As lactate became limiting, the OD and methane concentration peaked for one retention time of the reactor, and then declined to a steady-state. The methane concentration stabilized but OD continually decreased while biofilm biomass increased for another 100 h after lactate was not detectable. These results indicate that biofilm cells were competitive for bulk-phase lactate, and that the biofilm growth mode contributed to more efficient, multi-species substrate utilization.

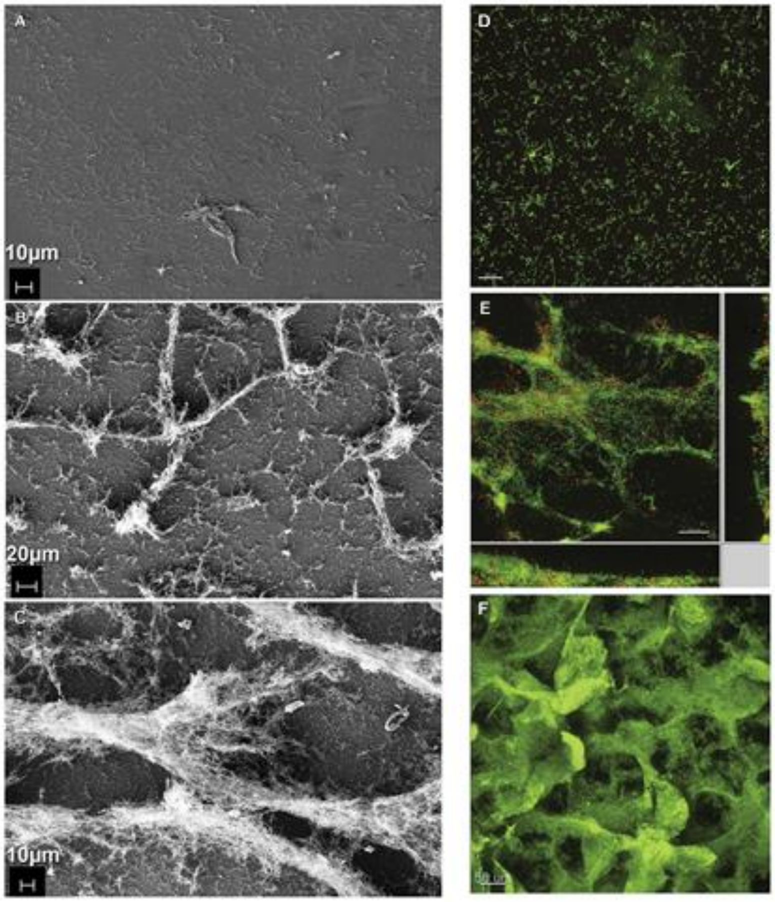

FIGURE 3 | Formation of coculture biofilm over time. (A–C) Electron micrographs of fixed coculture at **(A)** early (386X, 0 h; **B**) intermediate (243X, 48 h; **C**) steady-state (336X, 240 h) time points. **(D–F)** Fluorescence micrographs of coculture biofilm **(D,E)** embedded in polyacrylamide and hybridized with domain-specific oligonucleotide probes labeled green for *D. vulgaris* and red for *M. maripaludis* at **(D)** early (0 h) and **(E)** intermediate (48 h) time points. **(F)** Intact hydrated biofilm unfixed and stained with Acridine Orange at steady-state (240 h).

This is further demonstrated in that H_2 was not detectable in the reactor headspace at any point. Walker et al. (2009) observed a spike (50 Pa) followed by a constant low level of H_2 (less than 10 Pa) at steady-state when a planktonic-only system was not limited for lactate. Presumably all H_2 produced in our biofilm reactor was efficiently consumed. It should also be noted that H_2 was not detected when the lactate loading rate was increased (discussed below).

In aerobic biofilms, it has been shown that cells near the substratum can be limited in oxygen and metabolically inactive, i.e., not all the biofilm biomass is active (Xu et al., 2000). To assess the metabolic state of the syntrophic biofilm, intact, steady-state coculture biofilm was incubated with CTC (Stewart et al., 1994). The validity of this method for anaerobes has been debated with the primary concern that CTC is abiotically reduced in the presence of sulfide and cysteine (Stewart et al., 1994; Gruden et al., 2003; Halan et al., 2012). CT-formazan granules formed abiotically are poorly localized and rapidly photo-bleach, while CT-formazan of biogenic origin is an intracellular granule that is more resistant to photo-bleaching (Gruden et al., 2003). CCM contains 1 mM each of sodium sulfide and cysteine, but the biofilm was rinsed anoxically prior to staining in an anaerobic glovebag. The incubated biofilm was directly observed with CSLM, and the biofilm biomass showed respiratory potential based on formation of CT-formazan. However, portions of the intact biofilm were not visible via CSLM due to depth limitations (**Figure 5A**), therefore the biofilm was scraped for visualization (post-staining). Upon inspection of scraped biofilm, the entire biofilm biomass was stained (**Figures 5B,C**), and reduced CT-formazan granules could be observed in nearly all cells, localized inside the cell

Table 1 | Percent of *M. maripaludis* and *D. vulgaris* cells in planktonic and biofilm phases over time [row 1 early (0 h), 2 intermediate (48 h), 3 steady-state (240 h)] in a reactor containing both growth phases, a reactor where biofilm has been removed (row 4), a reactor with an increased loading rate (row 5), and a reactor containing a coculture of **A**pilA mutant *D. vulgaris* with wild-type *M. maripaludis* (row 6).

Rows		% *M. maripaludis* biofilm	% *D. vulgaris* biofilm	% *M. maripaludis* planktonic	% *D. vulgaris* planktonic
1	Biofilm and planktonic early	3% ± 0.8	97% ± 0.8	26% ± 13.7	69% ± 11.1
2	Biofilm and planktonic intermediate	22% ± 1.5	78% ± 1.5	23% ± 12.1	73% ± 10.6
3	Biofilm and planktonic steady state	31% ± 1.4	69% ±1.4	36% ±10.8	59% ±2.2
4	WT planktonic only	0	0	13% ± 1.9	82% ± 1.9
5	Biofilm and planktonic increased loading rate	18% ± 1.5	82% ± 1.5	22% ± 5.9	73% ± 3.3
6	,0,pilA planktonic only	0	0	19% ± 1.4	81% ± 1.4

Error is the 95% confidence interval. The number of images analyzed for each time point is early n = 146, intermediate n = 269, steady-state n = 2,118, biofilm removed n = 140, increased loading rate n = 174, and ,0,pilA n = 120.

with persistent fluorescence. These results indicate that the entire steady-state biofilm biomass retained respiratory potential and was metabolically active. The same results were obtained using FISH, where all biofilm cells exhibited strong fluorescence irrespective of location, and these results corroborated the idea that all cells were active (**Figure 5D**).

INCREASED LOADING RATE

To test the effect of a sudden input of nutrients on a stable community, the dilution rate was increased after 341 h to 0.109 h^{-1} (approximately 6-fold) in a biofilm reactor in steady-state. Methane levels increased within 1 h and peaked at ∼0.17 mM after 27 h (**Figure 4A**). The optical density increased slightly and then declined to just below steady-state levels, with an ∼20% decrease of *D. vulgaris* cells and ∼15% decrease in *M. maripaludis* cells in the planktonic phase based on cell counts. The system was monitored for four retention times (RT=9.9 h) with biofilm samples removed after 48 h, and the decreased planktonic biomass is likely a result of washout. The doubling time of *D. vulgaris* in CCM supplemented with sulfate is approximately 20 h ($k = 0.04\ h^{-1}$) while the doubling time of *M. maripaludis* with unlimited H_2 in CCM is 5 h ($k = 0.14\ h^{-1}$). Under these conditions as *D. vulgaris* was washed out of the reactor, H_2 was not produced at a rate that would allow the methanogen to divide before the entire reactor was turned over in 9.9 h. The total amount of biomass in the reactor did not change with increased loading, and while the planktonic populations began to washout, biomass was balanced by growth in the biofilm (**Figure 6B**). Under these conditions, biomass distribution in the biofilm shifted toward a greater percentage of *D. vulgaris* that increased by nearly 25% from 16.5 to 20.0 mg (**Figure 6B**), and this resembled pre-steady-state (i.e., when lactate was not entirely consumed) population structure most likely as a result of the increased loading rate for lactate (3 mM h^{-1}; **Table 1**). Despite the altered population ratio, the macrostructure of the biofilm remained similar to the steady-state structure (lactate loading rate 0.5 mM h^{-1}) with a *D. vulgaris* matrix intermixed with *M. maripaludis*.

In spite of lactate-excess, H_2 was still undetectable (limit of detection ∼ 0.0001 mM or 0.25 Pa) when the loading rate was increased. This is contrary to published results for excess lactate planktonic-only conditions where H_2 was continually 5–10 Pa at steady-state (Walker et al., 2009). These results suggest that the presence of biofilm caused a more efficient consumption or transfer of the produced H_2 gas between *D. vulgaris* and *M. maripaludis*. Biomass yield per methane produced (mg protein/mM CH_4) was significantly lower in lactate-excess conditions than in lactate-limited conditions (**Figure 6A**) and the same was true for biomass yield per lactate mass flux (mg protein/mM h^{-1} lactate). Essentially the same amount of biomass or carrying capacity was actively maintained under both conditions (i.e., lactate-excess versus lactate-limited) but the population distributions were different, and biofilm was able to increase metabolic flux without an increase in biomass. The carrying capacity, K, is defined as the maximum potential population size a given landscape is capable of supporting and is a common attribute used to describe population dynamics in ecology (Stilling, 2003; Berck et al., 2012). When additional lactate was available via an increased loading rate, the system was perturbed (washout of planktonic biomass) but the total biofilm biomass increased (**Figure 6B**). The total carrying capacity thus remained the same even though the population distribution and metabolic flux changed under lactate-excess conditions.

BIOFILM REMOVAL

In a separate biofilm reactor at steady-state, the biofilm coupons were removed after 432 h (**Figure 4B**) to test the stability and population structure of the planktonic community in the absence of biofilm. Upon biofilm removal, the planktonic optical density increased within 24 h, but methane levels did not increase for 50 h (**Figure 4B**). After a 50-h static period, methane concentrations increased rapidly but declined back to original steady-state levels (15 h time period). Lactate and H_2 were not detected, the OD increased, and similar levels of methane

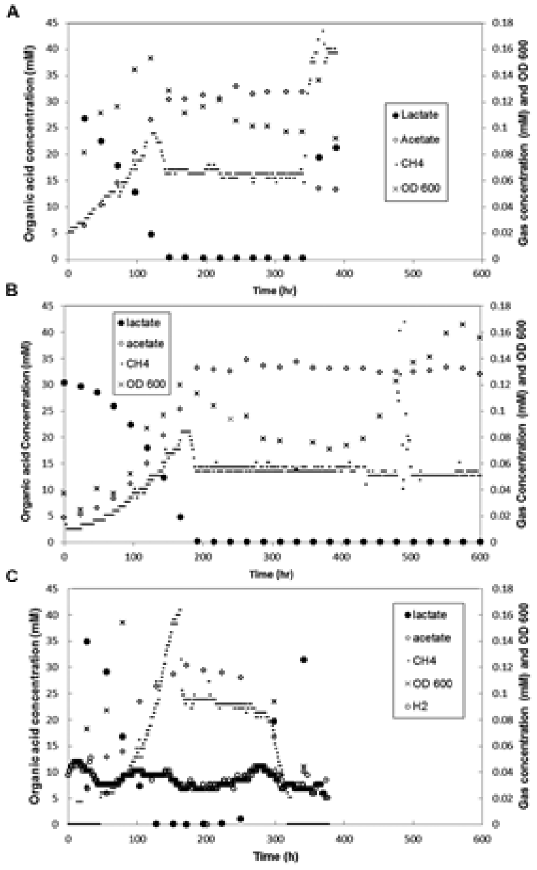

FIGURE 4 | Metabolite concentration over time in coculture biofilm reactors (A) with both biofilm and planktonic phases in which loading rate was increased at 341 h, (B) that had biofilm coupons removed at 432 h (C) grown with ,0,*pilA* mutant *D. vulgaris* and wild-type *M. maripaludis*. Each graph is representative of one of two duplicate experiments.

were produced as the system attempted to reach a new steady-state. The planktonic-phase only reactor population was 82% *D. vulgaris* but both *D. vulgaris* and *M. maripaludis* increased in absolute number based on cell counts and OD (**Table 1** and **Figure 4B**). Although 1.4 times greater biomass was maintained in the planktonic phase alone than the planktonic phase of the base case, the total reactor biomass was 3.4 times lower than the total biofilm plus planktonic biomass in the base case reactor (**Figure 6B**). The biomass yield was significantly lower than in the base case, and similar to total biomass yields in lactate-excess conditions (**Figure 6A**). Without a biofilm community, the carrying capacity of the system was significantly reduced under lactate-limiting conditions and the population distribution was less even.

To further investigate the role of biofilm in carrying capacity and stability, a mutant *D. vulgaris*, ,0,*pilA*, was grown in coculture with wild-type *M. maripaludis*. The ,0,*pilA D. vulgaris* lacks a presumptive type IV pilus and is deficient in biofilm formation (Figure S5). In batch coculture experiments, total methane production and growth were the same as wild-type coculture (data not shown). However, in continuous culture, the ,0,*pilA* coculture did not form biofilm and the coculture grew as a planktonic-phase with similar levels of methane produced compared to wild-type coculture (0.09 mM at steady-state; **Figure 4C**). At 175 h, the biomass yield of ,0,*pilA* coculture was similar to the planktonic-only wild-type coculture reactor (**Figure 6A**), and the total biomass was slightly higher than planktonic-only wild-type coculture (**Figure 6B**) with a similar distribution of *D. vulgaris* (**Table 1**). However, the mutant coculture did not stabilize and completely washed out of the reactor within 400 h (**Figure 4C**). In addition, in contrast to wild-type, H_2 was detectable (50–120 Pa) over the whole 350 h of continuous culture until cells were too few to count in the planktonic phase (**Figure 4C**). This result further demonstrates the role of biofilm structure in facilitating and stabilizing syntrophic interactions. In the absence of biofilm (either physically removing the biofilm or biofilm deficient coculture), the community was not stable, H_2 production and consumption were not balanced, and the carrying capacity declined for the methanogen.

In another δ-*Proteobacterium*, *Geobacter sulfurreducens*, PilA has been shown to be involved in extracellular electron transfer and biofilm formation (Richter et al., 2012), while in an aerobic δ-*Proteobacterium*, *Myxococcus xanthus*, PilA was shown to interact with biofilm EPS (Wei et al., 2012). Further work is needed to determine the role of type IV pili in facilitating interactions between SRB and hydrogenotrophic methanogens, but it seems likely that the pilus functions in attachment of cells to surfaces (biotic or abiotic) that directly or indirectly facilitates metabolic exchange.

DISCUSSION

The primary objective of this work was to characterize the relationship between function and structure of a syntrophic biofilm community. Previous work suggests that specific structural patterns can be expected in interacting communities (Nielsen et al., 2000; Gu et al., 2013; Momeni et al., 2013), and that these patterns are dependent upon the nature of the interaction. We observed a structured syntrophic biofilm with complex ridges and channels, where both partners were highly intermixed. Similar biofilm structures have been observed in mixed communities and are also presumed to be a direct result of interaction type (Nielsen et al., 2000; Molin and Tolker-Nielsen, 2003), so it is reasonable to expect that structure affects community function and vice versa. Several results reported here indicate that syntrophic lactate oxidation and transfer of the H_2 intermediate dictated the biofilm structure. Biofilm structures were never observed to exceed 50 μm in at least one dimension, and the BAM for this community predicted that biofilm thicker than 50 μm would experience lactate diffusion limitation at the substratum. These results suggest that lactate diffusion governed *D. vulgaris* biofilm structure. This type of structure would also have the same positive effect on H_2 diffusing away from the SRB, where a buildup of the inhibitory by-product would prevent further lactate oxidation. Monoculture

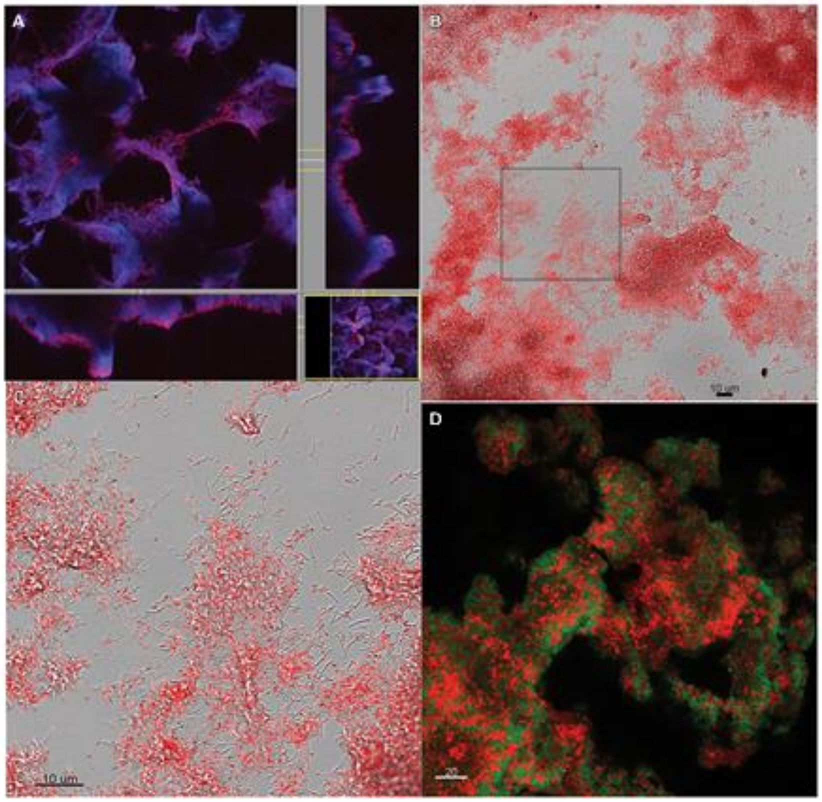

FIGURE 5 | Coculture biofilm (A) stained with CTC while intact and hydrated and showing all biomass stained with DAPI in blue, and CTC in red, or purple where both DAPI and CTC are present (B) scraped from the slide after CTC staining. (C) Zoomed in from the inset in (B) showing individual grains of red fluorescent CT-formazan in each cell. (D) Coculture biofilm scraped from the substratum, fixed and hybridized with domain-specific probes for *D. vulgaris* (green) and *M. maripaludis* (red).

biofilms of *D. vulgaris* grown with sulfate and lactate similarly form only thin biofilms, yet they do not form tall structures in the way that syntrophic *D. vulgaris* does. These results suggest that syntrophic interactions drive the observed structural features.

When we consider the structure–function relationship from the point of the methanogen, the results suggest that the biofilm structure was driven by H_2. In monoculture with H_2, *M. maripaludis* did not form biofilm, however, when grown syntrophically the methanogen did join the H_2-producing SRB biofilm. While it is possible that *D. vulgaris* biofilm simply provided a more suitable surface for attachment of *M. maripaludis*, it is also very likely that H_2 drove the interaction specifically. We have recently shown chemotaxis toward H_2 gas (hydrogenotaxis) in *M. maripaludis* (Brileya et al., 2013) and the response is especially strong under H_2-limited conditions. H_2 produced by SRB in the biofilm could diffuse to the aqueous and gas phases of the reactor, making it possible for planktonic *M. maripaludis* to scavenge the energy source without joining the biofilm. In spite of this option, more methanogen biomass was observed in the biofilm than the planktonic phase, whenever biofilm was present in the system. This suggests that some benefit is gained by interacting directly or closely with the SRB in the biofilm. These observations are supported by the lack of H_2 detected during cultivation of wild-type populations as coculture biofilm. The results of the mutant coculture experiment further support a benefit from close interaction, since the mutant SRB lacked a pilus that presumably helped interactions directly through attachment or motility in the biofilm. The lack of direct interaction in biofilm resulted in detectable H_2, and therefore inefficient transfer of the intermediate. It was recently shown that motility is an important determinant for structuring mixed biofilms when a motile *Bacillus* could infiltrate a *Staphylococcus* biofilm (Houry et al., 2012).

Analysis of cell-associated carbohydrates showed that *M. maripaludis* likely reallocates carbon in the syntrophic biofilm, given that the coculture biofilm had 10-fold less cell-associated carbohydrate than a monoculture *M. maripaludis* pellicle. One

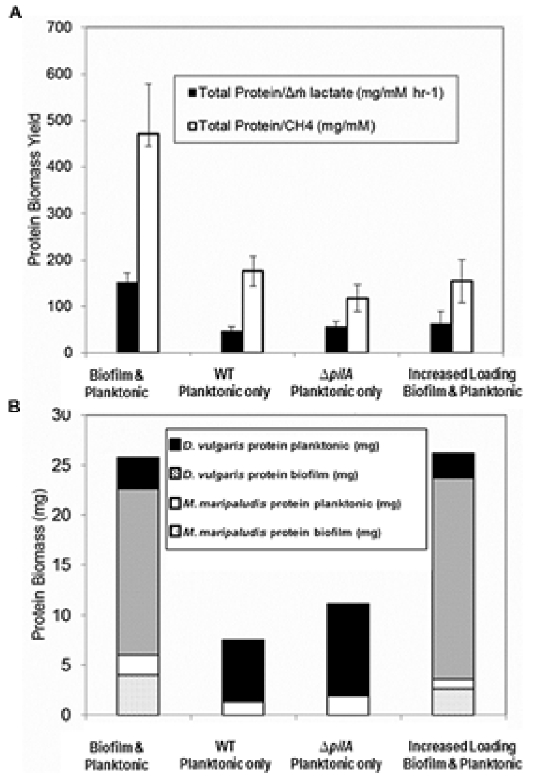

FIGURE 6 | (A) Biomass yield per lactate mass flux and per methane for reactors containing coculture with biofilm and planktonic phases (base case; $n = 8$), planktonic phase only after biofilm was removed ($n = 14$), ,0,*pilA* mutant coculture planktonic phase only ($n = 7$), and both biofilm and planktonic phases at an increased loading rate ($n = 2$). Error bars represent 95% confidence interval. **(B) Biomass distribution of each cell type in biofilm and planktonic phases for the same culture conditions based upon cell volume ratios and cell counts respectively.** Unpaired two-tailed *t*-test results indicate total protein/0,ṁ lactate difference is significant between coculture biofilm and planktonic (base case) versus all other conditions ($p < 0.005$), but that planktonic only versus increased loading rate is not significant ($p = 0.4$). Total Protein/CH_4 unpaired two-tailed *t*-test results were significant between biofilm and planktonic (base case) versus all other conditions [versus WT planktonic and ,0,*pilA* planktonic ($p < 0.005$), biofilm and planktonic (base case) versus increased loading rate ($p = 0.05$), planktonic only versus increased loading rate ($p = 0.4$)].

possible explanation is that a thick extracellular matrix would increase H_2 mass transfer resistance, so the methanogen produced less carbohydrate to facilitate in H_2 diffusion through the biofilm. Another possible explanation for altered carbon allocation is that *M. maripaludis* produced less EPS when grown as syntrophic biofilm to facilitate repositioning within the biofilm. *M. maripaludis* has only been shown to sense and swim toward H_2 gas in liquid (Brileya et al., 2013), but it has not been shown to swarm, so it remains unclear whether individuals could move through a dense EPS matrix toward a higher concentration of H_2.

Pure mutualism refers to the fact that the relationship is obligate and the growth rates of both populations are limited only by the concentrations of critical substrates produced by the partner (Meyer et al., 1975). The case of a SRB that oxidizes organic carbon to H_2 and a methanogen that consumes the H_2 is a variation that can be termed mutualism via product inhibition (Dean, 1985). Historically, microbial interactions have been studied in terms of competition for substrate and the competition coefficients are typically a ratio of the yield coefficients (Dean, 1985). Thus, stable or even unstable equilibria do not exist in terms of one population 'winning' over the other. However, these equations are based upon chemostats with only bulk-phase populations and not biofilms with inherent variability. Positive interactions could stabilize many more microbial interactions than previously thought (Shindala et al., 1965; Megee et al., 1972), particularly for biofilms. Our results support that community stability is a result of syntrophic interaction in biofilm. When lactate-loading rate was increased, causing washout conditions in the aqueous phase, biomass in the biofilm increased while planktonic biomass decreased. The washout situation highlights a complication of mutualistic interaction under flow conditions in which a population with a slower specific growth rate produces the limiting substrate of another population. Biomass retention in biofilm and close interaction represent logical ecological solutions to this problem. Community members are able to stay in a desirable location, rather than be washed away to potentially unfavorable environments. The mutant coculture could not form biofilm, and possibly close interactions, and therefore was unable to form a stable syntrophy with tight coupling between H_2 production and consumption.

Macroecologists and microbial ecologists alike have modeled mutualism to gain insight into inter-population dynamics, and results predict stability of cooperative populations under only specific density-dependent conditions (Boucher, 1988). Experiments with mutualistic microorganisms have revealed many adaptations to syntrophic relationships, including alternative electron-transport pathways, differences in gene expression patterns in the presence of a syntrophic partner, and rapid evolution resulting in optimized biomass production (Shimoyama et al., 2009; Walker et al., 2009, 2012; Hillesland and Stahl, 2010; Plugge et al., 2011; Bernstein et al., 2012; Lawrence et al., 2012; Sieber et al., 2012). In this syntrophic system, while we observed that biofilm growth mode promoted the greatest biomass retention and allowed the system to reach increased carrying capacity, we also observed that this biomass was metabolically functional, in spite of lactate limitation. CTC staining and FISH indicated that the whole biofilm biomass had respiratory potential. When additional lactate was added via an increased loading rate, the biofilm community responded within 1 h by increasing electron flux from lactate to methane. It is quite interesting to consider this result in the context of a low-nutrient environment, where it seems likely that a natural biofilm community could remain poised for episodic nutrient availability. Our results indicate that in a mixed community, syntrophs are able to rapidly cycle electrons or carbon.

In this model syntrophic system, structured biofilm promoted maximum carrying capacity, contributed to cooperative resource sharing (i.e., improved H_2 transfer) and provided greater community stability when compared to planktonic-only populations. Although both biofilms and syntrophic communities are inherently variable and heterogeneous, these culture conditions are environmentally relevant. Mixed culture biofilm reactors can be used to experimentally explore ecological and evolutionary phenomena in a more constrained setting. It remains to be seen what genetic and metabolic controls are responsible for the observed responses in this system, and future work is planned to understand how specific biofilm structures and interactions can impact meso- and macro-scale processes including greenhouse gas production, biogeochemical cycling, and waste conversion.

AUTHOR CONTRIBUTIONS

Kristen A. Brileya designed and performed experiments, analyzed and interpreted data, drafted and revised the manuscript. Laura B. Camilleri performed experiments, analyzed and interpreted data, and revised the manuscript. Grant M. Zane designed and performed experiments to create the mutant *,O,pilA D. vulgaris*, and revised the manuscript. Judy D. Wall designed experiments to create the mutant *,O,pilA D. vulgaris*, interpreted the data for this manuscript, and made critical revisions to the manuscript. Matthew W. Fields designed experiments, interpreted data, drafted and revised the manuscript.

ACKNOWLEDGMENTS

The authors are grateful for thoughtful discussions with Dr. Chris Walker, Dr. Sergey Stolyar, and Prof. David Stahl. Thanks to the Stahl laboratory for cultures of *M. maripaludis*. We are deeply indebted to Betsey Pitts for tirelessly sharing her knowledge of confocal and fluorescence microscopy and image analysis, and also to Dr. Roland Hatzenpichler and Dr. Sebastian Lücker for their suggestions and discussions about FISH and 3D-FISH. We thank Dr. Ross Carlson for the use of HPLC with much appreciated assistance from Dr. Hans Bernstein and Kris Hunt. This work was supported as a component of ENIGMA, a scientific focus area program supported by the U.S. Department of Energy, Office of Science, Office of Biological and Environmental Research, Genomics: GTL Foundational Science through contract DE-AC02-05CH11231 between Lawrence Berkeley National Laboratory and the U.S. Department of Energy. Kristen A. Brileya and Laura B. Camilleri were additionally supported by a NSF-IGERT fellowship in Geobiological Systems at Montana State University (DGE 0654336). The confocal microscope equipment used was purchased with funding from the NSF-Major Research Instrumentation Program and the M.J. Murdoch Charitable Trust. The FIB-SEM image was acquired with the help of Alice Dohnalkova and Bruce Arey through a user proposal funded by the Environmental Molecular Sciences Laboratory at Pacific Northwest National Lab. Zeiss FE-SEM images were acquired using equipment in the Image and Chemical Analysis Laboratory (ICAL) at Montana State University.

SUPPLEMENTARY MATERIAL

The Supplementary Material for this article can be found online at: http://www.frontiersin.org/journal/10.3389/fmicb.2014.00693/abstract

REFERENCES

Al-Ahmad, A., Follo, M., Selzer, A. C., Hellwig, E., Hannig, M., and Hannig, C. (2009). Bacterial colonization of enamel in situ investigated using fluorescence in situ hybridization. *J. Med. Microbiol.* 58, 1359–1366. doi: 10.1099/jmm.0.011213-0

Berck, P., Levy, A., and Chowdhury, K. (2012). An analysis of the world's environment and population dynamics with varying carrying capacity, concerns and skepticism. *Ecol. Econ.* 73, 103–112. doi: 10.1016/j.ecolecon.2011.09.019

Bernstein, H. C., Paulson, S. D., and Carlson, R. P. (2012). Synthetic *Escherichia coli* consortia engineered for syntrophy demonstrate enhanced biomass productivity. *J. Biotech.* 157, 159–166. doi: 10.1016/j.jbiotec.2011.10.001

Boucher, D. H. (1988). *The Biology of Mutualism*. New York: Oxford University Press.

Brenner, K., and Arnold, F. H. (2011). Self-organization, layered structure, and aggregation enhance persistence of a synthetic biofilm consortium. *PLoS ONE* 6:e16791. doi: 10.1371/journal.pone.0016791

Brileya, K. A., Camilleri, L. B., and Fields, M. W. (2014). "3D-Fluorescence in situ hybridization of intact, anaerobic biofilm," in *Engineering and Analyzing Multicellular Systems*, eds L. Sun and W. Shou (New York: Springer), 189–197.

Brileya, K. A., Connolly, J. M., Downey, C., Gerlach, R., and Fields, M. W. (2013). Chemotaxis toward hydrogen gas by *Methanococcus maripaludis*. *Sci. Rep.* 3, 1–7. doi: 10.1038/srep03140

Bryant, M., Campbell, L., Reddy, C., and Crabill, M. (1977). Growth of *Desulfovibrio* in lactate or ethanol media low in sulfate in association with H2-utilizing methanogenic bacteria. *Appl. Environ. Microbiol.* 33, 1162–1169.

Canfield, D. E., Stewart, F. J., Thamdrup, B., De Brabandere, L., Dalsgaard, T., Delong, E. F., et al. (2010). A cryptic sulfur cycle in oxygen-minimum-zone waters off the Chilean coast. *Science* 330, 1375–1378. doi: 10.1126/science.1196889

Chaplin, M. F., and Kennedy, J. F. (1994). *Carbohydrate Analysis: A Practical Approach*, 2nd Edn. Oxford: Irl Press.

Clark, M. E., Edelmann, R. E., Duley, M. L., Wall, J. D., and Fields, M. W. (2007). Biofilm formation in *Desulfovibrio vulgaris* Hildenborough is dependent upon protein filaments. *Environ. Microbiol.* 9, 2844–2854. doi: 10.1111/j.1462-2920.2007.01398.x

Clark, M. E., He, Q., He, Z., Huang, K. H., Alm, E. J., Wan, X. F., et al. (2006). Temporal transcriptomic analysis as *Desulfovibrio vulgaris* Hildenborough transitions into stationary phase during electron donor depletion. *Appl. Environ. Microbiol.* 72, 5578–5588. doi: 10.1128/AEM.00284-06

Clark, M. E., He, Z., Redding, A. M., Joachimiak, M. P., Keasling, J. D., Zhou, J. Z., et al. (2012). Transcriptomic and proteomic analyses of *Desulfovibrio vulgaris* biofilms: carbon and energy flow contribute to the distinct biofilm growth state. *BMC Genomics* 13:138. doi: 10.1186/1471-2164-13-138

Daims, H., Lücker, S., and Wagner, M. (2006). daime, a novel image analysis program for microbial ecology and biofilm research. *Environ. Microbiol.* 8, 200–213. doi: 10.1111/j.1462-2920.2005.00880.x

Dean, A. M. (1985). "The dynamics of microbial commensalisms and mutualisms," in *The Biology of Mutualism*, ed. D.H. Boucher (Oxford: Oxford University Press), 270–300.

Flemming, H.-C., and Wingender, J. (2010). The biofilm matrix. *Nat. Rev. Microbiol.* 8, 623–633.

Gokhale, C. S., and Traulsen, A. (2012). Mutualism and evolutionary multiplayer games: revisiting the Red King. *Proc. Biol. Sci.* 279, 4611–4616. doi: 10.1098/rspb.2012.1697

Gross, R., Hauer, B., Otto, K., and Schmid, A. (2007). Microbial biofilms: new catalysts for maximizing productivity of long-term biotransformations. *Biotechnol. Bioeng.* 98, 1123–1134. doi: 10.1002/bit.21547

Gruden, C., Fevig, S., and Abu-Dalo, M. (2003). 5-Cyano-2, 3-ditolyl tetrazolium chloride (CTC) reduction in a mesophilic anaerobic digester: measuring redox behavior, differentiating abiotic reduction, and comparing FISH response as an activity indicator. *J. Microbiol. Methods* 52, 59–68. doi: 10.1016/S0167-7012(02)00134-3

Gu, H., Hou, S., Yongyat, C., De Tore, S., and Ren, D. (2013). Patterned biofilm formation reveals a mechanism for structural heterogeneity in bacterial biofilms. *Langmuir* 29, 11145–11153. doi: 10.1021/la402608z

Halan, B., Buehler, K., and Schmid, A. (2012). Biofilms as living catalysts in continuous chemical syntheses. *Trends Biotech.* 30, 453–465. doi: 10.1016/j.tibtech.2012.05.003

Hall-Stoodley, L., Costerton, J., and Stoodley, P. (2004). Bacterial biofilms: from the natural environment to infectious diseases. *Nat. Rev. Microbiol.* 2, 95–108. doi: 10.1038/nrmicro821

Hall-Stoodley, L., Hu, F. Z., Gieseke, A., Nistico, L., Nguyen, D., Hayes, J., et al. (2006). Direct detection of bacterial biofilms on the middle-ear mucosa of children with chronic otitis media. *JAMA* 296, 202–211. doi: 10.1001/jama.296.2.202

Hansen, S. K., Rainey, P. B., Haagensen, J. A. J., and Molin, S. (2007). Evolution of species interactions in a biofilm community. *Nature* 445, 533–536. doi: 10.1038/nature05514

Hillesland, K. L., and Stahl, D. A. (2010). Rapid evolution of stability and productivity at the origin of a microbial mutualism. *Proc. Natl. Acad. Sci. U.S.A.* 107, 2124–2129. doi: 10.1073/pnas.0908456107

Houry, A., Gohar, M., Deschamps, J., Tischenko, E., Aymerich, S., Gruss, A., et al. (2012). Bacterial swimmers that infiltrate and take over the biofilm matrix. *Proc. Natl. Acad. Sci. U.S.A.* 109, 13088–13093. doi: 10.1073/pnas.1200791109

Jakubovics, N. S. (2010). Talk of the town: interspecies communication in oral biofilms. *Mol. Oral Microbiol.* 25, 4–14. doi: 10.1111/j.2041-1014.2009.00563.x

Kato, S., Hashimoto, K., and Watanabe, K. (2011). Methanogenesis facilitated by electric syntrophy via (semi)conductive iron-oxide minerals. *Environ. Microbiol.* 14, 1646–1654. doi: 10.1111/j.1462-2920.2011.02611.x

Kato, S., and Watanabe, K. (2010). Ecological and evolutionary interactions in syntrophic methanogenic consortia. *Microbes Environ.* 25, 145–151. doi: 10.1264/jsme2.ME10122

Lawrence, D., Fiegna, F., Behrends, V., Bundy, J. G., Phillimore, A. B., Bell, T., et al. (2012). Species interactions alter evolutionary responses to a novel environment. *PLoS Biol.* 10:e1001330. doi: 10.1371/journal.pbio.1001330

Leloup, J., Fossing, H., Kohls, K., Holmkvist, L., Borowski, C., and Jørgensen, B. B. (2009). Sulfate-reducing bacteria in marine sediment (Aarhus Bay, Denmark): abundance and diversity related to geochemical zonation. *Environ. Microbiol.* 11, 1278–1291. doi: 10.1111/j.1462-2920.2008.01855.x

Lowry, O. H., Rosebrough, N. J., Farr, A. L., and Randall, R. J. (1951). Protein measurement with the Folin phenol reagent. *J. Biol. Chem.* 193, 265–275.

McInerney, M. J., Sieber, J. R., and Gunsalus, R. P. (2009). Syntrophy in anaerobic global carbon cycles. *Curr. Opin. Biotechnol.* 20, 623–632. doi: 10.1016/j.copbio.2009.10.001

Megee, R. D. III, Drake, J. F., Fredrickson, A. G., and Tsuchiya, H. M. (1972). Studies in intermicrobial symbiosis, *Saccharomyces cerevisiae* and *Lactobacillus casei*. *Can. J. Microbiol.* 18, 1733–1742. doi: 10.1139/m72-269

Meyer, J. S., Tsuchiya, H. M., and Fredrickson, A. G. (1975). Dynamics of mixed populations having complementary metabolism. *Biotechnol. Bioeng.* 17, 1065–1081. doi: 10.1002/bit.260170709

Moissl-Eichinger, C., and Huber, H. (2011). Archaeal symbionts and parasites. *Curr. Opin. Microbiol.* 14, 364–370. doi: 10.1016/j.mib.2011.04.016

Molin, S., and Tolker-Nielsen, T. (2003). Gene transfer occurs with enhanced efficiency in biofilms and induces enhanced stabilisation of the biofilm structure. *Curr. Opin. Biotech.* 14, 255–261. doi: 10.1016/S0958-1669(03)00036-3

Møller, S., Sternberg, C., Andersen, J. B., Christensen, B. B., Ramos, J. L., Givskov, M., et al. (1998). In situ gene expression in mixed-culture biofilms: evidence of metabolic interactions between community members. *App. Environ. Microbiol.* 64, 721–732.

Momeni, B., Brileya, K. A., Fields, M. W., and Shou, W. (2013). Strong inter-population cooperation leads to partner intermixing in microbial communities. *Elife* 2:e00230. doi: 10.7554/eLife.00230

Moreau, J. W., Zierenberg, R. A., and Banfield, J. F. (2010). Diversity of dissimilatory sulfite reductase genes (dsrAB) in a salt marsh impacted by long-term acid mine drainage. *Appl. Environ. Microbiol.* 76, 4819–4828. doi: 10.1128/AEM.03006-09

Neef, L., van Weele, M., and van Velthoven, P. (2010). Optimal estimation of the present-day global methane budget. *Global Biogeochem. Cycles* 24, 1–10. doi: 10.1029/2009GB003661

Nielsen, A. T., Tolker-Nielsen, T., Barken, K. B., and Molin, S. (2000). Role of commensal relationships on the spatial structure of a surface-attached microbial consortium. *Environ. Microbiol.* 2, 59–68. doi: 10.1046/j.1462-2920.2000.00084.x

Perez-Osorio, A. C., Williamson, K. S., and Franklin, M. J. (2010). Heterogeneous rpoS and rhlR mRNA levels and 16S rRNA/rDNA (rRNA gene) ratios within *Pseudomonas aeruginosa* biofilms, sampled by laser capture microdissection. *J. Bacteriol.* 192, 2991–3000. doi: 10.1128/JB.01598-09

Plugge, C. M., Zhang, W., Scholten, J. C. M., and Stams, A. J. M. (2011). Metabolic flexibility of sulfate-reducing bacteria. *Front. Microbiol.* 2:81. doi: 10.3389/fmicb.2011.00081

Poli, A., Anzelmo, G., and Nicolaus, B. (2010). Bacterial exopolysaccharides from extreme marine habitats: production, characterization and biological activities. *Mar. Drugs* 8, 1779–1802. doi: 10.3390/md8061779

Purdy, K. J., Embley, T. M., and Nedwell, D. B. (2002). The distribution and activity of sulphate reducing bacteria in estuarine and coastal marine sediments. *Antonie Van Leeuwenhoek* 81, 181–187. doi: 10.1023/A:1020550215012

Raskin, L., Rittmann, B. E., and Stahl, D. A. (1996). Competition and coexistence of sulfate-reducing and methanogenic populations in anaerobic biofilms. *Appl. Environ. Microbiol.* 62, 3847–3857.

Richter, L. V., Sandler, S. J., and Weis, R. M. (2012). Two isoforms of *Geobacter sulfurreducens* PilA have distinct roles in pilus biogenesis, cytochrome localization, extracellular electron transfer, and biofilm formation. *J. Bacteriol.* 194, 2551–2563. doi: 10.1128/JB.06366-11

Schlesinger, W. H., and Bernhardt, E. S. (2013). *Biogeochemistry: An Analysis of Global Change*, 3rd Edn. Waltham, MA: Academic Press.

Shimoyama, T., Kato, S., Ishii, S., and Watanabe, K. (2009). Flagellum mediates symbiosis. *Science* 323, 1574. doi: 10.1126/science.1170086

Shindala, A., Bungay, H. R. III, Krieg, N. R., and Culbert, K. (1965). Mixed-culture interactions I. Commensalism of *Proteus vulgaris* with *Saccharomyces cerevisiae* in continuous culture. *J. Bacteriol.* 89, 693–696.

Sieber, J. R., McInerney, M. J., and Gunsalus, R. P. (2012). Genomic insights into syntrophy: the paradigm for anaerobic metabolic cooperation. *Annu. Rev. Microbiol.* 66, 429–452. doi: 10.1146/annurev-micro-090110-102844

Stams, A. J. M., and Plugge, C. M. (2009). Electron transfer in syntrophic communities of anaerobic bacteria and archaea. *Nat. Rev. Microbiol.* 7, 568–577. doi: 10.1038/nrmicro2166

Stewart, P. S. (2003). Diffusion in biofilms. *J. Bacteriol.* 185, 1485–1491. doi: 10.1128/JB.185.5.1485-1491.2003

Stewart, P. S., and Franklin, M. J. (2008). Physiological heterogeneity in biofilms. *Nat. Rev. Microbiol.* 6, 199–210. doi: 10.1038/nrmicro1838 Stewart,

P. S., Griebe, T., Srinivasan, R., Chen, C. I., Yu, F. P., deBeer, D., et al. (1994). Comparison of respiratory activity and culturability during monochloramine disinfection of binary population biofilms. *Appl. Environ. Microbiol.* 60, 1690–1692.

Stilling, P. D. (2003). *Ecology*, 4th Edn. Upper Saddle River, NJ: Prentice Hall Inc.

Stoecker, K., Dorninger, C., Daims, H., and Wagner, M. (2010). Double labeling of oligonucleotide probes for fluorescence in situ hybridization (DOPE-FISH) improves signal intensity and increases rRNA accessibility. *Appl. Environ. Microbiol.* 76, 922–926. doi: 10.1128/AEM.02456-09

Stolyar, S., Van Dien, S., Hillesland, K. L., Pinel, N., Lie, T. J., Leigh, J. A., et al. (2007). Metabolic modeling of a mutualistic microbial community. *Mol. Syst. Biol.* 3, 1–14. doi: 10.1038/msb4100131

Thauer, R. K., Kaster, A.-K., Seedorf, H., Buckel, W., and Hedderich, R. (2008). Methanogenic archaea: ecologically relevant differences in energy conservation. *Nat. Rev. Microbiol.* 6, 579–591. doi: 10.1038/nrmicro1931

van Groenigen, K. J., Osenberg, C. W., and Hungate, B. A. (2012). Increased soil emissions of potent greenhouse gases under increased atmospheric CO2. *Nature* 475, 214–216. doi: 10.1038/nature10176

Walker, C. B., He, Z., Yang, Z. K., Ringbauer, J. A., He, Q., Zhou, J., et al. (2009). The electron transfer system of syntrophically grown *Desulfovibrio vulgaris*. *J. Bacteriol.* 191, 5793–5801. doi: 10.1128/JB.00356-09

Walker, C. B., Redding-Johanson, A. M., Baidoo, E. E., Rajeev, L., He, Z., Hendrickson, E. L., et al. (2012). Functional responses of methanogenic archaea to syntrophic growth. *ISME* 6, 2045–2055. doi: 10.1038/ismej.2012.60

Wanner, O., and Gujer, W. (1986). A multispecies biofilm model. *Biotechnol. Bioeng.* 28, 314–328. doi: 10.1002/bit.260280304

Wei, H., Yang, Z., Lux, R., Zhao, M., Wang, J., He, X., et al. (2012). Direct visualization of the interaction between pilin and exopolysaccharides of *Myxococcus* *xanthus* with eGFP fused PilA protein. *FEMS Microbiol. Lett.* 326, 23–30. doi: 10.1111/j.1574-6968.2011.02430.x

Wilke, C. R., and Chang, P. (1955). Correlation of diffusion coefficients in dilute solutions. *AIChE J.* 1, 264–270. doi: 10.1002/aic.690010222

Xie, X., Johnson, T. M., Wang, Y., Lundstrom, C. C., Ellis, A., Wang, X., et al. (2013). Mobilization of arsenic in aquifers from the Datong Basin, China: evidence from geochemical and iron isotopic data. *Chemosphere* 90, 1878–1884. doi: 10.1016/j.chemosphere.2012.10.012

Xu, K. D., McFeters, G. A., and Stewart, P. S. (2000). Biofilm resistance to antimicrobial agents. *Microbiology* 146, 547–549.

Yeoh, H. T., Bungay, H. R., and Krieg, N. R. (1968). A microbial interaction involving combined mutualism and inhibition. *Can. J. Microbiol.* 14, 491–492. doi: 10.1139/m68-083

Zijnge, V., van Leeuwen, M. B. M., Degener, J. E., Abbas, F., Thurnheer, T., Gmür, R., et al. (2010). Oral biofilm architecture on natural teeth. *PLoS ONE* 5:e9321. doi: 10.1371/journal.pone.0009321

Conflict of Interest Statement: The authors declare that the research was conducted in the absence of any commercial or financial relationships that could be construed as a potential conflict of interest.

Received: 10 September 2014; accepted: 22 November 2014; published online: 15 December 2014.

Citation: Brileya KA, Camilleri LB, Zane GM, Wall JD and Fields MW (2014) Biofilm growth mode promotes maximum carrying capacity and community stability during product inhibition syntrophy. Front. Microbiol. 5:693. doi: 10.3389/fmicb.2014.00693

This article was submitted to Microbial Symbioses, a section of the journal Frontiers in Microbiology.

Copyright © 2014 Brileya, Camilleri, Zane, Wall and Fields. This is an open-access article distributed under the terms of the Creative Commons Attribution License (CC BY). The use, distribution or reproduction in other forums is permitted, provided the original author(s) or licensor are credited and that the original publication in this journal is cited, in accordance with accepted academic practice. No use, distribution or reproduction is permitted which does not comply with these terms.

APPENDIX E

3D-FLUORESCENCE IN SITU HYBRIDIZATION OF INTACT, ANAEROBIC BIOFILM

Contribution of Authors and Co-Authors

Manuscript in Appendix E

Author: Kristen A. Brileya

Contributions: Developed experimental design, performed experiments, analyzed data, wrote and revised the manuscript.

Co-Author: Laura B. Camilleri

Contributions: Developed experimental design, performed experiments, analyzed data, Wrote and revised the manuscript.

Co-Author: Matthew W. Fields

Contributions: Developed experimental design, analyzed data, wrote and revised the manuscript.

Manuscript Information Page

Kristen A. Brileya, Laura B. Camilleri, Matthew W. Fields

Engineering and Analyzing Multicellular Systems

Status of Manuscript:
____ Prepared for submission to a peer-reviewed journal
____ Officially submitted to a peer-review journal
____ Accepted by a peer-reviewed journal
__X_ Published in a peer-reviewed journal

Humana Press, Methods in Molecular Biology, Springer Science & Business Media; 2014; vol 1151, pgs 189-197. Doi: https://doi.org/10.1007/978-1-4939-0554-6_13

Chapter 13

3D-Fluorescence In Situ Hybridization of Intact, Anaerobic Biofilm

Kristen A. Brileya, Laura B. Camilleri, and Matthew W. Fields

Abstract

FISH (fluorescence in situ hybridization) is a valuable technique to visualize and quantify localization of different microbial species within biofilms. Biofilm conformation can be altered during typical sample preparation for FISH, which can impact observations in multispecies biofilms, including the relative positions of cells. Here, we describe methods to preserve 3-D structure during FISH for visualization of an anaerobic coculture biofilm of *Desulfovibrio vulgaris* Hildenborough and *Methanococcus maripaludis*.

Key words Biofilm structure, Multispecies biofilm, Population interactions, Sulfate-reducing bacteria, Methanogenic archaea

1 Introduction

FISH techniques based upon rRNA gene sequences have revolutionized the study of microorganisms in natural assemblages and environments and have allowed scientists and engineers to characterize the structure of microbial communities more quantitatively [1]. Techniques continue to improve in terms of sensitivity [2] and in situ hybridization can be used in combination with other methods [3] to elucidate information about metabolic activity, genetic potential, and environmental conditions [4–7]. Structure and local environments are particularly important in the study of microbial biofilms, and the application of FISH techniques to microbial assemblages provides insight into the complex structure-function relationships of microbial biofilms and/or aggregates.

Biofilms are typically defined as self-assembled groups of cells adhered to surfaces that are embedded within an exopolymer matrix. Matrices of well-studied biofilms are usually composed of exopolysaccharides (EPS) that can include carbohydrate, protein, DNA, and various appendages (i.e., pili, fimbriae) within the matrix [8]. As FISH techniques that can probe complex multispecies

Lianhong Sun and Wenying Shou (eds.), *Engineering and Analyzing Multicellular Systems: Methods and Protocols*,
Methods in Molecular Biology, vol. 1151, DOI 10.1007/978-1-4939-0554-6_13, © Springer Science+Business Media New York 2014

biofilms continue to emerge (e.g., ref. [9]), the maintenance of biofilm structure and integrity will be crucial to deciphering structure–function relationships. Here, we demonstrate the use of 3D-FISH on an anaerobic, coculture biofilm using the techniques previously described by Daims et al. [10].

2 Materials

2.1 Cover Slip Preparation

1. Absolute ethanol.
2. Acidic ethanol: Prepare fresh 99 mL of 70 % ethanol in a small beaker by adding 70 mL of absolute ethanol to 29 mL deionized water. Add 1 mL of 12 M HCl for a final concentration of 1 % (v/v).
3. Bind-Silane working solution: Add 1 mL of Bind-Silane (Amersham Biosciences, Uppsala, Sweden), 3 mL of 10 % (v/v) glacial acetic acid, and 296 mL of deionized water. Mix until the solution is clear. Store at 4 °C.
4. Cover slips (No. 1½, 24 × 50 mm).

2.2 Sample Preparation, Fixation, and Storage

1. 3× Phosphate-buffered saline (PBS): Prepare each of A. 200 mM NaH_2PO_4, B. 200 mM Na_2HPO_4, and C. 390 mM NaCl then adjust the pH of solution B to 7.2–7.4 with solution A. Next add 150 mL of the prepared phosphate buffer to 850 mL of solution C, and adjust the final pH to 7.2–7.4 with NaOH. To make 1× PBS dilute this solution with two volumes of deionized water.
2. 4 % Paraformaldehyde (PFA): Heat 33 mL of deionized water to 65 °C and add 2 g of paraformaldehyde while stirring (*see* **Note 1**). Add NaOH until the paraformaldehyde dissolves, then add 16.6 mL 3× PBS. Cool to room temperature and adjust pH to 7.2–7.4 then filter with a 0.2 μm filter. Store at −20 °C.
3. Glycerol.
4. Ice.

2.3 Polyacrylamide Embedding

1. Polyacrylamide (PAA) solution: Prepare 20 % (w/v) solution in water or 1× PBS. A 37.5:1 solution of Acrylamide: BIS Acrylamide (EMD Chemicals, Inc., Darmstadt, Germany) (*see* **Note 2**) is 40 % (w/v), so the 20 % PAA solution is prepared with an equal volume of water or 1× PBS. Store at 4 °C.
2. Ammonium persulfate (APS): A 10 % (w/v) solution is made by adding 1 g of APS (*see* **Note 3**) to 10 mL of deionized water. Store at 4 °C.
3. TEMED (Tetramethylethylenediamine) (*see* **Note 4**).

4. Polytetrafluoroethylene (PTFE) sheets: PTFE or Teflon™ (McMaster Carr, USA) can be obtained in a variety of dimensions and preparations. Use either polished "adhesive-ready" PTFE or a type that already has adhesive. Choose a thickness that is as tall as or taller than your biofilm, that your microscope objective has a long enough working distance to see through. For this study a 0.01 in. thick (~254 μm) film with adhesive was used. Cut small frames that fit around the perimeter of your cover slips.

2.4 *In Situ* Hybridization

1. 50, 80, 96 % (v/v) ethanol.
2. 5 M NaCl: Prepare 50 mL by dissolving 14.61 g of NaCl in water. Store at room temperature.
3. 1 M Tris–HCl buffer prepared in water, adjust pH with 10 N NaOH to 8.0. Store at room temperature.
4. High-quality molecular grade deionized formamide (*see* **Note 5**). Store at 4 °C or according to manufacturer's recommendation. Low-quality formamide that is contaminated with cations will reduce hybridization stringency.
5. Sodium dodecyl sulfate (SDS): Prepare a 10 % (w/v) solution by dissolving 2 g of SDS in 20 mL of deionized water. Store at room temperature.
6. 0.5 M Ethylenediaminetetraacetate (EDTA sodium salt) prepared in water, adjust pH with NaOH pellets to 8.0. As pH approaches 8.0, EDTA will dissolve slowly. At this point, use 10 N NaOH to raise pH with more control. Store at room temperature.
7. Fluorescently labeled oligonucleotide probe at 30 ng/μL for most fluorophores, or 50 ng/μL for probes labeled with fluorescein and its derivatives. For this example (Fig. 1), domain-level probes EUB338 (5′- GCT GCC TCC CGT AGG AGT -3′) double-labeled with Cy3 (5′and 3′) and ARCH915 (5′- GTG CTC CCC CGC CAA TTC CT -3′) double-labeled with Cy5 (5′and 3′) were used (Thermo Scientific Custom Biopolymers, Ulm, Germany). Store at −20 °C in the dark.
8. Ice-cold deionized water.
9. Citifluor AF1 Antifadent (Citifluor Ltd., London, UK).
10. Hybridization oven at 46 °C.
11. Water bath at 48 °C.
12. Oil free compressed air.
13. Microscope equipped with appropriate filter sets for selected fluorophore-labeled probe. A confocal laser scanning microscope (CLSM) is necessary to acquire optical sections through the depth of the biofilm. A long working distance objective is

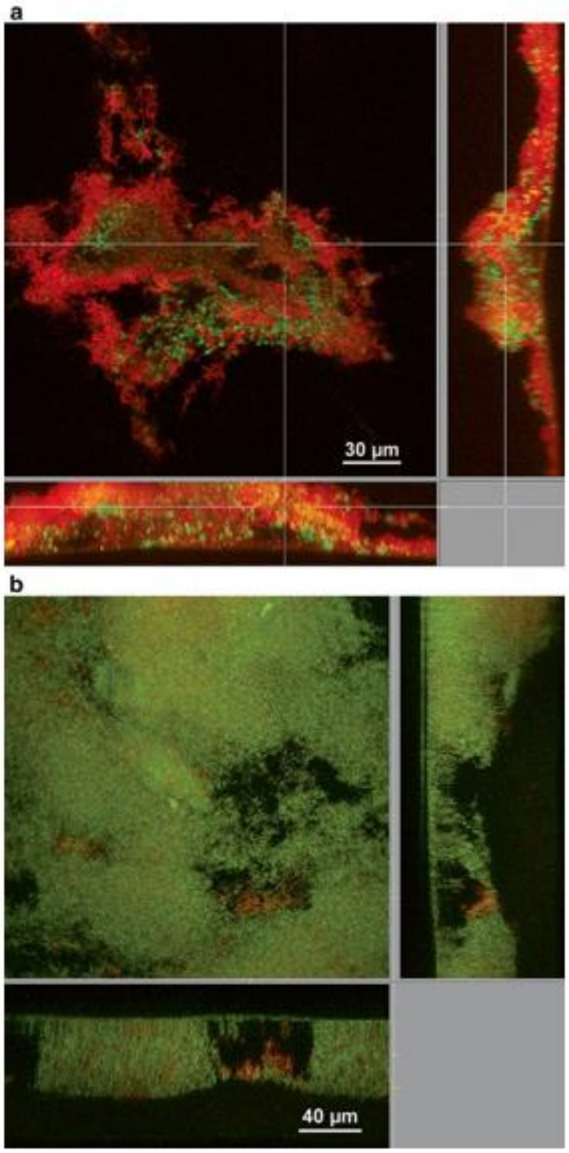

Fig. 1 (**a**) Coculture anaerobic biofilm embedded in polyacrylamide and hybridized to probes Arch915 (*green*) for *M. maripaludis* and Eub338 (*red*) for *D. vulgaris*. *Main panel* is biofilm as viewed from above, while *side panels* represent vertical cross sections. (**b**) *D. vulgaris* (Arch915—*Red*) and *M. maripaludis* (Eub338—*Green*) coculture biofilm embedded in polyacrylamide and viewed from above. Images were taken on a Leica TCS SP5 II upright confocal laser scanning microscope using a 63× long working distance water dipping objective. Digital reconstructions were done using Imaris v.7.6 (Bitplane, Zurich, CH). From colocalization analysis of these images using MetaMorph v. 7.6 (Molecular Devices, Sunnyvale, CA), we observed that the populations were distributed randomly through the depth of the biofilm

also required to obtain optical sections through the gel pad, such as the Leica 63× HCX APO L U-V-I water dipping objective (#506148, Leica Microsystems, Inc., Germany) used in the described example.

---

3 Methods

3.1 Cover Slip Pretreatment

1. Clean cover slips by dipping in a small beaker of acidic ethanol and drying on a lint-free tissue. To coat cover slips so that later they can be covalently attached to biofilm-embedded polyacrylamide gel, submerge the cover slips in the Bind-Silane solution and incubate at room temperature for 1 h. Rinse the cover slips in deionized water and then again in ethanol. Dry the cover slips on a lint-free tissue. Cover slips can be stored for several months at room temperature.

3.2 Sample Preparation, Fixation, and Storage

1. Whole biofilm grown on the microscope slide should be fixed immediately while still hydrated by placing in a 50 mL conical tube or slide holder with ice-cold 4 % PFA. Aqueous samples are typically fixed in three volumes of 4 % PFA to one volume of 1× PBS, especially if the biofilm has a low moisture content. A wet biofilm may be fixed directly in 4 % PFA. In both cases, make sure that the slide is submerged in the fixative solution. Fixation is typically for 3–12 h, and longer fixation times may render cells impermeable to the oligonucleotide probe (*see* **Note 6**).
2. Following fixation, slides should be stored at −20 °C in 1:1 glycerol:1× PBS. Do not store in ethanol as this will inhibit the polymerization of acrylamide during embedding.

3.3 Polyacrylamide Embedding

All of these steps must be done very quickly, so assemble all materials first in the fume hood. Leave the biofilm slide in the PBS:glycerol solution until you are ready to use it.

1. Lay pretreated cover slip on a paper towel and apply one of the PTFE frames to the edge by pressing gently with forceps.
2. Prepare a working PAA solution with 50 μL of 20 % PAA, 0.5 μL of 10 % APS, and 0.5 μL of TEMED. Immediately pipet this solution onto the biofilm and place the pretreated cover slip on the biofilm with the Teflon frame facing the solution and biofilm (Fig. 2). Make sure that there are no air bubbles as this will prevent the polymerization of acrylamide, then weight the slide down very lightly with a small serum bottle. Let the acrylamide solution polymerize for 10–15 min at room temperature. A larger volume may be necessary to cover the entire biofilm.

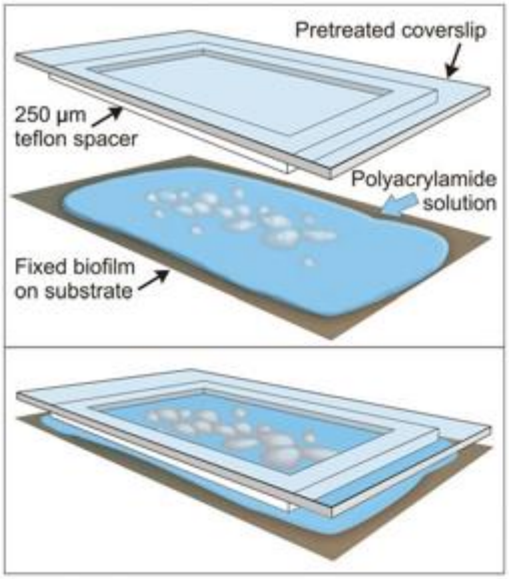

Fig. 2 Schematic showing assembly of the cover slip with Teflon frame and biofilm embedded in polyacrylamide

3. When the polyacrylamide has solidified to a gel, carefully separate the slide from the cover slip. The biofilm should now be upside down on the cover slip. To ensure that all of the biofilm came off the slide, you can examine it with light or fluorescent microscopy using an appropriate stain (*see* **Note 7**).

3.4 *In Situ* Hybridization

1. Dehydrate the whole cover slip and gel pad in an increasing ethanol series (5 min each in 50, 80, and 96 % ethanol). Dry gel pad completely by blowing oil-free compressed air on the surface for approximately 30 s. It is normal for the gel pad to turn white during dehydration.
2. Thaw oligonucleotide probes on ice in the dark and prepare hybridization buffer. Prepare hybridization buffer in a 1.5 mL centrifuge tube containing 5 M NaCl, 1 M Tris, deionized water, formamide, and 10 % SDS in the concentration appropriate for the probe as in selected column of Table 1. The appropriate formamide concentration is reported in the literature for previously published probes, and must be determined experimentally when a new probe is developed (e.g., ref. [11]).
3. Add 200 µL of hybridization buffer and 4 µL of probe to the surface of the gel pad and mix up and down by pipetting. The hybridization buffer will dome up on the surface of the gel for a short time, and it will not be difficult to mix in the probe,

Table 1
Volume in µL of each component of hybridization buffer to be used at each formamide concentration from 0 to 70 %

Form %	0 %	5 %	10 %	20 %	25 %	30 %	35 %	40 %	50 %	55 %	70 %
NaCl	180	180	180	180	180	180	180	180	180	180	180
Tris	20	20	20	20	20	20	20	20	20	20	20
H_2O	800	750	700	600	550	500	450	400	300	250	100
Form	0	50	100	200	250	300	350	400	500	550	700
SDS	1	1	1	1	1	1	1	1	1	1	1

Table 2
Volume of each component of washing buffer to be used at the corresponding formamide concentration from 0 to 70 %

Form %	0 %	5 %	10 %	20 %	25 %	30 %	35 %	40 %	50 %	55 %	70 %
NaCl	9 ml	6.3 ml	4.5 ml	2,150 µL	1,490 µL	1,020 µL	700 µL	460 µL	180 µL	100 µL	0
Tris (ml)	1	1	1	1	1	1	1	1	1	1	1
EDTA (µL)	0	0	0	500	500	500	500	500	500	500	500
H_2O (ml)	fill to 50	fill to 50	fill to 50	fill to 50	fill to 50	fill to 50	fill to 50	fill to 50	fill to 50	fill to 50	fill to 50
(SDS) (µL)	50	50	50	50	50	50	50	50	50	50	50

however take care to avoid touching the gel pad with the pipet tip. Work quickly to avoid exposing the probes to light and to prevent the hybridization buffer from evaporating.

4. Prepare a humid chamber hybridization tube (50 mL conical tube) by folding a Kimwipe tissue and laying it in the tube. Pour the rest of the hybridization buffer onto the tissue to keep the atmosphere in the chamber humid and at the desired concentration of formamide. Immediately transfer the cover slip into the hybridization tube, laying it on the tissue with the gel pad facing up, and incubate horizontally in the hybridization oven (46 °C) for 2–3 h. Longer hybridization times may be required for very thick or dense biofilms.
5. Prepare washing buffer in a 50 mL conical tube for the appropriate stringency according to one column of Table 2. Use the same concentration column as chosen for the hybridization

buffer, based on the reported value for the probe used, or the value determined for a newly developed probe. Warm the washing buffer in a water bath (48 °C).

6. After hybridization is complete, carefully and quickly transfer the embedded sample into the preheated washing buffer and incubate vertically for 35–40 min in the water bath (48 °C). The transfer must be done quickly and in the fume hood to avoid inhaling warm formamide and to prevent the wash buffer from cooling.
7. Dip the cover slip quickly in and out of ice-cold deionized water eight times to cool and wash the polyacrylamide pad and biofilm and dry immediately using oil-free compressed air.
8. Place the cover slip in the dark at room temperature for an additional 10 min to ensure it is dried completely. Do not over dry as the gel pad will crack.
9. Image the PAA embedded sample using a long working distance objective on a CLSM. Imaging can be done through the cover slip or through the gel pad.

4 Notes

1. Paraformaldehyde is a suspected carcinogen, wear gloves and a dust mask and work in a fume hood.
2. Acrylamide is known to cause cancer and birth defects. Wear gloves and work in a fume hood.
3. APS is a strong oxidant and irritant.
4. TEMED is highly flammable and corrosive.
5. Formamide is a known teratogen and causes irritation upon contact or inhalation. May cause unconsciousness. It is especially volatile when warm and should be used in the fume hood and handled with care.
6. Fixation time and requirements vary between cell types (e.g., Gram-negative, Gram-positive, or Archaea with or without an S layer) and should be tested on aqueous cultures first whenever possible. Fixation with one volume of 96 % ethanol mixed with one volume of 1× PBS may be preferable in some cases, and the fixed cells can be immediately stored at −20 °C. For some Gram-positive organisms, it may be necessary to treat with enzymes such as lysozyme, proteinase k, or achromopeptidase to permeabilize the cell.
7. To practice preparing the polyacrylamide gel pad and test the capabilities of your microscope, you can first try embedding and imaging fluorescent beads, for example, Constellation Microspheres (Invitrogen Molecular Probes, USA).

Acknowledgements

The authors wish to thank Betsey Pitts for microscopy assistance and Dr. Sebastian Lücker for thoughtful discussions. Special thanks to Peg Dirckx for preparing Figs. 1 and 2. This work was supported as a component of ENIGMA, a scientific focus area program supported by the U.S. Department of Energy, Office of Science, Office of Biological and Environmental Research, Genomics: GTL Foundational Science through contract DE-AC02-05CH11231 between Lawrence Berkeley National Laboratory and the U.S. Department of Energy. K.A.B. and L.B.C. were also supported by a NSF-IGERT fellowship in Geobiological Systems at Montana State University (DGE 0654336). The confocal microscopy equipment used was purchased with funding from the NSF-Major Research Instrumentation Program and the M.J. Murdock Charitable Trust.

References

1. Wagner M, Haider S (2012) New trends in fluorescence *in situ* hybridization for identification and functional analyses of microbes. Curr Opin Biotechnol 23:96–102
2. Pernthaler A, Pernthaler J, Amann R (2002) Fluoresecence in situ hybridization and catalyzed reporter deposition for the identification of marine bacteria. Appl Environ Microbiol 68:3094–3101
3. Wagner M (2009) Single-cell ecophysiology of microbes as revealed by Raman microspectroscopy or secondary ion mass spectrometry imaging. Annu Rev Microbiol 63:411–429
4. Dekas AE, Poretsky RS, Orphan VJ (2009) Deep-sea Archaea fix and share nitrogen in methane-consuming microbial consortia. Science 326:422–426
5. Gieseke A, Purkhold U, Wagner M, Amann R, Schramm A (2001) Community structure and activity dynamics of nitrifying bacteria in a phosphate-removing biofilm. Appl Environ Microbiol 67:1351–1362
6. Huang WE, Stoecker K, Griffiths R, Newbold L, Daims H, Whiteley AS, Wagner M (2007) Raman-FISH: combining stable-isotope Raman spectroscopy and fluorescence in situ hybridization for the single cell analysis of identity and function. Environ Microbiol 9: 1878–181889
7. Wagner M, Nielsen PH, Loy A, Nielsen JL, Daims H (2006) Linking microbial community structure with function: fluorescence in situ hybridization-microautoradiography and isotope arrays. Curr Opin Biotechnol 17:1–9
8. Branda SS, Vik A, Friedman L, Kolter R (2005) Biofilms: the matrix revisited. Trends Microbiol 13:20–26
9. Valm AM, Mark Welch JL, Rieken CW, Hasegawa Y, Sogin ML, Oldenbourg R, Dewhirst FE, Borisy V (2011) Systems-level analysis of microbial community organization through combinatorial labeling and spectral imaging. Proc Nat Acad Sci U S A 108: 4152–4157
10. Daims H, Lücker S, Wagner M (2006) daime, a novel image analysis program for microbial ecology and biofilm research. Environ Microbiol 8:200–213
11. Schramm A, Fuchs BM, Nielsen JL, Tonnolla M, Stahl DA (2002) Fluorescence in situ hybridization of 16S rRNA gene clones (Clone-FISH) for probe validation and screening of clone libraries. Environ Microbiol 4: 713–720